



Effects of Methyl Donor Nutrient Depletion on Gene Expression and DNA Methylation in Cervical Cancer Cell Line

MUNIRAH ISMAIL

Human Nutrition Unit

Department of Oncology and Metabolism

The Faculty of Medicine, Dentistry, and Health

University of Sheffield

A thesis submitted for the degree of Doctor of Philosophy

NOVEMBER 2021

Acknowledgement

Foremost, I would like to express my sincere gratitude to my supervisor, Dr Peter Grabowski, for the patient, encouragement and continuous support of my PhD study and research. His advice and guidance have helped me immensely during my time as PhD student. My sincere thanks also goes to Professor Hillary Powers for the help that she has provided throughout my time as a PhD student.

I would also like to thank all the staff members of the Department of Oncology and Metabolism, University of Sheffield. In particular, I would like to thank Mrs Barbara Mangnall and Mrs Joanna Chowdry for all the help, advice and support they continuously gave in order for me to successfully complete my laboratory experiments.

I am immensely grateful to Dr Paul Heath for his advice and guidance in the methylation array analysis, as well as Charlie Appleby-Mallinder and Matthew Wyles from SiTRAN.

I must express my gratitude to my aunt, Mrs Zarrin Abdullah, for her continued support and encouragement. I am extremely grateful by her willingness to continuously proofread my thesis.

Also, completing this work would have been all the more difficult were it not for the support and friendship provided by my housemates, Nadia and Asdya; and my friends at the University of Sheffield, Daniella Mariam, Zati Aqmar, Haslinda, Kamalia, Ejok and Atiqah.

I am very grateful to the Malaysian Ministry of Education, as this work would not have been possible without their financial support. I am especially indebted to my colleagues from the National University of Malaysia, who have been supportive and provided me with protected time to complete my thesis writing.

Last but not least, I would like to thank my parents and sisters, whose love and guidance are always with me in whatever I pursue.

Statement of Involvement

Certain measurements, which required the use of facilities to which there was limited researcher access, were made by others. These were: intracellular folate concentration, which was measured by Fraser Cocker, Senior Biomedical Scientist; and intracellular methionine concentration which was measured by Jennifer Watkinson, Lead Biomedical Scientist from the Department of Clinical Chemistry at the Children's Hospital in Sheffield.

Abstract

Cervical cancer arises when high-risk strains of human papilloma virus (HR-HPV) become integrated into the host genome in cervical epithelial cells and loss of episomal expression of the viral transcriptional regulator gene E2 occurs. However, not all women who acquire HPV infection develop cervical cancer: about 60% of HPV infections are transient and resolve on their own due to innate and adaptive immunity, indicating other risk factors. Among other known factors, dietary methyl donor nutrients that influence the methyl donor cycle may also be important in determining cervical cancer risk. They are required for the maintenance of DNA methylation, modification of which is associated with cancer progression through dysregulation of gene expression. The aim of this study is to identify molecular mechanisms by which alterations in methyl donor nutrients availability affect cervical cancer risk and progression.

A bioinformatics analysis was carried out to identify gene clusters susceptible to both methyl donor depletion and HPV integration using the DAVID, ClueGo and GeneMania software. The C4-II cervical cancer cell model of methyl donor depletion was used for this experimental study. Cells were grown for 8 days in complete medium, or medium depleted of folate, methionine or combined folate and methionine. The cell model was validated by measuring the intracellular folate, intracellular methionine and extracellular homocysteine concentrations. The *STAT1*, *RSAD2*, *OAS1*, *IFIT1* and *ISG15* genes expression were measured using RT-qPCR. A comprehensive DNA methylation profiling was performed using the Infinium Methylation EPIC BeadChip, followed by methylation data analysis with the RnBeads and bioinformatics software. Additionally, the TNF- α and IL-1 β cytokine production in THP-1 methyl donor depleted cells was measured using the Quantikine ELISA kit.

Gene clusters associated with host defence mechanisms, cell cycle, cell death and cell signalling were highly enriched. Additionally, a cluster of genes involved in antiviral defence induced by the type I interferon (IFN) pathway appeared to be most affected by methyl donor nutrients availability. These genes (*RSAD2*, *OAS1*, *IFIT1* and *ISG15*) were reported to be significantly upregulated with methionine or combined folate and methionine depletion; while *STAT1* gene expression was downregulated in all depleted conditions. Folate deficiency did not cause significant alteration to the expression of these genes. TNF- α and IL-1 β cytokine production was significantly reduced in all methyl donor depleted conditions. A majority of CpG sites were significantly hypomethylated in all conditions where methionine was deficient, while changes in folate depleted medium was not statistically significant. A high proportion of genes associated with host defence mechanisms, immune response as well as mitosis, cell differentiation, cell motility and angiogenesis were found to be hypomethylated.

This study highlights the importance of methionine over folate as a methyl donor in the regulation of gene expression, and also the regulatory functions of both folate and methionine on IFN-stimulated gene expression associated with antiviral immunity in a cervical cancer cell line. By identifying changes that occur in methyl donor regulated genes, there is a potential diagnostic or therapeutic approach based on epigenetic changes occurring due to nutrient availability for those who are in the at-risk group.

Table of Content

Acknowledgement	ii
Statement of Involvement.....	iii
Abstract.....	iv
Table of Content	v
List of Tables	x
List of Figures.....	xi
Abbreviations	xv
CHAPTER 1	1
INTRODUCTION	1
1.1 Cancer and its hallmark	1
1.2 Cervical cancer	2
1.2.1 Epidemiology of cervical cancer.....	2
1.2.2 Cervical cancer prevention program	4
1.2.3 Pathology of cervical cancer	5
1.2.4 Impact of HPV in the pathogenesis of cervical cancer	6
1.2.5 Cervical cancer risk factors	11
1.2.6 Diet and cervical cancer	14
1.3 DNA Methylation and Cancer	18
1.3.1 DNA methylation	18
1.3.2 Aberrant DNA methylation in cancer	20
1.3.3 DNA methyltransferase (DNMT)	23
1.3.4 Aberrant DNA methylation and cervical cancer	24
1.4 Methyl Donor Nutrients.....	28
1.4.1 One-carbon metabolism	28
1.4.2 Folate as a methyl donor	34
1.4.3 Methionine as methyl donor.....	42
1.4.4 Other micronutrients	45
1.5 Summary.....	47
1.6 Hypothesis and Objectives.....	48
1.6.1 Hypothesis.....	48
1.6.2 Objectives.....	48
CHAPTER 2.....	50
MATERIALS	50

2.1	Cell Lines	50
2.2	Media	50
2.3	Cell Culture	51
2.4	Depleted Media Preparation	51
2.5	Intracellular Folate Measurement	52
2.6	Intracellular Methionine Measurement	52
2.7	Homocysteine Measurement	52
2.8	RNA Extraction	52
2.9	cDNA Synthesis	53
2.10	Real-time quantitative PCR	53
2.11	Cytokine Production	54
2.12	DNA Extraction	54
2.13	Sodium Bisulphate Treatment	55
2.14	Methylation Array Profiling	55
2.15	Methylation Specific PCR Amplification	56
2.16	Gel Electrophoresis	56
CHAPTER 3		58
EFFECT OF METHYL DONOR NUTRIENT DEPLETION ON RNA EXPRESSION: A BIOINFORMATICS ANALYSIS		58
3.1	Introduction	58
3.2	Hypothesis and aims	62
3.3	Methods	63
3.3.1	Microarray dataset	63
3.3.2	Differentially expressed genes analysis	65
3.3.3	Functional and pathway enrichment analysis	65
3.3.4	Network analysis and visualization	67
3.4	Results	67
3.4.1	Effect of folate and methionine depletion on C4-II gene expression	67
3.4.2	Effect of HR-HPV integration in W12 cervical keratinocytes on gene expression	73
3.4.3	Effect of methyl donor nutrient depletion and chromosomal integration of HR- HPV in cervical cells gene expression	77
3.5	Discussion	87
3.6	Summary	92
CHAPTER 4		93
EFFECT OF METHYL DONOR DEPLETION ON THE EXPRESSION OF GENES ASSOCIATED WITH ANTIVIRAL IMMUNITY		93
4.1	Introduction	93

4.2	Hypothesis and aims	96
4.3	Methods	96
4.3.1	Preparation of media	96
4.3.2	Cell resuscitation	97
4.3.3	Cell subculture.....	97
4.3.4	Determination of cervical cancer cell growth characteristics in complete and depleted medium.....	97
4.3.5	C4-II sample preparation.....	97
4.3.6	Intracellular folate analysis	98
4.3.7	Intracellular methionine analysis	98
4.3.8	Intracellular and extracellular homocysteine analysis	99
4.3.9	C4-II RNA extraction.....	100
4.3.10	cDNA synthesis.....	101
4.3.11	Determination of primer efficiency using standard curve analysis.....	101
4.3.12	Determination of gene expression.....	103
4.3.13	Statistical analysis	104
4.4	Results.....	104
4.4.1	Effect of methyl donor depletion on C4-II cell growth.....	104
4.4.2	Effect of methyl donor depletion on intracellular folate.....	106
4.4.3	Effect of methyl donor depletion on intracellular methionine	107
4.4.4	Effect of methyl donor depletion on homocysteine export.....	108
4.4.5	Effect of methyl donor nutrient depletion on IFN-stimulated gene expression...	109
4.5	Discussion.....	119
4.5.1	Validation of cervical cancer cell model of methyl donor depletion	119
4.5.2	Effect of methyl donor depletion on the expression of interferon-stimulated genes	125
4.6	Summary	129
CHAPTER 5.....		130
EFFECT OF METHYL DONOR DEPLETION ON CYTOKINE PRODUCTION IN THE HUMAN THP-1 MONOCYTIC CELL LINE.....		130
5.1	Introduction.....	130
5.2	Hypothesis and Aim.....	136
5.3	Methods	136
5.3.1	Cell resuscitation	136
5.3.2	Cell subculture.....	136
5.3.3	Differentiation of THP-1 cell and sample collection	136
5.3.4	Determination of TNF- α concentration.....	137

5.3.5	Determination of IL-1 β concentration	139
5.3.6	Statistical analysis	140
5.4	Results.....	140
5.4.1	Effect of methyl donor depletion on TNF- α production	140
5.4.2	Effect of methyl donor depletion on IL-1 β production.....	142
5.5	Discussion	143
5.6	Summary	147
CHAPTER 6	148
EFFECT OF METHYL DONOR DEPLETION ON METHYLATION PROFILING	148
6.1	Introduction.....	148
6.2	Hypothesis and aim.....	152
6.3	Methods	152
6.3.1	C4-II sample preparation for methylation profiling	152
6.3.2	C4-II genomic DNA extraction.....	153
6.3.3	Sodium bisulphate treatment.....	154
6.3.4	C4-II cells methylation profiling.....	155
6.3.5	Methylation data analysis with RnBeads	156
6.3.6	Differentially methylated regions bioinformatics analysis	162
6.3.7	Designing methylation specific primers for PCR amplifications.....	162
6.3.8	Methylation specific PCR amplifications of selected genes	165
6.3.9	Gel electrophoresis	166
6.4	Results.....	166
6.4.1	Genomic DNA quality and quantity.....	166
6.4.2	RnBeads methylation data quality analysis.....	167
6.4.3	RnBeads methylation data filtration and normalisation.....	179
6.4.4	RnBeads exploratory analysis	179
6.4.5	RnBeads differential analysis.....	185
6.4.6	Bioinformatics analysis of differently methylated regions	188
6.4.7	Effect of methyl donor depletion on the methylation status of selected genes	193
6.5	Discussion	195
6.5.1	Methylation data quality control analysis and normalisation.....	195
6.5.2	Effect of methyl donor depletion on C4-II DNA methylation profile	197
6.5.3	Effect of methyl donor depletion on methylation status of selected genes	200
6.6	Summary	202
CHAPTER 7	204
DISCUSSION AND CONCLUSION	204

7.1	Discussion	204
7.2	Conclusion	211
7.3	Study Limitation	212
7.4	Future Works	213
	REFERENCES	215
	APPENDIX	271
	Appendix 1 Functional clustering analysis of upregulated DEGs from methyl donor depleted dataset.....	271
	Appendix 2 Functional clustering analysis of downregulated DEGs from methyl donor depleted dataset.....	276
	Appendix 3 Functional clustering analysis of common DEGs between methyl donor depleted and Epi-stage of HPV integration dataset	278
	Appendix 4 Functional clustering analysis of common DEGs between methyl donor depleted and Int-stage of HPV integration dataset	284

List of Tables

Table 3. 1	Selected GO_BP annotation clusters from both upregulated and downregulated DEGs of methyl donor depleted cells, associated with the hallmarks of cancer	69
Table 3. 2	Significant clusters annotated from common genes between methyl donor depletion and Epi-stage of HPV integration	78
Table 3. 3	Significant clusters annotated from common genes between methyl donor depletion and Int-stage of HPV integration	79
Table 3. 4	The changes in IFN-stimulated genes expression in methyl depleted C4-II cells and W12 episomal and integrated cervical keratinocytes cells	87
Table 4. 1	Reagent's mixture for cDNA synthesis	101
Table 4. 2	Positive control template serial dilution	102
Table 4. 3	Reagent's mixture for measuring primer efficiency using RT-PCR	103
Table 4. 4	Reagent's mixture for gene quantification using RT-qPCR	103
Table 4. 5	Doubling time of C4-II cervical cells grown in complete or methyl depleted media	106
Table 4. 6	Summary of C4-II cell count, Nanodrop and Bioanalyzer readings	110
Table 4. 7	Summary of the gene primers' standard curve slope, R2 and efficiency values	114
Table 5. 1	TNF- α Quantikine immunoassay control concentration	141
Table 5. 2	IL-1 β Quantikine immunoassay control concentration	142
Table 6. 1	Criteria selected for RnBeads analysis, pre-processing and differential modules	159
Table 6. 2	Specification of methylation specific primer pairs for <i>TP73</i> , <i>STAT1</i> and <i>DAPK1</i> genes	164
Table 6. 3	PCR amplification setup for each reaction	165
Table 6. 4	PCR amplification setting	166
Table 6. 5	C4-II genomic DNA yield and purity	167
Table 6. 6	Number of differently methylated regions according to sample group	188
Table 6. 7	Top ten GO-BP annotation clusters generated from gene promoter differently methylated regions	189

List of Figures

Figure 1. 1	Global cancer incidence and mortality in women (Sung et al., 2021).....	2
Figure 1. 2	Incidence and mortality rate of cervical cancer according to region in 2020.....	3
Figure 1. 3	HPV 16 structure and viral protein.....	7
Figure 1. 4	HPV-associated pathogenesis of cervical cancer	8
Figure 1. 5	Methylation of cytosine in carbon 5 to form 5-methylcytosine	19
Figure 1. 6	Methylation of CpG and gene expression	20
Figure 1. 7	The role of micronutrients in one-carbon metabolism and DNA methylation...	29
Figure 1. 8	Methyl donor depletion and cancer risks.....	33
Figure 3. 1	GO_BP terms network associated with upregulated DEGs in methyl donor depleted C4-II cervical cancer cell line.....	70
Figure 3. 2	GO_BP terms network associated with downregulated DEGs in methyl donor depleted C4-II cervical cancer cell line.....	71
Figure 3. 3	KEGG pathway network associated with DEGs in methyl donor depleted C4-II cervical cancer cell line	72
Figure 3. 4	GO_BP terms network associated with upregulated DEGs during the Epi-stage of HPV integration into W12 cervical keratinocytes cells.....	74
Figure 3. 5	GO_BP terms network associated with downregulated DEGs during the Epi- stage of HPV integration into W12 cervical keratinocytes cells.....	75
Figure 3. 6	GO_BP terms network associated with downregulated DEGs during the Int- stage of HPV integration into W12 cervical keratinocytes cells.....	76
Figure 3. 7	Venn diagram of common DEGs between methyl donor depletion and chromosomal integration of HPV dataset	77
Figure 3. 8	Network of biological processes affected by both methyl donor depletion and chromosomal integration of HPV at the Epi-stage.....	81
Figure 3. 9	Network of biological processes affected by both methyl donor depletion and chromosomal integration of HPV at the Int-stage.....	82
Figure 3. 10	Host defence mechanism affected by both methyl donor depletion and chromosomal integration of HPV at the Int-stage.....	83
Figure 3. 11	Network of KEGG pathways affected by both methyl donor depletion and chromosomal integration of HPV at the Epi-stage.....	84
Figure 3. 12	Network of KEGG pathways affected by both methyl donor depletion and chromosomal integration of HPV at the Int-stage.....	85

Figure 3. 13	Gene interaction network associated with methyl donor depletion and chromosomal integration of HPV	86
Figure 4. 1	Gene expression analysis workflow of five IFN-stimulated genes (ISGs) using quantitative RT-PCR	104
Figure 4. 2	C4-II growth curve in complete and depleted media	105
Figure 4. 3	Intracellular folate concentration of C4-II cells grown in complete and depleted media	106
Figure 4. 4	Intracellular methionine concentration of C4-II cells grown in complete and depleted media.....	108
Figure 4. 5	Extracellular homocysteine concentrations of C4-II cells grown in complete and depleted medium	109
Figure 4. 6	Determination of <i>STAT1</i> primer efficiency and specificity	111
Figure 4. 7	Determination of <i>RSAD2</i> primer efficiency and specificity.....	111
Figure 4. 8	Determination of <i>OAS1</i> primer efficiency and specificity	112
Figure 4. 9	Determination of <i>IFIT1</i> primer efficiency and specificity	112
Figure 4. 10	Determination of <i>ISG15</i> primer efficiency and specificity	113
Figure 4. 11	Determination of <i>GAPDH</i> primer efficiency and specificity.....	113
Figure 4. 12	Determination of <i>B2M</i> primer efficiency and specificity.....	114
Figure 4. 13	<i>STAT1</i> expression in complete and depleted media	115
Figure 4. 14	<i>RSAD2</i> expression in complete and depleted media	116
Figure 4. 15	<i>OAS1</i> expression in complete and methyl depleted media	117
Figure 4. 16	<i>IFIT1</i> expression in complete and methyl depleted media	118
Figure 4. 17	<i>ISG15</i> expression in complete and methyl depleted media.....	118
Figure 4. 18	Type 1 interferon signalling pathway involved in antiviral immunity.....	126
Figure 5. 1	Effect of methyl donor depletion on cytokines production workflow	138
Figure 5. 2	TNF- α standard curve	140
Figure 5. 3	The effect of methyl donor depletion on TNF- α concentration in THP-1 derived macrophages.....	141
Figure 5. 4	IL-1 β standard curve	142
Figure 5. 5	The effect of methyl donor depletion on IL-1 β concentration in THP-1 derived macrophages.....	143

Figure 6. 1	Bisulphite conversion process.....	154
Figure 6. 2	Infinium methylation EPIC BeadChip workflow	156
Figure 6. 3	Sample preparation and DNA methylation profiling workflow	157
Figure 6. 4	RnBeads analysis workflow.....	158
Figure 6. 5	User-generated csv file	158
Figure 6. 6	<i>DAPK1</i> primer sequence for methylation specific primers	163
Figure 6. 7	<i>TP73</i> primer sequence for methylation specific primer.....	163
Figure 6. 8	<i>STAT1</i> primer sequence for methylation specific primer	164
Figure 6. 9	Control boxplot for the staining probes	169
Figure 6. 10	Control boxplot for the hybridization probes.....	170
Figure 6. 11	Control boxplot for the extension probes.....	171
Figure 6. 12	Control boxplot for the target removal probes.....	172
Figure 6. 13	Control boxplot for the bisulphite conversion I probes	173
Figure 6. 14	Control boxplot for the bisulphite conversion II probes	174
Figure 6. 15	Control boxplot for the specificity I probes	175
Figure 6. 16	Control boxplot for the specificity II probes.....	176
Figure 6. 17	Control boxplot for the non-polymorphic probes	177
Figure 6. 18	Negative control boxplot.....	178
Figure 6. 19	Distribution of methylation β values before and after normalisation using the BMIQ method	179
Figure 6. 20	DNA methylation value distribution according to sample groups.....	180
Figure 6. 21	Heat map with hierarchical clustering of DNA methylation levels among sample groups	181
Figure 6. 22	Dimension reduction analysis of sample groups	182
Figure 6. 23	Relationship between average methylation and methylation variability of probe results for each sample group	183
Figure 6. 24	DNA methylation level for genomic region (gene) according to sample group	184
Figure 6. 25	DNA methylation level for genomic region (promoter) according to sample group	185
Figure 6. 26	DNA methylation level for genomic region (CpG islands) according to sample group	186
Figure 6. 27	Differential methylation analysis at individual CpG sites	187
Figure 6. 28	Venn diagram of common top ranking CpGs between methyl donor depleted conditions.....	188

Figure 6. 29	GO_BP terms network associated with DMRs for methionine depleted condition	190
Figure 6. 30	GO_BP terms network associated with DMRs for folate and methionine depleted condition	191
Figure 6. 31	GO_BP terms network associated with DMRs for 5% folate and methionine supplemented condition	192
Figure 6. 32	Post PCR amplification gel image for TP73 gene	194
Figure 6. 33	Post PCR amplification gel image for STAT1 gene	194
Figure 6. 34	Post PCR amplification gel image for DAPK1 gene	195

Abbreviations

CIN	cervical intraepithelial neoplasia
DEGs	differently expressed genes
DMEM	Dulbecco's Modified Eagle's Medium
DMR	differently methylated region
DNA	deoxyribonucleic acid
DNMT	DNA methyltransferase
DPBS	Dulbecco's phosphate buffer saline
F+M-	methionine depleted medium
F+M+	complete medium
FBS	fetal bovine serum
FDR	false discovery rate
F-M-	folate and methionine depleted medium
F-M+	folate depleted medium
GEO	Gene Expression Omnibus
GO	gene ontology
GO_BP	gene ontology terms to describe biological processes
HNSCC	head and neck squamous cell carcinoma
HPLC	high performance liquid chromatography
HPV	human papillomavirus
HR-HPV	high-risk human papillomavirus
IFN	interferon
IL	interleukin
ISG	interferon-stimulated genes
LPS	lipopolysaccharide
MSP	methylation specific PCR
NCBI	National Centre of Biotechnology Information
NK cells	natural killer cells
OC	oral contraceptives
OD	optical density
OSCC	oral squamous cell carcinoma
PCR	polymerase chain reaction
PMA	phorbol-12-myristate 13-acetate
qRT-PCR	quantitative real-time polymerase chain reaction
RIN	RNA integrity number
RNA	ribonucleic acid
RPMI	Roswell Park Memorial Institute medium
RQ	relative quantification
SAH	S-adenosyl homocysteine
SAM	S-adenosyl methionine
THF	tetrahydrofolate
TNF	tumour necrosis factor

CHAPTER 1

INTRODUCTION

Nutrients can regulate several biological processes in our bodies via modifying epigenetic mechanisms that are critical for gene expression such as DNA methylation. These epigenetic modifications may contribute to the status of our health and have been associated with the development of various cancers. A few nutrients in particular have been associated with the risk of cancer development via its function as methyl donor nutrients in the DNA methylation processes (Duthie et al., 2004; Mahmoud & Ali, 2019).

1.1 Cancer and its hallmark

According to the World Health Organization (WHO), cancer is defined as the abnormal growth of cells, in any part of the body, which has the potential to invade other organs or parts of the body. Cancer arises from the transformation of normal cells into tumour cells in a multi-stage process that generally progresses from a precancerous lesion to a malignant tumour, as a result of the interaction between a person's genetic factor and carcinogenic agents.

In the year 2000, Hanahan and Weinberg proposed six core hallmarks of cancer: the common traits that every single cancer including cervical cancer share which characterises the transformation from a normal cell to a cancer cell (Hanahan & Weinberg, 2000). These hallmarks of cancer are; firstly, cancer cells have their own growth signals, achieving an active proliferative state without relying on stimulatory signals. Secondly, cancer cells are insensitive to antigrowth signals. Thirdly, cancer cells are resistant to apoptosis. Fourthly, cancer cells have an infinite replicative potential. Fifthly, to maintain their viability, cancer cells require angiogenesis. Finally, cancer cells can move and travel to their surrounding tissue, resulting in tissue invasion and metastasis.

In 2011, Hanahan and Weinberg suggested two further hallmarks of cancer emerging from molecular studies and was involved in the pathogenesis of most cancers, namely the reprogramming of energy metabolism and the evasion of immune destruction (Hanahan & Weinberg, 2011). They also proposed two primary overarching characteristics of cancer that enable the acquisition of the eight hallmarks which are genome instability and mutation, and tumour-promoting inflammation. In addition, they identified four key intracellular signalling

networks which support cancer cell activity. These are motility circuits, proliferation circuits, viability circuits and cytoskeleton and differentiation circuits.

Understanding these core distinguishing characteristics of malignant cells is central to cancer research. As the scope for cancer research is very wide, this study attempts to better understand the hallmarks of cancer via intracellular networks by focussing on and exploring the role of methyl donors specifically in cervical cancer.

1.2 Cervical cancer

1.2.1 Epidemiology of cervical cancer

According to the International Agency for Research on Cancer (IARC) report in 2020, there was an estimated 604 000 newly diagnosed cervical cancer cases and 342 000 deaths caused by cervical cancer worldwide (Sung et al., 2021). It is the fourth most commonly diagnosed cancer in women (**Figure 1.1**). Additionally, mortality from cervical cancer is ranked fourth highest after breast, lung and colorectal cancer in women, however, it ranks second after breast cancer in countries with lower Human Development Index (HDI). When compared with the IARC report in 2018, there was an increase in incidence by 6% and mortality by 10% from cervical cancer worldwide (Bray et al., 2018). As global cervical cancer incidence and mortality appear to be on the rise; more in-depth studies should be conducted to better understand the underlying mechanisms of cervical cancer for its prevention.

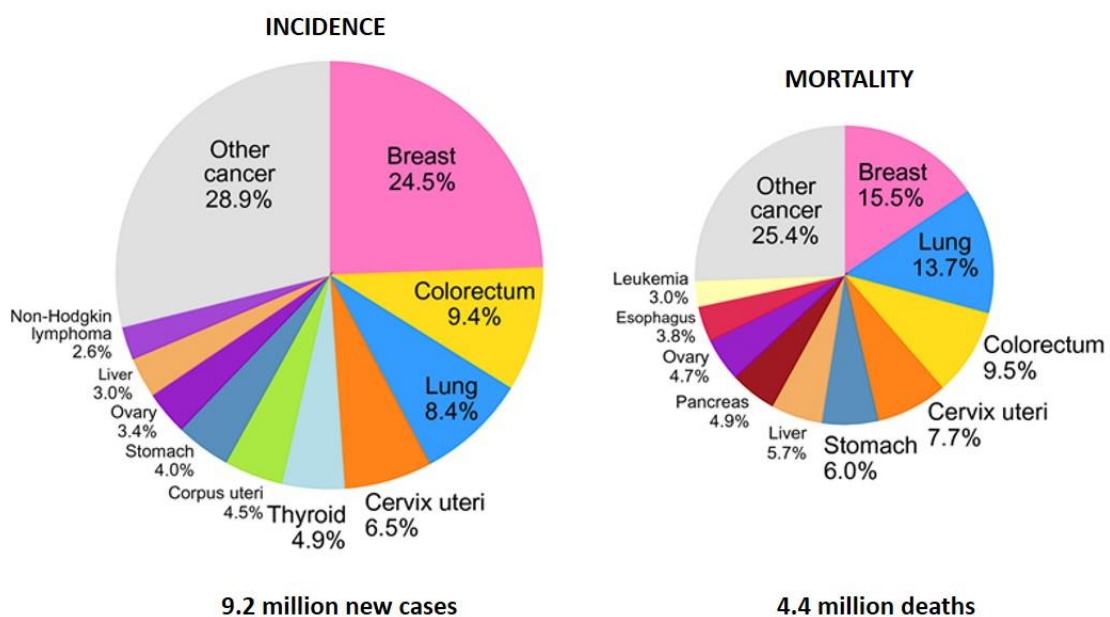


Figure 1.1 Global cancer incidence and mortality in women (Sung et al., 2021)

The World Health Organisation (WHO) reported that more than 85% of cervical cancer deaths occurred in low and middle income countries as there is limited access to preventive programs here, resulting in higher death rate (WHO, 2020). **Figure 1.2** shows that cervical cancer incidence and mortality occur highest in low and middle income countries such as Eastern, Southern and Central African countries, with Malawi reporting the highest cervical cancer mortality rates (Sung et al., 2021). In contrast, incidence of cervical cancer in northern America, Australia/New Zealand and western Asia is seven to ten times lower, with mortality rates varying up to 18 times (Ferlay et al., 2018). The HDI and poverty rates have been reported to account for more than 52% of geographical variation in cervical cancer mortality rates (Singh et al., 2012). Nonetheless, cervical cancer still remains as one of the biggest global threats to women’s health and lives despite the fact that neoplastic cell changes or its main cause, human papillomavirus (HPV) infections, can be screened earlier to enable preventative treatment in the development of invasive lesions and the introduction of HPV vaccination programs.

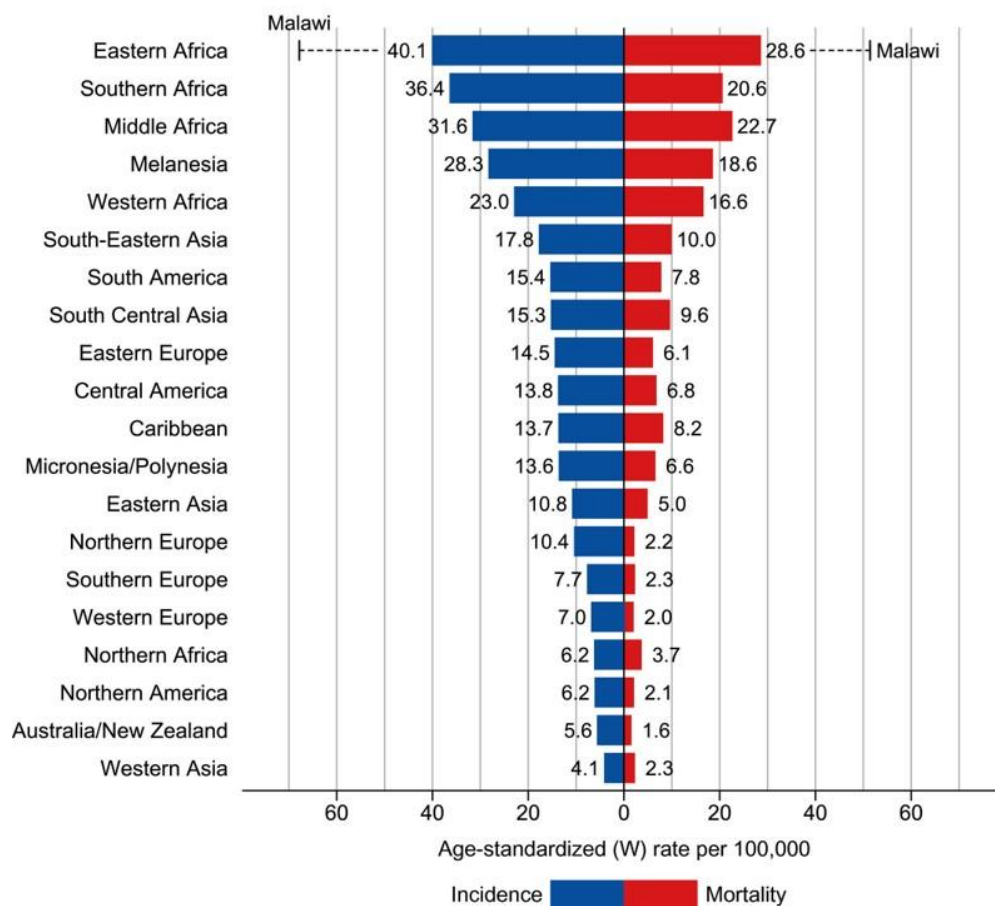


Figure 1.2 Incidence and mortality rate of cervical cancer according to region in 2020

Region-specific incidence and mortality age-standardized rates for cervical cancer in 2020. Rates are shown in descending order of the world (W) age-standardized incidence rate, and the highest national age-standardized for incidence and mortality are superimposed (Sung et al., 2021).

1.2.2 Cervical cancer prevention program

Infection by high-risk human papillomavirus (HR-HPV) is the main aetiology for the development of cervical cancer where the integration of the HPV genome into the host chromosome of cervical epithelial cells are key early events in the neoplastic progression of cervical lesions (Balasubramaniam et al., 2019; Da Silva et al., 2021). HPV has 12 oncogenic types classified as group 1 carcinogen by the International Agency for Research on Cancer Monographs (IARC, 2007). Thus, with a highly effective HPV vaccination program as well as secondary screening measures, cervical cancer should be considered nearly completely preventable. In order to reduce the burden of cervical cancer, WHO recommends 2 doses of vaccination against HPV for 9 to 13-year-old girls; and to prevent it, women aged 30 to 49 should be screened either through visual inspection with acetic acid in low-resource setting, a Papanicolaou smear (cervical cytology) every 3 to 5 years or a HPV test every 5 years, each with timely treatment of any detected precancerous lesions (WHO, 2017).

Large international randomised control clinical trials have shown that HPV vaccines are safe and highly effective against vaccine-type persistent infections and cervical precancerous lesions in women (Garland et al., 2007; Paavonen et al., 2009; Joura et al., 2015). Countries that have successfully implemented HPV vaccination programs have a reduction of 73-85% in HPV prevalence, and 41-57% reduction in high grade lesions among young women, less than 10 years after implementation of the HPV vaccination program (Drolet et al., 2019). Cervical screening at population-level has also been proven to be an effective measure against cervical cancer prevalence, with a sharp decline in age-standardised cervical cancer incidence in high-income countries, following the implementation of cytology-based screening (Franco et al., 2001; Bray et al., 2005). However, in terms of diagnostic effectiveness, HPV-based tests have shown to be more effective at detecting precancerous lesions and are likely to be more effective at preventing cervical cancer than visual inspection with acetic acid or cytology (Sankaranarayanan et al., 2009; Ronco et al., 2014; Ogilvie et al., 2017). In the United Kingdom, eligibility for the National Health Service (NHS) cervical cancer screening of individuals aged 25 to 49 years are every 3 years and those aged 50 to 64 every 5 years, with women aged 25 to 29 years having the highest incidence of cervical cancer and also those living in the most deprived areas (Wilding et al., 2020).

However, the successful implementation of these measures against cervical cancer varies across and within countries. Less than 30% of low and middle income countries have implemented national HPV vaccination programs compared to more than 85% among high

income countries (PATH, 2019). Additionally, only about 20% of women in low and middle income countries have ever been screened for cervical cancer compared to more than 60% in high income countries (Gakidou et al., 2008). These low and middle income countries do not have the technical or public health infrastructure to screen for HPV infection and/or to detect and remove pre-cancerous lesions. Vaccination against HPV for girls and young women, and in some countries also for young men, is a very effective means for cervical cancer prevention used in developed countries, but the high cost of HPV vaccination is a major barrier against its widespread use (Bruni et al., 2010; Jemal et al., 2011; Torre et al., 2015). Besides cost, the introduction to vaccine programs in low and middle income countries has also been restricted by paucity of adolescent health platforms, cultural challenges and difficulty in reaching the target population (Denny, 2015). Therefore, ongoing research to better understand the cervical cancer carcinogenesis process, as well as factors that contribute towards its risk and progression from pre-cancerous lesions to invasive cancer, is still crucial in order to develop more cost-effective preventative programs especially in low-and-middle income countries.

1.2.3 Pathology of cervical cancer

The cervix is the lower part of the uterus; it is cylindrical in shape and is connected to the vagina through the endocervical canal (Bermudez et al., 2015). This canal is lined with two types of epithelial cells, squamous cells (continuous with the vaginal epithelium, on the outer part of the cervix) and glandular cells (continuous with the endometrium, lining the cervical canal). The transition zone between these cells is called the squamocolumnar junction, where premalignant transformation usually occurs. These cell types generate the two main histological types of cervical cancer, squamous cell carcinomas (SCC) from squamous epithelial cells and adenocarcinoma (AC) from glandular epithelial cells (Pecorelli et al., 2009). In the revised International Federation of Gynaecology and Obstetrics (FIGO) staging of carcinoma of the cervix uteri, cervical cancer is divided into four stages. Stage I is when the cancerous cells are restricted within the cervix only; stage II is when the carcinoma appears outside the cervix but not in the pelvis; stage III is where the cancer has spread into the pelvis and the last most severe is stage IV where the cancer has moved beyond the pelvis into other organs (Pecorelli et al., 2009).

Cervical dysplasia, also known as cervical intraepithelial neoplasia (CIN), seen on cervical biopsy samples may regress spontaneously with the aid of the body's immune system; but also commonly progresses to the development of invasive cervical cancer, if it is not treated

at an early stage (Woodman et al., 2007). CIN can be categorized into three grades (Solomon & Nayar, 2004). CIN 1 is mild dysplasia or a low grade squamous intraepithelial lesion (LSIL), where undifferentiated cells are restricted within the lower third layer of the cervix. In CIN 2, moderate changes appear which are characterized by dyskaryotic cellular changes mostly affecting the lower two-third layer of the cervix. CIN 3 is a severe dysplasia or high grade squamous intraepithelial lesion (HSIL), where cell abnormalities have extended into the full thickness of the epithelium.

1.2.4 Impact of HPV in the pathogenesis of cervical cancer

In the past three to four decades, the natural history of cervical cancer has been well studied, and persistent infection of the cervix with the high-risk strain of HPV (HR-HPV) has been reported as a necessary causative factor for development of cervical cancer (zur Hausen, 2009; Okunade, 2020), with viral sequences detected in more than 95% of cases (Cancer Genome Atlas Research Network, 2017). More than 200 different types of HPV have been identified, though only 20 have been linked to the development of invasive cervical cancer (Burk et al., 2013; Galloway & Laimins, 2015; Cancer Genome Atlas Research Network, 2017; Liu et al., 2017). Specific viral types and intratypic variants have also been linked to increased risk of the disease (Burk et al., 2009; Tommasino, 2014; Mirabello et al., 2016).

HPV is a small, non-enveloped double-stranded DNA virus that belongs to the Papovaviridae family. Its genome codes for two capsid proteins L1 and L2, and six non-structural regulatory proteins (E1, E2, E4, E5, E6, E7), play a major role in the HPV life cycle and transformation of host cells into cancerous cells (**Figure 1.3**) (Woodman et al., 2007; Tommasino, 2014; de Sanjosé et al., 2018). The HPV virus is classified by the variation in the nucleotide sequence of the L1 capsid (Tommasino, 2014; Cancer Genome Atlas Research Network, 2017), with the most common oncogenic HPV types 16 and 18 being detected in 50% and 20% of cervical cancer cases, respectively (Tommasino, 2014). Although HPV 16 is the most prevalent type in cervical cancer, HPV 18 is typically associated with worse prognosis (Schwartz et al., 2001; Yang et al., 2014). Other HR-HPV that include HPV 31, 33, 34, 39, 45, 51, 52, 56, 58, 59, 66, 68 and 70; have also been classified as carcinogenic to humans (Li et al., 2011).

The HPV life cycle begins with the infection of the basal layer through microtraumas that compromises the epithelial barrier (**Figure 1.4**) (Stubenrauch & Laimins, 1999;

Balasubramaniam et al., 2019). At the beginning of infection, the HPV genome maintains a low copy number in the infected host basal cells. However, when the epithelial cells differentiate, the virus starts to replicate to a high copy number and expresses the L1 and L2 capsid proteins. This results in the production of new progeny virions that are released from the epithelial surface. For persistence, HPV needs to infect basal cells showing stem cell-like features that are still able to proliferate (Egawa et al., 2015). High-risk types of HPV are more prone to activate cell proliferation in basal and differentiated layers, promoting epithelial transformation. After integration of HPV DNA into the host genome, the overexpression of viral oncoproteins E6 and E7 are mainly responsible for the initial changes in epithelial cells (Balasubramaniam et al., 2019). E6 prevents the activity of the host's tumour suppressor p53, whilst E7 inhibits retinoblastoma (pRb), which controls cell division by blocking the activity of transcription factors. Inactivation of these host proteins disrupts both the DNA repair mechanisms and apoptosis, leading to rapid cell proliferation. Multiple genes involved in DNA repair, cell proliferation, growth factor activities, angiogenesis and mitogenesis genes become highly expressed in CIN and in cancer. This genomic instability encourages HPV-infected cells to progress towards invasive carcinoma. HPV integration also drives the carcinogenic process through the inactivation of E2 expression, the main inhibitor of E6 and E7, and the disruption of host genes because of the viral sequence insertion (McBride & Warburton, 2017). As for low-risk types of HPV, although E6 and E7 proteins are present, their role is limited to the increase of viral fitness and viral production, and is largely insufficient to trigger the development of neoplastic lesions or cancer (Schiffman et al., 2016).

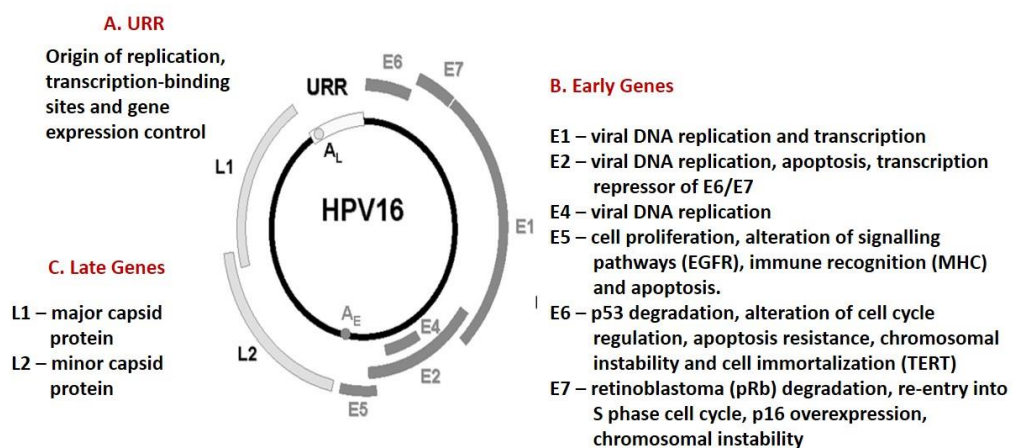


Figure 1.3 HPV 16 structure and viral protein

There are three functional regions in the HPV genome. **(A)** Upper regulatory region (URR) is a noncoding region containing the replication origin and transcription factor-binding sites that contribute to the regulation of DNA replication by controlling the viral gene transcription. **(B)** Early region that encodes for six proteins (E1, E2, E4, E5, E6, and E7) that are involved in viral replication and tumorigenesis. **(C)** Late region that encodes for capsid proteins L1 and L2. Adapted from (Stanley et al., 2007).

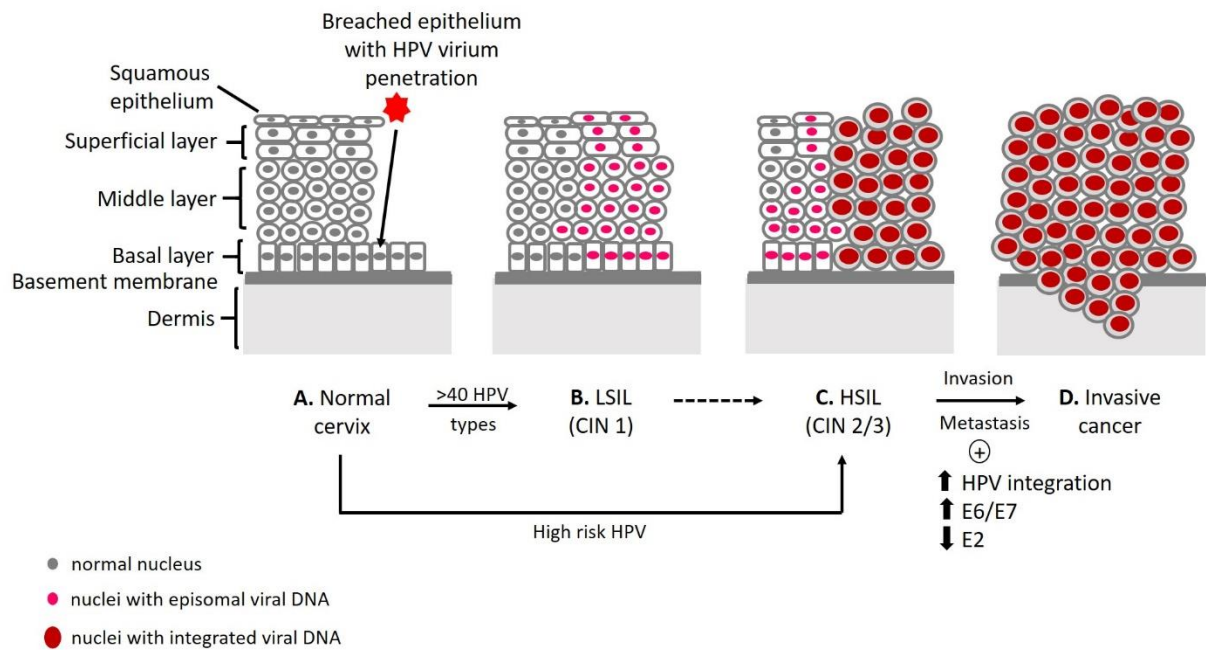


Figure 1.4 HPV-associated pathogenesis of cervical cancer

Distribution of normal and HPV-infected squamous epithelial cells at different stages of cervical dysplasia. The initial stage of carcinogenesis is controlled by viral HPV integration and host factors. (A) Basal cells in the cervical epithelium rest on the basement membrane, which is supported by the dermis. HPV is thought to access the basal cells through micro abrasions in the cervical epithelium. (B) Subsequently, early HPV genes E1, E2, E4, E5, E6 and E7 are expressed and the viral DNA replicates from the episomal DNA (pink nuclei). Low grade squamous intraepithelial lesions (LSIL) support productive viral replication. (C) As infection persists with the high-risk strain of HPV, there is a progression to high grade cervical intraepithelial neoplasia (HSIL) (D) The progression of untreated lesions to microinvasive and invasive cancer is associated with the integration of the HPV genome into the host chromosome (red nuclei), with associated loss or disruption of E2, and subsequent upregulation of E6 & E7 oncogene expression. Adapted from (Knoff et al., 2014).

Epidemiologic studies have reported that the risk of contracting a high-risk strain of HPV (HR-HPV) infection and cervical cancer is influenced by sexual activities including early exposure to sexual activity, having multiple sexual partners at any given time as well as having a history of other sexually transmitted infections, where the peak period for acquiring HPV infection is shortly after becoming sexually active (ACOG, 2017). However, the mere presence of the HR-HPV is not sufficient for neoplastic progression. About 85 to 90% of HR-HPV infections spontaneously regress, with only 10 to 15% that continue to persist, and consequently promote the progression of precancerous CIN to invasive cervical carcinoma (ICC), thus suggesting other conditions or cofactors that contribute towards cervical carcinogenesis (Łaniewski et al., 2020). Such conditions include the local microenvironment for cervical carcinogenesis, which has been reported to be essential for the control of persistent HPV infection and pathogenesis of cervical cancer (Egawa et al., 2015). HPV must be able to integrate into the host cells to initiate infection, which leads to epigenetic and genetic changes

in oncogenes and tumour suppressor genes within the basal epithelial cells, thus enabling viral replication (Gius et al., 2007). These changes then establish a conducive environment for neoplastic progression where the virus is able to evade the host immune system to ensure its continuous replication in the basal epithelial cells.

HPV type-specific persistent infections have been found to significantly increase the risk of cervical dysplasia thus increasing the risk of cervical cancer. A study was conducted among women to monitor the association between the course of HR-HPV infection and the development of cervical neoplasia over time (Cuschieri et al., 2005). They reported that women with type specific persistent infections were significantly more likely to develop cervical neoplasia than women who cleared the infection ($P=0.0001$) or were sequentially infected with different types ($P=0.001$). In a Columbian cohort study, 1728 women aged between 15 to 85 years with normal cytology at baseline were followed up every 6 months for an average of 9 years (Muñoz et al., 2009). The study concluded that viral load is the main determinant of persistence, where persistence of HPV 16 infections carries a higher risk of developing CIN 2/3. In another large-scale cohort study in Taiwan, 11 923 women aged 30 to 65 years old were followed up for 16 years to investigate the role of genotype-specific HPV persistence in predicting cervical cancer (Chen et al., 2011). Women with type-specific persistence of any carcinogenic HPV had greatly increased risk compared to women who were HPV-negative (hazard ratio=75.4, 85% CI=31.8-178.9).

Persistent HPV infections are defined as infections that are present at or before treatment and remain present after treatment, whilst incident HPV infections are defined as the detection of a new HPV genotype after treatment for CIN that was not present before or at the time of treatment (Rositch et al., 2014). In 2013, a systematic review and meta-analysis was conducted on HPV persistence patterns worldwide (Rositch et al., 2013). In this review, more than 100 000 women from 86 studies were examined to determine the patterns of persistent HPV infection among women who had not been given any treatment. It was estimated that approximately half of the HPV infections persist past 6 to 12 months. Additionally, HR-HPV persist for an average of 9.3 months, longer than low-risk HPV at 8.4 months, whilst HPV 16 was also found to persist longer at 12.4 months, compared to HPV 18 at 9.8 months. In a more recent systematic review, which included 45 studies with data on post-treatment HPV persistence among 6106 women, HPV persistence was found to be relatively shorter in duration with 25% of women who had a persistent HPV infection at 6 months after treatment, and 15% at 12 months post-treatment (Hoffman et al., 2017). HPV persistence values were relatively

lower as the women in these studies had received some form of treatment modalities, thus resulting in the clearance/elimination of a notable proportion of HPV infections. This study also reported a wide variation in the estimation of post-treatment HPV persistence depending on patient's age, HPV-type, detection method, treatment method and minimum HPV post-treatment testing interval. Furthermore, the median for HPV persistence was reported to be lower with increasing follow-up time, declining from 27% at 3 months after treatment to 21% at 6 months, 15% at 12 months, and 10% at 24 months. In addition to that, immune-competent persons infected with HPV generally have a slow progression to high-grade, precancerous lesions and subsequent carcinoma (Palefsky, 2007). However, most people with competent immune systems are able to clear HPV infections with no sequelae. Individuals who have compromised cell-mediated immunity, such as those with human immunodeficiency virus (HIV), AIDS, or solid-organ transplant recipients, have shown accelerated progression to high-grade lesions and, thus, are at an increased risk to develop HPV-associated carcinomas (Palefsky, 2007; Denny et al., 2012; Freiburger et al., 2015).

The progression of HPV-infected epithelial cells to invasive cancer is a long-term process associated with the accumulation of DNA alterations in host genes. CIN 1 is the stage when the virus persistently infects the cervical cells. The transition from precancerous lesions to invasive carcinoma takes at least 10 to 20 years (Wallin et al., 1999; Zielinski et al., 2001). CIN1 lesions that do not regress may develop into CIN2/3 within 2 to 3 years following infection (Winer et al., 2005). In terms of treatment, the American Society for Colposcopy and Cervical Pathology (ASCCP) recommends that women with a histological diagnosis of CIN 2 or 3 receive ablative or excisional treatment to eliminate CIN and associated HPV infection (Massad et al., 2013). Additionally, excisional treatment such as the loop electrosurgical excision procedure (LEEP) and conization appear to provide better HPV clearance than cryotherapy (Hoffman et al., 2017). Nonetheless, studies have shown that a proportion of CIN 2/3 cases still remain infected with HR-HPV even after treatment (Jancar et al., 2006; Kreimer et al., 2006). Recurrent CIN may result from inadequate treatment of precancerous cervical lesions, with incomplete removal of HPV infections resulting in HR-HPV infection persistence, re-infection with a new HR-HPV type, or persistence of another HPV type not associated with the primary cervical lesion (Tachezy et al., 2006).

Undoubtedly, there is a distinct impact of HPV on the pathogenesis of cervical cancer, although the specific mechanisms, including the genetic and epigenetics changes that occur during cervical carcinogenesis are not entirely understood. Thus, this study aims to shed light

on the epigenetic condition; on the role of methyl donor nutrients in DNA methylation and the regulation of gene expression, that is associated with the HPV mechanisms in neoplastic progression contributing towards cervical carcinogenesis.

1.2.5 Cervical cancer risk factors

In conjunction with infection of oncogenic types of HPV, there are several modifiable cofactors that could potentially influence the development of cervical cancer among women with positive HPV DNA. These include long-term use of oral contraceptives (OC), high parity and smoking.

The long-term use of OC as a risk factor for cervical cancer is not well established, where evidence for an association between cervical cancer and the use of oral or other hormonal contraceptives is not entirely consistent. In a study conducted to investigate the association between cervical carcinoma and the pattern of oral contraceptive use among 16 573 women with cervical cancer and 35 509 healthy women worldwide; reported long term use of oral contraceptives as a definite cofactor for cervical cancer but its role as a causal factor could not be established (International Collaboration of Epidemiological Studies of Cervical Cancer, 2007). In another study, they reported that the longer OC were used, the higher the chances were of developing cervical cancer (OR=1.47, 95%CI=1.02-2.12) (Bosch & de Sanjosé, 2007). The use of OC for a period of 5-9 years or more than 10 years could increase the risk of acquiring cervical cancer (OR=2.72, 95%CI=1.36-5.46) and (OR=4.48, 95%CI=2.24-9.36), respectively. Furthermore, two large prospective studies found evidence for a considerable increase in cervical cancer risk in OC users (Bond, 2014); whilst another study reported OC as a risk factor for CIN in a univariate analysis but when adjusted for HPV infection, its risk was found to be insignificant (Kjellberg et al., 2000). In contrast, a recent study, conducted to determine the risk factors associated with cervical cancer among 860 patients, concluded the role of oral contraceptives as controversial (Lukac et al., 2018).

A meta-analysis was conducted to evaluate the association between OC use and the risk of cervical cancer (Peng et al., 2017). This review of 16 case-control studies, included 15 619 participants consisting of 7433 cases and 8186 controls, did not find any significant risk of cervical cancer amongst individuals using OC (OR=1.12, 95%CI=0.90-1.38). Furthermore, no significant associations to cervical cancer risk were found for different durations of OC use (<5 years: OR=0.84; 95%CI, 0.68-1.04; 5-10 years: OR=1.06; 95%CI=0.66-1.71; >10 years: OR=1.25; 95%CI=0.76-2.06). Besides this, OC usage was not shown to increase the risk of

HPV infected cervical cancer among women (OR=1.09; 95%CI=0.80-1.49). On the other hand, a more recent systematic review and meta-analysis found that longer durations of OC usage was definitely associated with the risk of developing cervical cancer namely adenocarcinoma (Asthana et al., 2020). The overall risk of invasive cancer on OC use was found to be significant with unknown status of HPV with (OR =1.51, 95 %CI=1.35-1.68) and for unknown HPV as (OR=1.66, 95%CI=1.24-2.21). It was found that adenocarcinoma, squamous cell carcinoma and carcinoma in situ had significant association with (OR=1.77, 95 %CI=1.4-2.24), (OR=1.29, 95%CI=1.18-1.42) and (OR=1.7, 95%CI=1.18-2.44), respectively. Here it can be surmised that the use of OC may cause hormonal imbalances such as excess estrogen without progesterone, leading to a decrease in ovulation. This condition in turn, could cause a further reduction in progesterone levels, and the endometrial layer remains unshed. In response to this estrogenic effect, the endometrium cells crowd together and become abnormal leading to endometrial hyperplasia. This hyperplasia may lead to cancer, and since this phenomenon occurs in the endometrium, therefore long-term use of OC was found to be more associated with the risk of developing adenocarcinoma as compared to squamous cell carcinoma. Therefore, long term OC usage has the potential to influence the development of cervical cancer among women with positive HPV DNA.

Besides the use of OC, high parity has also been associated with cervical cancer incidence (Muñoz et al., 2006). The International Collaboration of Epidemiological Studies of Cervical Cancer combined individual data on 11 161 women with invasive carcinoma, 5402 women with cervical intraepithelial neoplasia (CIN) 3/carcinoma in situ and 33 542 women without cervical carcinoma from 25 epidemiological studies (International Collaboration of Epidemiological Studies of Cervical Cancer, 2006). They reported that there was an association between the number of full-term pregnancies with the risk of invasive cervical carcinoma. The relative risk for invasive cervical carcinoma among parous women was (RR=1.76, 95%CI=1.53-2.02) for ≥ 7 full-term pregnancies compared with 1-2, after controlling for age at first full-term pregnancy. On the other hand, no significant trend was found with increasing number of births among parous women for CIN 3/carcinoma in situ. Furthermore, early age at first full-term pregnancy was also associated with the risk of both invasive cervical carcinoma and CIN 3/carcinoma in situ. The RR for first full-term pregnancy at age < 17 years compared with ≥ 25 years was (RR=1.77, 95%CI=1.42-2.23) for invasive cervical carcinoma, and (RR=1.78, 95% CI=1.26-2.51) for CIN 3/carcinoma in situ, after controlling for number of full-term pregnancies. They also reported similar results in analyses restricted to HR-HPV positive cases and controls whereas conversely, no relationship was found between

cervical HPV positivity and number of full-term pregnancies, or age at first full-term pregnancy among controls. In addition, a European Prospective Investigation into Cancer and Nutrition (EPIC) cohort study involving 308 036 women, also reported that the number of full-term pregnancies was positively associated with CIN 3/carcinoma in situ risk (P-trend = 0.03), although no association was found with invasive cervical cancer (Roura et al., 2016). A possible biological mechanism explanation for the association between high parity and cervical carcinoma incidence could be that, the elevated levels of estrogen and especially progesterone during pregnancy are responsible for the alterations in the squamo-columnal junction occurring during pregnancy, maintaining the transformation zone on the exocervix for many years (Muñoz et al., 2002; International Collaboration of Epidemiological Studies of Cervical Cancer, 2006; Jensen et al., 2013). This would facilitate direct exposure to HPV, hence contributing to HPV persistence and progression to cervical neoplasia and cancer. Another possible mechanism is the immunosuppression linked to pregnancy which might enhance the role of HPV in cervical carcinogenesis.

Smoking is another factor that has long been associated with cervical cancer risk. In the European Prospective Investigation into Cancer and Nutrition (EPIC) cohort study, a total of 308 036 women were followed up for 9 years and the relationship between smoking and the risk of contracting cervical cancer was determined (Roura et al., 2014). After accounting for previous HPV infection, a strong association was found between smoking and the risk of CIN 3 and invasive cervical cancer, where quitting the smoking habit protected women against cervical cancer and is associated with a 2-fold risk reduction. A meta-analysis was conducted to evaluate the association between cigarette smoking and the risk of cervical cancer in Japanese women based on a systematic review of epidemiological evidence (Sugawara et al., 2019). A total of five studies were selected where all indicated that cigarette smoking had a strong positive association to the risk of cervical cancer. They reported that the relative risk (RR) for individuals who had ever-smoked relative to never-smokers was (RR=2.03, 95%CI=1.49-2.57). In addition, four studies also demonstrated dose-response relationships between cigarette smoking and the risk of cervical cancer. Besides that, passive smoking has also been associated with an increased risk of cervical cancer in a meta-analysis (Su et al., 2018). Su et al.'s meta-analysis consisted of a total of 14 eligible studies, with a total of 384 995 participants. The pooled ORs of passive smoking with cervical cancer risk was (OR=1.70, 95% CI=1.40-2.07, I² = 64.3%). However, biological mechanisms linking passive smoking with cervical neoplasm are not well characterized, though several mechanisms were considered to have a significant role. Incessant smoking may weaken the immune function (Sabra et al., 2017), thus increasing

the risk of HPV infection, where HPV is regarded as the most essential causative factor for cervical cancer (zur Hausen, 2009; Okunade, 2020). A study on women smokers reported that the count of cervical Langerhans' cells, CD8 and total lymphocytes showed a decrease of 6-16% following the reduction in the amount of smoking per day (Szarewski et al., 2001). Furthermore, nicotine has been proved to promote tumour development (Warren & Singh, 2013). Finally, pharmacokinetic interactions with smoke may well have a significant impact on the efficacy and toxicity of anticancer drugs (Condoluci et al., 2016). In short, there is epidemiological evidence that smoking positively influences the development of cervical cancer in women.

In summary, there is a lot of evidence which shows that long-term use of OC, high parity and smoking are definite risk factors for the development of cervical cancer and pre-cancer. However, these risk factors do not act independently but rather act as co-factors that interact with HPV to induce cervical carcinogenesis.

1.2.6 Diet and cervical cancer

In addition to long-term use of oral contraceptives (OC), high parity and smoking, dietary behaviour is also one of the modifiable cofactors that could potentially influence the development of cervical cancer among women. Dietary factors may be determinants of the persistence of HPV infections, or may affect the progression from infection to pre-cancerous lesion and invasive neoplasms. However, the evidence linking dietary behaviour with cervical cancer risk is quite limited. Early studies have failed to take into account the importance of HPV infection as a causal factor, and therefore, results from these studies may be confounded and need to be considered cautiously.

Ono et al. recently reviewed relevant literature to identify recent epidemiological studies and clinical trials in order to improve understanding of the role of individual antioxidant nutrients at different stages of cancer development from normal cervical cells, to CINs to invasive cancer (Ono et al., 2020). They suggest that the intake of vitamins A and D and carotenoids may inhibit early cervical cancer development, whilst the intake of folate may prevent or inhibit HPV infection from progressing to various grades of CIN. Furthermore, the intake of vitamins C, E, fruits and vegetables may widely inhibit the process of cervical cancer development. However, as most of the literature are epidemiological studies, further research

using experimental approaches is needed to clarify the effects of dietary and nutrient intake in detail.

García-Closas et al. had conducted a systematic review and qualitative classification of observational studies to provide epidemiologic evidence about the role of diet and nutrition on the risk of HPV persistence and cervical neoplasia, whilst taking HPV infection into account (García-Closas et al., 2005). A total of 23 observational studies that controlled for HPV and 6 randomised trials were included in the review. They concluded that there was a fairly consistent inverse association between fruits and vegetables and HPV persistence. As for nutrients, evidence for this inverse association was considered strongly consistent for lycopene (but not for other carotenoids nor for retinol) and vitamin E; and moderately consistent for vitamins B₁₂ and C. Furthermore, an increased risk associated with plasma homocysteine, which is inversely associated with folate, vitamin B₁₂ and vitamin B₆, was also considered strongly consistent. However, no consistent protective effect of folic acid was observed. In short, though there was evidence of association between diet and nutrition with HPV persistence and cervical neoplasia, the findings are not conclusive and are limited due to the observational designs of these studies which are suitable to identify association, but not demonstrate causality.

In the European Prospective Investigation into Cancer and Nutrition (EPIC) study, a total of 299 649 women were followed up for 9 years to determine the association between both fruit and vegetable intake and specific dietary nutrients and the incidence of cervical cancer (González et al., 2011). It was found that increasing fruit intake by 100 g daily could significantly lower the risk of acquiring invasive squamous cervical cancer (HR=0.83, 95% CI=0.72-0.98). However, there was an inverse association between vegetable intake (HR=0.85, 95% CI=0.65-1.10) as well as for the intake of garlic, onion, citrus fruits, vitamin C, E and retinol, and the incidence of cervical cancer; however, it was not statistically significant. Beta-carotene, vitamin D and folic acid intake was not associated with cancer risk. In a more recent systematic review and meta-analysis to determine the association of fruit and vegetable intake with the occurrence of CIN and invasive cancer, 18 studies have been identified: 17 case-control studies (n=9014 cases, n=29 088 controls) and one cohort study (n=299 651) (Tomita et al., 2021). They found no association between fruit and vegetable intake with CIN. The pooled adjusted ORs for cervical cancer were (OR=0.61, 95% CI=0.52-0.73) for vegetables and (OR=0.80 95% CI=0.70-0.93) for fruits, though no association was observed when the pooled effect was estimated among studies that were adjusted for HPV. They concluded that the consumption of fruits and vegetables was not associated with incidence of cervical cancer

among studies that controlled for HPV infection. However, the level of evidence could possibly be limited as only one cohort study was included in the analysis.

In 1997, the World Cancer Research Fund (WCRF) and American Institute for Cancer Research (AICR) published a comprehensive review of published scientific literature on diet, nutrition, physical activity and cancer (World Cancer Research Fund/American Institute for Cancer Research, 1997). However, at the time, there were few large prospective cohort studies, whereas the method of pooling studies and meta-analysis was still in its infancy (Clinton et al., 2019). Thus, the epidemiologic evidence was mostly from ecologic and case-control studies that are often significantly confounded by systemic biases; though the accumulated evidence was supported by laboratory investigations in a limited but rapidly growing array of experimental cancer models. A decade later, they published their second report (World Cancer Research Fund/American Institute for Cancer Research, 2007), followed by the third report in 2018 (World Cancer Research Fund/American Institute for Cancer Research, 2018); where a more systematic literature review was conducted to summarize and update the evidence from prospective studies and randomised controlled trials on the association between foods, nutrients, vitamins, minerals, physical activity, overweight and obesity with the risk of cancer. The main aim is to guide and establish a non-biased approach with meticulous methods for collecting, organizing, and systematically reviewing the evidence for each of the major cancer types. The PubMed database was searched and studies relevant to the inclusion criteria were identified. Data from each study were extracted including study design, characteristics of study population, mean age, distribution by sex, country, recruitment year, methods of exposure assessment, definition of exposure, definition of outcome, method of outcome assessment, study size, length of follow up, lost to follow-up, analytical methods and whether methods for correction of measurement error were used. The results were summarised in tables and figures. Furthermore, an additional analysis such as the dose-response meta-analysis was performed when there were at least two new reports of trials or two new reports of cohort studies with enough data identified for dose-response meta-analysis, and if there were in total five cohort studies or five randomised controlled trials. This was followed by an evaluation process based on the evidence and systematic reviews provided for each cancer, by an international and multidisciplinary panel of experts. Through a rigorous review process coupled with annual summits; conclusions were formalized, recommendations for cancer prevention are defined, and priority areas for future research are proposed (Clinton et al., 2019).

In the WCRF/AICR second report, there is limited-suggestive evidence linking the intake of carrots with invasive cervical cancer, based on four hospital-based case-control studies (World Cancer Research Fund/American Institute for Cancer Research, 2007). On the other hand, the evidence linking non-starchy vegetables, fruits, milk, retinol, vitamin E, and alcohol intake cannot be concluded due to limited evidence. In their more recent third report (World Cancer Research Fund/American Institute for Cancer Research, 2018), only one new study reported on uterine cervix cancer mortality and the intake of carrot or pumpkin combined (Iso & Kubota, 2007). In this study, carrot or pumpkin intake was not associated with uterine cervical cancer mortality. The hazard ratio comparing ≥ 3 -4 times/week of carrot intake to < 1 time/week intake was (HR=1.10, 95%CI=0.31-3.93). However, the number of cases was low and the analysis was only adjusted for age and study area. Similarly, for dietary retinol and beta-carotene intake, one new study (European Prospective Investigation into Cancer and Nutrition Study, EPIC) was identified and both nutrients were not associated with carcinoma in situ and invasive squamous cervical cancer risk (González et al., 2011). The hazard ratio was (HR=0.98, 95%CI=0.93-1.02) per 200 $\mu\text{g/day}$ intake of dietary retinol, and (HR=1.00, 95%CI=0.94-1.06) per 1500 $\mu\text{g/day}$ intake of dietary beta-carotene. Furthermore, the Women's Health Initiative-Dietary Modification Trial (WHI-DM trial) conducted in 2007 also did not support a significant effect of low-fat dietary intervention on cervix cancer prevention (Prentice et al., 2007). The study was designed to promote dietary change with the goal of reducing intake of total fat to 20% of energy and increasing consumption of fruits and vegetables to at least 5 servings daily and grains to at least 6 servings daily. Comparison group participants were not asked to make dietary changes. Postmenopausal women (age 50 to 79 years) with $\geq 33\%$ of total energy from fat were randomly assigned to the intervention group (n = 19 541) or the comparison group (n=29 294). After an average of 8.1 years of follow up, they reported a non-significant reduction in cervix cancer risk with the low-fat dietary intervention (HR=0.46, 95% CI=0.15-1.42). Based on current evidence by the WCRF/AICR, compared to various other types of cancer, there is no evidence to support the association between foods, nutrients, vitamins and mineral intake with cervical cancer. Nonetheless, there is substantial evidence from large population studies that have reported a reduction in various other cancer incidence and mortality by following a dietary pattern similar to the 2007 WCRF/IACR Cancer Prevention Recommendations (Romaguera et al., 2012; Vergnaud et al., 2013; Kohler et al., 2016). A diet based on these recommendations is likely to be dense in nutrients; containing foods and beverages with relatively high concentrations of vitamins and minerals and other dietary constituents such as dietary fibre, without excessive salt, saturated or trans fats, added

sugars or refined starch; thereby promoting good nutritional health and protecting against nutrient deficiency and non-communicable diseases.

Most of the current literature is based on epidemiological studies with clinical data; and only few experimental studies have been reported. Thus, the mechanisms through which diet and nutrition influence cancer development are unclear. However, there are several mechanisms that have been proposed to explain the protective role of specific nutrients against cancer. It was hypothesized that nutrients with antioxidant effects could reduce the risk of invasive cancer by diminishing the damage caused by reactive oxygen species (ROS) to the DNA, protein and lipids; as well as by boosting the immune system (Ono et al., 2020). The metabolism of normal, cancerous cells and inflammatory processes produce higher levels of ROS which could increase the risk of mutation by altering cellular functions. Another possible mechanism is the role of methyl donor nutrients such as folate, choline and methionine in maintaining normal DNA synthesis and repair, as well as DNA methylation and gene expression (Mahmoud & Ali, 2019). There has been particular interest in the possible role of folate as a determinant of cervical cancer risk (Piyathilake et al., 2004; Piyathilake et al., 2007), and its role in DNA methylation and gene expression (Flatley et al., 2009).

Hence, the crux of this study is to investigate the effect of methyl donor nutrients such as folate and methionine in DNA methylation and gene expression. The fundamental study to determine the role of these nutrients and the molecular mechanism by which they could contribute to cancer carcinogenesis might support more empirical nutritional studies towards cancer prevention in the future.

1.3 DNA Methylation and Cancer

1.3.1 DNA methylation

DNA methylation is an epigenetic mechanism involving the transfer of a methyl group onto the C5 position of the cytosine to form 5-methylcytosine (Moore et al., 2013; Hervouet et al., 2018). It is a reversible modification that occurs independently of the DNA sequence, and is essential in the directive of cellular phenotype by regulating gene transcription. DNA methylation is associated to a number of biological events that include embryonic development, parental imprinting genes, transposon silencing, X-chromosome inactivation and repression of oncogenic genes. DNA methylation can generally be observed in a condensed chromatin and when it occurs in promoters, it is associated with transcriptional gene silencing. DNA

methylation is processed by two distinct mechanisms: (i) the inheritance DNA methylation where, following DNA replication, it allows DNA methylation marks to be maintained on the new strand with the parental methylated strand being used as a matrix and (ii) de novo DNA methylation which, on the other hand, occurs on both strands independently of DNA replication. Additionally, de novo DNA methylation occurs mainly during embryogenesis, where DNA methylation profiles are established, and the DNA methylation inheritance machinery further maintains it after DNA replication and cell division.

The majority of DNA methylation occurs on cytosines that precede a guanine nucleotide or CpG sites. The reaction is catalysed by a family of DNA methyltransferases (DNMTs) that transfer a methyl group from S-adenosyl methionine (SAM) to the fifth carbon of cytosine residue to form 5-methylcytosine (**Figure 1.5**) (Moore et al., 2013). Initially, DNMTs will bind non-specifically to DNA, whereupon specific DNA target sites are identified, and SAM is recruited by DNMTs. The DNMTs will then incorporate the methyl group onto the carbon-5 position of the targeted cytosine, converting SAM to S-adenosyl-homocysteine (SAH), and DNMT enzymes are released. As DNA methylation usually takes place on gene promoter regions, this reaction leads to gene silencing, whereas DNA demethylation is associated with transcription activation and gene expression.

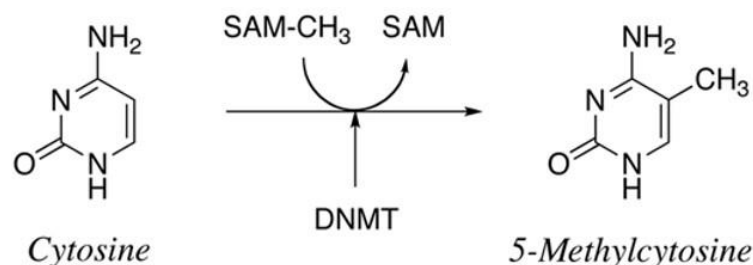


Figure 1.5 Methylation of cytosine in carbon 5 to form 5-methylcytosine

DNA methylation is catalysed by a family of DNA methyltransferases (DNMTs) that transfer a methyl group (CH_3) from S-adenosyl methionine (SAM) to the fifth carbon of cytosine residue to form 5-methylcytosine, thus converting SAM to S-adenosyl homocysteine (SAH).

Several mechanisms have been proposed to account for the transcriptional repression by DNA methylation (Das & Singal, 2004; Moore et al., 2013). The first mechanism involves direct interference with the binding of specific transcription factors to their recognition sites in their respective promoters. Several transcription factors, including AP-2, c-Myc/Myn, the cyclic AMP-dependent activator CREB, E2F, and NF κ B recognize sequences that contain CpG residues, and the binding of each has been shown to be inhibited by methylation (Tate & Bird,

1993). The second mode of repression involves a direct binding of specific transcriptional repressors to methylated DNA, such as methyl-binding proteins, histone deacetylases (HDACs), and histone methyltransferases that leads to chromatin repression, thus restricting its accessibility for transcription (**Figure 1.6**). Methyl binding proteins such as MeCP1, MBD1, MBD2, and MBD4 that bind to 5m-CpG through a motif called the methyl CpG binding domain (MBD), and Kaiso that binds through a zinc finger motif have been shown to repress transcription in both *in vitro* and cell culture assays by interacting with histone deacetylase complexes (Prokhortchouk & Hendrich, 2002).

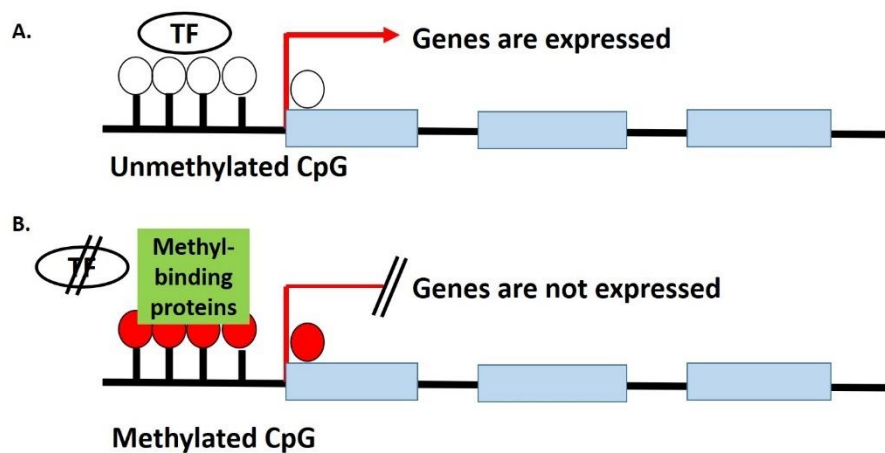


Figure 1.6 Methylation of CpG and gene expression

(A) CpG is not methylated, thus the transcription factor (TF) is activated and the gene is expressed (B) CpG is methylated, the transcription factor (TF) cannot be activated due to transcriptional repressor such as methyl-binding proteins, thus the gene is silenced.

1.3.2 Aberrant DNA methylation in cancer

Under normal conditions, a cell's DNA methylation pattern is dynamically balanced by methylation and demethylation. However, the presence of pathological conditions such as inflammation, oxidative stress and cancer could disrupt this balance, which is characterized by aberrant DNA methylation due to excessive methylation or deficient demethylation (Song & He, 2012). Aberrant DNA methylation has been detected in numerous cancers, consisting of two main features; global DNA hypomethylation, with local DNA hypermethylation especially in the promoter region of tumour suppressor genes (Jones & Baylin, 2007; Kanwal & Gupta, 2012). Cancer-associated DNA hypermethylation and hypomethylation occur early in tumorigenesis and both typically increase with tumour progression (Ehrlich, 2019).

In the intergenic regions and repetitive sequences of the human genome, CpG sites are sparse and mostly methylated. The hypomethylation of CpG sites in this area may result in genomic instability and loss of gene imprinting, which could eventually lead to the development of neoplastic cells (Kulis et al., 2013). Evidently, various human cancers frequently display global DNA hypomethylation (Ehrlich, 2002), which could occur passively through loss of the maintenance DNA methyltransferase, or actively by TET enzyme-mediated oxidation of methyl cytosine, followed by base excision repair (Tahiliani et al., 2009; Cortellino et al., 2011; Smith & Meissner, 2013). Almost half of the 25 examined breast adenocarcinomas exhibited hypomethylation in satellite 2 DNA, which is located in the long region of heterochromatin adjacent to the centromere of chromosome 1, and is normally highly methylated (Narayan et al., 1998). Ovarian epithelial carcinoma also exhibited hypomethylation in satellite 2 DNA of both chromosomes 1 and 16, demonstrating a statistically significant correlation between the extent of this satellite DNA hypomethylation and the degree of malignancy ($P < 0.01$) (Qu et al., 1999).

There is growing evidence indicating that global hypomethylation may lead to genome instability and DNA breakage (Jung & Pfeifer, 2015) as it would have a direct impact on chromatin integrity. This is supported by a study on mice carrying a hypomorphic allele of DNMT1 where DNA hypomethylation was associated with the development of tumours displaying a higher frequency of chromosomal rearrangements (Gaudet et al., 2003). The association between DNA hypomethylation and genomic rearrangements has also been observed in human cell lines (Vilain et al., 1999; Vilain et al., 2000). Alternatively, DNA hypomethylation could result in transcriptional activation of oncogenes thus leading to tumour initiation and development (Feinberg & Tycko, 2004; Wilson et al., 2007). Examples of oncogenes that are linked to cancer and activated via hypomethylation are protease urokinase, mesothelin, cancer-testis genes, claudin4, S100A4, heparinase, and the proopiomelanocortin gene (Funaki et al., 2015). Besides this, Zhou et al. suggested that a decrease in rDNA promoter methylation levels accompanied by rDNA chromatin decondensation, can result in an increase of ribosomal RNA (rRNA) synthesis in the development of human cervical cancer (Zhou et al., 2016). The ribosome serves as the centre of biological protein synthesis, and thus the production rate of the rRNA is tightly related to cellular growth and proliferation. The balance between the cell growth and ribosome production is maintained in normal cells by regulation of transcription of rRNA genes at an appropriate level whereas this balance in cancer cells is upset and rRNA synthesis is deregulated.

On the other hand, gene promoters are rich in CpG sites that are sometimes densely packed forming what is known as CpG islands. These islands are mostly unmethylated in order to allow gene transcription. Aberrant hypermethylation of these CpG sites may silence the expression of genes that are critical to cell homeostasis, DNA integrity, or genome stability, resulting in cancer development and progression (Bakshi et al., 2018). Numerous studies have reported frequent focal DNA hypermethylation in various cancers (Ehrlich, 2002) including breast (Hon et al., 2012), colorectal (Berman et al., 2011) and bladder (Jürgens et al., 1996) cancer. Pathogenic activation of Wnt signalling is often involved in early stages of carcinogenesis (Toh et al., 2017), where promoter DNA hypermethylation in one or more genes, including *APC*, *AXIN2*, *SFRP1-5*, *WIF1*, *DKK1* and *DKK3* is associated with the activation of this pathway in colorectal cancer (Novellademunt et al., 2015). Additionally, in cancer, DNA hypermethylation tends to target tumour suppressor genes, resulting in growth selection and uncontrolled cell proliferation (Qi & Xiong, 2018; Rahmani et al., 2018; Yamashita et al., 2018). Many tumour suppressor genes are deactivated via this mechanism including the *APC* (Mekky et al., 2018), *p16*, *Rb*, *VHL*, *E-cadherin*, *hLMH1* (Curtis & Goggins, 2005), *BRCA1* (Esteller, 2003); as well as several other genes that are involved in DNA repair, *MGMT*; cell cycle, *p16INK4a*, *p15INK4b*; apoptosis, *DAPK* and antioxidation, *GSTP1* (Sproul & Meehan, 2013). The extent to which DNA *de novo* methylation contributes to cancer development and progression varies among different types of cancer; very high in colon cancer, while rarer in brain tumours (Estécio & Issa, 2011).

Developmental or disease-associated DNA hypermethylation is able to modulate gene expression in various ways including silencing of the CpG-rich promoter, and silencing or downregulating an enhancer; both leading to the downregulation of gene expression by DNA hypermethylation (Ehrlich, 2019). Other than that, DNA hypermethylation could also facilitate transcription in gene bodies by suppressing cryptic promoter; protect borders of promoter or enhancer against unwanted expansion or contraction; regulate protein coding gene by controlling lincRNA genes; and control the use of alternate promoters or alternative splicing.

In short, global DNA methylation and DNA hypermethylation have been detected in various cancers, and is associated with cancer carcinogenesis. However specific mechanisms that lead to aberrant DNA methylation is yet to be fully understood. As the process of DNA methylation is dependent on the activity of a group of enzymes called DNA methyltransferases (DNMTs), as well as the presence of methyl donors, aberrant DNMTs and methyl donor availability could also influence the balance between methylation and demethylation. This

study, therefore, aims to help fill the knowledge gap on mechanisms associated with cancer risk by determining the effect of methyl donor depletion on these mechanisms.

1.3.3 DNA methyltransferase (DNMT)

DNA methylation is catalysed by a family of enzymes called DNA methyltransferases (DNMTs), consisting of DNMT1, DNMT3a, DNMT3b, and DNMT3L.

Essentially, DNMT1 is a maintenance methyltransferase that binds specifically to hemimethylated DNA and is responsible for conserving the DNA methylation pattern from one generation to the next; whilst DNMT3a and DNMT3b are de novo methyltransferases that establish DNA methylation patterns by targeting unmethylated cytosine bases to initiate methylation (Wu & Zhao, 2018). However, several studies have suggested that DNMT1 could also play a critical role in de novo DNA methylation, whilst DNMT3a and DNMT3b, though highly expressed in developing embryos, are also required to maintain DNA methylation patterns in adult tissues. Several studies have also reported that deleting or silencing DNMT1 and DNMT3b genes at the same time, leads to a greater reduction in DNA methylation, compared to the deletion or silencing of only one gene, thus supporting the de novo methyltransferase's critical role in maintaining DNA methylation (Rhee et al., 2002; Leu et al., 2003; Sowińska & Jagodzinski, 2007). Furthermore, in a study conducted using mouse embryonic stem cells with systematic gene knockouts of DNA methyltransferases to delineate its role, DNMT3a and DNMT3b were not able to induce an efficient de novo DNA methylation in the absence of DNMT1 (Liang et al., 2002). Moreover, close cooperation between DNMT1 and DNMT3s was reported for the methylation of specific genes in cancer cells. For example, it was reported that DNMT1 and DNMT3a were necessary for the methylation of the *CASP8* promoter in glioma cells (Datta et al., 2005; Hervouet et al., 2010). Other studies also have supported the cooperativity between DNMTs in de novo DNA methylation (Pradhan et al., 1999; Fatemi et al., 2002; Lorincz et al., 2002). In contrast to these three distinct DNMTs, DNMT3L is a catalytically inactive member of the DNMT3 family, which is mainly expressed during development, and is required for gene imprinting and the regulation of DNMT3a/b (Hervouet et al., 2018).

The dysregulation of DNMTs is associated with cellular transformation and cancer risk. It is suggested that the absence of inactive DNMTs, mainly DNMT1, will induce passive demethylation of the CpG sites and subsequently aberrant gene expression (Hervouet et al., 2018), where Gaudet et al. demonstrated that the deletion or reduction of DNMT1 leads to

substantial genome-wide hypomethylation and chromosomal instability (Gaudet et al., 2003). However, a decrease of DNMT1 concentration was rarely observed in solid tumours, in spite of global DNA hypomethylation and a decrease in maintaining methylation activity in cancer. Instead, DNMT1 was found to be overexpressed in patients with breast (Shin et al., 2016), liver (Saito et al., 2003), pancreas (Peng et al., 2006), and oesophagus (Zhao et al., 2011) cancer. This may be due to post-transcriptional and post-translational modifications of DNMT1, as well as its interaction with non-coding RNA and non-coding microRNA, that could modulate its activity in cancers. For instance, casein kinase-1 could induce the S146 phosphorylation of DNMT1 and decrease the DNA binding capacity of this enzyme (Sugiyama et al., 2010). S127 and S143 phosphorylation mediated by PKC and AKT were observed in glioma and provoked the disruption of DNMT1/PCNA/UHRF1 complex and a consecutive global DNA hypomethylation (Hervouet et al., 2010). On the other hand, overexpression of DNMTs in a variety of tumours could result in hypermethylation and oncogenic activation (Esteller, 2008). This is also supported by the overexpression of DNMT3a or DNMT3b in various cancers that have been shown to lead to DNA methylation-dependent silencing of numerous critical gene targets including tumour suppressors and pro-apoptotic genes (Mizuno et al., 2001; Butcher & Rodenhiser, 2007; Ibrahim et al., 2011; Kobayashi et al., 2011; Sandhu et al., 2015). Additionally, somatic mutation and deletion of DNMTs have also been associated with malignant transformation (Zhang & Xu, 2017).

Interestingly, viral oncoproteins have also been reported to bind and regulate DNMT1 enzymatic activity *in vitro*. Both DNMT1/E1A (in adenovirus) and DNMT1/E7 (in papillomavirus) interactions increase inheritance DNA methylation. Although mechanisms governing this phenomenon are still unclear, it has been proposed that viral oncoproteins might promote DNMT1 DNA binding and SAM recruitment (Burgers et al., 2007), thus contributing towards aberrant DNA methylation profiles in virus-associated cancers.

1.3.4 Aberrant DNA methylation and cervical cancer

Numerous clinical, epidemiological and molecular studies have shown that persistent infection with HR-HPV genotypes is an indispensable, but not sufficient prerequisite for the development of cervical cancer (Łaniewski et al., 2020; Da Silva et al., 2021), suggesting additional factors that create a conducive local microenvironment for malignant transformation. HPV integration into the host genome has led to dysregulation of both viral and host gene expression, followed by epigenetic modifications that are critical events in the carcinogenic process. A great number of studies have reported epigenetic modifications that contribute towards the progression of

pre-cancerous lesions to an invasive cervical cancer, where alterations in DNA methylation, an epigenetic mechanism crucial for regulating gene transcription has been demonstrated in cervical cancer and its precursors (Dueñas-González et al., 2005; Szalmas & Konya, 2009).

In cervical cancer, hypermethylation of genes that are essential in maintaining cellular processes have been reported, and may occur independently of HPV infection status (Szalmas & Konya, 2009; Wentzensen et al., 2009). Evidently, DNA hypermethylation that occurs in cancer cells seems to target tumour suppressor genes explicitly, silencing these genes which results in growth selection and uncontrolled cell proliferation. Examples include the hypermethylation of *FHIT*, a gene involved in cell cycle regulation and apoptosis (Ki et al., 2008); *DAPK*, a gene involved in apoptosis (Yang et al., 2010); *RARβ2*, a gene involved in the signalling pathway for cell growth suppression (Jha et al., 2010); *APC*, a tumour suppressor protein involved in the Wnt/βcatenin pathway (Dong et al., 2001); *p73*, a gene involved in cell cycle regulation and apoptosis (Liu et al., 2004) and *MGMT*, a DNA repair protein that protects human genome against mutation (Kim et al., 2010). Additionally, it appears that DNA hypermethylation occurs early in tumorigenesis and typically increases with tumour progression. Hypermethylation of *CCNA1*, a gene associated with the regulation of cell cycle, has been reported in HSIL (36.6%) and invasive cancer (93.3%) (Kitkumthorn et al., 2006; Yang et al., 2010). In another study conducted among 308 women with normal or various degrees of cervical neoplasia, a cluster of three tumour suppressor genes, *CDH1*, *DAPK*, and *HIC1*, displayed a significantly increased frequency of promoter methylation with progressively more severe cervical neoplasia ($P < 0.05$) (Flatley et al., 2009). A decline in *CADMI* gene expression has also been reported in high grade CIN and squamous cell carcinoma, where a severity of cervical dysplasia is correlated with a higher number of methylated genes (Overmeer et al., 2008), whilst hypermethylation of E-Cadherin promoter has been reported in 89% of invasive cancer, 26% in CIN III and none in normal tissues (Shivapurkar et al., 2007).

In a more recent study, Clarke et al. performed DNA methylation profiling on 50 formalin-fixed, paraffin-embedded tissue specimens from women with benign HPV-16 infection and histologically confirmed CIN3, and cancer (Clarke et al., 2017). This study reported that *ADCYAPI*, *ASCL1*, *CADMI*, *DCC*, *ATP10*, *DBC1*, *HS3T2*, *MOS*, *SOX1*, *SX17* and *TMEFF2* genes showed higher levels of methylation when compared to healthy controls. A study by Kremer et al. also reported hypermethylation levels of *ASCL1*, *LHX8*, and *ST6GALNAC5*, where DNA hypermethylation increased with the severity of cervical

cancer (Kremer et al., 2018). Moreover, Verlaet et al. showed that DNA methylation usually occurs at the pre-tumorigenic stage and reaches the highest level after tumorigenesis induced by HR-HPV (Verlaet et al., 2018).

In addition to that, Ma et al. performed a bioinformatics analysis to identify the aberrantly methylated and differentially expressed genes (DEGS), and their related pathways in cervical cancer (Ma et al., 2020). Gene expression profile dataset (33 cervical cancer and 24 normal samples) and methylation profile dataset (6 cervical cancer and 20 normal samples) were extracted from the Gene Expression Omnibus (GEO) database. They reported 2 upregulated-hypomethylated oncogenes and 8 downregulated-hypermethylated tumour suppressor genes. Hypomethylated and highly expressed genes were significantly enriched in cell cycle and autophagy. On the other hand, hypermethylated and lowly expressed genes were found in the estrogen receptor and Wnt/ β -catenin signalling pathways, where *ESR1*, *EPB41L3*, *EDNRB*, *ID4* and *PLAC8* were the hub genes. This finding indicates the relationship between CpG methylation status and its impact on gene expression in cervical cancer.

Several studies have also shown that cervical cancer frequently displays global DNA hypomethylation, though compared to hypermethylation, the literature is quite limited. A study was conducted in 1994, to determine the relationship between the degree of DNA hypomethylation and the grade of neoplasia in 41 patients with abnormal cervical epithelial cells (Kim et al., 1994). It was reported that the degree of DNA hypomethylation increases with the grade of cervical neoplasia ($P < 0.0001$), where the extent of methyl group incorporation was reduced threefold and sevenfold in the DNA from cervical dysplasia and cancer, respectively, compared with the DNA from normal cervical tissue ($P = 0.006$). Similar findings were reported in a study conducted by Fowler et al., involving 83 patients with normal and different stages of cervical neoplasia (Fowler et al., 1998). They found that the largest increase in hypomethylation appeared in the early stage of cervical neoplasia and was stable through CIN3, and then increased again when the disease progressed to cancer. Furthermore, global DNA hypomethylation was greater in women with invasive cervical cancer than all other groups ($P < 0.05$) (Flatley et al., 2009). Additionally, in a study to evaluate characteristics of global hypomethylation in the evolution of cervical cancer, L1 hypomethylation levels showed progressive significant increase when comparing normal epithelium (59.4 +/- 8.86%) to carcinoma in situ (64.37 +/- 7.32%) and squamous cell carcinoma (66.3 +/- 7.26%) ($P < 0.005$) (Shuangshoti et al., 2007). Similar to DNA hypermethylation, hypomethylation occurs early in tumorigenesis and typically increases with tumour progression.

There are several theories as to the presence of aberrant methylation profiles in cervical cancer. It is proposed that aberrant methylation patterns can be induced by viral E6 and E7 oncoproteins of HR-HPVs, to bring about alterations in a wide range of cellular genes, particularly those involved in cell cycle regulation, apoptosis, DNA damage repair and cell adhesion, senescence and survival of cells; including *TP53* and *RBI* tumour suppressor genes in cervical cancer (McCormick et al., 2015; Cardoso et al., 2017; Sen et al., 2018). HR-HPV integration drives the carcinogenic process through the inactivation of E2, leading to E6 and E7 overexpression, as well as the disruption of host genes due to viral sequence insertion (McBride & Warburton, 2017). DNA methylation of the HPV genome at the long control region (LCR), where the E2 binding site is located and contains CpG sites for potential methylation; will result in the loss of E2 function, leading to the overexpression of E6 and E7 oncoproteins (Yang, 2013). Furthermore, as cervical neoplasm severity increases, CpG hypermethylation of HPV LCR also increases (Ding et al., 2009). Studies of invasive cervical cancers consistently show that the L1 gene of HPV-16 and HPV-18 is hypermethylated, and hypermethylation increases with the severity of the disease (Yang, 2013).

Previous studies have suggested that epigenetic alterations associated with E6 and E7 activities are common events during the early steps of epithelial malignancy and have been described as potential biomarkers for cervical cancer (Clarke et al., 2012; Verlaat et al., 2017). Both E6 and E7 viral oncoproteins act together to promote the hypermethylation of cellular genes. E6 promotes degradation of *p53* and releases of Sp1 transcription factors, which bind to the DNMT1 gene promoter, activating its expression. E7 oncoproteins form a stable complex with *pRB*, releasing the transcription factor E2F, which binds to the DNMT1 gene promoter, thus activating its expression. Both these mechanisms lead to the production of DNMT enzymes, which promotes the hypermethylation and the silencing of cellular genes (Sen et al., 2018). However, Poomipark et al. proposed a contrasting hypothesis, where methyl donor status regulates DNA methylation, which in turn could affect the incidence of cervical cancer (Poomipark et al., 2016). In this present study, human cervical cancer cells (C4-II) were incubated in media and after significant depletion of the methyl donor for 8 days, DNMT3a and DNMT3b were reported to be downregulated, which is associated with DNA global hypomethylation. The effects of methyl donor depletion on DNMT expression are reversible, suggesting the idea that the intake of methyl donors mediates gene expression and influences cervical cancer progression.

1.4 Methyl Donor Nutrients

DNA methylation involves the addition of methyl groups by S-adenosylmethionine (SAM) to cytosine residue. Numerous studies have indicated DNA methylation adaptability to environmental factors including diet and nutritional elements, whereby methyl donor nutrients availability have been shown to modify DNA methylation either globally or at specific CpG sites by inducing the formation of methyl donors, acting as co-enzymes, or modifying DNMT enzymatic activity (Sapienza & Issa, 2016; Mahmoud & Ali, 2019; Ghazi et al., 2020).

1.4.1 One-carbon metabolism

Methyl donor nutrients may modify DNA methylation via its effect on the one-carbon (1C) metabolism (Mahmoud & Ali, 2019; Ghazi et al., 2020), which comprises a series of interlinking metabolic pathways that are central to cellular function (Clare et al., 2019). 1C metabolism includes the methionine cycle, folate cycle and transsulfuration pathways, and is compartmentalized between the cytoplasm, nucleus, and mitochondria. This complex network of biochemical reactions facilitates the transfer of 1C moieties in the form of methenyl, formyl, and methyl groups required for cellular processes. Such processes include molecular biosynthesis of proteins, polyamines, creatine, phospholipids; genomic maintenance via regulation of nucleotide pools; epigenetic control of gene expression by methylation of DNA, RNA, and histones; and redox defence (Lucock, 2000; Ducker & Rabinowitz, 2017). Micronutrients that mediate the 1C metabolism include essential methyl donors such as methionine, folate (B9), choline and betaine; and other B vitamins (B₂, B₃, B₆, and B₁₂) that act as cofactors in this mechanism (Clare et al., 2019; Mahmoud & Ali, 2019; Ghazi et al., 2020).

The production of S-adenosylmethionine (SAM), is generated from methionine, that partly depends on the availability of methyl donor nutrients from the diet; or produced endogenously by homocysteine re-methylation via two pathways namely, the folate and the betaine pathway (**Figure 1.7**) (Roje, 2006; Clare et al., 2019). Methionine is converted into SAM, a universal methyl donor involved in numerous downstream cellular reactions, by methionine adenosyltransferase (MAT). In order for DNA methylation to occur, an activated DNMT enzyme will catalyse the transfer of a methyl group from SAM to carbon 5 of cytosine in DNA to produce methylated DNA. Once the methyl group is transferred, SAM is converted to S-adenosylhomocysteine (SAH), which is hydrolysed back to homocysteine and adenosine through a reversible reaction catalysed by S-adenosylhomocysteine hydrolase (AHCY) to complete the methionine cycle.

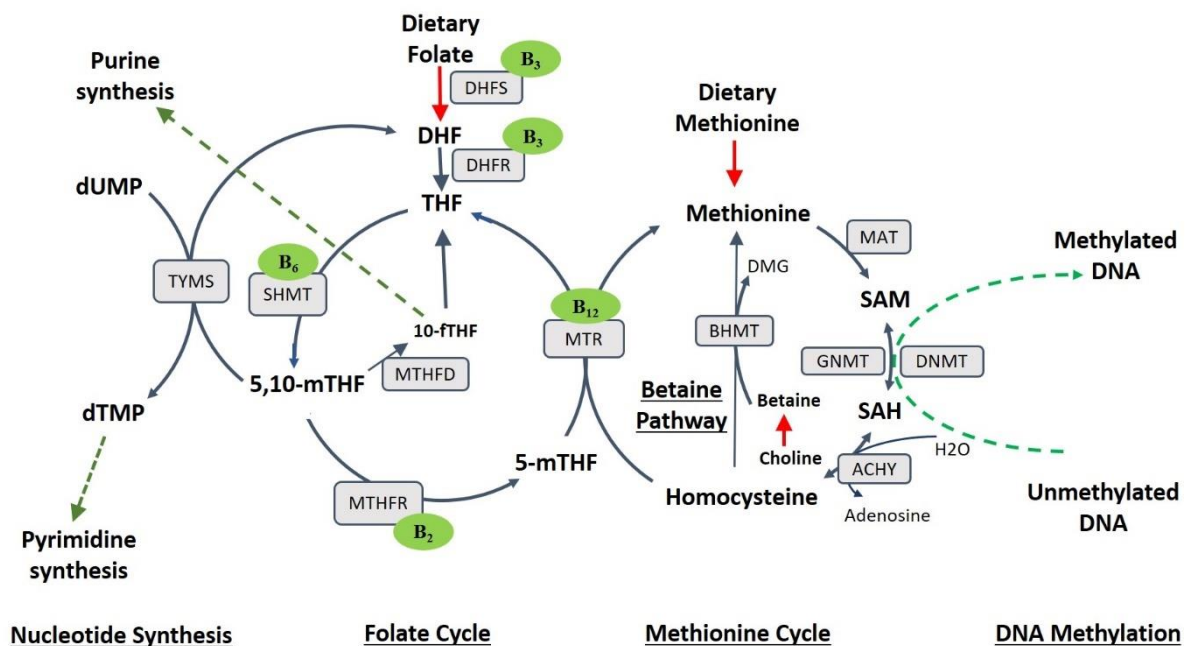


Figure 1.7 The role of micronutrients in one-carbon metabolism and DNA methylation

Methionine, whether from diet or endogenously synthesised, is critical for the synthesis of S-adenosyl methionine (SAM), which acts as a DNA methyltransferase (DNMT) cofactor and a universal methyl donor for DNA methylation. The enzyme that catalyses this reaction is methionine adenosyltransferase (MAT). Methionine can be obtained endogenously from homocysteine re-methylation, that can occur via two pathways: (1) Folate, where dietary folate is converted to dihydrofolate (DHF) by the dihydrofolate synthase (DHFS) enzyme, then to tetrahydrofolate (THF) by the dihydrofolate reductase (DHFR) enzyme; where vitamin B₃ acts as a cofactor in both steps. THF is then converted to 5,10-methylenetetrahydrofolate (5,10-mTHF) by the enzyme serine hydroxymethyltransferase (SHMT) that requires vitamin B₆ as a coenzyme. This reaction is followed by a reduction of 5,10-mTHF to 5-mTHF, via the enzyme methylenetetrahydrofolate reductase (MTHFR) and the co-enzyme vitamin B₂. 5-mTHF acts as a methyl donor for homocysteine re-methylation. To complete the cycle, 5-mTHF is transformed back to THF by the enzyme 5-methyltetrahydrofolate-homocysteine methyltransferase (MTR) that utilizes B₁₂ as a co-enzyme. (2) Betaine-homocysteine S-methyltransferase (BHMT) catalyses the re-methylation of homocysteine by using betaine, obtained from diet or via choline oxidation, as a methyl donor, resulting in methionine and dimethylglycine (DMG). The transfer of the methyl group from SAM to DNA results in S-adenosyl homocysteine (SAH) in the presence of glycine N-methyltransferase (GNMT), that can be reversibly converted to homocysteine and adenosine by the enzyme S-adenosylhomocysteine hydrolase (AHCY). An activated DNA methyltransferase (DNMT) enzyme will catalyse the transfer of a methyl group to carbon 5 of cytosine in DNA to produce methylated DNA. Folate is also required for purine and pyrimidine nucleoside thymidine synthesis in the DNA synthesis/repair mechanism. In the pyrimidine synthesis, thymidylate synthase (TYMS) will transfer a methyl group from 5,10-mTHF to convert deoxyuridine monophosphate (dUMP) to thymidine monophosphate (dTMP), whilst 10-formyltetrahydrofolate (10-fTHF) acts as methyl donor in the *de novo* purine synthesis.

In the folate pathway, dietary folate is reduced to its active form, tetrahydrofolate (THF) by the dihydrofolate reductase (DHFR) enzyme, that utilizes vitamin B₃ as its cofactor (**Figure 1.7**) (Ducker & Rabinowitz, 2017; Clare et al., 2019). In the folate cycle, THF is converted to

5,10-methylenetetrahydrofolate (5,10-mTHF) by the vitamin B₆-dependent enzyme, serine hydroxymethyltransferase (SHMT); followed by a reduction to 5-mTHF by the vitamin B₂-dependent enzyme, methylenetetrahydrofolate reductase (MTHFR). Alternatively, 5-mTHF can be converted to 10-formyltetrahydrofolate (10-fTHF), through a series of reactions catalysed by methylenetetrahydrofolate dehydrogenase (MTHFD). Demethylation of 5-mTHF completes the folate cycle, as 1C is donated for re-methylation of homocysteine to methionine, in the methionine cycle. This reaction is catalysed by the 5-methyltetrahydrofolate-homocysteine methyltransferase (MTR) enzyme that requires the vitamin B₁₂ co-enzyme. In the betaine pathway, betaine-homocysteine S-methyltransferase (BHMT), a vitamin B₆-dependent enzyme catalyses the transfer of a methyl group from betaine to homocysteine, resulting in the production of dimethylglycine (DMG) and methionine (Finkelstein & Martin, 1984; Clare et al., 2019).

The conversion of SAM to SAH by glycine N-methyltransferase (GNMT), and SAH to homocysteine by S-adenosylhomocysteine hydrolase (AHCY), acts as the negative feedback to this mechanism (Liteplo, 1988). This reaction is considered as a negative regulator of the DNA methylation process since SAH has a higher affinity to DNMTs than SAM, resulting in an inhibition of DNMT activity. In addition, the conversion of SAH to homocysteine is a reversible chemical reaction that could produce high levels of homocysteine in the body, and this is associated with reduced DNMT activity. The negative regulation of 1C metabolism is resolved by the re-methylation of homocysteine to methionine, via the folate-dependent pathway or the diet-derived betaine or choline pathway (Soda, 2018), thus demonstrating the essential role of folate and choline/betaine to this mechanism, and in the regulation of DNA methylation. Alternatively, homocysteine can undergo degradation via the two-step transsulfuration pathway, with vitamin B₆ as the cofactor (Clare et al., 2019). SAM coordinates transsulfuration by acting as an allosteric inhibitor of MTHFR and activator of cystathionine β -synthase (CBS), the first enzyme within the transsulfuration pathway that mediates the condensation of serine with homocysteine to yield cystathionine. The second step, catalysed by cystathionine γ -lyase, produces cysteine, a precursor for glutathione, which is a major redox-regulating system in cells.

In addition to DNA methylation, folate also plays an essential role in the DNA synthesis/repair mechanism, through its involvement in purine and pyrimidine nucleoside thymidine synthesis (Shuvalov et al., 2017). In *de novo* purine synthesis where 10-fTHF acts as the 1C donor, reactions catalysed by phosphoribosylglycinamide formyltransferase, converts

glycinamide ribonucleotide to formylglycinamide ribonucleotide; whilst phosphoribosylaminoimidazolecarboxamide formyltransferase, convert aminoimidazolecarboxamide to formylaminoimidazolecarboxamide ribonucleotide, to provide C2 and C8 atoms for purine ring synthesis, that leads to the formation of inosine monophosphate (IMP). IMP is the precursor of adenosine monophosphate (AMP) and guanosine monophosphate (GMP), required for purine nucleotide synthesis. On the other hand, the central precursor for generating pyrimidines is the uridine monophosphate (UMP) synthesis, which does not require 1C cofactors. UMP is converted to deoxyuridine monophosphate (dUMP) via uridine diphosphate by nucleoside diphosphate kinase. Then, thymidylate synthase (TYMS) transfers 1C from 5,10-mTHF, converting dUMP to thymidine monophosphate (dTMP). The 5,10-mTHF is oxidized to DHF, and subsequently reduced to THF, completing the metabolic loop.

A deficiency in folate may alter the balance of DNA precursors, leading to dUMP accumulation and incorporation of uracil onto DNA in place of thymine. Normally, any misincorporated uracil to the DNA strand will be extracted by uracil DNA glycosylase, a DNA repair enzyme. However, subsequent removal of the base-free sugar by DNA repair enzymes may cause a transient breakage in the DNA molecule, which is then sealed by DNA ligase. In a condition where folate is continuously limited, uracil misincorporation and repair may occur continually. This repeated breakage of the DNA molecule might ultimately lead to chromosomal damage and malignant transformation (**Figure 1.8**) (Blount et al., 1997; Catala et al., 2019). In previous studies using human cell culture, folate depletion has led to a reduction in DNA synthesis and progressively increases uracil misincorporation (2 to 3-fold) in PBMC *ex vivo* (Duthie & Hawdon, 1998), in human colonocytes (Duthie et al., 2008), and in SV40-immortalised human colon epithelial cells (HCEC) (Duthie et al., 2000). It was reported that the effect of folate deficiency on DNA stability in HCEC cells was highly sensitive to folate availability, with uracil concentrations declining to baseline levels after repleting the cells with folate at concentrations normally observed in both human blood and colon tissue (10 ng/mL) (Duthie et al., 2000). Furthermore, McGlynn et al. conducted a study to determine the association between folate status and uracil misincorporation in isolated colonocytes from colonoscopy patients (40 adenomatous polyps, 16 hyperplastic polyps and 53 control samples) (McGlynn et al., 2013). Within adenoma cases, there was a trend (P-trend < 0.001) of decreasing colonocyte folate (pg/10⁵ cells, mean ± CI) from the site distal to the polyp (16.9 ± 2.4), to the site adjacent to the polyp (14.7 ± 2.3), to the polyp (12.8 ± 2.0). Correspondingly, there were increases in uracil misincorporation (P-trend < 0.001) across the 3 sites. These findings highlight

the importance of folate adequacy via its role in DNA synthesis/repair mechanism, that might impact cancer risks.

Additionally, folate, methionine, choline and the B vitamins have been shown to modify DNA methylation either globally or at specific CpG sites by inducing the formation of methyl donors, acting as co-enzymes, or modifying DNMT enzymatic activity (Mahmoud & Ali, 2019; Ghazi et al., 2020). Furthermore, studies have suggested an interdependency of these nutrients, such that a disturbance to one methyl donor pathway brings about changes in others. Although many studies have demonstrated that altering methyl donor status can induce changes in DNA methylation, results are not entirely consistent.

Several studies have associated folate intake with lower risk of colorectal and prostate cancer (Giovannucci et al., 1993; Su & Arab, 2001; Giovannucci, 2002; Stevens et al., 2006); and folate supplementation has been found to modify DNA methylation status to provide a protective effect against diseases including cancer (Keyes et al., 2007; Wallace et al., 2010; Cartron et al., 2012). However, there are studies that have reported conflicting results (Song et al., 2000; Kotsopoulos et al., 2008; Qin et al., 2013; Gylling et al., 2014), indicating that the mechanisms associated with folate effect on DNA methylation are more complex than previously thought and confounded by other dietary, genetic, or tissue-related factors. Nonetheless, several studies have suggested that folate might provide cancer-protecting effects for specific cancers by inducing promoter methylation of proto-oncogenes (Wallace et al., 2010; Vineis et al., 2011; Caiazza et al., 2015). As for methionine, there is even more limited evidence with conflicting results on dietary methionine status and its effect on DNA methylation, especially in human studies (Mahmoud & Ali, 2019). A meta-analysis to determine the association between methionine and breast cancer risk found that methionine intake might be inversely associated with breast cancer risk, especially among post-menopausal women (Wu et al., 2013). On the other hand, high intake of methionine has been associated with increased risk of cancer (Vidal et al., 2012), with dietary methionine restriction currently being studied as an enhancer for chemotherapy treatment in metastatic cancer (Thivat et al., 2007; Durando et al., 2010). This could be due the cyclical nature of the methionine cycle, where excessive methionine might inhibit the re-methylation of homocysteine, thus disrupting the one-carbon cycle and negatively impacting DNA methylation (Regina et al., 1993). Contradicting results have also been reported regarding methionine availability on DNA hypermethylation/hypomethylation and cancer risk/progression in animal studies, indicating

other confounding dietary, genetic and tissue-related factors (Uekawa et al., 2009; Amaral et al., 2011; Miousse et al., 2017).

In short, 1C metabolism demonstrates the essential role of micronutrients in cellular pathways, and fluctuations in these nutrients can influence SAM/SAH ratios, thus impacting the epigenome through DNA methylation processes. This can have a long-term effect on gene expression, which could contribute to pathogenesis or progression of cancer (**Figure 1.8**). Several studies have reported the effects of supplementation or deficiency of these nutrients on global or gene-specific alterations in DNA methylation, which are further discussed in the next section.

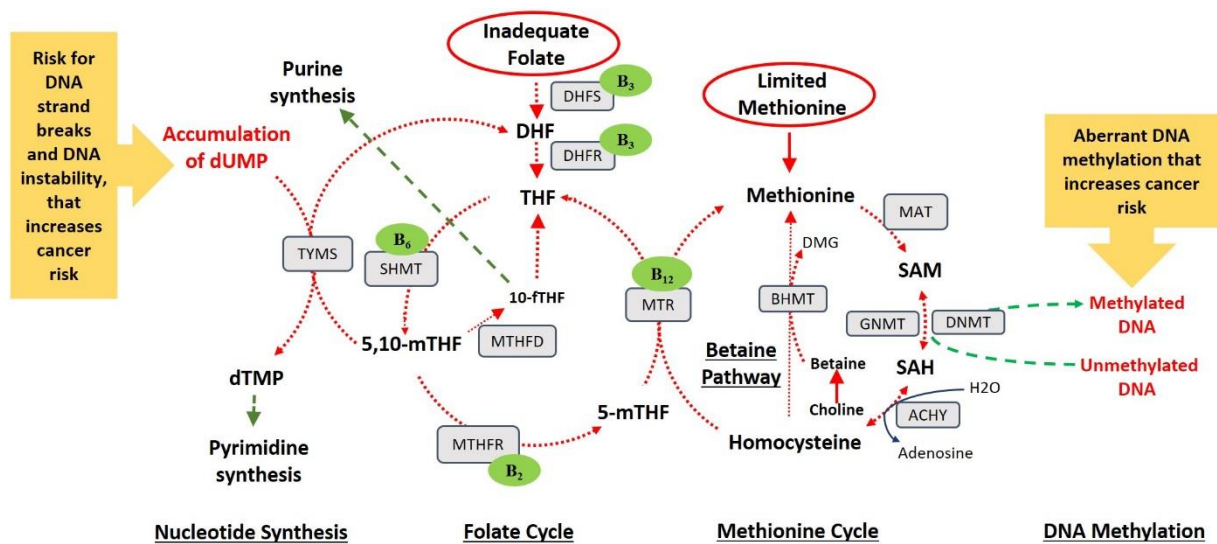


Figure 1.8 Methyl donor depletion and cancer risks

The depletion of methyl donor nutrients could impair DNA methylation, leading to aberrant DNA methylation and increased cancer risk. Additionally, folate depletion may alter the balance of DNA precursors, leading to dUMP accumulation and the incorporation of uracil onto DNA in place of thymine. Misincorporated uracil is usually removed by uracil DNA glycosylase, a DNA repair enzyme, however, subsequent removal of the base-free sugar by DNA repair enzymes may cause a transient breakage in the DNA molecule, which is then sealed by DNA ligase. In a condition where folate is continuously limited, uracil misincorporation and repair may occur continually. This repeated breakage of the DNA molecule might ultimately lead to chromosomal damage and malignant transformation.

A study to determine the influence of methyl donor nutrients on DNA methylation, DNMT expression and global gene expression was previously undertaken in this department (Poomipark, 2013; Poomipark et al., 2016). Initially, a cervical cancer cell model of folate and methionine depletion was developed, where C4-II cervical cancer cell lines were grown in complete media, folate depleted media or combined folate and methionine depleted media.

Disturbance to the methyl cycle was confirmed by significant reduction in intracellular folate and intracellular methionine concentration, as well as an increase in extracellular homocysteine concentration, after 8 days of culture ($P < 0.05$). In comparison to the cells grown in complete media, a significant downregulation of DNMT3a and DNMT3b gene expression was reported in the absence of both folate and methionine; which they associated with the reduction in global DNA methylation (18%). Furthermore, effects of folate and methionine depletion on DNMT3s' expression were reversed by transferring depleted cells to complete medium, suggesting reversible modulating effects of dietary methyl donor intake on gene expression, which may be relevant for cervical cancer progression. Additionally, a genome wide microarray analysis was performed where a preliminary bioinformatics analysis identified an upregulation of genes important for cell death, cell motion, protein kinase cascade, signal transduction, cell communication, blood vessel development, and focal adhesion; whilst genes important for regulation of the cell cycle, condensed chromosome, cytoskeleton organization, DNA metabolic process, lipid biosynthesis and chromosome organization were downregulated in combined folate and methionine depletion. However, current literature suggests that in addition to methyl donor availability, the integration of HR-HPV into the host genome and subsequent dysregulation of gene expression is an important event in cervical cancer growth and progression. Thus, this current study is an extension to the previous work by Poomipark et al., where the focus is on the inter-connected mechanisms of multiple factors, particularly methyl donor availability and genomic changes caused by HR-HPV integration in cervical cancer progression, which is still not entirely understood.

1.4.2 Folate as a methyl donor

Folate, or also known as vitamin B₉, is the generic name for a group of related compounds with similar nutritional properties, where 5-methyltetrahydrofolate (5-mTHF) is the active form of vitamin B₉. It is an essential water soluble B vitamin where rich sources include leafy green vegetables, beans, peas, lentils, fruits like lemons, bananas, and melons, and fortified or enriched products, such as breads and cereals (Donnelly, 2001). On the other hand, folic acid is the synthetic form of the vitamin, also known as pteroylmonoglutamic acid. It is used in supplements and added to processed food products, as it is more stable in foods than natural folates, and is better absorbed. At least 53 countries have implemented the fortification of dietary staples such as bread and cereals with folic acid (Crider et al., 2011). Current dietary reference values (DRVs) for the UK state that the amount of folate required to meet the requirements of 97.5% of the UK population is 200µg/day for adults and that women should take 400µg/day. The Recommended Dietary Allowance (RDAs) for the USA and the Joint Food

and Agriculture Organization of the United Nation/World Health Organization Nation (FAO/WHO) is set at 400µg/day for adults and 600µg/day for pregnant women (Geissler & Powers, 2011). The upper limit for folate is 1000 µg/day, which is one fifth of the minimum amount known to mask B₁₂ deficiency (Crider et al., 2011). Serum levels, are thought to reflect recent intake, where deficiency is categorized as less than 7 nmol/L to less than 10 nmol/L. In contrast, red blood cell (RBC) folate represents folate status over months with levels less than 315 to 363 nmol/L suggesting deficiency (de Benoist, 2008).

Folates comprise an aromatic pteridine ring linked to p-aminobenzoic acid and one or more glutamate residues (Tibbetts & Appling, 2010). Naturally-occurring folates are broken down in the gut by folate conjugase in the mucosal brush borders from folate polyglutamates to the monoglutamate form. Upon absorption, the monoglutamates are converted in the mucosal cells to 5-methyltetrahydrofolic acid (5-mTHF), which is usually the only form found in plasma. 5-mTHF is taken up by cells but cannot be retained intracellularly unless it is metabolised to tetrahydrofolate (THF). Dietary folate bioavailability ranges from 10% to 98% and is influenced by intestinal pH, enzymatic activity, presence of alcohol and other inhibitors, malabsorption disorders, and the food matrix. In contrast, folic acid is not conjugated and is therefore better absorbed. However, before it can become active, folic acid has to be reduced to THF and methylated.

Due to its role as a methyl donor in 1C metabolism, folate has been studied extensively as a possible mechanism for cancer development (Mahmoud & Ali, 2019; Ghazi et al., 2020). *In vitro* studies in various human cancer cell lines have demonstrated folate potential in modulating global and gene-specific DNA methylation patterns, and subsequently contributing towards cancer risk. In the study by Stempak et al., they examined the effects of isolated folate deficiency on DNA methylation using untransformed NIH/3T3 and CHO-K1 cells, and human HCT116 and Caco-2 colon cancer cells (Stempak et al., 2005). Both folic acid deficient (0 µM) HCT116 and Caco-2 cells reported a downregulation of DNMT1 and DNMT3a expression. However, there was no significant changes to DNMT activity or global DNA methylation. In contrast, Wasson et al. reported a significant increase in global DNA hypomethylation in SW620 colorectal cancer cells cultured in folate-free medium for 14 days, compared to cells grown in medium containing 3 µmol/L folic acid (Wasson et al., 2006). They also observed that folate-deprived cells showed a significantly higher DNA hypomethylation in the region of the *p53* gene. These effects of folate depletion were reversed upon folic acid repletion (3 µmol/L). On the other hand, folate supplementation has been shown to increase DNA methylation.

Lubecka-Pietruszewska et al. reported that increased folic acid concentrations (4-8mg/L) led to a dose-dependent promoter methylation of tumour suppressors *PTEN*, *APC*, and *RAR β 2*, in MCF-7 and MDA-MB-231 breast cancer cell lines (Lubecka-Pietruszewska et al., 2013). This may be linked to the increased DNA methylation detected within their promoter regions. In another study by Li et al., folic acid supplementation of 20 and 40 mmol/L demonstrated an increased SAM to SAH ratio in an *in vitro* model of human neuroblastoma cells (SH-SY5Y) (Li et al., 2015). This was followed by the downregulation of the abnormally phosphorylated tau protein, by inhibiting the demethylation reactions of PP2A, that plays a role in the regulation of the tau protein. In short, the effects of folate availability on DNA methylation in various human cancer cell lines appears to be cell-, site-, and gene-specific, and thus could lead to the differences in findings.

In an animal study, the effect of folate status has also been reported to modulate DNA methylation pattern, though with conflicting results. Global DNA hypomethylation was reported in 3 different murine studies in response to either a folate-deficient or a folate-rich diet provided at different stages of growth (Chen et al., 2011; Ly et al., 2011; Sie et al., 2011). In another study that uses the *Apc*^{+/-} *Msh2*^{-/-} mice murine model of intestinal tumorigenesis, no effect was observed for DNA methylation either globally or at a specific site, with 8 mg/kg folic acid supplementation (Song et al., 2000). However, it does significantly decrease the number of small intestinal adenomas (by 2.7-fold; P=0.004) and colonic foci (by 2.8-fold; P= .028) and colonic adenomas (by 2.8-fold; P=0.1); though this effect was only observed when the folate supplementation was administered prior to the establishment of neoplastic foci. Sie et al. reported an increase in global DNA methylation and the reduced risk of colorectal adenocarcinoma in the rat's offspring with maternal folic acid supplementation (control=2 mg/kg; supplemented=5 mg/kg); however, post-weaning supplementation significantly decreased global DNA methylation in the colon of the offspring at 14-weeks of age, and may increase cancer risk (Sie et al., 2011). On the other hand, the administration of a folate-deficient diet (0 mg/kg) for 4 to 6 weeks in rats at the weaning stage, have been found to induce DNA strand break and selective hepatic *p53* promoter hypomethylation, that was thought to play an integral role in carcinogenesis (Kim et al., 1997). Similar findings were reported by McKay et al., where a 0.4 mg/kg folate-deficient diet was fed to maternal and post-weaning rats. They reported that folate deficiency induces *p53* promoter hypomethylation in adult rats, and *APC* promoter hypermethylation in the *APC*^{+/^{min}} offspring, that may modulate colorectal carcinogenesis (McKay et al., 2011). Additionally, diet that is rich in folate was also observed to increase gene-specific methylation in genes that has been associated with cancer

development including *p16* in mouse colon (Keyes et al., 2007), and proto-oncogenes such as *PDGF-B*, *Ras*, and *survivin* in a mouse model of gliomagenesis (Cartron et al., 2012). Though there is evidence to suggest that folate availability may alter the DNA methylation process, it is still unclear whether its effects lead to an increased or decreased risk in developing cancer.

Similarly, in human studies, there are inconsistencies in the evidence linking folate availability towards cancer risk and progression. These discrepancies could be due to the variation in research methodologies including dosage used, intake mode of either from diet or folic acid supplementation, timing and duration of supplementation, as well as specific tissues factors (Kotsopoulos et al., 2008; Burr et al., 2017; Zhao et al., 2017; Pieroth et al., 2018). Furthermore, the measured folate serum or plasma concentration reflect recent dietary intake rather than long term folate status which is better reflected by red cell folate concentration. Additionally, other external factors such as age, genetic and epigenetic background, alcohol intake, and comorbidities could also impact the outcome of folate study (Guo et al., 2015; Yi et al., 2016). Studies have shown that polymorphism of the gene that encodes the enzyme methylenetetrahydrofolate reductase (MTHFR), where a C to T substitution at base 677 of the gene (677C→T; rs1801133), produces an enzyme with lower folate-processing capacity. Individuals with the TT genotype have significantly lower blood folate concentrations for the same dietary intake of folate (Molloy et al., 1997). A meta-analysis (Tsang et al., 2015) estimated that, compared to CC, the TT genotype confers a 16% lower red blood cell folate and a 13% lower serum (or plasma) folate measured using a microbiological assay and a serum (or plasma) difference of 20% when assessed using protein-binding assays.

In epidemiological studies, there is evidence that supports the association between folate intake and cancer risk, albeit conflictive. High folate intake has been observed to lower the risks of colorectal cancer in adults (Giovannucci et al., 1993). This association was also supported by the NHANES (National Health and Nutrition Examination Survey) Epidemiologic Follow-up Study (NHEFS) findings (Su & Arab, 2001). In this study, a total of 14 407 participants were followed up for 20 years. They reported that dietary folate intake was significantly inversely associated with colon cancer in men (RR=0.40, 95% (CI)=0.18, 0.88) who consumed more than 249 µg/day of folate and that there was a significant dose-response relationship (P=0.03), though no association was found in women. However, a prospective study involving 88 758 women reported lower colorectal cancer risk in women who consumed more than 400 µg/day (RR=0.81, 95%CI=0.62-1.07), which is more apparent in participants with a family history of colon cancer (RR=0.48, 95%CI=0.28-0.83) (Fuchs et al., 2002). Similar findings were reported

in the Cancer Prevention Study II Nutrition Cohort study involving 43 512 men and 56 011 women, where folate intake was associated with a reduced risk of prostate cancer (Stevens et al., 2006). In contrast, a prospective case-control study of 331 cases and 662 matched controls nested within the population-based Northern Sweden Health and Disease Study associated low plasma folate concentrations with lower risk of colorectal cancer (Gylling et al., 2014). A meta-analysis to examine the association between folate consumption and colorectal cancer risk was performed involving 7 cohort and 9 case-control studies; and the researcher concluded that dietary folate has a more protective effect on colorectal cancer than supplemental folate (Sanjoaquin et al., 2005). However, this association is confounded by other factors including gender, diet, and alcohol intake. In addition to that, a significant association between folate status and DNA hypomethylation was reported in 376 women diagnosed with CIN (Piyathilake et al., 2011). On the other hand, there are limited studies that link folate availability and cervical cancer. In a 1991 case-control study, in order to further examine the role of folate in cervical cancer risks, Potischman et al. collected serum samples from 330 cases at different stages of CIN and cervical cancer, and 555 controls with normal cervical cytology (Potischman et al., 1991). It was observed that there was no difference in folate concentration between the groups, suggesting that folate concentrations and stages of cervical neoplasia did not correlate. Similarly, in a nested-case control study, serum folate status was also not associated with cervical cancer incidence (Alberg et al., 2000). Observational studies have also reported the association between global DNA hypomethylation and increased risk of colorectal (Pufulete et al., 2003), cervical (Piyathilake et al., 2006), and bladder (Moore et al., 2008) cancer, but its association with low folate intake or blood concentrations was not evident. Moreover, observational studies of folate intake often do not distinguish between natural folates and folic acid and may be subject to other confounding factors.

Similarly, there are conflictive findings in folic acid supplementation in clinical trials. Qin et al. conducted a meta-analysis on randomized trials to determine the effect of folic acid supplementation and cancer risk (Qin et al., 2013). They did not report any significant effect on total cancer incidence (13 trials, n=49 406, RR=1.05; 95% CI:=0.99-1.11, P=0.13) as well as in colorectal cancer (7 trials, n=33 824), other gastrointestinal cancers (2 trials, n=20,228), prostate cancer (5 trials, n=27 065), other genitourinary cancers (2 trials, n=20 228), lung cancer (5 trials, n=31 864), breast cancer (4 trials, n=19 800), haematological malignancy (3 trials, n=25 670) and total cancer mortality (6 trials, n=31 930). However, they did observe a significantly reduced risk for melanoma (3 trials, n=19, 128). Folic acid supplementation of 1 mg/day for 3 years did not reduce the risk of adenoma recurrence amongst the 1021 men and

women diagnosed with colorectal adenoma (Cole et al., 2007). Additionally, they suggested that it might actually increase the risk of colorectal neoplasia. This finding was supported by another study by Oliai Araghi et al., in a multicentre, double-blind randomized placebo-controlled trial designed to assess the effect of 2 to 3 years of daily supplementation of folic acid (400 µg) and vitamin B₁₂ (500 µg) in 2524 participants. In this long-term follow up trial, the supplementation was associated with increased risk of colorectal cancer in adults aged 65 and above (Oliai Araghi et al., 2019). Similar findings were reported where there was increased lung cancer incidence with 800 µg/day folic acid and 400 µg/day vitamin B₁₂ supplementation (Ebbing et al., 2009). However, folate doses in these two studies were twice the recommended daily folate intake of 400 µg/day (Institute of Medicine Standing Committee on the Scientific Evaluation of Dietary Reference, 1998), suggesting a dose-dependent response to folate intake. This hypothesis is supported by a dose-response meta-analysis involving 14 prospective studies with 677 858 individuals, that discovered a potential J-shaped correlation between folate intake and breast cancer risk ($P=0.007$) and revealed that a daily folate intake of 200-320 µg/day was associated with a lower breast cancer risk; however, the breast cancer risk increased significantly with a daily folate intake of more than 400 µg/day (Zhang et al., 2014). There are also limited clinical trials that examine the association between folic acid supplementation and cervical cancer risks. In a 1982 study by Butterworth et al., 47 women who had mild or moderate CIN were administered supplements of folic acid or placebo daily for 3 months. (Butterworth et al., 1982). They discovered that the cervical cytology of women who received folic acid supplementation appeared to be better than the placebo group ($P<0.05$); and subsequently concluded that CIN severity was decreased with folate intake.

In human studies, controlled feeding trials were also undertaken to determine if folate supplementation and depletion affected DNA methylation patterns. In a prospective randomized trial, 20 patients with adenomas were randomized to receive either folate (5 mg/day) or placebo for 1 year after polypectomy. Folate supplementation significantly increased the serum, red blood cell and colonic mucosal folate concentrations ($p < 0.02$), as well as in the extent of genomic DNA methylation, after only 6 months of supplementation (Kim et al., 2001). Pufulete et al. showed that 400 µg/day of folic acid supplementation for 10 weeks in patients with colorectal adenomas led to an increase in DNA methylation in leukocytes (31%) and colonic mucosa (25%) (Pufulete et al., 2005). Similarly, supplementation of 600 µg/day for 2 years significantly increased tissue folate and global DNA methylation in 20 post-polypectomy patients (O'Reilly et al., 2016). In addition to dose and duration of folic acid

supplementation, the inconsistencies in findings could also be contributed to the type of methylation assays that were used and what they actually measure (Crary-Dooley et al., 2017).

Compared with global DNA methylation, gene-specific methylation analyses in response to folate status have demonstrated more consistent findings. Wallace et al. reported that the use of 1 mg/day of folic acid supplementation for 3 years increased the methylation of proto-oncogenes *ERα* and *SFRP1* promoter region, in adults who had previous cases of colorectal adenomas (Wallace et al., 2010). Similarly, folate levels were associated with hypermethylation of the tumour suppressor *RASSF1A* and *MTHFR* in lung cancer patients aged 35–70 years (Vineis et al., 2011). A genome-wide methylation analysis of primary breast tumours from 162 women measured 1413 autosomal CpG loci associated with 773 cancer-related genes (Christensen et al., 2010). This study found that higher folate intake was associated with higher levels of CpG loci methylation, especially in the *IL17RB* CpG locus, which is a gene that is commonly associated with the signalling cascade that promotes cancer cell survival, proliferation, and migration (Bastid et al., 2020).

In the context of folate status and HR-HPV induced cervical cancer, evidence suggests that the role of folate in DNA methylation may be important for HPV gene expression in host cells. The chromosome site sensitive to folate deficiency coincides with a HPV-16 integrating site in primary cervical carcinomas (Wilke et al., 1996). In 2004, a study was conducted on a cohort of 345 women who were at risk of CIN progression, to investigate the association between folate status and HR-HPV infection (Piyathilake et al., 2004). After 24 months, with the measurement of folate status and at least three consecutive visit HPV test results, it was found that women with a high folate status tended to show a negative result for the HR-HPV test (OR=2.50, 95% CI=1.18-5.30, P=0.02). Then in 2007, to find out whether circulating folate concentrations influenced the risk of CIN in high stage cytological abnormality (CIN \geq 2) among women with HR-HPV; another research was conducted on the same population (Piyathilake, 2007). The findings were that low red blood cell folate HPV-16 infected women (OR=9, 95%CI=3.3-24.8) were more likely to show a high CIN stage compared to non HPV-16 infected women who had high red blood cell folate (Piyathilake, 2007). In addition, another study also demonstrated that folate status was significantly lower in women with HR-HPV infection than those with no infection (P=0.03) (Flatley et al., 2009). Pathak et al.'s study of 100 human cervical biopsy samples consisting of normal, SIL, and cervical cancer also found that low folate status modulated the risk of HPV infection and cervical cancer (Pathak et al., 2014).

Folate deficiency has also been reported to have a negative effect on certain immune functions. In a study conducted using PHA-activated human T lymphocytes, folate depletion was found to reduce proliferation of T lymphocytes and CD8(+), whilst folate repletion of folate-deficient cells rapidly restored T lymphocyte CD8(+) proliferation (Courtemanche et al., 2004). Folate deficiency was also associated with reduced maturation of dendritic cells, lower secretion of IL-12, TNF- α , IL-6 and IL-1 β by dendritic-stimulated cells with LPS, and impaired differentiation of CD4+ T lymphocytes. The secretion of cytokines inducing the development of Th1 was also reduced (Wu et al., 2017). On the other hand, oral high-dose administration of folic acid (160 μ g/d to 10 mg/d) reduced the inflammatory response in mice with allergic dermatitis by suppressing T cell proliferation and the secretion of the proinflammatory and Th2 cytokines IL-4, IL-5, IL-9, IL-13, IL-17, IL-33; TNF α and TSLP in a dose-dependent manner (Makino et al., 2019). In a study conducted among 105 healthy postmenopausal women; amongst those with a diet low in folate (< 233 μ g/d), those who used folic acid-containing supplements had significantly greater NK cytotoxicity (P = 0.01) (Troen et al., 2006). However, those who consumed a folate-rich diet and used folic acid supplements > 400 μ g/d had reduced NK cytotoxicity compared with those with a low-folate diet and no supplements (P = 0.02). This conflicting result could be due to the presence of unmetabolized folic acid in 78% of plasma samples. In addition, an inverse relation was also found between the presence of unmetabolized folic acid in plasma and NK cytotoxicity which was stronger among women 60 years or older and more pronounced with increasing unmetabolized folic acid concentrations (P-trend = 0.002). However, the specific mechanism by which folate deficiency could impair the immune response is unclear.

To conclude, it is still unclear as to whether dietary folate or folic acid supplementation results in changes in healthy tissues that can predispose one to cancer. In conjunction to folate status, other factors such as age, gender, family history, ethnic group and lifestyle factors may provoke processes related to cancer risk, and could lead to inconsistencies in research findings especially in human studies. However, it is evident that folate can play a preventative role against cancer to a certain extent by inducing promoter methylation of proto-oncogenes; however, different tissues, genes and CpG sites are not equally susceptible to DNA methylation changes in response to folate intake. Thus, a more in-depth analysis on the underlying molecular and epigenetic mechanisms for this potential association, is very much warranted.

1.4.3 Methionine as methyl donor

Methionine is a component of dietary proteins and it breaks down in the small intestine generating free methionine that is absorbed and subsequently used for protein synthesis, and is also converted to SAM, a crucial methyl group donor for numerous reactions including DNA methylation and metabolic reaction (Chaturvedi et al., 2018). It is one of the eight essential amino acids that can be obtained from protein-rich sources such as meat, fish, eggs, soy, and dairy (Ravanel et al., 1998). As humans are unable to synthesise methionine, it must be obtained from diet (Finkelstein, 1990). Unlike other essential amino acids that must be consumed, methionine can be recycled via the re-methylation of homocysteine, in the presence of other methyl donors such as folate and choline/betaine as well as vitamin B₁₂ (Clare et al., 2019).

Though limited, evidence on dietary methionine status and its effect on DNA methylation metabolites and precursors have been reported with conflicting results (Mahmoud & Ali, 2019; Ghazi et al., 2020). This is supported in several animal studies, where there is a significant discordance between effects of dietary methionine intake on hepatic levels of methionine, SAM and SAH. In the study to evaluate the effects of increasing levels of dietary methionine intake on the metabolites and enzymes of methionine metabolism in rat liver, the researcher reported a lack of hepatic methionine induction and significant reduction in the SAM:SAH ratio, in response to methionine-rich diet intake for 7 days (Finkelstein & Martin, 1986). In contrast, a 20-fold increase in hepatic and plasma methionine as well as 80% increase in the SAM:SAH ratio were reported in rats fed a methionine-rich diet for 14 days (Regina et al., 1993); whilst, those fed for 10 days showed an 8-fold increase in hepatic SAM to SAH ratio (Rowling et al., 2002). The discrepancies in these findings indicate the complex nature of the effect of methionine, that could be due to variation in tissues as well as factors such as age or duration of exposure to methionine.

Compared to folate, there is limited evidence with regards to the effect of methionine availability on DNA hypermethylation/hypomethylation and cancer risk and progression; and again, results have been inconsistent. In the rat models to determine effects of methionine-supplemented diet, those given a high methionine diet did not report any changes to promoter methylation of *p53* (Amaral et al., 2011) and cystathionine beta-synthase (Uekawa et al., 2009). Whilst, in a prospective study by Vineis et al., the effect of methionine on the methylation patterns in candidates' genes were investigated in lung cancer patients and a set of controls. Methionine was associated exclusively with decreasing methylation levels of *p16^{INK4a}*, *RASSF1A*, and *MTHFR* in former smokers and *RASSF1A* and *GSTP1* in current smokers

(Vineis et al., 2011). The *RASSF1A* and *p16^{INK4a}* are well-known tumour suppressors that are frequently hypermethylated in several malignancies especially lung cancer. On the other hand, Bassett et al. and Fanidi et al. found no association between methionine intake and lung cancer risk (Bassett et al., 2012; Fanidi et al., 2018).

Similarly, epidemiological studies to determine the protective effects of dietary methionine intake against cancer were also found to be inconsistent (Zhou et al., 2013). In the American Cancer Society Cancer Prevention Study II Nutrition Cohort study, a total of 66 561 postmenopausal women were examined to determine the relationship between alcohol, dietary and total folate intake, multivitamin use, dietary methionine and breast cancer (Feigelson et al., 2003). They found no association between the risk of breast cancer and dietary folate, total folate, multivitamin use, or methionine intake. Supporting that finding, Tao et al. also did not report any significant association between methionine and the methylation status of TSG including *E-cadherin*, *p16^{INK4a}*, and *RAR β 2* in breast cancer (Tao et al., 2011). In contrast, a dose-response meta-analysis reported a significant inverse relationship between dietary methionine intake and breast cancer risk among post-menopausal women but not in pre-menopausal women (Wu et al., 2013). Furthermore, the risk was reduced by 4% for every 1 gram per day increment in dietary methionine intake. In their study, Vidal et al. reported that higher dietary methionine intake was associated with the risk of prostate cancer (OR=2.1, 95%CI=1.1-3.9), where the risk was most pronounced in men with a lower Gleason score (OR=2.75; 95%CI 1.32- 5.73) (Vidal et al., 2012). However, this association was only apparent in men who carried at least one *MTHFR* A1298C allele (OR=6.7, 95%CI=1.6-27.8), compared to *MTHFR* A1298A noncarrier men (OR=0.9, 95%CI=0.24-3.92, P-interaction=0.045). In addition to that, a meta-analysis of 8 prospective studies involving 431 029 participants and 6331 colorectal cancer cases observed a significant inverse association between dietary methionine intake and the risk of colorectal cancer with a longer follow-up time (RR=0.81, 95%CI=0.70-0.95), in Western studies (RR= 0.83, 95% CI=0.73-0.95) and in men (RR=0.75, 95% CI=0.57-0.99) (Zhou et al., 2013).

Being a precursor to SAM, methionine is a major driver of DNA methylation. Thus, fluctuations in methionine is expected to significantly alter the methylation status of DNA (Zhang, 2018). However, the lack of correlation between research findings could be due to the cyclic nature of the 1C metabolism, where excessive methionine might negatively impact DNA methylation by inhibiting homocysteine re-methylation to maintain a balance of the SAM to SAH ratio (Mahmoud & Ali, 2019). Additionally, the availability of other methyl donors could

also compensate for the absence of exogenous methionine by the re-methylation of homocysteine, where it should be considered as a confounding variable in research methodologies. Furthermore, as the effect of methionine appears to be tissue-specific, this further contributes towards inconsistencies in research findings. Finally, variations in age, gender and genetics could also be partly responsible for the conflicting findings, especially in human studies.

Interestingly, recent studies are currently exploring the effect of dietary methionine restriction as an enhancer to the effect of cancer chemotherapy regimen in metastatic cancer (Thivat et al., 2007; Durando et al., 2010), melanoma, and glioma (Thivat et al., 2007). Methionine restriction has been reported to be effective against carcinomas (Birnbaum et al., 1957), and has led to the inhibition of colonic tumour growth (Kominou et al., 2006) and prostatic intraepithelial neoplasia (Sinha et al., 2014), in preclinical studies using rat models. It is suggested that normal cells can synthesize sufficient methionine for growth requirements from homocysteine, 5-methyltetrahydrofolate and vitamin B₁₂ via the methionine cycle, thus they are relatively resistant to exogenous methionine restriction. However, many cancer-cell types require exogenous methionine for survival, and therefore methionine restriction is a promising avenue for treatment (Chaturvedi et al., 2018).

In contrast, the role of methionine in the immune system via its function as one carbon cycle is less studied. However, in a recent study by Roy et al., methionine has been identified as a key nutrient affecting epigenetic reprogramming in CD4⁺ T helper (Th) cells (Roy et al., 2020). It is reported that methionine is rapidly taken up by activated T cells and serves as the major substrate for biosynthesis of the universal methyl donor S-adenosyl-L-methionine (SAM), where dietary methionine is required to maintain intracellular SAM pools in T cells. Methionine restriction reduced histone H3K4 methylation (H3K4me₃) at the promoter regions of key genes involved in Th17 cell proliferation and cytokine production. In their mouse model of multiple sclerosis, dietary methionine restriction reduced the expansion of pathogenic Th17 cells *in vivo*, leading to reduced T cell-mediated neuroinflammation and disease onset. In another study, SAM has been suggested as an essential metabolite for inflammatory macrophages, where a high SAM:SAH ratio supports histone H3 lysine 36 trimethylation for IL-1 β production (Yu et al., 2019).

In short, the literature on the role of methionine as a methyl donor in cancer risk and progression is very limited, and the author of this study could not find any other studies

that relates its status to cervical cancer. Furthermore, current evidence cannot conclusively determine the direction of the association between dietary methionine and cancer risk, whereby studies to further understand the underlying molecular and epigenetic mechanisms for this potential association is very much needed.

1.4.4 Other micronutrients

In addition to folate and methionine, choline and betaine, a quaternary ammonium compound, is also involved in 1C metabolism where it serves as a methyl donor via the betaine pathway (Mahmoud & Ali, 2019; Ghazi et al., 2020). Though the human body can synthesise choline *de novo*, the quantity produced is not sufficient to meet the body's requirement (Ueland, 2011). The daily recommended intake of choline is 425 mg for women and 550 mg for men (Institute of Medicine Standing Committee on the Scientific Evaluation of Dietary Reference, 1998). Food sources that are rich in choline include fish, poultry, eggs, cruciferous vegetables, and dairy products. On the other hand, betaine can be obtained from dietary sources such as sugar beets or formed inside the body through irreversible oxidation of choline (Craig, 2004). Betaine, the direct methyl donor, contains three methyl groups and acts as a more efficient methyl donor than choline, which has only one methyl group. In the betaine pathway, the betaine-homocysteine S-methyltransferase (BHMT) enzyme mediates the transfer of the methyl group from betaine to remethylate homocysteine to methionine. Several observational studies in humans have reported an inverse correlation between choline/betaine intake or plasma levels with homocysteine levels (Melse-Boonstra et al., 2005; Chiuve et al., 2007; Lee et al., 2010). Furthermore, betaine supplementation has been shown to lower homocysteine levels in clinical trials; in 15 healthy subjects with 6 g/day of betaine for 3 weeks (Brouwer et al., 2000) and obese subjects with 6 g/day of betaine for 12 weeks (Schwab et al., 2002); though, doses given are much higher than the recommended daily intake.

Choline and betaine availability has been reported to influence global and gene-specific DNA methylation patterns (Zeisel, 2017), that are associated with the development of cancer (Stefanska et al., 2012). Maternal choline deficiency has significantly reduced methylation levels of the promoter region of genes regulating cell cycle (*CDKN3*) (Niculescu et al., 2006), calcium binding (*Calb1*) (Mehedint, et al., 2010b), and angiogenesis (*VEGF-C* and *ANGPT2*) (Mehedint, et al., 2010a); where the active transcription of these genes is associated with oncogenesis. In an animal study, choline-deficient rats reported an increased level of SAH, reduced hepatic DNMT activity and DNA methylation; as well as an increased incidence of developing liver cancer (da Costa et al., 1993; da Costa et al., 1995). Hypomethylation in the

promoter region of the oncogene *c-myc* was found in the hepatocellular carcinoma tissue of choline-deficient rats, whereas the promoters of several TSG (*p53*, *p16^{INK4a}*, *PtprO*, *Cdh1*, and *Cx26*) were hypermethylated (Shivapurkar & Poirier, 1983; Tsujiuchi et al., 1999; Tryndyak et al., 2011). In human studies, low intake of choline and/or betaine has been associated with the risk of developing breast (Du et al., 2017), colon (Lu et al., 2015), nasopharyngeal (Zeng et al., 2014), and liver (Zhou et al., 2017) cancer. However, the European Prospective Investigation into Cancer and Nutrition (EPIC) cohort study reported that, in participants with folate concentrations below the median of 11.3 nmol/l, a high betaine concentration was associated with the reduced risk of colorectal cancer (OR=0.71, 95%CI=0.50–1.00, *P*-trend = 0.02), which was not observed for those with a higher folate status (Nitter et al., 2014). This suggests that choline and betaine may compensate for the loss of the methyl group, due to folate deficiency. In a meta-analysis involving 11 epidemiological studies, a significant protective effect of dietary choline and betaine for cancer was observed against several types of cancer, where the pooled relative risks (RRs) of cancer were (RR=0.82, 95% CI=0.70-0.97) for choline consumption only, (RR=0.86, 95%CI=0.76-0.97) for betaine consumption only and (RR=0.60, 95%CI=0.40-0.90) for choline plus betaine consumption, respectively (Sun et al., 2016). They also found that an increment of 100 mg/day of choline plus betaine intake helped reduce cancer incidence by 11% (RR=0.89, 95% CI=0.87-0.92), through a dose-response analysis. In short, cumulative literature suggests a significant association of choline and betaine to methyl metabolism and DNA methylation and accordingly to gene regulation in carcinogenesis.

The B vitamins are water soluble vitamins. As humans are unable to synthesize B vitamins on their own, sufficient quantities need to be consumed from diet (Calderón-Ospina & Nava-Mesa, 2020). Meat, wholegrains, eggs, dairy products, legumes, nuts, dark leafy vegetables, as well as fruits such as citrus fruits, avocados, and bananas are rich sources of these vitamins (Institute of Medicine Standing Committee on the Scientific Evaluation of Dietary Reference, 1998). Though vitamins B₂, B₆, and B₁₂ are essential cofactors in 1C metabolism, there is very limited literature available with regards to its status, intake or supplementary effects on DNA methylation and gene expression in the development of cancer (Mahmoud & Ali, 2019; Ghazi et al., 2020). Most of the studies were conducted as secondary measures to the impact of other methyl donors such as folate or as a combined model of other micronutrients. Nonetheless, low levels of vitamins B₂, B₆, and B₁₂ in humans have been linked to cancers such as oesophageal cancer (Qiang et al., 2018), CIN (Piyathilake et al., 2014), colorectal cancer (Otani et al., 2005; Wei et al., 2005), and prostate cancer (Hultdin et al., 2005).

Amongst these three vitamins, B₁₂ or also known as cobalamin, is the most studied. In an animal study designed to examine the effect of folic acid in the absence and presence of vitamin B₁₂ deficiency on global methylation patterns, vitamin B₁₂ depletion was reported to induce global hypomethylation even when combined with a diet high in folate (Kulkarni et al., 2011), which highlights its essentiality as a cofactor in 1C metabolism and DNA methylation. Vitamin B₁₂ plays an important role in the re-methylation of homocysteine to methionine by acting as a cofactor for the 5-methyltetrahydrofolate-homocysteine methyltransferase (MTR) enzyme, where its deficiency has been associated with high levels of homocysteine (Ray et al., 2000; Robertson et al., 2005), suggesting that low vitamin B₁₂ levels could lead to DNA hypomethylation. Additionally, vitamin B₁₂ intake was found to be effective in reducing circulating levels of homocysteine (Gonin et al., 2003; Azadibakhsh et al., 2009) suggesting a reversible mechanism to this effect, that could potentially modify the risk of diseases. However, current literature shows inconsistencies in the association among vitamin B₁₂ intake, DNA methylation, and cancer. Vitamin B₁₂ is associated with a reduced risk of developing rectal (Gylling et al., 2014) carcinomas but an increased risk of prostate (Hultdin et al., 2005) and esophageal cancer (Qiang et al., 2018). In a study by Colacino et al., the methylation scores for several TSG in tumours from individuals with head and neck cancer were calculated and compared to dietary intake of vitamin B₁₂, where reduced TSG methylation was observed in individuals with a high intake of vitamin B₁₂ (Colacino et al., 2012). Squamous cell lung cancer (Piyathilake et al., 2000) and breast cancer (Johanning et al., 2002; Vineis et al., 2011) tissue also showed a localized deficiency of vitamin B₁₂, which may have resulted in the global DNA hypomethylation that was observed in these two studies. In women positive for human papilloma virus (HPV), high vitamin B₁₂ levels is shown to reduce the risk of CIN by maintaining a high degree of methylation on the HPV *E6* gene (Piyathilake et al., 2014). On the other hand, no association was observed between the intake of vitamin B₁₂ and the promoter methylation of *E-cadherin*, *p16^{INK4a}*, and *RARβ2* genes in breast tumour tissues (Tao et al., 2011). In short, though studies have reported the association between vitamin B intake and reduced cancer risk, findings are inconsistent as to whether this protective effect is associated with an induced hypo- or hypermethylation either globally or at the candidate gene level.

1.5 Summary

Numerous clinical, epidemiological and molecular studies have shown that persistent infection with high-risk HPV genotypes is an indispensable, but not sufficient prerequisite for the

development of cervical cancer. This suggests that the cervical carcinogenesis process triggered by HPV infection depends on other associated risk factors, that creates a conducive local microenvironment for malignant transformation. Dysregulation of both viral and host gene expression due to viral DNA integration into the cell's genome, as well as epigenetic modifications are crucial events in the carcinogenic process; where alterations in DNA methylation, an epigenetic mechanism crucial for regulating gene transcription has been demonstrated in cervical cancer and its precursors. Current literature suggests that methyl donors play an important role in regulating DNA expression and thereby influence cancer risk including cervical cancer. A low concentration of methyl donor nutrients can cause altered methylation status of DNA, which may be DNMT-mediated. Folate and other B vitamins deficiency may also affect nucleotide synthesis. The disruption in DNA methylation and nucleotide synthesis could affect the expression of genes, reduce DNA integrity and increase DNA damage. These changes are not only able to increase cancer risk, but also influence its progression. However, the effects and mechanisms of methyl donor nutrients in relation to cancer, including cervical cancer pathogenesis and progression are as yet unclear. The existence HR-HPV infection as a major risk factor for cervical cancer pathogenesis, and the following genomic changes caused by this infection, further complicates matters. Thus, this study aims to explore the role of key methyl donor nutrients in cervical cancer risk and progression via its function in DNA methylation.

1.6 Hypothesis and Objectives

1.6.1 Hypothesis

It is hypothesised that the absence of one or more donor nutrients will affect DNA methylation processes and gene expression associated with cervical cancer risk and progression.

1.6.2 Objectives

The main objective of the study is to determine the effect of methyl donor depletion on mechanisms associated with cancer risk and progression in cervical cancer cells *in vitro*. The specific objectives are:

- i. to identify cervical cancer-associated gene networks and pathways that are affected by both methyl donor nutrient depletion, and by chromosomal integration of HR-HPV in cervical cells using bioinformatics analysis.
- ii. to compare C4-II cervical cancer cell growth characteristics in complete, folate depleted, methionine depleted or combined folate-and-methionine depleted media.

- iii. to validate the C4-II cell model of methyl donor depletion by analysing intracellular folate concentration, intracellular methionine concentration, and homocysteine export.
- iv. to determine the effect of methyl donor nutrient depletion on the expression of IFN-stimulated genes using quantitative RT-PCR.
- v. to determine the effect of methyl donor nutrient depletion on cytokine production in differentiated macrophages, derived from the THP-1 cell line.
- vi. to investigate how the availability of folate and methionine impacts globally and specifically on DNA methylation in a C4-II cervical cancer cell model of methyl donor depletion.

CHAPTER 2

MATERIALS

2.1 Cell Lines

The C4-II cervical cancer cell line was used in this experiment. The cell line was obtained from HPA Culture Collections, United Kingdom. The C4-II cells were initially derived from a cervical carcinoma of a 41-year-old Caucasian female. It has been found that this cell line harbours human papillomavirus 18 (HPV-18) DNA sequences and is able to express HPV-18 RNA. C4-II is reported to be most identical to cervical cancer primary tissues in gene expression when compared to other cervical cancer cell lines, with global correlation to primary cervical cancer tissue of $R=0.52$, as compared to eight other cervical cancer cell lines (Carlson et al., 2007). The global correlation of transcriptional profiles provided a quantitative assessment on how well the cell lines model tissue, where a higher Pearson correlation coefficient denoted a better model of cervical tissue.

The THP-1 human leukemic monocyte cell line was also used in this experiment. The cell line was obtained from HPA Culture Collections, United Kingdom. The THP-1 cells were initially derived from a one-year-old male infant suffering from acute monocytic leukaemia (Tsuchiya et al., 1980).

2.2 Media

Dulbecco's Modified Eagle's Medium (DMEM) with GlutaMax I (GIBCO: Ref. No. 074-91212A) was used as the culture medium for C4-II cell lines. The medium was customized without methionine, folate and choline. The complete medium (F+M+) was supplemented with 30 mg/L of L-methionine, 4 mg/L of folic acid and 4 mg/L of choline chloride to ensure it contained sufficient nutrients for normal cell growth. 10% foetal bovine serum (FBS) and 1% penicillin/streptomycin antibiotics were also added to the media.

The methyl donor depleted medium was prepared by supplementing it with 4 mg/L of choline chloride, 10% FBS and 1% penicillin/streptomycin antibiotics (F-M-). As for the methionine depleted medium (F+M-) and folate depleted medium (F-M+) preparation, an additional supplementation of 4 mg/L of folic acid and 30 mg/L of L-methionine were added respectively. Additionally, 0.2 mg/L of folic acid and 1.5 mg/L of L-methionine were added to

the F-M- medium to prepare the 5% folate and methionine medium (F+M+5%). The Roswell Park Memorial Institute (RPMI) 1640 medium (Lonza: Cat. No. 12-115Q) was also used to maintain the THP-1 cell line culture.

2.3 Cell Culture

Automated cell counter (TC10) (Bio-Rad: USA)

Centrifuge, RT6000B refrigerated centrifuge (Sorvall: USA)

CO2 incubator (Sanyo: UK)

Counting slides, dual chamber for cell counter (Bio-Rad: Cat. No. 145-0011)

Dulbecco's phosphate buffered saline (DPBS) without Ca and Mg (Lonza: Cat. No. BE17-512F)

Haemocytometer (Hawksley: UK)

Microscope (Jenoptik: Germany)

Pipette, PIPETMAN Classic (Gilson: USA)

Serological pipettes (Fisherbrand, ThermoFisher Scientific)

Tissue culture flasks (Nunc, ThermoFisher Scientific)

Tissue culture plates (Falcon, ThermoFisher Scientific)

Trypan blue (SIGMA: CAS 72-57-1)

Trypsin-EDTA, 0.25% (GIBCO: Cat. No. 25200056)

Water bath, JB Nova (Grant: UK)

2.4 Depleted Media Preparation

Analytical weighing scale (Ohaus Pioneer: Switzerland)

Choline chloride (SIGMA: PCode 101640083)

Filter receiver and storage bottle, 500 ml polystyrene with PE cap (Scientific Laboratory Supplies: Ref. No. 4550500)

Foetal bovine serum (FBS) (Gold PPA: Cat. No. A15-151 or SeraLab: Code EU-000-S)

Folinic acid, folic acid calcium salt hydrate (SIGMA: CAS 1492-18-8)

Hydrochloric acid, 1M

HyPure cell culture grade water, endotoxin-free (HyClone: Cat. No. SH30529.03)

Indicator papers pH 6.4-8.0 narrow range (Whatman: Cat. No. 2600-103A)

Laboratory diaphragm pump, Capex 8C (Charles Austen Pump Ltd: UK)

L-Methionine (SIGMA: CAS 63-68-3)

Magnetic stirrer and hotplate (Medline Scientific Limited, UK)

Nalgene rapid-flow bottle top filter, 0.2µ PES membrane (500ml) (Thermo Scientific: Ref. No. 5954520)

Penicillin/ Streptomycin, 1% (GIBCO: Cat. No. 15140-122)

Sodium bicarbonate solution 7.5% (Gibco: Ref. No. 25080-060 25080-102)

2.5 Intracellular Folate Measurement

Centrifuge, MIKRO 22R (Hettich Zentrifugen: Germany)

Precellys lysing kit (Bertin technologies: Ref. No. KT03961-1-003.2)

Precellyse®24 lysis and homogenization machine (Bertin technologies: France)

Sonicator, UCD-200TM (Bioruptor Diagenode: Belgium)

2.6 Intracellular Methionine Measurement

Centrifuge, MIKRO 22R (Hettich Zentrifugen: Germany)

Precellys lysing kit (Bertin technologies: Ref. No. KT03961-1-003.2)

Precellyse®24 lysis and homogenization machine (Bertin technologies: France)

Sonicator, UCD-200TM (Bioruptor Diagenode: Belgium)

2.7 Homocysteine Measurement

Centrifuge, MIKRO 22R (Hettich Zentrifugen: Germany)

Homocysteine plasma control Bi-Level (CHROMSYSTEMS: Ref. No. 0071)

HPLC analysis of homocysteine kit (CHROMSYSTEMS: Order No. 45000)

HPLC system (Jasco: UK)

Precellys lysing kit (Bertin technologies: Ref. No. KT03961-1-003.2)

Precellyse®24 lysis and homogenization machine (Bertin technologies: France)

Sonicator, UCD-200TM (Bioruptor Diagenode: Belgium)

2.8 RNA Extraction

2-mercaptoethanol (Sigma Aldrich: Cat. No. M6250-10mL)

Centrifuge, MIKRO 22R (Hettich Zentrifugen: Germany)

Ethanol undenatured absolute (SERVA: Cat. No. 39556.01)

Microlance, BD microlance 3 (Becton Dickinson: Ref. No. 301300)

NanoDrop ND-1000 spectrophotometer (Thermo Fisher Scientific: USA)

Pipette, PIPETMAN Classic (Gilson: USA)

RNeasy Plus Mini Kit (Qiagen: Ref. No. 74134)
Syringe, 1 mL (Terumo)
TubeOne 10 µL graduated filter tip (Star Lab: Cat. No. S1111-370)
TubeOne 1000 µL XL graduated filter tip (Star Lab: Cat. No. S1122-1830)
TubeOne 200 µL graduated filter tip (Star Lab: Cat No. S1120-8810)
Vortex (IKA Genius 3: UK)
Water, sterile nuclease free (Fisher Scientific: Cat. No. BP2484-50)

2.9 cDNA Synthesis

0.2 mL PCR Tube, Domed Cap, Natural (StarLab: Cat. No. 11402-4300)
Microcentrifuge tubes, 0.5 mL (Scientific Laboratories Supplies : UK)
Mini Spin Centrifuge (Eppendorf: Germany)
Pipette, PIPETMAN Classic (Gilson: USA)
Precision DNase Kit (PrimerDesign: Cat. No. DNASE-50)
Precision nanoScript2 Reverse Transcription Kit (PrimerDesign: Cat. No. RT-nanoScript2)
Thermal cycler, Thermo Hybaid PCR Express (Thermo Scientific: USA)
TubeOne 10 µL graduated filter tip (Star Lab: Cat. No. S1111-370)
TubeOne 200 µL graduated filter tip (Star Lab: Cat No. S1120-8810)
Vortex (IKA Genius 3: UK)

2.10 Real-time quantitative PCR

Custom designed, pre-optimised RT-PCR Primer Mix (PrimerDesign: Cat. No SY-hu-600)
Human gene positive control (PrimerDesign: Cat. No. hu-Std)
MicroAmp fast 96-well reaction plate (Applied Biosystem: Cat. No. 4346907)
MicroAmp optical adhesive film (Applied Biosystem: Cat No. 4311971)
Microcentrifuge tubes, 0.5 mL (Scientific Laboratories Supplies : UK)
Mini PCR plater spinner, MPS 1000 (Labnet: US)
Mini spin centrifuge (Eppendorf: Germany)
Pipette, PIPETMAN Classic (Gilson: USA)
PrecisionPLUS 2X qPCR Mastermix (PrimerDesign: Cat. No. PPLUS-R-SY-12ML)
RNase/DNase free water (PrimerDesign: Cat. No. RNase/DNase free water)
StepOne Plus Real-Time PCR System (Applied Biosystem, US)
TubeOne 10 µL graduated filter tip (Star Lab: Cat. No. S1111-370)
TubeOne 1000 µL XL graduated filter tip (Star Lab: Cat. No. S1122-1830)

TubeOne 200 µL graduated filter tip (Star Lab: Cat No. S1120-8810)

Vortex (IKA Genius 3: UK)

2.11 Cytokine Production

Graduated cylinder, 100 mL & 500 mL

Centrifuge, MIKRO 22R (Hettich Zentrifugen: Germany)

Human IL-1 β Quantikine ELISA Kit (R & D System: Cat. No. DLB50)

Human TNF- α Quantikine ELISA Kit (R & D System: Cat. No. DTA00C)

LPS-EB ultrapure (InvivoGen: Cat. No. Tlr1-3pelps)

Plate reader, EnSight multimode plater reader (PerkinElmer: USA)

Phorbol 12-Myristate 13-Acetate (PMA) (Sigma: Cat. No. P8193)

Pipette, PIPETMAN Classic (Gilson: USA)

Quantikine Immunoassay Control Group 1 (R & D System: Cat. No. QC01-1)

TubeOne 1.5 mL natural flat cap microcentrifuge tubes (Star Lab: Cat. No. 51615-5500)

TubeOne 1000 µL XL graduated filter tip (Star Lab: S1122-1830)

TubeOne 200 µL tip (Star Lab: S1111-0700)

Vortex (IKA Genius 3, UK)

Vortex, Genie 2 Vortex Mixer (Scientific Industries : USA)

2.12 DNA Extraction

2-Propanol (SIGMA: Cat. No. 19516-25ML)

Centrifuge, Eppendorf 5810 R (Eppendorf: Germany)

Dulbecco's phosphate buffered saline (DPBS) without Ca and Mg (Lonza: Cat. No. BE17-512F)

Ethanol (SIGMA-ALDRICH: Cat. No. 51976-100ML)

NanoDrop ND-1000 spectrophotometer (Thermo Fisher Scientific: USA)

Nuclease free water, Ambion (Thermo Fisher Scientific: P/N AM9937)

Pipette, PIPETMAN Classic (Gilson: USA)

PureLink RNase A (Invitrogen: Ref. No. 12091-021)

Qiagen Blood and Cell Culture DNA Midi Kit (Qiagen: Cat. No. 13343)

Shaker

Tris-EDTA buffer solution (SIGMA-ALDRICH: Cat. No. 93283-100ML)

TubeOne 10 µL graduated filter tip (Star Lab: S1111-370)

TubeOne 1000 µL XL graduated filter tip (Star Lab: S1122-1830)

TubeOne 200 μ L tip (Star Lab: S1111-0700)

Vortex (IKA Genius 3: UK)

Water bath, Grant JB1 unstirred (Grant: UK)

2.13 Sodium Bisulphate Treatment

Centrifuge, MIKRO 22R (Hettich Zentrifugen: Germany)

Eppendorf, 0.2 mL (Scientific Laboratories Supplies: UK)

Eppendorf, 0.5 mL (Scientific Laboratories Supplies: UK)

Ethanol undenatured absolute (SERVA: Cat. No. 39556.01)

EZ DNA Methylation Kit (ZYMO RESEARCH: Cat. No. D5001 & D5002)

Nuclease free water, Ambion (Thermo Fisher Scientific: P/N AM9937)

Pipette, PIPETMAN Classic (Gilson: USA)

Thermal cycler, Thermo Hybaid PCR Express (Thermo Scientific: USA)

TubeOne 1.5 mL natural flat cap microcentrifuge tubes (Star Lab: Cat. No. 51615-5500)

TubeOne 10 μ L graduated filter tip (Star Lab: S1111-370)

TubeOne 1000 μ L XL graduated filter tip (Star Lab: S1122-1830)

TubeOne 200 μ L tip (Star Lab: S1111-0700)

Vortex (IKA Genius 3: UK)

Vortex, Genie 2 Vortex Mixer (Scientific Industries : USA)

Water, sterile nuclease free (Fisher Scientific: Cat. No. BP2484-50)

2.14 Methylation Array Profiling

2-Propanol (SIGMA: Cat. No. 19516-25ML)

96-well 0.8 mL Polypropylene Deepwell Storage Plate (Thermo Scientific: AB-0859)

96-well sealing mat (ThermoFisher Scientific: Cat. No. AB-0566)

Centrifuge, 3-16PK (SIGMA: Germany)

Centrifuge, ALC PK 120 (DJB Labcare: UK)

Centrifuge, Laborzentrifugen Model 1K15 microcentrifuge (SIGMA: Germany)

Ethanol undenatured absolute (SERVA: Cat. No. 39556.01)

Formamide (SIGMA-ALDRICH: Cat. No. 000000011814320001)

High Speed Microplate Shaker (Illumina: USA)

Hybridization Oven (Illumina: USA)

Infinium Hybridization Chambers and Gaskets (Illumina: USA)

Infinium Methylation EPIC BeadChip Kit, 16 samples (Illumina: Cat. No. WG-317-1001)

Infinium Multi-sample Alignment Mixture (Illumina: USA)
Infinium Staining Set (Illumina: USA) Manual Heat Sealer, ALPS 25 (Thermo Scientific: USA)
Microsample incubator, Hybex (SciGene: USA)
Pipette, PIPETMAN Classic (Gilson: USA)
Sodium hydroxide, 0.1N
Te-Flow flow-through chambers, with black frames, spacers, glass back plates and clamps
Thermal cycler, Q Cycler II single block (Quanta Biotech: Canada)
Tris-EDTA buffer solution (SIGMA-ALDRICH: Cat. No. 93283-100ML)
TubeOne 10 µL graduated filter tip (Star Lab: S1111-370)
TubeOne 1000 µL XL graduated filter tip (Star Lab: S1111-6700)
TubeOne 200 µL tip (Star Lab: S1111-0700)

2.15 Methylation Specific PCR Amplification

Custom SeqPrimers (Eurofins Genomics)
Eppendorf, 0.2 mL (Scientific Laboratories Supplies: UK)
Eppendorf, 0.5 mL (Scientific Laboratories Supplies: UK)
Pipette, PIPETMAN Classic (Gilson: USA)
Thermal cycler, Biometra Thermocycler T-Gradient ThermoBlock (Analytik Jena: Germany)
Tris-EDTA buffer solution (SIGMA-ALDRICH: Cat. No. 93283-100ML)
TubeOne 10 µL graduated filter tip (Star Lab: S1111-370)
TubeOne 1000 µL XL graduated filter tip (Star Lab: S1111-6700)
TubeOne 200 µL tip (Star Lab: S1111-0700)
Vortex (IKA Genius 3: UK)
ZymoTaq DNA Polymerase (ZYMO RESEARCH: Cat. No. E2002)

2.16 Gel Electrophoresis

Agarose, Ultra-Pure (Invitrogen: Ref. No. 16500-100)
Analytical weighing scale (Ohaus Pioneer: Switzerland)
Centrifuge, MIKRO 22R (Hettich Zentrifugen: Germany)
Ethidium bromide solution (Fluka: Cat. No. 46067)
Gel-Doc imager (BioRad: USA)
HyperLadder 100bp (Bioline: Cat. No. BIO-33056)
Laboratory Sealing Film Parafilm M
Measuring cylinder, 100 ml & 2000ml

Microwave, iGenix IG2008 (Igenix: UK)
Pipette, PIPETMAN Classic (Gilson: USA)
PowerPac basic (BioRad: USA)
Sub-Cell GT comb, 15 well, (BioRad: US)
TBE running buffer (Alfa Aesar: Cat. No. J62788)
TubeOne 10 μ L graduated filter tip (Star Lab: S1111-370)
TubeOne 200 μ L tip (Star Lab: S1111-0700)
Vortex (IKA Genius 3: UK)
Wide mini sub cell GT electrophoresis tank (BioRad: USA)

CHAPTER 3

EFFECT OF METHYL DONOR NUTRIENT DEPLETION ON RNA EXPRESSION: A BIOINFORMATICS ANALYSIS

3.1 Introduction

Human papillomavirus (HPV) infection is the main aetiological factor in the process of cervical carcinogenesis (Bosch et al., 2002; zur Hausen, 2009; Okunade, 2020), with viral sequences detected in more than 95% of cases (Cancer Genome Atlas Research Network, 2017). However, not all HPV infections suffered by women culminate in cervical cancer. Compared to low-risk strains of HPV, high-risk types HPV (HR-HPV) are more prone to activate cell proliferation in basal and differentiated layers, activating several pathways that promote epithelial transformation to become malignant.

HPV infection is a risk factor for malignancy of the uterine cervix as it has a pivotal role in carcinogenesis via the activation of its genomic products (Balasubramaniam et al., 2019). The initial targets of the virus are the basal cells that are vulnerable via microtraumas (Stubenrauch & Laimins, 1999). At the beginning of infection, the HPV virion proceeds into the host's cell by interacting with specific receptors such as alpha-6 integrin (Narisawa-Saito & Kiyono, 2007). Viral DNA replication starts in the basal layers, whilst maintaining a low copy number in the infected host basal cells. However, when the epithelial cells differentiate, the virus starts to replicate to a high copy number and expresses the L1 and L2 capsid proteins. This results in the production of new progeny virions that are released from the epithelial surface. For persistence, HPV needs to infect basal cells showing stem cell-like features that are still able to proliferate (Egawa et al., 2015). The expression of the early oncoproteins promotes replication and separation of recently synthesized DNA, therefore guaranteeing that infected stem cells stay in the lesion for an extended period of time. High-risk HPV types also have developed several mechanisms to avoid host immune response, which is important for viral persistence and progression to HPV-associated neoplastic diseases (Kanodia et al., 2007; Stanley et al., 2012).

Although the integration of viral DNA into the host's genome can lead to neoplastic alteration of infected cells, the existence of HPV DNA in the cell by itself is not enough to induce cancer (Narisawa-Saito & Kiyono, 2007). The overexpression of viral oncoproteins E6 and E7 are mainly responsible for the initial changes in epithelial cells (Balasubramaniam et

al., 2019). E6 prevents the activity of the host's tumour suppressor p53, whilst E7 inhibits retinoblastoma (pRb), which controls cell division by blocking the activity of transcription factors. Inactivation of these host proteins disrupts both the DNA repair mechanisms and apoptosis, leading to rapid cell proliferation. Multiple genes involved in DNA repair, cell proliferation, growth factor activities, angiogenesis and mitogenesis genes become highly expressed in cervical intraepithelial neoplasia (CIN) and in cancer. This genomic instability encourages HPV-infected cells to progress towards invasive carcinoma. HPV integration also drives the carcinogenic process through the inactivation of E2 expression, the main inhibitor of E6 and E7, and the disruption of host genes because of the viral sequence insertion (McBride & Warburton, 2017). Studies have suggested that epigenetic alterations associated with E6 and E7 activity are common events during the early steps of epithelial malignancy and have been described as potential biomarkers for cervical cancer (Clarke et al., 2012; Verlaat et al., 2017).

However, not all women who acquire HR-HPV infection developed cervical cancer. About 85 to 90% of HR-HPV infections spontaneously regress, with only 10 to 15% that continue to persist, and consequently promote the progression of precancerous cervical intraepithelial neoplasia to invasive cervical carcinoma, thus suggesting other conditions or cofactors that contribute towards cervical carcinogenesis (Łaniewski et al., 2020). Such conditions include the presence of conducive local microenvironment for cervical carcinogenesis, which have been reported to be essential for the control of persistent HPV infection and pathogenesis of cervical cancer (Egawa et al., 2015).

Studies have reported epigenetic modifications that also contribute towards the progression from pre-cancerous lesions to an invasive cancer. Alterations in DNA methylation, an epigenetic mechanism crucial for regulating gene transcription, have been demonstrated in cervical cancer and its precursors (Dueñas-González et al., 2005; Szalmas & Konya, 2009). Aberrant DNA methylation has been detected in numerous cancers, consisting of two main features; global DNA hypomethylation, with local DNA hypermethylation especially in the promoter region of tumour suppressor genes (Jones & Baylin, 2007; Kanwal & Gupta, 2012). In the intergenic regions and repetitive sequences of the human genome, CpG sites are sparse and mostly methylated. The hypomethylation of CpG sites in this area may result in genomic instability and loss of gene imprinting, which could eventually lead to the development of neoplastic cells (Kulis et al., 2013). On the other hand, gene promoters are rich in CpG sites that are sometimes densely packed forming what is known as CpG islands. These islands are mostly unmethylated in order to allow gene transcription. Aberrant hypermethylation of these

CpG sites may silence the expression of genes that are critical to cell homeostasis, DNA integrity, or genome stability, resulting in cancer development and progression (Bakshi et al., 2018). Several studies have shown that cervical cancer frequently displays global DNA hypomethylation, though compared to hypermethylation, the literature is quite limited (Kim et al., 1994; Fowler et al., 1998; Shuangshoti et al., 2007). Besides that, a cross-sectional study conducted among 308 women having normal cervix with different degrees of CIN severity found that global DNA hypomethylation is higher in women with invasive cervical cancer than all other groups ($P < 0.05$), whilst *CDHI*, *DAPK*, and *HIC1* tumour suppressor genes showed a significantly higher frequency of promoter methylation with progressively more severe cervical neoplasia ($P < 0.05$) (Flatley et al., 2009).

Hypermethylation of genes that are essential in maintaining cellular processes have been reported in cervical carcinoma, and may occur independently of HPV infection status (Szalmas & Konya, 2009; Wentzensen et al., 2009). Evidently, DNA hypermethylation that occurs in cancer cells seems to target tumour suppressor genes explicitly, silencing these genes which results in growth selection and uncontrolled cell proliferation. Examples include the hypermethylation of *FHIT*, a gene involved in cell cycle regulation and apoptosis (Ki et al., 2008); *DAPK*, a gene involved in apoptosis (Yang et al., 2010); *RAR β 2*, a gene involved in the signalling pathway for cell growth suppression (Jha et al., 2010); *APC*, a tumour suppressor protein involved in the Wnt/ β catenin pathway (Dong et al., 2001); *p73*, a gene involved in cell cycle regulation and apoptosis (Liu et al., 2004) and *MGMT*, a DNA repair protein that protects human genome against mutation (Kim et al., 2010). Additionally, hypermethylation of *CCNA1*, a gene associated with the regulation of cell cycle, has been reported in HSIL (36.6%) and invasive cancer (93.3%) (Kitkumthorn et al., 2006; Yang et al., 2010). A decline in *CADMI* gene expression has been reported in high grade CIN and squamous cell carcinoma, where a severity of cervical dysplasia is correlated with a higher number of methylated genes (Overmeer et al., 2008), whilst hypermethylation of the E-Cadherin promoter has been reported in 89% of invasive cancer, 26% in CIN III and none in normal tissues (Shivapurkar et al., 2007). In a bioinformatic study conducted using available gene expression profile and methylation profile in GEO database, it was reported that in cervical cancer samples, hypomethylated and highly expressed genes were significantly enriched in cell cycle and autophagy. On the other hand, hypermethylated and lowly expressed genes were found in estrogen receptor pathway and Wnt/ β -catenin signalling pathway, where *ESR1*, *EPB41L3*, *EDNRB*, *ID4* and *PLAC8* were the hub genes (Ma et al., 2020).

Numerous studies have indicated DNA methylation adaptability to environmental factors including diet and nutritional elements (Sapienza & Issa, 2016; Mahmoud & Ali, 2019). DNA methylation involves the addition of methyl groups by S-adenosylmethionine (SAM) to cytosine residues; a biological process that depends on the availability of methyl groups and accordingly the function of methyl donors and acceptors (Ducker & Rabinowitz, 2017; Mahmoud & Ali, 2019). The production of SAM, which is generated from methionine, partly depends on the availability of methyl-donor nutrients from diet. In addition to methionine, other methyl donor nutrients include folate and vitamin B₁₂, which participate in the generation of methionine via the methionine-synthase pathway, and choline and betaine, which are substrates in the betaine:homocysteine methyltransferase pathway.

Methyl donor nutrients availability has been shown to modify DNA methylation either globally or at specific CpG sites by inducing the formation of methyl donors, acting as coenzymes, or modifying DNMT enzymatic activity (Mahmoud & Ali, 2019; Ghazi et al., 2020). In a study conducted by our department previously, combined folate and methionine depletion of C4-II cervical cancer cells has led to a significant downregulation of DNMT3a and DNMT3b, which was associated with an 18% reduction in global DNA methylation compared with controls (Poomipark et al., 2016). Low folate status was also associated with HR-HPV infection ($P=0.031$) and with a diagnosis of CIN or invasive cervical cancer ($P<0.05$) (Flatley et al., 2009). In another long-term prospective follow up study, higher folate status has been reported to provide a protective effect against the natural history of HR-HPV (Piyathilake et al., 2004). Several other studies have also associated folate intake with lower risk of colorectal and prostate cancer (Giovannucci et al., 1993; Su & Arab, 2001; Giovannucci, 2002; Stevens et al., 2006); and folate supplementation has been found to modify the DNA methylation status to provide a protective effect against diseases including cancer (Keyes et al., 2007; Wallace et al., 2010; Cartron et al., 2012). However, there are studies that reported conflicting results (Song et al., 2000; Kotsopoulos et al., 2008; Qin et al., 2013; Gylling et al., 2014), indicating that the mechanisms associated with folate effect on DNA methylation are more complex than previously thought and confounded by other dietary, genetic, or tissue-related factors.

In addition to folate, methionine that serves as a precursor of SAM is an integral part of DNA methylation (Mahmoud & Ali, 2019). However, there are limited and inconsistencies in the evidence on dietary methionine status and its effect on DNA methylation, especially in human studies. This could be due to the cyclical nature of the SAM-SAH cycle, where excessive methionine might inhibit the re-methylation of homocysteine, thus disrupting the one-carbon

cycle and negatively impacting DNA methylation (Regina et al., 1993). Furthermore, there are inconsistencies in the epidemiological findings on the protective effect of dietary methionine against cancer (Zhou et al., 2013), where a high intake of methionine has been associated with increased risk of cancer (Vidal et al., 2012), with dietary methionine restriction currently being studied as an enhancer for chemotherapy treatment in metastatic cancer (Thivat et al., 2007; Durando et al., 2010). On the other hand, a meta-analysis to determine the association of vitamin B₆, vitamin B₁₂ and methionine with breast cancer risk found that methionine intake might be inversely associated with breast cancer risk, especially among post-menopausal women. They reported that the combined relative risk of breast cancer for the highest versus lowest category of dietary methionine intake was (RR=0.94, 95%CI=0.89-0.99, P=0.03). They also reported a linear dose-response relationship, where the risk of breast cancer decreased by 4% (P=0.05) for every 1 g per day increment in dietary methionine intake (Wu et al., 2013). Based on these findings, much more information is needed in order to determine the direction of the association between dietary methionine and cancer risk. Hence, exploring the underlying molecular and epigenetic mechanisms involving this nutrient might improve our understanding on this issue.

In summary, the effects and mechanisms of methyl donor nutrients in relation to cancer (including cervical cancer) pathogenesis and progression are as yet unclear. The existence of HR-HPV infection as a major risk factor for cervical cancer pathogenesis, and the following genomic changes caused by this infection, further complicates matters. Therefore, an extensive analysis of gene expression that combines both factors; methyl donor availability and HPV integration, might provide a better understanding of the aetiology of cervical cancer development and progression. The results of this study's of the bioinformatics analysis on genome-wide gene expression are focused on differential expression and functional classes of genes that were significantly more expressed within the total gene set present on the microarray. This approach permits projections to biological processes in the cells. It has been indicated that network and pathway analysis of gene expression is associated with observed phenotypes, which suggests that gene expression analysis can be a proxy for cellular processes.

3.2 Hypothesis and aims

Both methyl donor availability and HR-HPV infection may modulate cervical cancer growth and progression. Although broad knowledge about the mechanisms by which HR-HPV types initiate transformation of epithelial cells exists, the inter-connected mechanisms of multiple

factors, such as methyl donor availability and genomic changes caused by HR-HPV integration, to promote malignant transformation is still not entirely understood. This observation leads to the hypothesis that both phenotypes of cervical cancer cells and a panel of genes involved in fundamental cellular pathways and epigenetic alterations are potentially influenced by methyl donor status and chromosomal integration of HPV; that can be identified by *in silico* approaches.

In order to test this hypothesis, the aim of this study is to identify cervical cancer-associated gene networks and pathways that are affected by both methyl donor nutrient depletion, and chromosomal integration of HR-HPV in cervical cells using bioinformatics analysis.

3.3 Methods

3.3.1 Microarray dataset

In order to identify potential gene network and pathways that are affected by both methyl donor depletion and the integration of HR-HPV into cervical cells, two microarray datasets have been selected, each representing a condition being investigated; the effect of folate and methionine depletion on C4-II cervical cancer cell line (Poomipark, 2013) and the effect of HPV-16 integration into W12 cervical keratinocytes (Pett et al., 2006). Both datasets involve genome-wide microarray analysis in cervical cells using GeneChip HG-U133 Plus 2.0 Arrays (Affymetrix, UK).

a. Effect of folate and methionine depletion on C4-II cervical cancer cells

The microarray raw data was obtained from previous work in the department (Poomipark, 2013), where a genome-wide microarray project was performed using the cervical cancer C4-II cell line. The C4-II cells were derived from human cervical tumour and obtained from HPA Culture Collections, United Kingdom. The C4-II cells were grown in Waymouth MB standard medium (M+F+) (containing 900 nM folic acid and 300 µM methionine) or folate and methionine depleted medium (M-F-) (estimated to contain < 30 nM folic acid and ~20 µM methionine) for eight days, in triplicate for each condition. The medium was supplemented with 10% foetal bovine serum (FBS), 200 nM L-glutamine and 1% penicillin/streptomycin antibiotics. The C4-II RNA from all six samples were extracted using the RNeasy mini kit from Qiagen, where its purity and integrity were determined using the Agilent 2100 Bioanalyzer and Agilent RNA 6000 Nano Kit. The RNA from each sample was prepared using the GeneChip®

3' IVT Express Kit protocol, followed by genome-wide microarray analysis performed using GeneChip HG-U133 Plus 2.0 Arrays (Affymetrix, UK). The array was scanned to define the probe signals and stored as a CEL image file using the GeneChip® Scanner 3000. The M+F+ and M-F- samples probe array images were merged for probe intensities and normalised by GeneChip® Command Console® Software (Affymetrix, UK).

b. HR-HPV integration and episomal loss effect on cervical keratinocytes

A search for a second dataset was conducted to identify a study in which microarrays indicate alterations in the proliferative phenotype of cervical cancer. Gene expression databases maintain and provide data of gene expression profiles that are nowadays regularly released in a usable format (Sullivan et al., 2010). This has facilitated genomic queries and analysis for researchers and systematic exploration of experimental results of genes expressed in a variety of experiments (Barrett et al., 2013).

The search was conducted on PubMed at the NCBI database (<http://www.ncbi.nlm.nih.gov/pubmed/>) for studies involving HPV integration into cervical cells (published until 12/2015) with publicly available microarray data. At this point of time, the only microarray study that fulfilled the selection criteria was the study conducted by Pett et. al, that measured the changes in gene expression during the episomal and integrated stage of HPV-16 into W12 cervical keratinocyte cells (Pett et al., 2006). The transcription profile of the study (GSE4289) was downloaded from the National Centre for Biotechnology Information Gene Expression Omnibus (GEO) database. This dataset is composed of genome-wide microarray analysis on the W12 cervical keratinocyte cell line containing the high-risk human papillomavirus 16 (HPV-16), using the Affymetrix Human Genome U133 Array. The W12 cells were derived from a low-grade squamous intraepithelial lesion (LG-SIL), which resulted from an *in vivo* infection with HPV-16. This W12 accurately models cervical neoplastic progression during long-term culture, with a spontaneous transition from cells containing only episomal HPV-16 to a population containing only integrated HPV-16. Total RNA from the W12 samples representing the three different stages of HPV-16 cervical infection progression, each in duplicate, namely:

- i. episomal: low-grade cervical intraepithelial neoplasia, in the form of pure episomal HPV-16 at an early stage;
- ii. mixed: high-grade cervical intraepithelial neoplasia, in which cells have mixed episomal and integrated HPV-16 genome and;

- iii. integrated: invasive cancer with cervical keratinocytes containing pure integrated HPV-16 after long-term cultivation.

were used to generate biotin-label cRNA for microarray analysis using the GeneChip HG-U133 Plus 2.0 Arrays (Affymetrix, UK). Two biological replicates were performed for each sample.

3.3.2 Differentially expressed genes analysis

A comparison between expression of genes in M+F+ conditions and M-F- conditions in the methyl donor depletion dataset was made using the Qlucore Software version 3.1 and was considered differentially expressed if $P < 0.05$ with a fold change of more than 1.5. In the second microarray dataset, the time-dependent and HPV-16 episome loss changes in gene expression were compared in the three above-mentioned states and differentially expressed genes were also determined using the Qlucore Software version 3.1 and were considered differentially expressed if $P < 0.05$ with a fold change of more than 1.5. An adjustment for multiple testing was performed using False Discovery Rate (FDR). The db2db software from bioDBnet (<https://biodbnet-abcc.ncifcrf.gov/db/db2db.php>) was used to convert identifiers from Affymetrix ID to Gene Symbol for the GSE4289 dataset.

The differentially expressed genes (DEGs) from both datasets were imported into a Microsoft Excel spreadsheet for data cleaning prior to performing the bioinformatics analysis, where probes without an official gene name were removed. Three sets of DEGs lists were generated; upregulated genes, downregulated genes and a combination of both genes from both datasets. A list of common genes between the two microarray datasets was identified using Venny 2.1 (<http://bioinfogp.cnb.csic.es/tools/venny/>).

3.3.3 Functional and pathway enrichment analysis

In order to identify functions and pathways affected by either methyl donor depletion, chromosomal integration of HPV or both conditions, the lists of DEGs were uploaded to the DAVID Bioinformatics Resource 6.8 software (<http://david.abcc.ncifcrf.gov/>). DAVID bioinformatics resources are aimed at extracting biological meaning systematically from large gene or protein lists with the help of an integrated biological knowledge base and analytic tools (Huang et al., 2007). DAVID functional annotation clustering tools are able to group the list of genes into subsets that are characterized by common expression patterns or co-expression over a set of experimental conditions, to determine expression patterns in the dataset. This approach

is known as clustering and assumes that genes with similar expression patterns are assigned to the same cluster according to the principle of homogeneity. Gene Ontology (GO) terms are applied to describe biological processes (GO_BP), molecular function (GO_MF) and subcellular location (GO_CC) of genes. The GO consortium defines and utilizes a standard vocabulary to ascribe functional categories to genes, such as the biological processes and pathways that are influenced according to the conditions of the given set of genes. This analysis yields various gene lists that are significantly overrepresented in the analysed groups of genes and are broadly classified into several catalogues with respect to the GO annotation (Ashburner et al., 2000; Huang et al., 2007; Gene Ontology, 2015).

Clusters were ordered according to all cluster members' global participation in the enriched function related to the complete gene list. A higher score for each cluster denotes that the cluster members are implicated in more significant or enriched functions. Thus, each cluster containing enriched functions was assigned an enrichment score representing its relative functional importance. A modified Fisher's exact test was used to calculate P-values to demonstrate the probability that a gene was annotated to a GO term randomly and was normally used as the reference for assigning a certain function to a module. An adjustment for multiple testing was performed using False Discovery Rate (FDR). FDR is calculated by an algorithm and reflects the expected proportion of false positives in the list of declared significant clusters. The functional enrichment analysis for the screened DEGs was performed by DAVID, where $FDR < 0.05$ was chosen as the cut-off point.

The DAVID functional annotation clustering tool was used to group the DEGs into subsets characterized by their functional biological process (GO_BP) (Ashburner et al., 2000; Huang et al., 2007; Gene Ontology, 2015). A maximum of 3000 genes were uploaded (the maximum number of genes allowed to be uploaded into the system); and high to medium classification stringency settings were applied to determine the clusters. Clusters with a P-value of less than 0.05, a False Detection Rate (FDR) < 0.05 and an enrichment score of 1.3 or more were selected for further discussion, based on the protocol set by Huang et al. (Huang et al., 2009). A higher enrichment score for a group indicates that the gene members in the group are involved in more important (enriched) terms in a given study; and as the enrichment score of 1.3 is equivalent to the non-log scale of 0.05, groups with a score of 1.3 or more should be given more consideration.

3.3.4 Network analysis and visualization

The Cytoscape program (version 3.4.0) was the main platform used to visualize gene interaction networks and biological pathways (Shannon et al., 2003). Firstly, ClueGo, a cytoscape plug-in (<http://www.ici.upmc.fr/cluego/cluegoDownload.shtml>) was used to facilitate the biological interpretation and to visualize functionally grouped terms in the form of networks and charts. This software allows the integration of several databases such as GO term and KEGG pathways to generate a functionally organized GO/pathway term network, where each term in the network was connected based on kappa statistics (Bindea et al., 2009). The Cohen's kappa coefficient measures inter-rater agreement for categorical items. In ClueGo, the kappa score is used to define term-term interrelations (edges) and functional groups, based on shared genes between the terms. The networks generated by ClueGo could also be visualized at different levels of specificity by selecting the various restriction criteria provided in the software. The lists of DEGs were uploaded to the ClueGo plug-in via Cytoscape with the following settings;

- i. Pathway with P-value < 0.05
- ii. Benjamini-Hochberg correction method for multiple testing
- iii. GO term grouping (functional grouping) based on kappa score
- iv. GO term fusion option – a fusion of GO parent-child term based on similar associated genes in order to highlight the more representative term and prevent redundancy
- v. GO tree interval – min:3 and max:8

Secondly, the lists of common DEGs between the methyl donor depletion dataset and the chromosomal integration of HPV dataset were uploaded into GeneMania via the Cytoscape platform to compute gene interaction networks (Warde-Farley et al., 2010). The MCODE v1.2 (Molecular Complex Detection) plugin for Cytoscape was used for identifying sub-networks of co-expressed genes. This method can detect densely connected nodes as a sub-network/cluster and is based on periphery and density edges of sub-networks (Bader & Hogue, 2003). The density values were set at 0.

3.4 Results

3.4.1 Effect of folate and methionine depletion on C4-II gene expression

In the microarray analysis to compare gene expression between C4-II cervical cancer cells grown in a combined folate and methionine depleted medium (F-M-) and complete medium (F+M+), 54 675 probes were detected. During data cleaning, 551 probes were removed as they did not have official gene names, and a total of 6127 probes were identified to be significantly

different, with a P-value of less than 0.05 and a fold change of 1.5 or more. The number of up- and down-regulated probes was 3970 and 2157 respectively. Functional clustering analysis was performed using the DAVID software to identify overrepresented biological processes (GO_BP). A total of 41 clusters from upregulated DEGs and 15 clusters from the downregulated DEGs were identified ($P < 0.05$, Benjamini-Hochberg < 0.05 , enrichment score > 1.3) (**Appendix 1 and 2**). Each significant cluster was given a name to represent their main biological function and selected clusters that might be associated with the hallmarks of cancer are presented in **Table 3.1**. The majority of the upregulated annotation clusters are associated with cell death, host defence and immune function. The biological processes associated with the cell cycle were significantly enriched for the downregulated annotation clusters.

In order to facilitate the biological interpretation of the differences in gene expression between methyl-depleted (F-M-) and complete (F+M+) conditions, the DEGs were also uploaded to the ClueGo plug-in via the Cytoscape platform in order to visualize the functionally grouped terms in the form of networks. Two databases, the GO_BP term and KEGG pathways were selected during the ClueGo analysis. **Figure 3.1** and **Figure 3.2** represent the GO term network of biological processes that are enriched due to folate and methionine depletion. Similar to the findings in DAVID, biological processes associated with immune responses and cell death were significantly enriched. However, the ClueGo analysis also detected terms related to cell cycle as being upregulated. The ClueGo analysis of the downregulated DEGs revealed that several biological processes associated with the cell cycle were highly enriched. In addition, ClueGo also identified several other significant GO_BP terms associated with host defence, DNA damage, DNA repair and cell signalling that were downregulated due to folate and methionine depletion.

The lists of all DEGs (combined up- and down-regulated genes) were used to identify KEGG pathways networks that were enriched in folate and methionine depleted conditions (**Figure 3.3**). It appears that genes that are affected by methyl donor depletion are involved in several pathways associated with the development of cancer or hallmarks of cancer, such as pathways in cancer, viral carcinogenesis, p53 signalling, cell cycle, cellular senescence and apoptosis.

Table 3. 1 Selected GO_BP annotation clusters from both upregulated and downregulated DEGs of methyl donor depleted cells, associated with the hallmarks of cancer

Annotation Cluster	Overrepresented Biological Process	Enrichment Score
	<i>Upregulated</i>	
8	cell death	10.75
9	response to biotic stimulus	10.73
11	response to type 1 interferon	10.15
12	viral process	9.36
15	regulation of cell signalling	8.37
16	positive regulation of cell death	8.34
18	innate immune response	7.87
19	positive regulation of cell signalling	6.22
20	regulation of viral process	6.21
21	negative regulation of cell signalling	6.02
22	negative regulation of cell death	5.56
23	regulation of kinase activity	5.06
24	viral genome replication	5.04
26	immune system development	4.68
28	stress-activated MAPK kinase	4.22
30	endopeptidase activity	3.88
31	cellular response to biotic stimulus	3.77
33	regulation of cell motility/migration	3.71
38	T cell cytokine production	3.20
39	immune response activation and signalling	3.15
40	MAPK cascade	3.06
	<i>Downregulated</i>	
1	mitotic cell cycle	31.96
2	mitotic nuclear division	29.02
3	chromosome segregation	26.33
4	negative regulation of mitotic cell cycle	7.76
5	regulation of mitosis process	7.45
6	meiotic cell cycle	7.08
11	chromosome localization	4.8

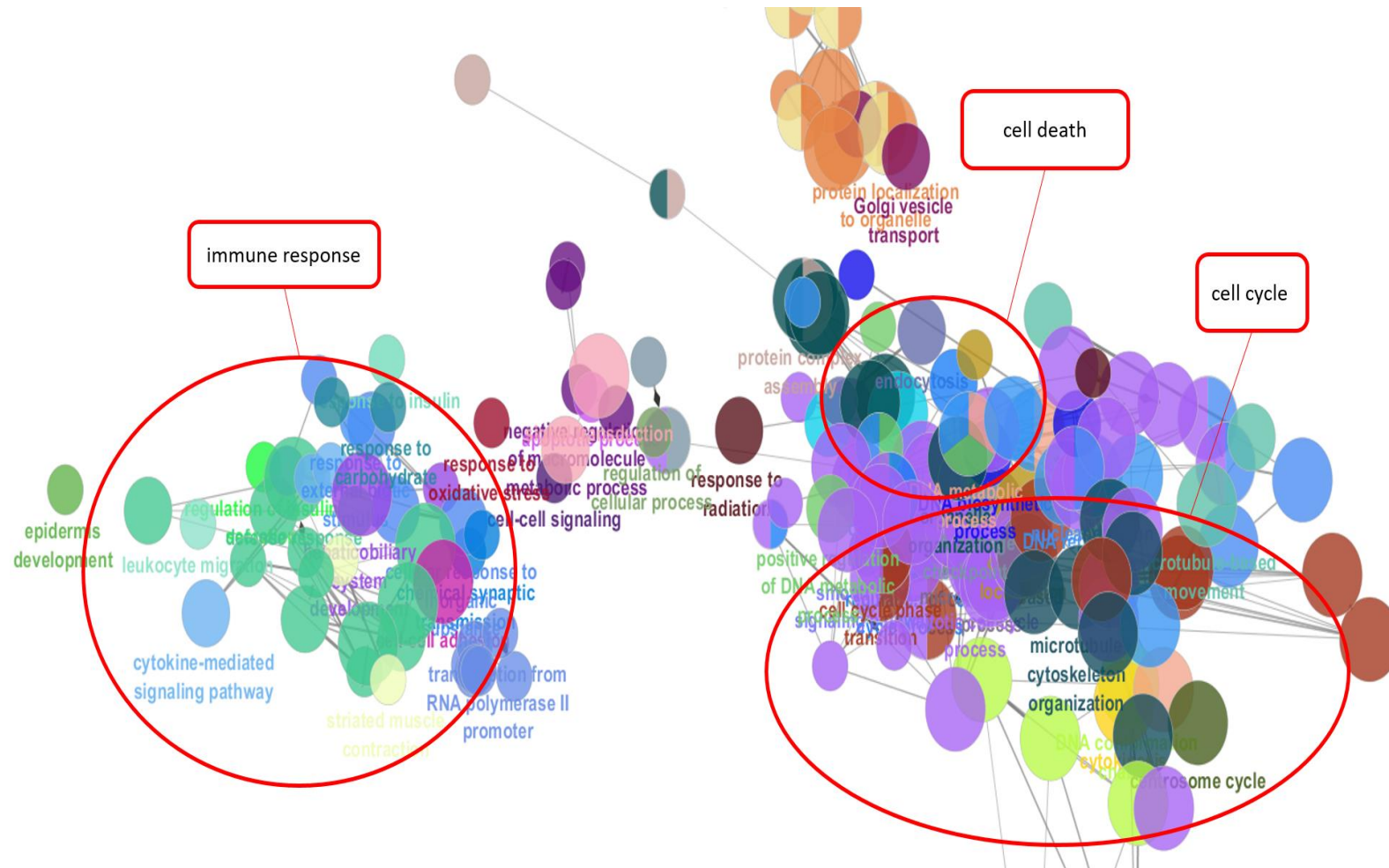


Figure 3.1 GO_BP terms network associated with upregulated DEGs in methyl donor depleted C4-II cervical cancer cell line

This figure represents a network of biological processes (GO_BP terms) that is enriched due to folate and methionine depletion. Each node represents a specific biological process (GO_BP terms) that is enriched in this analysis. Node size reflects the significance level of the enriched terms; bigger nodes indicate higher levels of significance. The node colour indicates a specific GO term, and similar coloured nodes indicate that these GO terms are from the same GO parent-child terms. Kappa score was used to link (edges) the enriched terms (nodes), where it defined term-term interrelations (edges) and functional groups, based on shared genes between the terms.

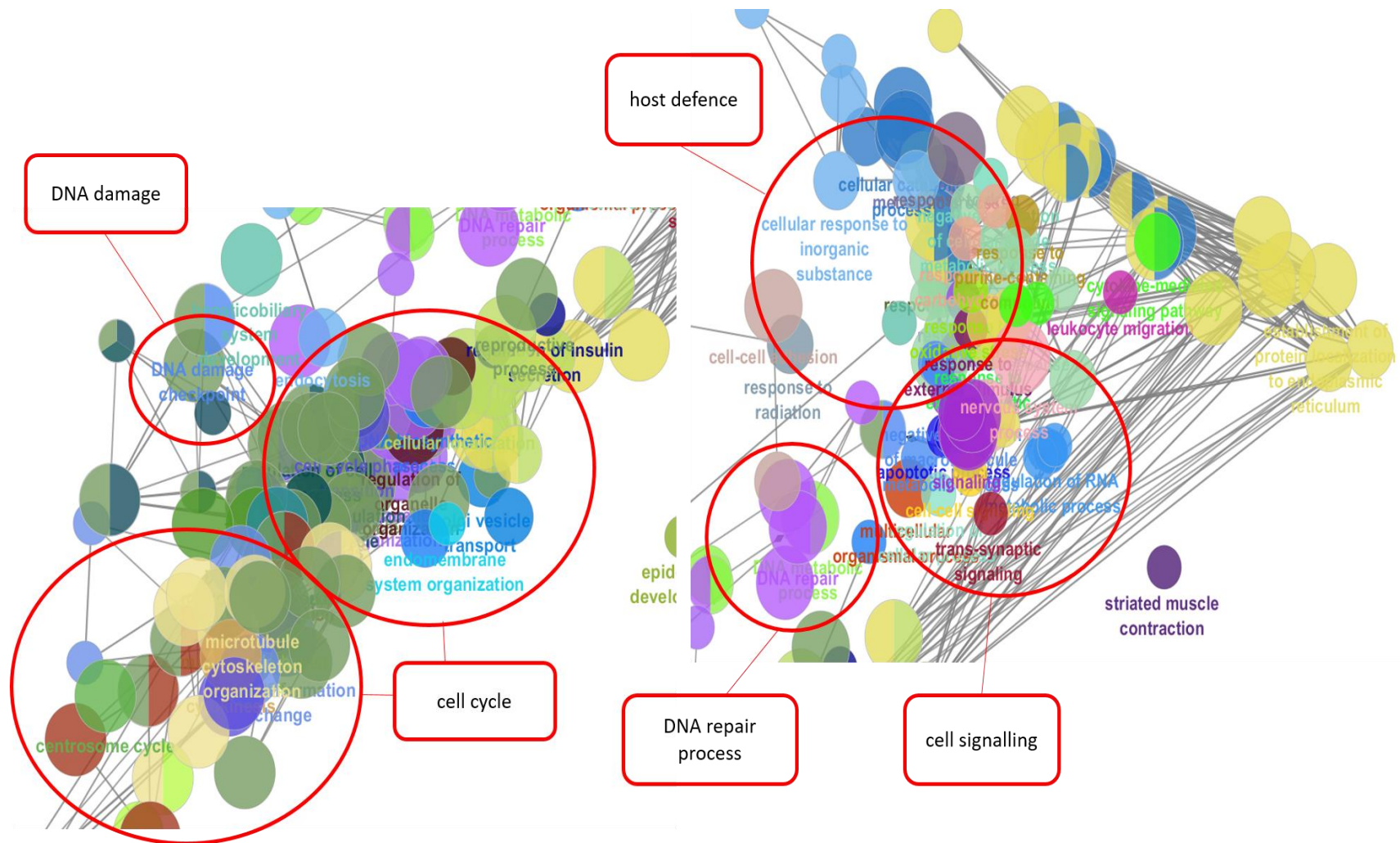


Figure 3.2 GO_BP terms network associated with downregulated DEGs in methyl donor depleted C4-II cervical cancer cell line

This figure represents a network of biological processes (GO_BP terms) that is enriched due to folate and methionine depletion. Each node represents a specific biological process (GO_BP terms) that is enriched in this analysis. Node size reflects the significance level of the enriched terms; bigger nodes indicate higher levels of significance. The node colour indicates a specific GO term, and similar coloured nodes indicate that these GO terms are from the same GO parent-child terms. Kappa score was used to link (edges) the enriched terms (nodes) where it defined term-term interrelations (edges) and functional groups, based on shared genes between the terms.

3.4.2 Effect of HR-HPV integration in W12 cervical keratinocytes on gene expression

From the 54 675 probes detected in the microarray, 3559 probes were identified to have a significant difference in gene expression between pure episomal to the mixed episomal-integrated stage (Epi-stage) with a fold change of 1.5 or more ($P < 0.05$). Also 3555 probes significantly changed gene expression from the mixed episomal-integrated stage to the fully integrated stage (Int-stage) ($P < 0.05$). A total of 2121 upregulated and 1438 downregulated DEGs at the Epi-stage were submitted into the ClueGo software to identify functional biological processes (GO_BP) that were affected during the initial integration of HPV into the W12 cervical keratinocytes (**Figure 3.4 and Figure 3.5**).

This analysis revealed several GO terms that might be associated with the hallmarks of cancer such as cell proliferation and differentiation, angiogenesis, cell signalling, immune response and viral life cycle, that were significantly enriched from the upregulated Epi-stage gene set. A similar analysis with the downregulated Epi-stage gene set has identified GO_BP terms related to immune response and response to stress that were significantly enriched. A ClueGo analysis was also conducted using the Int-stage gene set. None of the GO terms for the biological process appear to be significant for the upregulated group of genes. However, several terms associated with cell signalling and immune response were significantly enriched from the downregulated group of genes (**Figure 3.6**).

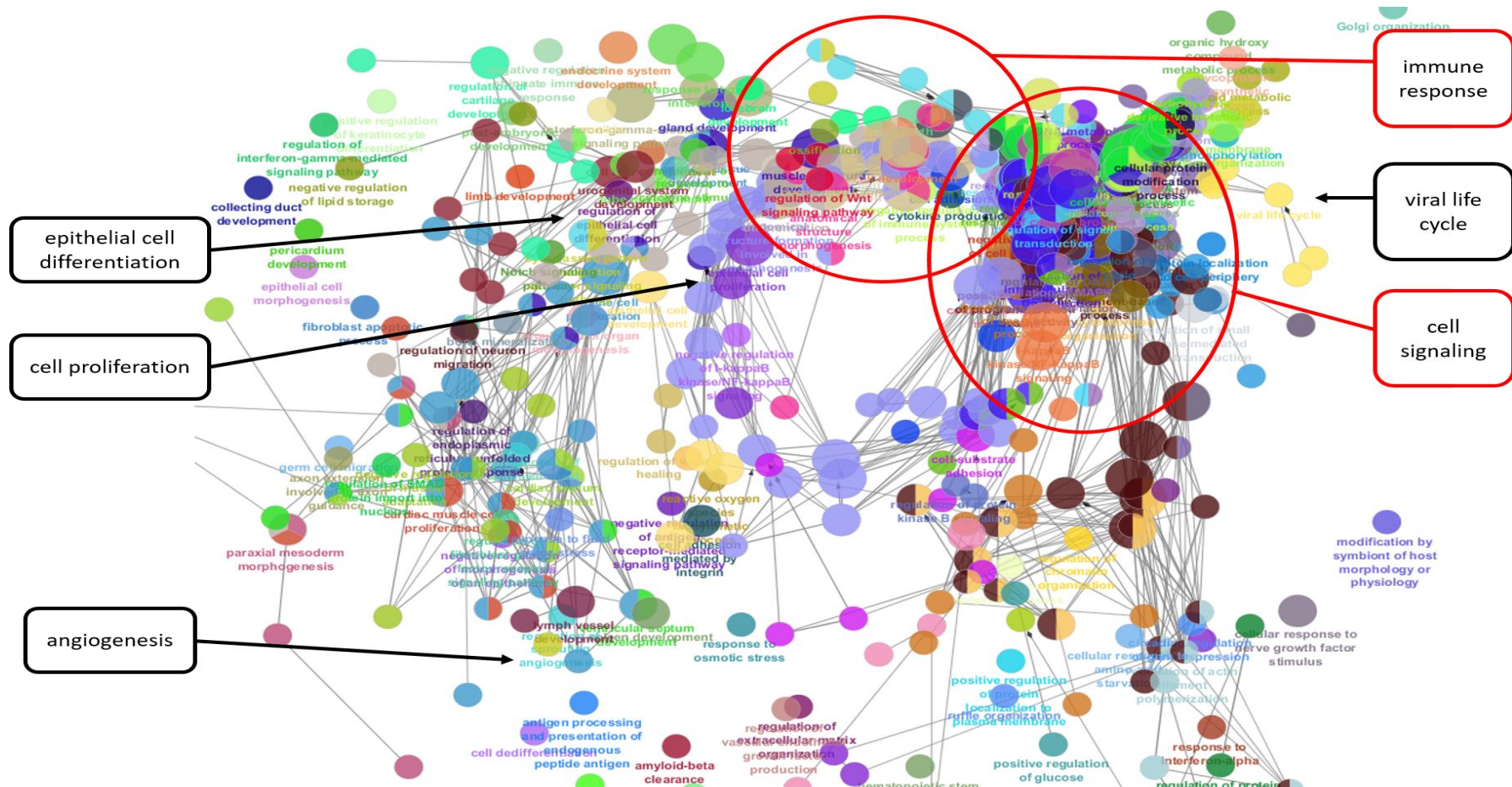


Figure 3.4 GO_BP terms network associated with upregulated DEGs during the Epi-stage of HPV integration into W12 cervical keratinocytes cells

This figure represents a network of biological processes (GO_BP terms) that is enriched at the beginning stage of HPV integration (episomal) into W12 cells. Each node represents a specific biological process (GO_BP terms) that is enriched in this analysis. Node size reflects the significance level of the enriched terms; bigger nodes indicate higher levels of significance. The node colour indicates a specific GO term, and similar coloured nodes indicate that these GO terms are from the same GO parent-child terms. Kappa score was used to link (edges) the enriched terms (nodes) where it defined term-term interrelations (edges) and functional groups, based on shared genes between the terms.

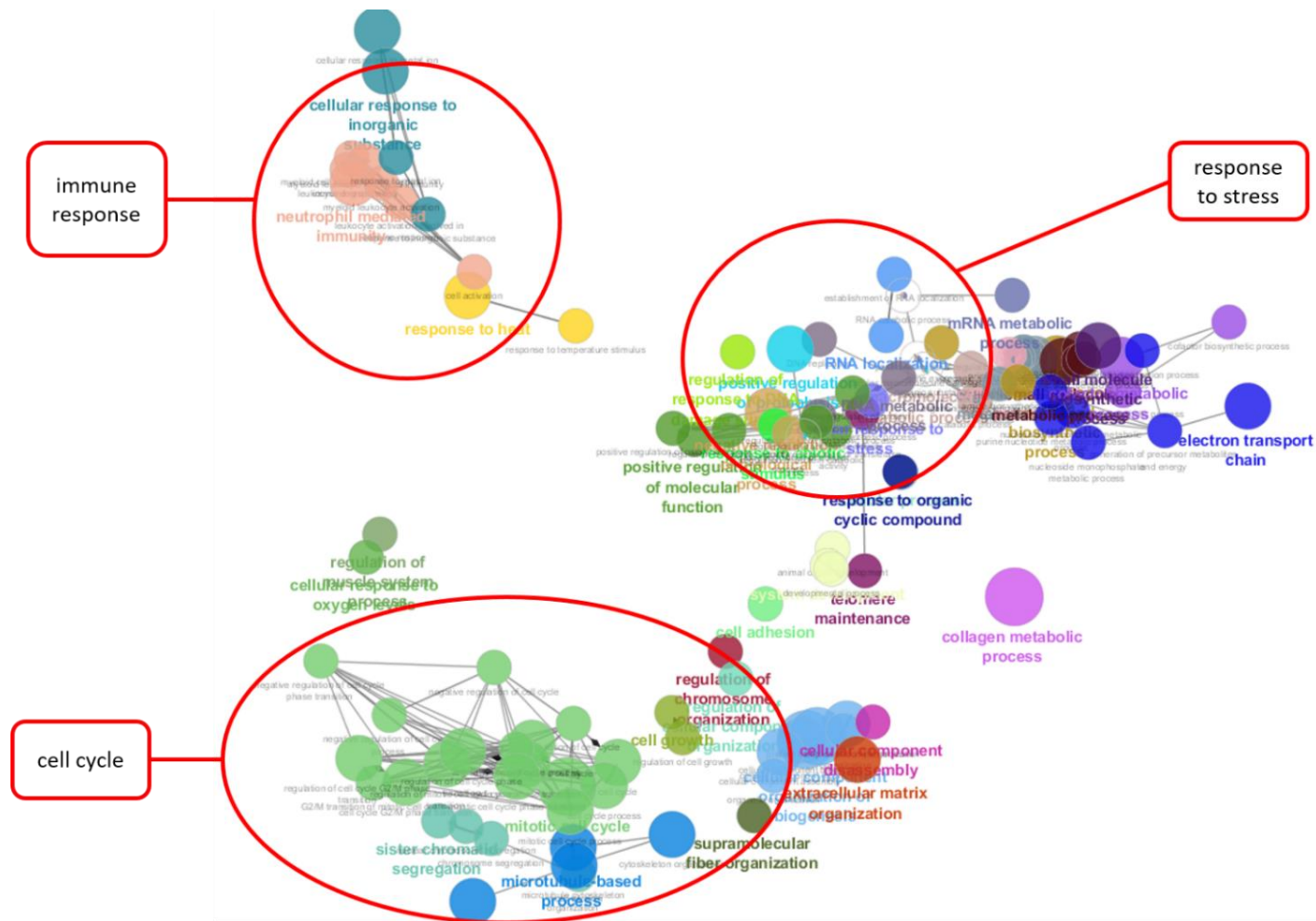


Figure 3. 5 GO_BP terms network associated with downregulated DEGs during the Epi-stage of HPV integration into W12 cervical keratinocytes cells

This figure represents a network of biological processes (GO_BP terms) that is enriched at the beginning stage of HPV integration (episomal) into W12 cells. Each node represents a specific biological process (GO_BP terms) that is enriched in this analysis. Node size reflects the significance level of the enriched terms; bigger nodes indicate higher levels of significance. The node colour indicates a specific GO term, and similar coloured nodes indicate that these GO terms are from the same GO parent-child terms. Kappa score was used to link (edges) the enriched terms (nodes) where it defined term-term interrelations (edges) and functional groups, based on shared genes between the terms.

3.4.3 Effect of methyl donor nutrient depletion and chromosomal integration of HR-HPV in cervical cells gene expression

The lists of DEGs from both datasets were uploaded into the Venny 2.0 software to identify genes that are mutually affected by the absence of folate and methionine; and also by the chromosomal integration of HPV into the cervical cell. Venny identified 635 genes that were commonly affected by methyl donor depletion and the beginning of HPV integration (Epi-stage). A total of 557 genes were also affected by both the methyl donor depletion and the late stage of HPV integration (Int-stage) (**Figure 3.7**).

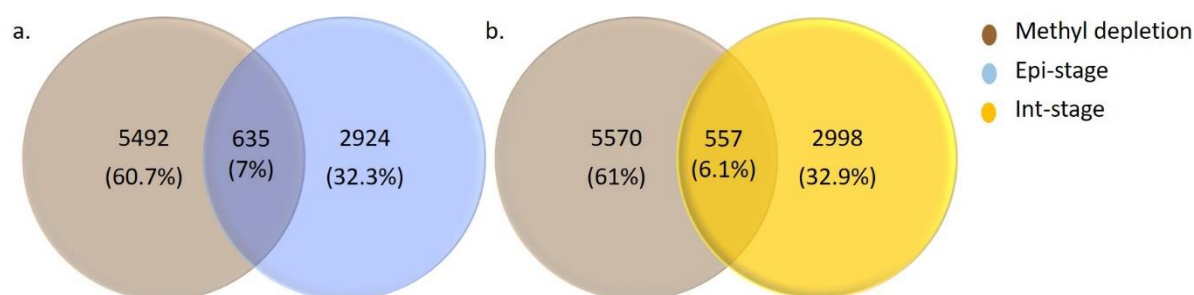


Figure 3.7 Venn diagram of common DEGs between methyl donor depletion and chromosomal integration of HPV dataset

Figure (a) shows common DEGs between methyl donor depletion and Epi-stage of HPV integration; (b) shows common DEGs between methyl donor depletion and Int-stage of HPV integration.

The lists of mutually affected genes were further clustered according to their biological functions using the DAVID software. A total of 226 clusters were identified from the methyl donor depletion and Epi-stage of HPV integration common DEGs (**Appendix 3**). Of these, eleven clusters were found to be significant ($P < 0.05$) with $FDR < 0.05$ (**Table 3.2**). Interestingly, of these eleven clusters, six are associated with cellular host defence mechanisms, indicating that genes involved in host defence mechanisms are also affected by the absence of methyl donors. The analysis also identified three significantly enriched clusters associated with the cell cycle; one cluster involving regulation of cell signalling and two clusters related to response to oxygen. In addition, several clusters associated with cancer hallmarks such as cell cycle, apoptosis, angiogenesis and motility were found to be considered highly enriched (enrichment score > 1.3) (Huang et al., 2009), though these findings were not statistically significant ($P > 0.05$).

Table 3.2 Significant clusters annotated from common genes between methyl donor depletion and Epi-stage of HPV integration

Annotation Cluster	Overrepresented Biological Process	Gene Count	P-value	FDR
1	Enrichment Score: 9.02			
	interspecies interaction between organisms	66	6.6e-10	6.2e-7
	symbiosis, encompassing mutualism through parasitism	66	6.6e-10	6.2e-7
	viral process	64	1.2e-9	9.7e-7
2	multi-organism cellular process	64	1.6e-9	1.1e-6
	Enrichment Score: 8.09			
3	organelle fission	47	5.8e-9	2.7e-6
	nuclear division	45	6.9e-9	3.0e-6
	mitotic nuclear division	37	1.3e-8	4.4e-6
4	Enrichment Score: 8.09			
	response to biotic stimulus	58	7.8e-9	3.1e-6
	response to external biotic stimulus	56	8.4e-9	2.9e-6
5	response to other organism	56	8.4e-9	2.9e-6
	Enrichment Score: 7.84			
	response to type I interferon	16	5.7e-9	2.9e-6
6	cellular response to type I interferon	15	2.3e-8	7.2e-6
	type I interferon signalling pathway	15	2.3e-8	7.2e-6
7	Enrichment Score: 6.82			
	interferon-gamma-mediated signalling pathway	16	8.2e-9	3.1e-6
	response to interferon-gamma	20	2.2e-7	6.3e-5
8	cellular response to interferon-gamma	17	1.9e-6	4.1e-4
	Enrichment Score: 6.03			
	response to cytokine	51	2.9e-7	7.8e-5
9	cytokine-mediated signalling pathway	40	3.1e-7	8.1e-5
	cellular response to cytokine stimulus	43	8.7e-6	1.5e-3
10	Enrichment Score: 5.09			
	chromosome segregation	27	2.5e-6	1.1e-3
	sister chromatids segregation	21	8.8e-6	1.5e-3
11	nuclear chromosome segregation	24	1.1e-5	1.8e-3
	Enrichment Score: 4.47			
12	regulation of cell communication	125	1.8e-5	2.7e-3
	regulation of signal transduction	114	3.4e-5	4.5e-3
	regulation of signalling	124	6.1e-5	7.4e-3
13	Enrichment Score: 4.21			
	regulation of viral process	22	2.7e-5	3.8e-3
	regulation of symbiosis, encompassing mutualism through parasitism	23	3.1e-5	4.2e-3
14	regulation of multi-organism cellular process	25	2.8e-4	2.6e-2
	Enrichment Score: 3.47			
15	cellular response to oxygen level	15	1.1e-4	1.2e-2
	cellular response to hypoxia	13	4.6e-4	3.4e-2
	cellular response to decreased oxygen levels	13	7.4e-4	4.8e-2
16	Enrichment Score: 3.20			
	response to oxygen level	22	3.5e-4	2.8e-2
	response to hypoxia	20	7.1e-4	4.7e-2
	response to decreased oxygen levels	20	1.0e-3	5.9e-2

The functional annotation clustering of the common DEGs between methyl donor depletion and invasive stage of HPV integration (Int-stage) identified 224 clusters (**Appendix**

4), with eight clusters that are statistically significant ($P < 0.05$; $FDR < 0.05$) (**Table 3.3**). Of these, five clusters were associated with host defence mechanisms together with single clusters involving regulation of cell signalling, cellular metabolism and catabolic processes. Several other clusters that might be associated with cancer processes were also identified, such as relating to cell cycle, proliferation and differentiation; apoptosis, angiogenesis and motility. Although these clusters are not significant, they were still highly enriched in the analysis (enrichment score > 1.3).

Table 3.3 Significant clusters annotated from common genes between methyl donor depletion and Int-stage of HPV integration

Annotation Cluster	Overrepresented Biological Process	Gene Count	P-value	FDR
1	Enrichment Score: 10.8			
	response to external biotic stimulus	57	8.1e-12	1.1e-8
	response to other organism	57	8.1e-12	1.1e-8
2	response to biotic stimulus	57	6.1e-11	5.6e-8
	Enrichment Score: 10.78			
	response to type 1 interferon	18	5.9e-12	1.1e-8
3	cellular response to type 1 interferon	7	2.8e-11	3.1e-8
	type 1 interferon signalling pathway	7	2.8e-11	3.1e-8
	Enrichment Score: 9.38			
4	viral process	59	3.5e-10	2.1e-7
	interspecies interaction between organisms	60	4.3e-10	2.4e-7
	symbiosis, encompassing mutualism through parasitism	60	4.3e-10	2.4e-7
	multi-organism cellular process	59	4.6e-10	2.3e-7
5	Enrichment Score: 6.04			
	negative regulation of cellular metabolic process	94	2.1e-6	4.3e-4
	negative regulation of metabolic process	96	1.4e-5	2.1e-3
6	negative regulation of macromolecule metabolic process	89	2.7e-5	3.5e-3
	Enrichment Score: 4.88			
	regulation of viral process	21	9.3e-6	4.3e-3
7	regulation of symbiosis, encompassing mutualism through parasitism	22	9.6e-6	2.1e-3
	regulation of multi-organism cellular process	25	2.6e-5	3.5e-3
	Enrichment Score: 4.80			
8	catabolic process	83	3.5e-6	6.7e-4
	cellular catabolic process	68	1.9e-5	2.7e-3
	organic substance catabolic process	72	2.3e-4	1.9e-2
9	Enrichment Score: 3.79			
	immune system development	40	8.2e-5	6.7e-3
	hemopoiesis	36	2.0e-4	2.7e-2
10	hematopoietic or lymphoid organ development	37	2.6e-4	1.9e-2
	Enrichment Score: 3.5			
	regulation of signal transduction	96	2.8e-4	2.1e-2
11	regulation of cell communication	104	3.1e-4	2.3e-2
	regulation of signalling	105	3.7e-4	2.6e-2

ClueGo analysis was also conducted on the common DEGs between methyl donor depletion and chromosomal integration of HPV. Totals of 635 and 557 common DEGs were submitted to the ClueGo software to visualize the functionally grouped terms in the form of networks that are affected during the episomal (Epi-stage) and invasive (Int-stage) stages of HPV integration, respectively. This analysis revealed several functional groups of terms significantly enriched at the episomal stage of HPV integration that might be associated with the hallmarks of cancer such as cell cycle, cell death, viral cycle, host defence, immune response and wound healing (**Figure 3.8**). Similarly, several terms related to host defence and immune response were significantly enriched during the invasive stage (Int-stage) of HPV integration (**Figure 3.9**). In addition, biological processes associated with cell differentiation and the response to stress were also enriched. A close-up view of the network, depicting the Int-stage functional processes affected by both methyl donor depletion and chromosomal integration of HPV, shows in more detail the commonly affected biological mechanisms associated with host defence (**Figure 3.10**).

ClueGo analysis using the KEGG database was conducted to identify pathways that are affected by both methyl donor depletion and chromosomal integration of HPV into cervical cells (**Figure 3.11** and **Figure 3.12**). It appears that the depletion of methyl donors affects several pathways associated with cell cycle, cell cycle checkpoints, senescence, interferon signalling and interleukin signalling at the episomal stage (Epi-stage) of HPV integration. The interferon and interleukin signalling pathways, as well as pathways in antiviral mechanisms were significantly enriched in the methyl donor depleted condition at the invasive stage (Int-stage) of HPV integration.

In addition to identifying overrepresented biological processes and pathways, the interactions of genes with significant change in expression were investigated by submitting the common DEGs between the two datasets into the visualization Cytoscape tool using the GeneMania database. This created a massive gene interaction network composed of 532 nodes and 14 788 edges (for the methyl depletion and Epi-stage gene set) and 468 nodes and 11 882 edges (for the methyl depletion and Int-stage gene set). In order to identify functional modules of genes and their interaction from this enormous network, the MCODE plug-in was used to detect densely connected nodes (where groups of genes that are densely connected to each other are most probably involved in similar biological functions or pathways), to create sub-networks/clusters that might be of interest. Each cluster was given a score and the sub-networks with the highest score are presented in **Figure 3.13**.

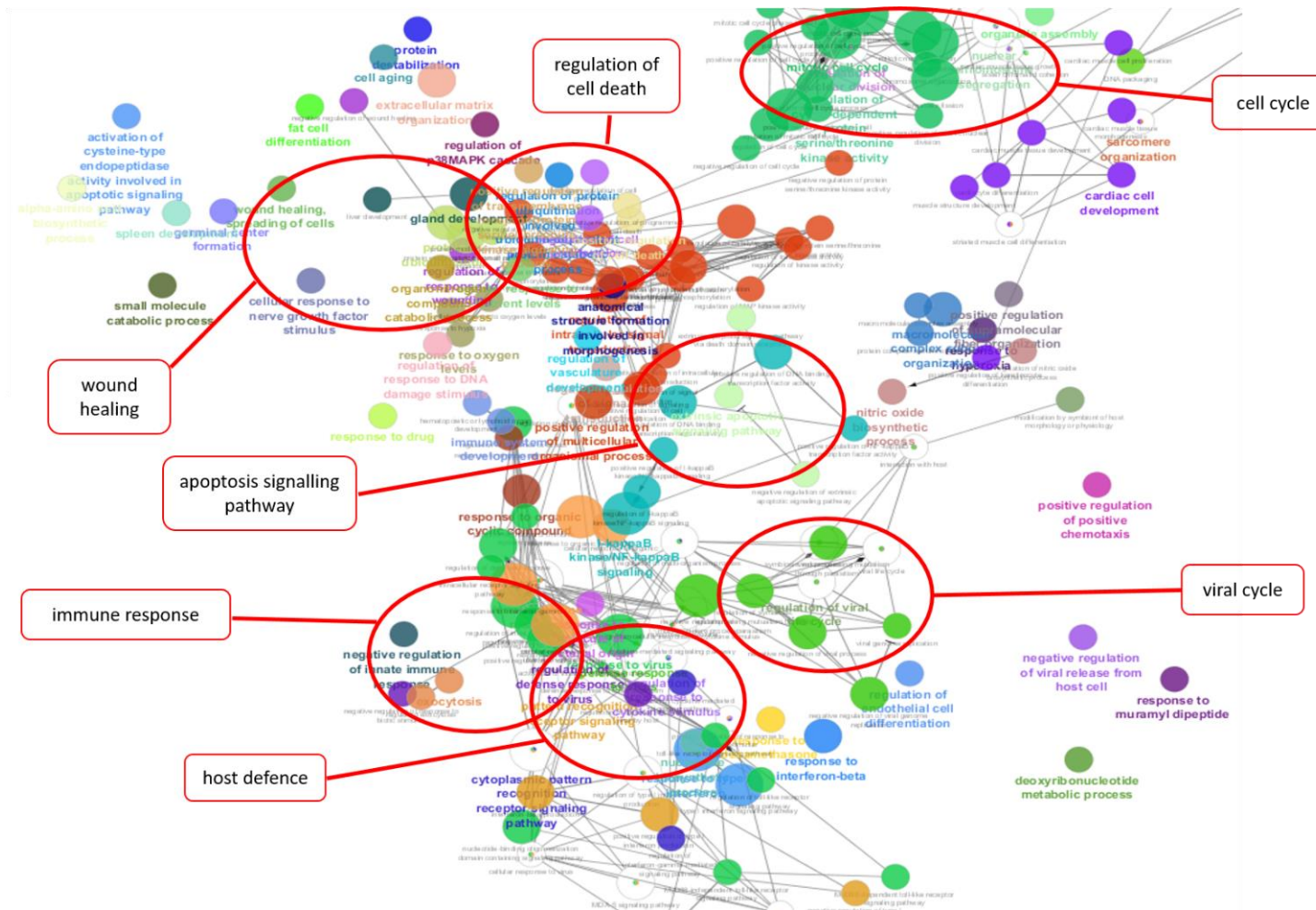


Figure 3.8 Network of biological processes affected by both methyl donor depletion and chromosomal integration of HPV at the Epi-stage

This figure represents a network of biological processes (GO_BP terms) that is enriched by both methyl donor depletion and the beginning stage (episomal) of HPV integration. Each node represents a specific biological process (GO_BP terms) that is enriched in this analysis. Node size reflects the significance level of the enriched terms; bigger nodes indicate higher levels of significance. The node colour indicates a specific GO term, and similar coloured nodes indicate that these GO terms are from the same GO parent-child terms. Kappa score was used to link (edges) the enriched terms (nodes) where it defined term-term interrelations (edges) and functional groups, based on shared genes between the terms.

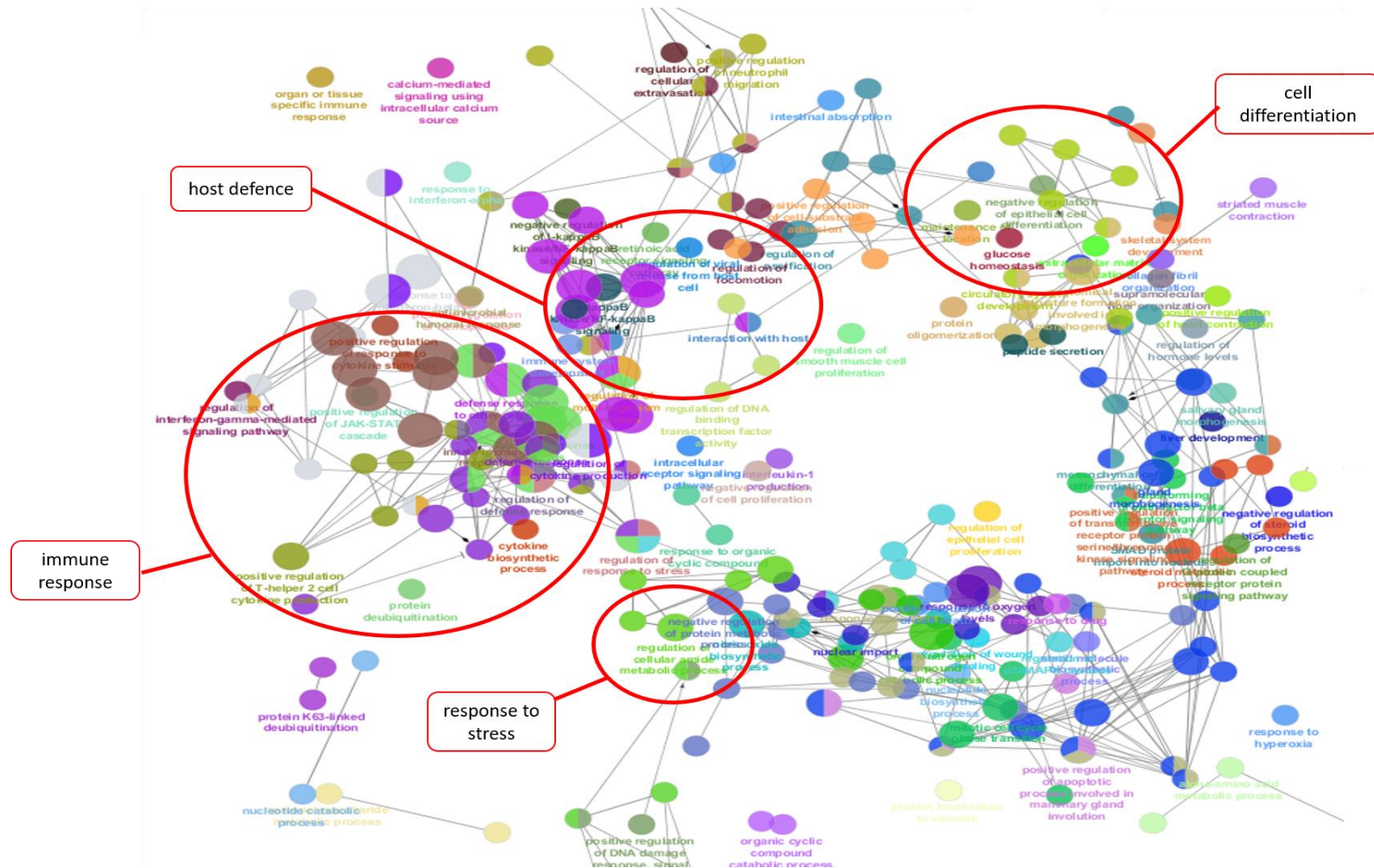


Figure 3.9 Network of biological processes affected by both methyl donor depletion and chromosomal integration of HPV at the Int-stage

This figure represents a network of biological processes (GO_BP terms) that is enriched by both methyl donor depletion and later stage (integrated) of HPV integration. Each node represents a specific biological process (GO_BP terms) that is enriched in this analysis. Node size reflects the significance level of the enriched terms; bigger nodes indicate higher levels of significance. The node colour indicates a specific GO term, and similar coloured nodes indicate that these GO terms are from the same GO parent-child terms. Kappa score was used to link (edges) the enriched terms (nodes) where it defined term-term interrelations (edges) and functional groups, based on shared genes between the terms.

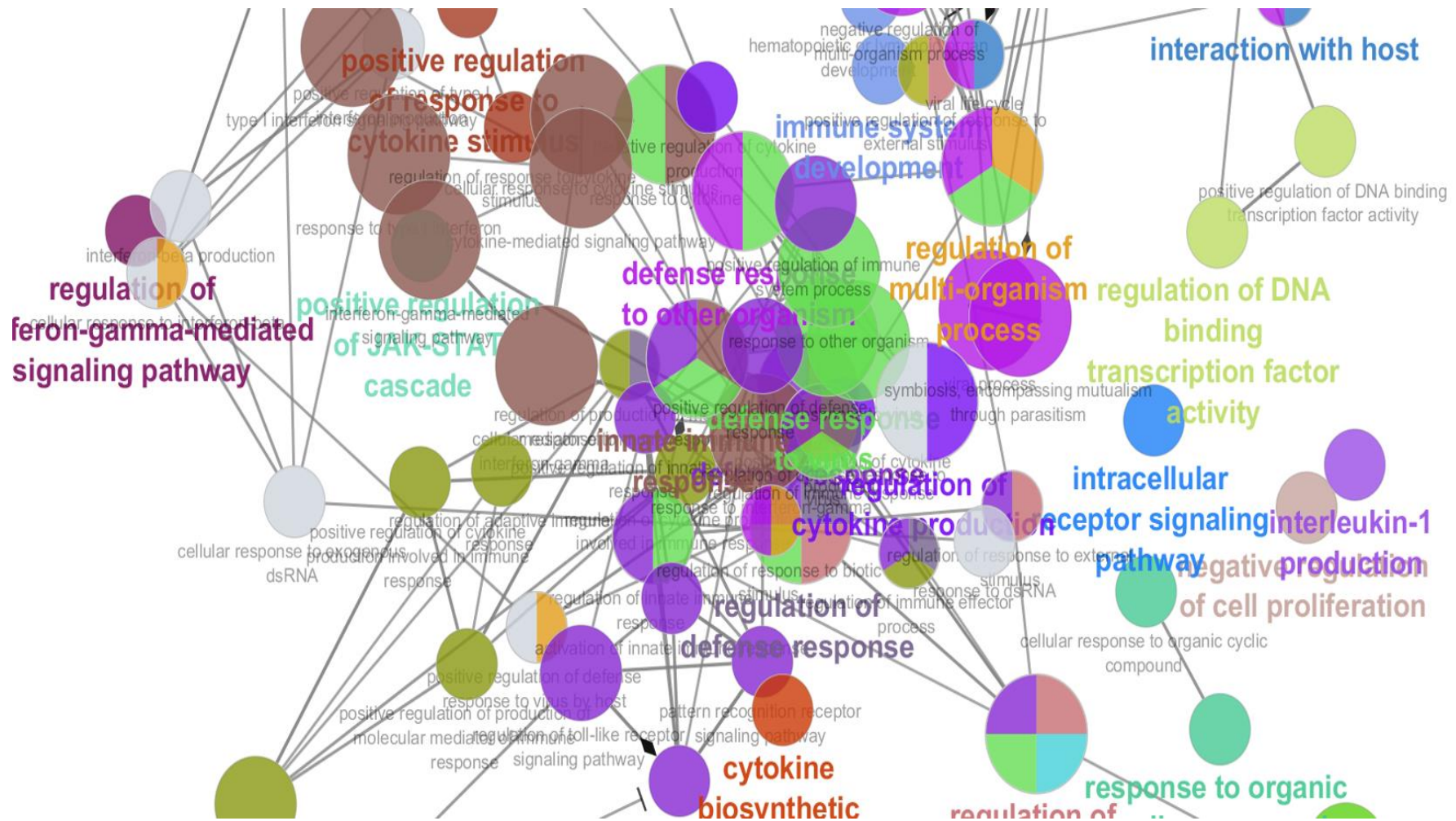


Figure 3.10 Host defence mechanism affected by both methyl donor depletion and chromosomal integration of HPV at the Int-stage

This figure represents a closer look at the network of biological processes (GO_BP terms) associated with host defence mechanisms that are enriched by both methyl donor depletion and later stage (integrated) of HPV integration. Each node represents a specific biological process (GO_BP terms) that is enriched in this analysis. Node size reflects the significance level of the enriched terms; bigger nodes indicate higher levels of significance. The node colour indicates a specific GO term, and similar coloured nodes indicate that these GO terms are from the same GO parent-child terms. Kappa score was used to link (edges) the enriched terms (nodes) where it defined term-term interrelations (edges) and functional groups, based on shared genes between the terms.

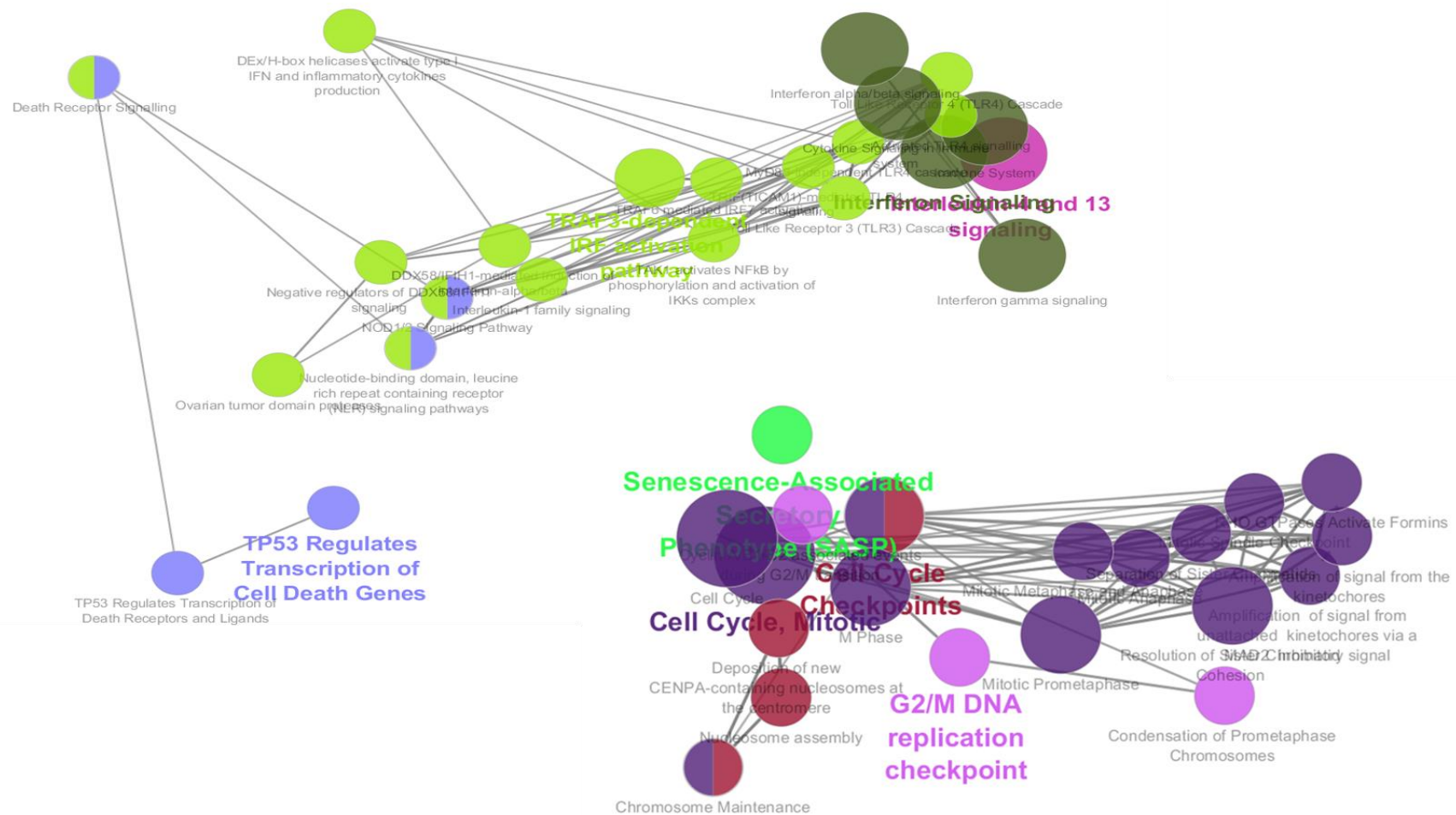


Figure 3.11 Network of KEGG pathways affected by both methyl donor depletion and chromosomal integration of HPV at the Epi-stage

This figure represents a network of KEGG pathways that is enriched by both methyl donor depletion and the beginning stage (episomal) of HPV integration. Each node represents a specific KEGG pathway that is enriched in this analysis. Node size reflects the significance level of the enriched pathway; bigger nodes indicate higher levels of significance. The node colour indicates a specific KEGG pathway, and similar coloured nodes indicate a similar or closely related pathway. Kappa score was used to link (edges) the enriched pathway (nodes) where it defined pathway-pathway interrelations (edges) and functional pathways, based on shared genes between the pathways.

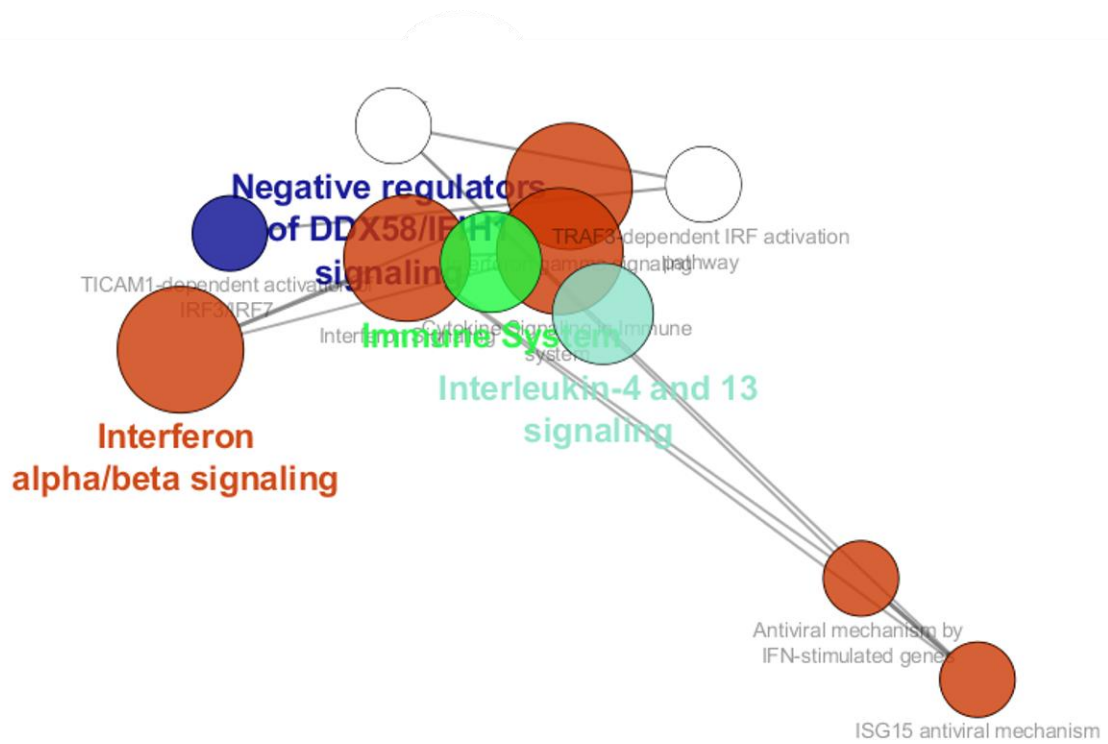


Figure 3. 12 Network of KEGG pathways affected by both methyl donor depletion and chromosomal integration of HPV at the Int-stage

This figure represents a network of KEGG pathways that is enriched by both methyl donor depletion and later stage (integrated) of HPV integration. Each node represents a specific KEGG pathway that is enriched in this analysis. Node size reflects the significance level of the enriched pathway; bigger nodes indicate higher levels of significance. The node colour indicates a specific KEGG pathway, and similar coloured nodes indicate a similar or closely related pathway. Kappa score was used to link (edges) the enriched pathway (nodes) where it defined pathway-pathway interrelations (edges) and functional pathways, based on shared genes between the pathways.

Among the genes identified in the MCODE sub-networks are; *STAT1* that is involved in cytokine-induced signalling pathways and can act as an antiviral and antibacterial mediator, growth inhibitor and inducer of apoptosis (Verhoeven et al., 2020) as well as genes associated with innate immunity such as *OAS1* (Kristiansen et al., 2011), *MX1*, *MX2* (Haller & Kochs, 2011; Boerner et al., 2015), *IFIT1*, *IFIT3* (Pidugu et al., 2019b), *ISG15* (Burks et al., 2015) and *RSAD2* (Kurokawa et al., 2019) that are directly implicated in the elimination of viruses and induced by the type I interferon (IFN) pathway.

The changes in expression of selected IFN-stimulated genes (ISGs) in methyl depleted C4-II cells, as well as in W12 cervical keratinocytes cells at the episomal and integrated stage of HPV chromosomal integration are shown in **Table 3.4**. These ISGs (*OAS1*, *MX1*, *MX2*, *IFIT1*, *IFIT3*, *ISG15* and *RSAD2*) were all upregulated in methyl donor depleted C4-II cells.

ISG15 appears most affected with a fold change of 13.1, followed by *IFIT1* and *RSAD2*, where the genes were upregulated with fold changes of 12.1 and 8.1 respectively. In the W12 cervical keratinocytes cells, these ISGs were also upregulated at the earlier stage of HPV integration (Epi-Stage), but interestingly, appears to be downregulated at the later stage of HPV chromosomal integration (Int-stage).

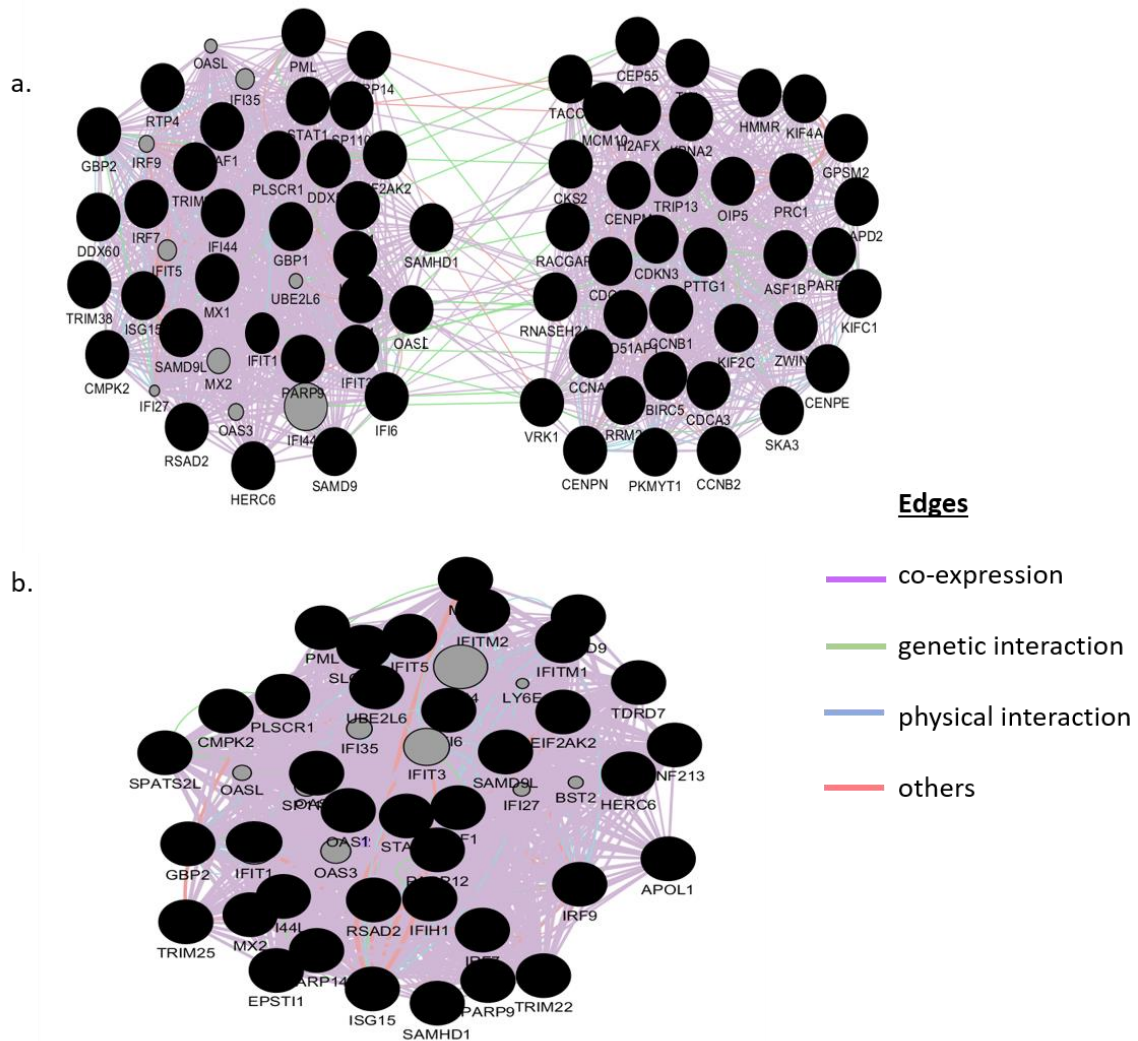


Figure 3.13 Gene interaction network associated with methyl donor depletion and chromosomal integration of HPV

Common DEGs between methyl donor depletion and chromosomal integration were uploaded into GeneMania generating massive gene networks. The MCODE plug-in was then used to identify densely connected nodes as a sub-network/cluster via mathematical modelling, from the large GeneMania gene network, indicating potential gene or a network of genes of interest. This figure shows the MCODE subnetwork with the highest score generated from (a) common DEGs of methyl donor depletion and beginning stage (episomal) of chromosomal HPV integration (b) common DEGs of methyl donor depletion and later stage (integrated) of chromosomal HPV integration. Genes (nodes) are linked (edges) to one another, illustrating the relationship between genes (i.e. co-expression, genetic interaction, physical interaction or others) based on publicly available databases. Black nodes represent the DEGs while grey nodes represent relevant genes that have similar functions to the DEGs.

Table 3. 4 The changes in IFN-stimulated genes expression in methyl depleted C4-II cells and W12 episomal and integrated cervical keratinocytes cells

IFN-stimulated genes (ISG)	Methyl Depletion Dataset	Epi-Stage Dataset	Int-Stage Dataset
	Fold change	Fold change	Fold change
<i>ISG15</i>	13.1	2.4	1.3
<i>IFIT1</i>	12.1	2.0	1.4
<i>RSAD2</i>	8.1	5.4	1.3
<i>OAS1</i>	7.0	2.0	1.3
<i>IFIT3</i>	6.6	2.0	1.3
<i>MX1</i>	4.2	3.2	1.4
<i>MX2</i>	3.2	3.0	3.2

3.5 Discussion

To the knowledge of this researcher, this study is one of the pioneering works in the field of cervical cancer research. Besides the work by (Poomipark, 2013, Poomipark et al., 2016), there is no other known literature with regards to the effects of methyl donor nutrients on cervical cancer gene expression. A study was previously conducted on head and neck squamous cell carcinoma (HNSCC) that was grown in complete or folate, methionine and choline deficient media in order to investigate the effects of methyl donor depletion on intracellular processes (Hearnden et al., 2018). An increment in doubling-time and apoptosis was observed, with a reduction in cell proliferation in methyl depleted cells as compared to those grown in complete medium. However, it was reported that the decrease in cell proliferation rate detected in methyl donor-deficient cultures did not account entirely for the reduction in the cell number observed. Cell death, through apoptosis, also increased in the methyl donor depleted conditions, while cell necrosis remained unchanged. Here it is noted that Hearnden et al.'s finding is for HNSCC and not cervical cancer which is the focus of this study.

Due to its role methyl donor in 1C metabolism, folate has been studied extensively as a possible mechanism for cancer development. There is evidence to suggest that altered folate status influences the risk of cancer and there are plausible mechanisms to support this. Furthermore, *in vitro*, *in vivo* and clinical trials in various other human cancer, especially colon have demonstrated folate potential in modulating global and gene-specific DNA methylation patterns, and subsequently contributing towards cancer risk (Mahmoud & Ali, 2019; Ghazi et al., 2020). On the other hand, studies of methyl donors other than folate have indicated a complex interaction between methyl donor availability and function, whereby deficiency in one methyl donor may be compensated for by another, to maintain a functional methyl cycle

(Niculescu & Zeisel, 2002). However, very few studies have examined effects of depletion of more than a single methyl donor, where the opportunity for such compensation is minimised.

In the initial work conducted in the department, a genome-wide microarray analysis was performed to determine the effects of folate and methionine depletion on C4-II cervical cancer cells gene expression; where the up-and-downregulated genes were analysed separately using the DAVID Bioinformatics Resources 6.7 software (Poomipark, 2013). This analysis identified a high proportion of genes associated with cell death, cell communication, and cell motion that were upregulated, whilst a high proportion of genes associated with regulation of the cell cycle, cytoskeleton organisation, and chromosome organisation were downregulated. Additionally, signalling pathways leading to cell motility, including the Wnt signalling pathway and focal adhesion was also identified as potential pathways that are affected by folate and methionine depletion.

As an extension to Poomipark's study, this study aims to identify cervical cancer-associated gene networks and pathways that are affected not only by methyl donor nutrient depletion, but also by chromosomal integration of HR-HPV in cervical cells using bioinformatics analysis. Based on current literature, both methyl donor availability (Flatley et al., 2009; Mahmoud & Ali, 2019) and persistent infection of HR-HPV (Balasubramaniam et al., 2019; Okunade, 2020) may modulate cervical cancer growth and progression. Although there is broad knowledge about the mechanisms by which high risk HPV types initiate transformation of cervical epithelial cells to become malignant, the inter-connected mechanisms of multiple factors, such as methyl donor availability and genomic changes caused by HR-HPV integration to promote malignant transformation, are still not entirely understood. This observation leads to the hypothesis that both phenotypes of cervical cancer cells and a panel of genes involved in fundamental cellular pathways and epigenetic alterations are potentially influenced by methyl donor status and chromosomal integration of HPV; that can be identified using bioinformatic approaches. Thus, a secondary dataset that measured the changes in gene expression during initial and later stages of HPV chromosomal integration into cervical cells was combined with the original methyl donor depletion dataset, in order to identify gene networks and pathways that are not only affected by methyl donor depletion but also due to chromosomal integration of HPV. In order to draw stronger inferences, the methyl donor depletion datasets were analysed by pooling both up-and-down regulated genes, where an in-depth bioinformatics analysis was conducted using an updated version of the DAVID Bioinformatics Resources 6.8 software, as well as the ClueGo software and GeneMania with

MCODE plugin, in order to identify networks of genes, biological processes and pathways that are overrepresented.

In this study, initial bioinformatics analysis on the methyl donor depletion dataset revealed similarities to Poomipark's findings, where up-regulated genes showed an overrepresentation of biological processes associated with cell death, cell signalling, and cell motion; and down-regulated genes depicted an overrepresentation of biological processes associated with regulation of the cell cycle, cytoskeleton organisation, and chromosome organisation (**Table 3.1, Figure 3.1 to Figure 3.3**) (Poomipark, 2013). However, this study's analysis also identified a high proportion of genes associated with viral activity, host defence and immune function that were upregulated with folate and methionine deficiency. This suggests that the absence of methyl donors may lead to a dysregulation of gene expression that affects biological processes, which are important in the development and progression of cervical cancer. On the other hand, the observed downregulation of the cell cycle could also be indicative of cytostatic cells due to nutrient depletion. Methyl donors are essential in the synthesis of purine and pyrimidine, which in turn are required for DNA production. Additionally, the depletion of methyl donor nutrients results in low levels of S-adenosylmethionine (SAM), and this could lead to cell cycle arrest, primarily at the G1 phase of the cell cycle, as has previously been reported in human and murine B cells with reduced levels of methionine and SAM (Lin et al., 2014). This study's findings support numerous findings in other various cancers which show that the availability of methyl donor nutrients can modify DNA methylation either globally or at specific CpG sites. Methyl donor nutrients may regulate the DNA methylation pattern by inducing the formation of methyl donors, acting as coenzymes, or modifying DNMT enzymatic activity (Sapienza & Issa, 2016; Mahmoud & Ali, 2019).

The secondary dataset measures the changes in gene expression during the episomal and integrated stage of HPV-16 integration into W12 cervical keratinocyte cells (Pett et al., 2006). This W12 accurately models cervical neoplastic progression during long-term culture, with spontaneous transition from cells containing only episomal HPV-16 to a population containing only integrated HPV-16. Hanahan and Weinberg proposed a set of hallmarks which comprised the common traits shared by every single cancer, that facilitate the transformation from a normal cell to a cancer cell (Hanahan & Weinberg, 2000, 2011). These include (1) having specific growth signals to achieve an active proliferative state without reliance on outside stimuli (2) non-receptive towards antigrowth signals (3) able to resist apoptosis (4) have the potential to

replicate infinitely (5) have the potential to support angiogenesis to maintain viability (6) have the ability to invade surrounding tissues, (7) reprogramming of energy metabolism and (8) evasion of immune destruction, resulting in cancer metastasis. In order to attain these eight hallmarks, an additional two characteristics of cancer were proposed; genome instability and mutation together with tumour-promoting inflammation. With these hallmarks in view, this study's analysis of the secondary dataset revealed several overrepresented biological processes including cell proliferation and differentiation; angiogenesis, cell signalling, immune response and viral life cycle that are consistent with the hallmarks of cancer, and are significantly upregulated at the beginning stage (episomal) of HPV chromosomal integration (**Figure 3.4 and Figure 3.5**). On the other hand, a high proportion of genes related to immune response and response to stress were down-regulated. In the later stage (integrated) of HPV chromosomal integration (**Figure 3.6**), several terms associated with cell signalling and immune response were significantly enriched from the down-regulated group of genes. This finding suggests that when HPV integrates with cervical keratinocytes, numerous epigenetic modifications occur, which may facilitate the transformation of a normal cell to a cancer cell.

Human papillomavirus DNA contains six genes including E7, E6, E5, E4, E2 and E1 which are expressed at the early stage of HPV integration into the host genome, followed by L1 and L2 genes. Studies have suggested that epigenetic alterations associated with E6 and E7 activity are common events during the early steps of epithelial malignancy and have been described as potential biomarkers for cervical cancer (Clarke et al., 2012; Verlaat et al., 2017). The episomal loss of E2 that occurs during viral DNA integration into the host genome, leads to an upregulation of HPV-produced oncoproteins E6 and E7, which in turn induce the silencing of the p53 and pRb tumour-suppressor genes (McBride & Warburton, 2017; Balasubramaniam et al., 2019). Inactivation of these host proteins disrupts both the DNA repair mechanisms and apoptosis, leading to rapid cell proliferation. Multiple genes involved in DNA repair, cell proliferation, growth factor activities, angiogenesis and mitogenesis genes become highly expressed in cervical intraepithelial neoplasia (CIN) and in cancer.

Finally, the principal findings of this study are that combined folate and methionine deficiency might be associated with dysregulation of several genes associated with host defence mechanisms and immune response. Specifically, it has highlighted several genes of innate immunity that are directly implicated in the elimination of viruses and induced by the type I interferon (IFN) pathway (**Table 3.4 and Figure 3.13**). As persistent HR-HPV infection has a pivotal role in the carcinogenesis of cervical cancer (Balasubramaniam et al., 2019), the host's

immune system's ability to manage HPV infection is crucial in order to prevent its progression to cancer (Hu & Ma, 2018). A previous study reported that the activation of type 1 interferons during HPV viral infection is able to prevent the transformation of premalignant cells *in vitro* by maintaining the expression of tumour suppressor gene p53 (Takaoka et al., 2003), a gene that is inhibited by E6 overexpression (Balasubramaniam et al., 2019). The bioinformatics analysis in this study has raised the question of whether methyl donor availability may influence an individual's susceptibility towards HPV infection and persistence, and cervical cancer development via its impact on DNA methylation.

Interferons (IFN) are cytokines that are released in response to pathogens including viruses, bacteria, parasites and tumour cells, thus modulating the immune response and providing antiviral, anti-proliferative and antiangiogenic effects (Muller et al., 2017). In addition, these cytokines are also involved in the cell cycle, differentiation and apoptosis (Dunn et al., 2006; Parker et al., 2016). IFN are divided into 2 subtypes; type 1 interferons that are induced during viral infection, and type 2 interferons that are not virus inducible and are restricted to mitogen or cytokine-activated lymphoid cells such as T lymphocytes and natural killer (NK) cells (Kim et al., 2000; Parker et al., 2016). In order to activate their target genes, IFNs need to bind to receptors associated with JAK1 and TYK2 and undergo phosphorylation, which activates the STATs (Di Franco et al., 2017). These STATs heterodimers will then associate with a DNA-binding protein such as ISGF-3 or IRF-9, forming an active complex on the interferon response element (ISRE), thus inducing several IFN-stimulated genes including *MX* and *ISG15* (Bluyssen et al., 1996; Stark et al., 1998). As the IFNs are involved in the activation of a number of signalling pathways in tumour cells including cell proliferation, differentiation, survival and invasion; the downregulation or silencing of IFN genes, and their receptors or associated signalling molecules such as *STAT1*, allows the continued growth of tumour cells (Hasthorpe et al., 1997; Levy & Gilliland, 2000; Wagner et al., 2004). In this study, *STAT1* as well as several ISGs including *ISG15*, *MX1*, *MX2*, *RSAD2*, *OAS1*, *IFIT1* and *IFIT3*, were upregulated in the absence of folate and methionine when compared to cells grown in complete media, indicating that the expression of these genes might be regulated by the presence of methyl donor nutrients. Interestingly, with folate and methionine depletion, the selected IFN-stimulated genes (ISGs) expression was upregulated; and a similar pattern was observed during the episomal stage (Epi-stage) of HPV integration in W12 cervical keratinocytes cells. However, these genes appeared to be downregulated during the later stage of HPV integration (Int-stage).

Overall, the findings from this study have highlighted the potential role of host defence mechanisms, specifically with regards to functions of type 1 interferon in cancer development or progression, which in turn may be modulated by methyl donor nutrients. Though, the microarray datasets chosen for the bioinformatics analysis involved two different types of cervical cell lines, C4-II cervical cancer cells and W12 cervical keratinocytes cells, and they were not grown under identical conditions, both cell lines were derived from cervical tissues, making them fairly comparable. The findings from this bioinformatics analysis generates interesting further hypotheses such as

- i. methyl donor depletion leads to an altered immune response in C4-II cervical cancer cells,
- ii. methyl donor depletion reduces growth activity of C4-II cervical cancer cells,
- iii. methyl donor depletion leads to increased apoptosis in C4-II cervical cancer cells,

which calls for further investigation using laboratory methods.

3.6 Summary

HPV infection plays a major role in cervical carcinogenesis via the activation of its genomic products. However, not all women who acquire HR-HPV infection develop cervical cancer. Most infections spontaneously regress, with only a small percentage that continue to persist, and consequently promote the progression of precancerous CIN to invasive cervical carcinoma, thus suggesting other conditions or cofactors that contribute towards cervical carcinogenesis. This includes alterations in DNA methylation, where methyl donor nutrients availability has been shown to modify DNA methylation either globally or at specific CpG sites by inducing the formation of methyl donors, acting as coenzymes, or modifying DNMT enzymatic activity. This study has identified genes that are involved in cell host defence mechanisms and cell level oncogenic processes, which are mutually sensitive to methyl donor nutrient availability. This has raised the question of whether methyl donor availability may influence an individual's susceptibility towards HPV infection and persistence, and cervical cancer development via its impact on DNA methylation. More extensive work and experimental study need to be conducted in order to validate these bioinformatics findings. Nonetheless, these findings highlight the potential to identify pathways; linked to methyl donor nutrient metabolism that might modify the risk of cervical cancer, through effects on host defence against HPV infection.

CHAPTER 4

EFFECT OF METHYL DONOR DEPLETION ON THE EXPRESSION OF GENES ASSOCIATED WITH ANTIVIRAL IMMUNITY

4.1 Introduction

The development of invasive cervical cancer from HPV-infected epithelial cells is a long-term process associated with the accumulation of DNA alterations in the host cell genes (Balasubramaniam et al., 2019; Yuan et al., 2021). Once the HPV enters the host basal squamous cells, it must integrate into the host cell to initiate infection. This then leads to a series of genetic events that enables viral replication, thus establishing a conducive environment for neoplastic progression (Gius et al., 2007). However, in order to ensure continuous replication in the basal epithelial cells, the HPV virus must evade the host immune system. Studies have suggested that high-risk HPV types have developed several mechanisms to avoid host immune response, which is important for viral persistence and progression to HPV-associated neoplastic diseases (Kanodia et al., 2007; Stanley et al., 2012).

Generally, once HPV infection occurs, the host cell activates the innate and adaptive immune systems that are controlled by the major histocompatibility complex (MHC) class I and class II molecules (Balasubramaniam et al., 2019). The MHC molecules present the antigen to the T cells; cytotoxic T cells that are able to directly kill cells that are infected with a virus, and helper T cells that stimulate the responses of other cells including macrophages, B cells and cytotoxic T cells. The macrophages, Langerhans cells and the natural killer cells triggers the regulation of toll-like receptors (TLR), which in turn elicits antiviral responses via interferon-regulatory factor (IRF) to produce the necessary cytokines (Carmody & Chen, 2007; DeCarlo et al., 2012). TLR 3, 4, 7, 8, and 9 play a major role in antiviral immunity by triggering the downstream production of interferons (IFN) (Sato et al., 2009). However, the overexpression of HPV E6 and E7 oncoproteins may down-regulate TLR 9, thus impairing the interferon response (Hasan et al., 2007). In the presence of HPV products; TLR expression becomes irregular, Langerhans cells fail to present the antigens efficiently, tumour-associated macrophages aggregate resulting in an unsuccessful immune response by the host (Deligeoroglou et al., 2013). It also downregulates the expression of microenvironment components which are necessary for natural-killer cells response and antigen presentation to cytotoxic cells. Additionally, HPV promotes T-helper cell 2 (Th2) and T-regulatory cell

phenotypes and reduces Th1 phenotypes, leading to suppression of cellular immunity and lesion progression to cancer.

Furthermore, HPV also avoids the immune system by downregulating the expression of interferon, upregulates interleukin IL-10 and transforming growth factor TGF- β 1 to produce a local immunosuppressive environment, which, along with altered tumour surface antigens, forms an immunosuppressive network that inhibits the antitumor immune response (Torres-Poveda et al., 2014). When HPV enters the cervical epithelium, phagocytosis takes place when the dendritic cells of the host immune system engulf the HPV antigen. The phagolysosome then sends the antigen to bind with the MHC molecules' cell surface. The antigen presenting cells (APC) will then activate CD4+ and T cells, enabling the pro-inflammatory and antiviral cytokines such as IFN- γ and tumour necrosis factor alpha (TNF- α). However, the activation of APC will also stimulate the production of Tregs (regulatory T cells). Tregs will activate interleukin IL-10 and transforming growth factor beta (TGF)- β 1, which will inhibit the function of APC. It is reported that the transformation of normal epithelial cells to pre-cancerous lesions and cancer is associated to the amount of Treg cells produced, where women with persistent HPV-16 infection have been observed to have significantly higher Tregs than HPV-negative women.

Interestingly, the bioinformatics analysis in **Chapter 3** indicates that the combined folate and methionine deficiency might be associated with dysregulation of several genes associated with host defence mechanisms and immune responses, highlighting several genes related to antiviral defence that are induced by the type I interferon (IFN) pathway. Interferons (IFNs) are cytokines produced by the innate immune system in response to viral infection (Takaoka et al., 2003). Events such as persistent viral infection increases IFNs production, initiating a signalling cascade through the Janus kinase signal transducer and activator of transcription (JAK-STAT) pathway (Sadler & Williams, 2008). Phosphorylated *STAT1* and *STAT2* will bind with IRF9 to form a complex known as IFN-stimulated gene factor 3 (ISGF3), resulting in the transcription of numerous IFN-stimulated genes (ISGs) (Darnell et al., 1994; Sadler & Williams, 2008; Schneider et al., 2014). Activation of type 1 IFNs induces the production of antiviral proteins such as myxovirus-resistance protein (Mx), GTPase, RNA-dependent Protein Kinase (PKR), ribonuclease L (RNase L), Oligo-adenylate Synthetase (OAS) and Interferon Stimulated Gene (ISG) (Sadler & Williams, 2008; Schneider et al., 2014). These antiviral proteins are crucial for antiviral activities in host cells, which include the inhibition of virus entry, prevention of virus replication and obstruction of viral egress

(Schneider et al., 2014). On the other hand, genes induced by IFNs also participates in cell growth and regulation, and apoptosis (Kalvakolanu, 2000). Studies on cell culture have found that IFN- α , IFN- β and IFN- γ directly induce caspase-mediated apoptosis in a variety of tumour cell types, leading to experimental studies on the use of type 1 IFN treatment in various cancers (Herzer et al., 2009). However, as precise molecular mechanisms of action of IFNs in cancer treatment are far from being elucidated, it severely hinders the further application of IFNs in cancer therapy.

In this chapter, the expression of five IFN-stimulated genes (ISGs) identified in **Chapter 3** will be validated using real-time quantitative PCR (qRT-PCR). In order to measure the changes in gene expression of cells grown in methyl depleted conditions, an appropriate cervical cancer model of folate and methionine depletion that demonstrate a functional methyl donor deficiency is required. A depletion of folate and methionine is directly reflected by a reduction in intracellular measurements of these two nutrients, when compared to the control (Poomipark et al., 2016). In addition, a depletion of these nutrients will disrupt the supply of methyl groups to the one carbon cycle, thus re-methylation of homocysteine cannot occur, causing an increase in homocysteine levels. An elevation of the extracellular homocysteine levels is a reflection of increased intracellular homocysteine, caused by disturbance of the one carbon cycle (Nakano et al., 2005; Poomipark et al., 2016; Hearnden et al., 2018).

A cervical cancer cell model of methyl donor depletion was previously developed in the department (Poomipark, 2013; Poomipark et al., 2016). The cancer cell model was generated by culturing the C4-II cervical cancer cell lines for 12 days in Waymouth medium depleted of folate or folate and methionine. Intracellular folate, intracellular methionine and extracellular homocysteine were measured in order to determine the functional impact of these depletions on one carbon cycle. It has been observed that in folate or folate and methionine depleted conditions, the amount of intracellular folate in C4-II cells was significantly affected at day 4, and the level of folate showed a decreasing trend after 8 and 12 days of culture. Similarly, there was a significant reduction of intracellular methionine in C4-II cells with both folate and methionine deficiency. An increase in extracellular homocysteine was also demonstrated, which indicates an impairment of homocysteine re-methylation, causing the rise of homocysteine exports.

This cancer model by (Poomipark et al., 2016), was used to generate the microarray dataset that was used in **Chapter 3** bioinformatics analysis, and thus will be used in this chapter

to validate the microarray findings. In this study, the cervical cells were adapted to DMEM medium which excludes key methyl donor nutrients. Changes were made with the medium as there was no cost-effective commercial sources of a basal Waymouth medium at the time when this study was conducted, which excludes key methyl donor nutrients without some residue of these nutrients being present; while it was possible to obtain a basal DMEM medium that was fully modifiable. In the experimental approach of this study, the adapted cervical cancer cell model of methyl donor depletion will be used extensively, utilising not only solely folate and folate-and-methionine depletion, but also a depletion of only methionine. Thus, a validation of this model is required.

4.2 Hypothesis and aims

It is hypothesized that the folate and methionine depletion in cervical cancer cells will upregulate the IFN-stimulated genes (ISGs). In order to test this hypothesis, three objectives were generated:

- a. to compare C4-II cervical cancer cell growth characteristics in complete, folate depleted, methionine depleted or combined folate-and-methionine depleted media.
- b. to validate the C4-II cell model of methyl donor depletion by analysing intracellular folate concentration, intracellular methionine concentration, and homocysteine export.
- c. to determine the effect of methyl donor nutrient depletion on the expression of IFN-stimulated genes using quantitative RT-PCR.

4.3 Methods

4.3.1 Preparation of media

The DMEM medium was prepared by adding 49.3 mL of sodium bicarbonate and 4 mg/L of choline chloride to 1 L of sterile water. The powdered medium was added, and the mixture was then placed on a magnetic stirrer for 10 minutes to ensure that it was fully dissolved (F-M-). In order to prepare methionine depleted media (F+M-) and folate depleted media (F-M+), an additional supplementation of 4 mg/L of folic acid and 30 mg/L of L-methionine were added respectively. The complete medium (F+M+) was supplemented with both L-methionine and folic acid to ensure it contained sufficient nutrients for normal cell growth. Lastly, hydrochloric acid was gradually added to achieve a pH of 7.4. The dissolved medium was then filtered into a 500 mL sterile bottle. 10% foetal bovine serum (FBS) and 1% penicillin/streptomycin antibiotics were added to the medium prior to use.

4.3.2 Cell resuscitation

The C4-II cells contained in Cryo tubes were moved from liquid nitrogen and partially submerged in the water bath at 37°C to allow them to thaw. Cells were then transferred into a new centrifuge tube containing 5 mL of pre-warmed complete DMEM medium. The suspension was centrifuged at 1000 rpm for 5 minutes, at room temperature. The supernatant was discarded and 10 mL of fresh and pre-warmed complete DMEM medium was added into the centrifuge tube. The cell suspension was transferred into a new flask and incubated at 37°C with 5% carbon dioxide.

4.3.3 Cell subculture

C4-II cells were observed under the microscope to assess the degree of confluency as well as signs of contamination. The spent medium was removed and the cell monolayer was washed with 10 mL DPBS. Then, 2 mL of trypsin-EDTA was pipetted into the culture flask and the flask was swirled to ensure the surface of the flask was fully covered with trypsin. The cells were then incubated for 10 to 15 minutes. The flask was observed under a microscope to ensure that all cells were detached and floating. Cells were then suspended in 2 mL of pre-warmed complete DMEM medium. The cell suspension (1 mL) was transferred into a new flask containing 10 mL of fresh pre-warmed standard DMEM medium and incubated at 37°C with 5% carbon dioxide. The cells were sub-cultured when they reached 80-90% confluence.

4.3.4 Determination of cervical cancer cell growth characteristics in complete and depleted medium

C4-II cervical cancer cells were resuscitated, cultured and maintained as described in **section 4.3.2** and **section 4.3.3**. Complete and depleted media were prepared as described in **section 4.3.1**. Cells were seeded in a 12-well plate at a starting cell density of 5×10^4 cells/well in four different types of media; complete medium (F+M+), folate depleted medium (F-M+), methionine depleted medium (F+M-) or folate and methionine depleted medium (F-M-). Cells were then incubated at 37°C with 5% carbon dioxide. Eight similar sets of 12-well plates were prepared and cell growth was observed and measured daily for eight days. At day four, half of the spent media in each well was replaced.

4.3.5 C4-II sample preparation

C4-II cervical cancer cells were resuscitated, cultured and maintained as described in **section 4.3.2** and **section 4.3.3**. At passage 118, the cells were trypsinised, and then the cells were

suspended in 10% FBS in DPBS. The cell suspension was collected into a centrifuge tube, followed by centrifugation at 1000 rpm for 5 minutes, at room temperature. The cells were then re-suspended in 1 mL of 10% FBS in DPBS. Then, 20 μ L of cell suspension was added to 20 μ L of trypan blue in a microfuge tube for cell counting. Cells were counted using an automated cell counter. The number of total cells, live cells and cell viability (%) were recorded. Cells were seeded at 8×10^5 (F+M+ and F-M+) in 1 T75 flask or 1.6×10^6 (F+M- and F-M-) in 2 T75 flasks in fresh pre-warmed DMEM medium. Cells were then incubated at 37°C with 5% carbon dioxide for 8 days. At day 4 of culture, half of the spent media was replaced with fresh pre-warmed DMEM medium.

4.3.6 Intracellular folate analysis

C4-II cervical cancer cells were cultured in complete and depleted media as described in **section 4.3.5**. At least 5×10^6 cells were harvested at day 4 and 8 of culture. After trypsinisation, cells were suspended in 10% FBS in DPBS. The cell suspension was collected into a centrifuge tube, followed by centrifugation at 1000 rpm for 5 minutes at room temperature. The supernatant was discarded and the cells were re-suspended in 500 μ L of 0.5% (w/v) ascorbic acid. Cells were counted using an automated cell counter. The numbers of total cells, live cells and cell viability (%) were recorded. Cells were disrupted using a sonicator at high pulse for 10 minutes. The cells were then homogenized with 2 cycles of precellys (1 cycle: 6000 rpm/pulse: 2 x 30 sec / pause: 20 sec), followed by centrifugation at 16 000 x g for 10 minutes at 4°C. The supernatant was collected and diluted at a 1:10 ratio in separate tubes and all samples were stored at -80°C until analysis. Intracellular folate was measured in units of ng/ml using the Architect *i2000SR* Immunoassay Analyzer in the Department of Clinical Chemistry, Sheffield Children's Hospital. Intracellular folate concentration was presented as pmol/ 10^6 cells.

4.3.7 Intracellular methionine analysis

C4-II cervical cancer cells were cultured in standard and depleted media as described in **section 4.3.5**. At least 2×10^7 cells were harvested at day 4 and 8 of culture. After trypsinisation, cells were suspended in 10% FBS in DPBS. The cell suspension was collected into a centrifuge tube, followed by centrifugation at 1000 rpm for 5 minutes at room temperature. The supernatant was discarded and the cells were re-suspended in 300 μ L of DPBS. Cells were counted using an automated cell counter. The number of total cells, live cells and cell viability (%) were recorded. Cells were disrupted using a sonicator at high pulse for 10 minutes. The cells were then homogenized with 2 cycles of precellys (1 cycle: 6000 rpm/pulse: 2 x 30 sec / pause: 20

sec), followed by centrifugation at 16 000 x g for 10 minutes at 4°C. All samples were stored at -80°C until analysis. Methionine was measured using the Biochrom 30 amino acid analyser at the Department of Clinical Chemistry, Sheffield Children’s Hospital, using a Biosys software v2.05 and analysed using the EZChrom Elite software v3.4. The intracellular methionine was measured in units of nmol/L and presented as pmol/10⁶ cells.

4.3.8 Intracellular and extracellular homocysteine analysis

C4-II cervical cancer cells were cultured in complete and depleted media as described in **section 4.3.5**. At least 2 x 10⁷ cells were harvested at day 4 and 8 of culture; and the culture media was also collected. The measurements of intracellular and extracellular homocysteine were performed with reverse-phase high-performance liquid chromatography using the CHROMSYSTEMS HPLC Kit. The plasma calibrator, controls and derivatisation reagents were reconstituted as per manufacturer’s instructions. The sample, controls or plasma calibrator (100 µL) were transferred into light protected reaction vials, followed by 25 µL internal standard and 75 µL reduction reagent. The mixtures were vortexed for 2 seconds and incubated for 10 minutes at room temperature. Then, 100 µL of precipitation reagent was pipetted into each vial. The mixtures were vortexed for 30 seconds and centrifuged at 9000 x g for 6 minutes. The supernatants (50 µL) were transferred into new light protected vials and 100 µL of derivatisation mix was added to each vial. The mixtures were vortexed briefly and incubated for 10 minutes at 50-55°C. The prepared samples, controls and calibrator (25 µL) were then injected into the HPLC system. The absorbance of the eluted compounds was monitored using EX = 385 nm and EM = 515 nm. The retention times of the analyte internal standard and homocysteine at a flow rate of 1.5 ml/min were approximately 3.3 minutes and 3.9 minutes, respectively. The chromatogram readings were recorded using the Azur HPLC Software, where the quantification was performed using automatic peak area integration. The homocysteine concentrations were calculated using the calibrator and internal standard readings as stated in the formula below. The concentration of homocysteine was reported in µmol/L.

$$C_{\text{Sample}} [\mu\text{mol/L}] = \frac{A_{\text{Sample}} \times IS_{\text{Calibrator}}}{A_{\text{Calibrator}} \times IS_{\text{Sample}}} \times C_{\text{Calibrator}}$$

A_{Sample} = peak area/height of substance A in the chromatogram of the sample

A_{Calibrator} = peak area/height of substance A in the chromatogram of the calibrator

IS_{Sample} = peak area/height of Internal Standard in the chromatogram of the sample

$IS_{\text{Calibrator}}$ = peak area/height of Internal Standard in the chromatogram of the calibrator

$C_{\text{Calibrator}}$ = the concentration C of substance A in the calibrator (15 μ mol/L)

4.3.9 C4-II RNA extraction

C4-II cervical cancer cells were cultured in complete and depleted media as described (see section 4.3.5). Cells were seeded at 8×10^5 in 1 T75 flask (F+M+ and F-M+) or 1.6×10^6 in 2 T75 flasks (F+M- and F-M-), and harvested at day 4 and 8 of culture. The number of cells required for RNA extraction is optimised at $3\text{-}4 \times 10^6$ cells/sample, and not exceeding 1×10^7 cells/sample. Once cell counting was completed, the cell suspensions were centrifuged at 1000rpm for 5 minutes at room temperature. The supernatant was discarded and the cell pellet was stored at -80°C until further analysis.

RNA was extracted using the RNeasy Plus Mini Kit from Qiagen, following the protocol provided by the manufacturer. Briefly, cells were then lysed with 350 μ L Buffer RLT and homogenized by passing the lysate for 5 times through a 20-gauge needle fitted with a syringe. The RLT Buffer contains guanidine-isothiocyanate which inactivates RNases, ensuring isolation of intact RNA. Then, genomic DNA was removed by passing the lysate through a gDNA eliminator spin column at 10 000 x g for 30 seconds. In order to bind the RNA, 350 μ L of 70% ethanol was added to the flow-through and the sample was transferred to the RNeasy spin column. The sample was centrifuged at 10 000 x g for 15 seconds. Buffer RW1 was added to the spin column followed by centrifugation at 10 000 x g for 15 seconds. Then, 500 μ L of Buffer RPE was added to the spin column followed by centrifugation at 10 000 x g for 15 seconds. The washing step with Buffer RPE was repeated twice. An additional centrifugation was run for 1 minute at full speed to eliminate any possibility of buffer carryover. RNA was then eluted with 40 μ L of RNase-free water by centrifugation at 10 000 x g for 1 minute.

The extracted RNA samples were treated with DNase to remove DNA contaminants using the Precision DNase kit by PrimerDesign, following the protocol provided by the manufacturer. Briefly, 5 μ L of DNase reaction buffer and 1 μ L of DNase enzyme were added to each RNA sample, followed by 10 minutes of incubation at 30°C . The DNase was then inactivated by incubating the sample for 5 minutes at 55°C . Purified RNA was stored at -20°C . RNA quality was determined using a Nanodrop spectrophotometer. Pure RNA has a A_{260}/A_{280} ratio of 1.9-2.1. Purified RNA samples were also sent to the Sheffield Institute for Translational

Neuroscience (SiTran) where their quantity and integrity were determined using the Agilent 2100 Bioanalyzer.

4.3.10 cDNA synthesis

The cDNA was synthesised from 1µg of RNA using the Precision nanoScript2 Reverse Transcription Kit by PrimerDesign, following the protocol provided by the manufacturer, which involves a two-step reverse transcription process. First, in the annealing step, 1 µL of oligo-dT primer was added to a volume of RNA template that provides 1 µg of RNA. RNase/DNase free water was added to make a final volume of 10 µL for each sample. The samples were incubated at 65°C for 5 minutes followed by immediate cool-down in an ice water bath. In the extension step, a mixture of reagents as stated in **Table 4.1** was prepared and 10 µL of the mixture was added to each sample on ice. Samples were mixed briefly by vortexing, followed by a pulse spin and incubation at 42°C for 20 minutes. The reaction was then inactivated by incubating the sample for 10 minutes at 75°C. cDNA was stored at -20°C.

Table 4. 1 Reagent's mixture for cDNA synthesis

Component	1 reaction
nanoScript2 4X Buffer	5 µL
dNTP mix 10mM	1 µL
RNase/DNase free water	3 µL
nanoScript2 enzyme	1 µL
Final volume	10 µL

4.3.11 Determination of primer efficiency using standard curve analysis

In order to determine the expression of *STAT1*, *RSAD2*, *OAS1*, *IFIT1* and *ISG15* genes using quantitative RT-PCR, a custom designed primer mix for each gene was obtained from PrimerDesign. A standard curve analysis was conducted for each primer to measure the efficiency with which a given set of primers amplified the target gene. The standard curve for each gene of interest was performed using custom-designed primer mix, positive control template and master mix with SYBR green gene detection kit from PrimerDesign, following the protocol provided by the manufacturer. Sequences for forward (F) and reverse (R) primers are presented as follows:

STAT1: F: CCCTTCTGGCTTTGGATTGAAAG
R: CGGCTGCTGGTCCTTCAAC

RSAD2: F: GTGAGAATTGTGGAGAAGATGCTC
R: CCAGAATAAGGTAGGAGTCTTTCATC

OAS1 : F: TGTGTGTGTCCAAGGTGGTA
R: TGATCCTGAAAAGTGGTGAGAG

IFIT1 : F: GAAGCCTGGCTAAGCAAAACC
R: CTCCAGACTATCCTTGACCTGATGA

ISG15 : F: GCGAACTCATCTTTGCCAGTA
R: CAGGTCTGACACCGACATG

All reagents were removed from the freezer and thawed on ice. The lyophilised primer mix was re-suspended with 660 µL of RNase/DNase free water, and positive control template with 500 µL of template preparation buffer. Each tube was vortexed thoroughly and allowed to stand for 5 minutes, before vortexing it again prior to use (Tube 1). Then, a 10-fold serial dilution for 6 points was prepared by adding 10 µL of positive control template to 90 µL of template preparation buffer (**Table 4.2**).

Table 4.2 Positive control template serial dilution

Positive control template	Copy number
Tube 1	2×10^5 per µL
Tube 2	2×10^4 per µL
Tube 3	2×10^3 per µL
Tube 4	2×10^2 per µL
Tube 5	20 per µL
Tube 6	2 per µL

A reaction mixture containing master mix and primer mix was prepared following PrimerDesign protocol (**Table 4.3**), and 15 µL of the mixture was pipetted onto a 96-well plate. Then, 5 µL of each positive control template was added into the well in triplicate, starting with the lowest copy number. A non-template reaction was also prepared by replacing the positive control template with 5 µL of RNase/DNase free water. The plate was then sealed with a plastic cover and vortexed thoroughly. The StepOne Plus Real-Time PCR System was used to run the analysis. First, the enzyme was activated at 95°C for 2 minutes. This was followed by 40 cycles of denaturation step at 95°C for 10 seconds and extension step at 60°C for 60 seconds. A post PCR melt curve was also conducted to prove the specificity of the primers. A good set of primers will report an efficiency of between 90 to 110%, where the slope of the graph should be between -3.1 to -3.6.

Table 4. 3 Reagent's mixture for measuring primer efficiency using RT-PCR

Component	1 reaction
PrecisionPLUS master mix	10 μ L
Primer mix	1 μ L
RNase/DNase free water	4 μ L
Final volume	15 μL

4.3.12 Determination of gene expression

The expression of *STAT1*, *RSAD2*, *OAS1*, *IFIT1* and *ISG15* genes was determined using quantitative RT-PCR as described. The relative quantification of each gene of interest was performed using custom-designed primer mix and master mix with the SYBR green gene detection kit from PrimerDesign, following the protocol provided by the manufacturer. cDNA templates and reagents were thawed on ice and mixed thoroughly prior to use. cDNA samples were thawed and diluted to a concentration of 25ng/ μ L with RNase/DNase free water and were mixed thoroughly by vortex. A PCR reaction mixture containing master mix and primer mix was prepared following the PrimerDesign protocol (**Table 4.4**), and 17.5 μ L of the mixture was pipetted onto a 96-well plate. Then, 2.5 μ L of cDNA templates were added into the well in triplicate. For each gene, a non-template reaction was also prepared by replacing the cDNA template with RNase/DNase free water. The plate was then sealed with a plastic cover and vortexed thoroughly. The StepOne Plus Real-Time PCR System was used to run the analysis. First, the enzyme was activated at 95°C for two minutes. This was followed by 40 cycles of the denaturation step at 95°C for 10 seconds and the extension step at 60°C for 60 seconds. A post PCR melt curve was also performed. The expression of GAPDH and B2M was conducted with exactly the same procedures in order to achieve a valid internal control for data normalisation. The delta Cq method was used to calculate relative quantification of gene expression between the samples grown in complete (F+M+, control) and depleted media (Livak & Schmittgen, 2001). **Figure 4.1** summarises the gene expression analysis workflow.

Table 4. 4 Reagent's mixture for gene quantification using RT-qPCR

Component	1 reaction
PrecisionPLUS master mix	10 μ L
Primer mix	1 μ L
RNase/DNase free water	6.5 μ L
Final volume	17.5 μL

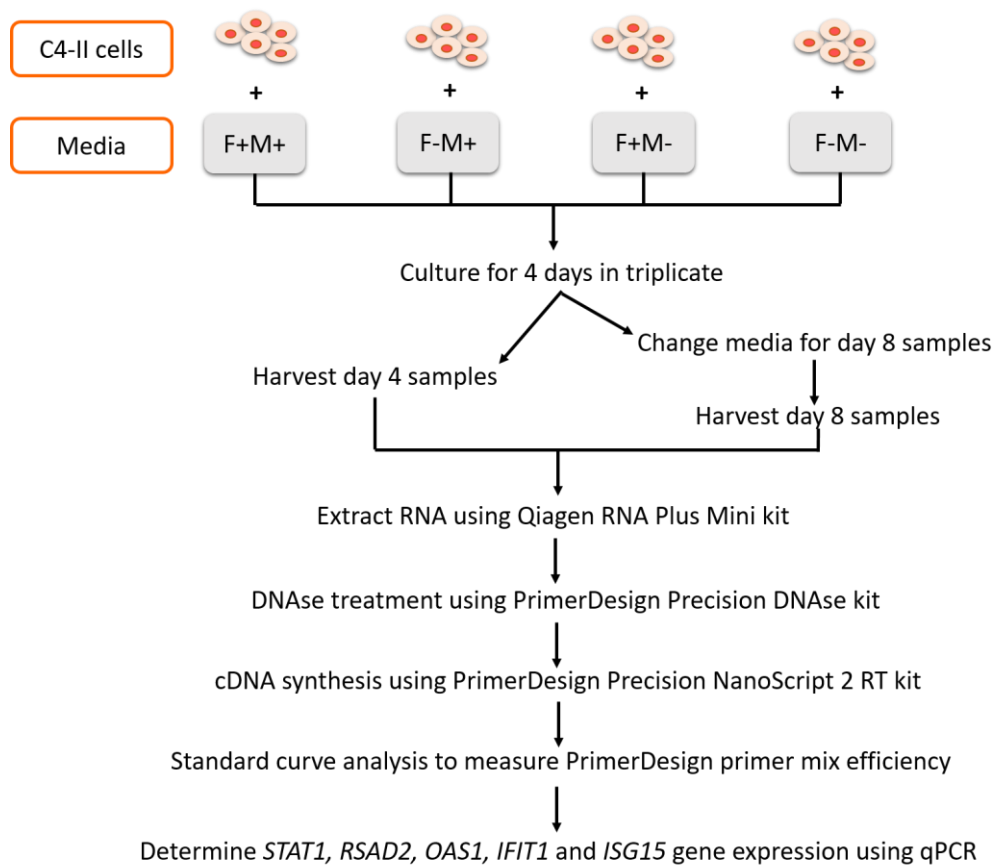


Figure 4.1 Gene expression analysis workflow of five IFN-stimulated genes (ISGs) using quantitative RT-PCR

4.3.13 Statistical analysis

Statistical analysis was conducted using GraphPad Prism 7. Three independent experiments were carried out and expressed as mean \pm SEM. The two-way ANOVA statistical analysis was used to determine the effect of time and methyl donor depletion treatment on outcome of variables. If the effect of time or treatment was significant, one-way ANOVA analysis was carried out, followed by Bonferroni's post hoc test. P value <0.05 was considered to be significant for all statistical analysis.

4.4 Results

4.4.1 Effect of methyl donor depletion on C4-II cell growth

In this experiment, the effect of methyl donor depletion on C4-II cervical cancer cell growth was measured. The cells were grown in four different media; complete (F+M+), folate depleted (F-M+), methionine depleted (F+M-) or folate and methionine depleted (F-M-) medium for eight days. It was observed that C4-II cells grown in complete (F+M+) and folate depleted medium (F-M+) reached about 95% and 90% confluence by day eight, respectively. On the

other hand, cells grown in methionine (F+M-) or folate and methionine depleted medium (F-M+) only reached around 20% confluency. It was also observed that cells grown in methionine depleted (F+M-) or folate and methionine depleted (F-M-) medium were sparse and small, with less cell adherence and visible cell debris. In contrast, cells grown in complete or only folate depletion media grew more consistently and; with better cell adherence.

The two-way ANOVA confirmed that C4-II cell growth was influenced by both time and methyl donor depletion treatment ($P < 0.0001$), with a significant interaction between these factors ($P < 0.0001$) (**Figure 4.2**). Cells grew at a similar rate in complete (F+M+) and folate depleted (F-M+) conditions up day 4, from which time cells grown in the F+M+ medium grew faster. By day eight, the number of cells was greater in complete medium (F+M+) compared to any other conditions ($P < 0.001$). Contrarily, cells grown in methionine (F+M-) or folate and methionine depleted (F-M-) medium appeared to be stagnant, with a significantly lower number of cells when compared with cells in complete (F+M+) ($P < 0.0001$) and folate depleted (F-M+) medium ($P < 0.0001$). Overall, C4-II cells grew at a slower rate in folate depleted medium (F-M+) than in complete medium (F+M+), and cell growth was much worse with methionine depletion (F+M-) or folate and methionine depletion (F-M-) (**Table 4.5**).

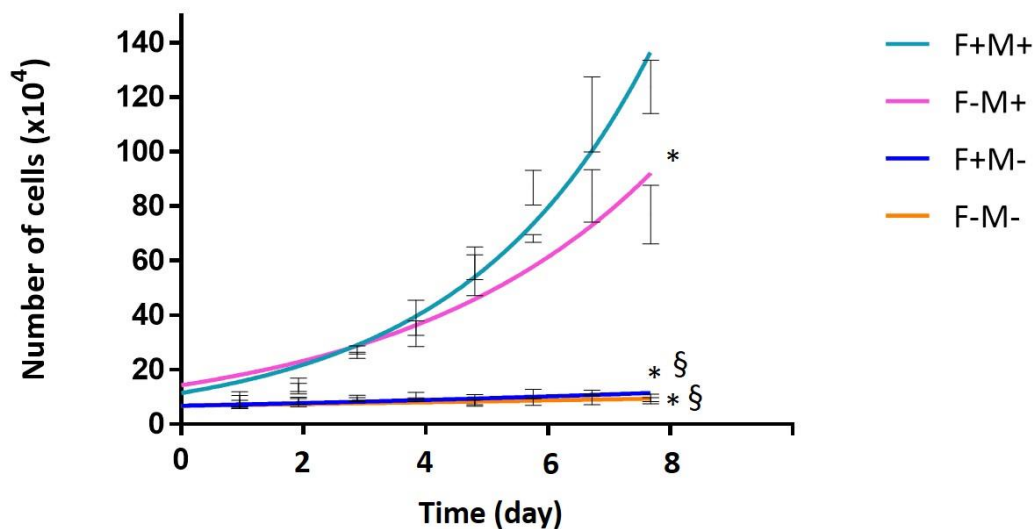


Figure 4. 2 C4-II growth curve in complete and depleted media

This figure shows C4-II cell growth in complete medium (F+M+), folate depleted medium (F-M+), methionine depleted medium (F+M-) and folate and methionine depleted medium (F-M-). Each value shows mean of three-independent experiments and error bars show SEM.

* significantly different from control (F+M+), § significantly different from F-M+, $P < 0.05$ (one-way ANOVA, Bonferroni's post hoc test).

Table 4.5 Doubling time of C4-II cervical cells grown in complete or methyl depleted media

C4-II cervical cancer cell	Doubling Time (hours)			
	F+M+	F-M+	F+M-	F-M-
	54	72	254	415

4.4.2 Effect of methyl donor depletion on intracellular folate

In this experiment, intracellular folate concentration of C4-II cervical cancer cells grown in complete and methyl depleted media for over eight days was measured. In order to make the data comparable, the intracellular folate concentration was corrected for cell number and calculated as pmol/10⁶cells. It was observed that C4-II cells grown in folate depleted media (F-M+ or F-M-) showed at least a 90% decrease in intracellular folate within four days of culture, as compared to those grown in media that contains folate (F+M+ or F+M-). Cells grown in folate depleted media (F-M+ or F-M-) for only four days had an intracellular folate concentration of 2.5 – 3.4 pmol/10⁶ cells compared with 32.3 pmol/10⁶ cells in cells grown in complete medium (F+M+) (**Figure 4.3**).

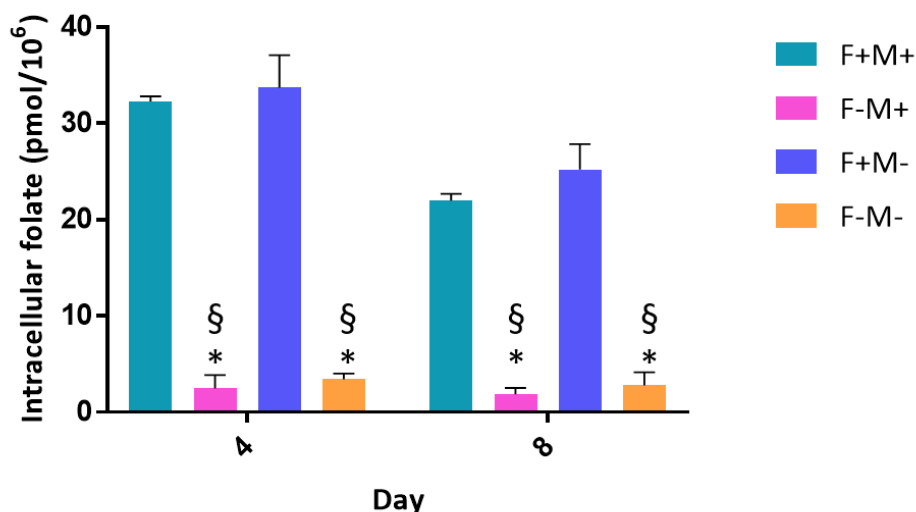


Figure 4.3 Intracellular folate concentration of C4-II cells grown in complete and depleted media

This figure shows intracellular folate concentrations of C4-II cells grown in complete medium (F+M+), folate depleted medium (F-M+), methionine depleted medium (F+M-) and folate and methionine depleted medium (F-M-). Each value shows mean of three-independent experiments and error bars show SEM.

* significantly different from control (F+M+), § significantly different from F-M+, P<0.0001 (one-way ANOVA, Bonferroni's post hoc test).

The two-way ANOVA analysis confirmed that there is a significant difference between methyl donor availability ($P < 0.0001$) over the period of eight days ($P < 0.0001$), with significant interaction between methyl donor status and time ($P = 0.0004$). On days four and eight, cells grown in folate depleted media (F-M+ or F-M-) had significantly lower intracellular folate concentrations than cells grown with folate (F+M+ or F+M-) ($P < 0.0001$), but were not different from one another. The folate concentrations in all four types of media were also assayed; this showed that folate depleted media (F-M+ or F-M-) contained an average folate concentration of 0.3 mg/L and 0.6 mg/L, respectively. In contrast, media with folate (F+M+ or F+M-) had an average folate concentration of 5.6 mg/L and 5.7 mg/L, respectively.

4.4.3 Effect of methyl donor depletion on intracellular methionine

In this experiment, intracellular methionine concentrations of C4-II cervical cancer cells grown in complete and methyl depleted media for over eight days were measured. In order to make the data comparable, the intracellular methionine concentration was corrected for cell number and calculated as pmol/ 10^6 cells. It was observed that C4-II cells grown in methionine depleted media (F+M- or F-M-) showed at least a 71% decrease in intracellular methionine within four days of culture, as compared to those grown in media that contained methionine (F+M+ or F-M+). Cells grown in methionine depleted media (F+M- or F-M-) for only four days had an intracellular methionine concentration of 55 – 64 pmol/ 10^6 cells compared with 222 pmol/ 10^6 cells in cells grown in complete medium (F+M+) (**Figure 4.4**).

The two-way ANOVA analysis confirmed a significant difference between methyl donor availability ($P < 0.0001$) over the period of eight days ($P = 0.0016$). On days four and eight, cells grown in methionine depleted medium (F+M- or F-M-) had significantly lower intracellular methionine concentration than cells grown with methionine (F+M+ or F-M+) ($P < 0.001$), but were not different from one another. The methionine concentrations in all four types of media were also assayed; this showed that media with methionine (F+M+ or F-M+) had an average methionine concentration of 29 mg/L and 27 mg/L, respectively. The methionine concentration in methionine depleted media (F+M- or F-M-) was extremely low, close to the lowest limitation of the assay (1.45 – 45.4 nmol/L).

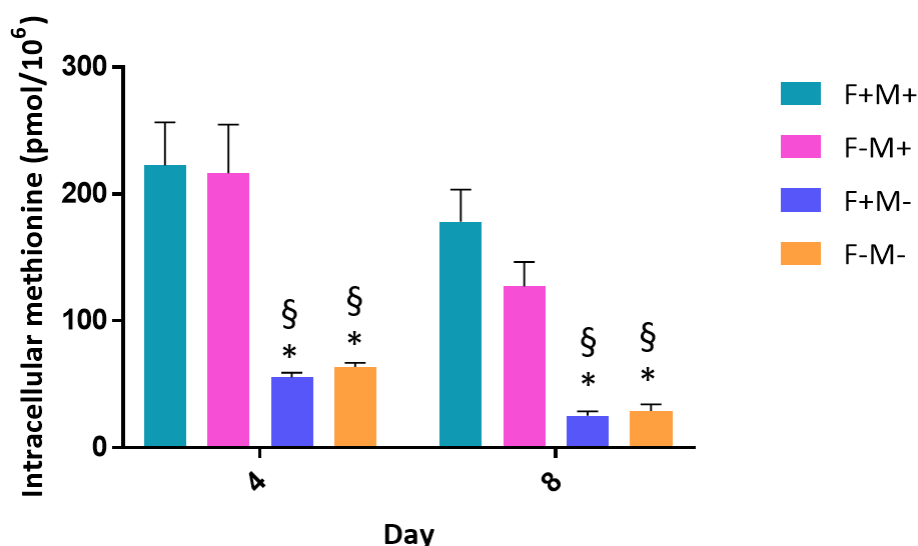


Figure 4.4 Intracellular methionine concentration of C4-II cells grown in complete and depleted media

This figure shows intracellular methionine concentrations of C4-II cells grown in complete medium (F+M+), folate depleted medium (F-M+), methionine depleted medium (F+M-) and folate and methionine depleted medium (F-M-). Each value shows mean of three-independent experiments and error bars show SEM.

* significantly different from control (F+M+), § significantly different from F-M+, $P < 0.001$ (one-way ANOVA, Bonferroni's post hoc test).

4.4.4 Effect of methyl donor depletion on homocysteine export

In this experiment, intracellular and extracellular homocysteine concentrations of C4-II cervical cancer cells grown in complete and methyl depleted media for over eight days were measured.

Figure 4.5 shows the extracellular homocysteine concentrations in the media for C4-II cells that were grown under different methyl donor availability conditions.

The two-way ANOVA analysis confirmed that there is a significant difference between methyl donor availability ($P < 0.0004$) over the period of eight days ($P < 0.0001$), with significant interaction between methyl donor status and time ($P = 0.0006$). There were no significant differences between the homocysteine levels in complete and in any of the methyl depleted conditions at day four. However, by day eight, the concentration of homocysteine in the medium was higher for cells grown in folate depleted medium (F-M+) ($P < 0.0001$), methionine depleted medium (F+M-) ($P = 0.005$) and folate and methionine depleted medium (F-M-) ($P = 0.0008$) than for control cells grown in complete medium (F+M+). The concentration of intracellular homocysteine was also measured. However, the concentration was either not

detectable or gave extremely low values (less than 1.0 $\mu\text{mol/L}$) which was close to the lowest limitation of this assay (1.0-200 $\mu\text{mol/L}$).

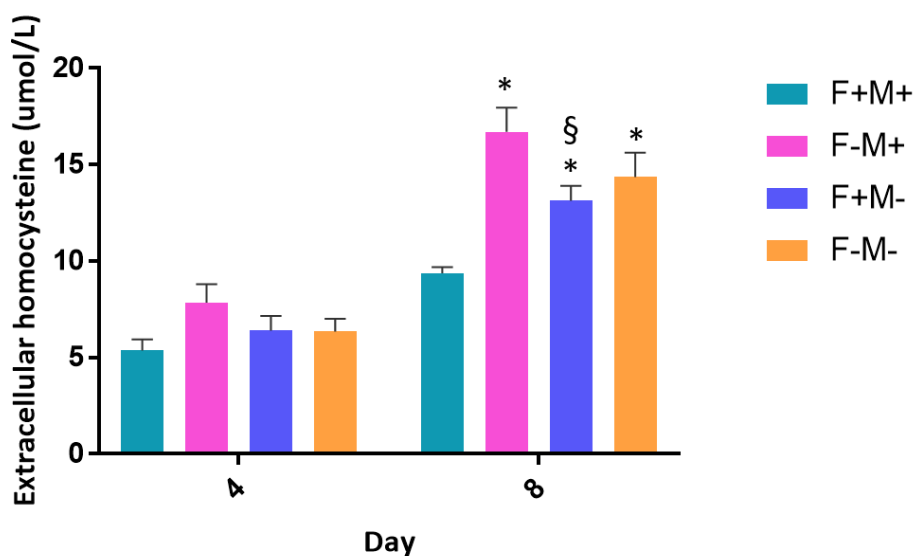


Figure 4.5 Extracellular homocysteine concentrations of C4-II cells grown in complete and depleted medium

This figure shows extracellular homocysteine concentrations of C4-II cells grown in complete medium (F+M+), folate depleted medium (F-M+), methionine depleted medium (F+M-) and folate and methionine depleted medium (F-M-). Each value shows mean of three-independent experiments and error bars show SEM.

* significantly different from control (F+M+), § significantly different from F-M+, $P < 0.01$ (one-way ANOVA, Bonferroni's post hoc test).

4.4.5 Effect of methyl donor nutrient depletion on IFN-stimulated gene expression

a. Quantification and determination of RNA quality

C4-II RNA quality and quantity were determined by spectrophotometry (NanoDrop; Thermo Scientific) and microfluidic analysis (Agilent Technologies' Bioanalyzer), and the readings are summarized in **Table 4.6**. All samples have a $A_{260}:A_{280}$ ratio value range between 2.0 and 2.1, confirming the purity of these samples to be within an acceptable range. The integrity and size distribution of total RNA in each sample were determined by the RNA integrity number (RIN) value from the Agilent Bioanalyzer; higher RIN numbers indicates quality RNA. Control group (F+M+) sample and their biological replicates generated a RIN value of 10. Sample from the depleted groups and their biological replicates had a slightly lower RIN value ranging from 9.6 to 10, however the integrity of these samples was still within an acceptable range.

Table 4. 6 Summary of C4-II cell count, Nanodrop and Bioanalyzer readings

Media	Cell Count		NanoDrop	Bioanalyzer	
	Live cell counts	% cell viability	260:280	RIN	ng/uL
Day 4					
F+M+	2.82 x 10 ⁶	98	2.09	10.0	719.0
	3.62 x 10 ⁶	98	2.10	10.0	630.0
	1.76 x 10 ⁶	97	2.10	10.0	301.0
F-M+	2.19 x 10 ⁶	99	2.09	10.0	578.0
	2.46 x 10 ⁶	97	2.10	10.0	1100.0
	1.99 x 10 ⁶	98	2.10	10.0	419.0
F+M-	3.26 x 10 ⁶	96	2.03	9.6	503.0
	3.76 x 10 ⁶	91	2.04	9.9	310.0
	3.44 x 10 ⁶	97	2.10	10.0	294.0
F-M-	3.56 x 10 ⁶	97	2.02	9.8	594.0
	4.53 x 10 ⁶	94	2.01	9.8	262.0
	3.36 x 10 ⁶	97	2.03	9.8	347.0
Day 8					
F+M+	4.03 x 10 ⁶	97	2.09	10.0	1357.0
	4.40 x 10 ⁶	96	2.09	10.0	1319.0
	3.39 x 10 ⁶	91	2.01	10.0	631.0
F-M+	3.68 x 10 ⁶	91	2.10	10.0	445.0
	3.89 x 10 ⁶	96	2.10	9.9	2075.0
	5.43 x 10 ⁶	95	2.00	10.0	314.0
F+M-	1.96 x 10 ⁶	97	2.01	9.9	225.0
	0.81 x 10 ⁶	96	2.01	9.6	43.0
	1.69 x 10 ⁶	94	2.03	9.7	146.0
F-M-	1.42 x 10 ⁶	92	2.10	10.0	288.0
	1.56 x 10 ⁶	91	2.01	9.6	26.0
	1.41 x 10 ⁶	95	2.03	9.7	125.0

b. Determination of primer efficiency using standard curves analysis

In order to determine the efficiency and specificity of the custom-designed primers, a standard curve analysis was conducted together with a post-melt curve for all genes including the reference genes which is presented in **Figures 4.6 - 4.12**. The primers for all genes delivered an efficiency that is within the acceptable range (between 90 and 110%); with a slope of -3.1 to -3.6 (**Table 4.7**).

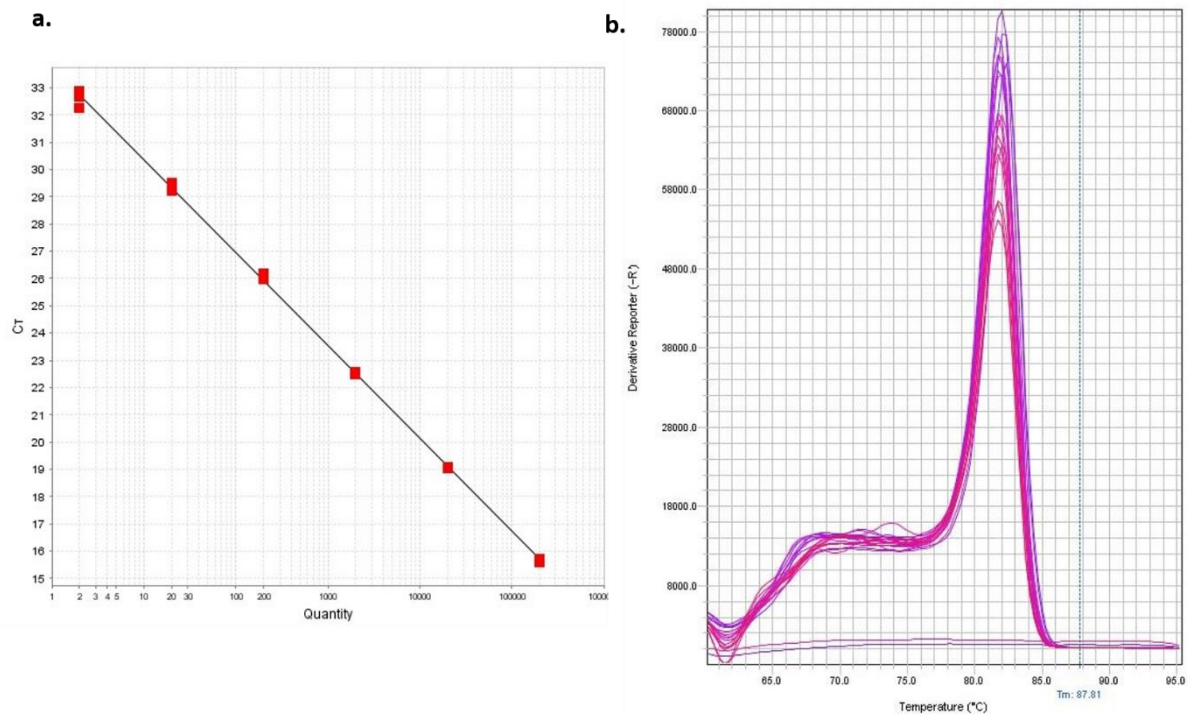


Figure 4.6 Determination of *STAT1* primer efficiency and specificity

(a) the standard curve for *STAT1*, where the y-axis represents the threshold of cycle (Ct) value, and the x-axis represents copy number of the positive control with slope:-3.409, R^2 :0.999, Eff%:96.498. (b) the post-melt curve analysis, where a single peak typically represents a pure single amplicon.

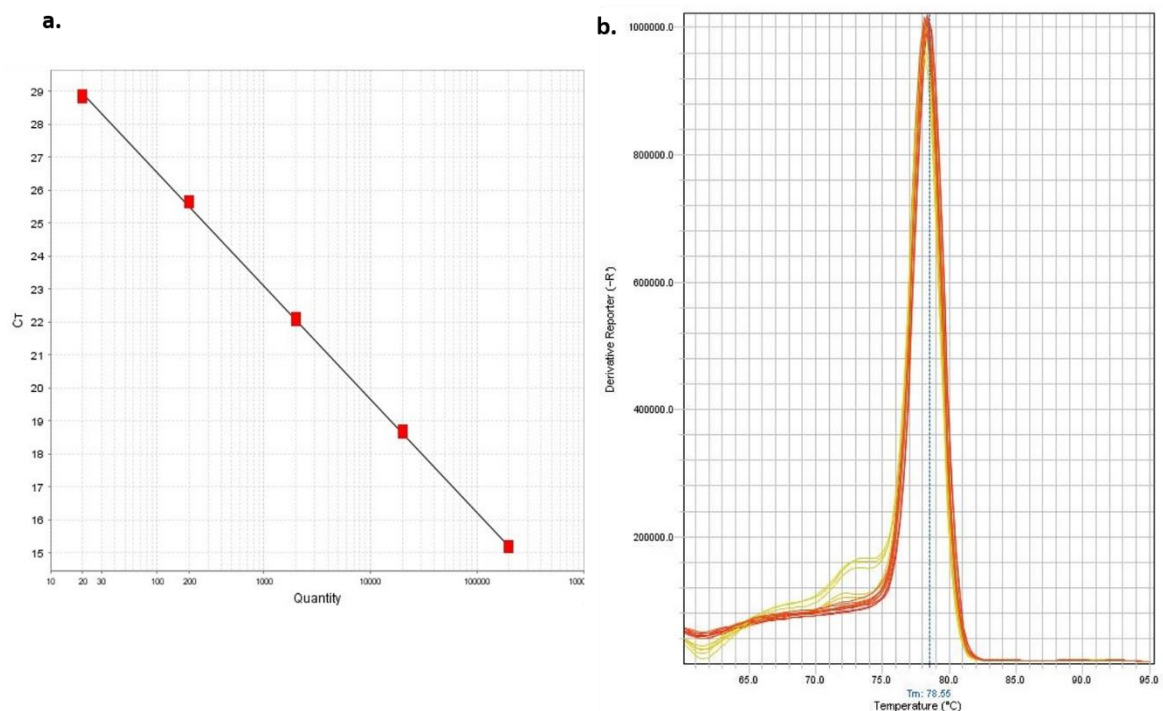


Figure 4.7 Determination of *RSAD2* primer efficiency and specificity

(a) the standard curve for *RSAD2*, where the y-axis represents the threshold of cycle (Ct) value, and the x-axis represents copy number of the positive control with slope:-3.429, R^2 : 1.0, Eff%:95.718. The lowest level of standard was not detectable and has been omitted (b) the post-melt curve analysis, where a single peak typically represents a pure single amplicon.

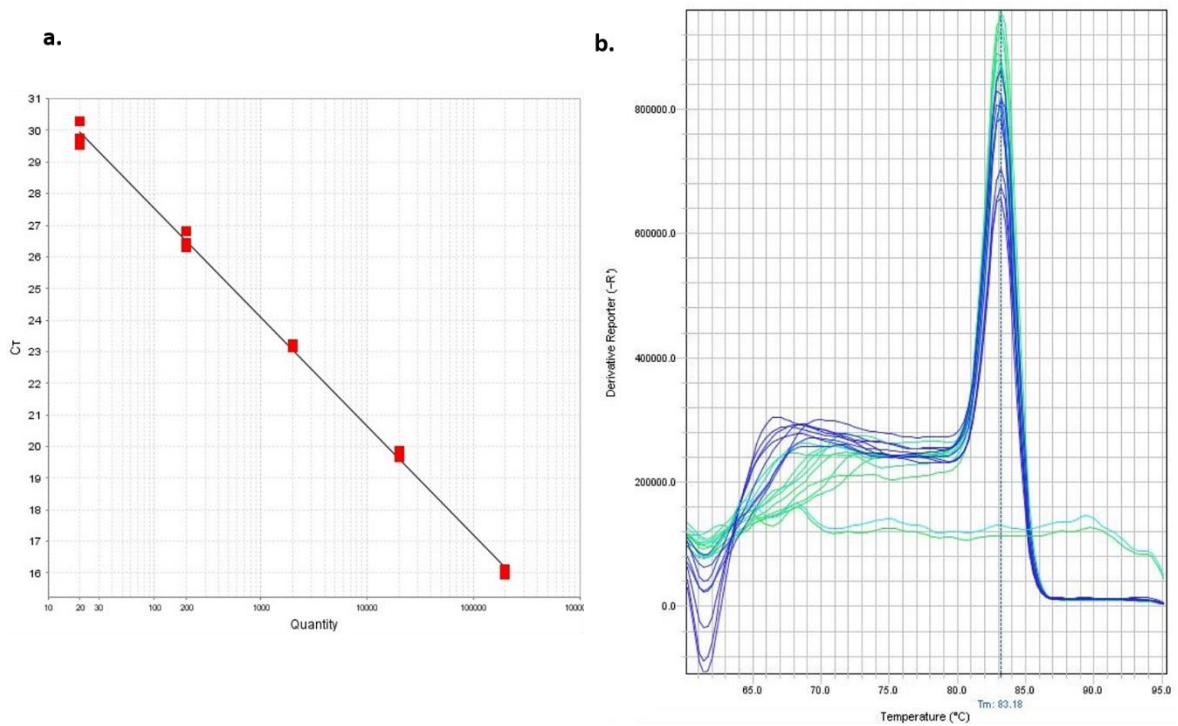


Figure 4.8 Determination of *OASI* primer efficiency and specificity

(a) the standard curve for *OASI*, where the y-axis represents the threshold of cycle (Ct) value, and the x-axis represents copy number of the positive control with slope:-3.445, R^2 :0.998, Eff%:95.101. The lowest level of standard was not detectable and has been omitted (b) the post-melt curve analysis, where a single peak typically represents a pure single amplicon.

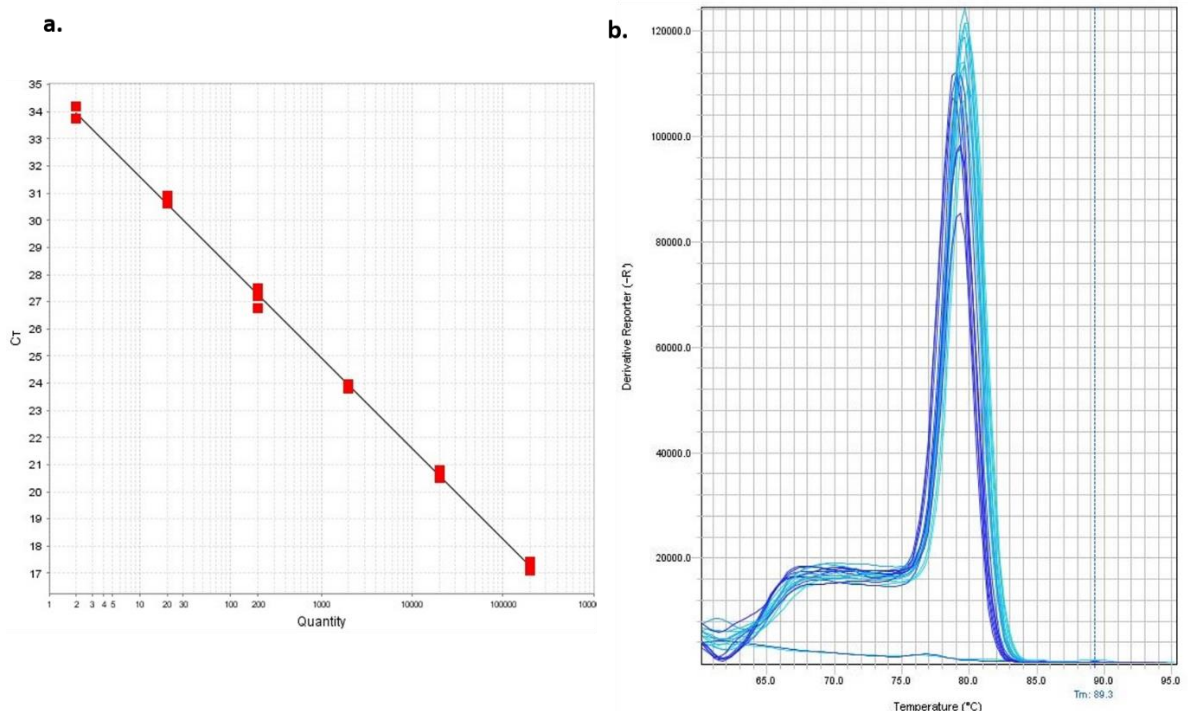


Figure 4.9 Determination of *IFIT1* primer efficiency and specificity

(a) the standard curve for *IFIT1*, where the y-axis represents the threshold of cycle (Ct) value, and the x-axis represents copy number of the positive control with slope:-3.338, R^2 :0.999, Eff%:99.33. (b) the post-melt curve analysis, where a single peak typically represents a pure single amplicon.

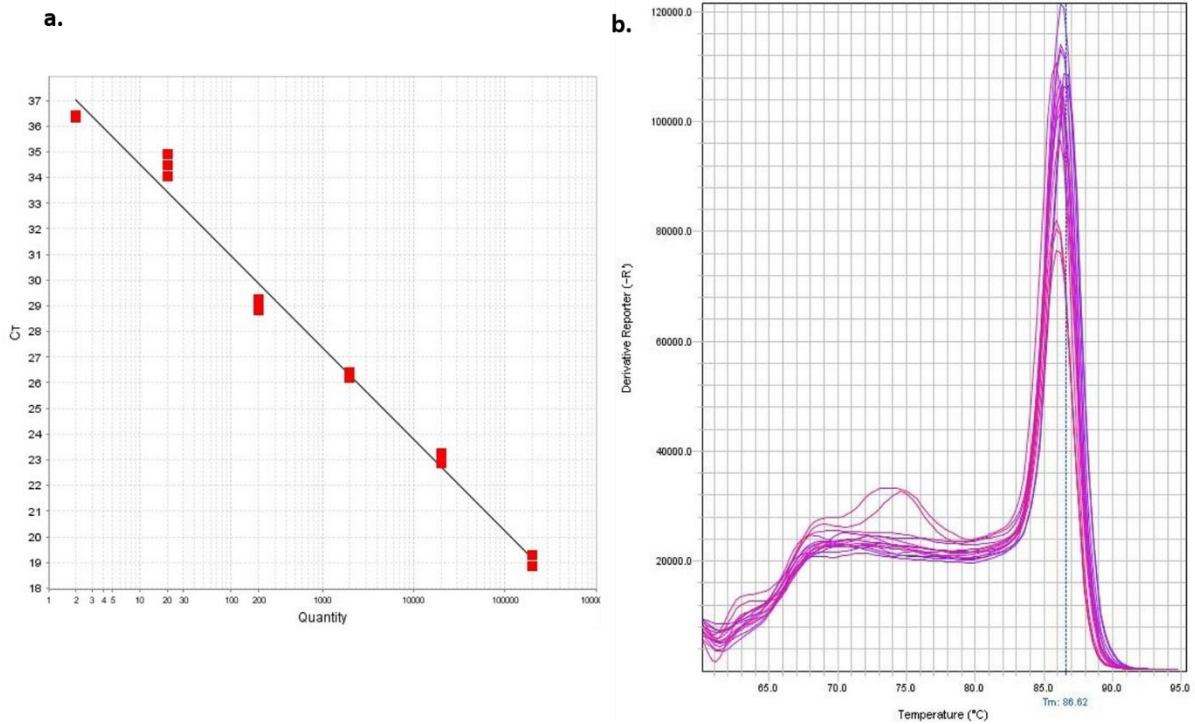


Figure 4.10 Determination of *ISG15* primer efficiency and specificity

(a) the standard curve for *ISG15*, where the y-axis represents the threshold of cycle (Ct) value, and the x-axis represents copy number of the positive control with slope:-3.572, R^2 :0.988, Eff%:90.53. (b) the post-melt curve analysis, where a single peak typically represents a pure single amplicon.

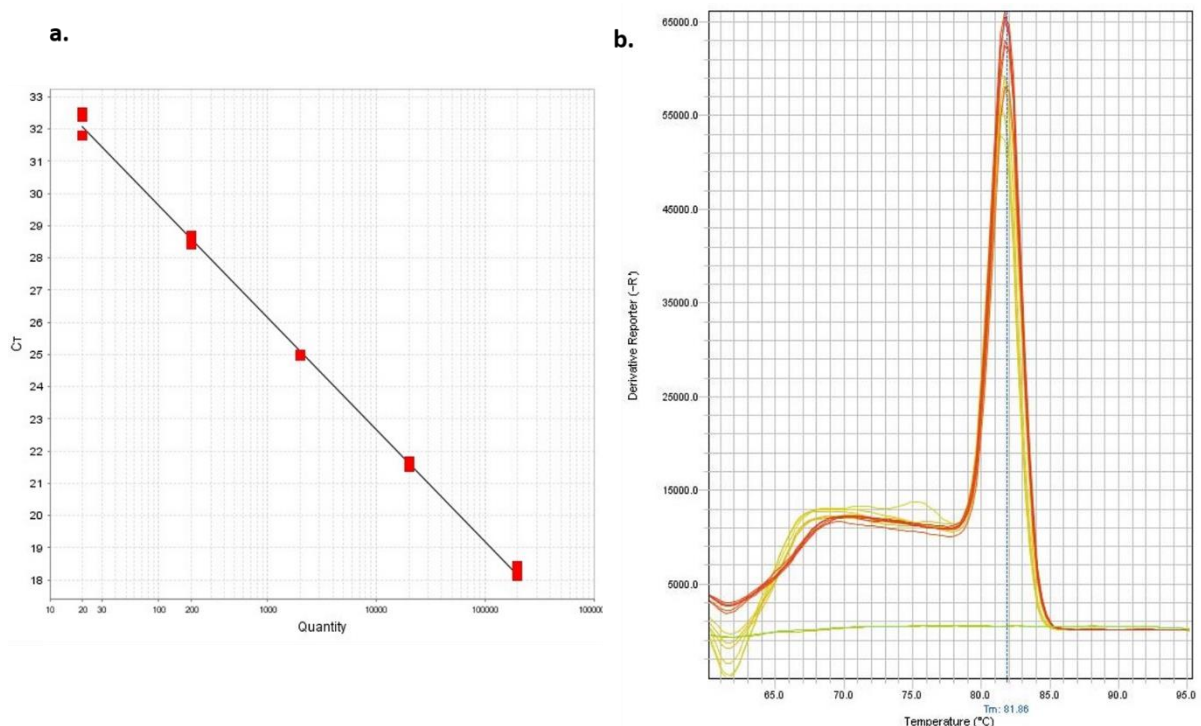


Figure 4.11 Determination of *GAPDH* primer efficiency and specificity

(a) the standard curve for *GAPDH*, where the y-axis represents the threshold of cycle (Ct) value, and the x-axis represents copy number of the positive control with slope:-3.48, R^2 :0.998, Eff%:93.801; The lowest level of standard was not detectable and had been omitted (b) the post-melt curve analysis, where a single peak typically represents a pure single amplicon.

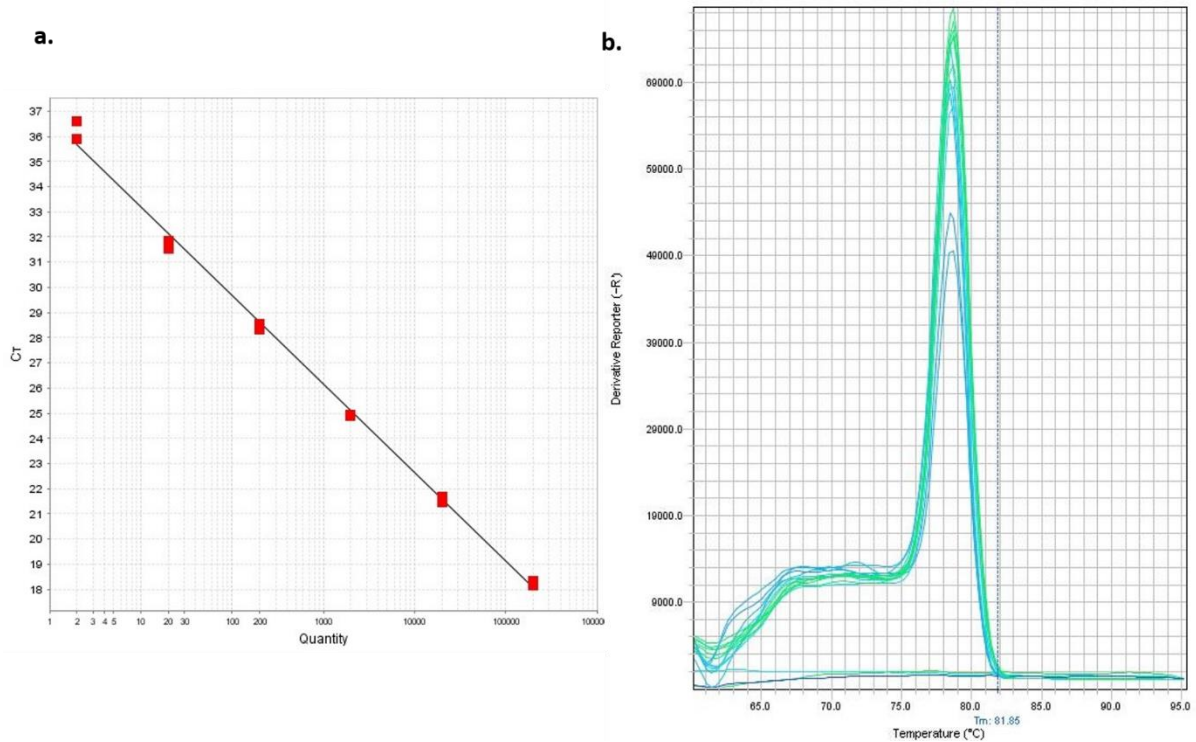


Figure 4. 12 Determination of *B2M* primer efficiency and specificity

(a) the standard curve for *B2M*, where the y-axis represents the threshold of cycle (Ct) value, and the x-axis represents copy number of the positive control with slope:-3.52, R^2 :0.997, Eff%:92.367. (b) the post-melt curve analysis, where a single peak typically represents a pure single amplicon.

Table 4. 7 Summary of the gene primers' standard curve slope, R2 and efficiency values

Gene	Slope	R ²	Efficiency
<i>STAT1</i>	-3.409	0.999	96.5
<i>RSAD2</i>	-3.429	1.000	95.7
<i>OAS1</i>	-3.445	0.998	95.1
<i>IFIT1</i>	-3.338	0.999	99.3
<i>ISG15</i>	-3.572	0.988	90.5
<i>GAPDH</i>	-3.480	0.998	93.8
<i>B2M</i>	-3.520	0.997	92.4

c. Relative quantification of gene expression in complete and methyl depleted conditions

In this experiment, the relative quantification (RQ) real-time PCR of gene expression was examined in C4-II cervical cancer cells. Each gene was normalised to the *GAPDH* and *B2M* reference genes to eliminate any systematic errors due to differences between samples (an internal control) and; C4-II in complete medium (F+M+) was used as the positive control condition.

Figure 4.13 presents the effect of methyl donor depletion on *STAT1* gene expression. In the microarray studies (**Chapter 3**), *STAT1* was significantly upregulated by 6.9-fold in folate and methionine depleted medium (F-M-). The two-way ANOVA analysis confirmed that there is a significant difference between methyl donor availability ($P=0.0126$) over the period of eight days ($P=0.0002$), with significant interaction between methyl donor status and time ($P=0.0072$). At day four, *STAT1* was significantly upregulated, by 6.4-fold, in methionine depletion (F+M-) ($P=0.0356$) and by 8.1-fold in folate and methionine depletion (F-M-) ($P=0.0078$). *STAT1* was also upregulated in folate depleted cells (F-M+) however, the difference was not significant ($P=0.9962$). Contrary to the microarray findings, the quantitative PCR analysis found that *STAT1* was downregulated in all three methyl depleted conditions at day eight. One-way ANOVA analysis also confirmed that there was no significant difference between the control (F+M+) and any of the depleted conditions at day eight ($P>0.05$).

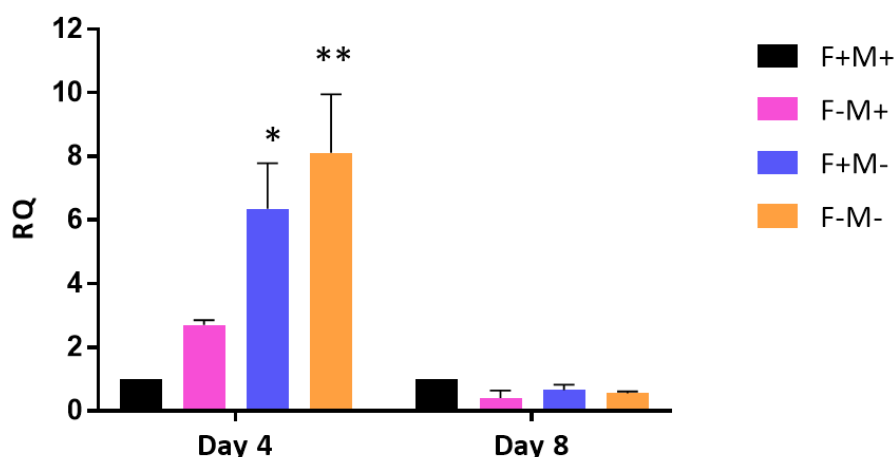


Figure 4. 13 *STAT1* expression in complete and depleted media

This figure shows *STAT1* expression in complete medium (F+M+), folate depleted medium (F-M+), methionine depleted medium (F+M-) and folate and methionine depleted medium (F-M-). Each value shows mean of three-independent experiments and error bars show SEM.

* significantly different from control (F+M+), $P<0.05$; ** significantly different from control (F+M+), $P<0.01$ (one-way ANOVA, Bonferroni's post hoc test).

The effects of methyl donor depletion on *RSAD2* gene expression are presented in **Figure 4.14**. This gene was observed to be significantly upregulated in the microarray analysis by 8.1fold (**Chapter 3**). In the quantitative PCR analysis, the two-way ANOVA analysis confirmed that there is a significant difference between methyl donor status ($P=0.0004$), however the gene expression was not significantly influenced by time ($P=0.6586$) or interaction ($P=0.6860$). At day four, *RSAD2* was significantly upregulated by 9.8-fold in methionine depletion (F+M-) ($P=0.0007$), and by 12.0-fold in folate and methionine depletion (F-M-)

($P=0.0001$). However, there was no significant difference between *RSAD2* gene expression in complete (F+M+) and only folate depleted conditions (F-M+). Similarly, the *RSAD2* expression was upregulated at day eight by 11.3-fold with methionine depletion (F+M-) ($P=0.0098$) and by 11.0-fold in both folate and methionine depletion (F-M-) ($P=0.0090$). Again, there was no significant difference between *RSAD2* gene expression in complete (F+M+) and only folate depleted conditions (F-M+).

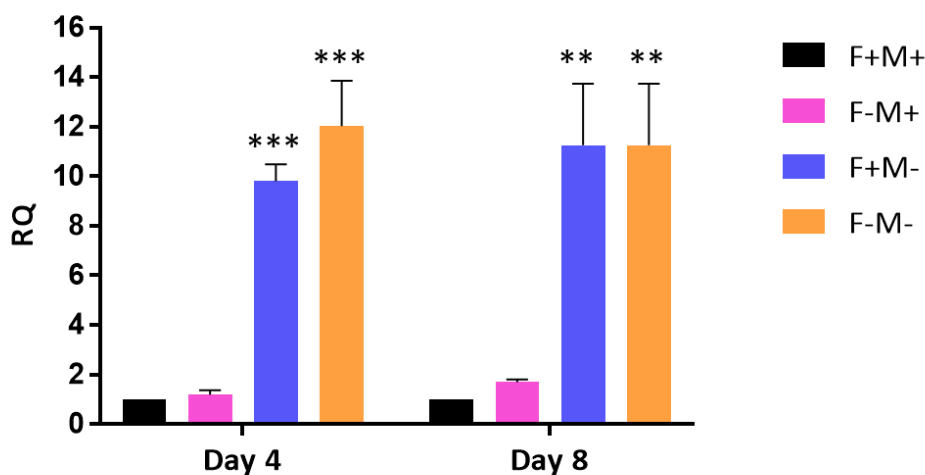


Figure 4.14 *RSAD2* expression in complete and depleted media

This figure shows *RSAD2* expression in complete medium (F+M+), folate depleted medium (F-M+), methionine depleted medium (F+M-) and folate and methionine depleted medium (F-M-). Each value shows mean of three-independent experiments and error bars show SEM.

** significantly different from control (F+M+), $P<0.01$; *** significantly different from control (F+M+), $P<0.001$ (one-way ANOVA, Bonferroni's post hoc test).

Figure 4.15 presents the effect of methyl donor depletion on *OAS1* gene expression. This gene was observed to be significantly upregulated in the previous microarray analysis (**Chapter 3**) by 7.0-fold, in combined folate and methionine depletion after eight days of culture. The two-way ANOVA analysis confirmed that there is a significant difference between methyl donor availability ($P<0.0001$) over the period of eight days ($P=0.0176$), with significant interaction between methyl donor status and time ($P=0.0149$). At day four, *OAS1* was most affected by folate and methionine depletion (F-M-) ($P=0.0002$), associated with 10.1-fold increase in expression. It was also upregulated by 7.1-fold in methionine depleted medium (F+M-) ($P=0.0030$). At day eight, *OAS1* expression was upregulated by 7.6-fold in methionine depletion (F+M-) ($P=0.0007$), and by 4.7-fold in both folate and methionine depletion (F-M-) ($P=0.0227$). Similar to the previous genes, there was no significant difference between *OAS1* gene expression in complete (F+M+) and only folate depleted condition (F-M+).

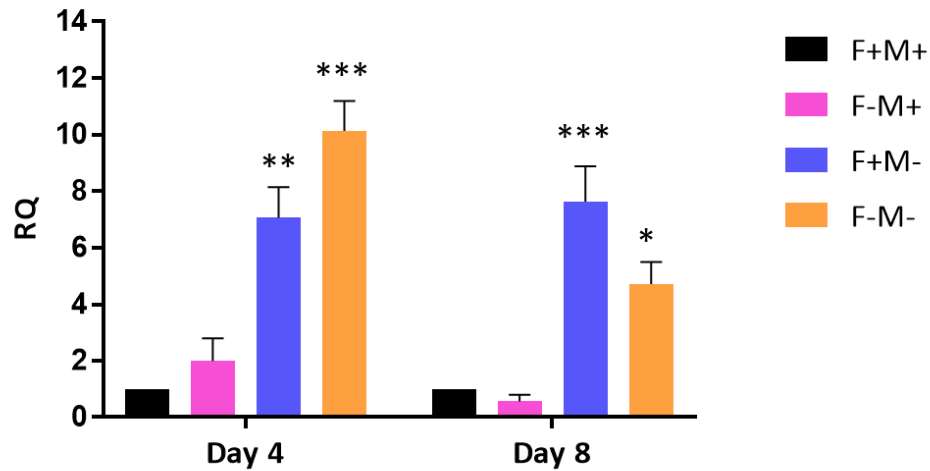


Figure 4.15 *OAS1* expression in complete and methyl depleted media

This figure shows *OAS1* expression in complete medium (F+M+), folate depleted medium (F-M+), methionine depleted medium (F+M-) and folate and methionine depleted medium (F-M-). Each value shows mean of three-independent experiments and error bars show SEM.

* significantly different from control (F+M+), $P < 0.05$; ** significantly different from control (F+M+), $P < 0.01$; *** significantly different from control (F+M+), $P < 0.001$ (one-way ANOVA, Bonferroni's post hoc test).

The effects of methyl donor depletion on *IFIT1* gene expression are presented in **Figure 4.16**. This gene was observed to be significantly upregulated in the microarray analysis by 12.1-fold (**Chapter 3**). In the quantitative PCR analysis, the two-way ANOVA analysis confirmed that there is a significant difference between methyl donor availability ($P = 0.0044$) over the period of eight days ($P = 0.0043$), but there was no significant interaction between methyl donor status and time ($P = 0.0978$). At day four, *IFIT1* was significantly upregulated by 7.2-fold methionine only depletion (F+M-) ($P = 0.0222$), and by 8.0-fold in folate and methionine depletion (F-M-) ($P = 0.0115$). The *IFIT1* gene expression was upregulated at day eight by 4.9-fold in methionine only depletion (F+M-) ($P = 0.0294$) and by 4.8-fold in both folate and methionine depletion (F-M-) ($P = 0.0312$). Again, there was no difference between *IFIT1* gene expression in complete (F+M+) and only folate depleted condition (F-M+).

Figure 4.17 presents the effects of methyl donor depletion on *ISG15* gene expression. Microarray analysis (**Chapter 3**) found *ISG15* to be significantly upregulated by 13.1-fold, in folate and methionine depleted medium (F-M-). The two-way ANOVA analysis confirmed that there is a significant difference between methyl donor status ($P = 0.0001$), however the gene expression was not significantly influenced by time ($P = 0.3587$) or interaction ($P = 0.4540$). At day four, *ISG15* was significantly upregulated by 6.7-fold for methionine depleted medium (F+M-) ($P = 0.0027$) and, by 5.3-fold in depletion of both folate and methionine depletion (F-M-

) ($P=0.0150$). Similarly, the *ISG15* expression was upregulated at day eight by 8.5-fold in methionine only depleted condition (F+M-) ($P=0.0209$) and by 8.4-fold in both folate and methionine (F-M-) ($P=0.0211$). There was no significant difference between *ISG15* gene expression in complete (F_M+) and only folate depleted condition (F-M+).

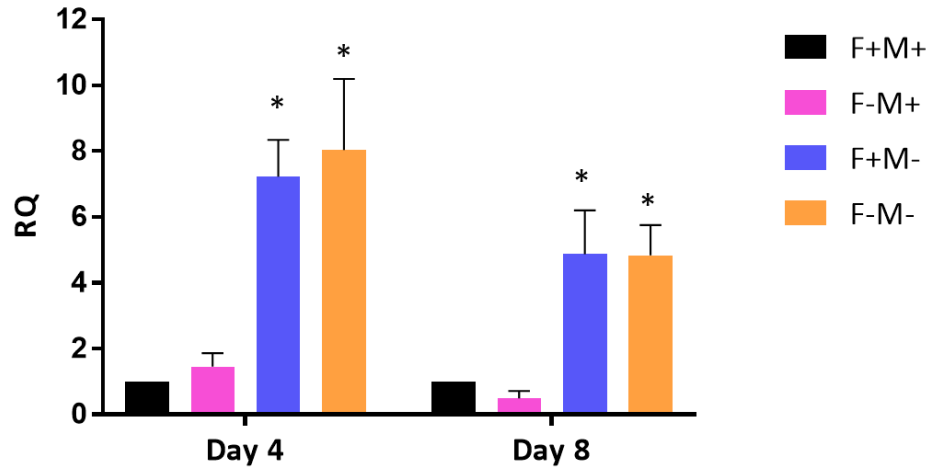


Figure 4.16 *IFIT1* expression in complete and methyl depleted media

This figure shows *IFIT1* expression in complete medium (F+M+), folate depleted medium (F-M+), methionine depleted medium (F+M-) and folate and methionine depleted medium (F-M-). Each value shows mean of three-independent experiments and error bars show SEM.

* significantly different from control (F+M+), $P<0.05$ (one-way ANOVA, Bonferroni's post hoc test).

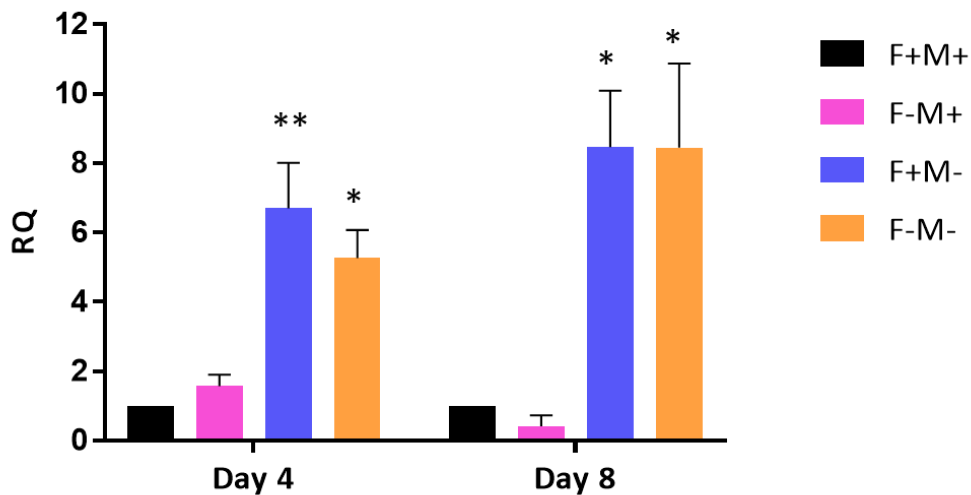


Figure 4.17 *ISG15* expression in complete and methyl depleted media

This figure shows *ISG15* expression in complete medium (F+M+), folate depleted medium (F-M+), methionine depleted medium (F+M-) and folate and methionine depleted medium (F-M-). Each value shows mean of three-independent experiments and error bars show SEM.

* significantly different from control (F+M+), $P<0.05$; ** significantly different from control (F+M+), $P<0.01$ (one-way ANOVA, Bonferroni's post hoc test).

4.5 Discussion

The bioinformatics analysis of the microarray datasets indicated an upregulation of genes associated with antiviral response in folate and methionine depletion. Though microarray data provides the opportunity for comparing whole genome profiling between samples, the quality of gene expression data varies greatly with platform and procedures being used (Morey et al., 2006). In addition, microarray may report false positives/negatives even with FDR correction (Miron et al., 2006). In this study, the quantitative RT-PCR technique was used to further investigate the gene expression results obtained from microarray analysis. In order to conduct this experiment, the methyl donor depletion cancer cell model was first validated prior to gene expression analysis. Three representations of methyl donor depletion were used; folate depletion (F-M+), methionine depletion (F+M-) and folate and methionine depletion (F-M-). DMEM media was customized to be made without folate, methionine and choline, and methyl donor nutrients were added accordingly to achieve the required state of depletion. The presence of folate and methionine in the growth serum being used together with the DMEM media, will provide a minimal amount of these nutrients to the cells, maintaining some growth in the depleted cells. The media and intracellular nutrient levels were assayed in order to confirm deficiency.

4.5.1 Validation of cervical cancer cell model of methyl donor depletion

In order to validate the methyl donor depletion cervical cancer cell model, an experiment to determine C4-II cervical cancer cell growth, intracellular folate concentration, intracellular methionine concentration and homocysteine concentration in complete and depleted media was conducted.

a. Effect of methyl donor depletion on C4-II cervical cancer cell growth

In the first part of the experiment where the effects of methyl donor depletion on cell growth was measured, cells treated with complete and folate depleted media appeared to grow at a similar rate up till day four, where the rate of growth in folate deprived cells started to decrease with a significantly lower number of cells at day eight (**Figure 4.2**). In contrast, the number of C4-II cells in methionine, and folate and methionine depleted media appeared to be stagnant throughout the culture period. A similar outcome was seen by Poomipark, who conducted a similar experiment to determine the effects of methyl donor depletion on C4-II cervical cancer cell growth (Poomipark, 2013; Poomipark et al., 2016). She had grown the C4-II cervical cancer cell line in Waymouth complete media, folate depleted media, and folate and methionine

depleted media for 12 days. It was clearly seen that the cells grew at a similar rate up to day four, regardless of the treatment they received. However, from day five onwards, cells grown in the complete media grew at a faster rate compared to cells in folate or folate and methionine depleted media. It was reported that the growth rate was significantly different for all three treatments ($P < 0.001$) and it was influenced by time and treatment ($P < 0.001$). A significant interaction was also detected between time and treatment ($P < 0.001$).

When comparing cell growth of C4-II cells in the current experiments to Poomipark, cells grown in DMEM complete medium grow at a faster rate than cells grown in Waymouth complete medium (doubling rate 54 vs 66 hours); possibly because of the nutritional differences between the media (**Table 4.5**). DMEM folate depleted medium also appears to support cell growth better than Waymouth folate depleted medium (doubling time 72 vs 87 hours); possibly because DMEM folate depleted medium has a higher folate content (0.3-0.6 mg/L) than Waymouth folate depleted medium (estimated < 0.01 mg/L). Contrarily, the deficiencies of both folate and methionine caused a longer doubling time in DMEM (415 vs 122 hours); possibly because DMEM methionine depleted medium has a lower methionine content (< 1.45 mg/L) than Waymouth folate depleted medium (estimated ~ 3 mg/L). Again, these differences could also be due to other nutritional differences between DMEM and Waymouth medium formulation.

An unpublished work from this department also found that the use of different media can affect the growth of cells differently (Shafie, 2014). In this experiment, C4-II cervical cancer cells grown in three different standard media (Waymouth, DMEM and RPMI) for 14 days demonstrated doubling times of 57, 26 and 33 hours respectively. The same study also measured the growth of C4-II cells in folate and methionine depleted RPMI medium compared to complete Waymouth and DMEM medium. It appears that all the C4-II cells followed linear a growth curve from day 0 to 6, after which the cells started to grow exponentially in all media except RPMI depleted medium. The doubling time for cells grown in RPMI depleted media was 247 hours, compared to 415 hours in the current study and 122 hours in Poomipark's study. Additionally, it has been demonstrated that in DMEM medium, a depletion of methyl donors (folate and methionine) to 5% or less of standard levels is required to significantly affect the doubling time of C4-II cells (Shafie, 2014); while a depletion to 25% or 50% of standard levels did not significantly affect C4-II cell growth. Furthermore, a measurement of MTT (3-(4, 5-dimethylthiazolyl-2)-2, 5-diphenyltetrazolium bromide) reported that a depletion to 25% or 50% of standard levels did not significantly affect cell proliferation as compared to the depletion

of less than 5% of standard levels. Besides the medium used, other study had also indicated that the growth of cells can also differ depending on cell passage number and investigator laboratory expertise (Kwist et al., 2016).

There are other depletion models of methyl donor nutrients in cancer cells that have been developed at different levels of depletion. The effect of folate depletion appears to be conditional upon types of cells being used as well as the severity of folate depletion (Kim, 2005). In a more recent study, two head and neck squamous cell carcinoma (HNSCC) cell lines, UD-SCC2 (HPV-16-positive) and UPCI-SCC72 (HPV-negative) cells were cultured in complete RPMI medium as well as; at different levels of folate, methionine and choline depletion for eight days (0%, 5%, 10% and 40% of complete methyl donor concentrations). The methyl donors for the depleted cells were gradually reduced during the first four days of culture (Hearnden et al., 2018). Both cell lines reported a significant dose-dependent reduction in cell number ($P < 0.001$) after seven days of culture, though UPCI-SCC72 was more susceptible to methyl donor depletion. The doubling time for cells grown in complete medium was 39 hours, but 86 hours for cells with 90% methyl donor depletion, 124 hours for 95% depletion and 741 hours for 100% depletion. They conclude that with methyl donor depletion, there was a significant reduction in proliferation and migratory capacity. In addition, there was an upregulation of genes associated with apoptosis and an increasing level of apoptosis, suggesting that a methyl donor deficient diet may significantly affect the growth of established HNSCC.

Evidence shows that severe deficiencies of folate and/or methionine would impair cell growth, and this was also observed in this study. Folate does not only provide methyl donors to the one carbon cycle for the methylation process, but it is also essential for DNA synthesis and repair by providing 5,10-methylene tetrahydrofolate to convert uracil into thymine (Grant et al., 2002). Thus, its deficiency inhibits DNA synthesis and cell proliferation, while increasing DNA damage (Duthie et al., 2008). Furthermore, methionine an essential amino acid that cannot be synthesized by animals, plays an important role in the synthesis of virtually all eukaryotic proteins (Brosnan & Brosnan, 2006). The depletion of methyl donor nutrients results in low levels of S-adenosylmethionine (SAM), and this could lead to cell cycle arrest, primarily at the G1 phase of the cell cycle, as has previously been reported in human and murine B cells with reduced levels of methionine and SAM (Lin et al., 2014). Consequently, methionine deficiency has been found to suppress cell proliferation rates and affects cell differentiation in various cell lines (Castellano et al., 2017; Saito et al., 2017). Inhibition of cell proliferation was also found in methionine deficient neuroblastoma, where the cells were arrested at the G2 phase of the cell

cycle (Hu & Cheung, 2009; Hoffman et al., 2019). In the current study, only cell viability data based on cell count was recorded. An additional analysis to determine cell proliferation rate in the current study might provide a more accurate and comprehensive data on the effect of methyl donor depletion in C4-II cell growth.

The role that folate plays in DNA synthesis and cell division is well understood and this is the basis for the use of anti-folate drugs in cancer treatment. A decrease in methyl donor availability is expected to lead to a fall in cell proliferation and this is what was observed in this study. Compared to folate, evidence on methionine is limited. However, it is suggested that normal cells can synthesize sufficient methionine for growth requirements from homocysteine, 5-methyltetrahydrofolate and vitamin B₁₂ via the methionine cycle, thus they are relatively resistant to exogenous methionine restriction. However, many cancer-cell types require exogenous methionine for survival (Chaturvedi et al., 2018), thus it could explain the severe growth retardation in methionine-deficient C4-II cervical cancer cells observed in this study. Additionally, recent studies are currently exploring the effect of dietary methionine restriction as an enhancer to the effect of cancer chemotherapy regimen in metastatic cancer (Thivat et al., 2007; Durando et al., 2010), melanoma, and glioma (Thivat et al., 2007). Methionine restriction has been reported to be effective against carcinomas (Birnbaum et al., 1957), and has led to the inhibition of colonic tumour growth (Komninou et al., 2006) and prostatic intraepithelial neoplasia (Sinha et al., 2014), in preclinical studies using rat models.

b. Effect of methyl donor nutrient depletion on intracellular folate, intracellular methionine and homocysteine concentrations

In this study, the depletion of folate and/or methionine leads to a significant reduction in intracellular folate and methionine concentrations at day four of culture, with a significant elevation of extracellular homocysteine at day eight, thus confirming the disturbance to the methyl cycle caused by methyl donor depletion (Nakano et al., 2005; Poomipark, 2013; Poomipark et al., 2016; Hearnden et al., 2018).

Similar to this study, Poomipark et al. reported that with folate, or folate and methionine depletion, the level of intracellular folate concentration in C4-II cells was significantly reduced by 90% at day four of culture; with a decreasing trend from day 8 to 12 of culture (**Figure 4.3**) (Poomipark et al., 2016). There was a significant difference between folate availability ($P < 0.0001$) over the period of 12 days ($P < 0.001$), with significant interaction between folate status and time ($P < 0.001$). At day four, the intracellular folate concentration in complete

medium (F+M+) was 2 pmol/10⁶ cells, whilst folate depleted medium (F-M+ and F-M-) had concentrations of 0.1 – 0.3 pmol/10⁶ cells. In this study, the overall concentration of intracellular folate was much higher with 2.5 – 3.4 pmol/10⁶ cells for folate depleted conditions (F-M+ and F-M-); and 32.3 pmol/10⁶ cells in complete medium. As mentioned above, this is possibly because DMEM complete and folate depleted medium have a higher folate content (5.6-5.7 mg/L and 0.3-0.6 mg/L, respectively) than in Waymouth medium (0.4mg/L and <0.01mg/L, respectively).

A significant reduction of intracellular methionine concentration was also detected in C4-II cells when the media was depleted of both folate and methionine, with a significant difference between methionine depletion treatment (P=0.001) over the period of 12 days (P=0.05) (**Figure 4.4**) (Poomipark et al., 2016). The intracellular methionine concentration of folate and methionine deprived cells fell to 100 pmol/10⁶ cells at day four of culture as compared to cells grown in complete medium, which reported a concentration of 300 pmol/10⁶ cells. In this study, there was a lower intracellular concentration of methionine overall, with 55 – 64 pmol/10⁶ cells in methionine depleted cells (F+M- and F-M-) and 222 pmol/10⁶ cells in complete medium. As mentioned above, this is possibly because DMEM complete and methionine depleted medium has a lower methionine content (30 mg/L and <1.45 mg/L, respectively) than in Waymouth medium (45mg/L and ~3 mg/L, respectively).

Consistent with this study, an elevated extracellular homocysteine was also reported with a significant effect of time (P<0.001) and methyl donor depletion treatment (P<0.001), with significant interaction between treatment and time (P<0.001) (**Figure 4.5**) (Poomipark et al., 2016). Both folate depletion, and folate and methionine depletion showed a significant increase of extracellular homocysteine at day 12, while only folate depletion showed a significant difference at day eight of culture, when compared to the cells grown in complete medium. Contrarily, this study reported a significant increase in extracellular homocysteine for all methyl depleted conditions at day eight. This is possibly due to other nutritional differences between the medium used, especially the presence of other methyl donor nutrients such as choline.

The *in vitro* cancer cell model of methyl donor depletion developed by Hearnden and colleagues using the UD-SCC2 HNSCC cell line containing HPV-16 referred to above, found an elevated concentration of extracellular homocysteine, measured using HPLC, in 95% methyl donor depleted condition after three days of culture (Hearnden et al. 2018). At day seven, the

difference between homocysteine concentrations in complete medium and depleted medium reached a statistical significance ($P < 0.05$). Comparing cells grown in complete and depleted media, intracellular methionine was reduced at day three of culture and a significant difference ($p < 0.05$) was detected at day seven of culture. A similar trend was observed for intracellular choline and betaine.

There are studies of the effects of folate and methionine depletion in other cancer and non-cancer cell models. A study of isolated human umbilical vein endothelial cells (HUVECs) grown in different folate (0 to 0.4 mg/L) or methionine (at 0, 15 mg/L or 30 mg/L) medium concentrations in order to investigate the role of homocysteine in atherosclerosis reported that folate deficiency leads to increased homocysteine export, with strong negative correlation between intracellular folate and extracellular homocysteine concentrations ($R = -0.71$, $P < 0.005$) (Nakano et al., 2005). A higher methionine concentration in the medium was also found to further exacerbate the impact of folate depletion on homocysteine export.

Similar to the current study, intracellular folate concentration of NIH/3T3 mouse fibroblast cells and CHO-K1 Chinese hamster ovary cells fell significantly by 91% and 94% respectively, when grown in folate depleted medium for 12 days (Stempak et al., 2005). In the same study, two human colon adenocarcinoma cell lines, HCT116 and Caco-2 grown in folate depleted RPMI medium for 20 days also showed significant reductions in intracellular folate concentrations of 88% and 98%, respectively. These cells were grown in either RPMI medium containing 0 (depleted) or 0.9 mg/L (complete) folic acid. Folate depleted cells were still able to grow, but at a significantly slower rate than cells in complete medium. In another study, the effect of long-term folate depletion on a prostate cancer cell line derived from transgenic adenoma of the mouse prostate (TRAMP) demonstrates that folate depletion (0.04mg/L) significantly reduced intracellular folate concentration by 50 to 60% after 20 population doublings, with less than 10ng/5 x 10⁶ cells as compared to complete cells (20-70ng/5 x 10⁶ cells) (Bistulfi et al., 2010). As in other studies, folate depleted cells still grew, but at a significantly slower rate than cells in complete medium. It has been suggested that folate deficiency may trigger an increase in the expression of folate receptor genes as a compensatory mechanism, which in turn supports minimal cell growth (Kelemen, 2006).

This study has shown that C4-II cervical cancer cells grown in folate and /or methionine depleted DMEM medium had exhibit disruption of the methyl cycle, characterized by elevated extracellular homocysteine concentrations. The folate concentration in folate depleted media

was reported to be (0.3 – 0.6 mg/L) compared to medium with folate (5.6 – 5.7 mg/L). The methionine concentration in methionine depleted media was reported to be (<1.45 mg/L) compared to the medium with methionine (27 – 29 mg/L). In comparison with Poomipark's, this model appears to represent a more severe methionine depletion than folate. However, the depletion of these methyl donor nutrients presented an appropriate level of intracellular methyl donor nutrient depletion for the determination of associated differences in gene expression.

4.5.2 Effect of methyl donor depletion on the expression of interferon-stimulated genes

In this study, the expression of four IFN-stimulated genes (ISGs) i.e. *RASD2*, *OAS1*, *IFIT1* and *ISG15* as well as *STAT1* in C4-II cervical cancer cells grown in complete and methyl depleted medium were determined using quantitative RT-PCR. C4-II cells grown in methionine depleted medium (F+M- and F-M-) showed a significant upregulation of all ISGs at day four and eight of culture (**Figure 4.13 to Figure 4.17**). On the other hand, *STAT1* was significantly upregulated at day four but was downregulated in all three methyl depleted conditions at day eight.

Events such as persistent viral infection increases IFNs production, initiating a signalling cascade through the Janus kinase signal transducer and activator of transcription (JAK-STAT) pathway (Sadler & Williams, 2008). **Figure 4.18** shows stimulation of ISGs by type 1 IFN signalling pathway in the event of a viral infection. It is suggested that the suppression of type 1 IFN signalling may help developing tumours evade the critical early step of immune recognition and clearance (Schneider et al., 2014).

Radical S-adenosyl methionine domain-containing 2 (*RSAD2*), also known as viperin (virus inhibitory protein, endoplasmic reticulum associated, or IFN inducible) is an antiviral protein gene (Helbig & Beard, 2014); where its function also depends upon S-adenosylmethionine (SAM) availability (Feld et al., 2011). *RSAD2* is stimulated by type I, II and III interferons (IFN), double-stranded DNA analogs, RNA analogs, and by infection with many RNA and DNA viruses (Nasr et al., 2012). An overexpression of this gene is associated with an increased apoptosis in response to CD40 ligation in HPV-infected epithelial cervical cells (Tummers et al., 2014). CD40 is a cell surface receptor that belongs to the tumour necrosis factor-R (TNF-R) that acts as a molecular signal in adaptive immune response (Elgueta et al., 2009). It is also suggested that *RSAD2* may function as a signal for innate antiviral immunity pathways by stimulating CD-40 ligand-mediated induction of the NF- κ B; a key regulator of

inflammatory immune response involved in regulating cytokine production, in carcinoma cells (Moschonas et al., 2012). However, the suppression of viruses by *RSAD2* may be dependent on its activity as a radical S-adenosylmethionine (SAM) enzyme (Duschene & Broderick, 2010; Shaveta et al., 2010). SAM has been shown to improve IFN signalling and antiviral defence, as it participates in many methylation reactions, such as STAT1-DNA binding leading to an increase in IFN activity (Bing et al., 2014). This suggests that methyl donor availability may be critical for the expression of *RSAD2* and mutations in SAM domains, as DNA methylation triggered by methyl donor status might affect both cancer-protecting genes and the HPV genome, as the disease progresses.

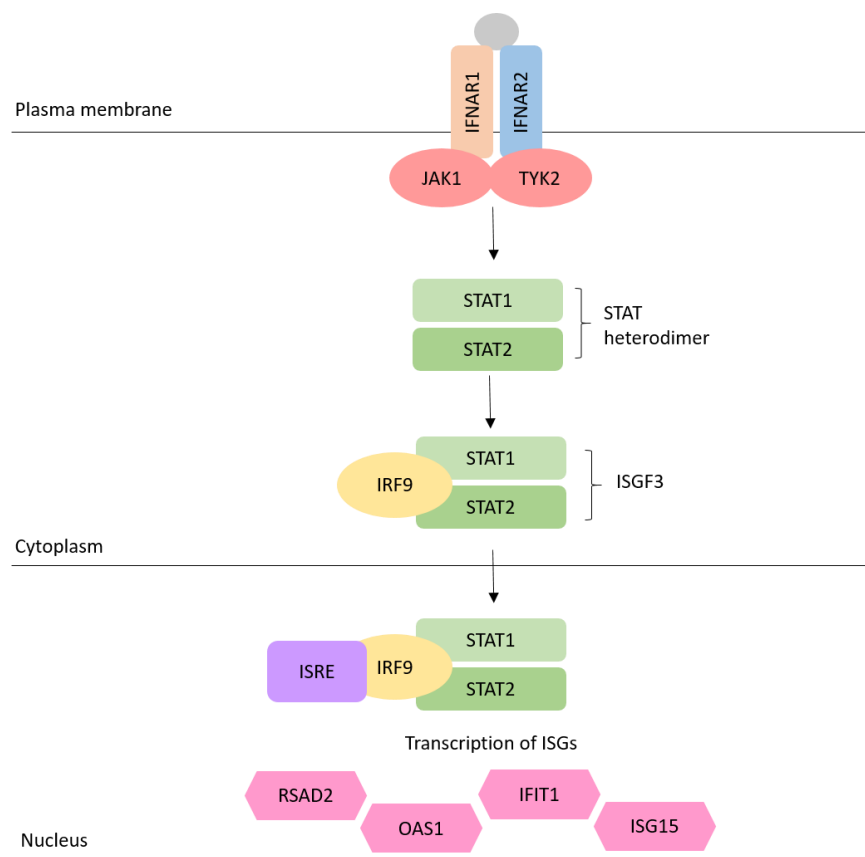


Figure 4. 18 Type 1 interferon signalling pathway involved in antiviral immunity

In the event of viral infection, IFNs production increases and binds with receptor IFNAR1 and IFNAR2, activating a signalling cascade through the Janus kinase signal transducer and activator of transcription (JAK-STAT) pathway via JAK1 and TYK2 kinases. This leads to phosphorylation of *STAT1* and *STAT2*. Together with IFN regulatory factor 9 (IRF9), the STAT heterodimer forms IFN-stimulated transcription factor (ISGF3). Once this complex arrives in the nucleus, it induces the IFN-stimulated genes (ISG) from interferon-stimulated response element (ISRE) to order to mediate antiviral response. This figure was adapted from (Sadler & Williams, 2008).

Oligoadenylate-synthase 1 (*OAS1*) is also an antiviral gene involved in the detection of foreign RNA, that can precipitate indiscriminate cleavage of both host and viral RNA and the

production of additional pathogen-associated molecular patterns (PAMPs), which reinforce the innate immune response (Sadler & Williams, 2008). *OAS1* has been found to catalyse the synthesis of 2'-5'-linked oligomers of adenosine from ATP, which specifically activate the latent form of RNaseL leading to RNA degradation (Maia et al., 2016). Changes to the *OAS1* gene have been associated with various diseases, caused by viral infections. For example, the polymorphism of *OAS1* leads to susceptibility of SARS disease and progression (Hamano et al., 2005). It has been reported that the downregulation of *OAS1* expression is significantly correlated with poor pathologic differentiation, lymph node metastasis, distant metastasis, and advanced TNM stages of colorectal cancer (Kuang et al., 2017). Furthermore, it is suggested that the low level of *OAS1* in breast and prostate cancer disrupts the *OAS1*/RNaseL apoptosis pathway (Maia et al., 2016).

Tetratricopeptide repeats 1 protein (*IFIT1*) inhibits virus replication by binding and regulating the functions of cellular and viral proteins and RNAs (Fensterl & Sen, 2015). *IFIT1* inhibits the replication of viruses by competing with the viral DNA binding sites, preventing the translation of viral mRNA. In the context of *IFIT1* gene expression and cancer, an association of the downregulation of *IFIT1* gene expression is reported in ovarian cancer, where it is associated with a progression and poor cancer prognosis (Gyorffy et al., 2008). On the other hand, *IFIT1* was also upregulated in various cancers including colorectal, gastric and oesophageal, where it is associated with a progression and poor cancer prognosis (Yu et al., 2015; Borg et al., 2016). Recently, a study to determine the mechanism and clinical significance of *IFIT1* and *IFIT3* expression on oral squamous cell carcinoma (OSCC) cells associated the overexpression of *IFIT1* with increased cell proliferation and invasive activity (Pidugu et al., 2019b). They also reported significantly higher percentages of advanced tumour stage, lymph node metastasis, perineural invasion, lymphovascular invasion, and extranodal extension in patients with tumour elevated *IFIT1*. OSCC patients with high *IFIT1* levels showed a significantly lower 5-year survival rate than those with lower *IFIT1* levels.

Interferon stimulated gene 15 (*ISG15*) is part of ubiquitin-like pathway that modulates the function of numerous protein targets. The expression of this gene is associated with the regulation of type 1 IFN and activation of Natural Killer (NK) cells, both of which are important mediators of tumour immunity (Liang et al., 2014). *ISG15* has been found to suppress tumour growth both by increasing the number of infiltrating NK cells, and enhancing major histocompatibility complex (MHC) class I expression in breast cancer cells (Burks et al., 2015). However, several studies have reported elevated *ISG15* levels in various

cancer cells including breast, oral squamous cell and endometrium (Desai et al., 2006; Bektas et al., 2008; Laljee et al., 2013). There is also an association of *ISG15* in hepatocellular carcinoma (HCC) with increased tumour grades, increases metastases and reduced survival rates suggesting its potential to promote tumour growth (Li et al., 2014).

Besides the ISGs, the signal transducer and activator of transcription 1 (*STAT 1*) gene is also a crucial component of IFN signalling, mediating cellular responses towards cytokines and other growth factors (Zhang & Liu, 2017). The *STAT1* protein is a functional transcription factor that facilitates crosstalk between signal transduction pathways; involved in activation of specific genes such as interferon regulatory factor 1 (*IRF1*) and antigen peptide transporter 1 (*TAP1*) (Ramana et al., 2000). *STAT1* plays an important role in biological processes of normal cells such as cell death promotion, cell growth inhibition, immune system stimulation and cell differentiation regulation (Zhang & Liu, 2017). A deficiency of *STAT1* has been found to impair TNF- α/β response, resulting in lethal viral disease in patients with mutated *STAT1* alleles (Dupuis et al., 2003; Jouanguy et al., 2007). This suggests that the impairment of *STAT1* increases the susceptibility to viral disease by disrupting the *STAT1*-dependent responses.

In the context of cancer, *STAT1* plays a crucial role as a tumour suppressor, through its capacity to induce the immune system and promote tumour immune surveillance (Koromilas & Sexl, 2013). Studies have reported a downregulation of *STAT1* in various cancer cells including lung, colorectal, gastric and oesophageal (Chen et al., 2015; Zhang et al., 2014; Zhang et al., 2017), while an increase of *STAT1* expression in patients with breast and gastrointestinal cancers has been associated with a better cancer prognosis (Widschwendter et al., 2002; Deng et al., 2012). Several mechanisms for *STAT1* tumour suppressor function have been proposed, including promoting apoptosis and cell cycle arrest, improving immune-surveillance and reducing metastasis and angiogenesis (Zhang & Liu, 2017). However, an elevated *STAT1* expression appears to worsen the clinical outcome of some cancers and several studies have highlighted the oncogenic potential of *STAT1* (Duarte et al., 2012; Magkou et al., 2012), with aberrant expression of this gene identified in breast and, head and neck cancers (Buettner et al., 2002; Greenwood et al., 2012). In this study, differing results have been yielded regarding *STAT1* expression in methyl depleted conditions. In the microarray analysis, *STAT1* was significantly upregulated in the absence of folate and methionine. Contrarily, quantitative RT-PCR analysis of *STAT1* gene expression did not indicate a significant difference between complete and methyl depleted medium. This could possibly be due to the limitation of the microarray method being used, where a false positive/negative might be reported even with

FDR correction (Miron et al., 2006). Additionally, the quantitative RT-PCR gives a better idea of the true effect size of the regulation of a particular gene and/or compare the expression of different genes; where microarray is hybridization based and therefore the orders of magnitude are limited.

The IFN-induced genes play a critical role during viral infection through their ability to mediate antiviral activities. However, due to the conflicting findings regarding some of these genes, it is difficult to conclude if their functions promote tumour suppression or growth. Additionally, a number of ISGs also participate in cell growth regulation and apoptosis process, where the severe depletion of methyl donor might led to the upregulation of these genes (Kalvakolanu, 2000). More extensive work and experimental study needs to be conducted in order to validate the mechanistic nature of these ISGs and its functional impact in host defence and immune function. Nonetheless, in this study, the ISGs *RASD2*, *OAS1*, *IFIT1* and *ISG15* were found to be significantly upregulated with folate and methionine depletion in the microarray analysis, and this was validated by quantitative RT-PCR analysis. This suggests a potentially important role of methyl donor nutrients in regulating IFN-stimulated genes in cervical cells, especially during the initial phase of HPV viral infection.

4.6 Summary

In this chapter, it has been observed that depletion of folate, methionine or both nutrients have significantly reduced the growth rate of C4-II cervical cancer cells, with a greater effect from the deficit of methionine than folate. The C4-II cervical cancer cell model of methyl donor depletion was validated by a significant reduction of intracellular folate concentration in folate depleted media (F-M+ and F-M-) and a significant reduction of intracellular methionine concentration with methionine depletion (F+M- and F-M-) at both day four and eight of culture. The elevated extracellular homocysteine at day eight of culture also indicates a functional depletion of methyl donors. Similar to the microarray analysis, all IFN-stimulated genes (*RSAD2*, *OAS1*, *IFIT1*, *ISG15*) showed a significant upregulation in the folate and methionine depleted condition after eight days of culture. In addition, it demonstrated that methionine depletion affects the expression of these genes in a similar manner. In contrast, the absence of folate did not cause a significant alteration to the gene expression. This study highlights the regulatory functions of methyl donor nutrients on IFN-stimulated gene expression associated with antiviral immunity and also the importance of methionine as a methyl donor in the regulation of gene expression.

CHAPTER 5

EFFECT OF METHYL DONOR DEPLETION ON CYTOKINE PRODUCTION IN THE HUMAN THP-1 MONOCYTIC CELL LINE

5.1 Introduction

Persistent infection of the cervix with HR-HPV has been reported as a necessary causative factor for development of cervical cancer (zur Hausen, 2009; Okunade, 2020), however, HPV infections usually resolve spontaneously, without causing symptoms or illness (Farzaneh et al., 2006; Ferlay et al., 2015). Nonetheless, a small proportion of high-risk HPV infections may persist and progress to pre-cancerous intraepithelial lesions and cervical cancer (Nagai et al., 2001; Łaniewski et al., 2020). The fact that several women infected with HPV never develop cervical cancer indicates that HPV is a necessary factor, but not a sufficient cause for the carcinogenesis. Studies have reported that other variables, such as immune response, genetic predisposition and environmental, are involved in the increased risk for cervical carcinoma (Castellsagué et al., 2002; Tamandani et al., 2009; Mayadev et al., 2018). Cellular immunity is necessary for clearing HPV-infected and HPV-transformed tumour cells, where HPV infection abrogates initial steps of the innate immune system, involving Toll-like receptor signalling and cytokine synthesis and secretion. Although some viral infections elicit strong host immune responses and are consequently eliminated, HPV have been reported to effectively evade such immune recognition, thereby allowing the establishment of persistent viral infection (Stanley & Sterling, 2014).

Several tissue cell types of the immune system secrete cytokines, which are small polypeptides or proteins that have pleotropic functions at the local tissue level or occasionally at systemic level (Paradkar et al., 2014). Cytokines function synergistically and control the growth, differentiation or activation of different cell types. Cytokines are essential in defending against HPV infection, and act through cytokine receptors on the cell membrane or soluble plasma or tissue fluid receptors. Initially, cytokines were only considered as the immune system's messenger molecules whose function was to guide leucocytes to the inflammation sites. Recent literature however, has shown that when dysregulated, cytokines have been associated with most neoplastic tissues and they may even have a role in malignant transformation, proliferation, survival, angiogenesis, invasion and metastasis. Now almost 50 cytokines have been identified and some of these or their receptors are significantly altered in carcinogenesis and metastasis of cervical cancer. However, the association and mechanism

between cytokine production and the development of cervical neoplasia is controversial and poorly understood, as in-depth knowledge about the natural history of the HPV life cycle, the specific host immune response and other factors including experimental conditions are still lacking (Otani et al., 2019).

Several cytokines have been identified to play an important role in modulating the immune responses against HPV infection and may contribute to the progression of cervical cancer (Paradkar et al., 2014). Cytokine activation is presumed to occur shortly after establishment of HPV infection, leading to mucosal expression of candidate antiviral (INF- α), type-1 (IFN- γ and IL-12), regulatory (IL-10), and proinflammatory (IL-1 α , IL-1 β , IL-6, IL-8, MIP1- α , and TNF- α) cytokines (Scott et al., 2013). These cytokines help to modulate viral replication and polarize the immune response to a Th1 (cellular) or Th2 (humoral) pattern. Classically, Th1-type cytokines generate immune-stimulating responses, where the production of interleukin (IL)-2 and interferon gamma (IFN- γ) have been associated with the clearance of HPV infection and regression of cervical intraepithelial neoplasia (CIN), while tumour necrosis factor alpha (TNF- α) is known to have antiviral properties (Bleotu et al., 2013; Torres-Poveda et al., 2016). They mainly induce cell mediated immunity and work as tumour suppressing cytokines. In contrast, Th2-type cytokines are immuno-inhibitory, and include IL-4, IL-5, IL-6, IL-8, and IL-10 for cell mediated immunity and primarily induce humoral immunity (Bais et al., 2007); where an excess Th2 response may counteract Th1-mediated actions, leading to HPV persistence and progression of squamous intraepithelial lesion (SIL) (Wang et al., 2018).

It has been reported that HPV positive patients with CIN experience a pronounced shift from Th1 cytokine production to Th2 cytokine production, which suggests that the cytokine response to HPV infection influences the disease outcome (Conesa-Zamora, 2013). Additionally, Peghini et al. also reported that immunostimulatory signals (Th1 cytokine profile) are hampered whereas proinflammatory and immunosuppressor signals (Th2 cytokine profile) are stimulated in cervical cancer (Peghini et al., 2012). Th1 cytokines i.e. IL-1 (IL1-RN and IL-1 β), TNF- α , interferon, are potent activators of cell-mediated immunity that may precede HPV clearance, while Th2 cytokines i.e. IL-4, IL-6, IL-10 and TNF- β impair the immune response, leading to an inefficient virus elimination and chronic infection (Torres-Poveda et al., 2014). Furthermore, alteration in cytokine production has been observed in cervical pre-cancer and cancer stages, where some of these alterations could be specifically associated with HPV-related carcinogenesis. It is reported that the cytokine response in peripheral monocyte blood

culture differs significantly in the presence or absence of high-risk strains of HPV (Bais et al., 2007). They also found that the amount of cytokines differed based on the degree of neoplasia. On the other hand, several studies have also reported that increased levels of Th1-type cytokines, including TNF- α and IL-1 β , have been associated with persistent HPV infection and metastasis (Mota et al., 1999; zur Hausen, 2002; Bailey et al., 2014). It has been suggested that whilst Th1 cytokines are crucial for inducing an adequate anti-tumour immune response, continuous expression of Th1 cytokines can promote the chronic inflammatory process which causes generation of reactive oxygen and nitrogen species (Paradkar et al., 2014). These changes induce DNA damage and make the cells susceptible to neoplasia.

Tumour necrosis factor- α (TNF- α) is a multifunctional cytokine produced by monocytes and macrophages and plays an important role in promoting inflammatory response, cell proliferation, and inducing apoptosis (Das et al., 2018). It is a polypeptide that directly kills or inhibits tumour cells and plays an important role in the development and progression of tumours and is an important proinflammatory cytokine. The loss of TNF- α could lead to immune-surveillance failure, thus leading to HPV infection related cervical cancer development. In a study conducted among 75 cervical cancer cases, 25 CIN cases, and 50 healthy female controls; the gradient downregulation of TNF- α correlated with progression of the disease from normal/CIN/cervical cancer (Das et al., 2018). However, TNF- α has contradictory roles in the evolution and treatment of malignant disease (Balkwill, 2002). TNF- α selectively destroys tumour blood vessels with powerful anti-tumour actions when locally administered in high doses. In contrast, TNF- α may act as an endogenous tumour promoter when chronically produced, contributing to tissue remodelling and stromal development necessary for tumour growth and spread. Additionally, whilst the role of TNF- α in orchestrating an antitumor immune response against HPV expressing cervical cancer cells has been reported, results involving different study populations belonging to different ethnicity and pathological types are equivocal and inconclusive (Basile et al., 2001; Tjong et al., 2001; Das et al., 2018).

TNF- α expression is influenced by multiple pro-inflammatory and inflammatory cytokines such as IFN- γ and NF- $\kappa\beta$ which are the most important. Interferon gamma (IFN- γ) induces TNF- α production through promoter-dependent transcription (Vila-del Sol et al., 2008). IFN- γ produced by naive Th cells contributes to antitumor activity and has both direct toxic effect on cancer cells and antiangiogenic activity (Ramanakumar et al., 2010). Besides this, recent works using *in vitro* systems reported that TNF- α induction is dependent of nuclear factor-kappa B (NF- $\kappa\beta$) activation and expression (Wu et al., 2016). Being the central key pro-

inflammatory molecule, the role of NF- κ B in immune modulation and carcinogenicity has been established, though with conflicting results on its function as protector or promoter of cancer carcinogenesis (Pikarsky & Ben-Neriah, 2006). NF- κ B expression has been shown to be upregulated in cervical cancer (Prusty et al., 2005; Pallavi et al., 2015). Additionally, SNPs in the promoter region of the TNF- α gene were strongly associated with altered levels of gene expression and consequently, have been associated with susceptibility to HPV infection and cervical cancer (Duarte et al., 2005). Therefore, the negative or positive side of the deregulation of TNF- α expression in the pathogenesis of HPV linked cervical carcinogenesis requires a critical evaluation of other cofounding variables.

Another important group of cytokines that play an important role in modulating the immune responses against HPV infection is the interleukin-1 (IL-1) family (IL-1 α and IL-1 β) which are mediators of acute inflammation. Both, IL-1 α and IL-1 β have pro-inflammatory characteristics that induce the production of other inflammatory molecules (Paradkar et al., 2014). However, conflicting effects of IL-1 β in terms of tumour development have been observed. Due to the induction of type 1 and type 17 antigen-specific T cell responses, IL-1 β exerts anti-tumorigenic effects (Bent et al., 2018). Contrarily, IL-1 β within the tumour microenvironment can promote carcinogenesis, tumour growth, and metastasis by different key mechanisms such as driving chronic non-resolved inflammation, endothelial cell activation, tumour angiogenesis, and the induction of immune-suppressive cells. Clinically, a correlation between high levels of IL-1 β and worsening prognosis in cancer patients was observed, where studies have reported that high levels of IL-1 α/β in plasma and cervicovaginal secretions of women with CIN and cervical cancer (Qian et al., 2010). Similar to TNF- α , the impact of IL-1 β deregulation in the pathogenesis of HPV-linked cervical carcinogenesis requires a critical evaluation of other cofounding factors.

As stated earlier, in addition to HR-HPV infection, other variables such as immune response may contribute towards increased risk of cervical carcinoma. In **Chapter 4**, it was found that methionine and folate deficiency alter the expression of genes associated with host defence and immune response. The B vitamins including folate are involved in many functions but work predominantly as co-factors to enzymes involved in energy metabolism and the synthesis of organic molecules. Folate in particular, acts as a one carbon donor in nucleotide synthesis and DNA methylation, and through this function may play an essential role for the immune system (Depeint et al., 2006; Elmadfa & Meyer, 2019). Folate deficiency has been reported to have a negative effect on certain immune functions. In a study conducted using

PHA-activated human T lymphocytes, folate depletion was found to reduced proliferation of T lymphocytes and CD8(+), whilst folate repletion of folate-deficient cells rapidly restored T lymphocyte CD8(+) proliferation (Courtemanche et al., 2004). Folate deficiency was also associated with reduced maturation of dendritic cells, lower secretion of IL-12, TNF- α , IL-6 and IL-1 β by dendritic-stimulated cells with LPS, and impaired differentiation of CD4+ T lymphocytes. The secretion of cytokines inducing the development of Th1 was also reduced (Wu et al., 2017). On the other hand, oral high-dose administration of folic acid (160 μ g/d to 10 mg/d) reduced the inflammatory response in mice with allergic dermatitis by suppressing T cell proliferation and the secretion of the proinflammatory and Th2 cytokines IL-4, IL-5, IL-9, IL-13, IL-17, IL-33; TNF α and TSLP in a dose-dependent manner (Makino et al., 2019).

Whereas, in a human study conducted among 105 healthy postmenopausal women, dietary and supplemental intakes of folate and folic acid in relation to an index of immune function, natural killer cell (NK) cytotoxicity were determined; and among women with a diet low in folate (< 233 μ g/d), those who used folic acid-containing supplements had significantly greater NK cytotoxicity (P = 0.01) (Troen et al., 2006). However, those who consumed a folate-rich diet, and in addition were taking folic acid supplements of > 400 μ g/d had reduced NK cytotoxicity compared with those consuming a low-folate diet and no supplements (P = 0.02). This conflicting result could be due to the presence of unmetabolized folic acid in plasma, where unmetabolized folic acid was detected in 78% of plasma samples. This study also found an inverse relation between the presence of unmetabolized folic acid in plasma and NK cytotoxicity. This inverse relation was stronger among women 60 years or older and more pronounced with increasing unmetabolized folic acid concentrations (P-trend = 0.002). This indicates that in addition to folate or folic acid intake, there are other variables which may influence the effect of this nutrient towards immune responses.

In contrast, the role of methionine in the immune system via its function as one carbon cycle is less studied. However, in a recent study by Roy et al., methionine has been identified as a key nutrient affecting epigenetic reprogramming in CD4+ T helper (Th) cells (Roy et al., 2020). It is reported that methionine is rapidly taken up by activated T cells and serves as the major substrate for biosynthesis of the universal methyl donor S-adenosyl-L-methionine (SAM), where dietary methionine is required to maintain intracellular SAM pools in T cells. Methionine restriction reduced histone H3K4 methylation (H3K4me3) at the promoter regions of key genes involved in Th17 cell proliferation and cytokine production. In their mouse model of multiple sclerosis, dietary methionine restriction reduced the expansion of pathogenic Th17

cells *in vivo*, leading to reduced T cell-mediated neuroinflammation and disease onset. In another study, SAM has been suggested as an essential metabolite for inflammatory macrophages, where high a SAM:SAH ratio supports histone H3 lysine 36 trimethylation for IL-1 β production (Yu et al., 2019).

In order to explore the effect of methyl donor nutrient depletion directly on the immune system, the THP-1 cell line was used as the cell model for methyl donor nutrient depletion in this pilot study. THP-1 cells have been widely used as an *in vitro* model of human monocytes and macrophages in the study of inflammation-related immune responses (Daigneault et al., 2010; Chanput et al., 2014). Several studies have compared THP-1 cells with peripheral blood mononuclear cell (PBMC)-derived macrophages, and found that both exhibit similar morphological and functional properties (Daigneault et al., 2010; Mehta et al., 2010; Schroecksnadel et al., 2011). Therefore, THP-1 derived macrophages could be a suitable alternative for PBMC-derived macrophages in terms of cytokine production, cell morphology and macrophage surface markers. However, studies have also identified that the type of reagents used during the differentiation protocol affects the macrophage phenotype. Among the differentiation reagents, phorbol-12-myristate 13-acetate (PMA) has been observed to be most effective in obtaining THP-1 derived macrophages that are similar to PBMC-derived macrophages (Chanput et al., 2012; Bastiaan-Net et al., 2013; Chanput et al., 2013). A study comparing the effect of THP-1 cell differentiation using 1,25-dihydroxyvitamin D₃ (VD₃) or PMA with PBMC monocytes-derived macrophages on cell morphology and adhesion, surface markers expression and phagocytic activity found differences between these groups (Daigneault et al., 2010). However, a THP-1 differentiation protocol using 200 nM of PMA for 3 days, followed by 5 days of rest in a culture media without PMA developed THP-1 derived macrophages that closely resembled PBMC monocytes-derived macrophages. In a more recent study, a modified differentiation protocol with 20 ng/ml PMA and at least 48 hours incubation have been shown to enhance macrophage differentiation of THP-1 cells without induced cell death with a viability of 92.2% (Biriken et al., 2018).

Additionally, in this study, the THP-1 cells were adapted to DMEM medium. Changes were made with the medium as there was no cost-effective commercial sources of a basal RPMI medium at the point when the study was conducted, which excludes key methyl donor nutrients without some residue of these nutrients being present; while it was possible to obtain a basal DMEM medium that was fully modifiable.

5.2 Hypothesis and Aim

It is hypothesized that folate and/or methionine depletion will alter the production of cytokines in THP-1 derived macrophages. In order to test this hypothesis, the objective of this experiment is to determine the effect of methyl donor nutrient depletion on cytokine production in differentiated macrophages, derived from the THP-1 cell line.

5.3 Methods

5.3.1 Cell resuscitation

The THP-1 cells from liquid nitrogen were partially submerged in the water bath at 37°C to allow them to thaw. Cells were then transferred into a new centrifuge tube containing 5 mL of pre-warmed RPMI medium. The suspension was centrifuged at 1000 rpm for 5 minutes, at room temperature. The supernatant was discarded and the cells were re-suspended in 5 mL of pre-warmed RPMI medium. Then 20 µL of cell suspension was added to 20 µL of trypan blue in a microfuge tube for cell counting. Cells were counted using an automated cell counter. The number of total cells, live cells and cell viability (%) were recorded. Cells were seeded at 2×10^5 cells/mL, in 20 mL of pre-warmed RPMI medium. Cells were then incubated at 37°C and 5% carbon dioxide.

5.3.2 Cell subculture

THP-1 cells were observed under the microscope to assess the degree of confluency as well as signs of contamination. The cell suspension was transferred into a 50 mL falcon tube and centrifuged at 1000 rpm for 5 minutes, at room temperature. Then, 20 µL of cell suspension was added to 20 µL of trypan blue in a microfuge tube for cell counting. Cells were counted using an automated cell counter. The number of total cells, live cells and cell viability (%) were recorded. Cells were seeded at 2×10^5 cells/mL, in 20 mL of pre-warmed RPMI medium. Cells were then incubated at 37°C and 5% carbon dioxide. The cells were sub-cultured every three days to maintain optimal cell growth.

5.3.3 Differentiation of THP-1 cell and sample collection

THP-1 cells were resuscitated, cultured and maintained as described in **section 5.3.1 and 5.3.2**. Prior to setting up the experiment, the THP-1 cells that were initially cultured in RPMI medium were gradually adapted to the complete DMEM medium for a total of five passages with the following ratios of DMEM to RPMI: 50:50, 75:25, 87.5:12.5 and 100:0. At passage 19, the

THP-1 cell suspension was transferred into a 50 mL falcon tube and centrifuged at 1000 rpm for 5 minutes to pellet the cells. The cells were then re-suspended in 5 mL of 10% FBS in DPBS. Then, 20 μ L of cell suspension was added to 20 μ L of trypan blue for cell counting. Cells were counted using an automated cell counter. The numbers of total cells, live cells and cell viability (%) were recorded. Then 2 mL of fresh pre-warmed DMEM medium was pipetted into a 12-well plate and cells were seeded at 8×10^5 cells/well. The cells were seeded in four different DMEM media with three biological replicates: complete media (F+M+), folate depleted (F-M+), methionine depleted, (F+M-) and folate and methionine depleted media (F-M-).

In order to differentiate THP-1 cells into macrophages, cells were stimulated with 200nM of phorbol-12-myristate 13-acetate (PMA), followed by incubation at 37°C and 5% carbon dioxide for 3 days, where the newly formed macrophages will adhere to the surface of the well plate (Daigneault et al., 2010). The PMA-containing medium was replaced with fresh pre-warmed complete and depleted media, and the THP-1 derived macrophages were further incubated for 5 days. These cells were then stimulated with 10ng/ml of ultra-pure LPS for 20 hours in the incubator, to stimulate cytokine production. The spent media was collected and centrifuged at 10 000 x g for 10 minutes at 4°C. The supernatants were transferred into new tubes and stored as aliquots in -80°C. The experimental design of this study is summarized in **Figure 5.1**.

5.3.4 Determination of TNF- α concentration

The concentration of TNF- α in THP-1 samples were determined using the Quantikine ELISA Kit by R & D System, following the protocol provided by the manufacturer. Additionally, the Quantikine Immunoassay Control Group 1 by R & D Systems was used as the quantitative control in this experiment, where its concentration is known.

The TNF- α standard was reconstituted with 1.5 mL of distilled water to produce a stock solution at 10 000 pg/mL. The stock solution was allowed to sit for 15 minutes with gentle agitation prior to making 2-fold serial dilutions for 8 points, in order to generate a standard curve for result interpretation. The controls (Quantikine Immunoassay Control Group 1) were reconstituted by adding 2 mL of distilled water to each control vial and mixed thoroughly by vortex. Frozen THP-1 samples (**from section 5.3.3**) were thawed and centrifuged at 10 000 x g for 10 minutes at 4°C prior to use. Excess microplate strips were removed and 50 μ L of Assay

Diluent RD1F was added to each well, followed by 200 μL of standards, controls or samples in duplicate. The plate was covered with adhesive strip and incubated for 2 hours at room temperature. Then, each well was aspirated completely and washed with 400 μL of Wash Buffer for 3 times. In the next step, 200 μL of Human TNF- α Conjugate was added to each well, covered with a new adhesive strip and incubated for 1 hour at room temperature. Again, each well was aspirated completely and washed with 400 μL of Wash Buffer 3 times. Then, 200 μL of Substrate Solution was added to each well. After 20 minutes of incubation at room temperature, 50 μL of Stop Solution was immediately added into each well, where the colour should change from blue to yellow. The optical density (OD) of each well was determined within 30 minutes, using a microplate reader set to 450 nm and 540 nm.

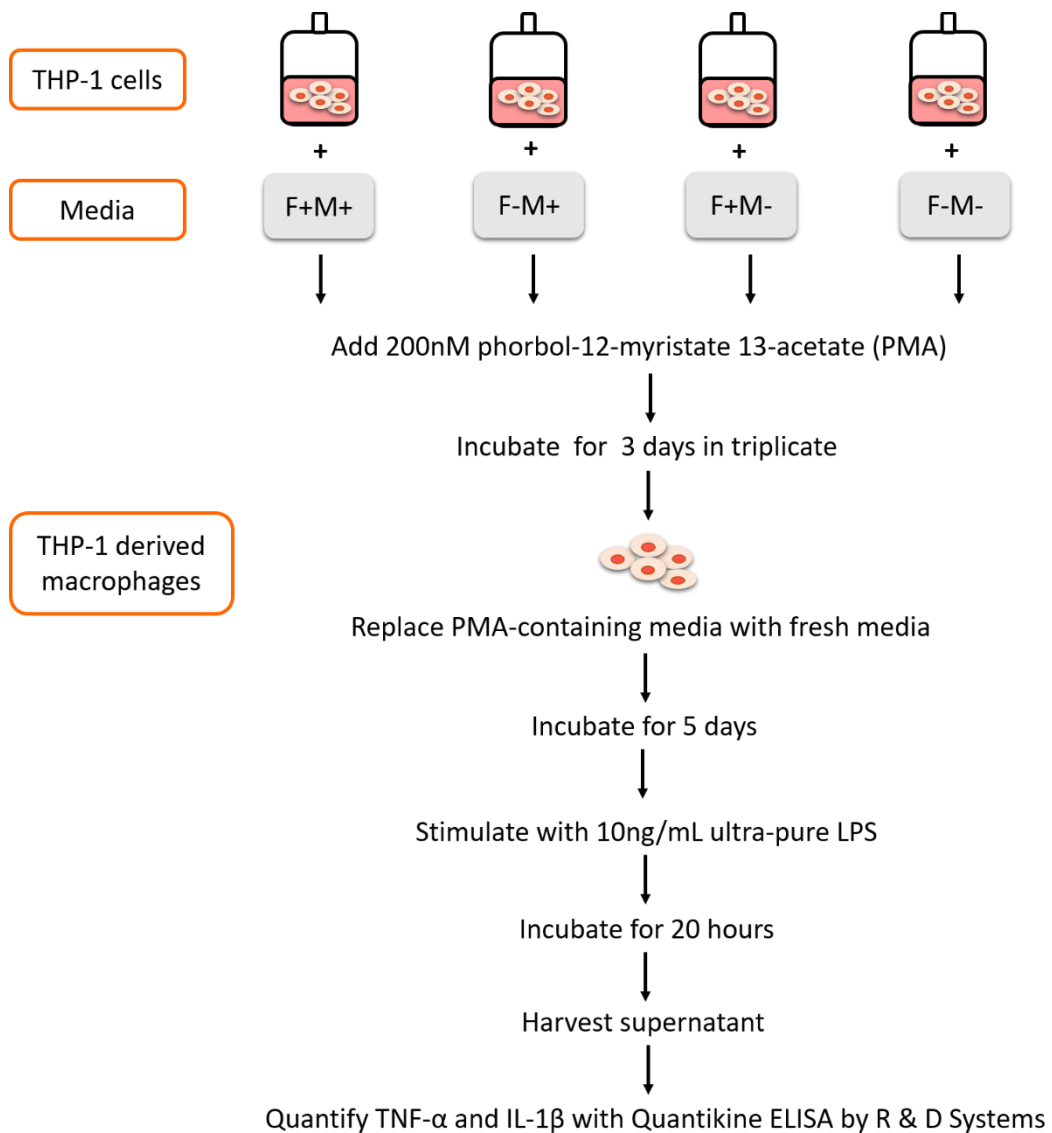


Figure 5.1 Effect of methyl donor depletion on cytokines production workflow

The average OD readings for each TNF- α standard, control and THP-1 sample duplicates were calculated and subtracted with the average zero standard OD readings. In order to correct for any optical imperfections in the plate, the readings were then corrected by subtracting the average OD readings at 450 nm with average OD readings at 540 nm. A linearized standard curve was constructed by plotting the log of the TNF- α concentration versus the log of the TNF- α standard OD. The best fit line was determined with linear regression using GraphPad Prism software. The sample and control results were interpolated from the generated standard curve.

5.3.5 Determination of IL-1 β concentration

The concentration of IL-1 β in THP-1 samples were measured using the Quantikine ELISA kit by R & D Systems, following the protocol provided by the manufacturer. Additionally, the Quantikine Immunoassay Control Group 1 by R & D Systems was used as the quantitative control in this experiment, where its concentration is known.

The IL-1 β standard was reconstituted with 1.5 mL of distilled water to produce a stock solution at 250 pg/mL. The stock solution was allowed to sit for 15 minutes with gentle agitation prior to making 2-fold serial dilutions for 8 points in order to generate a standard curve for result interpretation. The controls (Quantikine Immunoassay Control Group 1) were reconstituted by adding 1.5 mL of distilled water to each control vial and mixed thoroughly by vortex. Frozen THP-1 samples (**from section 5.3.3**) were thawed and centrifuged at 10 000 x g for 10 minutes at 4°C prior to use. Excess microplate strips were removed and 200 μ L of standards, controls or samples were pipetted into the wells in duplicate. The plate was covered with adhesive strip and incubated for 2 hours at room temperature. Then, each well was aspirated completely and washed with 400 μ L of Wash Buffer for 3 times. In the next step, 200 μ L of Human IL-1 β Conjugate was added to each well, covered with a new adhesive strip and incubated for 1 hour at room temperature. Again, each well was aspirated completely and washed with 400 μ L of Wash Buffer 3 times. Then, 200 μ L of Substrate Solution was added to each well. After 20 minutes of incubation at room temperature, 50 μ L of Stop Solution was immediately added into each well, where the colour should change from blue to yellow. The optical density (OD) of each well was determined within 30 minutes, using a microplate reader set to 450 nm and 540 nm.

The average OD readings for each IL-1 β standard, control and THP-1 sample duplicates were calculated and subtracted with the average zero standard OD readings. In order to correct for any optical imperfections in the plate, the readings were then corrected by subtracting the average OD readings at 450 nm with average OD readings at 540 nm. A linearized standard curve was constructed by plotting the log of the IL-1 β concentration versus the log of the standard OD. The best fit line was determined with linear regression using GraphPad Prism software. The sample and control results were interpolated from the standard curve.

5.3.6 Statistical analysis

Statistical analysis was conducted using GraphPad Prism 7. Three independent experiments were carried out and expressed as mean \pm SEM. One-way ANOVA was used to determine the effect of methyl donor depletion on outcome variables, followed by Bonferroni's post hoc test. P-value <0.05 was considered to be significant for all statistical analysis.

5.4 Results

5.4.1 Effect of methyl donor depletion on TNF- α production

Based on the corrected optical density (OD) readings for TNF- α standards, a linearized standard curve was constructed by plotting the log of the TNF- α concentration versus the log of the standard OD. The best fit line was determined with linear regression using GraphPad Prism software (**Figure 5.2**).

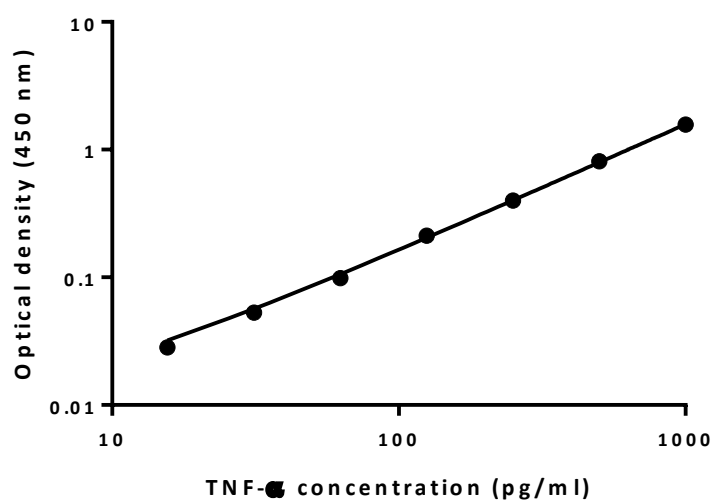


Figure 5.2 TNF- α standard curve

The standard curve $R^2 = 0.9997$; $y = 0.001574 (x) + 0.007557$

The sample and control results were interpolated from the standard curve. **Table 5.1** shows the concentration of TNF- α in the controls provided by Quantikine. All controls were within the acceptable range. **Figure 5.3** shows the concentration of TNF- α produced by differentiated macrophages that were grown in complete and depleted media, after 20 hours of LPS stimulation. Results showed that the concentration of TNF- α was highest in macrophages cultured in complete media (F+M+) with an average reading of 592pg/ml. The folate depleted macrophage (F-M+) reported the lowest reading where the TNF- α concentration was significantly reduced by almost 50% (321pg/ml) as compared to the macrophages grown in complete media (P=0.0002). Similarly, macrophages grown in methionine depleted (F+M-) and folate and methionine depleted media (F-M-) also showed a significant reduction of TNF- α concentration, with average readings of 349pg/ml (P=0.0004) and 366pg/ml (P=0.0007), respectively. Clearly, the deficiency of either folate, methionine or both nutrients significantly reduced the production of TNF- α by THP-1 derived macrophages.

Table 5.1 TNF- α Quantikine immunoassay control concentration

Immunoassay control group 1	TNF- α concentration (pg/mL)	
	Acceptable range ($\pm 3SD$)*	Result
Low	68-128	82
Medium	230-388	293
High	467-765	544

*Acceptable range determined by Quantikine Immunoassay Control Group 1 protocol by R & D Systems

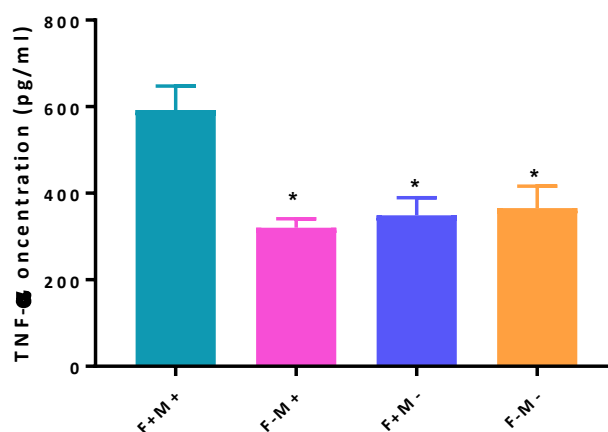


Figure 5.3 The effect of methyl donor depletion on TNF- α concentration in THP-1 derived macrophages

This figure shows the TNF- α concentrations of THP-1 derived macrophages grown in complete medium (F+M+), folate depleted medium (F-M+), methionine depleted medium (F+M-) and folate and methionine depleted medium (F-M-). Each value shows mean of three-independent experiments and error bars show SEM.

* significantly different from control (F+M+), P < 0.001 (one-way ANOVA, Bonferroni's post hoc test).

5.4.2 Effect of methyl donor depletion on IL-1 β production

Based on the corrected optical density (OD) readings for IL-1 β standards, a linearized standard curve was constructed by plotting the log of the IL-1 β concentration versus the log of the standard OD. The best fit line was determined with linear regression using GraphPad Prism software (**Figure 5.4**). The sample and control results were interpolated from the standard curve. **Table 5.2** shows the concentration of the IL-1 β in the controls provided by Quantikine. All the controls were within the acceptable range.

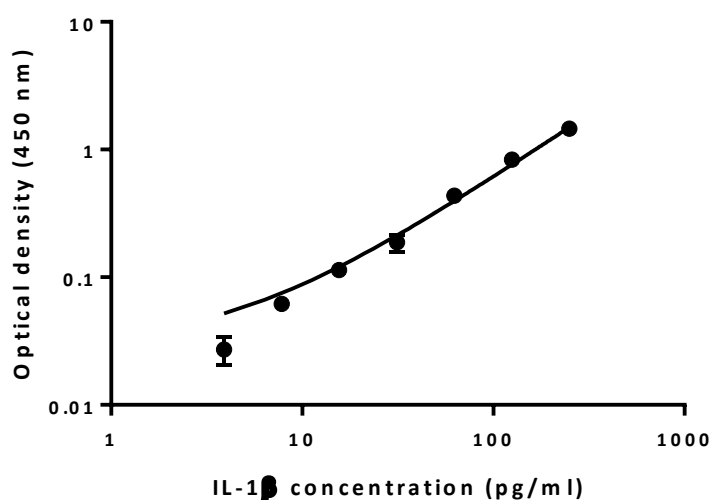


Figure 5.4 IL-1 β standard curve

The standard curve $R^2 = 0.9941$; $y = 0.005867 (x) + 0.02921$

Table 5.2 IL-1 β Quantikine immunoassay control concentration

Immunoassay control group 1	IL-1 β concentration (pg/mL)	
	Acceptable range ($\pm 3SD$)*	Result
Low	10-35	18
Medium	44-74	58
High	85-153	116

*Acceptable range determined by Quantikine Immunoassay Control Group 1 protocol by R & D Systems

Figure 5.5 shows the concentration of IL-1 β produced by differentiated macrophages grown in standard and depleted media, after 20 hours of LPS stimulation. Results show that the concentration of IL-1 β is significantly reduced in folate and/or methionine depletion as compared to those grown in complete medium. The folate and methionine depleted macrophage (F-M-) showed the lowest IL-1 β concentration (47pg/ml) as compared to the macrophages grown in complete medium (F+M+) (251pg/ml) ($P < 0.0001$). Similarly, macrophages grown in

only methionine depleted media (F+M-) also showed a reduction of IL-1 β concentration of almost 80%, with an average reading of 51pg/ml (P<0.0001). Macrophages grown in folate depleted media (F-M+) also showed a significant decrease (P<0.0001), though the average reading is higher (193pg/ml) compared to macrophages in other depleted conditions. This finding indicates that the production IL-1 β by THP-1 derived macrophages are significantly affected especially in methionine depleted or combined folate-and-methionine depleted conditions.

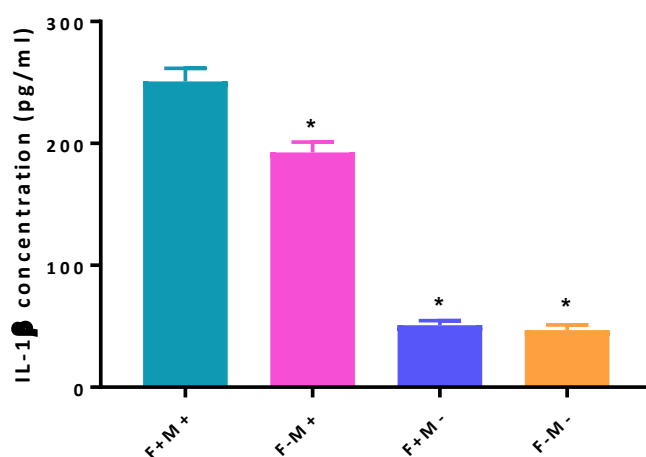


Figure 5.5 The effect of methyl donor depletion on IL-1 β concentration in THP-1 derived macrophages

This figure shows the IL-1 β concentrations of THP-1 derived macrophages grown in complete medium (F+M+), folate depleted medium (F-M+), methionine depleted medium (F+M-) and folate and methionine depleted medium (F-M-). Each value shows mean of three-independent experiments and error bars show SEM.

* significantly different from control (F+M+), P < 0.0001 (one-way ANOVA, Bonferroni's post hoc test).

5.5 Discussion

Monocytes and macrophages produce cytokines in response to different stimuli, such LPS (Laskin & Pendino, 1995). The proinflammatory molecules released by macrophages in the inflamed regions orchestrate the enhancement of monocyte recruitment from blood to tissue. Recruited monocytes differentiate into macrophages to continue the inflammatory response (Shi & Pamer, 2011). Due to this, THP-1 cells have been widely used as an *in vitro* model of human monocytes and macrophages in the study of inflammation-related immune responses (Daigneault et al., 2010; Chanput et al., 2014). Several studies have compared THP-1 cells with peripheral blood mononuclear cell (PBMC)-derived macrophages, and found that both exhibit similar morphological and functional properties (Daigneault et al., 2010; Mehta et al., 2010;

Schroecksnadel et al., 2011). Therefore, THP-1 derived macrophages could be a suitable alternative for PBMC-derived macrophages in terms of cytokine production, cell morphology and macrophage surface markers. In this study, it was found that combined folate and methionine deficiency might be associated with dysregulation of several genes associated with host defence mechanisms and immune response. In order to investigate the impact of methyl donor nutrient depletion on immune response, the THP-1 derived macrophages were cultured in complete and methyl depleted media, and cytokine production was assayed after LPS stimulation. The objective was to investigate the effect of folate, methionine or combined folate and methionine depletion on the production of two key inflammatory cytokines, TNF- α and IL-1 β , that have been associated have been associated with persistent HPV infection and metastasis (Mota et al., 1999; zur Hausen, 2002; Bailey et al., 2014).

A deficiency of folate, methionine or combined folate and methionine has been demonstrated to significantly reduce the production of TNF- α and IL-1 β cytokines in THP-1 derived macrophages. There are limited data that measures the impact of methyl donor depletion on the production of cytokines. However, recent study has reported that methyl donor availability might alter LPS-induced inflammatory response in human THP-1 monocyte or macrophage cells. In a study conducted by Samblas et al., they reported that folic acid and choline decreased the CCL2 mRNA levels; whilst a mixture of folic acid, choline and vitamin B₁₂ reduced CD40 expression, but increased SERPINE1 expression (Samblas et al., 2018). Additionally, folic acid, choline and vitamin B₁₂ also increased methylation levels in CpGs located in IL1B, SERPINE1 and IL18 genes. Both current and previous finding highlights the potential of methyl donor nutrient regulatory functions in immune response towards external stimuli.

In accordance with this study, other studies have reported a correlation between cytokine dysregulation and the incidence of cervical neoplasia, as well as advancement from pre-cancer (LSIL, HSIL) to tumour development, invasion and metastasis. These studies have shown that predominantly Th2-type cytokines (as compared to Th1-type cytokines) being produced in a number of cancers. A study to investigate the mRNA expression of 20 different cytokines in 10 different cervical cancer cell lines (i.e. SiHa, HeLa, CaSki and 5 other primary cell lines obtained from cervical cancer patients) as well as 3 normal cervical epithelial cells; and based on RT-PCR and Southern blotting analysis discovered that both normal and cancerous cells produce TGF- β , IL-4, IL-12, p35 and IL15. However, TNF- α , IL-10 and

RANTES were only present in normal cell lines (Hazelbag et al., 2001). Another study compared the cytokine profiles of 90 patients with advanced cervical cancer and healthy controls, including between pre- and post-neoadjuvant chemo-radiation treatment. PBMC was isolated from participants' blood samples, and cytokine levels were measured after stimulation with phytohemagglutinin (Sharma et al., 2009). Prior to treatment, cancer patients showed significantly lower Th1-type cytokine (IL-2 and IFN- γ) and higher Th2-type cytokine (IL-4 and IL-10) levels, as compared to healthy controls. However, after completing the chemo-radiation treatment, these patients showed a significant increase in both IL-2 and IFN- γ , which remained significant during follow-up. Previous studies have also reported that excessive production of Th2-type cytokines inhibits the function of T lymphocytes, which recognize tumour cells (Hung et al., 1998; Lin & Karin, 2007; Swann & Smyth, 2007). These cytokines suppress class I and II major histocompatibility complex (MHC) molecules, thus impairing tumour antigen presentation to CD8⁺ CTL and to CD4⁺-dependent antigen presentation.

Tumour necrosis factor alpha (TNF- α) are pro-inflammatory cytokines that are mainly derived from macrophages and they are involved in a range of biological activities. Higher levels of expression are associated with the HPV persistence and the development of HPV-related cancers (Aggarwal et al., 2006; Scott et al., 2013). It has been observed that elevated TNF- α concentrations due to pathological conditions is associated with malignancy, whilst moderate secretion of this cytokine is necessary for cell protection and disease prevention via the regulation on immune response (Zuo et al., 2011). In this study, there is a significant reduction of TNF- α concentration in methyl donor depleted conditions, suggesting that the depletion of these nutrients directly impacts pro-inflammatory responses towards external stimuli, thus could influence the development and progression of cervical cancer through modulation of infectivity of HPV.

Interleukin-1 beta (IL-1 β) plays an important role in the development of cancer, participating in the interleukin-1 (IL-1) signalling pathways that initiate the polarization of CD4⁺ T cells, activating Th1 and Th17 cells. IL-1 β , as one of the cytokines from the IL-1 family, is considered crucial in resolving acute inflammation by activating its adaptive anti-tumour response. On the other hand, this cytokine has also been observed to support carcinogenesis in chronic inflammation, which is the case in HPV infection. In addition, IL-1 β produced in the tumour microenvironment, mostly by tumour-infiltrating macrophages, has been found to induce the development of tumour and metastasis (Bent et al., 2018).

Several studies have found that subjects with higher plasma IL-1 β levels are at a higher risk of cancer, whilst cancer patients with high IL-1 β expression have a worse prognosis than those without (Lewis et al., 2006; Landvik et al., 2009; Qian et al., 2010). It has been reported that IL-1 β encourages tumour cell invasion, angiogenesis and inhibits the host immune response (Saijo et al., 2002; Song et al., 2003). In breast cancer cells, IL-1 β has been reported to combine with the oestrogen receptor (ER) α causing transcriptional activation (Speirs et al., 1999). Moreover, IL-1 β has not only been found to mediate adhesion and invasion, it can also activate the NF- κ B and ERK signalling pathways which encourages resistance to chemotherapy in pancreatic cancer cells (Kate et al., 2006; Angst et al., 2008). It has been observed that this cytokine can also impair antiviral activity via interferon and the activation of *STAT1* in the liver and modulate immune responses in hepatitis virus related hepatocellular carcinoma (Tian et al., 2000; Tanaka et al., 2003). In this study, the deficiency of folate, methionine or both methyl donors significantly reduced the production of IL-1 β . Again, this suggests that a depletion of methyl donor nutrients directly impacts the innate immune system, which could influence the development and progression of cervical cancer through modulation of infectivity of HPV.

The THP-1 cell model has been widely used in studies as it is able to demonstrate or mimic the human *in vivo* immune response, however it does not truly represent the effect of cervical tissue responses towards external stimuli. A known limitation of the use of cell lines in research is the difference to the natural environment, however previous studies have found that LPS mimics the inflammatory environment when added to THP-1 (Ahmad et al., 2018). Despite this, direct extrapolation to human disease is not possible because more proinflammatory molecules and more than one cell type are involved in the human body response towards external stimuli.

Other important limitation to note is that this experiment was conducted on the assumption that the cell model of methyl donor depletion using THP-1 would be applicable and the measurements of the cell growth and viability in different media condition as well as folate, methionine and homocysteine concentration have not been undertaken. Previous study has reported that methyl donors did not affect THP-1 cell viability (Samblas et al., 2018). However, compared to Samblas et al., this study had cultured THP-1 cells in DMEM media instead of RPMI as recommended by the ATCC. Thus, an additional analysis on THP-1 cell viability and proliferation rate in the DMEM as well as in presence of folate and/or methionine depletion may provide a better understanding on whether the difference in the amount of cytokines produced between the standard and depleted conditions is due to the depletion of these nutrients

at cellular levels or simply caused by cells poor viability in the depleted conditions or the change in type of media. Ideally, with more time and funding, a more comprehensive cytokine profile, that represents both Th-1 and Th-2 type cytokine responses towards external stimuli in methyl donor depleted conditions, could provide a more in-depth understanding on the effect of methyl donor deficiency on immune response. Nonetheless, regardless of these limitations, methyl donor nutrients modulation significantly altered the production of cytokine, highlighting potential regulatory functions of methyl donor nutrients in the immune response mechanism, and subsequently on cervical cancer risk and progression.

5.6 Summary

A deficiency of folate, methionine or combined folate-and-methionine has been demonstrated in this study to significantly reduce the production of cytokines in THP-1 derived macrophages. This additional investigation demonstrates that cytokine production in the humoral immune system is also affected by methyl donor nutrient depletion. Cytokine production is down-regulated in conditions of scarcity, therefore for an appropriate immune response there is a need for adequate methyl donor nutrient availability. The impact of this decrease in cytokine production in methyl donor nutrient depleted conditions on cervical cancer progression needs to be considered in the context of similar alterations in gene regulation within cervical epithelial cells as demonstrated in **Chapter 3**. In the context of cervical cancer risk and progression, it is not yet possible to confirm whether the depletion of these nutrients is beneficial or detrimental and this would require further investigation.

CHAPTER 6

EFFECT OF METHYL DONOR DEPLETION ON METHYLATION PROFILING

6.1 Introduction

Numerous clinical, epidemiological and molecular studies have shown that persistent infection with high-risk HPV genotypes is an indispensable, but not sufficient prerequisite for the development of cervical cancer (Łaniewski et al., 2020; Da Silva et al., 2021). This suggests that the cervical carcinogenesis process triggered by HPV infection depends on other associated risk factors, including environmental and/or other factors the cells may experience, creating a conducive local microenvironment for malignant transformation. Dysregulation of both viral and host gene expression due to viral DNA integration into the cell's genome, as well as epigenetic modifications are crucial events in the carcinogenic process. This includes epigenetic changes such as DNA methylation, histone modification and gene silencing (Ramassone et al., 2018).

Alterations in DNA methylation, an epigenetic mechanism crucial for regulating gene transcription has been demonstrated in cervical cancer and its precursors (Dueñas-González et al., 2005; Szalmas & Konya, 2009). Aberrant DNA methylation has been detected in numerous cancers, consisting of two main features; global DNA hypomethylation, with local DNA hypermethylation (Jones & Baylin, 2007; Kanwal & Gupta, 2012). In the intergenic regions and repetitive sequences of the human genome, CpG sites are sparse and mostly methylated. The hypomethylation of CpG sites in this area may result in genomic instability and loss of gene imprinting, which could eventually lead to the development of neoplastic cells (Kulis et al., 2013). On the other hand, gene promoters are rich in CpG sites, that are sometimes densely packed to form CpG islands. Normally, these CpG islands are not methylated, thus allowing transcription to occur, resulting in the expression of genes. Methylation at the CpG islands inhibits transcription binding factors to DNA, stopping the transcription process and ultimately suppressing the expression of genes. Aberrant hypermethylation of these CpG sites may silence the expression of genes that are crucial for cell homeostasis, DNA integrity or genome stability, and is associated with cancer development and progression (Bakshi et al., 2018). Several studies have shown that cervical cancer frequently displays global DNA hypomethylation, though compared to hypermethylation, the literature is quite limited (Kim et al., 1994; Fowler et al., 1998; Shuangshoti et al., 2007). Besides that, a cross-sectional study conducted among 308 women having normal cervix with different degrees of CIN severity found that global DNA

hypomethylation is higher in women with invasive cervical cancer than all other groups ($P < 0.05$), whilst *CDH1*, *DAPK*, and *HIC1* tumour suppressor genes showed a significantly higher frequency of promoter methylation with progressively more severe cervical neoplasia ($P < 0.05$) (Flatley et al., 2009).

The hypermethylation of genes that are essential in maintaining cellular processes have been reported in cervical carcinoma, and may occur independently of HPV infection status (Szalmas & Konya, 2009; Wentzensen et al., 2009). Evidently, DNA hypermethylation that occurs in cancer cells seems to target tumour suppressor genes explicitly, silencing these genes which results in growth selection and uncontrolled cell proliferation. Examples include the hypermethylation of *FHIT*, a gene involved in cell cycle regulation and apoptosis (Ki et al., 2008); *DAPK*, a gene involved in apoptosis (Yang et al., 2010); *RAR β 2*, a gene involved in the signalling pathway for cell growth suppression (Jha et al., 2010); *APC*, a tumour suppressor protein involved in the Wnt/ β catenin pathway (Dong et al., 2001); *p73*, a gene involved in cell cycle regulation and apoptosis (Liu et al., 2004) and *MGMT*, a DNA repair protein that protects human genome against mutation (Kim et al., 2010). Additionally, hypermethylation of *CCNA1*, a gene associated with regulation of cell cycle, has been reported in HSIL (36.6%) and invasive cancer (93.3%) (Kitkumthorn et al., 2006; Yang et al., 2010). A decline in *CADMI* gene expression has been reported in high grade CIN and squamous cell carcinoma, where a severity of cervical dysplasia is correlated with a higher number of methylated genes (Overmeer et al., 2008), whilst hypermethylation of E-Cadherin promoter has been reported in 89% of invasive cancer, 26% in CIN III and none in normal tissues (Shivapurkar et al., 2007).

In a more recent study, Clarke et al. performed DNA methylation profiling on 50 formalin-fixed, paraffin-embedded tissue specimens from women with benign HPV-16 infection and histologically confirmed CIN3, and cancer (Clarke et al., 2017). This study reported that *ADCYAPI*, *ASCL1*, *CADMI*, *DCC*, *ATP10*, *DBC1*, *HS3T2*, *MOS*, *SOX1*, *SX17* and *TMEFF2* genes showed higher levels of methylation when compared to healthy controls. A study by Kremer et al. also reported hypermethylation levels of *ASCL1*, *LHX8*, and *ST6GALNAC5*, where DNA hypermethylation increased with the severity of cervical cancer (Kremer et al., 2018). Moreover, Verlaat et al. showed that DNA methylation usually occurs at the pre-tumorigenic stage and reaches the highest level after tumorigenesis induced by HR-HPV (Verlaat et al., 2018). In a bioinformatic study conducted using available gene expression profile and methylation profile in GEO database, it was reported that in cervical cancer samples, hypomethylated and highly expressed genes were significantly enriched in cell

cycle and autophagy. On the other hand, hypermethylated and lowly expressed genes were found in estrogen receptor pathway and Wnt/ β -catenin signalling pathway, where *ESR1*, *EPB41L3*, *EDNRB*, *ID4* and *PLAC8* were the hub genes (Ma et al., 2020).

DNA methylation involves the addition of methyl groups by S-adenosylmethionine (SAM) to cytosine residues; a biological process that depends on the availability of methyl groups and accordingly the function of methyl donors and acceptors (Ducker & Rabinowitz, 2017; Mahmoud & Ali, 2019). The production of SAM, which is generated from methionine, partly depends on the availability of methyl-donor nutrients from diet. In addition to methionine, other methyl donor nutrients include folate and vitamin B₁₂, which participate in the generation of methionine via the methionine– synthase pathway, and choline and betaine, which are substrates in the betaine:homocysteine methyltransferase pathway.

Methyl donor nutrients availability has been shown to modify DNA methylation either globally or at specific CpG sites by inducing the formation of methyl donors, acting as coenzymes, or modifying DNMT enzymatic activity (Mahmoud & Ali, 2019; Ghazi et al., 2020). In a study conducted by our department previously, combined folate and methionine depletion of C4-II cervical cancer cells has led to a significant downregulation of DNMT3a and DNMT3b, which was associated with an 18% reduction in global DNA methylation compared with controls (Poomipark et al., 2016). Low folate status was also associated with HR-HPV infection (P=0.031) and with a diagnosis of CIN or invasive cervical cancer (P<0.05) (Flatley et al., 2009). In another long-term prospective follow up study, higher folate status has been reported to provide a protective effect against the natural history of HR-HPV (Piyathilake et al., 2004). Several other studies have also associated folate intake with lower risk of colorectal and prostate cancer (Giovannucci et al., 1993; Su & Arab, 2001; Giovannucci, 2002; Stevens et al., 2006); and folate supplementation has been found to modify the DNA methylation status to provide a protective effect against diseases including cancer (Keyes et al., 2007; Wallace et al., 2010; Cartron et al., 2012). However, there are studies that reported conflicting results (Song et al., 2000; Kotsopoulos et al., 2008; Qin et al., 2013; Gylling et al., 2014), indicating that the mechanisms associated with folate effect on DNA methylation are more complex than previously thought and confounded by other dietary, genetic, or tissue-related factors. Thus, a genome wide methylation array which investigates thousands of CpG sites simultaneously could provide a better understanding of the interaction between DNA methylation and folate availability.

In addition to folate, methionine that serves as a precursor of SAM is an integral part of DNA methylation (Mahmoud & Ali, 2019). However, there are limited and inconsistencies in the evidence on dietary methionine status and its effect on DNA methylation, especially in human studies. This could be due to the cyclical nature of the SAM-SAH cycle, where excessive methionine might inhibit the re-methylation of homocysteine, thus disrupting the one-carbon cycle and negatively impacting DNA methylation (Regina et al., 1993). Furthermore, there are inconsistencies in the epidemiological findings on the protective effect of dietary methionine against cancer (Zhou et al., 2013), where a high intake of methionine has been associated with increased risk of cancer (Vidal et al., 2012), with dietary methionine restriction currently being studied as an enhancer for chemotherapy treatment in metastatic cancer (Thivat et al., 2007; Durando et al., 2010). On the other hand, a meta-analysis to determine the association of vitamin B₆, vitamin B₁₂ and methionine with breast cancer risk found that methionine intake might be inversely associated with breast cancer risk, especially among post-menopausal women (Wu et al., 2013). They reported that the combined relative risk of breast cancer for the highest versus lowest category of dietary methionine intake was (RR=0.94, 95%CI=0.89-0.99, P=0.03). They also reported a linear dose-response relationship, where the risk of breast cancer decreased by 4% (P=0.05) for every 1 g per day increment in dietary methionine intake. Additionally, conflicting results regarding the effect of methionine availability on DNA hypermethylation/hypomethylation and cancer risk/progression have been reported in several animal studies, indicating other confounding dietary, genetic and tissue-related factors (Uekawa et al., 2009; Amaral et al., 2011; Miousse et al., 2017). Data on methionine status and cervical cancer is even more scarce. Based on these findings, much more information is needed in order to determine the direction of the association between dietary methionine and cancer risk.

As above, the literature suggests that methyl donor nutrients have the capacity to modulate genes related to cervical carcinogenesis via an effect on DNA methylation. However, little is known with regards to the impact of these nutrients' availability, especially methionine on DNA methylation profile of cervical cancers. Most studies to date have only identified the presence of aberrant DNA methylation in cervical cancer, or the effect of methyl donor availability in other cancers. Using high-throughput technologies, there are opportunities to provide a comprehensive view of DNA methylation pattern. To the researcher's knowledge, this is the first study that profile a genome-wide DNA methylation in cervical cancer, in order to explore the impact of methyl donor depletion on DNA methylation profiles. In addition to three methyl donor depleted conditions used in the previous chapters (F-M+, F+M- and F-M-), the C4-II cells were also grown in 5% folate and methionine repleted media (F+M+5%). Based

on unpublished work in the department, it has been demonstrated that a depletion of folate and methionine to 5% or less of standard levels is required to significantly affect the doubling time of C4-II cells (Shafie, 2014), where the doubling time for C4-II cells in complete media is 29.2 hours, 31.2 hours at 50% depletion, 30.1 hours at 75% depletion and 66.6 hours at 95% depletion of methionine and folate. The rationale for including the M+F+5% was to determine the impact of 5% repletion on DNA methylation profile; if there was a differential effect on DNA methylation pattern compared with the observed impact on cell division in Shafie's data.

6.2 Hypothesis and aim

It is hypothesized that folate and/or methionine depletion will alter the methylation profile of C4-II cervical cancer cells. In order to test this hypothesis, three objectives were generated:

- i. to investigate how the availability of folate and methionine impacts globally and specifically on DNA methylation in a C4-II cervical cancer cell model of methyl donor depletion by methylation profiling.
- ii. to identify functions and pathways from the methylation profile, that are affected by methyl donor nutrient depletion using a bioinformatics approach.
- iii. to determine the effect of methyl donor nutrient depletion on the methylation status of selected genes using methylation specific PCR.

6.3 Methods

6.3.1 C4-II sample preparation for methylation profiling

The C4-II cells were rejuvenated in complete medium and were sub-cultured for a total of three passages before being utilised for this experiment as describe in **section 4.3.2** and **section 4.3.3**. At passage 119, the C4-II cells were grown at a starting density of 1×10^6 cells in each T75 flask. The maximum amount of starting material was 2×10^7 cells; therefore, the cell culture procedure was optimised to yield between $1-1.5 \times 10^7$ cells in the complete medium, with a lower number of cells expected in the depleted media. C4-II cells were cultured for eight days in five different media; complete medium (F+M+), folate depleted medium (F-M+), methionine depleted medium (F+M-), folate and methionine depleted medium (F-M-), and 5% folate and methionine supplemented medium (F+M+5%), where half of the spent media were replaced at day four.

The complete (F+M+) and folate depleted (F-M+) cells were grown in one T75 flask, while the methionine depleted (F+M-), folate and methionine depleted (F-M-) and 5% folate

and methionine supplemented (F+M+5%) cells were grown in two T75 flasks due to their slow growth rate. C4-II cells were grown separately on three different occasions yielding three sets of samples for each medium, except for cells grown in complete medium where four biological replicates were prepared (total of 16 samples). The additional replicate for C4-II cells grown in complete media were added due to an empty slot available on the Infinium DNA Methylation EPIC BeadChip.

6.3.2 C4-II genomic DNA extraction

A maximum of 1.8×10^7 cells were harvested at day eight of culture for each C4-II sample. DNA extraction was performed using the Qiagen Blood and Cell Culture DNA Midi Kit, following the protocol provided by the manufacturer. After trypsinisation, cell suspensions were transferred to new tubes and centrifuged at $1500 \times g$ for 10 minutes at 4°C . The supernatant was removed and cells were re-suspended with 4 mL of cold DPBS, followed by centrifugation at $1500 \times g$ for 10 minutes at 4°C . The supernatant was discarded and cells were re-suspended with 2 ml of cold DPBS. Then, 20 μL of cell suspension was added to 20 μL of trypan blue for cell counting. Cells were counted using an automated cell counter. The numbers of total cells, live cells and cell viability (%) were recorded. A maximum of 2 mL cell suspension was prepared in a new 10 mL screw cap tube. Buffer C1 (2 mL) and distilled water (6 mL) were added to the cell suspension, followed by an incubation period of 10 minutes on ice. Lysed cells were centrifuged at $1300 \times g$ for 15 minutes at 4°C . The supernatant was removed and cells were re-suspended with 1 mL Buffer C1 and 3 ml distilled water. Cells were centrifuged again at $1300 \times g$ for 15 min at 4°C . The supernatant was removed and lysed cells were stored at -20°C .

Frozen lysed cells were thawed and completely re-suspended in 5 mL of Buffer G2 by vortex for 30 seconds at maximum speed. Then, 95 μL of protease was added to the lysed cells and incubated for 60 minutes at 50°C . Lysed cells were then vortexed at maximum speed for 10 seconds and immediately loaded into the genomic tip, allowing for gravity flow rate. The genomic tips were equilibrated with 4 mL of Buffer QBT and allowed to empty by gravity flow prior to use. The genomic tips were washed with 7.5 mL of Buffer QC, allowing the buffer to move by gravity flow. The genomic DNA was eluted with 5 mL Buffer QF into a new 10 mL collection tube by gravity flow. Genomic DNA was precipitated with 3.5 mL isopropanol, followed by centrifugation at $5000 \times g$ for 10 minutes at 4°C . The supernatant was removed and genomic DNA was washed with 2 mL of cold 70% ethanol. The mixture was vortexed

briefly prior to centrifugation at 5000 x g for 10 minutes at 4°C. All supernatants were removed using a pipette and genomic DNA was air dried for 10 minutes. Genomic DNA was re-suspended in 1 mL of Tris-EDTA buffer and incubated on a shaker overnight, at room temperature, to dissolve the DNA. The genomic DNA purity and yield were determined using a Nanodrop spectrophotometer. A genomic DNA 260:280 value of 1.7-1.9 was considered acceptable for downstream analysis. The samples were stored at -80°C.

6.3.3 Sodium bisulphate treatment

The required volume of each genomic DNA sample to provide 500 ng of DNA was calculated and treated with sodium bisulphite, which converts unmethylated cytosine to uracil (**Figure 6.1**). Sodium bisulphite treatment was performed using the EZ DNA Methylation Kit, following the protocol provided by the manufacturer.

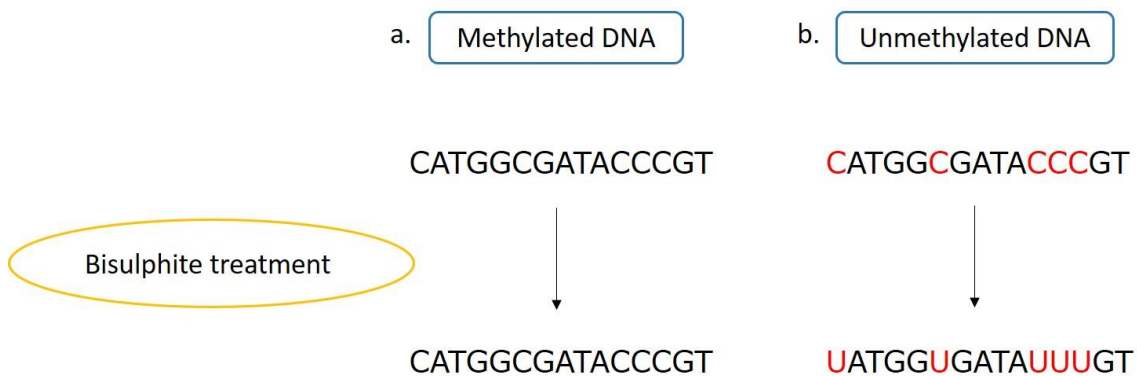


Figure 6.1 Bisulphite conversion process

The figure shows the effect of bisulphite treatment on (a) methylated DNA, where cytosine remains the same, whilst for (b) unmethylated DNA, the cytosine is converted to uracil.

Frozen genomic DNA was thawed and vortexed for 5 seconds prior to use. Then, 5 µL of M-Dilution Buffer was added to each genomic DNA sample and the total volume was adjusted to 50 µL with nuclease free water. DNA was incubated for 15 minutes at 37°C. CT-Conversion Reagent (100 µL) was added to the DNA samples, followed by an incubation period of 16 hours at 50°C. Samples were then incubated on ice (4°C) for at least 10 minutes. The Zymo-Spin™ IC Column was placed into the provided Collection Tube and 400 µL of M-Binding Buffer was added to the column. DNA samples were then loaded into the column and mixed by inverting several times. Samples were centrifuged at 10 000 x g for 30 seconds at

4°C, and the flow-through was discarded. Then, 100 µL M-Wash Buffer was added to the column, followed by centrifugation at 10 000 x g for 60 seconds at 4°C. M-Desulphonation Buffer (200 µL) was added to the column and left to stand at room temperature (20-30°C) for 15 minutes, followed by centrifugation at 10 000 x g for 30 seconds at 4°C. Then, 200 µL M-Wash Buffer was added to the column and centrifuged at 10 000 x g for 30 seconds at 4°C. This step was repeated twice. Finally, samples were eluted by adding 10 µL of M-Elution Buffer directly to the column matrix and centrifuged at 10 000 x g for 30 seconds at 4°C. The samples were stored at -80°C.

6.3.4 C4-II cells methylation profiling

Methylation profiling was performed using the Infinium DNA Methylation EPIC BeadChip Kit, following the protocol provided by the manufacturer at the Sheffield Institute for Translational Neuroscience (SiTran). This analysis involved eight processes as described in **Figure 6.2**. In the first step of DNA amplification, 4 µl of bisulphite-treated DNA was used. This was followed by the DNA fragmentation, DNA precipitation and DNA resuspension procedures. DNA samples were then dispensed onto the BeadChip for hybridization. Two 8 x 1 BeadChips were used to analyse the 16 C4-II samples (BeadChip ID: S/N 201465930010 and S/N 201465930033). The BeadChip was then washed and stained prior to imaging. Imaging was carried out using the Illumina iScan System. The summary of the C4-II sample preparation and DNA methylation procedures are presented in **Figure 6.3**.

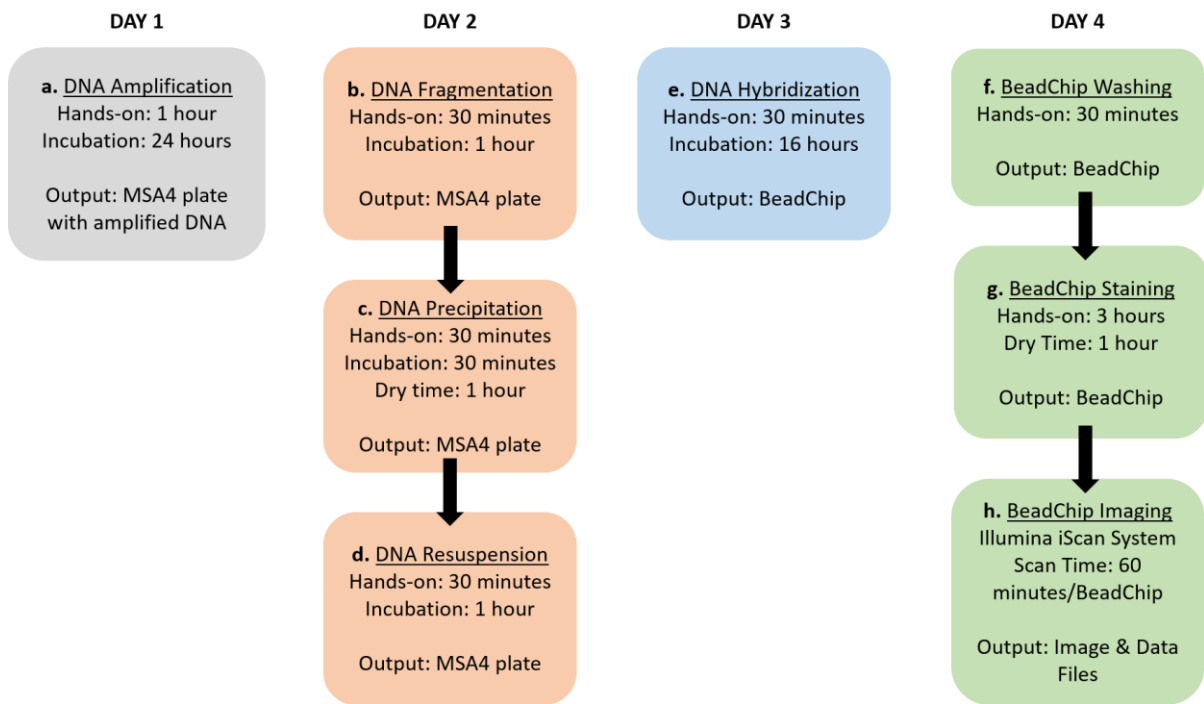


Figure 6.2 Infinium methylation EPIC BeadChip workflow

6.3.5 Methylation data analysis with RnBeads

The methylation data analysis and interpretation were performed using RnBeads software, via the R platform (version 3.4.3) (<https://cran.r-project.org/>). This software utilizes the R programming language to execute a comprehensive methylation analysis pipeline involving seven working modules (Assenov et al., 2014). RnBeads uses a sample annotation table (CSV file) generated by the user to define the input data files (IDAT file) as well as other experimental conditions that are relevant to the methylation analysis. The software then pools all samples' data as one object (*RnBSet*) which provides the basis for its analysis. It also tracks each working module and generates an interactive report as the analysis progresses. Ghostscript software was used to generate plots and graphs in the RnBeads analysis (<https://www.ghostscript.com/download/gsdnld.html>). The RnBeads analysis workflow is summarized in **Figure 6.4**.

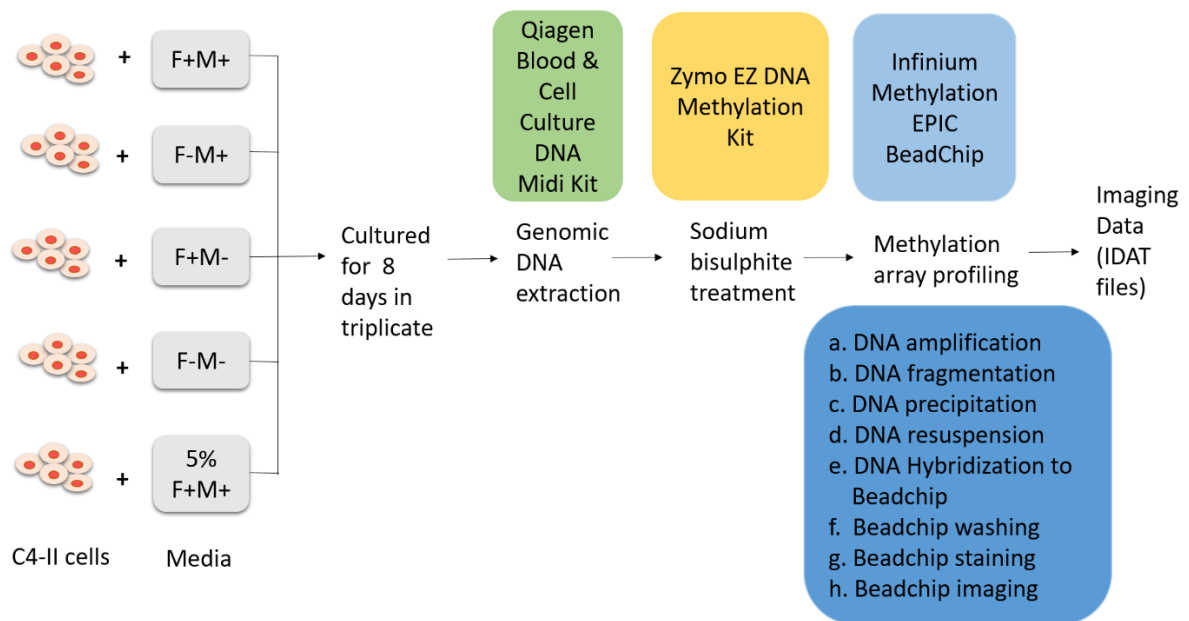


Figure 6.3 Sample preparation and DNA methylation profiling workflow

C4-II cells were grown in complete medium (F+M+), folate depleted medium (F-M+), methionine depleted medium (F+M-), folate and methionine depleted medium (F-M-) and 5% folate and methionine supplemented medium (F+M+5%) for eight days in triplicate. The sample genomic DNA was extracted and treated with sodium bisulphite. Finally, methylation array profiling was performed producing imaging data that requires further analysis for interpretation.

A file documenting details of each sample, including sample name, sample group, BeadChip sentrix ID and position was created and saved in csv format prior to the analysis, using Microsoft Excel (**Figure 6.5**).

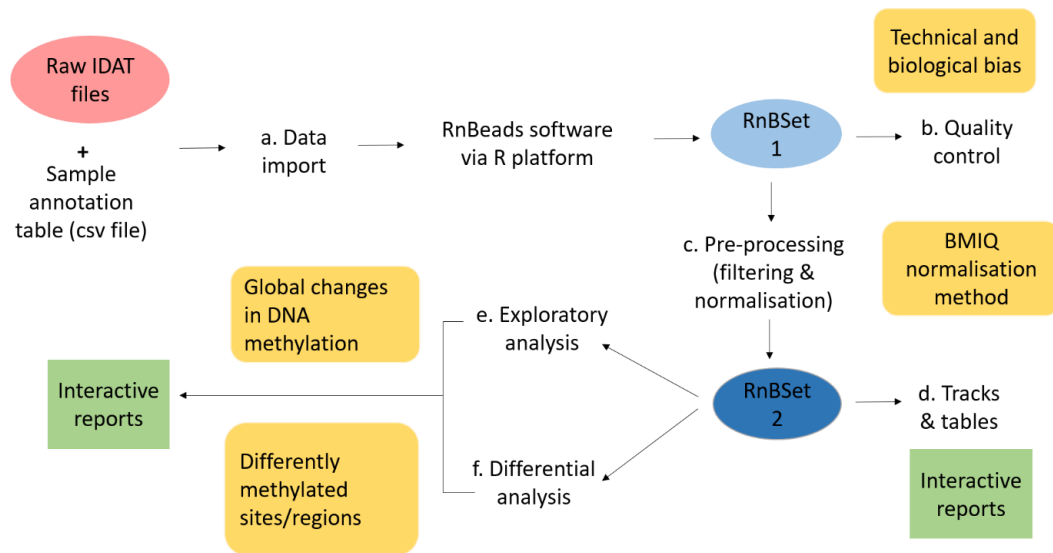


Figure 6.4 RnBeads analysis workflow

This figure shows the RnBeads analysis workflow starting from (a) data import, where the imaging results (IDAT files) and sample annotation table (csv file) were imported into the RnBeads software. The software then pools all samples' data as one object (*RnBSet1*) which provides the basis for the analysis. (b) Quality control module was run to identify technical and biological biases. (c) Low quality data was filtered out, and data normalisation using the BMIQ method was conducted creating a secondary RnBSet. (d) Each working module is tracked and generates an interactive report as the analysis progresses. (e) By using RnBSet2, exploratory analysis was conducted in order to identify global changes in DNA methylation and (f) differential analysis to identify specific differently methylated sites/regions.

[Header]			
Investigator Name	Scientist		
Project Name	Methylation		
Experiment Name	Methylation experiment		
Date	8/3/2018		
[Data]			
Sample_Name	Sample_Group	Sentrix_ID	Sentrix_Position
S1.C.8.1 TB1	F+M+	201465930010	R01C01
S2.C.8.1 TC1	F+M+	201465930010	R06C01
S3.C.8.1 TC1	F+M+	201465930033	R03C01
S5.C.8.6 TB1	F+M+	201465930033	R08C01
S1.C.8.2 TB1	M+F-	201465930010	R02C01
S2.C.8.2 TC1	M+F-	201465930010	R07C01
S3.C.8.2 TC1	M+F-	201465930033	R04C01
S1.C.8.5 TC1	M+F+ 5%	201465930010	R05C01
S2.C.8.5 TC1	M+F+ 5%	201465930033	R02C01
S3.C.8.5 TC1	M+F+ 5%	201465930033	R07C01
S1.C.8.4 TB1	M-F-	201465930010	R04C01
S2.C.8.4 TB1	M-F-	201465930033	R01C01
S3.C.8.4 TC1	M-F-	201465930033	R06C01
S1.C.8.3 TB1	M-F+	201465930010	R03C01
S2.C.8.3 TB1	M-F+	201465930010	R08C01
S3.C.8.3 TC1	M-F+	201465930033	R05C01

Figure 6.5 User-generated csv file

This figure shows the csv file detailing sample information including sample name, group and position on the BeadChip. This allows RnBeads software to identify sample during the analysis.

The RnBeads analysis was conducted using R by inputting the following command;

```
--source(http://bioconductor.org/biocLite.R)
--biocLite(c("RnBeads","RnBeads.hg19","RnBeads.hg38"))
--a
--library(RnBeads)
--install.packages("shiny")
--install.packages("doParallel")
--install.packages("devtools")
--install.packages("RPMM")
--devtools::install_github("daattali/shinyjs")
--suppressPackageStartupMessages(library(RnBeads))
--rnb.run.dj()
```

The last command opens the RnBeads data juggler webpage, where the analysis was conducted. On the webpage analysis tab, a file path to the results folder was created. The analysis was conducted using 8 core processors, with a black and white theme. The file path to the user-generated csv file and IDAT files were added via the webpage input data; and the Illumina EPIC platform was selected. Prior to running the analysis, criteria were selected for the analysis, pre-processing and differential modules as shown in **Table 6.1**. The imaging IDAT files and csv file were imported into RnBeads software for data analysis and interpretation.

Table 6. 1 Criteria selected for RnBeads analysis, pre-processing and differential modules

Analysis	Pre-processing	Differential
Predefined option profile = 450k_full	Pre-processing = enable	Differential = enable
Analysis name = RnBeads Analysis	Filtering.greedyicut = enable	Differential.comparison.column = Sample_Group
Set assembly = hg38	Filtering.sex.chromosome.removal = enable	Differential.site.test.method = limma
Set region = include all options	Filtering. SNP = 3 SNPs	Differential report sites = enable
Set identifiers column = Sample_Name	Normalisation method = bmiq	Differential.variability.method = diffVar
Set colours = YIBI	Normalisation background method = none	

In order to minimize technical, biological and/or measurement biases, RnBeads performs a quality control analysis to identify potential quality issues within the results; followed by data filtration and normalisation during the pre-processing step (Assenov et al., 2014). As the Infinium BeadChips contain built-in quality control probes, the software simply detects and plots signals intensity readings of these probes to provide information on the quality of the sample assay. The data was presented as a control boxplot showing the distribution of signal intensity readings for each of the quality control probes for both red (methylated signals) and green channels (un-methylated signals) (Assenov et al., 2014; Morris & Beck, 2015). The expected intensity level (high, medium or background) is given in the plot labels, and low-quality samples appear as outliers. The background intensity level of 1000 to 2000 is considered within the acceptable range (Assenov et al., 2014).

Next, based on the filtration criteria that have been selected, the software performed a two-step filtering process on samples, CpG sites and DNA methylation measurements. First, probes that could bias the normalisation procedure such as probes that overlap with SNPs with a high chance of influencing DNA methylation measurement were removed (Nordlund et al., 2013). RnBeads also removed probes with highest impurity, identified using the Greedycut algorithm. Briefly, Greedycut is an iterative algorithm that filters out the probes with the highest fraction of unreliable measurements one at a time. The methylation β values were considered to be unreliable when its corresponding detection P-value was not below the threshold T : $p \geq T = 0.05$.

Secondly, the methylation β values were normalised using the BMIQ normalisation method, in order to reduce background noise and eliminate systematic biases in the methylation array procedure (Teschendorff et al., 2013). This method uses a three-state beta-mixture model to assign probes to methylation states. It is followed by the transformation of probabilities into quantiles. A methylation-dependent dilation transformation was then carried out in order to preserve the monotonicity and continuity of the data. This method reduces the technical variation and bias of type 2 probe values and eliminates the type 1 enrichment bias caused by the lower dynamic range of type 2 probes. Finally, a second filtering procedure, where samples, CpGs and DNA methylation measurements with too many missing values that should be correctly included in the normalisation procedure, but not the downstream analysis, were removed.

The RnBeads software performed two types of methylation analysis i.e exploratory and differential methylation analysis. In the exploratory analysis, global changes in DNA methylation were identified by visual inspection of the DNA methylation data (Assenov et al., 2014). The global distribution of DNA methylation levels is presented as density plots. This allows the identification of sample groups that deviate from the characteristic bimodal shape, where highly methylated loci and essentially un-methylated loci can be distinguished. In order to visualise the of associations between sample groups and global trends in DNA methylation data, hierarchically clustered heat map was generated, followed by dimension reduction analysis using principal component analysis and multidimensional scaling. As this experiment involves biological and technical replicates, a pairwise correlation was used to assess the reproducibility between the experiments, where the results are presented as scatter plots to facilitate the detection of hypervariable samples within and across sample groups. Besides single CpG measurements, RnBeads also computed DNA methylation profiles regional levels including gene, promoter and CpG islands.

In the differential analysis, DNA methylation differences between control and treated groups were analysed at the individual CpG level, as well as between predefined genomic regions. The Limma package were employed and fitted using an empirical Bayes approach on derived M-values, in order to determine P-values (Du et al., 2010; Ritchie et al., 2015). The P-values were then corrected for multiple testing using the false discovery rate (FDR) method. The P-values at the genomic regions are calculated by combining the uncorrected, individual CpG P values using an extension of Fisher's method; followed by multiple testing correction using the FDR method. The combined measurements across a larger genomic region, provides a higher statistical power for the analysis, resulting in more interpretable sets of differentially methylated regions. Additionally, the RnBeads differential analysis also generated a combined rank score for each of the analysed CpG sites, creating a priority-ranked list of sites or regions that were most affected by the treatment given. This combined rank is defined as the maximum (i.e., worst) of three individual rankings i.e. by DNA methylation mean difference; the relative difference in mean DNA methylation levels, calculated as the absolute value of the logarithm of the quotient of mean DNA methylation levels; and by the sites or region differential methylation P-values (Assenov et al., 2014).

6.3.6 Differentially methylated regions bioinformatics analysis

The list of differentially methylated regions (DMRs) (based on combined adjusted $P < 0.05$) for the gene promoter region was extracted from the RnBeads output into an Excel spreadsheet, followed by data cleaning prior to performing bioinformatics analysis. Three sets of data were generated by comparing the methylation profiles of cells grown in complete (F+M+) to those grown in methionine depleted (F+M-), folate and methionine depleted (F-M-) or 5% folate and methionine supplemented (F+M+5%) media. A list of genes that were common between these groups was identified using Venny 2.1 (<http://bioinfogp.cnb.csic.es/tools/venny/>). There was no significant difference for all CpG sites, for cells grown in folate depleted medium (F-M+) compared to the control group (F+M+) (combined adjusted $P > 0.05$).

In order to identify functions and pathways affected by methyl donor depletion, the list of differentially methylated regions (DMRs) was uploaded to the DAVID Bioinformatics Resource 6.8 software (see section 3.3.3). The DAVID functional annotation clustering tool was used to group the genes into subsets that are characterised by functional biological processes (GO_BP). Based on the RnBeads combined rank score, the top 3000 genes were uploaded, and high to medium classification stringency settings were applied to determine the clusters (Huang et al., 2009). The lists of DMRs were also uploaded to ClueGo plug-in via the Cytoscape platform to facilitate the biological interpretation of differences in methylation profiles between complete and depleted medium (see section 3.3.4).

6.3.7 Designing methylation specific primers for PCR amplifications

The methylation specific primers for *TP73*, *DAPK1* and *STAT1* genes were designed using the Methprimer web tool (<http://www.urogene.org/cgi-bin/methprimer/methprimer.cgi>) (Li & Dahiya, 2002) and purchased from Eurofins. The ensemble ID and promoter location for each gene of interest were identified from the RnBeads output. Then, the promoter sequences for these genes were retrieved from the ensemble database (Zerbino et al., 2018) and uploaded into the Methprimer software. MSP primers options were selected to generate forward and reverse primers for both methylated and un-methylated bases. Primers with comparable fragment length and similar T_m values were chosen. **Figures 6.6 – 6.8** present the primer sequences for all three genes. These primer pairs contain at least one CpG near their 3' end, and several non-CpG C's. The designed primers for the methylated and un-methylated alleles also contain the same CpGs in their sequence. The PCR product size for all three sets of MSP primers is expected to be between 162 - 273 base pairs (**Table 6.2**). The *TP73* and *DAPK1* primer pairs'

The forward and reverse primers were rehydrated with 10mM Tris-EDTA pH 8.0, according to the manufacturer's instructions (stock solution). The re-suspended primers were kept in aliquots at -20°C. The primer stock solutions were diluted with 10 mM Tris-EDTA pH 8.0 prior to use at 1:10 for PCR amplification.

6.3.8 Methylation specific PCR amplifications of selected genes

Methylation specific PCR (MSP) amplifications for *TP73*, *STAT1* and *DAPK1* genes were carried out using the ZymoTaq Polymerase Kit, following the protocol provided by the manufacturer. Extracted genomic DNA of C4-II cells grown in complete medium (F+M+), folate depleted medium (F-M+) and methionine depleted medium (F+M-), that was previously prepared for methylation profiling (see section 6.3.1 and 6.3.2) were used in this experiment. Genomic DNA samples were treated with bisulphite (see section 6.3.3) and stored in -80°C. Frozen modified DNA samples and other reagents were thawed and vortexed for 5 seconds prior to use. For each sample, two reaction tubes were prepared (for methylated and unmethylated) according to **Table 6.3**. A no template was also included to ensure there was no contamination in the mastermix.

Table 6.3 PCR amplification setup for each reaction

Reagent	Volume	Final Concentration
2X Reaction Buffer	25 µL	1X
dNTP Mix	0.5 µL	0.25 mM each dNTP
Forward Primer (10 µM)	5 µL	0.3 to 1µM
Reverse Primer (10 µM)	5 µL	0.3 to 1µM
Template DNA	4 µL	< 200 ng/50µl (4 ng/µL)
ZymoTaq™ DNA Polymerase (5 U/µl)	0.4 µL	2 U/50µL
ddH2O	10.1 µL	-
Total volume	50 µL	

A touchdown PCR method was used to increase the PCR specificity of the annealing primer-template without the need for optimisation, which also aims to increase the sensitivity and yield (Korbie & Mattick, 2008). The StepOne Plus Real-Time PCR System was used to run the analysis. First, the enzyme was activated at 95°C for 10 minutes in order to denature the DNA and to enable the use of hot start Taq polymerase. This was followed by 30 to 40 cycles of denaturation, annealing and extension steps. The initial annealing step are set at 5°C above the primer T_m, and the temperature declines gradually with each cycle until it falls to the primer T_m. The final extension step was carried out for 7 minutes at 72°C (**Table 6.4**). Amplified DNA was stored at -20°C.

Table 6.4 PCR amplification setting

Step	Temperature	Duration
Initial denaturation	95 °C	10 min
Denaturation	94 to 96 °C	30 sec
Annealing	Variable (T _m provided by manufacturer)	30 to 40 sec
Extension	72 °C 30-40 cycles	30 to 60 sec. for ≤ 1kb (45 sec)
Final extension	72 °C	7 min
Hold	4 °C	> 4 min

6.3.9 Gel electrophoresis

In order to determine that the bisulphite-treated DNA was successfully amplified, gel electrophoresis was performed using 10µl of the PCR product. A 1x10 TBE running buffer was prepared by adding 200 mL of 1x10 TBE to 1800 mL of distilled water. Autoclave tape was used to make sides for the gel cast, and a gel comb was inserted. Three grams of agarose gel was measured and mixed with 150 mL of 1x10 TBE in a conical flask. The conical flask was covered with Saran wrap and microwaved for 1 minute set at high. Then, 10 µL of ethidium bromide was added, and the agarose solution was carefully mixed. The agarose solution was poured into the cast and left 20-30 minutes to allow it to set. The comb and autoclave tape were removed and the cast was placed into the electrophoresis tank. The tank and gel cast were then covered with 1x10 TBE buffer. Samples were prepared by adding 2 µL loading dye to 10 µL of sample. Then, 5 µL of DNA ladder was pipetted into the first well, followed by 12 µL of samples. The electrophoresis was conducted for approximately 50 minutes at 100 volts. The gel was then imaged with BioRad Gel Doc Imager.

6.4 Results

6.4.1 Genomic DNA quality and quantity

The genomic DNA purity and yield were determined using Nanodrop Spectrophotometry and the results are presented in **Table 6.5**. The genomic DNA 260:280 values are between 1.7-1.9, which are considered acceptable for the downstream analysis.

Table 6.5 C4-II genomic DNA yield and purity

Sample Group	ng/UL	A260	A280	260:280
F+M+ Rep 1	54.51	1.090	0.592	1.84
F+M+ Rep 2	56.44	1.129	0.593	1.91
F+M+ Rep 3	190.23	3.805	2.002	1.90
F+M+ Rep 4	51.78	1.036	0.521	1.99
F-M+ Rep 1	132.17	2.643	1.405	1.88
F-M+ Rep 2	101.84	2.037	1.086	1.88
F-M+ Rep 3	120.33	2.407	1.266	1.90
F+M- Rep 1	28.92	0.578	0.304	1.90
F+M- Rep 2	73.45	1.469	0.764	1.92
F+M- Rep 3	82.78	1.656	0.877	1.89
F-M- Rep 1	34.42	0.688	0.38	1.81
F-M- Rep 2	63.1	1.262	0.665	1.90
F-M- Rep 3	71.04	1.421	0.735	1.93
F+M+5% Rep 1	15.35	0.307	0.162	1.89
F+M+5% Rep 2	19.29	0.386	0.195	1.98
F+M+5% Rep 3	194.72	3.894	2.046	1.90

Sample groups consist of C4-II genomic DNA, grown in complete medium (F+M+), folate depleted medium (F-M+), methionine depleted medium (F+M-), folate and methionine depleted medium (F-M-) and 5% folate and methionine supplemented medium (F+M+5%). Cells were grown in triplicate (Rep 1 – Rep 3) for each condition, except for cells grown in complete medium where 4 replicates are prepared (Rep 1 – Rep 4).

6.4.2 RnBeads methylation data quality analysis

RnBeads performed the quality control module to identify technical and biological biases from the methylation data. This module identifies low quality datasets and removes them from the downstream analysis. Unfortunately, the scanner was not able to detect one of the samples from folate and methionine depleted conditions (F-M-) during the imaging procedure and it had to be removed from the RnBeads analysis.

In this data quality analysis, one sample of the 5% folate and methionine supplemented group (F+M+5%) and a sample from the control group (F+M+) were found to be of poor quality (**Figures 6.9 – 6.17**). They consistently returned a lower-than-average intensity readings for a majority of the quality control parameters indicating inefficient staining, hybridisation; A, T, C and G extensions, bisulphite conversion and allele-specific extension processes. In addition, these two samples also returned a lower-than-average intensity reading for non-polymorphic probes, which indicates inefficiencies at all steps of the methylation procedure. This could be due to technical assay failure, as only one replicate (each from F+M+ and F+M+5%) are

reported to have quality issues. Thus, these two samples were removed from the downstream analysis, as they might introduce biases to the downstream analysis.

The quality control module also generated a negative control boxplot showing the distributions of intensity readings for approximately 600 negative control probes present on the Infinium BeadChip. These probes estimate the background signal level for both green (unmethylated) and red (methylated) channels, by monitoring signals at bisulphite-converted sequences that do not contain CpGs. The negative control probe intensity readings are expected to be normally distributed with a relatively low mean (< 1000), as shown in **Figure 6.18**.

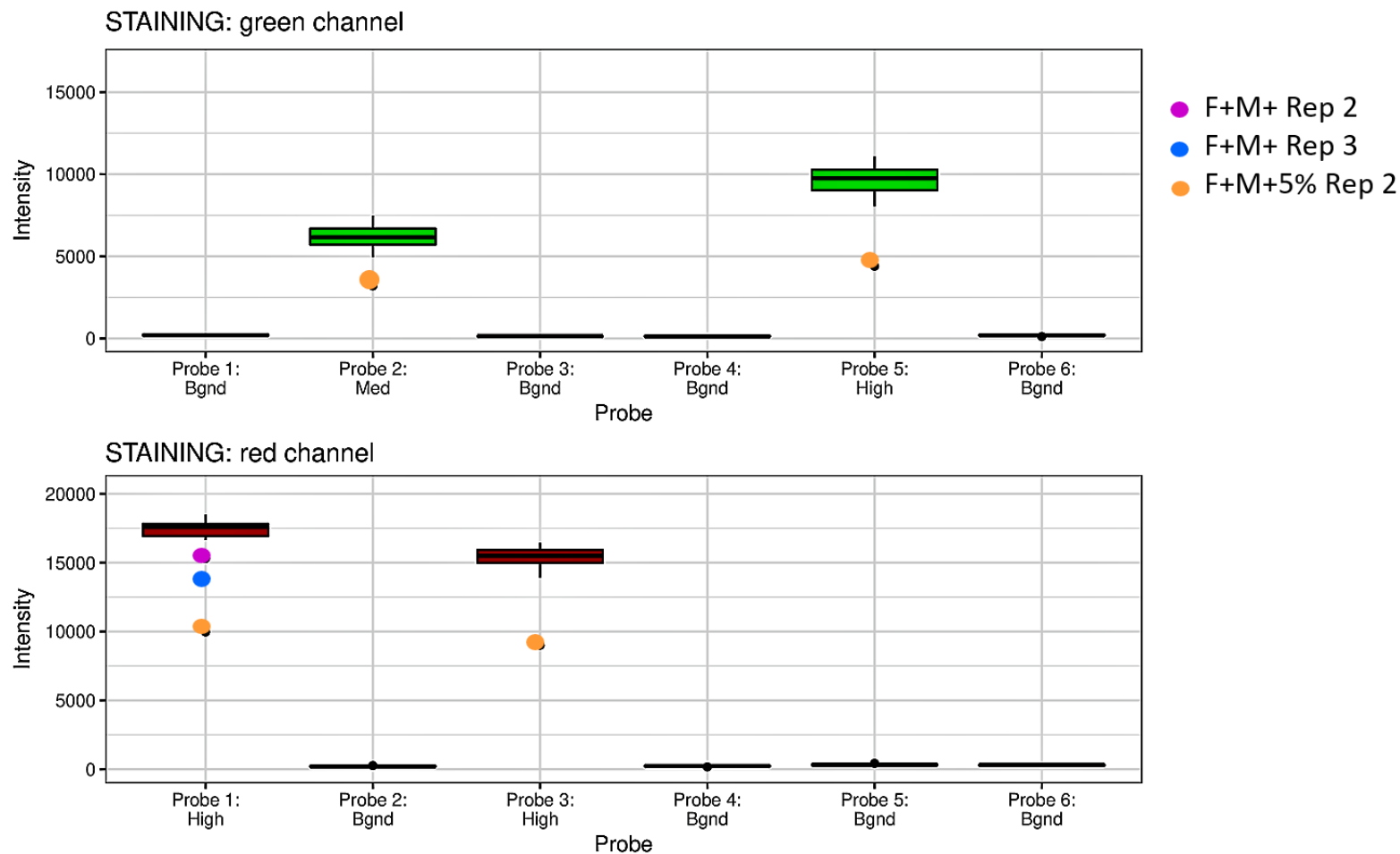


Figure 6.9 Control boxplot for the staining probes

This figure presents the quality control boxplot generated from the staining probes, which monitors the efficiency of the staining step. The boxplot shows the distribution of signal intensity readings for both red (methylated signals) and green (un-methylated signals) channels, for six staining probes. Each probe has a given intensity readings at high, medium or background level; low quality samples appear as outliers. In this figure, two samples from the F+M+ group and one sample from the F+M+5% have been identified as outliers, indicating an inefficient staining process for these samples.

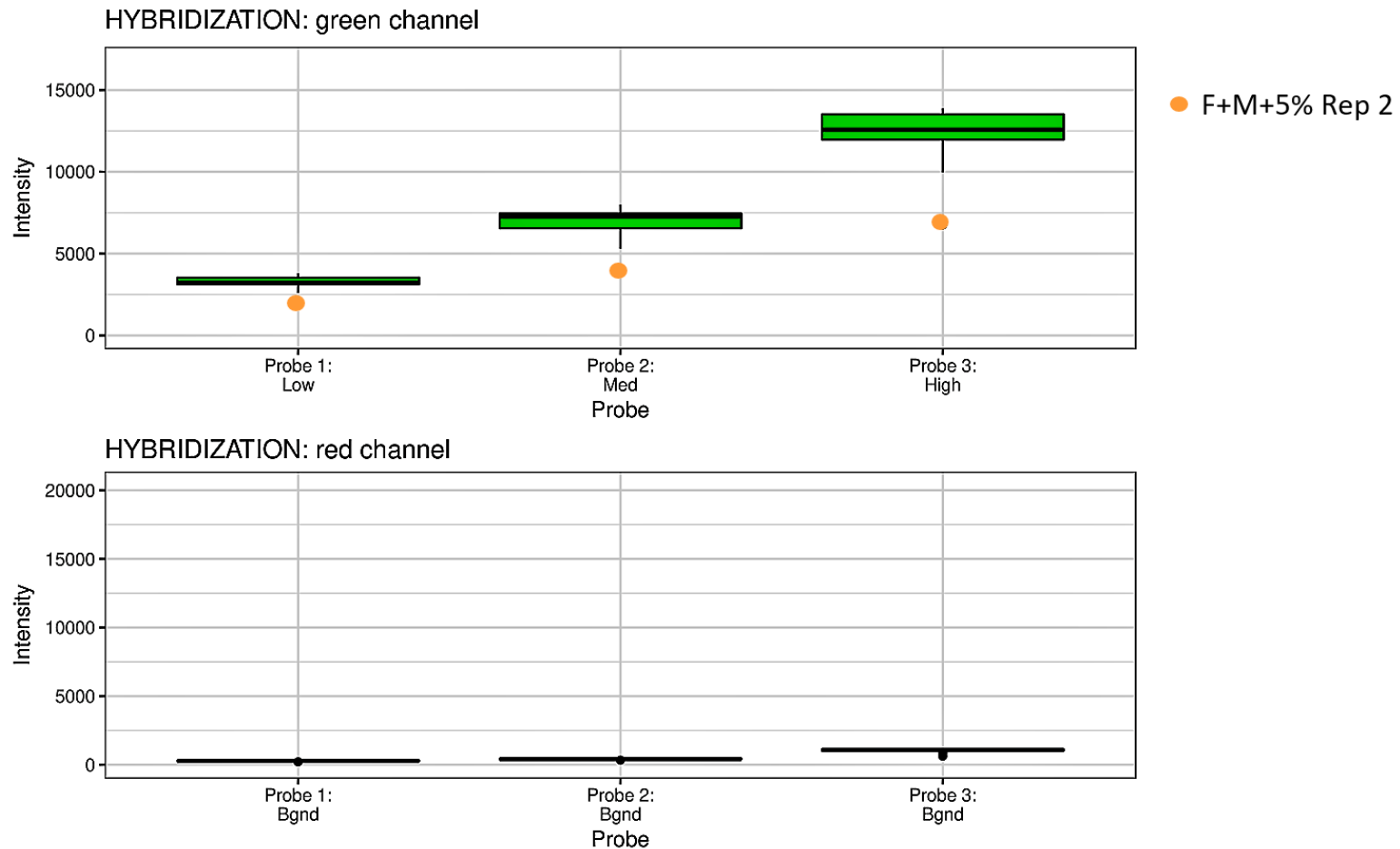


Figure 6. 10 Control boxplot for the hybridization probes

This figure presents the quality control boxplot generated from the hybridisation probes, which monitors the overall performance of the hybridisation step using synthetic targets as the reference. These targets are present in the hybridisation buffer at low, medium and high concentrations, resulting in three well separated intensity readings intervals in the green channels (un-methylated signals). In contrast, the methylated signals (red channels) are set at background level. Low quality samples appear as outliers. In this figure, one sample from F+M+5% is identified as an outlier, indicating an inefficient hybridisation process for that sample.

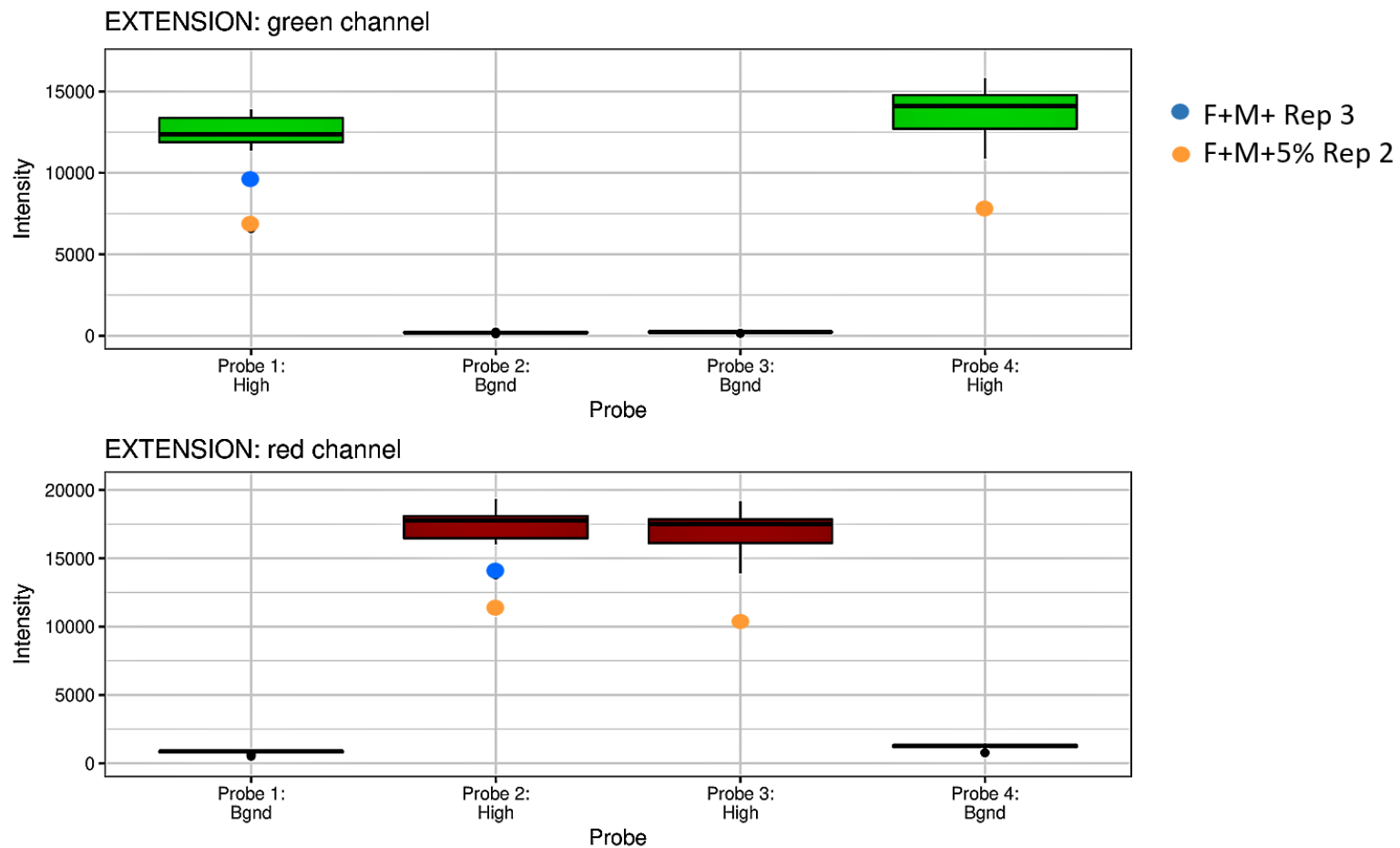


Figure 6.11 Control boxplot for the extension probes

This figure presents the quality control boxplot generated from the extension probes, which monitors the efficiency of A, T, C and G nucleotides extension from a hairpin probe. The boxplot shows the distribution of signal intensity readings for both red (methylated signals) and green (un-methylated signals) channels, for four extension probes. Each probe has a given intensity at high level or background level; low quality samples appear as outliers. In this figure, one sample from the F+M+ group and one sample from F+M+5% have been identified as outliers, indicating an inefficient extension process for both samples.

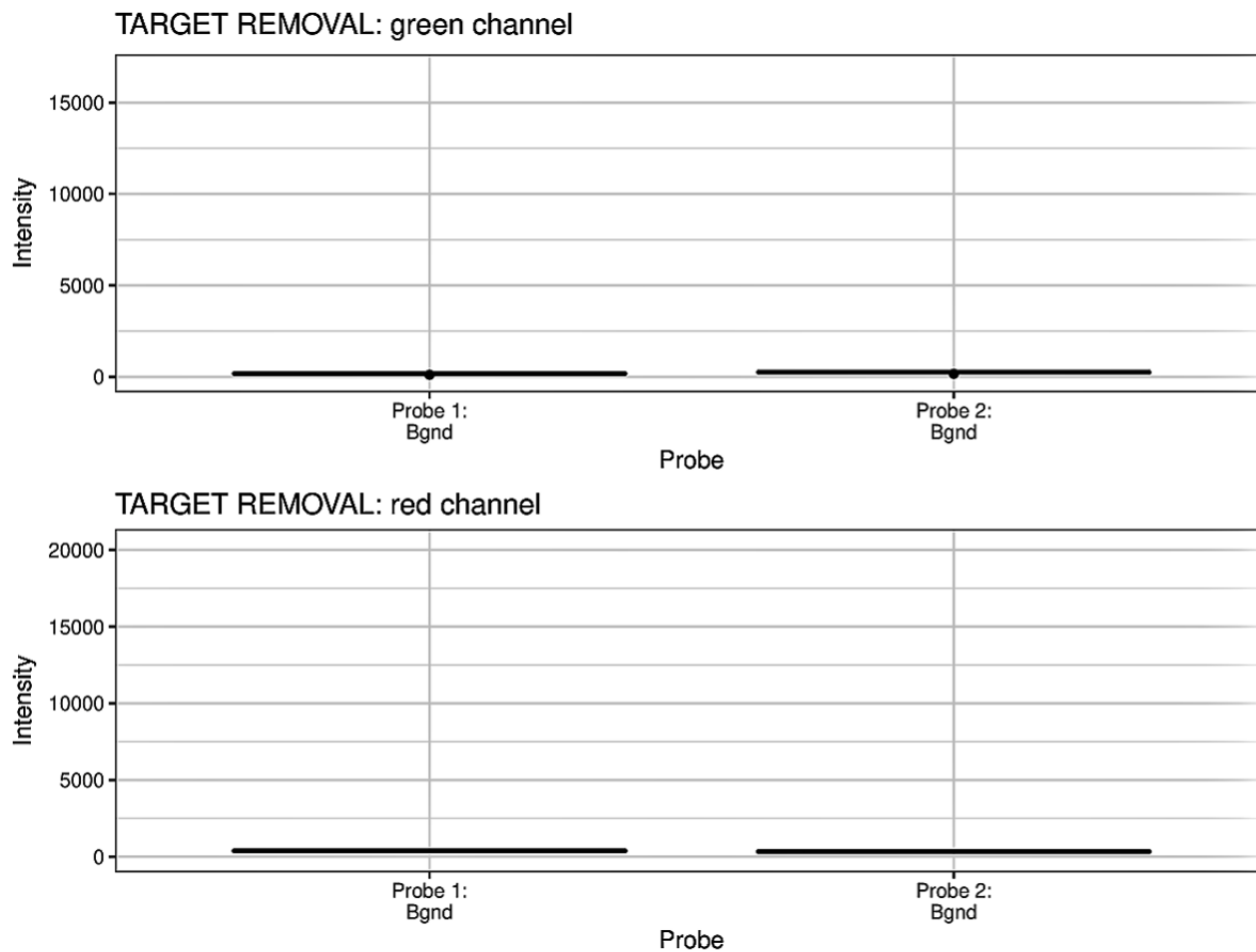


Figure 6. 12 Control boxplot for the target removal probes

This figure presents the quality control boxplot generated from the target removal probes, which monitors the efficiency of the stripping step after the extension process. The boxplot shows the distribution of signal intensity readings for both red (methylated signals) and green (un-methylated signals) channels, for two target removal probes, set at background level. In this figure, no outliers were detected indicating an efficient stripping process for all samples.

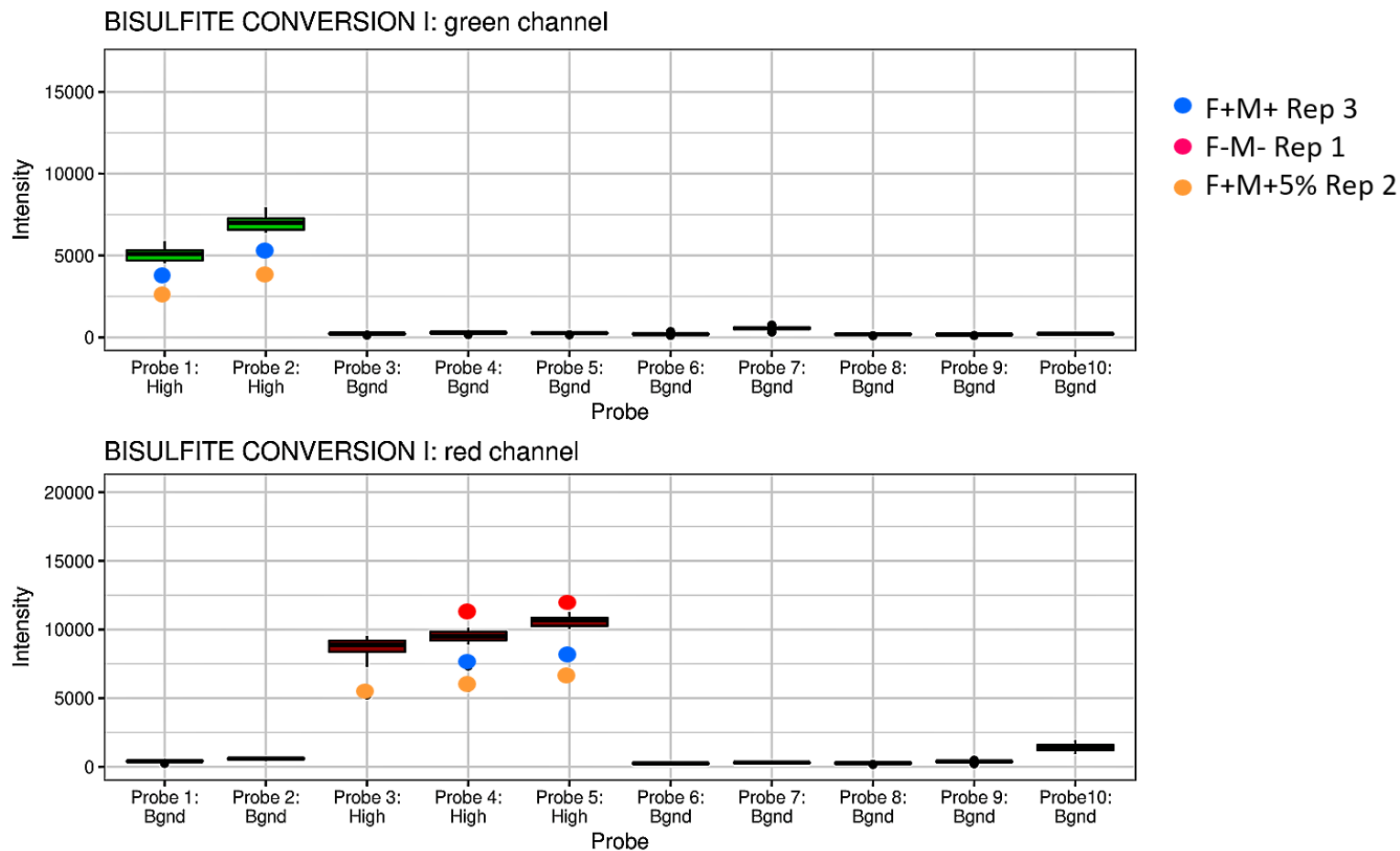


Figure 6.13 Control boxplot for the bisulphite conversion I probes

This figure presents the quality control boxplot generated from the bisulphite conversion I probes, which monitors the overall performance of the bisulphite conversion step. The boxplot shows the distribution of signal intensity readings for both red (methylated signals) and green (un-methylated signals) channels, for ten bisulphite conversion probes. Each probe has a given intensity readings at high level or background level; low quality samples appear as outliers. In this figure, one sample from the F+M+ group and one sample from F+M+5% have been identified as outliers, indicating an inefficient bisulphite conversion process; while one sample from the F-M- group shows a much higher intensity readings compared to the average values.

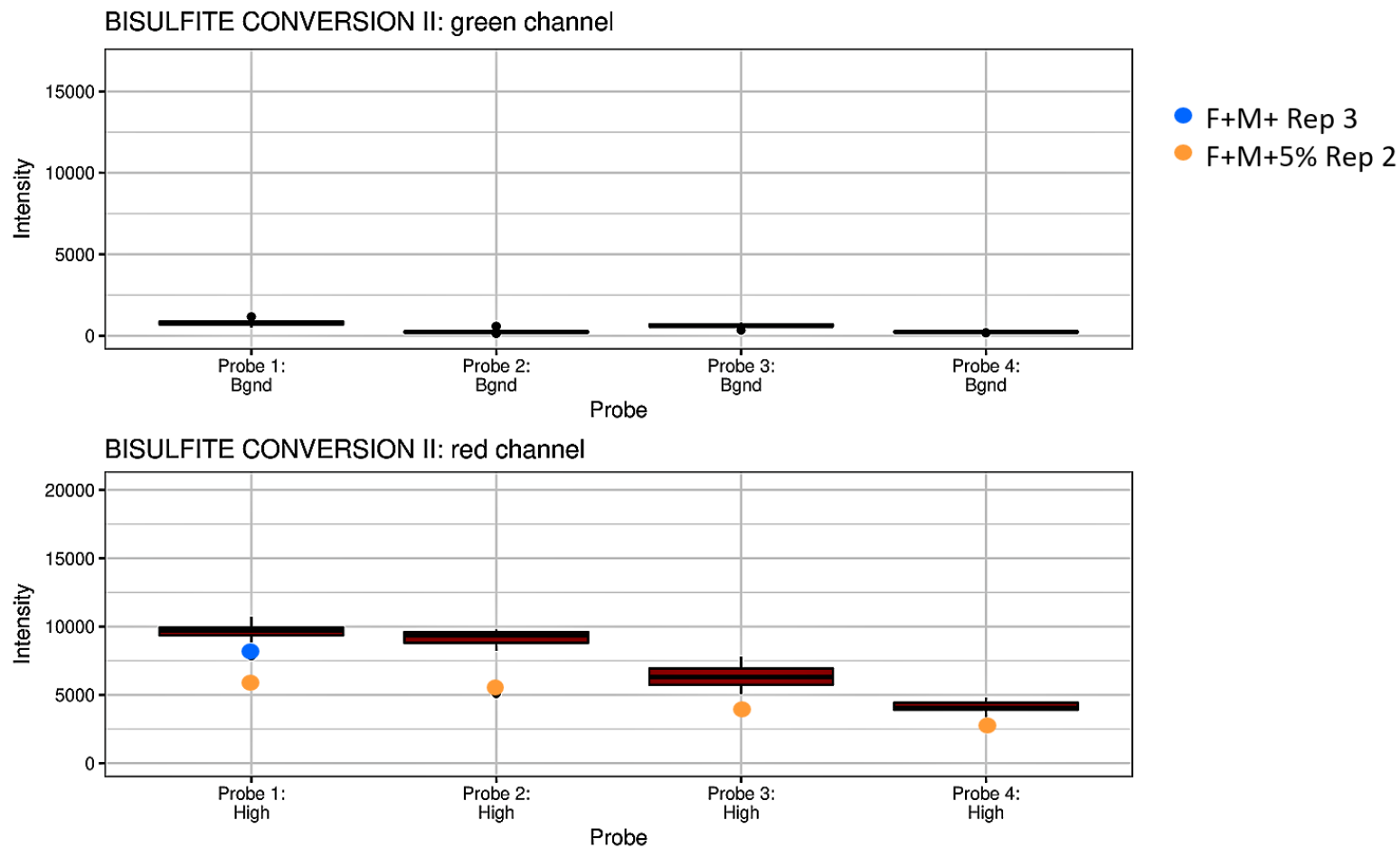


Figure 6. 14 Control boxplot for the bisulphite conversion II probes

This figure presents the quality control boxplot generated from the bisulphite conversion II probes, which also monitors the overall performance of the bisulphite conversion step. The boxplot shows the distribution of signal intensity readings set at high level for the red channel (methylated signals) and background level for the green channel (un-methylated signals). Low quality samples appear as outliers. In this figure, one sample from F+M+ group and one sample from F+M+5% have been identified as outliers, indicating an inefficient bisulphite conversion process for these samples.

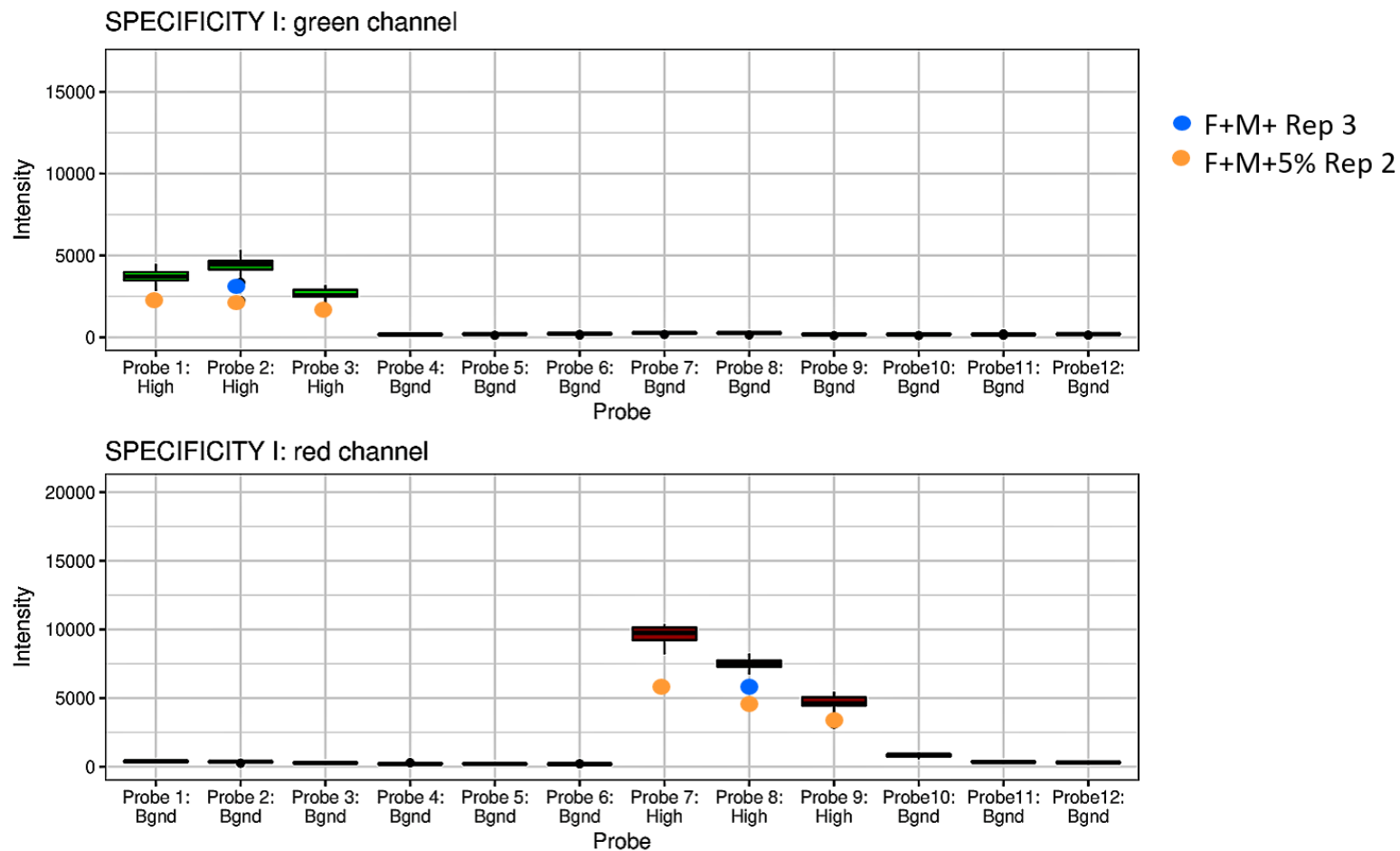


Figure 6. 15 Control boxplot for the specificity I probes

This figure presents the quality control boxplot generated from the specificity I probes, which monitors the allele-specific extension step. The boxplot shows the distribution of signal intensity readings for both red (methylated signals) and green (un-methylated signals) channels, for 12 specificity probes. Each probe has a given intensity readings at high level or background level; low quality samples appear as outliers. In this figure, one sample from F+M+ group and one sample from F+M+5% have been identified as outliers, indicating an inefficient allele-specific extension process for both samples.

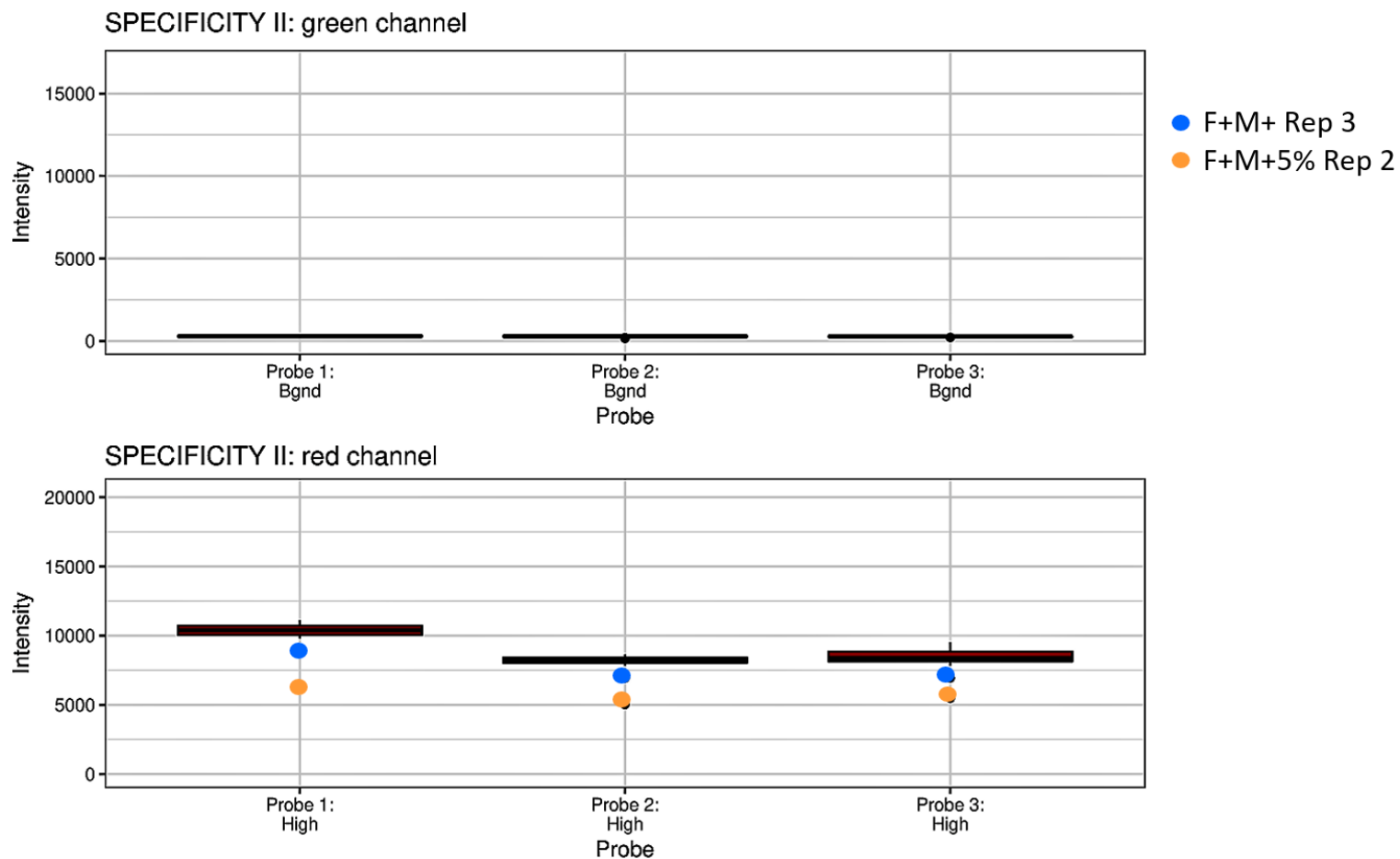


Figure 6. 16 Control boxplot for the specificity II probes

This figure presents the quality control boxplot generated from the specificity II probes, which also monitors the allele-specific extension step. The boxplot shows the distribution of signal intensity signals set at high level for the red channel (methylated signals) and background level for the green channel (unmethylated signals). Low quality samples appear as outliers. In this figure, one samples from F+M+ group and one sample from F+M+5% have been identified as outliers, indicating an inefficient allele-specific extension process.

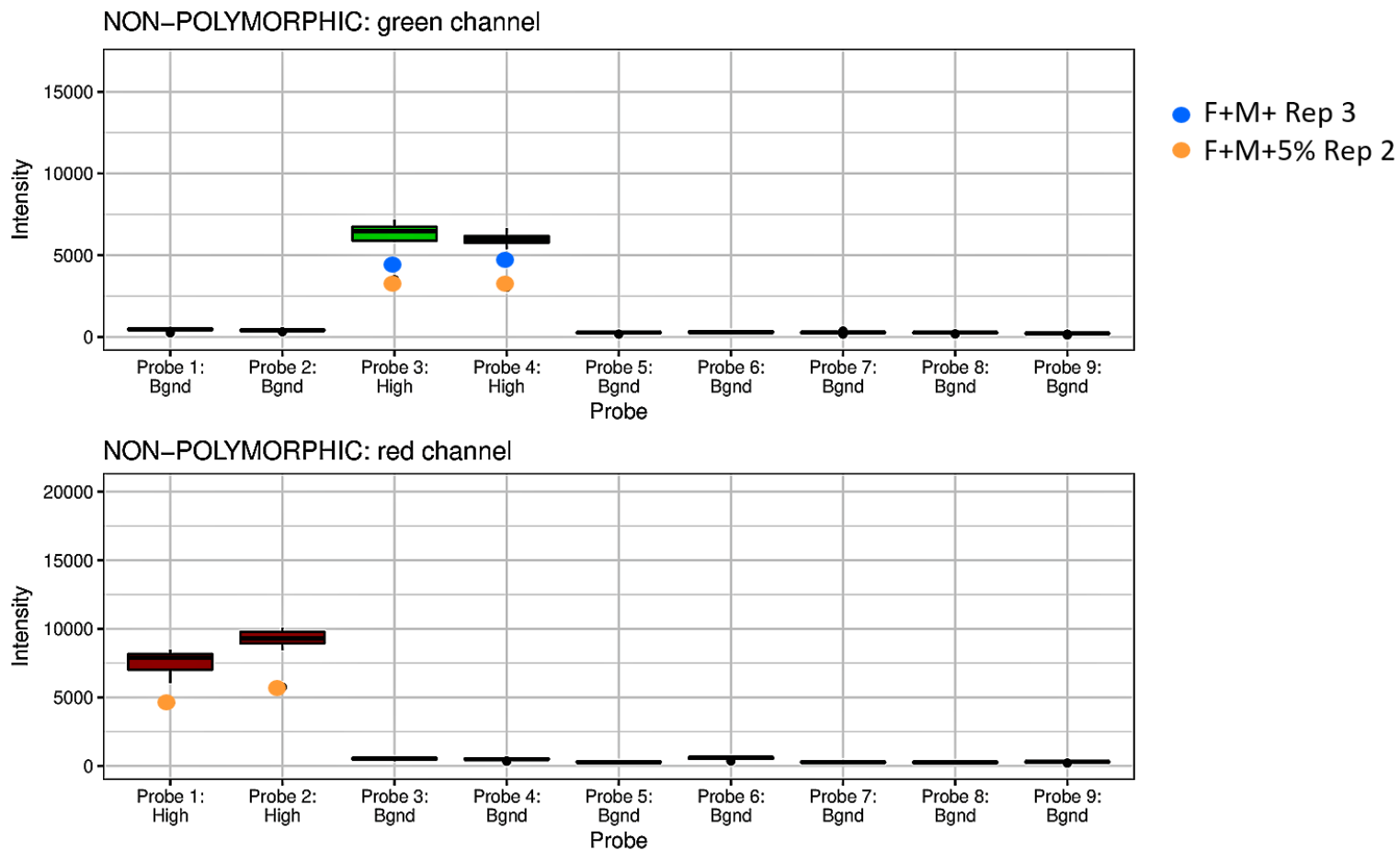


Figure 6. 17 Control boxplot for the non-polymorphic probes

This figure presents the quality control boxplot generated from the non-polymorphic probes, which monitors the efficiency of all steps of the methylation procedures by querying a non-polymorphic base in the genome (one probe for each nucleotide). The boxplot shows the distribution of signal intensity readings for both red (methylated signals) and green (un-methylated signals) channels, for nine non-polymorphism probes. Each probe has a given intensity readings at high level or background level; low quality samples appear as outliers. In this figure, one sample from F+M+ group and one sample from F+M+5% have been identified as outliers, indicating an overall inefficient process of methylation procedures.

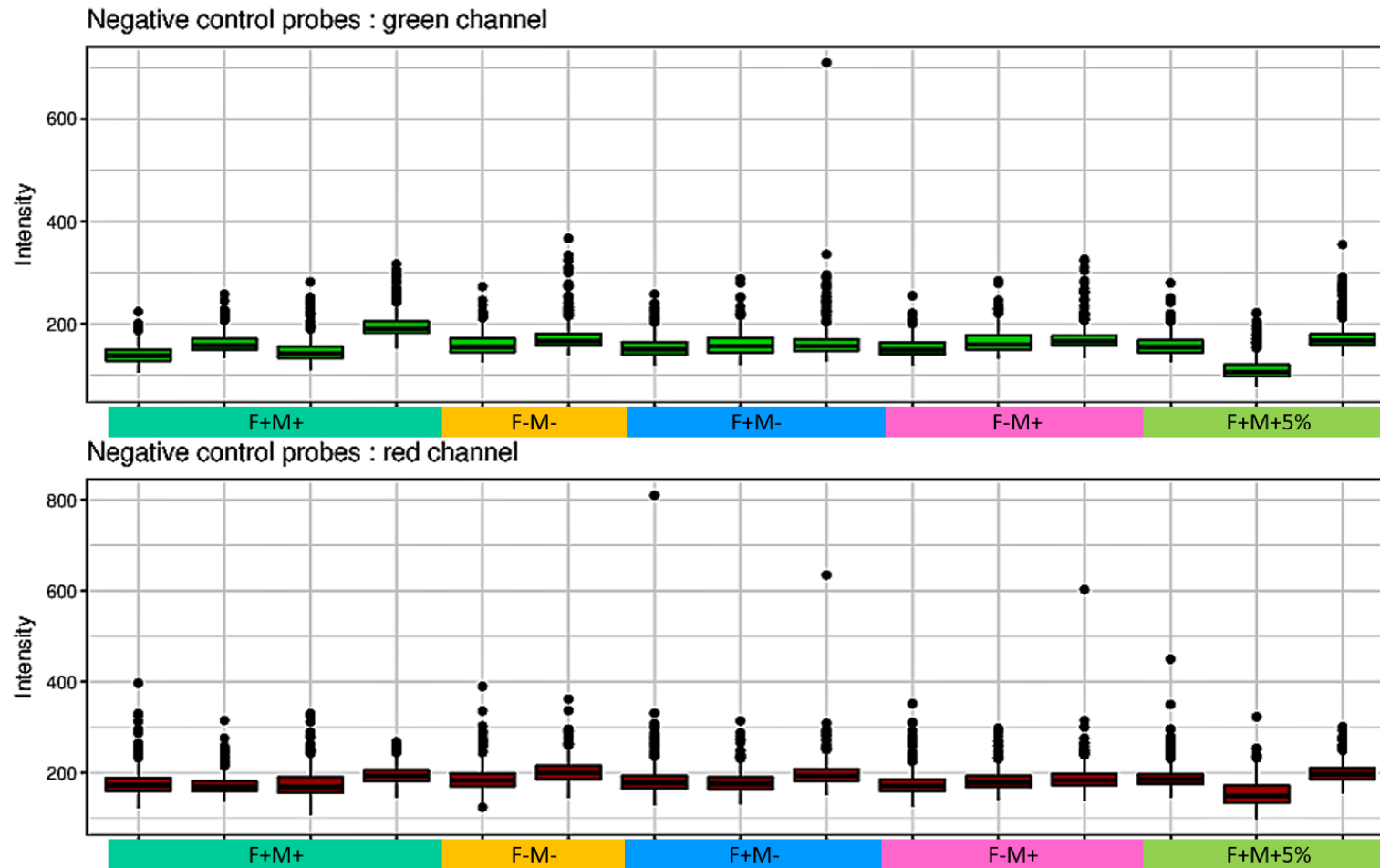


Figure 6. 18 Negative control boxplot

This figure presents the negative control boxplot for all sample replicates, generated from approximately 600 negative control probes designed to estimate background signal levels for both red (methylated signals) and green (un-methylated signals) channels. The negative control probes' intensity readings are expected to be normally distributed with a relatively low mean (< 1000), as shown in this figure.

6.4.3 RnBeads methylation data filtration and normalisation

The filtering step was executed in two stages. First, 20 151 probes that could bias the normalisation procedure were removed. Of these 17 371 sites were removed because they overlapped with SNPs while the other 2 780 probes were excluded as they were identified to be unreliable by the GreedyCut algorithm. The methylation β values were then normalised using the BMIQ normalisation method (Figure 6.19). Finally, the second filtering step was executed, removing an additional 21 980 probes from the downstream analysis. Of the total 866 895 probes measured, 824 764 probes (95%) were retained for the following exploratory and differential analysis.

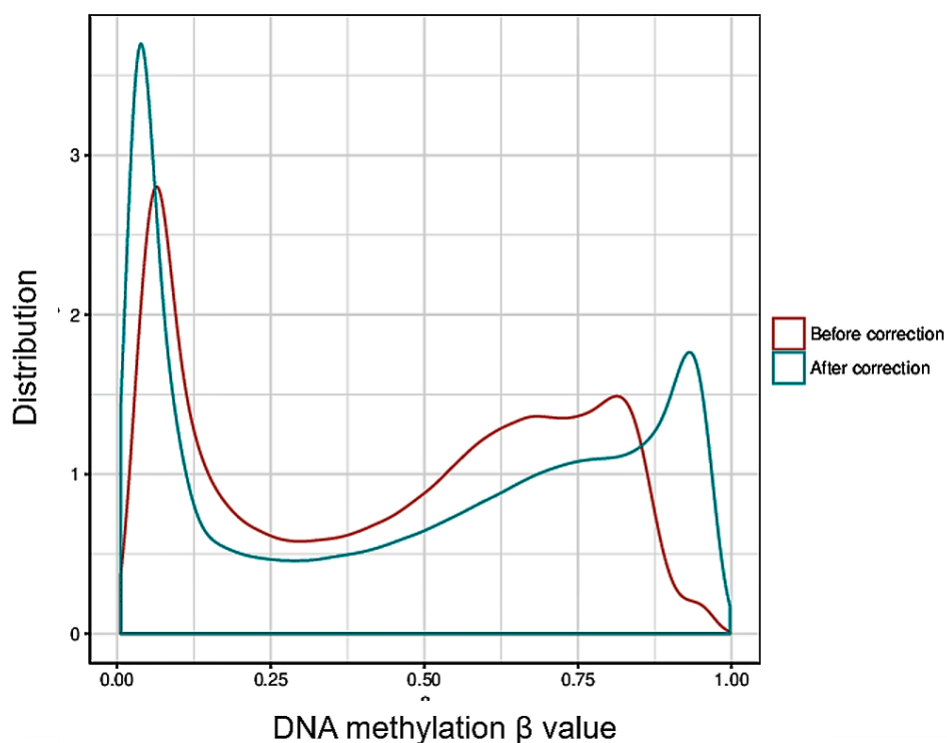


Figure 6.19 Distribution of methylation β values before and after normalisation using the BMIQ method

This method uses a three-state beta-mixture model to assign probes to methylation states. It is followed by the transformation of probabilities into quantiles. A methylation-dependent dilation transformation was then carried out in order to preserve the monotonicity and continuity of the data. This method reduces the technical variation and bias of type II probe values and eliminates the type I enrichment bias caused by the lower dynamic range of type II probes.

6.4.4 RnBeads exploratory analysis

In the exploratory analysis, global changes in DNA methylation were identified by visual inspection of DNA methylation data plots. In the C4-II cells grown in complete medium (F+M+), the global distribution of DNA methylation is characteristically bimodal with discrete

peaks at approximately 6% and 95% (**Figure 6.20**). C4-II cells grown in only folate depleted medium (F-M+) showed a similar distribution of DNA methylation values to control group (F+M+). However, with methionine depletion (F+M-), more sites appeared to be hypomethylated, with the peak for highly methylated loci shifted from 95% in the control group to approximately 75%. C4-II cells grown in combined folate and methionine depleted medium (F-M-) and 5% folate and methionine supplemented medium (F+M+5%) also had a similar hypomethylation trend, with the peak of the highly methylated loci shifted to approximately 70%, and with a higher distribution of the essentially un-methylated loci.

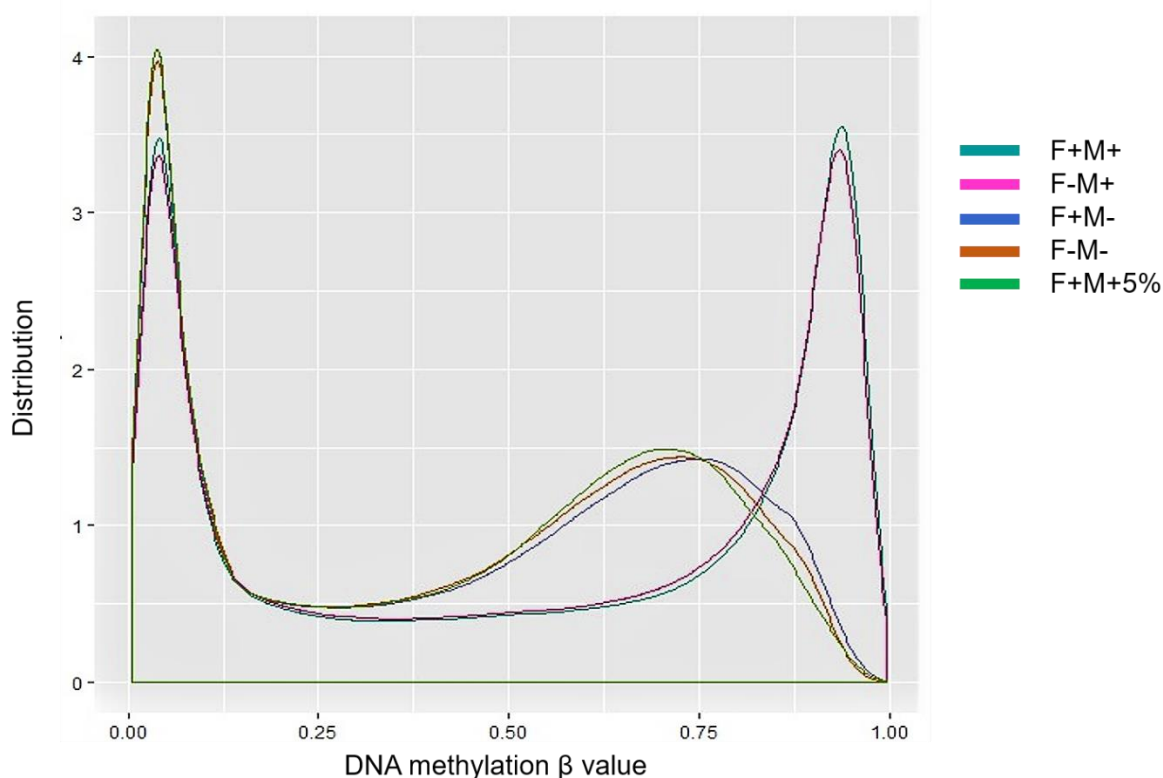


Figure 6.20 DNA methylation value distribution according to sample groups

This figure shows the distribution of DNA methylation values of C4-II cells grown in complete medium (F+M+), folate depleted medium (F-M+), methionine depleted medium (F+M-), folate and methionine depleted medium (F-M-), and 5% folate and methionine supplemented medium (F+M+5%). A DNA methylation value of 0.00 represents essentially un-methylated loci, while 1.00 represents the highly methylated loci.

A hierarchically clustered heat map was generated in order to provide a global assessment of sample subtypes in the data set. In addition, dimension reduction using principal component analysis and multidimensional scaling was also carried out, allowing the visualisation of associations between sample group and global trends in DNA methylation data. In both analyses, there was a relative similarity of DNA methylation profiles between C4-II

cells grown in complete medium (F+M+) and folate depleted medium (F-M+); as well as between C4-II cells grown in methionine depleted medium (F+M-), folate and methionine depleted medium (F-M-) and 5% folate and methionine supplemented medium (F+M+5%). Put another way, in both these plots there was distinct separation between methionine replete samples (F+M+ and F-M+) and methionine deficient sample groups (F+M-, F-M- and F+M+5%) (**Figures 6.21 and 6.22**). A pairwise correlation was used in order to assess the variability within the sample replicates. **Figure 6.23** shows the relationship between average methylation and methylation variability of probes, where minimal variability was detected within sample replicates, for all sample groups.

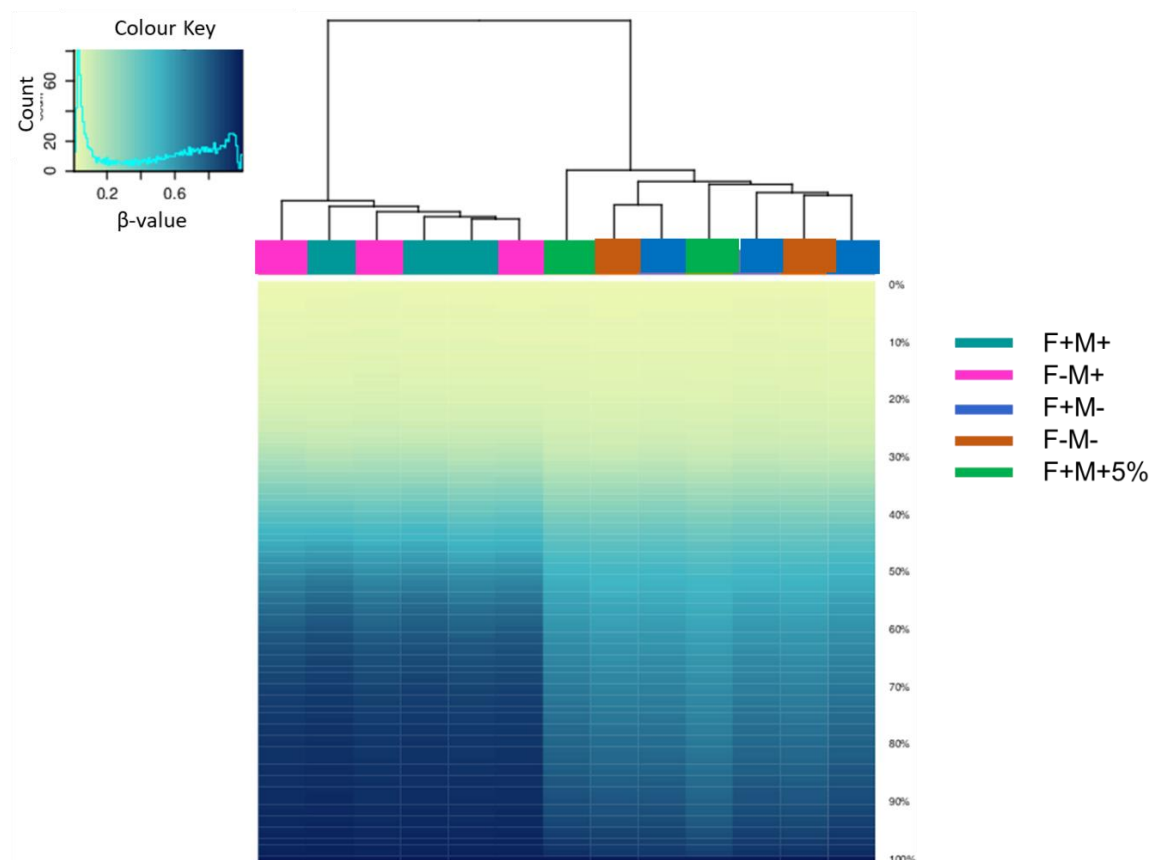


Figure 6. 21 Heat map with hierarchical clustering of DNA methylation levels among sample groups

This figure shows the hierarchical clustering of samples based on all methylation values, using average linkage and Manhattan distance, where it displays methylation percentiles per sample. The sample groups consist of C4-II cells grown in complete medium (F+M+), folate depleted medium (F-M+), methionine depleted medium (F+M-), folate and methionine depleted medium (F-M-), and 5% folate and methionine supplemented medium (F+M+5%). The colour key range represents the β values, from low (light blue – essentially un-methylated) to high (darker blue – highly methylated). The fluorescent blues line represents the distribution of DNA methylation values. There is a distinct separation between methionine replete samples (F+M+ and F-M+) and methionine deficient sample groups (F+M-, F-M- and F+M+5%). It appears that the depletion of folate alone had little impact, while those grown in methionine deficient media are clustered differently from control group.

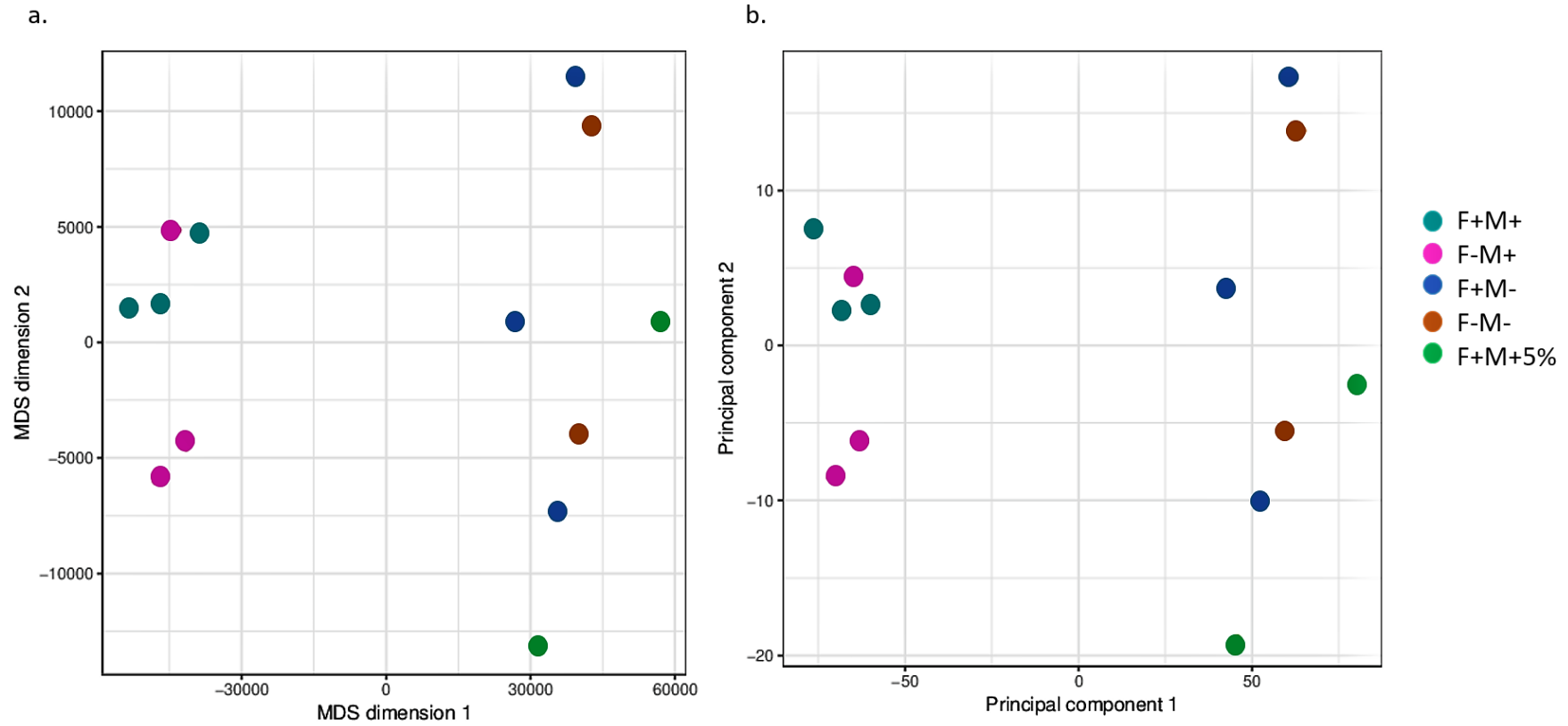


Figure 6.22 Dimension reduction analysis of sample groups

This figure shows the relative similarities and differences of DNA methylation profiles between sample groups. The scatter plot (a) visualizes the samples transformed into 2-dimensional space after performing Kruskal's non-metric multidimensional scaling and (b) shows values of selected principal components. The sample groups consist of C4-II cells grown in complete medium (F+M+), folate depleted medium (F-M+), methionine depleted medium (F+M-), folate and methionine depleted medium (F-M-), and 5% folate and methionine supplemented medium (F+M+5%). There is a distinct separation between methionine replete samples (F+M+ and F-M+) and methionine deficient sample groups (F+M-, F-M- and F+M+5%). It appears that the depletion of folate alone had little impact, while those grown in methionine deficient media are clustered differently from control group.

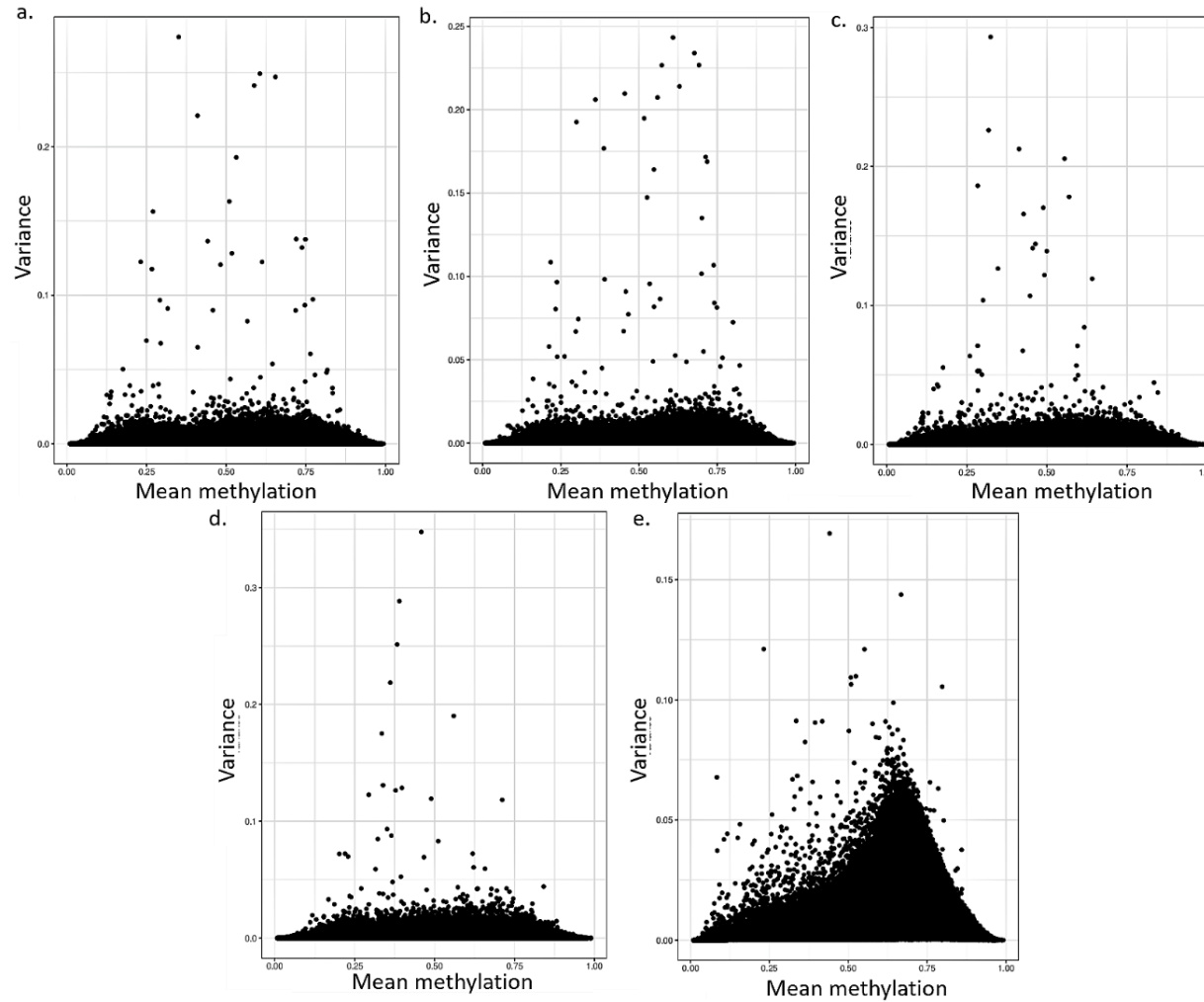


Figure 6.23 Relationship between average methylation and methylation variability of probe results for each sample group

This scatter plot shows the pairwise correlation between probe mean methylation and the variance within each sample biological replicates. The figures show the minimal variability within each sample replicates, for all sample groups; **(a)** complete medium (F+M+), **(b)** folate depleted medium (F-M+), **(c)** methionine depleted medium (F+M-), **(d)** folate and methionine depleted medium (F-M-), and **(e)** 5% folate and methionine supplemented medium (F+M+5%). Every point corresponds to one probe.

Other than single CpG measurements, RnBeads also generated DNA methylation profile analyses for predefined genomic regions including gene, promoter and CpG islands. RnBeads produced composite plots of DNA methylation levels within these genomic regions and these plots were used to identify global changes in DNA methylation that affect gene promoters differently when compared to intragenic or intergenic regions. Based on this analysis, taking regional averages over all annotated genes, DNA methylation levels were again seen to be generally higher in complete (F+M+) and folate depleted (F-M+) media than in the other three conditions (F+M-, F-M- and F+M+5%) (Figure 6.24). Similar trends were also observed for both gene promoter regions and CpG islands (Figures 6.25 and 6.26).

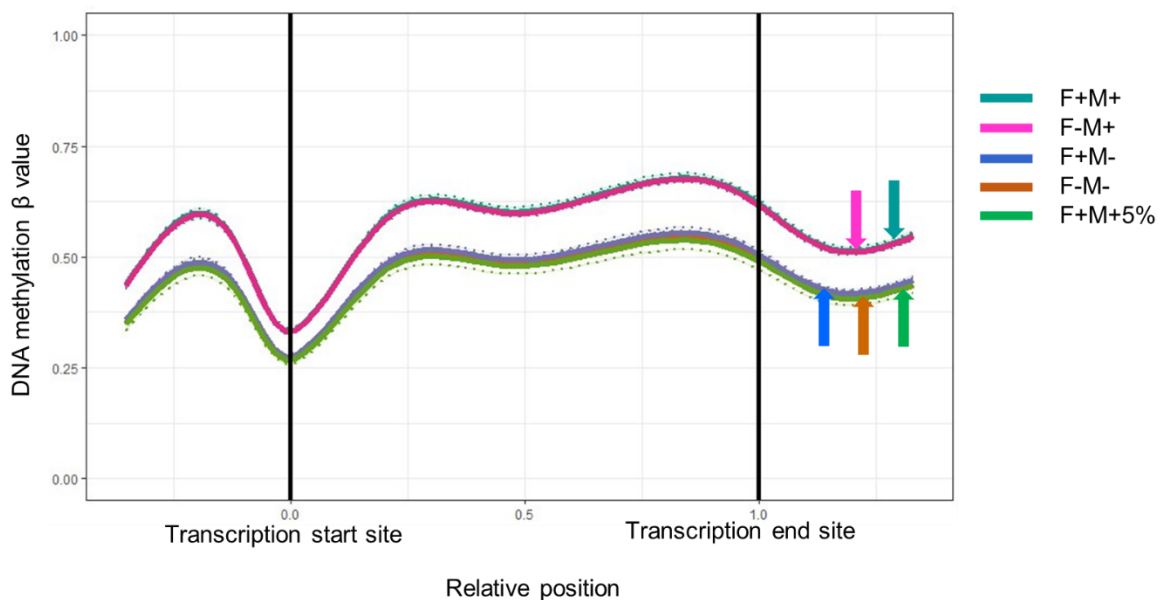


Figure 6. 24 DNA methylation level for genomic region (gene) according to sample group

This figure shows the regional methylation profile according to sample groups, presented as a composite plot. The relative coordinates of 0 and 1 correspond to the start and end coordinates of that region respectively. Coordinates smaller than 0 and greater than 1 denote flanking regions normalized by region length. Horizontal lines indicate region boundaries. For scatterplot smoothing, generalised additive models with cubic spine smoothing were used. Deviation bands indicate 95% confidence intervals. The sample groups consist of C4-II cells grown in complete medium (F+M+), folate depleted medium (F-M+), methionine depleted medium (F+M-), folate and methionine depleted medium (F-M-), and 5% folate and methionine supplemented medium (F+M+5%).

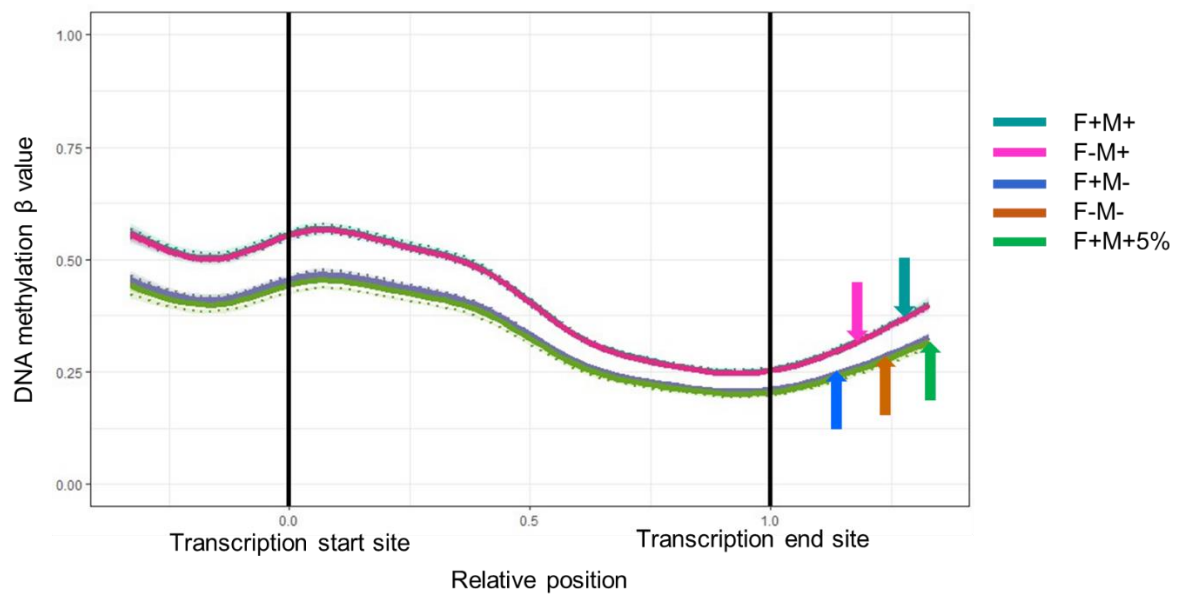


Figure 6.25 DNA methylation level for genomic region (promoter) according to sample group

This figure shows the regional methylation profile according to sample groups, presented as a composite plot. The relative coordinates of 0 and 1 correspond to the start and end coordinates of that region respectively. Coordinates smaller than 0 and greater than 1 denote flanking regions normalized by region length. Horizontal lines indicate region boundaries. For scatterplot smoothing, generalised additive models with cubic spine smoothing were used. Deviation bands indicate 95% confidence intervals. The sample groups consist of C4-II cells grown in complete medium (F+M+), folate depleted medium (F-M+), methionine depleted medium (F+M-), folate and methionine depleted medium (F-M-), and 5% folate and methionine supplemented medium (F+M+5%).

6.4.5 RnBeads differential analysis

In the differential analysis, DNA methylation differences were analysed at the individual CpGs level. It was found that there were no significant differences between cells grown in folate depleted medium (F-M+) and control group (F+M+) (**Figure 6.27a**). In contrast, in all the other three groups where methionine is depleted, regardless in the presence or absence of folate, there was a significant difference in CpG methylation, with a majority of CpG sites were hypomethylated (**Figures 6.27b to 6.27d**). A total of 470 487 CpG sites were differently methylated in C4-II cells grown in methionine depleted medium (F+M-), when compared with cells grown in complete medium (F+M+) (adjusted $P < 0.05$). Of these, 1730 CpGs were found to be hypermethylated. C4-II cells grown in both folate and methionine depleted medium (F-M-) had a higher number of differently methylated sites (515 066) than cells grown in only methionine depleted medium (F+M-), but with lower number of CpGs (1557) being hypermethylated. When the medium was repleted with 5% of folate and methionine (F+M+5%), a total of 513 954 sites were found to be differently methylated, when compared to the control group (F+M+) with 1705 sites hypermethylated.

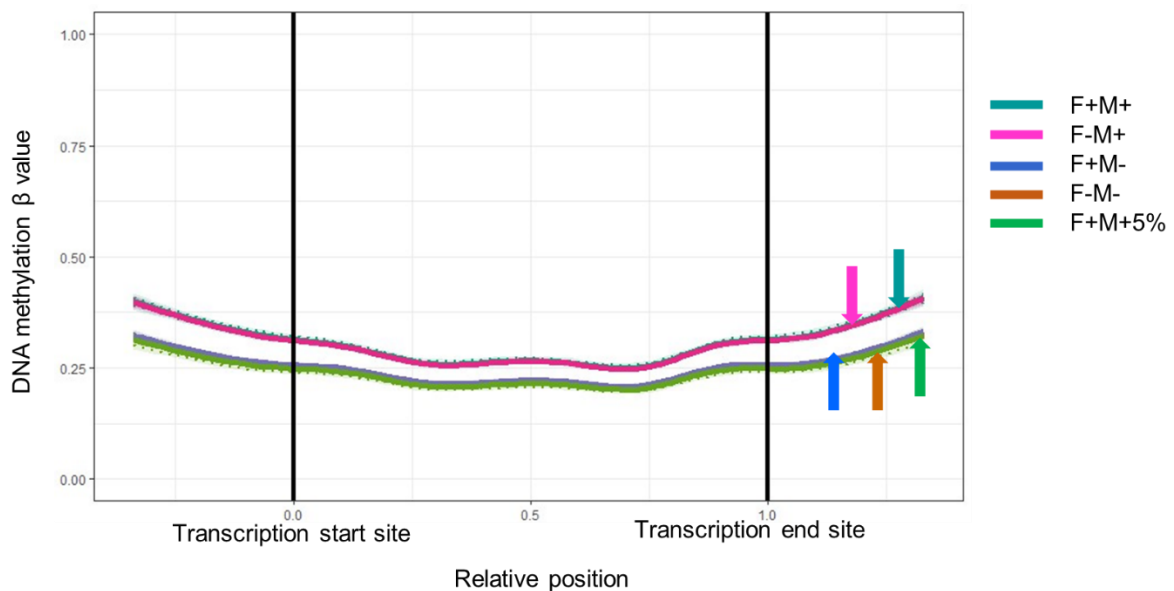


Figure 6.26 DNA methylation level for genomic region (CpG islands) according to sample group

This figure shows the regional methylation profile according to sample groups, presented as a composite plot. The relative coordinates of 0 and 1 correspond to the start and end coordinates of that region respectively. Coordinates smaller than 0 and greater than 1 denote flanking regions normalized by region length. Horizontal lines indicate region boundaries. For scatterplot smoothing, generalised additive models with cubic spine smoothing were used. Deviation bands indicate 95% confidence intervals. The sample groups consist of C4-II cells grown in complete medium (F+M+), folate depleted medium (F-M+), methionine depleted medium (F+M-), folate and methionine depleted medium (F-M-), and 5% folate and methionine supplemented medium (F+M+5%).

The RnBeads differential analysis also generates a combined rank score for each of the analysed CpG sites, creating a priority-ranked list of sites that were most affected by the given treatment. Based on these priority-ranked lists, Venny 2.0 has identified several top ranking CpG sites that were affected in all three methionine depleted conditions i.e. methionine depleted medium (F+M-), folate and methionine depleted medium (F-M-) and 5% folate and methionine supplemented medium (F+M+5%) all of which are hypomethylated (**Figure 6.28**). Individual inspection of these top-ranking sites using the UCSC genome browser identified several interesting genes that corresponded to these CpG sites including *TP73*, *STAT1* and *DAPK1*.

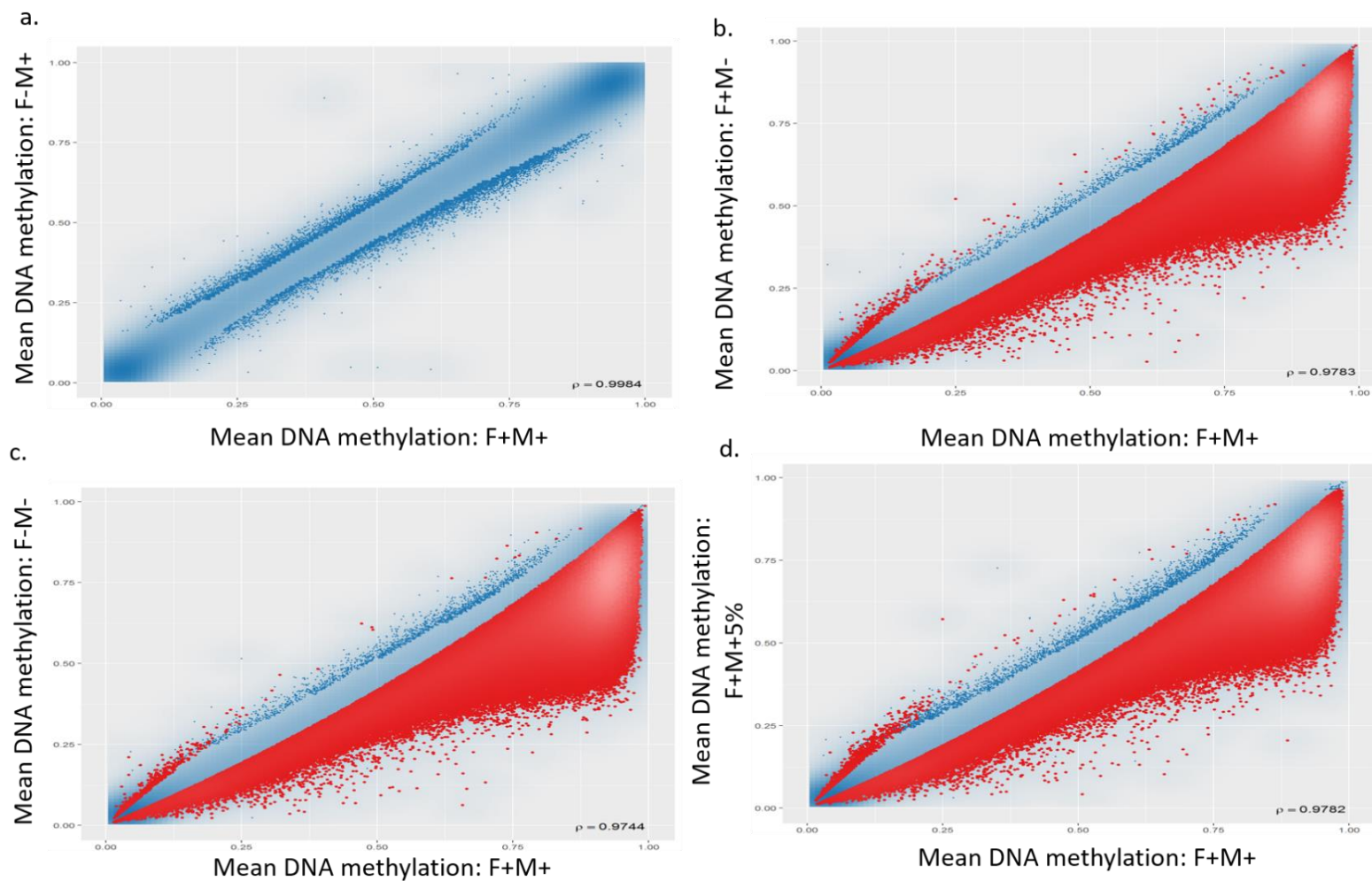


Figure 6.27 Differential methylation analysis at individual CpG sites

This figure shows the scatter plot of groupwise mean DNA methylation levels across CpG sites, where comparison was made between C4-II cell grown in complete medium (F+M+) and (a) folate depleted medium (F-M+), (b) methionine depleted medium (F+M-), (c) folate and methionine depleted medium (F-M-), and (d) 5% folate and methionine supplemented medium (F+M+5%). Differentially methylated CpG sites identified based on adjusted P value < 0.05 are highlighted in red.

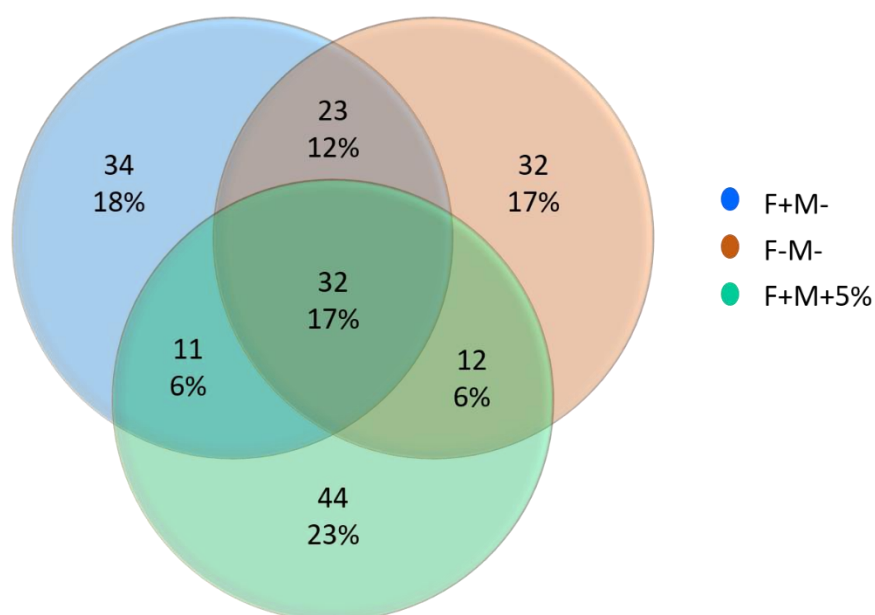


Figure 6.28 Venn diagram of common top ranking CpGs between methyl donor depleted conditions

This figure shows the common top 100 ranked CpG sites that were identified based on RnBeads combined ranking score, between methionine depleted medium (F+M-), folate and methionine depleted medium (F-M-) and 5% folate and methionine supplemented medium (F+M+5%).

In addition to single CpGs, the RnBeads differential analysis was also performed for sets of predefined genomic regions such as CpG islands, gene, and promoter regions. **Table 6.6** presents the number of differently methylated regions (combined adjusted $P < 0.05$) for methionine depleted cells (F+M-), folate and methionine depleted cells (F-M-) and 5% folate and methionine supplemented cells (F+M+5%), when compared with the control group (F+M+).

Table 6.6 Number of differently methylated regions according to sample group

	Differently Methylated Regions		
	Gene	Promoter	CpG islands
F+M+ with F+M-	23 845	21 397	10 451
F+M+ with F-M-	26 032	24 168	11 030
F+M+ with F+M+5%	25 752	23 389	11 028

6.4.6 Bioinformatics analysis of differently methylated regions

Additionally, a bioinformatics analysis was carried out in order to identify functions and pathways that are affected by the methyl donor depletion. Functional clustering analysis was performed using the DAVID software to determine overrepresented biological processes (GO_BP) from top 3000 (based on RnBeads combined rank score) gene promoter differently

methyated regions, all of which were hypomethylated. Each cluster was given a name to represent their main biological function and the top ten clusters for each methyl donor depletion condition are presented in **Table 6.7**. Similar to findings in **Chapter 3**, several clusters associated with host defence and immune responses were identified to be affected in C4-II cells grown in methionine depletion medium (F+M-), folate and methionine depleted medium (F-M), as well as in the 5% folate and methionine supplemented medium (F+M+5%).

Table 6.7 Top ten GO-BP annotation clusters generated from gene promoter differently methylated regions

Overrepresented Biological Process					
Methionine depletion (F+M-)	*ES	Folate and methionine depletion (F-M-)	*ES	5% folate and methionine supplementation (F+M+5%)	*ES
Multicellular organismal process	8.37	Multicellular organismal process	7.95	Single organism process	6.21
Immune response	5.60	Response to stress	6.26	Cellular response to organic substance	3.03
Defence response	5.09	Inflammatory response	5.25	Reproduction process	2.68
Localization	4.81	Defence response	5.18	Homeostatic process	2.25
Lipid metabolic process	4.40	Homeostatic process	5.17	System development	2.16
Inflammatory response	4.09	Localization	5.12	Lipid localisation	2.14
Cholesterol metabolic response	3.98	Cell motility	4.14	Response to wounding	1.96
Ion transport	3.45	Lipid metabolic process	3.78	Angiogenesis	1.92
Anion transport	3.20	Regulation of inflammatory response	3.54	Lipid metabolic process	1.79
Leukocyte activation	3.11	Leukocyte migration	3.22	Cellular response to cytokine stimulus	1.78

*ES: enrichment score, P<0.05 with Benjamini-Hochberg correction

The lists of differently methylated regions (DMRs) were also uploaded to the ClueGo plug-in via the Cystoscape platform, to visualize the functionally grouped terms in the form of networks, using the GO_BP term database. **Figures 6.29** to **Figure 6.31** represent the GO term network of biological processes that are enriched for all three methyl depleted conditions. Similar to the findings in DAVID, biological processes associated with immune responses and host defence were significantly enriched. Additionally, ClueGo analysis also detected terms related to mitosis, cell differentiation, cell motility and angiogenesis that was affected by methyl donor depletion.

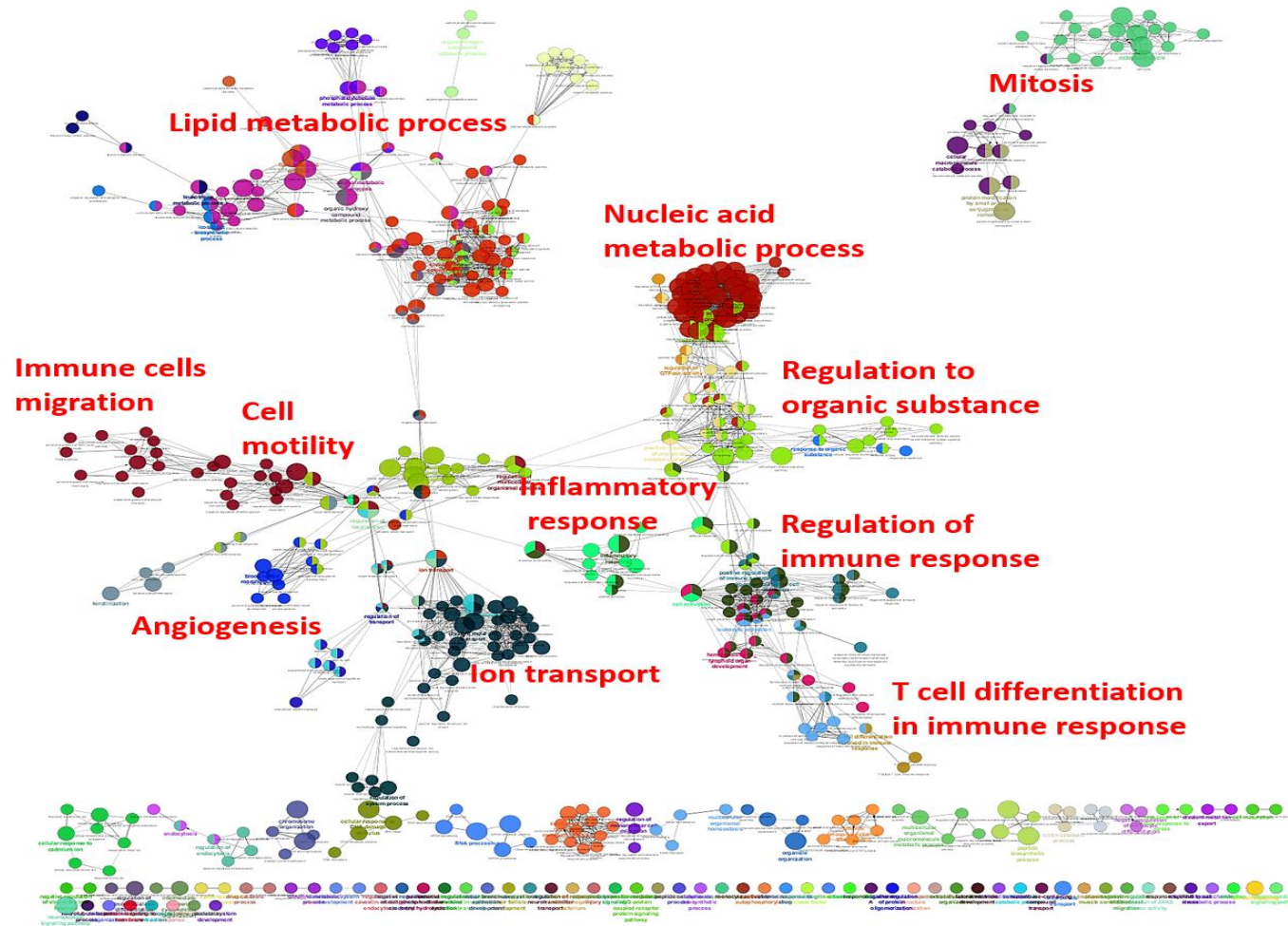


Figure 6. 29 GO_BP terms network associated with DMRs for methionine depleted condition

This figure represents network of biological process (GO_BP terms) that are enriched by methionine depletion. Each node represents a specific biological process (GO_BP terms) that are enriched in this analysis. Node size reflects the significance level of the enriched terms; bigger nodes indicate higher levels of significance. The node colour indicates a specific GO term, and similar coloured nodes indicate that these GO terms are from the same GO parent-child terms. Kappa score was used to link (edges) of the enriched terms (nodes) where it defined term-term interrelations (edges) and functional groups, based on shared genes between the terms.

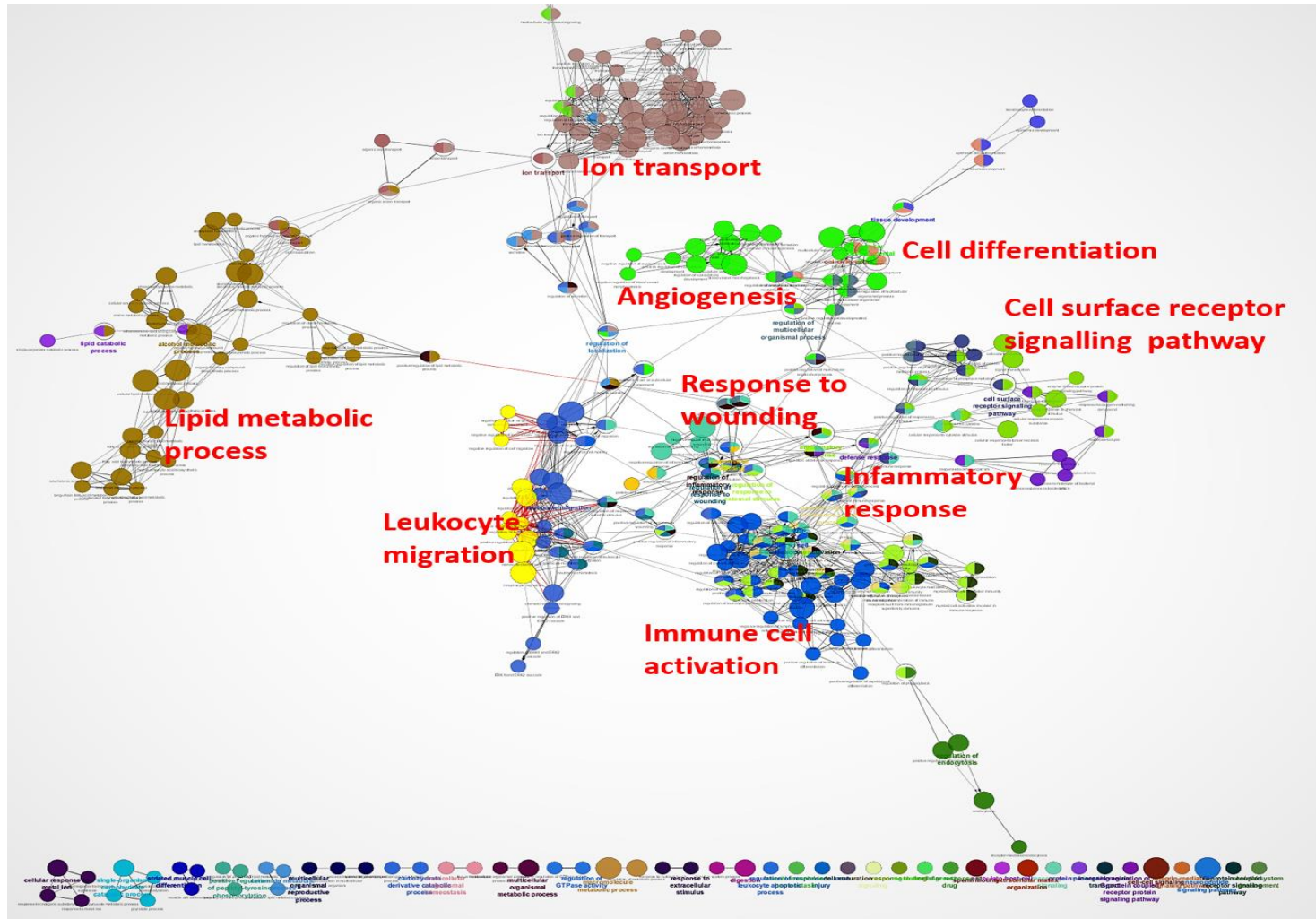


Figure 6. 30 GO_BP terms network associated with DMRs for folate and methionine depleted condition

This figure represents network of biological process (GO_BP terms) that are enriched by folate and methionine depletion. Each node represents a specific biological process (GO_BP terms) that are enriched in this analysis. Node size reflects the significance level of the enriched terms; bigger nodes indicate higher levels of significance. The node colour indicates a specific GO term, and similar coloured nodes indicate that these GO terms are from the same GO parent-child terms. Kappa score was used to link (edges) of the enriched terms (nodes) where it defined term-term interrelations (edges) and functional groups, based on shared genes between the terms.

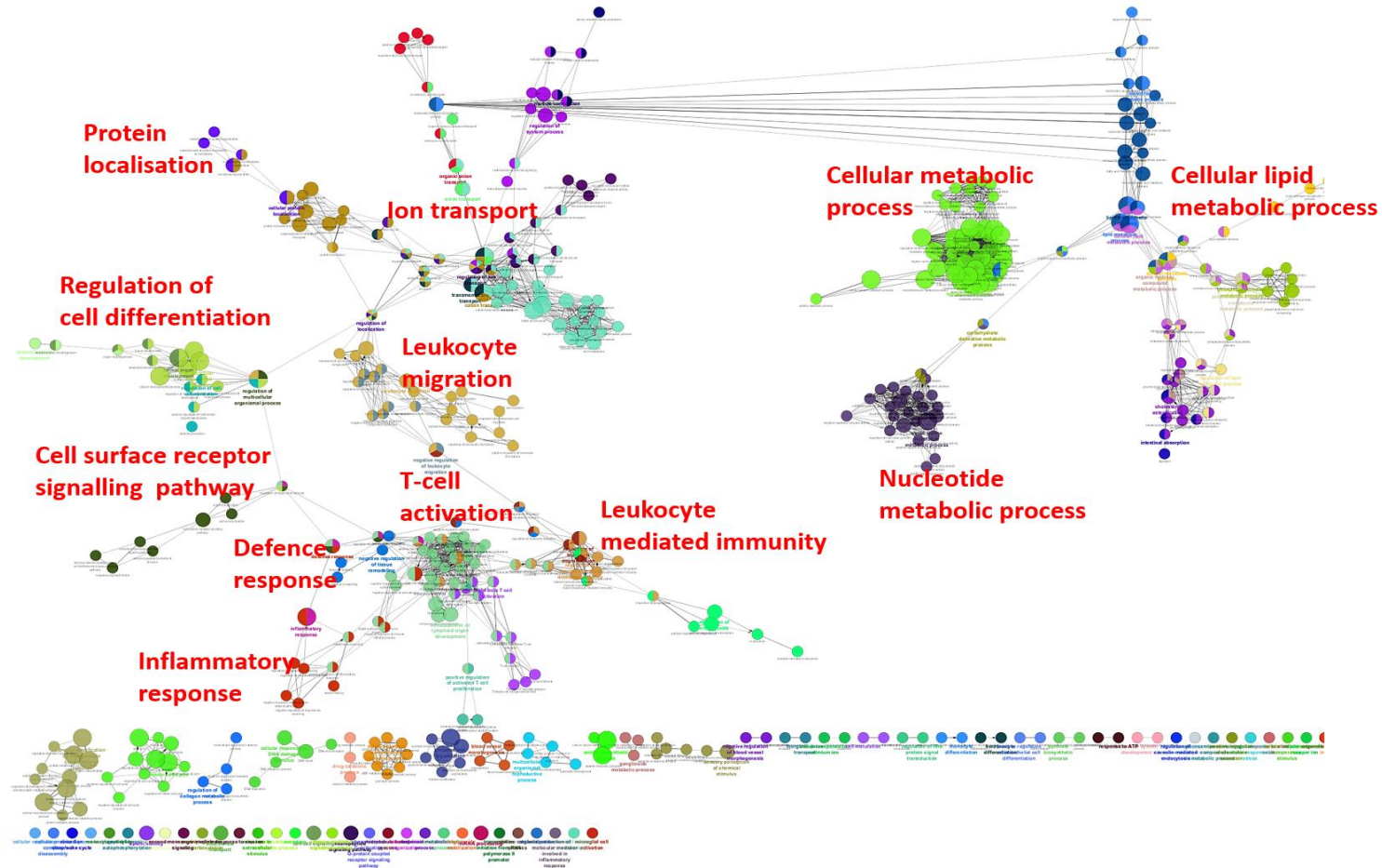


Figure 6. 31 GO_BP terms network associated with DMRs for 5% folate and methionine supplemented condition

This figure represents network of biological process (GO_BP terms) that are enriched by 5% folate and methionine supplementation. Each node represents a specific biological process (GO_BP terms) that are enriched in this analysis. Node size reflects the significance level of the enriched terms; bigger nodes indicate higher levels of significance. The node colour indicates a specific GO term, and similar coloured nodes indicate that these GO terms are from the same GO parent-child terms. Kappa score was used to link (edges) of the enriched terms (nodes) where it defined term-term interrelations (edges) and functional groups, based on shared genes between the terms.

6.4.7 Effect of methyl donor depletion on the methylation status of selected genes

Methylation specific PCR (MSP) were carried out in order to determine the effect of methyl donor depletion on the methylation status of *TP73*, *STAT1* and *DAPK1* genes. This technique involves sodium bisulphite treatment whereby un-methylated cytosine were converted to uracil, whilst methylated cytosine remained unchanged. The differences were then detected by PCR using specific primer sets for both un-methylated and methylated DNA. Bisulphite treated DNA samples from methionine depleted conditions (F+M-), folate and methionine depleted conditions (F-M-) and control groups (F+M+) were amplified using methylation specific primers. Finally, gel electrophoresis was carried out to determine if PCR amplifications of bisulphite-treated DNA were successful.

PCR amplification for target gene *TP73* was effective where single strong bands were present between 100-200 base pairs for all samples amplified with methylated primer pairs (**Figure 6.32**). As the expected product size was 162 base pairs in length, it is assumed that the region of interest has been successfully amplified. In contrast, with the un-methylated primer pairs, faint bands were present in methionine depleted samples only (F+M-). It appears that the *TP73* gene in C4-II cells are highly methylated in the presence of both folate and methionine (F+M+), as well as in folate depleted conditions (F-M+) and methionine depleted conditions (F+M-). However, in methionine depleted condition (F+M-), *TP73* also appears to be partially methylated, where there were traces of this gene being un-methylated.

A similar result can be seen for target gene *STAT1*. All samples amplified with methylated primer pairs produced single strong bands between 250-300 base pairs, where the expected product size was 273 base pairs (**Figure 6.33**). At the same time, faint bands were also present in all samples amplified with un-methylated primer pairs, with the bands present stronger for methionine depleted samples (F+M-), compared to complete (F+M+) or folate depleted samples (F-M+). Unfortunately, the bisulphite-treated DNA for *DAPK1* was not successfully amplified, though very faint bands could be detected in the samples amplified by un-methylated primers (**Figure 6.34**).

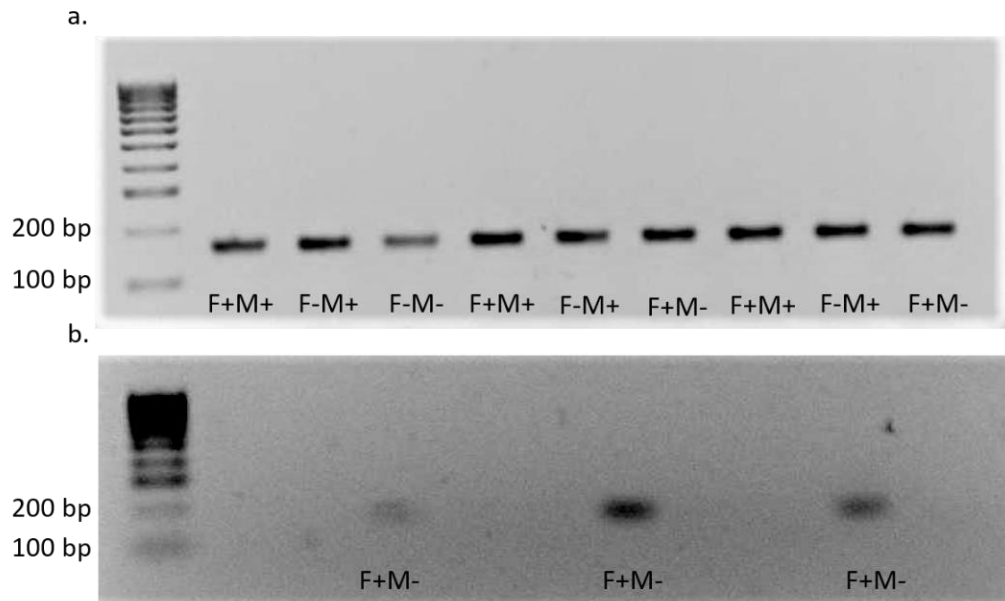


Figure 6.32 Post PCR amplification gel image for TP73 gene

This figure shows the post PCR amplification gel image for the *TP73* gene with (a) methylated primers, (b) un-methylated primers, where the expected product size is 162 and 163 base pairs, respectively. Three biological replicates were prepared for each condition; complete (F+M+), folate depleted (F-M+) and methionine depleted (F+M-).

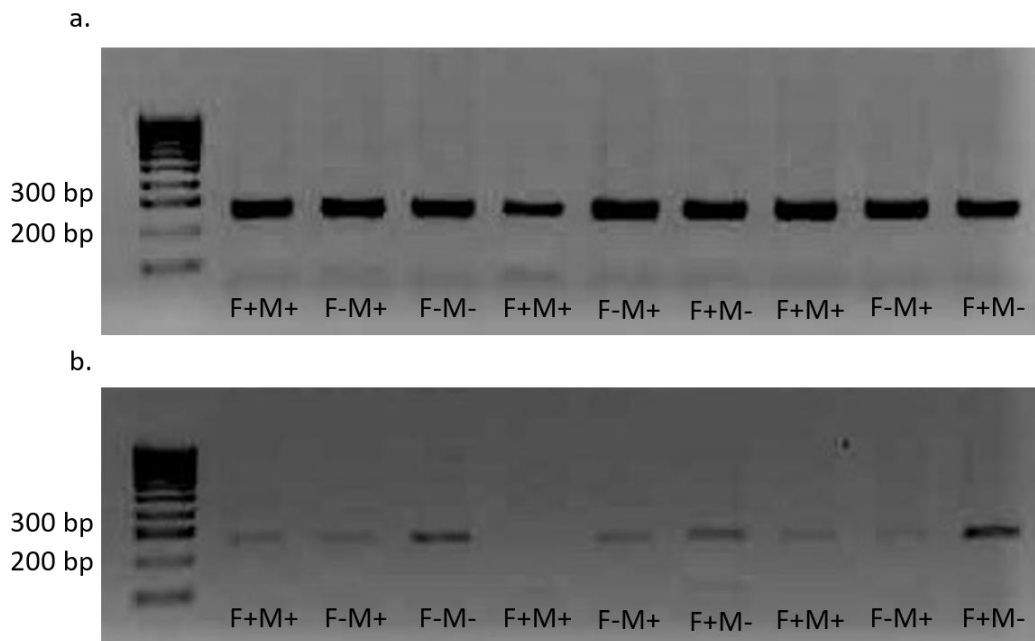


Figure 6.33 Post PCR amplification gel image for STAT1 gene

This figure shows the post PCR amplification gel image for the *STAT1* gene with (a) methylated primers, (b) un-methylated primers, where the expected product size is 273 base pairs. Three biological replicates were prepared for each condition; complete (F+M+), folate depleted (F-M+) and methionine depleted (F+M-).

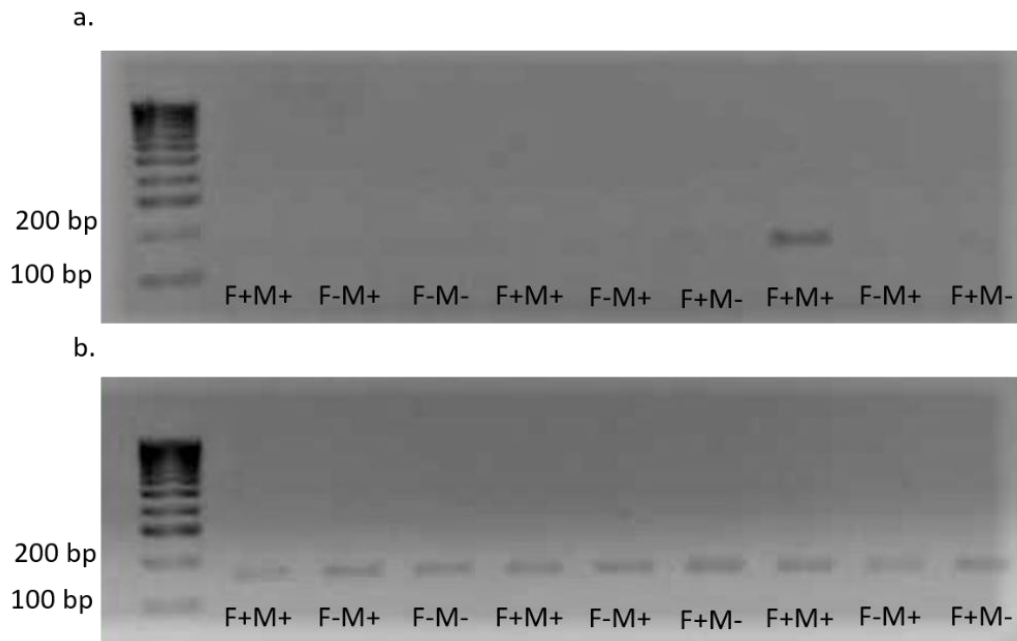


Figure 6.34 Post PCR amplification gel image for DAPK1 gene

This figure shows the post PCR amplification gel image for the *DAPK1* gene with (a) methylated primers, (b) un-methylated primers, where the expected product size is 164 and 167 base pairs, respectively. Three biological replicates were prepared for each condition i.e. complete (F+M+), folate depleted (F-M+) and methionine depleted (F+M-)

6.5 Discussion

In this work, the DNA methylation profile of C4-II cervical cancer cells was studied, aiming to acquire an understanding of the underlying epigenetic changes associated with folate and/or methionine depletion that are relevant to cervical cancer risk and progression. To the best of this researcher's knowledge, this is the first study that has been conducted in order to determine the impact of folate and methionine depletion on the genome wide methylation profile of cervical cancer cells. The use of the Infinium EPIC BeadChip has allowed the determination of methylation status on more than 850 000 single CpG sites, as well as other pre-defined regions with the help of RnBeads software.

6.5.1 Methylation data quality control analysis and normalisation

The Infinium EPIC BeadChip used in this study is one of the most advanced methylation arrays that investigates a total of 863 904 individual CpG sites, as well as 2932 non-CpG sites and 59 single nucleotide polymorphisms (SNPs); superseding the previous 450k Human Methylation array. It inherited the 450k Human Methylation array design and more than 90% of its probes. Additionally, this array includes additional probes related to the Functional Annotation of the Mammalian Genome (FANTOM5) and Encyclopaedia of DNA elements (ENCODE)

enhancers which greatly increases the power of this microarray to study enhancer/regulatory regions (Zhou et al., 2017).

The array used in this study also contains built-in quality control probes which ensure reliable and comparable data. Infinium EPIC BeadChip analysis of DNA methylation relies on the bisulphite conversion method. This method involves treating DNA with bisulphite, which converts un-methylated cytosine into uracil, while methylated cytosine remains unchanged. It was observed that some of the Infinium probes do not perform as expected, possibly due to effect of DNA polymorphisms on sequence, and competing off-target hybridization events (**Figure 6.9 to Figure 6.17**) (Byun et al., 2009; Dedeurwaerder et al., 2014; Naeem et al., 2014). This includes probes with internal SNPs close to the 3' end of the probe, probes with non-unique mapping to the bisulphite-converted genome; and probes with off-target hybridization due to partial overlap with non-unique elements (Laird et al., 2016). A total of three sample had to be removed from the downstream analysis as; one sample cannot be scanned during imaging procedure and two sample were of very low quality, as they might introduce biases to the downstream analysis.

This study used the Illumina BeadChip that comprises two different probe designs (type one and type two probes) and the methylation values generated from these two designs displayed a widely different distribution. The type two probes were found to have a much lower dynamic range compared to type one probes (Teschendorff et al., 2013; Dedeurwaerder et al., 2014). Furthermore, a study to compare type two probe methylation values with bisulphite pyrosequencing has indicated that type two probe values are biased and generally less reproducible. To correct for this bias, the Beta Mixture Quantile dilation (BMIQ) method was used to adjust the beta-values of type two design probes into a statistical distribution characteristic of type one probes (**Figure 6.19**) (Teschendorff et al., 2013). This method was validated on cell-line data, fresh frozen and paraffin-embedded tumour tissue samples, and was found give a favourable comparison with two other normalisation methods: the peak-based correction (PBC) method and the subset quantile normalization (SWAN) method. BMIQ reduced the technical variation and bias of type two probe values and successfully removed the type one enrichment bias caused by the lower dynamic range of type two probes (Teschendorff et al., 2013).

6.5.2 Effect of methyl donor depletion on C4-II DNA methylation profile

This study has demonstrated that in conditions where methionine is deficient, a majority of CpG sites were hypomethylated globally in C4-II cervical cancer cell (**Figure 6.20 and Figure 6.27**). In contrast, C4-II cells grown in folate depleted condition presented a similar methylation profile to the control sample (F+M+), without any significant difference between their individual CpG methylation status. The dimension reduction analysis using principal component analysis and multidimensional scaling has separated the C4-II samples into two distinct groups, demonstrating a strong negativity related to the presence of methionine and a strong positivity relating to the absence of methionine (**Figure 6.22**). This suggests that one of the components or associations between these sample groups could be related to the availability of methionine. Furthermore, the bioinformatics analysis of this study revealed that biological processes associated with immune responses and host defence mechanisms as well as mitosis, cell differentiation, cell motility and angiogenesis were affected by methionine deficiency (**Figure 6.29 to Figure 6.31**). This supports the finding from Chapter 3, suggesting that the genes involved in these processes are aberrantly methylated leading to dysregulation their expression. The 95% methyl donor depletion (M+F+5%) was observed to strongly inhibits C4-II cell division (Shafie, 2014); and this was also observed during sample preparation, where C4-II cells had to be cultured in multiple flasks in order to obtain sufficient DNA for analysis, due to their slow growth rate. Additionally, this 5% folate and methionine medium supplementation did not improve the global hypomethylated state of the C4-II cells, though there was a reduction in the number of differently methylated sites as compared to a complete depletion of folate and methionine (F-M-) (**Table 6.6**).

Overall, this study found that compared to folate depletion, methionine availability is crucial in maintaining DNA methylation pattern. The DNA methylation process is regulated by SAM availability, where it serves as a universal methyl donor. This metabolite is synthesized from methionine and ATP by methionine adenosyltransferase (MATs) (Clare et al., 2019). In the event where SAM donates a methyl group for DNA methylation, it will be converted to SAH, after which it functions as a potent inhibitor of all methyltransferases. Thus, the intracellular SAM:SAH ratio has been found to be tightly regulated by the metabolism of methionine (Shiraki et al., 2014; Janke et al., 2015). A study was conducted to determine the effect of methionine depletion on methionine metabolism in human embryonic stem cells (ECSs) and induced pluripotent stem cells (iPSCs), where the importance of methionine availability in the regulation of cell maintenance and differentiation was highlighted (Shiraki et al., 2014). It was reported that methionine deficiency causes a rapid decrease in intracellular

SAM, which leads to a decrease in H3K4me3 and global reduction in DNA methylation in human ESCs and iPSCs cells. Therefore, a measurement of intracellular SAM to SAH ratio in this study's cervical cancer model of methyl donor depletion might provide a better understanding on the effect of folate and methionine depletion on the one carbon cycle metabolites.

Additionally, the deprivation of methionine was also found to affect the human ESCs and iPSCs cells growth with cell cycle arrest at the G0/G1 phase (Shiraki et al., 2014). This is followed by an increase in cell apoptosis after a methionine depletion of 24 hours. Their gene expression analysis revealed that genes associated with the cell cycle were increased by 3-fold, while for apoptosis they were increased 2-fold. Similarly, the bioinformatic analysis in this study also showed a high proportion of CpG associated with mitosis and cell differentiation to be highly hypomethylated. Shiraki et al. suggested that the p53-p38 signalling pathway was triggered as an early response to methionine depletion at 5 hours, while the p38 activation partially accounts for the cell-cycle arrest leading to apoptosis of ESCs/iPSCs cells, in long-term methionine deficiency.

In contrast to methionine depletion, high methionine is expected to increase DNA methylation. However, excessive methionine may actually disrupt the one carbon cycle by inhibiting the re-methylation of homocysteine. Studies of SAM treatment on different types of cancer cell lines have been found to be effective in suppressing the cell's ability to invade and proliferate. In a study by Shukeir et al., the highly invasive human prostate cancer cells PC-3 and DU-145 were cultured in media which had been supplemented with either 100 μ M or 250 μ M of SAM (Shukeir et al., 2015). The methylation profile was analysed using the Illumina Methylation 450K Kit, and data analysis was performed using Genome studio software. A total of 73 CpG sites were found to be significantly hypermethylated following treatment with SAM, and these sites corresponded to 51 genes involved in key intracellular pathways that could affect tumour growth and metastasis. These genes included the known prostate cancer oncogene, *CTSH*, and cervical cancer oncogene, *TTC23*. Signal transduction regulators like *STAT3*, *STAT5A* and *STAT5B* were also found to be hypermethylated. A functional analysis of the hypermethylated genes identified signalling pathways that are involved in cell proliferation, migration, invasiveness, angiogenesis and metastasis, such as JAK/STAT, ERK/MAPK, WNT/ β -catenin, mTOR, PPARG, VEGF, Gap and tight junction. In another *in vitro* study conducted using MDA-MB-231 and Hs578T breast cancer cell lines, the administration of

SAM caused a significant dose-dependent decrease in cell proliferation, invasion, migration, anchorage-independent growth and increased apoptosis (Mahmood et al., 2018).

In the study conducted by (Poomipark et al., 2016), the C4-II cervical cancer cells were grown in complete, folate depleted, and folate and methionine depleted medium for four, eight and twelve days. The 5-methylcytosine levels were then measured using an immunocytochemistry method with flow cytometric detection in order to determine the effect of methyl donor depletion on global DNA methylation. Similar to the current study, Poomipark et al. reported that in folate and methionine depleted conditions, there was a significant reduction of global DNA methylation by 18% when compared to the complete condition. A significant effect of time ($P=0.016$) was also reported, where the mean global DNA methylation was reported to be lower at day twelve (17.5%) as compared to day four (2.0%) and day eight (13.6%) of culture. A reduction in global DNA methylation was also shown in cells grown in only folate depleted conditions, although the finding was not statistically significant. Nonetheless, the DNA methylation analysis using the flow cytometry method are only able to determine the impact of methyl donor depletion globally, and was not able to identify specific genes that were affected. On the other hand, DNA methylation profiling conducted in this study allowed a more comprehensive analysis on the impact of methyl donor nutrient depletion, where the methylation status of specific CpG sites was determined. Subsequently, data generated from DNA methylation profiling can be scrutinised for patterns or perturbations using bioinformatics approach, in order to identify molecular mechanisms that are affected by methyl donor depletion. It is also a more robust analysis that allow for the discovery of results that are not anticipated or intended by the research design, yet could provide critical insights into biology and pathophysiology. Poomipark et al. also reported that genes associated with methionine metabolite enzymes, including DNMT3a and DNMT3b, were significantly downregulated in folate and methionine depleted media, and the effect was reversed by methyl donor repletion, suggesting the global hypomethylation observed in their study could be, in part, due to the dysregulated DNMTs gene expression. In this study, it was observed that the DNA methylation level of the DNMT3b gene promoter region was significantly reduce in methionine depleted media (F+M-, F-M- and F+M+5%), when compared to the control (F+M+). Other DNMTs (DNMT1 and DNMT3a) were also hypomethylated, however the difference was not statistically significant.

This study also demonstrates that the deprivation of folate in C4-II cells did not cause any significant changes to DNA methylation profiles when compared to the control group.

Folate is only one of several substrates for methylation and it is possible that the DNA methylation profile is maintained to some extent by the presence of other methyl donors. In their study, Craciunescu et al. showed that choline supplementation mitigated effects of folate depletion on the rate of mitosis of neural progenitor cells in mice (Craciunescu et al., 2010). As the medium used to grow the C-4 II cells are rich in choline, this may have compensated for the depletion of folate and maintained methionine synthesis and therefore SAM synthesis, through the betaine pathway. An additional analysis to determine intracellular choline and betaine in this model of methyl donor depletion might provide useful insight to this finding.

Furthermore, previous studies had reported that cells grown in folate depleted media still grew, but at a significantly slower rate than cells in complete medium. Stempak et al. had grown two human colon adenocarcinoma cell lines, HCT116 and Caco-2 grown in folate depleted RPMI medium for 20 days in media containing 0 (depleted) or 0.9 mg/L (complete) folic acid (Stempak et al., 2005). In another study, prostate cancer cell line derived from transgenic adenoma of the mouse prostate (TRAMP) were also grown in folate depleted media (0.04mg/L) (Bistulfi et al., 2010). In both studies, folate depleted cells still grew, but at a significantly slower rate than cells in complete medium. It has been suggested that folate deficiency may trigger an increase in the expression of folate receptor genes as a compensatory mechanism, which in turn supports its function to a certain extent (Kelemen, 2006).

Though folate depletion appears to have little impact on DNA methylation, previous studies has also highlighted its importance in supporting DNA synthesis and repair, faults in which are associated with cancer risk and progression (Duthie et al., 2000; Rampersaud et al., 2002; Narayanan et al., 2004). In the absence of folate, the deoxyuridine monophosphate (dUMP) accumulates and the production of purine and pyrimidine is reduced, causing more uracil to be incorporated into DNA by DNA polymerase. The DNA repair activity to remove this uracil may cause transient nicks to be formed, and two opposing nicks could lead to chromosome breaks, thus damaging the DNA strand. This causes DNA to be unstable and ultimately increases the risk of cancer and other cognitive defects associated with folate deficiency in humans.

6.5.3 Effect of methyl donor depletion on methylation status of selected genes

In this study, the *TP73* and *STAT1* genes were found to be highly methylated in all media conditions in the methylation specific PCR (MSP) analysis, with partial non-methylation in methionine depleted conditions (F+M-). In contrast, the CpG sites of these two genes were

reported to be significantly hypomethylated in methionine depleted conditions (F+M-, F-M- and F+M+5%), when compared to the control (F+M+) via the methylation array.

The MSP technique consists mainly of two procedures; firstly the conversion of un-methylated cytosine to uracil with sodium bisulphite treatment, followed by detection of the bisulphite induced sequence differences with PCR, by using specific primer sets for both un-methylated and methylated DNA (Ku et al., 2011). Compared to other techniques, MSP is a quick and cost-effective method to assess the methylation pattern of almost any CpG sites within CpG islands. It requires a very small amount of DNA and is sensitive to 0.1% of methylated alleles in a given CpG island locus. However, this method is not able to quantify the methylation levels, but only indicates the presence or absence of methylation. Furthermore, sequences that have been incompletely converted during the bisulphite treatment, which usually occurs in DNA samples that lacks methylation or have a low level of methylation, are frequently co-amplified during MSP, resulting in an overestimation of DNA methylation (Sasaki et al., 2003). This could be one of the possible explanations for the contradicting results in the methylation status of *TP73* and *STAT1* in this study.

Additionally in this technique, the design of a good primer pairs is a crucial in order to obtain reliable PCR results (Derks et al., 2004). The designed methylation specific PCR primer pairs should have at least one CpG near their 3'ends in order to distinguish between methylated and un-methylated sequences. They should also contain several non-CpG C's, which favours amplification of the bisulphite-modified sequences. Furthermore, the designed primers for the methylated and un-methylated alleles should also contain the same CpGs in their sequences. Additionally, the resulting PCR product should not exceed 300 base pairs, as bisulphite treatment could cause fragmentation of DNA samples (Li & Dahiya, 2002). The differences between the melting temperatures for the designed primer pairs are preferably less than 5° C in order to improve the PCR efficiency (Derks et al., 2004). In this study, the designed primers fulfilled all these criteria, except for the difference between the *STAT1* primer pair melting temperatures which exceeded 5°C.

The tumour protein 73 (*TP73*) gene belong to the p53 tumour suppressor family which regulates genomic integrity, cellular proliferation and apoptosis. This gene plays an important role in cell homeostasis, as it partially compensates for the loss of p53 function (Vilgelm et al., 2010). Unlike *TP53*, which is mutated in more than 50% of all human tumours, *TP73* is rarely mutated (less than 1%) but rather overexpressed as compared with normal tissue (Gomez et al.,

2018). A meta-analysis reported that *TP73* expression in cervical cancer is significantly higher than that in normal cervical squamous epithelium, which may play an important role in the occurrence and development of cervical cancer (Feng et al., 2017). Genetic alterations in *TP73* were also suggested to contribute to the development of cervical cancer in an HPV-infected transformation zone under prolonged exposure to events related to pregnancy (Craveiro et al., 2004).

Similarly, signal transducer and activator of transcription 1 (*STAT1*) also plays a crucial role as a tumour suppressor, through its capacity to control immune system function and promote tumour immune surveillance (Koromilas & Sexl, 2013). *STAT1* was reported to be highly methylated in serum samples of cervical cancer patients (Jha et al., 2016). Additionally, the loss of activation and/or expression of *STAT1* occurs in malignant cells derived from various histological types of tumours, such as breast cancer, oesophageal cancer, colorectal cancer, lung cancer, melanoma, and gastric cancer (Adamkova et al., 2007; Zhang et al., 2014; Chen et al., 2015; Zhang et al., 2017).

However, there are conflicting views on *TP73* and *STAT1* functions in promoting or preventing malignancies, as there are a relatively large number of factors that are known to dictate how these genes affect the malignant phenotypes and clinical behaviours of cancer. For example, *STAT1* can act as either a tumour suppressor or promoter in different types of cancer and contraindications have been reported in some types of cancer, such as breast cancer and leukaemia (Zhang & Liu, 2017). These variations resulted from differences in the genetics and environments of the patient cohorts, rather than from the specific type of cancer. On the other hand, the expression and activation ratio of *STAT1 α* and *STAT1 β* in different cancer types may promote a “switch” from a tumour survival to a tumour death phenotype. Additionally, it is important to note that the methylation of a single CpG site will not necessarily affect its protein expression. A study investigating *TP73* gene methylation status in invasive breast carcinoma cells found that a decrease in *TP73* methylation levels did not affect the expression of the p73 protein with an inverse correlation of $\rho=-0.42$; $P=0.039$ (Gomez et al., 2018). This also highlights the importance of validating the current study at the functional level.

6.6 Summary

In this study, it was found that a complete depletion of folate has little impact on DNA methylation in C4-II cervical cancer cells, whereas methionine depletion has a significant

impact on the regulation of DNA methylation. It also highlights the regulatory functions of methionine via DNA methylation on biological processes associated with host defence mechanisms, immune responses, as well as mitosis, cell differentiation, cell motility and angiogenesis; and the potential to identify pathways linked to methyl donor nutrient metabolism that might modify the risk of cervical cancer, through effects on cancer processes. Nonetheless, the importance of folate as methyl donor cannot be ignored. Furthermore, the role that folate plays in DNA synthesis and cell division is well understood and this is the basis for the use of anti-folate drugs in cancer treatment.

CHAPTER 7

DISCUSSION AND CONCLUSION

7.1 Discussion

Cervical cancer is classified as the fourth most common type of cancer that occurs uniquely in women, and constitutes a serious global public health problem (Sung et al., 2021). With an estimated occurrence of 604 000 new cases in 2020 and an overall incidence rate of 18.8/100 00 women, cervical cancer is the second most common type of cancer diagnosed and the third leading cause of cancer-associated deaths in women in the least developed countries. Furthermore, there was an increase in cervical cancer incidence by 6% and in mortality by 10% worldwide, since the IARC report in 2018 (Bray et al., 2018). Cervical cancer still remains as one of the biggest threats to women's health and lives worldwide despite the fact that either early neoplastic cell changes or human papillomavirus (HPV) infections, can be screened, enabling treatment to prevent the development of invasive lesions and; with the introduction of HPV vaccination programs that have been reported to be safe and highly effective against vaccine-type persistent infections and cervical precancerous lesions in women. The higher incidence and mortality in least developed countries could in part be explained by the absence of technical or public health infrastructure to screen for HPV infection and/or to detect and remove pre-cancerous lesions (Gakidou et al., 2008), the high cost of HPV vaccination (Torre et al., 2015), as well as paucity of adolescent health platforms, cultural challenges and difficulty in reaching the target population (Denny, 2015). Therefore, ongoing research to better understand the cervical cancer carcinogenesis process, as well as factors that contribute towards its risk and progression from pre-cancerous lesions to invasive cancer, are still crucial in order to develop more cost-effective preventative programs especially in low and middle income countries.

Numerous clinical, epidemiological and molecular studies have shown that persistent infection with high-risk HPV genotypes is an indispensable, but not sufficient prerequisite for the development of cervical cancer. About 85 to 90% of HPV infections spontaneously regress due to the bodies innate and adaptive immunity, with only 10 to 15% that continue to persist (Łaniewski et al., 2020; Da Silva et al., 2021). This suggests that additional factors are necessary in order to establish a conducive environment for neoplastic progression, where the virus is able to evade the host immune system to ensure its continuous replication in the basal epithelial

cells. Dysregulation of both viral and host gene expression due to viral DNA integration into the cell's genome, as well as epigenetic modifications, are key events in the carcinogenic process. Modification of the DNA methylation pattern, an epigenetic mechanism pivotal for regulating gene transcription, has been demonstrated in cervical cancer and its precursors (Dueñas-González et al., 2005; Szalmas & Konya, 2009), consisting of two main features. Global hypomethylation may lead to genome instability and DNA breakage as well as transcriptional activation of oncogenes (Feinberg & Tycko, 2004; Wilson et al., 2007; Jung & Pfeifer, 2015); whilst gene-specific hypermethylation may silence the expression of genes that are critical to cell homeostasis, DNA integrity, or genome stability, resulting in cancer development and progression (Bakshi et al., 2018). It has been hypothesized that aberrant methylation patterns can be induced by the overexpression of viral E6 and E7 oncoproteins of HR-HPVs (Sen et al., 2018).

On the other hand, Poomipark et al. proposed a contrasting hypothesis where methyl donor status regulates DNA methylation, that affects the incidence of cervical cancer (Poomipark et al., 2016). Methyl donor nutrients availability has been shown to modify DNA methylation either globally or at specific CpG sites by inducing the formation of methyl donors, acting as co-enzymes, or modifying DNMT enzymatic activity (Mahmoud & Ali, 2019; Ghazi et al., 2020). There has been particular interest in the possible role of folate as a determinant of cervical cancer risk as previous studies have associated low folate status with higher HR-HPV incidence and CIN stage (Piyathilake et al., 2004; Piyathilake et al., 2007), and its role in DNA methylation and gene expression (Flatley et al., 2009). Evidence on methionine status and its association with cervical cancer is lacking, though its intake has been associated with reduced risk of breast, prostate and colorectal cancer. Nonetheless, the specific mechanisms by which these methyl donor nutrients contribute to the development of cervical cancer are as yet unclear, with conflicting findings to their possible roles in preventing or promoting cancer development. Thus, the main aim of this study is to determine the effects methyl donor depletion, folate and methionine in particular, on mechanisms associated with cancer risk and progression in cervical cancer cells. The main findings in this study highlight the importance of methionine over folate as a methyl donor in the regulation of gene expression, and also the regulatory functions of both folate and methionine on IFN-stimulated gene expression associated with antiviral immunity in a cervical cancer cell line.

As previous studies have indicated, HR-HPV infection as well as methyl donor nutrient availability may modulate cervical cancer growth and progression. Thus, this study has identified and combined two microarray datasets, each representing the conditions mentioned above, in order to identify gene networks and pathways that are affected by both methyl donor nutrient depletion and chromosomal integration of HPV in cervical cells; which to our knowledge, has never been done before. Contrary to the more common hypothesis-testing approach; the hypothesis-generating approach used in this study involves background research, directly followed by experimental design and application to generate high-throughput data. This data is then scrutinised for patterns or perturbations, followed by data interpretation, and finally the hypotheses were refined and extended. Subsequently, these hypotheses are usually validated by experimental study. Though not common, this approach is becoming more widely used, especially with the development in high throughput technologies such as microarray analysis (Xu et al., 2019). The ability to combine high-throughput datasets that measure different sets of conditions, might provide a more robust analysis that also allows for the discovery of results that are not anticipated or intended by the original research design, and yet could provide critical insights into biology and pathophysiology. Interestingly, via this method, we have identified several IFN-stimulated genes that are involved in cell host defence mechanisms and genes that are involved in cell level oncogenic processes, which are mutually sensitive to methyl donor nutrient availability (**Figure 3.10 to Figure 3.13**); which has not been demonstrated in the original bioinformatics analysis (Poomipark, 2013). This has raised the question of whether methyl donor nutrients availability may influence an individual's susceptibility towards HPV infection and persistence, and cervical cancer development via its impact on DNA methylation.

Initial work to validate the bioinformatics findings was conducted, where four IFN-stimulated genes (ISGs), *RSAD2*, *OAS1*, *IFIT1*, *ISG15* showed a significant upregulation in methionine or combined folate and methionine depleted condition after day four and eight of culture (**Figure 4.14 to Figure 4.17**). As there are no previous studies that look into this phenomenon, it is difficult to identify the specific mechanisms for this effect. However, the upregulation of these genes may be associated with the reduction in global DNA methylation observed in this study, where more than 470 000 CpG sites were found to be hypomethylated in methionine-deficient cells (**Figure 6.20 and Figure 6.27**). These ISGs and their signalling pathways play vital roles in the malignant transformation of cells in the tumour microenvironment. Although IFNs have been used as exogenous pharmaceuticals for the treatment of cancers, paradoxical findings revealed that constitutive expression of aberrantly regulated ISGs promotes neoplastic disease development and progression including skin, breast

and head and neck cancers (Cheon et al., 2014). Increased expression of ISGs has been reported in metastatic cancer cells compared to non-metastatic cells (Khodarev et al., 2009). On the other hand, the upregulation of ISGs expression has been associated with an improved clinical outcome (Danish et al., 2013; Zhang et al., 2016). This contradictory finding makes it difficult to speculate as to whether the upregulation of ISGs would be beneficial or detrimental in the treatment of cervical cancer. Additionally, several other factors are thought to influence the expression of IFN genes, such as the expression level of microRNAs (miRNAs) and non-coding RNAs (ncRNAs), and chromatin conformation (Aune et al., 2013; Kambara et al., 2014; Forster et al., 2015), which have been known to be affected by methyl donor deficiency. Changes in DNA methylation might also be accompanied by altered histone methylation and acetylation, with consequent effects on the accessibility of transcription factors to binding sites of chromatin.

Dysregulated cytokines production has been identified along with HPV infection in the pathogenesis of cervical neoplasia (Paradkar et al., 2014; Das et al., 2018; Otani et al., 2019). Thus, this study attempts to determine the functional impact of folate and/or methionine depletion on host defence mechanisms; whereby production of TNF- α and IL-1 β cytokines on THP-1 derived macrophages grown in folate and/or methionine depleted medium was assessed. A significant reduction of TNF- α and IL-1 β cytokines was demonstrated in the absence of folate, methionine or both nutrients (**Figure 5.4 and Figure 5.5**). A recent study had also observed that monocyte pre-treatment with specific methyl donors, particularly folic acid, reduced the inflammatory response in LPS-activated THP-1 macrophages, which could in part be mediated by increased DNA methylation in some CpG sites of important proinflammatory genes (Samblas et al., 2018). This demonstrates that cytokine production in the humoral immune system is also affected by methyl donor nutrient depletion. As cytokine production is down-regulated in conditions of folate and methionine scarcity, therefore, for an appropriate immune response against HR-HPV infection there might be a need for adequate methyl donor nutrient availability.

The functional significance of altered expression of IFN genes to cancer progression in response to methyl donor depletion is unclear, but there is evidence to support the notion that upregulation of IFN genes may be an important anti-tumour strategy in cancer. These antiviral proteins are crucial for antiviral activities in host cells, which include the inhibition of virus entry, prevention of virus replication and obstruction of viral egress (Schneider et al., 2014), thus it might play a pivotal role in HR-HPV viral infection and persistence that lead to

neoplastic progression. ISGs have been shown to act against HPV by directly binding with the key E1 replication protein, which is crucial for the synthesis of viral progeny DNA (Pidugu et al., 2019a). Furthermore, it is suggested that the suppression of Type 1 IFN signalling may help developing tumours evade the critical early step of immune recognition and clearance. Studies on cell culture have found that IFN- α , IFN- β and IFN- γ directly induce caspase-mediated apoptosis in a variety of tumour cell types, leading to experimental studies on the use of Type 1 IFN treatments in various cancers (Herzer et al., 2009; Kirkwood, 2002). However, as precise molecular mechanisms of IFNs action in cancer treatment is far from being elucidated, it severely hinders further application of IFNs in cancer therapy. Therefore, this study has highlighted the potential effect of methyl donor nutrients via its impact on DNA methylation in modulating IFN genes expression. Other recent studies are also exploring the role of methionine as a key nutrient in epigenetic reprogramming in CD4+ T helper (Th) cells (Roy et al., 2020). Methionine restriction has been found to reduce histone H3K4 methylation (H3K4me3) at the promoter regions of key genes involved in Th17 cell proliferation and cytokine production, that may lead to disease onset. Furthermore, SAM has been suggested as an essential metabolite for inflammatory macrophages, where a high SAM:SAH ratio supports histone H3 lysine 36 trimethylation for IL-1 β production (Yu et al., 2019). However, more extensive work and experimental study need to be conducted in order to validate the mechanistic nature of these ISGs and their functional impact in host defence and immune function. Nonetheless, the results of this study suggests that methyl donor availability may be critical for the expression of IFN-stimulated genes, as DNA methylation triggered by methyl donor status might affect both cancer-protecting genes and the HPV genome, as the disease progresses.

Additionally, instead of folate, this study highlights the importance of methionine in the regulation of DNA methylation. As discussed earlier, significant upregulation of ISGs were only observed in methionine-deficient cells. Furthermore, DNA methylation profiling has demonstrated that a majority of the CpG sites were hypomethylated globally in methionine (F+M-) or combined folate and methionine deficiencies (F-M-); whilst a depletion of only folate (F-M+) might not be sufficient to affect global DNA methylation (**Figure 6.20 and Figure 6.27**). It is possible that methyl donor depletion could lead to a reduction in DNMTs expression, resulting in the observed global DNA hypomethylation in this study. Poomipark et al. reported that the depletion of both folate and methionine in C4-II cervical cancer cells had a greater impact on the downregulation of DNMT3a and DNMT3b gene expression as well as DNMT1 protein expression, while folate depletion alone had little or no effect on the DNMT gene or protein expression (Poomipark et al., 2016). As folate is only one of several substrates in the

IC metabolism, it is possible that the DNA methylation profile is preserved to some extent at the expense of other methyl donor (Liu & Ward, 2010). Furthermore, others have shown interactions between the activities of dietary methyl donors (Niculescu & Zeisel, 2002), notably choline, that may mitigate effects of folate depletion. In their study, Craciunescu et al. showed that choline supplementation mitigated effects of folate depletion on the rate of mitosis of neural progenitor cells in mice (Craciunescu et al., 2010). As the medium used to grow the C-4 II cells is rich in choline, this may have compensated for the depletion of folate and maintained methionine synthesis and therefore SAM synthesis, through the betaine pathway. An additional analysis to determine intracellular choline and betaine in this model of methyl donor depletion might provide useful insight to this finding.

An important limitation to note is the severe depletion of folate and/or methionine in the cervical cancer model of methyl donor depletion of this study. The folate-deficient medium contained an average of 0.3 mg/L (F-M+) and 0.6 mg/L (F-M-) of folate, while the 5% folate repleted-medium was estimated to contain average folate concentrations of 0.6 mg/L (F-M+) and 0.9 mg/L (F-M-), respectively. This severe depletion of folate might not be reflective of the level of deficiency observed in real life humans. According to the National Diet and Nutrition Survey (NDNS), clinical threshold for folate deficiency in which there is a risk of disease is less than 305 nmol/L for RBC folate and less than 7 nmol/L for serum folate; whilst serum folate containing less than 13 nmol/L of folate indicates folate deficiency is possible (NDNS, 2020). In this NDNS report, serum folate concentration of less than 7 nmol/L is present in 11% of the adult UK population aged between 19 to 64 years and 13% of women of child bearing age (aged 16 to 49 years) indicating clinical deficiency of folate; whilst serum folate concentration of less than 13 nmol/L is present in 52% for both adults and women of child bearing age, indicating possible folate deficiency. The NDNS also reported that the percentage with mean folate intakes below the LRNI was 4% and 8% for adults aged 19 to 64 years and women of childbearing age, respectively. However, Rogers et al. reported that the prevalence of folate deficiency was more than 20% in many countries with lower income economies but was typically less than 5% in countries with higher income economies (Rogers et al., 2018). There is no data on folate status or intake in Eastern, Southern and Central African countries, where incidence of cervical cancer is highest. However, recent study in Brazil have reported that the mean folate intake was 375.8 µg/day, where only 1.7% reported folate levels below 6.8nmol/L (Steluti et al., 2017). This finding is attributed to the national folic acid fortification policy that was implemented 10 years ago. In contrast, a study in Iran reported a higher percentage (14.3%) of folate deficiency (<6.7nmol/L), with a lower mean intake of folate of

198.3 µg/day, among women of childbearing age in Golestan province, where a pilot project on folic acid fortification of flour is being implemented (Abdollahi et al., 2008). Extrapolating the finding of this study to individuals with folate deficiency, and based on the NDNS data stated above, it would suggest that as a consequence of this deficiency, significant numbers of sexually active women could be at risk of a poor immune response. This could affect their ability to combat HR-HPV infection, leading to HPV persistence and subsequently increase the risk of developing cervical cancer. Moreover, previous studies have also shown that low folate status is associated with higher HR-HPV incidence and CIN stage (Piyathilake et al., 2004; Piyathilake et al., 2007).

Adversely, there is very limited data on methionine intake. The findings of this study showed that methionine concentration in methionine depleted media (F+M- or F-M-) was extremely low, close to the lowest limitation of the assay (1.45 – 45.4 nmol/L) and could not be accurately determined. However, the impact of methionine depletion is more pronounced in the findings of this study. This suggests that methyl donor nutrient depletion might adversely impact immune function. On the other hand, literature on methionine intake and possible association with HPV infection and cervical cancer are scarce, indicating a need for it, so that findings on methyl donor nutrients studies can be better contextualized.

Nutrients can regulate several biological processes in our body via modifying epigenetic mechanisms that are critical for gene expression such as DNA methylation. The reversible characteristics of epigenetic marks, and their sensitivity to nutritional changes, create an attractive and promising field of study. However, the involvement of various nutrients interactions with DNA methylation also makes it a very complex field to study. Furthermore, the DNA methylation process itself appears to be gene-sensitive, tissue-dependent and could be affected by other pathological conditions and environmental factors. Thus, findings from this study must be interpreted with care and cannot be generalised to all types of cancer cells/tissues. This study suggests that a depletion of methyl donor nutrients directly impacts the innate immune system, which could influence the development and progression of cervical cancer through modulation of infectivity of HPV. It suggests the potential of these nutrients in influencing the expression of genes involved in immune response via demethylation, bringing about a more pronounced immune response in early stages of cervical cancer. Thus, it might prove to be more insightful to conduct further studies on methyl donor regulated gene expression and functional outcomes associated with immune response at various stages of cancer progression. In the context of cervical cancer risk and progression, it is not yet possible

to confirm whether the depletion of these nutrients is beneficial or detrimental, and therefore additional experimentation is required. However, identifying changes in methyl donor regulated genes could hold diagnostic or therapeutic potential based on epigenetic changes occurring due to nutrient availability for those who are in the at-risk group.

Accordingly, future research should be designed in a way that dissects the effect of single versus combined intake of methyl donors, dietary versus supplementary mode of intake, and dose response relationship. Furthermore, researchers should consider the differential response to methyl donors between healthy tissues and cancerous lesions where aberrant methylation profiles might exist and modify the outcome, hence proposing the validation study with primary cell. Finally, large scale clinical trials in both healthy people and cancer patients are needed in order to provide specific recommendations for methyl donor intake that maintains normal methylation profiles in each group. Nonetheless, this current research warrants future investigation with promising data on nutrients and epigenetic changes in relation to cancer risk.

7.2 Conclusion

It was hypothesised that the deficiency of folate and/or methionine influences the regulation of DNA methylation processes, thus effecting the expression of genes in the cervical cancer cell lines which could potentially influence cervical cancer risk and progression. The research to investigate this hypothesis can be considered in five parts:

- identification of cervical cancer-associated gene networks and pathways that are affected by both methyl donor nutrient depletion, and by chromosomal integration of HR-HPV in cervical cells using bioinformatics analysis.
- validation of the C4-II cervical cancer cell model of methyl donor depletion by analysing intracellular folate concentration, intracellular methionine concentration and extracellular homocysteine concentration.
- determination of the effect of methyl donor nutrient depletion on the expression of interferon stimulated genes, associated with host defence mechanisms using quantitative RT-PCR.
- determination of the effect of methyl donor nutrient depletion on cytokine production in differentiated macrophages, derived from the THP-1 cell line.
- investigation of how the availability of methionine and folate impacts globally and specifically on DNA methylation in a C4-II cervical cancer cell model of methyl donor depletion by methylation profiling and by methylation specific PCR.

The outcome of these investigations has

- shown a retardation of C4-II cervical cancer cells growth in response to folate depletion, with more severe effects for methionine and combined folate and methionine depletion.
- confirmed the reduction of intracellular folate in response to folate depletion; a decrease in intracellular methionine in response to methionine depletion; and the accumulation of extracellular homocysteine in response to folate, methionine or both nutrients' depletion, indicating a functional model of methyl donor nutrient depletion.
- identified genes that are involved in host defence and genes that are involved in cancer processes, both sets of which are sensitive to methyl donor nutrient availability.
- highlighted the role of host defence mechanisms, specifically with regards to the functions of type 1 interferon in preventing cancer progression, which in turn may be modulated by methyl donor nutrients availability.
- shown an upregulation in the expression of genes, associated with the type 1 interferon pathway immune responses towards external stimuli, in response to methionine only or combined folate and methionine depletion.
- shown a reduction of TNF α and IL-1 β cytokines production in response to methyl donor nutrient depletion in THP-1 derived macrophages.
- shown a reduction in DNA methylation globally in response to methionine or combined folate and methionine depletion. A 5% addition of folate and methionine did not reverse the effect of global DNA hypomethylation. A deficiency of folate alone did not present a significant change to the DNA methylation profile.
- shown inconsistent results in TP73 and STAT1 methylation status via methylation profiling and methylation specific PCR, which may be due to limitations in the method used.

7.3 Study Limitation

In general, the main limitations of this study are the result of time and cost constraints. Initially, this study was planned to start with the experimental phase using two established cell lines; C4-II and SiHa cervical cancer cell lines, with the findings to be confirmed using primary cells. However, we were not able to determine a functional impact of methionine and/or folate depletion at the cellular level using the SiHa cell line. Thus, further analysis using this cell line was not conducted. Additionally, there was a limitation in recruiting patients to obtain primary

samples, which was not feasible within this context, time, cost and access to clinical service. The main disadvantage of an established cell line is that, after a period of growth, cell characteristics can change and may become quite different from those found in the initial passages (Kaur & Dufour, 2012). Therefore, cell lines may not adequately represent primary cells and may provide different results. In this context, the biological responses in primary cells may be closer to an *in vivo* situation than the ones obtained with cell lines. On the other hand, primary cells are only useful within the first few passages and have a higher risk of contamination than cell lines.

The experiment on the effect of methyl donor depletion on cytokine production was conducted on the assumption that the THP-1 cells would experience a similar functional state of methyl donor depletion. The measurements of THP-1 cells and THP-1 derived macrophages cell viability in complete and depleted media, as well as intracellular folate, methionine and homocysteine concentrations were not carried out due to the limitations of time, cost and access to clinical service that could assist with the analysis. Nonetheless, in this pilot study, regardless of the absence of data on cell differentiation, methyl donor nutrient modulation significantly altered cytokine production, thus, a more robust experimental design can be developed where these issues are addressed, in order to further explore the impact of methyl donor depletion on cytokines production.

The cervical cancer cell model of methyl donor depletion in this study presents a severe deficiency of folate and/or methionine that might not be reflective towards the deficiency levels observed in human. Future work should consider the effects of methyl donor depletion at different levels of depletion, as well as in repleted conditions to determine the reversibility of the its effect.

This study uses the hypothesis-generating approach, instead of a hypothesis-driven approach in order to understand the molecular effects of methyl donor depletion on cervical cancer cells. As this approach is predictive in nature, the findings need to be validated via the hypothesis-testing approach, which will incur additional time and cost.

7.4 Future Works

This thesis has raised several interesting findings that can be further explored in the future, in order to provide a more robust understanding on the impact of methyl donor depletion on

cervical cancer risk and progression. As the current findings are based on an established cancer cell line, it is important to replicate these experiments using a primary cell culture; as biological responses in primary cells may be closer to an *in vivo* situation than the ones obtained with established cell lines. Additionally, effects of methyl donor depletion at different levels of depletion or in repletion could also be carried out. This could provide greater understanding on how levels of depletion severity may affect experimental outcome.

Additionally, in order to further understand the impact of methyl donor depletion on host defence mechanisms during an active stage of infection; future works can include the use of a methyl donor depleted cell model using normal primary cervical tissue culture, where HPV infection can be simulated, and its effects on the expression of IFN genes and cytokine productions can be assessed. Furthermore, a more comprehensive cytokine profile in epithelial cells that represents both Th-1 and Th-2 type cytokine responses towards external stimuli in methyl donor depleted conditions can be carried out.

In addition to its impact on host defence and immune system, the bioinformatics analysis also identified several key biological processes associated with the hallmarks of cancer that can be further explored in the future. This includes the impact of methyl donor depletion on cell proliferation and apoptosis, as the changes in the gene clusters could also be an indicative of cytostatic cells. Its findings can also strengthen the interpretation of this current work.

Besides folate and methionine, other methyl donor nutrients include choline and betaine, which are substrates in the betaine:homocysteine methyltransferase pathway. Previous studies have suggested an interdependency of these methyl donor nutrients, where the presence of choline could feed into the methionine and folate cycle to a certain extent, thus masking the effect of folate and/or methionine depletion. Thus, an experimental study that includes other methyl donor nutrients might be useful in order to explore the interaction between these nutrients in the one carbon cycle. Additionally, there are scarcity in current literature that examine the impact of methyl donor nutrients intake as a whole, and its impact on immune function, HPV infection and persistence, DNA methylation and cervical cancer. Thus, studies at the population level to determine this association could supports *in vivo* and *in vitro* findings.

REFERENCES

- Abdollahi, Z., Elmadfa, I., Djazayeri, A., Sadeghian, S., Freisling, H., Mazandarani, F. S., & Mohamed, K. (2008). Folate, vitamin B12 and homocysteine status in women of childbearing age: baseline data of folic acid wheat flour fortification in Iran. *Ann Nutr Metab*, 53(2), 143-150. <https://doi.org/10.1159/000170890>
- ACOG. (2017). Committee Opinion No. 704: Human Papillomavirus Vaccination. *Obstet Gynecol*, 129(6), 1. <https://doi.org/10.1097/aog.0000000000002052>
- Adamkova, L., Souckova, K., & Kovarik, J. (2007). Transcription protein STAT1: biology and relation to cancer. *Folia Biol (Praha)*, 53(1), 1-6.
- Aggarwal, B. B., Shishodia, S., Sandur, S. K., Pandey, M. K., & Sethi, G. (2006). Inflammation and cancer: how hot is the link? *Biochem Pharmacol*, 72(11), 1605-1621. <https://doi.org/10.1016/j.bcp.2006.06.029>
- Ahmad, R., Al-Roub, A., Kochumon, S., Akther, N., Thomas, R., Kumari, M., Koshy, M. S., Tiss, A., Hannun, Y. A., Tuomilehto, J., Sindhu, S. & Rosen, E. D. (2018). The synergy between palmitate and TNF- α for CCL2 production is dependent on the TRIF/IRF3 pathway: Implications for metabolic inflammation. *J Immunol*, 200(10), 3599-3611. <https://doi.org/10.4049/jimmunol.1701552>
- Alberg, A. J., Selhub, J., Shah, K. V., Viscidi, R. P., Comstock, G. W., & Helzlsouer, K. J. (2000). The risk of cervical cancer in relation to serum concentrations of folate, vitamin B12, and homocysteine. *Cancer Epidemiol Biomarkers Prev*, 9(7), 761-764.
- Amaral, C. L., Bueno Rde, B., Burim, R. V., Queiroz, R. H., Bianchi Mde, L., & Antunes, L. M. (2011). The effects of dietary supplementation of methionine on genomic stability and p53 gene promoter methylation in rats. *Mutat Res*, 722(1), 78-83. <https://doi.org/10.1016/j.mrgentox.2011.03.006>
- Angst, E., Reber, H. A., Hines, O. J., & Eibl, G. (2008). Mononuclear cell-derived interleukin-1 beta confers chemoresistance in pancreatic cancer cells by upregulation of cyclooxygenase-2. *Surgery*, 144(1), 57-65. <https://doi.org/10.1016/j.surg.2008.03.024>
- Ashburner, M., Ball, C. A., Blake, J. A., Botstein, D., Butler, H., Cherry, J. M., Davis, A. P., Dolinski, K., Dwight, S. S., Eppig, J. T., Harris, M. A., Hill, D. P., Issel-Tarver, L., Kasarskis, A., Lewis, S., Matese, J. C., Richardson, J. E., Ringwald, M., Rubin, G. M., & Sherlock, G. (2000). Gene ontology: tool for the unification of biology. The Gene Ontology Consortium. *Nat Genet*, 25(1), 25-29. <https://doi.org/10.1038/75556>
- Assenov, Y., Muller, F., Lutsik, P., Walter, J., Lengauer, T., & Bock, C. (2014). Comprehensive analysis of DNA methylation data with RnBeads. *Nat Methods*, 11(11), 1138-1140. <https://doi.org/10.1038/nmeth.3115>

- Asthana, S., Busa, V., & Labani, S. (2020). Oral contraceptives use and risk of cervical cancer- A systematic review & meta-analysis. *Eur J Obstet Gynecol Reprod Biol*, 247, 163-175. <https://doi.org/10.1016/j.ejogrb.2020.02.014>
- Aune, T., Collins, P., Collier, S., Henderson, M., & Chang, S. (2013). Epigenetic activation and silencing of the gene that encodes IFN- γ . *Front Immunol*, 4(112). <https://doi.org/10.3389/fimmu.2013.00112>
- Azadibakhsh, N., Hosseini, R. S., Atabak, S., Nateghiyan, N., Golestan, B., & Rad, A. H. (2009). Efficacy of folate and vitamin B12 in lowering homocysteine concentrations in hemodialysis patients. *Saudi J Kidney Dis Transpl*, 20(5), 779-788.
- Bader, G. D., & Hogue, C. W. (2003). An automated method for finding molecular complexes in large protein interaction networks. *BMC Bioinformatics*, 4, 2. <http://www.ncbi.nlm.nih.gov/pubmed/12525261>
- Bailey, S. R., Nelson, M. H., Himes, R. A., Li, Z., Mehrotra, S., & Paulos, C. M. (2014). Th17 cells in cancer: the ultimate identity crisis. *Front Immunol*, 5, 276. <https://doi.org/10.3389/fimmu.2014.00276>
- Bais, A. G., Beckmann, I., Ewing, P. C., Eijkemans, M. J., Meijer, C. J., Snijders, P. J., & Helmerhorst, T. J. (2007). Cytokine release in HR-HPV(+) women without and with cervical dysplasia (CIN II and III) or carcinoma, compared with HR-HPV(-) controls. *Mediators Inflamm*, 2007, 24147. <https://doi.org/10.1155/2007/24147>
- Bakshi, A., Bretz, C. L., Cain, T. L., & Kim, J. (2018). Intergenic and intronic DNA hypomethylated regions as putative regulators of imprinted domains. *Epigenomics*, 10(4), 445-461. <https://doi.org/10.2217/epi-2017-0125>
- Balasubramaniam, S. D., Balakrishnan, V., Oon, C. E., & Kaur, G. (2019). Key molecular events in cervical cancer development. *Medicina (Kaunas)*, 55(7). <https://doi.org/10.3390/medicina55070384>
- Balkwill, F. (2002). Tumor necrosis factor or tumor promoting factor? *Cytokine Growth Factor Rev*, 13(2), 135-141. [https://doi.org/https://doi.org/10.1016/S1359-6101\(01\)00020-X](https://doi.org/https://doi.org/10.1016/S1359-6101(01)00020-X)
- Barrett, T., Wilhite, S. E., Ledoux, P., Evangelista, C., Kim, I. F., Tomashevsky, M., Marshall, K. A., Phillippy, K. H., Sherman, P. M., Holko, M., Yefanov, A., Lee, H., Zhang, N., Robertson, C. L., Serova, N., Davis, S., & Soboleva, A. (2013). NCBI GEO: archive for functional genomics data sets--update. *Nucleic Acids Res*, 41(Database issue), D991-995. <https://doi.org/10.1093/nar/gks1193>

- Basile, J. R., Zacny, V., & Münger, K. (2001). The cytokines tumor necrosis factor-alpha (TNF-alpha) and TNF-related apoptosis-inducing ligand differentially modulate proliferation and apoptotic pathways in human keratinocytes expressing the human papillomavirus-16 E7 oncoprotein. *J Biol Chem*, 276(25), 22522-22528. <https://doi.org/10.1074/jbc.M010505200>
- Bassett, J. K., Hodge, A. M., English, D. R., Baglietto, L., Hopper, J. L., Giles, G. G., & Severi, G. (2012). Dietary intake of B vitamins and methionine and risk of lung cancer. *Eur J Clin Nutr*, 66(2), 182-187. <https://doi.org/10.1038/ejcn.2011.157>
- Bastiaan-Net, S., Chanput, W., Hertz, A., Zwittink, R. D., Mes, J. J., & Wichers, H. J. (2013). Biochemical and functional characterization of recombinant fungal immunomodulatory proteins (rFIPs). *Int Immunopharmacol*, 15(1), 167-175. <https://doi.org/10.1016/j.intimp.2012.11.003>
- Bastid, J., Dejou, C., Docquier, A., & Bonnefoy, N. (2020). The emerging role of the IL-17B/IL-17RB pathway in cancer. *Front Immunol*, 11, 718. <https://doi.org/10.3389/fimmu.2020.00718>
- Bektas, N., Noetzel, E., Veeck, J., Press, M. F., Kristiansen, G., Naami, A., Hartmann, A., Dimmler, A., Beckmann, M. W., Knuchel, R., Fasching, P. A., & Dahl, E. (2008). The ubiquitin-like molecule interferon-stimulated gene 15 (ISG15) is a potential prognostic marker in human breast cancer. *Breast Cancer Res*, 10(4), R58. <https://doi.org/10.1186/bcr2117>
- Bent, R., Moll, L., Grabbe, S., & Bros, M. (2018). Interleukin-1 Beta-A friend or foe in malignancies? *Int J Mol Sci*, 19(8), 2155. <https://doi.org/10.3390/ijms19082155>
- Berman, B. P., Weisenberger, D. J., Aman, J. F., Hinoue, T., Ramjan, Z., Liu, Y., Noushmehr, H., Lange, C. P., van Dijk, C. M., Tollenaar, R. A., Van Den Berg, D., & Laird, P. W. (2011). Regions of focal DNA hypermethylation and long-range hypomethylation in colorectal cancer coincide with nuclear lamina-associated domains. *Nat Genet*, 44(1), 40-46. <https://doi.org/10.1038/ng.969>
- Bermudez, A., Bhatla, N., & Leung, E. (2015). Cancer of the cervix uteri. *Int J Gynaecol Obstet*, 131 Suppl 2, S88-95. <https://doi.org/10.1016/j.ijgo.2015.06.004>
- Bindea, G., Mlecnik, B., Hackl, H., Charoentong, P., Tosolini, M., Kirilovsky, A., Fridman, W. H., Pages, F., Trajanoski, Z., & Galon, J. (2009). ClueGO: a Cytoscape plug-in to decipher functionally grouped gene ontology and pathway annotation networks. *Bioinformatics*, 25(8), 1091-1093. <https://doi.org/10.1093/bioinformatics/btp101>
- Bing, Y., Zhu, S., Yu, G., Li, T., Liu, W., Li, C., Wang, Y., Qi, H., Guo, T., Yuan, Y., He, Y., Liu, Z., & Liu, Q. (2014). Glucocorticoid-induced S-adenosylmethionine enhances the interferon signaling pathway by restoring STAT1 protein methylation in hepatitis B virus-infected cells. *The Journal of biological chemistry*, 289(47), 32639-32655. <https://doi.org/10.1074/jbc.M114.589689>

- Biriken, D., Yazihan, N., & Yılmaz, Ş. (2018). Investigation of cytokine and midkine responses of human THP-1 leukemia cells induced by phorbol-12-Myristate-13-Acetate (PMA) at different concentrations and times. *Mikrobiyol Bul*, 52(2), 147-155. <https://doi.org/10.5578/mb.66745>
- Birnbaum, S. M., Greenstein, J. P., & Winitz, M. (1957). Quantitative nutritional studies with water-soluble, chemically defined diets. II. Nitrogen balance and metabolism. *Arch Biochem Biophys*, 72(2), 417-427. [https://doi.org/10.1016/0003-9861\(57\)90217-5](https://doi.org/10.1016/0003-9861(57)90217-5)
- Bistulfi, G., Vandette, E., Matsui, S., & Smiraglia, D. J. (2010). Mild folate deficiency induces genetic and epigenetic instability and phenotype changes in prostate cancer cells. *BMC Biol*, 8, 6. <https://doi.org/10.1186/1741-7007-8-6>
- Bleotu, C., Chifiriuc, M. C., Grigore, R., Grancea, C., Popescu, C. R., Anton, G., & Cernescu, C. (2013). Investigation of Th1/Th2 cytokine profiles in patients with laryngo-pharyngeal, HPV-positive cancers. *Eur Arch Otorhinolaryngol*, 270(2), 711-718. <https://doi.org/10.1007/s00405-012-2067-7>
- Blount, B. C., Mack, M. M., Wehr, C. M., MacGregor, J. T., Hiatt, R. A., Wang, G., Wickramasinghe, S. N., Everson, R. B., & Ames, B. N. (1997). Folate deficiency causes uracil misincorporation into human DNA and chromosome breakage: implications for cancer and neuronal damage. *Proc Natl Acad Sci U S A*, 94(7), 3290-3295. <https://doi.org/10.1073/pnas.94.7.3290>
- Bluyssen, A. R., Durbin, J. E., & Levy, D. E. (1996). ISGF3 gamma p48, a specificity switch for interferon activated transcription factors. *Cytokine Growth Factor Rev*, 7(1), 11-17.
- Boerner, J. L., Nechiporchik, N., Mueller, K. L., Polin, L., Heilbrun, L., Boerner, S. A., Zoratti, G. L., Stark, K., LoRusso, P. M., & Burger, A. (2015). Protein expression of DNA damage repair proteins dictates response to topoisomerase and PARP inhibitors in triple-negative breast cancer. *PLoS One*, 10(3), e0119614. <https://doi.org/10.1371/journal.pone.0119614>
- Bond, S. (2014). Large prospective study finds no association between oral contraceptive use and breast cancer but increased risk for cervical cancer. *Journal of Midwifery & Women's Health*, 59(2), 218-219. https://doi.org/10.1111/jmwh.12179_3
- Borg, D., Hedner, C., Gaber, A., Nodin, B., Fristedt, R., Jirstrom, K., Eberhard, J., & Johnsson, A. (2016). Expression of IFITM1 as a prognostic biomarker in resected gastric and esophageal adenocarcinoma. *Biomark Res*, 4, 10. <https://doi.org/10.1186/s40364-016-0064-5>
- Bosch, F. X., & de Sanjosé, S. (2007). The epidemiology of human papillomavirus infection and cervical cancer. *Dis Markers*, 23(4), 213-227. <http://www.ncbi.nlm.nih.gov/pubmed/17627057>

- Bosch, F. X., Lorincz, A., Muñoz, N., Meijer, C. J., & Shah, K. V. (2002). The causal relation between human papillomavirus and cervical cancer. *J Clin Pathol*, *55*(4), 244-265. <https://doi.org/10.1136/jcp.55.4.244>
- Bray, F., Ferlay, J., Soerjomataram, I., Siegel, R. L., Torre, L. A., & Jemal, A. (2018). Global cancer statistics 2018: GLOBOCAN estimates of incidence and mortality worldwide for 36 cancers in 185 countries. *CA: A Cancer Journal for Clinicians*, *68*(6), 394-424. <https://doi.org/10.3322/caac.21492>
- Bray, F., Loos, A. H., McCarron, P., Weiderpass, E., Arbyn, M., Møller, H., Hakama, M., & Parkin, D. M. (2005). Trends in cervical squamous cell carcinoma incidence in 13 European countries: changing risk and the effects of screening. *Cancer Epidemiol Biomarkers Prev*, *14*(3), 677-686. <https://doi.org/10.1158/1055-9965.Epi-04-0569>
- Brosnan, J. T., & Brosnan, M. E. (2006). The sulfur-containing amino acids: an overview. *J Nutr*, *136*(6 Suppl), 1636s-1640s. <https://doi.org/10.1093/jn/136.6.1636S>
- Brouwer, I. A., Verhoef, P., & Urgert, R. (2000). Betaine supplementation and plasma homocysteine in healthy volunteers. *Arch Intern Med*, *160*(16), 2546-2547. <https://doi.org/10.1001/archinte.160.16.2546-a>
- Bruni, L., Diaz, M., Castellsagué, X., Ferrer, E., Bosch, F. X., & de Sanjosé, S. (2010). Cervical human papillomavirus prevalence in 5 continents: meta-analysis of 1 million women with normal cytological findings. *J Infect Dis*, *202*(12), 1789-1799. <https://doi.org/10.1086/657321>
- Buettner, R., Mora, L. B., & Jove, R. (2002). Activated STAT signaling in human tumors provides novel molecular targets for therapeutic intervention. *Clin Cancer Res*, *8*(4), 945-954.
- Burgers, W. A., Blanchon, L., Pradhan, S., de Launoit, Y., Kouzarides, T., & Fuks, F. (2007). Viral oncoproteins target the DNA methyltransferases. *Oncogene*, *26*(11), 1650-1655. <https://doi.org/10.1038/sj.onc.1209950>
- Burk, R. D., Chen, Z., & Van Doorslaer, K. (2009). Human papillomaviruses: genetic basis of carcinogenicity. *Public Health Genomics*, *12*(5-6), 281-290. <https://doi.org/10.1159/000214919>
- Burk, R. D., Harari, A., & Chen, Z. (2013). Human papillomavirus genome variants. *Virology*, *445*(1-2), 232-243. <https://doi.org/10.1016/j.virol.2013.07.018>
- Burks, J., Reed, R. E., & Desai, S. D. (2015). Free ISG15 triggers an antitumor immune response against breast cancer: a new perspective. *Oncotarget*, *6*(9), 7221-7231. <https://doi.org/10.18632/oncotarget.3372>

- Burr, N. E., Hull, M. A., & Subramanian, V. (2017). Folic acid supplementation may reduce colorectal cancer risk in patients with inflammatory bowel disease: a systematic review and meta-analysis. *J Clin Gastroenterol*, *51*(3), 247-253. <https://doi.org/10.1097/mcg.0000000000000498>
- Butcher, D. T., & Rodenhiser, D. I. (2007). Epigenetic inactivation of BRCA1 is associated with aberrant expression of CTCF and DNA methyltransferase (DNMT3B) in some sporadic breast tumours. *Eur J Cancer*, *43*(1), 210-219. <https://doi.org/10.1016/j.ejca.2006.09.002>
- Butterworth, C. E., Jr., Hatch, K. D., Gore, H., Mueller, H., & Krumdieck, C. L. (1982). Improvement in cervical dysplasia associated with folic acid therapy in users of oral contraceptives. *Am J Clin Nutr*, *35*(1), 73-82. <https://doi.org/10.1093/ajcn/35.1.73>
- Byun, H. M., Siegmund, K. D., Pan, F., Weisenberger, D. J., Kanel, G., Laird, P. W., & Yang, A. S. (2009). Epigenetic profiling of somatic tissues from human autopsy specimens identifies tissue- and individual-specific DNA methylation patterns. *Hum Mol Genet*, *18*(24), 4808-4817. <https://doi.org/10.1093/hmg/ddp445>
- Caiazza, F., Ryan, E. J., Doherty, G., Winter, D. C., & Sheahan, K. (2015). Estrogen receptors and their implications in colorectal carcinogenesis. *Front Oncol*, *5*, 19. <https://doi.org/10.3389/fonc.2015.00019>
- Calderón-Ospina, C. A., & Nava-Mesa, M. O. (2020). B Vitamins in the nervous system: current knowledge of the biochemical modes of action and synergies of thiamine, pyridoxine, and cobalamin. *CNS Neurosci Ther*, *26*(1), 5-13. <https://doi.org/10.1111/cns.13207>
- Cancer Genome Atlas Research Network. (2017). Integrated genomic and molecular characterization of cervical cancer. *Nature*, *543*(7645), 378-384. <https://doi.org/10.1038/nature21386>
- Cardoso, M. F. S., Castelletti, C. H. M., Lima-Filho, J. L., Martins, D. B. G., & Teixeira, J. A. C. (2017). Putative biomarkers for cervical cancer: SNVs, methylation and expression profiles. *Mutat Res*, *773*, 161-173. <https://doi.org/10.1016/j.mrrev.2017.06.002>
- Carlson, M. W., Iyer, V. R., & Marcotte, E. M. (2007). Quantitative gene expression assessment identifies appropriate cell line models for individual cervical cancer pathways. *BMC Genomics*, *8*, 117. <https://doi.org/10.1186/1471-2164-8-117>
- Carmody, R. J., & Chen, Y. H. (2007). Nuclear factor-kappaB: activation and regulation during toll-like receptor signaling. *Cell Mol Immunol*, *4*(1), 31-41.

- Cartron, P. F., Hervouet, E., Debien, E., Olivier, C., Pouliquen, D., Menanteau, J., Loussouarn, D., Martin, S. A., Campone, M., & Vallette, F. M. (2012). Folate supplementation limits the tumorigenesis in rodent models of gliomagenesis. *Eur J Cancer*, *48*(15), 2431-2441. <https://doi.org/10.1016/j.ejca.2012.01.002>
- Castellano, R., Perruchot, M. H., Tesseraud, S., Metayer-Coustard, S., Baeza, E., Mercier, Y., & Gondret, F. (2017). Methionine and cysteine deficiencies altered proliferation rate and time-course differentiation of porcine preadipose cells. *Amino Acids*, *49*(2), 355-366. <https://doi.org/10.1007/s00726-016-2369-y>
- Castellsagué, X., Bosch, F. X., & Muñoz, N. (2002). Environmental co-factors in HPV carcinogenesis. *Virus Res*, *89*(2), 191-199. [https://doi.org/10.1016/s0168-1702\(02\)00188-0](https://doi.org/10.1016/s0168-1702(02)00188-0)
- Catala, G. N., Bestwick, C. S., Russell, W. R., Tortora, K., Giovannelli, L., Moyer, M. P., Lendoiro, E., & Duthie, S. J. (2019). Folate, genomic stability and colon cancer: the use of single cell gel electrophoresis in assessing the impact of folate in vitro, in vivo and in human biomonitoring. *Mutat Res*, *843*, 73-80. <https://doi.org/10.1016/j.mrgentox.2018.08.012>
- Chanput, W., Mes, J. J., Savelkoul, H. F., & Wichers, H. J. (2013). Characterization of polarized THP-1 macrophages and polarizing ability of LPS and food compounds. *Food Funct*, *4*(2), 266-276. <https://doi.org/10.1039/c2fo30156c>
- Chanput, W., Mes, J. J., & Wichers, H. J. (2014). THP-1 cell line: an in vitro cell model for immune modulation approach. *Int Immunopharmacol*, *23*(1), 37-45. <https://doi.org/10.1016/j.intimp.2014.08.002>
- Chanput, W., Reitsma, M., Kleinjans, L., Mes, J. J., Savelkoul, H. F., & Wichers, H. J. (2012). Beta-Glucans are involved in immune-modulation of THP-1 macrophages. *Mol Nutr Food Res*, *56*(5), 822-833. <https://doi.org/10.1002/mnfr.201100715>
- Chaturvedi, S., Hoffman, R. M., & Bertino, J. R. (2018). Exploiting methionine restriction for cancer treatment. *Biochem Pharmacol*, *154*, 170-173. <https://doi.org/10.1016/j.bcp.2018.05.003>
- Chen, H. C., Schiffman, M., Lin, C. Y., Pan, M. H., You, S. L., Chuang, L. C., Hsieh, C. Y., Liaw, K. L., Hsing, A. W., & Chen, C. J. (2011). Persistence of type-specific human papillomavirus infection and increased long-term risk of cervical cancer. *JNCI: Journal of the National Cancer Institute*, *103*(18), 1387-1396. <https://doi.org/10.1093/jnci/djr283>
- Chen, J., Zhao, J., Chen, L., Dong, N., Ying, Z., Cai, Z., Ji, D., Zhang, Y., Dong, L., Li, Y., Jiang, L., Holtzman, M. J., & Chen, C. (2015). STAT1 modification improves therapeutic effects of interferons on lung cancer cells. *J Transl Med*, *13*, 293. <https://doi.org/10.1186/s12967-015-0656-0>

- Cheon, H., Borden, E. C., & Stark, G. R. (2014). Interferons and their stimulated genes in the tumor microenvironment. *Semin Oncol*, 41(2), 156-173. <https://doi.org/10.1053/j.seminoncol.2014.02.002>
- Chiuve, S. E., Giovannucci, E. L., Hankinson, S. E., Zeisel, S. H., Dougherty, L. W., Willett, W. C., & Rimm, E. B. (2007). The association between betaine and choline intakes and the plasma concentrations of homocysteine in women. *Am J Clin Nutr*, 86(4), 1073-1081. <https://doi.org/10.1093/ajcn/86.4.1073>
- Christensen, B. C., Kelsey, K. T., Zheng, S., Houseman, E. A., Marsit, C. J., Wrensch, M. R., Wiemels, J. L., Nelson, H. H., Karagas, M. R., Kushi, L. H., Kwan, M. L., & Wiencke, J. K. (2010). Breast cancer DNA methylation profiles are associated with tumor size and alcohol and folate intake. *PLoS Genet*, 6(7), e1001043. <https://doi.org/10.1371/journal.pgen.1001043>
- Clare, C. E., Brassington, A. H., Kwong, W. Y., & Sinclair, K. D. (2019). One-Carbon Metabolism: Linking Nutritional Biochemistry to Epigenetic Programming of Long-Term Development. *Annu Rev Anim Biosci*, 7(1), 263-287. <https://doi.org/10.1146/annurev-animal-020518-115206>
- Clarke, M. A., Luhn, P., Gage, J. C., Bodelon, C., Dunn, S. T., Walker, J., Zuna, R., Hewitt, S., Killian, J. K., Yan, L., Miller, A., Schiffman, M., & Wentzensen, N. (2017). Discovery and validation of candidate host DNA methylation markers for detection of cervical precancer and cancer. *International journal of cancer*, 141(4), 701-710. <https://doi.org/10.1002/ijc.30781>
- Clarke, M. A., Wentzensen, N., Mirabello, L., Ghosh, A., Wacholder, S., Harari, A., Lorincz, A., Schiffman, M., & Burk, R. D. (2012). Human papillomavirus DNA methylation as a potential biomarker for cervical cancer. *Cancer Epidemiol Biomarkers Prev*, 21(12), 2125-2137. <https://doi.org/10.1158/1055-9965.Epi-12-0905>
- Clinton, S. K., Giovannucci, E. L., & Hursting, S. D. (2019). The World Cancer Research Fund/American Institute for cancer research third expert report on diet, nutrition, physical activity, and cancer: impact and future directions. *The Journal of Nutrition*, 150(4), 663-671. <https://doi.org/10.1093/jn/nxz268>
- Colacino, J. A., Arthur, A. E., Dolinoy, D. C., Sartor, M. A., Duffy, S. A., Chepeha, D. B., Bradford, C. R., Walline, H. M., McHugh, J. B., D'Silva, N., Carey, T. E., Wolf, G. T., Taylor, J. M., Peterson, K. E., & Rozek, L. S. (2012). Pretreatment dietary intake is associated with tumor suppressor DNA methylation in head and neck squamous cell carcinomas. *Epigenetics*, 7(8), 883-891. <https://doi.org/10.4161/epi.21038>

- Cole, B. F., Baron, J. A., Sandler, R. S., Haile, R. W., Ahnen, D. J., Bresalier, R. S., McKeown-Eyssen, G., Summers, R. W., Rothstein, R. I., Burke, C. A., Snover, D. C., Church, T. R., Allen, J. I., Robertson, D. J., Beck, G. J., Bond, J. H., Byers, T., Mandel, J. S., Mott, L. A., Pearson, L. H., Barry, E. L., Rees, J. R., Marcon, N., Saibil, F., Ueland, P. M., & Greenberg, E. R. (2007). Folic acid for the prevention of colorectal adenomas: a randomized clinical trial. *Jama*, 297(21), 2351-2359. <https://doi.org/10.1001/jama.297.21.2351>
- Condoluci, A., Mazzara, C., Zoccoli, A., Pezzuto, A., & Tonini, G. (2016). Impact of smoking on lung cancer treatment effectiveness: a review. *Future Oncol*, 12(18), 2149-2161. <https://doi.org/10.2217/fon-2015-0055>
- Conesa-Zamora, P. (2013). Immune responses against virus and tumor in cervical carcinogenesis: treatment strategies for avoiding the HPV-induced immune escape. *Gynecol Oncol*, 131(2), 480-488. <https://doi.org/10.1016/j.ygyno.2013.08.025>
- Cortellino, S., Xu, J., Sannai, M., Moore, R., Caretti, E., Cigliano, A., Le Coz, M., Devarajan, K., Wessels, A., Soprano, D., Abramowitz, L. K., Bartolomei, M. S., Rambow, F., Bassi, M. R., Bruno, T., Fanciulli, M., Renner, C., Klein-Szanto, A. J., Matsumoto, Y., Kobi, D., Davidson, I., Alberti, C., Larue, L., & Bellacosa, A. (2011). Thymine DNA glycosylase is essential for active DNA demethylation by linked deamination-base excision repair. *Cell*, 146(1), 67-79. <https://doi.org/10.1016/j.cell.2011.06.020>
- Courtemanche, C., Elson-Schwab, I., Mashiyama, S. T., Kerry, N., & Ames, B. N. (2004). Folate deficiency inhibits the proliferation of primary human CD8+ T lymphocytes in vitro. *J Immunol*, 173(5), 3186-3192. <https://doi.org/10.4049/jimmunol.173.5.3186>
- Craciunescu, C. N., Johnson, A. R., & Zeisel, S. H. (2010). Dietary choline reverses some, but not all, effects of folate deficiency on neurogenesis and apoptosis in fetal mouse brain. *J Nutr*, 140(6), 1162-1166. <https://doi.org/10.3945/jn.110.122044>
- Craig, S. A. (2004). Betaine in human nutrition. *Am J Clin Nutr*, 80(3), 539-549. <https://doi.org/10.1093/ajcn/80.3.539>
- Crary-Dooley, F. K., Tam, M. E., Dunaway, K. W., Hertz-Picciotto, I., Schmidt, R. J., & LaSalle, J. M. (2017). A comparison of existing global DNA methylation assays to low-coverage whole-genome bisulfite sequencing for epidemiological studies. *Epigenetics*, 12(3), 206-214. <https://doi.org/10.1080/15592294.2016.1276680>
- Craveiro, R., Costa, S., Pinto, D., Salgado, L., Carvalho, L., Castro, C., Bravo, I., Lopes, C., Silva, I., & Medeiros, R. (2004). TP73 alterations in cervical carcinoma. *Cancer Genet Cytogenet*, 150(2), 116-121. <https://doi.org/10.1016/j.cancergencyto.2003.08.020>
- Crider, K. S., Bailey, L. B., & Berry, R. J. (2011). Folic acid food fortification-its history, effect, concerns, and future directions. *Nutrients*, 3(3), 370-384. <https://doi.org/10.3390/nu3030370>

- Curtis, C. D., & Goggins, M. (2005). DNA methylation analysis in human cancer. *Methods Mol Med*, *103*, 123-136. <https://doi.org/10.1385/1-59259-780-7:123>
- Cuschieri, K. S., Cubie, H. A., Whitley, M. W., Gilkison, G., Arends, M. J., Graham, C., & McGoogan, E. (2005). Persistent high risk HPV infection associated with development of cervical neoplasia in a prospective population study. *J Clin Pathol*, *58*(9), 946. <https://doi.org/10.1136/jcp.2004.022863>
- da Costa, K. A., Cochary, E. F., Blusztajn, J. K., Garner, S. C., & Zeisel, S. H. (1993). Accumulation of 1,2-sn-diradylglycerol with increased membrane-associated protein kinase C may be the mechanism for spontaneous hepatocarcinogenesis in choline-deficient rats. *J Biol Chem*, *268*(3), 2100-2105.
- da Costa, K. A., Garner, S. C., Chang, J., & Zeisel, S. H. (1995). Effects of prolonged (1 year) choline deficiency and subsequent re-feeding of choline on 1,2-sn-diradylglycerol, fatty acids and protein kinase C in rat liver. *Carcinogenesis*, *16*(2), 327-334. <https://doi.org/10.1093/carcin/16.2.327>
- Da Silva, M. L. R., De Albuquerque, B., Allyrio, T., De Almeida, V. D., Cobucci, R. N. O., Bezerra, F. L., Andrade, V. S., Lanza, D. C. F., De Azevedo, J. C. V., De Araújo, J. M. G., & Fernandes, J. V. (2021). The role of HPV-induced epigenetic changes in cervical carcinogenesis (Review). *Biomed Rep*, *15*(1), 60. <https://doi.org/10.3892/br.2021.1436>
- Daigneault, M., Preston, J. A., Marriott, H. M., Whyte, M. K., & Dockrell, D. H. (2010). The identification of markers of macrophage differentiation in PMA-stimulated THP-1 cells and monocyte-derived macrophages. *PLoS One*, *5*(1), e8668. <https://doi.org/10.1371/journal.pone.0008668>
- Danish, H. H., Goyal, S., Taunk, N. K., Wu, H., Moran, M. S., & Haffty, B. G. (2013). Interferon-induced protein with tetratricopeptide repeats 1 (IFIT1) as a prognostic marker for local control in T1-2 N0 breast cancer treated with breast-conserving surgery and radiation therapy (BCS + RT). *Breast J*, *19*(3), 231-239. <https://doi.org/10.1111/tbj.12097>
- Darnell, J. E., Jr., Kerr, I. M., & Stark, G. R. (1994). Jak-STAT pathways and transcriptional activation in response to IFNs and other extracellular signaling proteins. *Science*, *264*(5164), 1415-1421.
- Das, C. R., Tiwari, D., Dongre, A., Khan, M. A., Husain, S. A., Sarma, A., Bose, S., & Bose, P. D. (2018). Deregulated TNF-alpha levels along with HPV genotype 16 infection are associated with pathogenesis of cervical neoplasia in northeast Indian patients. *Viral Immunol*, *31*(4), 282-291. <https://doi.org/10.1089/vim.2017.0151>
- Das, P. M., & Singal, R. (2004). DNA Methylation and Cancer. *J Clin Oncol*, *22*(22), 4632-4642. <https://doi.org/10.1200/JCO.2004.07.151>

- Datta, J., Majumder, S., Bai, S., Ghoshal, K., Kutay, H., Smith, D. S., Crabb, J. W., & Jacob, S. T. (2005). Physical and functional interaction of DNA methyltransferase 3A with Mbd3 and Brg1 in mouse lymphosarcoma cells. *Cancer research*, *65*(23), 10891-10900. <https://doi.org/10.1158/0008-5472.CAN-05-1455>
- de Benoist, B. (2008). Conclusions of a WHO Technical Consultation on folate and vitamin B12 deficiencies. *Food Nutr Bull*, *29*(2 Suppl), S238-244. <https://doi.org/10.1177/15648265080292s129>
- de Sanjosé, S., Brotons, M., & Pavón, M. A. (2018). The natural history of human papillomavirus infection. *Best Pract Res Clin Obstet Gynaecol*, *47*, 2-13. <https://doi.org/10.1016/j.bpobgyn.2017.08.015>
- DeCarlo, C. A., Rosa, B., Jackson, R., Niccoli, S., Escott, N. G., & Zehbe, I. (2012). Toll-like receptor transcriptome in the HPV-positive cervical cancer microenvironment. *Clin Dev Immunol*, *2012*, 785825. <https://doi.org/10.1155/2012/785825>
- Dedeurwaerder, S., Defrance, M., Bizet, M., Calonne, E., Bontempi, G., & Fuks, F. (2014). A comprehensive overview of Infinium HumanMethylation450 data processing. *Brief Bioinform*, *15*(6), 929-941. <https://doi.org/10.1093/bib/bbt054>
- Deligeoroglou, E., Giannouli, A., Athanasopoulos, N., Karountzos, V., Vatopoulou, A., Dimopoulos, K., & Creatsas, G. (2013). HPV infection: immunological aspects and their utility in future therapy. *Infect Dis Obstet Gynecol*, *2013*, 540850. <https://doi.org/10.1155/2013/540850>
- Deng, H., Zhen, H., Fu, Z., Huang, X., Zhou, H., & Liu, L. (2012). The antagonistic effect between STAT1 and Survivin and its clinical significance in gastric cancer. *Oncol Lett*, *3*(1), 193-199. <https://doi.org/10.3892/ol.2011.423>
- Denny, L. (2015). Control of cancer of the cervix in low- and middle-income countries. *Ann Surg Oncol*, *22*(3), 728-733. <https://doi.org/10.1245/s10434-014-4344-8>
- Denny, L. A., Franceschi, S., de Sanjosé, S., Heard, I., Moscicki, A. B., & Palefsky, J. (2012). Human papillomavirus, human immunodeficiency virus and immunosuppression. *Vaccine*, *30* (5), F168-174. <https://doi.org/10.1016/j.vaccine.2012.06.045>
- Depeint, F., Bruce, W. R., Shangari, N., Mehta, R., & O'Brien, P. J. (2006). Mitochondrial function and toxicity: role of B vitamins on the one-carbon transfer pathways. *Chem Biol Interact*, *163*(1-2), 113-132. <https://doi.org/10.1016/j.cbi.2006.05.010>
- Derks, S., Lentjes, M. H., Hellebrekers, D. M., de Bruine, A. P., Herman, J. G., & van Engeland, M. (2004). Methylation-specific PCR unraveled. *Cell Oncol*, *26*(5-6), 291-299.

- Desai, S. D., Haas, A. L., Wood, L. M., Tsai, Y. C., Pestka, S., Rubin, E. H., Saleem, A., Nur, E. K. A., & Liu, L. F. (2006). Elevated expression of ISG15 in tumor cells interferes with the ubiquitin/26S proteasome pathway. *Cancer Res*, *66*(2), 921-928. <https://doi.org/10.1158/0008-5472.can-05-1123>
- Di Franco, S., Turdo, A., Todaro, M., & Stassi, G. (2017). Role of Type I and II interferons in colorectal cancer and melanoma. *Front Immunol*, *8*, 878. <https://doi.org/10.3389/fimmu.2017.00878>
- Ding, D. C., Chiang, M. H., Lai, H. C., Hsiung, C. A., Hsieh, C. Y., & Chu, T. Y. (2009). Methylation of the long control region of HPV16 is related to the severity of cervical neoplasia. *Eur J Obstet Gynecol Reprod Biol*, *147*(2), 215-220. <https://doi.org/10.1016/j.ejogrb.2009.08.023>
- Dong, S. M., Kim, H. S., Rha, S. H., & Sidransky, D. (2001). Promoter hypermethylation of multiple genes in carcinoma of the uterine cervix. *Clin Cancer Res*, *7*(7), 1982-1986.
- Donnelly, J. G. (2001). Folic acid. *Crit Rev Clin Lab Sci*, *38*(3), 183-223. <https://doi.org/10.1080/20014091084209>
- Drolet, M., Bénard, É., Pérez, N., & Brisson, M. (2019). Population-level impact and herd effects following the introduction of human papillomavirus vaccination programmes: updated systematic review and meta-analysis. *Lancet*, *394*(10197), 497-509. [https://doi.org/10.1016/s0140-6736\(19\)30298-3](https://doi.org/10.1016/s0140-6736(19)30298-3)
- Du, P., Zhang, X., Huang, C. C., Jafari, N., Kibbe, W. A., Hou, L., & Lin, S. M. (2010). Comparison of Beta-value and M-value methods for quantifying methylation levels by microarray analysis. *BMC Bioinformatics*, *11*, 587. <https://doi.org/10.1186/1471-2105-11-587>
- Du, Y. F., Lin, F. Y., Long, W. Q., Luo, W. P., Yan, B., Xu, M., Mo, X. F., & Zhang, C. X. (2017). Serum betaine but not choline is inversely associated with breast cancer risk: a case-control study in China. *Eur J Nutr*, *56*(3), 1329-1337. <https://doi.org/10.1007/s00394-016-1183-3>
- Duarte, C. W., Willey, C. D., Zhi, D., Cui, X., Harris, J. J., Vaughan, L. K., Mehta, T., McCubrey, R. O., Khodarev, N. N., Weichselbaum, R. R., & Gillespie, G. Y. (2012). Expression signature of IFN/STAT1 signaling genes predicts poor survival outcome in glioblastoma multiforme in a subtype-specific manner. *PLoS One*, *7*(1), e29653. <https://doi.org/10.1371/journal.pone.0029653>
- Duarte, I., Santos, A., Sousa, H., Catarino, R., Pinto, D., Matos, A., Pereira, D., Moutinho, J., Canedo, P., Machado, J. C., & Medeiros, R. (2005). G-308A TNF-alpha polymorphism is associated with an increased risk of invasive cervical cancer. *Biochem Biophys Res Commun*, *334*(2), 588-592. <https://doi.org/10.1016/j.bbrc.2005.06.137>

- Ducker, G. S., & Rabinowitz, J. D. (2017). One carbon metabolism in health and disease. *Cell Metab*, 25(1), 27-42. <https://doi.org/10.1016/j.cmet.2016.08.009>
- Dueñas-González, A., Lizano, M., Candelaria, M., Cetina, L., Arce, C., & Cervera, E. (2005). Epigenetics of cervical cancer. An overview and therapeutic perspectives. *Mol Cancer*, 4, 38. <https://doi.org/10.1186/1476-4598-4-38>
- Dunn, G. P., Koebel, C. M., & Schreiber, R. D. (2006). Interferons, immunity and cancer immunoediting. *Nat Rev Immunol*, 6(11), 836-848. <https://doi.org/10.1038/nri1961>
- Dupuis, S., Jouanguy, E., Al-Hajjar, S., Fieschi, C., Al-Mohsen, I. Z., Al-Jumaah, S., Yang, K., Chapgier, A., Eidenschenk, C., Eid, P., Al Ghonaium, A., Tufenkeji, H., Frayha, H., Al-Gazlan, S., Al-Rayes, H., Schreiber, R. D., Gresser, I., & Casanova, J. L. (2003). Impaired response to interferon-alpha/beta and lethal viral disease in human STAT1 deficiency. *Nat Genet*, 33(3), 388-391. <https://doi.org/10.1038/ng1097>
- Durando, X., Farges, M. C., Buc, E., Abrial, C., Petorin-Lesens, C., Gillet, B., Vasson, M. P., Pezet, D., Chollet, P., & Thivat, E. (2010). Dietary methionine restriction with FOLFOX regimen as first line therapy of metastatic colorectal cancer: a feasibility study. *Oncology*, 78(3-4), 205-209. <https://doi.org/10.1159/000313700>
- Duschene, K. S., & Broderick, J. B. (2010). The antiviral protein viperin is a radical SAM enzyme. *FEBS Lett*, 584(6), 1263-1267. <https://doi.org/10.1016/j.febslet.2010.02.041>
- Duthie, S. J., & Hawdon, A. (1998). DNA instability (strand breakage, uracil misincorporation, and defective repair) is increased by folic acid depletion in human lymphocytes in vitro. *Faseb j*, 12(14), 1491-1497.
- Duthie, S. J., Mavrommatis, Y., Rucklidge, G., Reid, M., Duncan, G., Moyer, M. P., Pirie, L. P., & Bestwick, C. S. (2008). The response of human colonocytes to folate deficiency in vitro: functional and proteomic analyses. *J Proteome Res*, 7(8), 3254-3266. <https://doi.org/10.1021/pr700751y>
- Duthie, S. J., Narayanan, S., Blum, S., Pirie, L., & Brand, G. M. (2000). Folate deficiency in vitro induces uracil misincorporation and DNA hypomethylation and inhibits DNA excision repair in immortalized normal human colon epithelial cells. *Nutr Cancer*, 37(2), 245-251. https://doi.org/10.1207/S15327914NC372_18
- Duthie, S. J., Narayanan, S., Sharp, L., Little, J., Basten, G., & Powers, H. (2004). Folate, DNA stability and colo-rectal neoplasia. *Proc Nutr Soc*, 63(4), 571-578. <http://www.ncbi.nlm.nih.gov/pubmed/15831129>

- Ebbing, M., Bønaa, K. H., Nygård, O., Arnesen, E., Ueland, P. M., Nordrehaug, J. E., Rasmussen, K., Njølstad, I., Refsum, H., Nilsen, D. W., Tverdal, A., Meyer, K., & Vollset, S. E. (2009). Cancer incidence and mortality after treatment with folic acid and vitamin B12. *Jama*, *302*(19), 2119-2126. <https://doi.org/10.1001/jama.2009.1622>
- Egawa, N., Egawa, K., Griffin, H., & Doorbar, J. (2015). Human papillomaviruses; epithelial tropisms, and the development of neoplasia. *Viruses*, *7*(7), 3863-3890. <https://doi.org/10.3390/v7072802>
- Ehrlich, M. (2002). DNA methylation in cancer: too much, but also too little. *Oncogene*, *21*(35), 5400-5413. <https://doi.org/10.1038/sj.onc.1205651>
- Ehrlich, M. (2019). DNA hypermethylation in disease: mechanisms and clinical relevance. *Epigenetics*, *14*(12), 1141-1163. <https://doi.org/10.1080/15592294.2019.1638701>
- Elgueta, R., Benson, M. J., de Vries, V. C., Wasiuk, A., Guo, Y., & Noelle, R. J. (2009). Molecular mechanism and function of CD40/CD40L engagement in the immune system. *Immunological reviews*, *229*(1), 152-172. <https://doi.org/10.1111/j.1600-065X.2009.00782.x>
- Elmadfa, I., & Meyer, A. L. (2019). The role of the status of selected micronutrients in shaping the immune function. *Endocr Metab Immune Disord Drug Targets*, *19*(8), 1100-1115. <https://doi.org/10.2174/1871530319666190529101816>
- Estéicio, M. R., & Issa, J. P. (2011). Dissecting DNA hypermethylation in cancer. *FEBS Lett*, *585*(13), 2078-2086. <https://doi.org/10.1016/j.febslet.2010.12.001>
- Esteller, M. (2003). Cancer epigenetics: DNA methylation and chromatin alterations in human cancer. *Adv Exp Med Biol*, *532*, 39-49. https://doi.org/10.1007/978-1-4615-0081-0_5
- Esteller, M. (2008). Epigenetics in cancer. *N Engl J Med*, *358*(11), 1148-1159. <https://doi.org/10.1056/NEJMra072067>
- Fanidi, A., Muller, D. C., Yuan, J. M., Stevens, V. L., Weinstein, S. J., Albanes, D., Prentice, R., Thomsen, C. A., Pettinger, M., Cai, Q., Blot, W. J., Wu, J., Arslan, A. A., Zeleniuch-Jacquotte, A., McCullough, M. L., Le Marchand, L., Wilkens, L. R., Haiman, C. A., Zhang, X., Han, J., Stampfer, M. J., Smith-Warner, S. A., Giovannucci, E., Giles, G. G., Hodge, A. M., Severi, G., Johansson, M., Grankvist, K., Langhammer, A., Krokstad, S., Næss, M., Wang, R., Gao, Y. T., Butler, L. M., Koh, W. P., Shu, X. O., Xiang, Y. B., Li, H., Zheng, W., Lan, Q., Visvanathan, K., Bolton, J. H., Ueland, P. M., Midttun, Ø., Ulvik, A., Caporaso, N. E., Purdue, M., Ziegler, R. G., Freedman, N. D., Buring, J. E., Lee, I. M., Sesso, H. D., Gaziano, J. M., Manjer, J., Ericson, U., Relton, C., Brennan, P., & Johansson, M. (2018). Circulating folate, vitamin B6, and methionine in relation to lung cancer risk in the lung cancer cohort consortium (LC3). *J Natl Cancer Inst*, *110*(1), 57-67. <https://doi.org/10.1093/jnci/djx119>

- Farzaneh, F., Roberts, S., Mandal, D., Ollier, B., Winters, U., Kitchener, H. C., & Brabin, L. (2006). The IL-10 -1082G polymorphism is associated with clearance of HPV infection. *BJOG*, *113*(8), 961-964. <https://doi.org/10.1111/j.1471-0528.2006.00956.x>
- Fatemi, M., Hermann, A., Gowher, H., & Jeltsch, A. (2002). DNMT3a and DNMT1 functionally cooperate during de novo methylation of DNA. *Eur J Biochem*, *269*(20), 4981-4984. <http://www.ncbi.nlm.nih.gov/pubmed/12383256>
- Feigelson, H. S., Jonas, C. R., Robertson, A. S., McCullough, M. L., Thun, M. J., & Calle, E. E. (2003). Alcohol, folate, methionine, and risk of incident breast cancer in the American Cancer Society Cancer Prevention Study II Nutrition Cohort. *Cancer Epidemiol Biomarkers Prev*, *12*(2), 161-164.
- Feinberg, A. P., & Tycko, B. (2004). The history of cancer epigenetics. *Nature Reviews Cancer*, *4*(2), 143-153. <https://doi.org/10.1038/nrc1279>
- Feld, J. J., Modi, A. A., El-Diwany, R., Rotman, Y., Thomas, E., Ahlenstiel, G., Titerence, R., Koh, C., Cherepanov, V., Heller, T., Ghany, M. G., Park, Y., Hoofnagle, J. H., & Liang, T. J. (2011). S-adenosyl methionine improves early viral responses and interferon-stimulated gene induction in hepatitis C nonresponders. *Gastroenterology*, *140*(3), 830-839. <https://doi.org/10.1053/j.gastro.2010.09.010>
- Feng, H., Sui, L., Du, M., & Wang, Q. (2017). Meta-analysis of TP73 polymorphism and cervical cancer. *Genet Mol Res*, *16*(1). <https://doi.org/10.4238/gmr16016571>
- Fensterl, V., & Sen, G. C. (2015). Interferon-induced IFIT proteins: their role in viral pathogenesis. *Journal of Virology*, *89*(5), 2462. <https://doi.org/10.1128/JVI.02744-14>
- Ferlay, J., Ervik, M., Lam, F., Colombet, M., Mery, L., Piñeros, M., Znaor, A., Soerjomataram, I., & Bray, F. (2018). Global cancer observatory: cancer today. *Lyon, France: International Agency for Research on Cancer*.
- Ferlay, J., Soerjomataram, I., Dikshit, R., Eser, S., Mathers, C., Rebelo, M., Parkin, D. M., Forman, D., & Bray, F. (2015). Cancer incidence and mortality worldwide: sources, methods and major patterns in GLOBOCAN 2012. *Int J Cancer*, *136*(5), E359-386. <https://doi.org/10.1002/ijc.29210>
- Finkelstein, J. D. (1990). Methionine metabolism in mammals. *J Nutr Biochem*, *1*(5), 228-237. [https://doi.org/10.1016/0955-2863\(90\)90070-2](https://doi.org/10.1016/0955-2863(90)90070-2)
- Finkelstein, J. D., & Martin, J. J. (1984). Methionine metabolism in mammals. Distribution of homocysteine between competing pathways. *J Biol Chem*, *259*(15), 9508-9513.
- Finkelstein, J. D., & Martin, J. J. (1986). Methionine metabolism in mammals. Adaptation to methionine excess. *J Biol Chem*, *261*(4), 1582-1587.

- Flatley, J. E., McNeir, K., Balasubramani, L., Tidy, J., Stuart, E. L., Young, T. A., & Powers, H. J. (2009). Folate status and aberrant DNA methylation are associated with HPV infection and cervical pathogenesis. *Cancer Epidemiol Biomarkers Prev*, *18*(10), 2782-2789. <https://doi.org/10.1158/1055-9965.EPI-09-0493>
- Forster, S. C., Tate, M. D., & Hertzog, P. J. (2015). MicroRNA as Type I Interferon-Regulated transcripts and modulators of the innate immune response. *Front Immunol*, *6*(334). <https://doi.org/10.3389/fimmu.2015.00334>
- Fowler, B. M., Giuliano, A. R., Piyathilake, C., Nour, M., & Hatch, K. (1998). Hypomethylation in cervical tissue: is there a correlation with folate status? *Cancer Epidemiol Biomarkers Prev*, *7*(10), 901-906.
- Franco, E. L., Duarte-Franco, E., & Ferenczy, A. (2001). Cervical cancer: epidemiology, prevention and the role of human papillomavirus infection. *Cmaj*, *164*(7), 1017-1025.
- Freiberger, D., Lewis, L., & Helfand, L. (2015). Human papillomavirus-related high-grade squamous intraepithelial lesions of the esophagus, skin, and cervix in an adolescent lung transplant recipient: a case report and literature review. *Transpl Infect Dis*, *17*(1), 98-102. <https://doi.org/10.1111/tid.12322>
- Fuchs, C. S., Willett, W. C., Colditz, G. A., Hunter, D. J., Stampfer, M. J., Speizer, F. E., & Giovannucci, E. L. (2002). The influence of folate and multivitamin use on the familial risk of colon cancer in women. *Cancer Epidemiol Biomarkers Prev*, *11*(3), 227-234.
- Funaki, S., Nakamura, T., Nakatani, T., Umehara, H., Nakashima, H., Okumura, M., Oboki, K., Matsumoto, K., Saito, H., & Nakano, T. (2015). Global DNA hypomethylation coupled to cellular transformation and metastatic ability. *FEBS Lett*, *589*(24 Pt B), 4053-4060. <https://doi.org/10.1016/j.febslet.2015.11.020>
- Gakidou, E., Nordhagen, S., & Obermeyer, Z. (2008). Coverage of cervical cancer screening in 57 countries: low average levels and large inequalities. *PLoS Med*, *5*(6), e132. <https://doi.org/10.1371/journal.pmed.0050132>
- Galloway, D. A., & Laimins, L. A. (2015). Human papillomaviruses: shared and distinct pathways for pathogenesis. *Curr Opin Virol*, *14*, 87-92. <https://doi.org/10.1016/j.coviro.2015.09.001>
- García-Closas, R., Castellsagué, X., Bosch, X., & González, C. A. (2005). The role of diet and nutrition in cervical carcinogenesis: a review of recent evidence. *Int J Cancer*, *117*(4), 629-637. <https://doi.org/10.1002/ijc.21193>

- Garland, S. M., Hernandez-Avila, M., Wheeler, C. M., Perez, G., Harper, D. M., Leodolter, S., Tang, G. W., Ferris, D. G., Steben, M., Bryan, J., Taddeo, F. J., Railkar, R., Esser, M. T., Sings, H. L., Nelson, M., Boslego, J., Sattler, C., Barr, E., & Koutsky, L. A. (2007). Quadrivalent vaccine against human papillomavirus to prevent anogenital diseases. *N Engl J Med*, 356(19), 1928-1943. <https://doi.org/10.1056/NEJMoa061760>
- Gaudet, F., Hodgson, J. G., Eden, A., Jackson-Grusby, L., Dausman, J., Gray, J. W., Leonhardt, H., & Jaenisch, R. (2003). Induction of tumors in mice by genomic hypomethylation. *Science*, 300(5618), 489-492. <https://doi.org/10.1126/science.1083558>
- Geissler, C., & Powers, H. (2011). *Human Nutrition*, (12 Ed.). Churchill Livingstone Elsevier.
- Gene Ontology Consortium (2015). Gene Ontology Consortium: going forward. *Nucleic Acids Res*, 43(Database issue), D1049-1056. <https://doi.org/10.1093/nar/gku1179>
- Ghazi, T., Arumugam, T., Foolchand, A., & Chuturgoon, A. A. (2020). The impact of natural dietary compounds and food-borne mycotoxins on dna methylation and cancer. *Cells*, 9(9), 2004. <https://doi.org/10.3390/cells9092004>
- Giovannucci, E. (2002). Epidemiologic studies of folate and colorectal neoplasia: a review. *J Nutr*, 132(8), 2350s-2355s. <https://doi.org/10.1093/jn/132.8.2350S>
- Giovannucci, E., Stampfer, M. J., Colditz, G. A., Rimm, E. B., Trichopoulos, D., Rosner, B. A., Speizer, F. E., & Willett, W. C. (1993). Folate, methionine, and alcohol intake and risk of colorectal adenoma. *J Natl Cancer Inst*, 85(11), 875-884. <https://doi.org/10.1093/jnci/85.11.875>
- Gius, D., Funk, M. C., Chuang, E. Y., Feng, S., Huettner, P. C., Nguyen, L., Bradbury, C. M., Mishra, M., Gao, S., Buttin, B. M., Cohn, D. E., Powell, M. A., Horowitz, N. S., Whitcomb, B. P., & Rader, J. S. (2007). Profiling microdissected epithelium and stroma to model genomic signatures for cervical carcinogenesis accommodating for covariates. *Cancer Res*, 67(15), 7113-7123. <https://doi.org/10.1158/0008-5472.Can-07-0260>
- Gomez, L. C., Sottile, M. L., Guerrero-Gimenez, M. E., Zoppino, F. C. M., Redondo, A. L., Gago, F. E., Orozco, J. I., Tello, O. M., Roque, M., Nadin, S. B., Marzese, D. M., & Vargas-Roig, L. M. (2018). TP73 DNA methylation and upregulation of DeltaNp73 are associated with an adverse prognosis in breast cancer. *J Clin Pathol*, 71(1), 52-58. <https://doi.org/10.1136/jclinpath-2017-204499>
- Gonin, J. M., Nguyen, H., Gonin, R., Sarna, A., Michels, A., Masri-Imad, F., Bommareddy, G., Chassaing, C., Wainer, I., Loya, A., Cary, D., Barker, L. F., Assefi, A., Greenspan, R., Mahoney, D., & Wilcox, C. S. (2003). Controlled trials of very high dose folic acid, vitamins B12 and B6, intravenous folinic acid and serine for treatment of hyperhomocysteinemia in ESRD. *J Nephrol*, 16(4), 522-534.

- González, C. A., Travier, N., Luján-Barroso, L., Castellsagué, X., Bosch, F. X., Roura, E., Bueno-de-Mesquita, H. B., Palli, D., Boeing, H., Pala, V., Sacerdote, C., Tumino, R., Panico, S., Manjer, J., Dillner, J., Hallmans, G., Kjellberg, L., Sanchez, M. J., Altzibar, J. M., Barricarte, A., Navarro, C., Rodriguez, L., Allen, N., Key, T. J., Kaaks, R., Rohrmann, S., Overvad, K., Olsen, A., Tjønneland, A., Munk, C., Kjaer, S. K., Peeters, P. H., van Duijnhoven, F. J., Clavel-Chapelon, F., Boutron-Ruault, M. C., Trichopoulou, A., Benetou, V., Naska, A., Lund, E., Engeset, D., Skeie, G., Franceschi, S., Slimani, N., Rinaldi, S., & Riboli, E. (2011). Dietary factors and in situ and invasive cervical cancer risk in the European prospective investigation into cancer and nutrition study. *Int J Cancer*, *129*(2), 449-459. <https://doi.org/10.1002/ijc.25679>
- Grant, G., Brand, G. M., Pirie, L., Narayanan, S., & Duthie, S. J. (2002). Impact of folate deficiency on dna stability. *The Journal of Nutrition*, *132*(8), 2444S-2449S. <https://doi.org/10.1093/jn/132.8.2444S>
- Greenwood, C., Metodieva, G., Al-Janabi, K., Lausen, B., Alldridge, L., Leng, L., Bucala, R., Fernandez, N., & Metodiev, M. V. (2012). STAT1 and CD74 overexpression is co-dependent and linked to increased invasion and lymph node metastasis in triple-negative breast cancer. *J Proteomics*, *75*(10), 3031-3040. <https://doi.org/10.1016/j.jprot.2011.11.033>
- Guo, S., Jiang, X., Chen, X., Chen, L., Li, X., & Jia, Y. (2015). The protective effect of methylenetetrahydrofolate reductase C677T polymorphism against prostate cancer risk: evidence from 23 case-control studies. *Gene*, *565*(1), 90-95. <https://doi.org/10.1016/j.gene.2015.03.067>
- Gylling, B., Van Guelpen, B., Schneede, J., Hultdin, J., Ueland, P. M., Hallmans, G., Johansson, I., & Palmqvist, R. (2014). Low folate levels are associated with reduced risk of colorectal cancer in a population with low folate status. *Cancer Epidemiol Biomarkers Prev*, *23*(10), 2136-2144. <https://doi.org/10.1158/1055-9965.Epi-13-1352>
- Gyorffy, B., Dietel, M., Fekete, T., & Lage, H. (2008). A snapshot of microarray-generated gene expression signatures associated with ovarian carcinoma. *Int J Gynecol Cancer*, *18*(6), 1215-1233. <https://doi.org/10.1111/j.1525-1438.2007.01169.x>
- Haller, O., & Kochs, G. (2011). Human MxA protein: an interferon-induced dynamin-like GTPase with broad antiviral activity. *J Interferon Cytokine Res*, *31*(1), 79-87. <https://doi.org/10.1089/jir.2010.0076>
- Hamano, E., Hijikata, M., Itoyama, S., Quy, T., Phi, N. C., Long, H. T., Ha, L. D., Ban, V. V., Matsushita, I., Yanai, H., Kirikae, F., Kirikae, T., Kuratsuji, T., Sasazuki, T., & Keicho, N. (2005). Polymorphisms of interferon-inducible genes OAS-1 and MxA associated with SARS in the Vietnamese population. *Biochem Biophys Res Commun*, *329*(4), 1234-1239. <https://doi.org/10.1016/j.bbrc.2005.02.101>
- Hanahan, D., & Weinberg, R. A. (2000). The hallmarks of cancer. *Cell*, *100*(1), 57-70. <http://www.ncbi.nlm.nih.gov/pubmed/10647931>

- Hanahan, D., & Weinberg, R. A. (2011). Hallmarks of cancer: the next generation. *Cell*, *144*(5), 646-674. <https://doi.org/10.1016/j.cell.2011.02.013>
- Hasan, U. A., Bates, E., Takeshita, F., Biliato, A., Accardi, R., Bouvard, V., Mansour, M., Vincent, I., Gissmann, L., Iftner, T., Sideri, M., Stubenrauch, F., & Tommasino, M. (2007). TLR9 expression and function is abolished by the cervical cancer-associated human papillomavirus type 16. *J Immunol*, *178*(5), 3186-3197. <https://doi.org/10.4049/jimmunol.178.5.3186>
- Hasthorpe, S., Holland, K., Nink, V., Lawler, C., & Hertzog, P. (1997). Mechanisms of resistance off NSCLC to interferons. *Int J Oncol*, *10*(5), 933-938.
- Hazelbag, S., Fleuren, G. J., Baelde, J. J., Schuurin, E., Kenter, G. G., & Gorter, A. (2001). Cytokine profile of cervical cancer cells. *Gynecol Oncol*, *83*(2), 235-243. <https://doi.org/10.1006/gyno.2001.6378>
- Hearnden, V., Powers, H. J., Elmogassabi, A., Lowe, R., & Murdoch, C. (2018). Methyl-donor depletion of head and neck cancer cells in vitro establishes a less aggressive tumour cell phenotype. *Eur J Nutr*, *57*(4), 1321-1332. <https://doi.org/10.1007/s00394-017-1411-5>
- Helbig, K. J., & Beard, M. R. (2014). The role of viperin in the innate antiviral response. *J Mol Biol*, *426*(6), 1210-1219. <https://doi.org/10.1016/j.jmb.2013.10.019>
- Hervouet, E., Lalier, L., Debien, E., Cheray, M., Geairon, A., Rogniaux, H., Loussouarn, D., Martin, S. A., Vallette, F. M., & Cartron, P.-F. (2010). Disruption of DNMT1/PCNA/UHRF1 interactions promotes tumorigenesis from human and mice glial cells. *PLoS One*, *5*(6), e11333-e11333. <https://doi.org/10.1371/journal.pone.0011333>
- Hervouet, E., Peixoto, P., Delage-Mourroux, R., Boyer-Guittaut, M., & Cartron, P. F. (2018). Specific or not specific recruitment of DNMTs for DNA methylation, an epigenetic dilemma. *Clin Epigenetics*, *10*, 17. <https://doi.org/10.1186/s13148-018-0450-y>
- Hervouet, E., Vallette, F. M., & Cartron, P. F. (2010). Impact of the DNA methyltransferases expression on the methylation status of apoptosis-associated genes in glioblastoma multiforme. *Cell death & disease*, *1*(1), e8-e8. <https://doi.org/10.1038/cddis.2009.7>
- Herzer, K., Hofmann, T. G., Teufel, A., Schimanski, C. C., Moehler, M., Kanzler, S., Schulze-Bergkamen, H., & Galle, P. R. (2009). IFN-alpha-induced apoptosis in hepatocellular carcinoma involves promyelocytic leukemia protein and TRAIL independently of p53. *Cancer Res*, *69*(3), 855-862. <https://doi.org/10.1158/0008-5472.can-08-2831>
- Hoffman, R. M., Hoshiya, Y., & Guo, W. (2019). Efficacy of methionine-restricted diets on cancers in vivo. *Methods Mol Biol*, *1866*, 75-81. https://doi.org/10.1007/978-1-4939-8796-2_7

- Hoffman, S. R., Le, T., Lockhart, A., Sanusi, A., Dal Santo, L., Davis, M., McKinney, D. A., Brown, M., Poole, C., Willame, C., & Smith, J. S. (2017). Patterns of persistent HPV infection after treatment for cervical intraepithelial neoplasia (CIN): a systematic review. *Int J Cancer*, *141*(1), 8-23. <https://doi.org/10.1002/ijc.30623>
- Hon, G. C., Hawkins, R. D., Caballero, O. L., Lo, C., Lister, R., Pelizzola, M., Valsesia, A., Ye, Z., Kuan, S., Edsall, L. E., Camargo, A. A., Stevenson, B. J., Ecker, J. R., Bafna, V., Strausberg, R. L., Simpson, A. J., & Ren, B. (2012). Global DNA hypomethylation coupled to repressive chromatin domain formation and gene silencing in breast cancer. *Genome Res*, *22*(2), 246-258. <https://doi.org/10.1101/gr.125872.111>
- Hu, J., & Cheung, N. K. (2009). Methionine depletion with recombinant methioninase: in vitro and in vivo efficacy against neuroblastoma and its synergism with chemotherapeutic drugs. *Int J Cancer*, *124*(7), 1700-1706. <https://doi.org/10.1002/ijc.24104>
- Hu, Z., & Ma, D. (2018). The precision prevention and therapy of HPV-related cervical cancer: new concepts and clinical implications. *Cancer Med*, *7*(10), 5217-5236. <https://doi.org/10.1002/cam4.1501>
- Huang, D. W., Sherman, B. T., & Lempicki, R. A. (2009). Systematic and integrative analysis of large gene lists using DAVID bioinformatics resources. *Nature protocols*, *4*(1), 44-57. <Go to ISI>://MEDLINE:19131956
- Huang, D. W., Sherman, B. T., Tan, Q., Kir, J., Liu, D., Bryant, D., Guo, Y., Stephens, R., Baseler, M. W., Lane, H. C., & Lempicki, R. A. (2007). DAVID Bioinformatics Resources: expanded annotation database and novel algorithms to better extract biology from large gene lists. *Nucleic Acids Res*, *35*(Web Server issue), W169-175. <https://doi.org/10.1093/nar/gkm415>
- Hultdin, J., Van Guelpen, B., Bergh, A., Hallmans, G., & Stattin, P. (2005). Plasma folate, vitamin B12, and homocysteine and prostate cancer risk: a prospective study. *Int J Cancer*, *113*(5), 819-824. <https://doi.org/10.1002/ijc.20646>
- Hung, K., Hayashi, R., Lafond-Walker, A., Lowenstein, C., Pardoll, D., & Levitsky, H. (1998). The central role of CD4(+) T cells in the antitumor immune response. *J Exp Med*, *188*(12), 2357-2368.
- IARC. (2007). Human papillomaviruses. *IARC Monogr Eval Carcinog Risks Hum*, *90*, 1-636.
- Ibrahim, A. E. K., Arends, M. J., Silva, A. L., Wyllie, A. H., Greger, L., Ito, Y., Vowler, S. L., Huang, T. H. M., Tavaré, S., Murrell, A., & Brenton, J. D. (2011). Sequential DNA methylation changes are associated with DNMT3b overexpression in colorectal neoplastic progression. *Gut*, *60*(4), 499. <https://doi.org/10.1136/gut.2010.223602>

- Institute of Medicine Standing Committee on the Scientific Evaluation of Dietary Reference. (1998). The National Academies Collection: Reports funded by National Institutes of Health. In *Dietary Reference Intakes for Thiamin, Riboflavin, Niacin, Vitamin B(6), Folate, Vitamin B(12), Pantothenic Acid, Biotin, and Choline*. National Academies Press (US). National Academy of Sciences. <https://doi.org/10.17226/6015>
- International Collaboration of Epidemiological Studies of Cervical Cancer. (2006). Cervical carcinoma and reproductive factors: collaborative reanalysis of individual data on 16,563 women with cervical carcinoma and 33,542 women without cervical carcinoma from 25 epidemiological studies. *Int J Cancer*, *119*(5), 1108-1124. <https://doi.org/10.1002/ijc.21953>
- International Collaboration of Epidemiological Studies of Cervical Cancer. (2007). Cervical cancer and hormonal contraceptives: collaborative reanalysis of individual data for 16 573 women with cervical cancer and 35 509 women without cervical cancer from 24 epidemiological studies. *The Lancet*, *370*(9599), 1609-1621. [https://doi.org/https://doi.org/10.1016/S0140-6736\(07\)61684-5](https://doi.org/https://doi.org/10.1016/S0140-6736(07)61684-5)
- Iso, H., & Kubota, Y. (2007). Nutrition and disease in the Japan Collaborative Cohort Study for Evaluation of Cancer (JACC). *Asian Pac J Cancer Prev*, *8*, 35-80.
- Jancar, N., Rakar, S., Poljak, M., Fujs, K., Kocjan, B. J., & Vrtacnik-Bokal, E. (2006). Efficiency of three surgical procedures in eliminating high-risk human papillomavirus infection in women with precancerous cervical lesions. *Eur J Gynaecol Oncol*, *27*(3), 239-242.
- Janke, R., Dodson, A. E., & Rine, J. (2015). Metabolism and epigenetics. *Annu Rev Cell Dev Biol*, *31*, 473-496. <https://doi.org/10.1146/annurev-cellbio-100814-125544>
- Jemal, A., Bray, F., Center, M. M., Ferlay, J., Ward, E., & Forman, D. (2011). Global cancer statistics. *CA Cancer J Clin*, *61*(2), 69-90. <https://doi.org/10.3322/caac.20107>
- Jensen, K. E., Schmiedel, S., Norrild, B., Frederiksen, K., Iftner, T., & Kjaer, S. K. (2013). Parity as a cofactor for high-grade cervical disease among women with persistent human papillomavirus infection: a 13-year follow-up. *Br J Cancer*, *108*(1), 234-239. <https://doi.org/10.1038/bjc.2012.513>
- Jha, A. K., Nikbakht, M., Parashar, G., Shrivastava, A., Capalash, N., & Kaur, J. (2010). Reversal of hypermethylation and reactivation of the RAR β 2 gene by natural compounds in cervical cancer cell lines. *Folia Biol (Praha)*, *56*(5), 195-200.
- Jha, A. K., Sharma, V., Nikbakht, M., Jain, V., Sehgal, A., Capalash, N., & Kaur, J. (2016). A comparative analysis of methylation status of tumor suppressor genes in paired biopsy and serum samples from cervical cancer patients among north indian population. *Genetika*, *52*(2), 255-259.

- Johanning, G. L., Heimburger, D. C., & Piyathilake, C. J. (2002). DNA methylation and diet in cancer. *J Nutr*, *132*(12), 3814s-3818s. <https://doi.org/10.1093/jn/132.12.3814S>
- Jones, P. A., & Baylin, S. B. (2007). The epigenomics of cancer. *Cell*, *128*(4), 683-692. <https://doi.org/10.1016/j.cell.2007.01.029>
- Jouanguy, E., Zhang, S. Y., Chapgier, A., Sancho-Shimizu, V., Puel, A., Picard, C., Boisson-Dupuis, S., Abel, L., & Casanova, J. L. (2007). Human primary immunodeficiencies of type I interferons. *Biochimie*, *89*(6-7), 878-883. <https://doi.org/10.1016/j.biochi.2007.04.016>
- Joura, E. A., Giuliano, A. R., Iversen, O. E., Bouchard, C., Mao, C., Mehlsen, J., Moreira, E. D., Jr., Ngan, Y., Petersen, L. K., Lazcano-Ponce, E., Pitisuttithum, P., Restrepo, J. A., Stuart, G., Woelber, L., Yang, Y. C., Cuzick, J., Garland, S. M., Huh, W., Kjaer, S. K., Bautista, O. M., Chan, I. S., Chen, J., Gesser, R., Moeller, E., Ritter, M., Vuocolo, S., & Luxembourg, A. (2015). A 9-valent HPV vaccine against infection and intraepithelial neoplasia in women. *N Engl J Med*, *372*(8), 711-723. <https://doi.org/10.1056/NEJMoa1405044>
- Jung, M., & Pfeifer, G. P. (2015). Aging and DNA methylation. *BMC Biol*, *13*, 7. <https://doi.org/10.1186/s12915-015-0118-4>
- Jürgens, B., Schmitz-Dräger, B. J., & Schulz, W. A. (1996). Hypomethylation of L1 LINE sequences prevailing in human urothelial carcinoma. *Cancer Res*, *56*(24), 5698-5703.
- Kalvakolanu, D. V. (2000). Interferons and cell growth control. *Histol Histopathol*, *15*(2), 523-537. <https://doi.org/10.14670/hh-15.523>
- Kambara, H., Niazi, F., Kostadinova, L., Moonka, D. K., Siegel, C. T., Post, A. B., Carnero, E., Barriocanal, M., Fortes, P., Anthony, D. D., & Valadkhan, S. (2014). Negative regulation of the interferon response by an interferon-induced long non-coding RNA. *Nucleic Acids Res*, *42*(16), 10668-10680. <https://doi.org/10.1093/nar/gku713>
- Kanodia, S., Fahey, L. M., & Kast, W. M. (2007). Mechanisms used by human papillomaviruses to escape the host immune response. *Curr Cancer Drug Targets*, *7*(1), 79-89. <https://doi.org/10.2174/156800907780006869>
- Kanwal, R., & Gupta, S. (2012). Epigenetic modifications in cancer. *Clin Genet*, *81*(4), 303-311. <https://doi.org/10.1111/j.1399-0004.2011.01809.x>
- Kate, M., Hofland, L. J., van Koetsveld, P. M., Jeekel, J., & van Eijck, C. H. (2006). Pro-inflammatory cytokines affect pancreatic carcinoma cell. Endothelial cell interactions. *Jop*, *7*(5), 454-464.

- Kaur, G., & Dufour, J. M. (2012). Cell lines: Valuable tools or useless artifacts. *Spermatogenesis*, 2(1), 1-5. <https://doi.org/10.4161/spmg.19885>
- Kelemen, L. E. (2006). The role of folate receptor alpha in cancer development, progression and treatment: cause, consequence or innocent bystander? *Int J Cancer*, 119(2), 243-250. <https://doi.org/10.1002/ijc.21712>
- Keyes, M. K., Jang, H., Mason, J. B., Liu, Z., Crott, J. W., Smith, D. E., Friso, S., & Choi, S. W. (2007). Older age and dietary folate are determinants of genomic and p16-specific DNA methylation in mouse colon. *J Nutr*, 137(7), 1713-1717. <https://doi.org/10.1093/jn/137.7.1713>
- Khodarev, N. N., Roach, P., Pitroda, S. P., Golden, D. W., Bhayani, M., Shao, M. Y., Darga, T. E., Beveridge, M. G., Sood, R. F., Sutton, H. G., Beckett, M. A., Mauceri, H. J., Posner, M. C., & Weichselbaum, R. R. (2009). STAT1 pathway mediates amplification of metastatic potential and resistance to therapy. *PLoS One*, 4(6), e5821. <https://doi.org/10.1371/journal.pone.0005821>
- Ki, K. D., Lee, S. K., Tong, S. Y., Lee, J. M., Song, D. H., & Chi, S. G. (2008). Role of 5'-CpG island hypermethylation of the FHIT gene in cervical carcinoma. *J Gynecol Oncol*, 19(2), 117-122. <https://doi.org/10.3802/jgo.2008.19.2.117>
- Kim, J. H., Choi, Y. D., Lee, J. S., Lee, J. H., Nam, J. H., & Choi, C. (2010). Assessment of DNA methylation for the detection of cervical neoplasia in liquid-based cytology specimens. *Gynecol Oncol*, 116(1), 99-104. <https://doi.org/10.1016/j.ygyno.2009.09.032>
- Kim, K. Y., Blatt, L., & Taylor, M. W. (2000). The effects of interferon on the expression of human papillomavirus oncogenes. *J Gen Virol*, 81(Pt 3), 695-700. <https://doi.org/10.1099/0022-1317-81-3-695>
- Kim, Y. I. (2005). Nutritional epigenetics: impact of folate deficiency on DNA methylation and colon cancer susceptibility. *J Nutr*, 135(11), 2703-2709. <http://www.ncbi.nlm.nih.gov/pubmed/16251634>
- Kim, Y. I., Baik, H. W., Fawaz, K., Knox, T., Lee, Y. M., Norton, R., Libby, E., & Mason, J. B. (2001). Effects of folate supplementation on two provisional molecular markers of colon cancer: a prospective, randomized trial. *Am J Gastroenterol*, 96(1), 184-195. <https://doi.org/10.1111/j.1572-0241.2001.03474.x>
- Kim, Y. I., Giuliano, A., Hatch, K. D., Schneider, A., Nour, M. A., Dallal, G. E., Selhub, J., & Mason, J. B. (1994). Global DNA hypomethylation increases progressively in cervical dysplasia and carcinoma. *Cancer*, 74(3), 893-899. [https://doi.org/10.1002/1097-0142\(19940801\)74:3<893::aid-cnrcr2820740316>3.0.co;2-b](https://doi.org/10.1002/1097-0142(19940801)74:3<893::aid-cnrcr2820740316>3.0.co;2-b)

- Kim, Y. I., Pogribny, I. P., Basnakian, A. G., Miller, J. W., Selhub, J., James, S. J., & Mason, J. B. (1997). Folate deficiency in rats induces DNA strand breaks and hypomethylation within the p53 tumor suppressor gene. *Am J Clin Nutr*, 65(1), 46-52. <https://doi.org/10.1093/ajcn/65.1.46>
- Kirkwood, J. (2002). Cancer immunotherapy: the interferon-alpha experience. *Semin Oncol*, 29(3 Suppl 7), 18-26.
- Kitkumthorn, N., Yanatatsanajit, P., Kiatpongsan, S., Phokaew, C., Triratanachat, S., Trivijitsilp, P., Termrungruanglert, W., Tresukosol, D., Niruthisard, S., & Mutirangura, A. (2006). Cyclin A1 promoter hypermethylation in human papillomavirus-associated cervical cancer. *BMC Cancer*, 6, 55. <https://doi.org/10.1186/1471-2407-6-55>
- Kjellberg, L., Hallmans, G., Åhren, A. M., Johansson, R., Bergman, F., Wadell, G., Ångström, T., & Dillner, J. (2000). Smoking, diet, pregnancy and oral contraceptive use as risk factors for cervical intra-epithelial neoplasia in relation to human papillomavirus infection. *British Journal of Cancer*, 82(7), 1332-1338. <https://doi.org/10.1054/bjoc.1999.1100>
- Knoff, J., Yang, B., Hung, C. F., & Wu, T. C. (2014). Cervical cancer: development of targeted therapies beyond molecular pathogenesis. *Current obstetrics and gynecology reports*, 3(1), 18-32. <https://doi.org/10.1007/s13669-013-0068-1>
- Kobayashi, Y., Absher, D. M., Gulzar, Z. G., Young, S. R., McKenney, J. K., Peehl, D. M., Brooks, J. D., Myers, R. M., & Sherlock, G. (2011). DNA methylation profiling reveals novel biomarkers and important roles for DNA methyltransferases in prostate cancer. *Genome Res*, 21(7), 1017-1027. <https://doi.org/10.1101/gr.119487.110>
- Kohler, L. N., Garcia, D. O., Harris, R. B., Oren, E., Roe, D. J., & Jacobs, E. T. (2016). Adherence to diet and physical activity cancer prevention guidelines and cancer outcomes: a systematic review. *Cancer Epidemiol Biomarkers Prev*, 25(7), 1018-1028. <https://doi.org/10.1158/1055-9965.Epi-16-0121>
- Komninou, D., Leutzinger, Y., Reddy, B. S., & Richie, J. P., Jr. (2006). Methionine restriction inhibits colon carcinogenesis. *Nutr Cancer*, 54(2), 202-208. https://doi.org/10.1207/s15327914nc5402_6
- Korbie, D. J., & Mattick, J. S. (2008). Touchdown PCR for increased specificity and sensitivity in PCR amplification. *Nature protocols*, 3(9), 1452-1456. <https://doi.org/10.1038/nprot.2008.133>
- Koromilas, A. E., & Sexl, V. (2013). The tumor suppressor function of STAT1 in breast cancer. *Jakstat*, 2(2), e23353. <https://doi.org/10.4161/jkst.23353>

- Kotsopoulos, J., Sohn, K. J., & Kim, Y. I. (2008). Postweaning dietary folate deficiency provided through childhood to puberty permanently increases genomic DNA methylation in adult rat liver. *J Nutr*, *138*(4), 703-709. <https://doi.org/10.1093/jn/138.4.703>
- Kreimer, A. R., Guido, R. S., Solomon, D., Schiffman, M., Wacholder, S., Jeronimo, J., Wheeler, C. M., & Castle, P. E. (2006). Human papillomavirus testing following loop electrosurgical excision procedure identifies women at risk for posttreatment cervical intraepithelial neoplasia grade 2 or 3 disease. *Cancer Epidemiol Biomarkers Prev*, *15*(5), 908-914. <https://doi.org/10.1158/1055-9965.Epi-05-0845>
- Kremer, W. W., Van Zummeren, M., Novianti, P. W., Richter, K. L., Verlaat, W., Snijders, P. J., Heideman, D. A., Steenbergen, R. D., Dreyer, G., & Meijer, C. J. (2018). Detection of hypermethylated genes as markers for cervical screening in women living with HIV. *J Int AIDS Soc*, *21*(8), e25165. <https://doi.org/10.1002/jia2.25165>
- Kristiansen, H., Gad, H. H., Eskildsen-Larsen, S., Despres, P., & Hartmann, R. (2011). The oligoadenylate synthetase family: an ancient protein family with multiple antiviral activities. *J Interferon Cytokine Res*, *31*(1), 41-47. <https://doi.org/10.1089/jir.2010.0107>
- Ku, J. L., Jeon, Y. K., & Park, J. G. (2011). Methylation-specific PCR. *Methods Mol Biol*, *791*, 23-32. https://doi.org/10.1007/978-1-61779-316-5_3
- Kuang, Y., Liu, S., Wang, C., & Hu, X. (2017). Low expression of 2'-5' oligoadenylate synthetase 1 predicted poor prognosis in colorectal cancer. *Int J Clin Exp Pathol*, *10*(3):3353-3360.
- Kulis, M., Queirós, A. C., Beekman, R., & Martín-Subero, J. I. (2013). Intragenic DNA methylation in transcriptional regulation, normal differentiation and cancer. *Biochimica et biophysica acta*, *1829*(11), 1161-1174. <https://doi.org/10.1016/j.bbagr.2013.08.001>
- Kulkarni, A., Dangat, K., Kale, A., Sable, P., Chavan-Gautam, P., & Joshi, S. (2011). Effects of altered maternal folic acid, vitamin B12 and docosahexaenoic acid on placental global DNA methylation patterns in Wistar rats. *PLoS One*, *6*(3), e17706. <https://doi.org/10.1371/journal.pone.0017706>
- Kurokawa, C., Iankov, I. D., & Galanis, E. (2019). A key anti-viral protein, RSAD2/VIPERIN, restricts the release of measles virus from infected cells. *Virus Res*, *263*, 145-150. <https://doi.org/10.1016/j.virusres.2019.01.014>
- Kwist, K., Bridges, W. C., & Burg, K. J. L. (2016). The effect of cell passage number on osteogenic and adipogenic characteristics of D1 cells. *Cytotechnology*, *68*(4), 1661-1667. <https://doi.org/10.1007/s10616-015-9883-8>

- Laird, P. W., Zhou, W., & Shen, H. (2016). Comprehensive characterization, annotation and innovative use of Infinium DNA methylation BeadChip probes. *Nucleic Acids Research*, *45*(4), e22-e22. <https://doi.org/10.1093/nar/gkw967>
- Laljee, R. P., Muddaiah, S., Salagundi, B., Cariappa, P. M., Indra, A. S., Sanjay, V., & Ramanathan, A. (2013). Interferon stimulated gene-ISG15 is a potential diagnostic biomarker in oral squamous cell carcinomas. *Asian Pac J Cancer Prev*, *14*(2), 1147-1150.
- Landvik, N. E., Hart, K., Skaug, V., Stangeland, L. B., Haugen, A., & Zienolddiny, S. (2009). A specific interleukin-1B haplotype correlates with high levels of IL1B mRNA in the lung and increased risk of non-small cell lung cancer. *Carcinogenesis*, *30*(7), 1186-1192. <https://doi.org/10.1093/carcin/bgp122>
- Łaniewski, P., İlhan, Z. E., & Herbst-Kralovetz, M. M. (2020). The microbiome and gynaecological cancer development, prevention and therapy. *Nat Rev Urol*, *17*(4), 232-250. <https://doi.org/10.1038/s41585-020-0286-z>
- Laskin, D. L., & Pendino, K. J. (1995). Macrophages and inflammatory mediators in tissue injury. *Annu Rev Pharmacol Toxicol*, *35*, 655-677. <https://doi.org/10.1146/annurev.pa.35.040195.003255>
- Lee, J. E., Jacques, P. F., Dougherty, L., Selhub, J., Giovannucci, E., Zeisel, S. H., & Cho, E. (2010). Are dietary choline and betaine intakes determinants of total homocysteine concentration? *Am J Clin Nutr*, *91*(5), 1303-1310. <https://doi.org/10.3945/ajcn.2009.28456>
- Leu, Y. W., Rahmatpanah, F., Shi, H., Wei, S. H., Liu, J. C., Yan, P. S., & Huang, T. H. (2003). Double RNA interference of DNMT3b and DNMT1 enhances DNA demethylation and gene reactivation. *Cancer Res*, *63*(19), 6110-6115.
- Levy, D. E., & Gilliland, D. G. (2000). Divergent roles of STAT1 and STAT5 in malignancy as revealed by gene disruptions in mice. *Oncogene*, *19*(21), 2505-2510. <https://doi.org/10.1038/sj.onc.1203480>
- Lewis, A. M., Varghese, S., Xu, H., & Alexander, H. R. (2006). Interleukin-1 and cancer progression: the emerging role of interleukin-1 receptor antagonist as a novel therapeutic agent in cancer treatment. *J Transl Med*, *4*, 48. <https://doi.org/10.1186/1479-5876-4-48>
- Li, C., Wang, J., Zhang, H., Zhu, M., Chen, F., Hu, Y., Liu, H., & Zhu, H. (2014). Interferon-stimulated gene 15 (ISG15) is a trigger for tumorigenesis and metastasis of hepatocellular carcinoma. *Oncotarget*, *5*(18), 8429-8441. <https://doi.org/10.18632/oncotarget.2316>

- Li, L. C., & Dahiya, R. (2002). MethPrimer: designing primers for methylation PCRs. *Bioinformatics*, *18*(11), 1427-1431.
- Li, N., Franceschi, S., Howell-Jones, R., Snijders, P. J., & Clifford, G. M. (2011). Human papillomavirus type distribution in 30,848 invasive cervical cancers worldwide: variation by geographical region, histological type and year of publication. *Int J Cancer*, *128*(4), 927-935. <https://doi.org/10.1002/ijc.25396>
- Li, W., Jiang, M., Xiao, Y., Zhang, X., Cui, S., & Huang, G. (2015). Folic acid inhibits tau phosphorylation through regulation of PP2A methylation in SH-SY5Y cells. *J Nutr Health Aging*, *19*(2), 123-129. <https://doi.org/10.1007/s12603-014-0514-4>
- Liang, G., Chan, M. F., Tomigahara, Y., Tsai, Y. C., Gonzales, F. A., Li, E., Laird, P. W., & Jones, P. A. (2002). Cooperativity between DNA methyltransferases in the maintenance methylation of repetitive elements. *Mol Cell Biol*, *22*(2), 480-491. <https://doi.org/10.1128/mcb.22.2.480-491.2002>
- Liang, K. C., Suzuki, Y., Kumagai, Y., & Nakai, K. (2014). Analysis of changes in transcription start site distribution by a classification approach. *Gene*, *537*(1), 29-40. <https://doi.org/10.1016/j.gene.2013.12.038>
- Lin, D. W., Chung, B. P., & Kaiser, P. (2014). S-adenosylmethionine limitation induces p38 mitogen-activated protein kinase and triggers cell cycle arrest in G1. *J Cell Sci*, *127*(Pt 1), 50-59. <https://doi.org/10.1242/jcs.127811>
- Lin, W. W., & Karin, M. (2007). A cytokine-mediated link between innate immunity, inflammation, and cancer. *J Clin Invest*, *117*(5), 1175-1183. <https://doi.org/10.1172/jci31537>
- Liteplo, R. G. (1988). DNA (cytosine) methylation in murine and human tumor cell lines treated with S-adenosylhomocysteine hydrolase inhibitors. *Cancer Lett*, *39*(3), 319-327. [https://doi.org/10.1016/0304-3835\(88\)90076-6](https://doi.org/10.1016/0304-3835(88)90076-6)
- Liu, J. J., & Ward, R. L. (2010). Folate and one-carbon metabolism and its impact on aberrant DNA methylation in cancer. *Adv Genet*, *71*, 79-121. <https://doi.org/10.1016/b978-0-12-380864-6.00004-3>
- Liu, P., Iden, M., Fye, S., Huang, Y. W., Hopp, E., Chu, C., Lu, Y., & Rader, J. S. (2017). Targeted, deep sequencing reveals full methylation profiles of multiple hpv types and potential biomarkers for cervical cancer progression. *Cancer Epidemiol Biomarkers Prev*, *26*(4), 642-650. <https://doi.org/10.1158/1055-9965.Epi-16-0368>
- Liu, S. S., Leung, R. C., Chan, K. Y., Chiu, P. M., Cheung, A. N., Tam, K. F., Ng, T. Y., Wong, L. C., & Ngan, H. Y. (2004). p73 expression is associated with the cellular radiosensitivity in cervical cancer after radiotherapy. *Clin Cancer Res*, *10*(10), 3309-3316. <https://doi.org/10.1158/1078-0432.Ccr-03-0119>

- Livak, K. J., & Schmittgen, T. D. (2001). Analysis of relative gene expression data using real-time quantitative PCR and the 2(-Delta Delta C(T)) Method. *Methods*, 25. <https://doi.org/10.1006/meth.2001.1262>
- Lorincz, M. C., Schübeler, D., Hutchinson, S. R., Dickerson, D. R., & Groudine, M. (2002). DNA methylation density influences the stability of an epigenetic imprint and DNMT3a/b-independent de novo methylation. *Mol Cell Biol*, 22(21), 7572-7580. <https://doi.org/10.1128/mcb.22.21.7572-7580.2002>
- Lu, M. S., Fang, Y. J., Pan, Z. Z., Zhong, X., Zheng, M. C., Chen, Y. M., & Zhang, C. X. (2015). Choline and betaine intake and colorectal cancer risk in Chinese population: a case-control study. *PLoS One*, 10(3), e0118661. <https://doi.org/10.1371/journal.pone.0118661>
- Lubecka-Pietruszewska, K., Kaufman-Szymczyk, A., Stefanska, B., & Fabianowska-Majewska, K. (2013). Folic acid enforces DNA methylation-mediated transcriptional silencing of PTEN, APC and RARbeta2 tumour suppressor genes in breast cancer. *Biochem Biophys Res Commun*, 430(2), 623-628. <https://doi.org/10.1016/j.bbrc.2012.11.103>
- Lucock, M. (2000). Folic acid: nutritional biochemistry, molecular biology, and role in disease processes. *Mol Genet Metab*, 71(1-2), 121-138. <https://doi.org/10.1006/mgme.2000.3027>
- Lukac, A., Sulovic, N., Smiljic, S., Ilic, A. N., & Saban, O. (2018). The prevalence of the most important risk factors associated with cervical cancer. *Materia socio-medica*, 30(2), 131-135. <https://doi.org/10.5455/msm.2018.30.131-135>
- Ly, A., Lee, H., Chen, J., Sie, K. K., Renlund, R., Medline, A., Sohn, K. J., Croxford, R., Thompson, L. U., & Kim, Y. I. (2011). Effect of maternal and postweaning folic acid supplementation on mammary tumor risk in the offspring. *Cancer Res*, 71(3), 988-997. <https://doi.org/10.1158/0008-5472.can-10-2379>
- Ma, X., Liu, J., Wang, H., Jiang, Y., Wan, Y., Xia, Y., & Cheng, W. (2020). Identification of crucial aberrantly methylated and differentially expressed genes related to cervical cancer using an integrated bioinformatics analysis. *Biosci Rep*, 40(5). <https://doi.org/10.1042/bsr20194365>
- Magkou, C., Giannopoulou, I., Theohari, I., Fytou, A., Rafailidis, P., Nomikos, A., Papadimitriou, C., & Nakopoulou, L. (2012). Prognostic significance of phosphorylated STAT-1 expression in premenopausal and postmenopausal patients with invasive breast cancer. *Histopathology*, 60(7), 1125-1132. <https://doi.org/10.1111/j.1365-2559.2011.04143.x>

- Mahmood, N., Cheishvili, D., Arakelian, A., Tanvir, I., Khan, H. A., Pepin, A. S., Szyf, M., & Rabbani, S. A. (2018). Methyl donor S-adenosylmethionine (SAM) supplementation attenuates breast cancer growth, invasion, and metastasis in vivo; therapeutic and chemopreventive applications. *Oncotarget*, *9*(4), 5169-5183. <https://doi.org/10.18632/oncotarget.23704>
- Mahmoud, A. M., & Ali, M. M. (2019). Methyl donor micronutrients that modify DNA methylation and cancer outcome. *Nutrients*, *11*(3). <https://doi.org/10.3390/nu11030608>
- Maia, C. J., Rocha, S. M., Socorro, S., Schmitt, F., & Santos, C. R. (2016). Oligoadenylate synthetase 1 (OAS1) expression in human breast and prostate cancer cases, and its regulation by sex steroid hormones. *Advances in Modern Oncology Research*, *2*(2016), 2.
- Makino, E., Fukuyama, T., Watanabe, Y., Tajiki-Nishino, R., Tajima, H., Ohnuma-Koyama, A., Takahashi, N., Ohtsuka, R., & Okazaki, Y. (2019). Subacute oral administration of folic acid elicits anti-inflammatory response in a mouse model of allergic dermatitis. *J Nutr Biochem*, *67*, 14-19. <https://doi.org/10.1016/j.jnutbio.2019.01.009>
- Massad, L. S., Einstein, M. H., Huh, W. K., Katki, H. A., Kinney, W. K., Schiffman, M., Solomon, D., Wentzensen, N., & Lawson, H. W. (2013). 2012 updated consensus guidelines for the management of abnormal cervical cancer screening tests and cancer precursors. *Obstet Gynecol*, *121*(4), 829-846. <https://doi.org/10.1097/AOG.0b013e3182883a34>
- Mayadev, J., Lim, J., Durbin-Johnson, B., Valicenti, R., & Alvarez, E. (2018). Smoking decreases survival in locally advanced cervical cancer treated with radiation. *Am J Clin Oncol*, *41*(3), 295-301. <https://doi.org/10.1097/coc.0000000000000268>
- McBride, A. A., & Warburton, A. (2017). The role of integration in oncogenic progression of HPV-associated cancers. *PLoS Pathog*, *13*(4), e1006211. <https://doi.org/10.1371/journal.ppat.1006211>
- McCormick, T. M., Canedo, N. H., Furtado, Y. L., Silveira, F. A., de Lima, R. J., Rosman, A. D., Almeida Filho, G. L., & Carvalho Mda, G. (2015). Association between human papillomavirus and Epstein - Barr virus DNA and gene promoter methylation of RB1 and CDH1 in the cervical lesions: a transversal study. *Diagn Pathol*, *10*, 59. <https://doi.org/10.1186/s13000-015-0283-3>
- McGlynn, A. P., Wasson, G. R., O'Reilly, S. L., McNulty, H., Downes, C. S., Chang, C. K., Hoey, L., Molloy, A. M., Ward, M., Strain, J. J., McKerr, G., Weir, D. G., & Scott, J. M. (2013). Low colonocyte folate is associated with uracil misincorporation and global DNA hypomethylation in human colorectum. *J Nutr*, *143*(1), 27-33. <https://doi.org/10.3945/jn.112.167148>

- McKay, J. A., Williams, E. A., & Mathers, J. C. (2011). Effect of maternal and post-weaning folate supply on gene-specific DNA methylation in the small intestine of weaning and adult *apc* and wild type mice. *Frontiers in genetics*, 2, 23. <https://doi.org/10.3389/fgene.2011.00023>
- Mehedint, M. G., Craciunescu, C. N., & Zeisel, S. H. (2010a). Maternal dietary choline deficiency alters angiogenesis in fetal mouse hippocampus. *Proc Natl Acad Sci USA*, 107(29), 12834-12839. <https://doi.org/10.1073/pnas.0914328107>
- Mehedint, M. G., Niculescu, M. D., Craciunescu, C. N., & Zeisel, S. H. (2010b). Choline deficiency alters global histone methylation and epigenetic marking at the *Re1* site of the calbindin 1 gene. *Faseb j*, 24(1), 184-195. <https://doi.org/10.1096/fj.09-140145>
- Mehta, S. R., Zhang, X. Q., Badaro, R., Spina, C., Day, J., Chang, K. P., & Schooley, R. T. (2010). Flow cytometric screening for anti-leishmanials in a human macrophage cell line. *Exp Parasitol*, 126(4), 617-620. <https://doi.org/10.1016/j.exppara.2010.06.007>
- Mekky, M. A., Salama, R. H., Abdel-Aal, M. F., Ghaliony, M. A., & Zaky, S. (2018). Studying the frequency of aberrant DNA methylation of APC, P14, and E-cadherin genes in HCV-related hepatocarcinogenesis. *Cancer Biomark*, 22(3), 503-509. <https://doi.org/10.3233/cbm-171156>
- Melse-Boonstra, A., Holm, P. I., Ueland, P. M., Olthof, M., Clarke, R., & Verhoef, P. (2005). Betaine concentration as a determinant of fasting total homocysteine concentrations and the effect of folic acid supplementation on betaine concentrations. *Am J Clin Nutr*, 81(6), 1378-1382. <https://doi.org/10.1093/ajcn/81.6.1378>
- Miousse, I. R., Pathak, R., Garg, S., Skinner, C. M., Melnyk, S., Pavliv, O., Hendrickson, H., Landes, R. D., Lumen, A., Tackett, A. J., Deutz, N. E. P., Hauer-Jensen, M., & Koturbash, I. (2017). Short-term dietary methionine supplementation affects one-carbon metabolism and DNA methylation in the mouse gut and leads to altered microbiome profiles, barrier function, gene expression and histomorphology. *Genes Nutr*, 12, 22. <https://doi.org/10.1186/s12263-017-0576-0>
- Mirabello, L., Yeager, M., Cullen, M., Boland, J. F., Chen, Z., Wentzensen, N., Zhang, X., Yu, K., Yang, Q., Mitchell, J., Roberson, D., Bass, S., Xiao, Y., Burdett, L., Raine-Bennett, T., Lorey, T., Castle, P. E., Burk, R. D., & Schiffman, M. (2016). HPV16 sublineage associations with histology-specific cancer risk using hpv whole-genome sequences in 3200 women. *J Natl Cancer Inst*, 108(9). <https://doi.org/10.1093/jnci/djw100>
- Miron, M., Woody, O. Z., Marcil, A., Murie, C., Sladek, R., & Nadon, R. (2006). A methodology for global validation of microarray experiments. *BMC Bioinformatics*, 7(1), 333. <https://doi.org/10.1186/1471-2105-7-333>

- Mizuno, S., Chijiwa, T., Okamura, T., Akashi, K., Fukumaki, Y., Niho, Y., & Sasaki, H. (2001). Expression of DNA methyltransferases DNMT1, 3A, and 3B in normal hematopoiesis and in acute and chronic myelogenous leukemia. *Blood*, *97*(5), 1172-1179. <https://doi.org/10.1182/blood.v97.5.1172>
- Molloy, A. M., Daly, S., Mills, J. L., Kirke, P. N., Whitehead, A. S., Ramsbottom, D., Conley, M. R., Weir, D. G., & Scott, J. M. (1997). Thermolabile variant of 5,10-methylenetetrahydrofolate reductase associated with low red-cell folates: implications for folate intake recommendations. *Lancet*, *349*(9065), 1591-1593. [https://doi.org/10.1016/s0140-6736\(96\)12049-3](https://doi.org/10.1016/s0140-6736(96)12049-3)
- Moore, L. D., Le, T., & Fan, G. (2013). DNA methylation and its basic function. *Neuropsychopharmacology*, *38*(1), 23-38. <https://doi.org/10.1038/npp.2012.112>
- Moore, L. E., Pfeiffer, R. M., Poscablo, C., Real, F. X., Kogevinas, M., Silverman, D., García-Closas, R., Chanock, S., Tardón, A., Serra, C., Carrato, A., Dosemeci, M., García-Closas, M., Esteller, M., Fraga, M., Rothman, N., & Malats, N. (2008). Genomic DNA hypomethylation as a biomarker for bladder cancer susceptibility in the Spanish Bladder Cancer Study: a case-control study. *Lancet Oncol*, *9*(4), 359-366. [https://doi.org/10.1016/s1470-2045\(08\)70038-x](https://doi.org/10.1016/s1470-2045(08)70038-x)
- Morey, J. S., Ryan, J. C., & Van Dolah, F. M. (2006). Microarray validation: factors influencing correlation between oligonucleotide microarrays and real-time PCR. *Biological procedures online*, *8*, 175-193. <https://doi.org/10.1251/bpo126>
- Morris, T. J., & Beck, S. (2015). Analysis pipelines and packages for Infinium HumanMethylation450 BeadChip (450k) data. *Methods (San Diego, Calif.)*, *72*, 3-8. <https://doi.org/10.1016/j.ymeth.2014.08.011>
- Moschonas, A., Ioannou, M., & Eliopoulos, A. G. (2012). CD40 stimulates a "feed-forward" NF-kappaB-driven molecular pathway that regulates IFN-beta expression in carcinoma cells. *J Immunol*, *188*(11), 5521-5527. <https://doi.org/10.4049/jimmunol.1200133>
- Mota, F., Rayment, N., Chong, S., Singer, A., & Chain, B. (1999). The antigen-presenting environment in normal and human papillomavirus (HPV)-related premalignant cervical epithelium. *Clin Exp Immunol*, *116*(1), 33-40.
- Muller, L., Aigner, P., & Stoiber, D. (2017). Type I interferons and natural killer cell regulation in cancer. *Front Immunol*, *8*, 304. <https://doi.org/10.3389/fimmu.2017.00304>
- Muñoz, N., Castellsagué, X., Berrington de González, A., & Gissmann, L. (2006). Chapter 1: HPV in the etiology of human cancer. *Vaccine*, *24*(3), S3/1-10. <https://doi.org/10.1016/j.vaccine.2006.05.115>

- Muñoz, N., Franceschi, S., Bosetti, C., Moreno, V., Herrero, R., Smith, J. S., Shah, K. V., Meijer, C. J., & Bosch, F. X. (2002). Role of parity and human papillomavirus in cervical cancer: the IARC multicentric case-control study. *Lancet*, *359*(9312), 1093-1101. [https://doi.org/10.1016/s0140-6736\(02\)08151-5](https://doi.org/10.1016/s0140-6736(02)08151-5)
- Muñoz, N., Hernandez-Suarez, G., Méndez, F., Molano, M., Posso, H., Moreno, V., Murillo, R., Ronderos, M., Meijer, C., & Muñoz, Á. (2009). Persistence of HPV infection and risk of high-grade cervical intraepithelial neoplasia in a cohort of Colombian women. *British Journal of Cancer*, *100*(7), 1184-1190. <https://doi.org/10.1038/sj.bjc.6604972>
- Naeem, H., Wong, N. C., Chatterton, Z., Hong, M. K., Pedersen, J. S., Corcoran, N. M., Hovens, C. M., & Macintyre, G. (2014). Reducing the risk of false discovery enabling identification of biologically significant genome-wide methylation status using the HumanMethylation450 array. *BMC Genomics*, *15*, 51. <https://doi.org/10.1186/1471-2164-15-51>
- Nagai, Y., Maehama, T., Asato, T., & Kanazawa, K. (2001). Detection of human papillomavirus DNA in primary and metastatic lesions of carcinoma of the cervix in women from Okinawa, Japan. *Am J Clin Oncol*, *24*(2), 160-166. <https://doi.org/10.1097/00000421-200104000-00013>
- Nakano, E., Taiwo, F. A., Nugent, D., Griffiths, H. R., Aldred, S., Paisi, M., Kwok, M., Bhatt, P., Hill, M. H., Moat, S., & Powers, H. J. (2005). Downstream effects on human low density lipoprotein of homocysteine exported from endothelial cells in an in vitro system. *J Lipid Res*, *46*(3), 484-493. <https://doi.org/10.1194/jlr.M400339-JLR200>
- Narayan, A., Ji, W., Zhang, X. Y., Marrogi, A., Graff, J. R., Baylin, S. B., & Ehrlich, M. (1998). Hypomethylation of pericentromeric DNA in breast adenocarcinomas. *Int J Cancer*, *77*(6), 833-838. [https://doi.org/10.1002/\(sici\)1097-0215\(19980911\)77:6<833::aid-ijc6>3.0.co;2-v](https://doi.org/10.1002/(sici)1097-0215(19980911)77:6<833::aid-ijc6>3.0.co;2-v)
- Narayanan, S., McConnell, J., Little, J., Sharp, L., Piyathilake, C. J., Powers, H., Basten, G., & Duthie, S. J. (2004). Associations between two common variants C677T and A1298C in the methylenetetrahydrofolate reductase gene and measures of folate metabolism and DNA stability (strand breaks, misincorporated uracil, and DNA methylation status) in human lymphocytes in vivo. *Cancer Epidemiol Biomarkers Prev*, *13*(9), 1436-1443. <http://www.ncbi.nlm.nih.gov/pubmed/15342443>
- Narisawa-Saito, M., & Kiyono, T. (2007). Basic mechanisms of high-risk human papillomavirus-induced carcinogenesis: roles of E6 and E7 proteins. *Cancer Sci*, *98*(10), 1505-1511. <https://doi.org/10.1111/j.1349-7006.2007.00546.x>
- Nasr, N., Maddocks, S., Turville, S. G., Harman, A. N., Woolger, N., Helbig, K. J., Wilkinson, J., Bye, C. R., Wright, T. K., Rambukwelle, D., Donaghy, H., Beard, M. R., & Cunningham, A. L. (2012). HIV-1 infection of human macrophages directly induces viperin which inhibits viral production. *Blood*, *120*(4), 778-788. <https://doi.org/10.1182/blood-2012-01-407395>

- NDNS. (2020). The National Diet and Nutrition Survey (NDNS) Report of Years 9 to 11 (2016/2017 to 2018/2019) of the Rolling Programme. P. H. England. <https://www.gov.uk/government/statistics/ndns-results-from-years-9-to-11-2016-to-2017-and-2018-to-2019>
- Niculescu, M. D., Craciunescu, C. N., & Zeisel, S. H. (2006). Dietary choline deficiency alters global and gene-specific DNA methylation in the developing hippocampus of mouse fetal brains. *Faseb j*, *20*(1), 43-49. <https://doi.org/10.1096/fj.05-4707com>
- Niculescu, M. D., & Zeisel, S. H. (2002). Diet, methyl donors and DNA methylation: interactions between dietary folate, methionine and choline. *J Nutr*, *132*(8), 2333S-2335S. <http://www.ncbi.nlm.nih.gov/pubmed/12163687>
- Nitter, M., Norgård, B., de Vogel, S., Eussen, S. J., Meyer, K., Ulvik, A., Ueland, P. M., Nygård, O., Vollset, S. E., Bjørge, T., Tjønneland, A., Hansen, L., Boutron-Ruault, M., Racine, A., Cottet, V., Kaaks, R., Kühn, T., Trichopoulou, A., Bamia, C., Naska, A., Grioni, S., Palli, D., Panico, S., Tumino, R., Vineis, P., Bueno-de-Mesquita, H. B., van Kranen, H., Peeters, P. H., Weiderpass, E., Dorronsoro, M., Jakszyn, P., Sánchez, M., Argüelles, M., Huerta, J. M., Barricarte, A., Johansson, M., Ljuslinder, I., Khaw, K., Wareham, N., Freisling, H., Duarte-Salles, T., Stepien, M., Gunter, M. J., & Riboli, E. (2014). Plasma methionine, choline, betaine, and dimethylglycine in relation to colorectal cancer risk in the European Prospective Investigation into Cancer and Nutrition (EPIC). *Ann Oncol*, *25*(8), 1609-1615. <https://doi.org/10.1093/annonc/mdu185>
- Nordlund, J., Backlin, C. L., Wahlberg, P., Busche, S., Berglund, E. C., Eloranta, M. L., Flaegstad, T., Forestier, E., Frost, B. M., Harila-Saari, A., Heyman, M., Jonsson, O. G., Larsson, R., Palle, J., Ronnblom, L., Schmiegelow, K., Sinnett, D., Soderhall, S., Pastinen, T., Gustafsson, M. G., Lonnerholm, G., & Syvanen, A. C. (2013). Genome-wide signatures of differential DNA methylation in pediatric acute lymphoblastic leukemia. *Genome Biol*, *14*(9), r105. <https://doi.org/10.1186/gb-2013-14-9-r105>
- Novellademunt, L., Antas, P., & Li, V. S. W. (2015). Targeting Wnt signaling in colorectal cancer. a review in the theme: cell signaling: proteins, pathways and mechanisms. *American Journal of Physiology-Cell Physiology*, *309*(8), C511-C521. <https://doi.org/10.1152/ajpcell.00117.2015>
- O'Reilly, S. L., McGlynn, A. P., McNulty, H., Reynolds, J., Wasson, G. R., Molloy, A. M., Strain, J. J., Weir, D. G., Ward, M., McKerr, G., Scott, J. M., & Downes, C. S. (2016). Folic acid supplementation in postpolypectomy patients in a randomized controlled trial increases tissue folate concentrations and reduces aberrant DNA biomarkers in colonic tissues adjacent to the former polyp site. *J Nutr*, *146*(5), 933-939. <https://doi.org/10.3945/jn.115.222547>

- Ogilvie, G. S., Krajden, M., van Niekerk, D., Smith, L. W., Cook, D., Ceballos, K., Lee, M., Gentile, L., Gondara, L., Elwood-Martin, R., Peacock, S., Stuart, G., Franco, E. L., & Coldman, A. J. (2017). HPV for cervical cancer screening (HPV FOCAL): complete round 1 results of a randomized trial comparing HPV-based primary screening to liquid-based cytology for cervical cancer. *Int J Cancer*, *140*(2), 440-448. <https://doi.org/10.1002/ijc.30454>
- Okunade, K. S. (2020). Human papillomavirus and cervical cancer. *J Obstet Gynaecol*, *40*(5), 602-608. <https://doi.org/10.1080/01443615.2019.1634030>
- Oliai Araghi, S., Kieft-de Jong, J. C., van Dijk, S. C., Swart, K. M. A., van Laarhoven, H. W., van Schoor, N. M., de Groot, L., Lemmens, V., Stricker, B. H., Uitterlinden, A. G., & van der Velde, N. (2019). Folic acid and vitamin B12 supplementation and the risk of cancer: long-term follow-up of the B vitamins for the Prevention Of Osteoporotic Fractures (B-PROOF) Trial. *Cancer Epidemiol Biomarkers Prev*, *28*(2), 275-282. <https://doi.org/10.1158/1055-9965.Epi-17-1198>
- Ono, A., Koshiyama, M., Nakagawa, M., Watanabe, Y., Ikuta, E., Seki, K., & Oowaki, M. (2020). The preventive effect of dietary antioxidants on cervical cancer development. *Medicina (Kaunas, Lithuania)*, *56*(11), 604. <https://doi.org/10.3390/medicina56110604>
- Otani, S., Fujii, T., Kukimoto, I., Yamamoto, N., Tsukamoto, T., Ichikawa, R., Nishio, E., & Iwata, A. (2019). Cytokine expression profiles in cervical mucus from patients with cervical cancer and its precursor lesions. *Cytokine*, *120*, 210-219. <https://doi.org/10.1016/j.cyto.2019.05.011>
- Otani, T., Iwasaki, M., Hanaoka, T., Kobayashi, M., Ishihara, J., Natsukawa, S., Shaura, K., Koizumi, Y., Kasuga, Y., Yoshimura, K., Yoshida, T., & Tsugane, S. (2005). Folate, vitamin B6, vitamin B12, and vitamin B2 intake, genetic polymorphisms of related enzymes, and risk of colorectal cancer in a hospital-based case-control study in Japan. *Nutr Cancer*, *53*(1), 42-50. https://doi.org/10.1207/s15327914nc5301_5
- Overmeer, R. M., Henken, F. E., Snijders, P. J., Claassen-Kramer, D., Berkhof, J., Helmerhorst, T. J., Heideman, D. A., Wilting, S. M., Murakami, Y., Ito, A., Meijer, C. J., & Steenbergen, R. D. (2008). Association between dense CADM1 promoter methylation and reduced protein expression in high-grade CIN and cervical SCC. *J Pathol*, *215*(4), 388-397. <https://doi.org/10.1002/path.2367>
- Paavonen, J., Naud, P., Salmerón, J., Wheeler, C. M., Chow, S. N., Apter, D., Kitchener, H., Castellsague, X., Teixeira, J. C., Skinner, S. R., Hedrick, J., Jaisamrarn, U., Limson, G., Garland, S., Szarewski, A., Romanowski, B., Aoki, F. Y., Schwarz, T. F., Poppe, W. A., Bosch, F. X., Jenkins, D., Hardt, K., Zahaf, T., Descamps, D., Struyf, F., Lehtinen, M., & Dubin, G. (2009). Efficacy of human papillomavirus (HPV)-16/18 AS04-adjuvanted vaccine against cervical infection and precancer caused by oncogenic HPV types (PATRICIA): final analysis of a double-blind, randomised study in young women. *Lancet*, *374*(9686), 301-314. [https://doi.org/10.1016/s0140-6736\(09\)61248-4](https://doi.org/10.1016/s0140-6736(09)61248-4)

- Palefsky, J. (2007). Human papillomavirus infection in HIV-infected persons. *Top HIV Med*, 15(4), 130-133.
- Pallavi, S., Anoop, K., Showket, H., Alo, N., & Mausumi, B. (2015). NFKB1/NFKB1a polymorphisms are associated with the progression of cervical carcinoma in HPV-infected postmenopausal women from rural area. *Tumour Biol*, 36(8), 6265-6276. <https://doi.org/10.1007/s13277-015-3312-7>
- Paradkar, P. H., Joshi, J. V., Mertia, P. N., Agashe, S. V., & Vaidya, R. A. (2014). Role of cytokines in genesis, progression and prognosis of cervical cancer. *Asian Pac J Cancer Prev*, 15(9), 3851-3864.
- Parker, B. S., Rautela, J., & Hertzog, P. J. (2016). Antitumour actions of interferons: implications for cancer therapy. *Nat Rev Cancer*, 16(3), 131-144. <https://doi.org/10.1038/nrc.2016.14>
- PATH. (2019). Global, HPV vaccine introduction overview: projected and current national introductions, demonstration/pilot projects, gender-neutral vaccination programs, and global HPV vaccine introduction maps (2006-2022). <https://www.path.org/resources/global-hpv-vaccine-introduction-overview/>
- Pathak, S., Bajpai, D., Banerjee, A., Bhatla, N., Jain, S. K., Jayaram, H. N., & Singh, N. (2014). Serum one-carbon metabolites and risk of cervical cancer. *Nutr Cancer*, 66(5), 818-824. <https://doi.org/10.1080/01635581.2014.916318>
- Pecorelli, S., Zigliani, L., & Odicino, F. (2009). Revised FIGO staging for carcinoma of the cervix. *Int J Gynaecol Obstet*, 105(2), 107-108. <https://doi.org/10.1016/j.ijgo.2009.02.009>
- Peghini, B. C., Abdalla, D. R., Barcelos, A. C., Teodoro, L., Murta, E. F., & Michelin, M. A. (2012). Local cytokine profiles of patients with cervical intraepithelial and invasive neoplasia. *Hum Immunol*, 73(9), 920-926. <https://doi.org/10.1016/j.humimm.2012.06.003>
- Peng, D. F., Kanai, Y., Sawada, M., Ushijima, S., Hiraoka, N., Kitazawa, S., & Hirohashi, S. (2006). DNA methylation of multiple tumor-related genes in association with overexpression of DNA methyltransferase 1 (DNMT1) during multistage carcinogenesis of the pancreas. *Carcinogenesis*, 27(6), 1160-1168. <https://doi.org/10.1093/carcin/bgi361>
- Peng, Y., Wang, X., Feng, H., & Yan, G. (2017). Is oral contraceptive use associated with an increased risk of cervical cancer? An evidence-based meta-analysis. *J Obstet Gynaecol Res*, 43(5), 913-922. <https://doi.org/10.1111/jog.13291>

- Pett, M. R., Herdman, M. T., Palmer, R. D., Yeo, G. S. H., Shivji, M. K., Stanley, M. A., & Coleman, N. (2006). Selection of cervical keratinocytes containing integrated HPV16 associates with episome loss and an endogenous antiviral response. *Proceedings of the National Academy of Sciences of the United States of America*, *103*(10), 3822-3827. <https://doi.org/10.1073/pnas.0600078103>
- Pidugu, V. K., Pidugu, H. B., Wu, M. M., Liu, C. J., & Lee, T. C. (2019a). Emerging functions of human IFIT proteins in cancer. *Front Mol Biosci*, *6*, 148. <https://doi.org/10.3389/fmolb.2019.00148>
- Pidugu, V. K., Wu, M. M., Yen, A. H., Pidugu, H. B., Chang, K. W., Liu, C. J., & Lee, T. C. (2019b). IFIT1 and IFIT3 promote oral squamous cell carcinoma metastasis and contribute to the anti-tumor effect of gefitinib via enhancing p-EGFR recycling. *Oncogene*. <https://doi.org/10.1038/s41388-018-0662-9>
- Pieroth, R., Paver, S., Day, S., & Lammersfeld, C. (2018). Folate and its impact on cancer risk. *Curr Nutr Rep*, *7*(3), 70-84. <https://doi.org/10.1007/s13668-018-0237-y>
- Pikarsky, E., & Ben-Neriah, Y. (2006). NF-kappaB inhibition: a double-edged sword in cancer? *Eur J Cancer*, *42*(6), 779-784. <https://doi.org/10.1016/j.ejca.2006.01.011>
- Piyathilake, C. J. (2007). Update on micronutrients and cervical dysplasia. *Ethn Dis*, *17*(2), S2-14-17. <http://www.ncbi.nlm.nih.gov/pubmed/17684808>
- Piyathilake, C. J., Azrad, M., Jhala, D., Macaluso, M., Kabagambe, E. K., Brill, I., Niveleau, A., Jhala, N., & Grizzle, W. E. (2006). Mandatory fortification with folic acid in the United States is not associated with changes in the degree or the pattern of global DNA methylation in cells involved in cervical carcinogenesis. *Cancer Biomark*, *2*(6), 259-266. <https://doi.org/10.3233/cbm-2006-2604>
- Piyathilake, C. J., Henao, O. L., Macaluso, M., Cornwell, P. E., Meleth, S., Heimbürger, D. C., & Partridge, E. E. (2004). Folate is associated with the natural history of high-risk human papillomaviruses. *Cancer Res*, *64*(23), 8788-8793. <https://doi.org/10.1158/0008-5472.CAN-04-2402>
- Piyathilake, C. J., Johanning, G. L., Macaluso, M., Whiteside, M., Oelschlager, D. K., Heimbürger, D. C., & Grizzle, W. E. (2000). Localized folate and vitamin B12 deficiency in squamous cell lung cancer is associated with global DNA hypomethylation. *Nutr Cancer*, *37*(1), 99-107. https://doi.org/10.1207/s15327914nc3701_13

- Piyathilake, C. J., Macaluso, M., Alvarez, R. D., Chen, M., Badiga, S., Siddiqui, N. R., Edberg, J. C., Partridge, E. E., & Johannig, G. L. (2011). A higher degree of LINE-1 methylation in peripheral blood mononuclear cells, a one-carbon nutrient related epigenetic alteration, is associated with a lower risk of developing cervical intraepithelial neoplasia. *Nutrition*, 27(5), 513-519. <https://doi.org/10.1016/j.nut.2010.08.018>
- Piyathilake, C. J., Macaluso, M., Brill, I., Heimburger, D. C., & Partridge, E. E. (2007). Lower red blood cell folate enhances the HPV-16-associated risk of cervical intraepithelial neoplasia. *Nutrition*, 23(3), 203-210. <https://doi.org/10.1016/j.nut.2006.12.002>
- Piyathilake, C. J., Macaluso, M., Chambers, M. M., Badiga, S., Siddiqui, N. R., Bell, W. C., Edberg, J. C., Partridge, E. E., Alvarez, R. D., & Johannig, G. L. (2014). Folate and vitamin B12 may play a critical role in lowering the HPV-16 methylation-associated risk of developing higher grades of CIN. *Cancer Prev Res (Phila)*, 7(11), 1128-1137. <https://doi.org/10.1158/1940-6207.Capr-14-0143>
- Poomipark, N. (2013). The influence of methyl donor status on cervical cancer cell behavior in vitro. University of Sheffield. <http://etheses.whiterose.ac.uk/id/eprint/4561>
- Poomipark, N., Flatley, J. E., Hill, M. H., Mangnall, B., Azar, E., Grabowski, P., & Powers, H. J. (2016). Methyl donor status influences DNMT expression and global DNA methylation in cervical cancer cells. *Asian Pac J Cancer Prev*, 17(7), 3213-3222.
- Potischman, N., Brinton, L. A., Laiming, V. A., Reeves, W. C., Brenes, M. M., Herrero, R., Tenorio, F., de Britton, R. C., & Gaitan, E. (1991). A case-control study of serum folate levels and invasive cervical cancer. *Cancer Res*, 51(18), 4785-4789.
- Pradhan, S., Bacolla, A., Wells, R. D., & Roberts, R. J. (1999). Recombinant human DNA (cytosine-5) methyltransferase expression, purification, and comparison of de novo and maintenance methylation. *J Biol Chem*, 274(46), 33002-33010. <https://doi.org/10.1074/jbc.274.46.33002>
- Prentice, R. L., Thomson, C. A., Caan, B., Hubbell, F. A., Anderson, G. L., Beresford, S. A., Pettinger, M., Lane, D. S., Lessin, L., Yasmeen, S., Singh, B., Khandekar, J., Shikany, J. M., Satterfield, S., & Chlebowski, R. T. (2007). Low-fat dietary pattern and cancer incidence in the Women's Health Initiative Dietary Modification Randomized Controlled Trial. *J Natl Cancer Inst*, 99(20), 1534-1543. <https://doi.org/10.1093/jnci/djm159>
- Prokhortchouk, E., & Hendrich, B. (2002). Methyl-CpG binding proteins and cancer: are MeCpGs more important than MBDs? *Oncogene*, 21(35), 5394-5399. <https://doi.org/10.1038/sj.onc.1205631>

- Prusty, B. K., Husain, S. A., & Das, B. C. (2005). Constitutive activation of nuclear factor -kB: preferential homodimerization of p50 subunits in cervical carcinoma. *Front Biosci*, *10*, 1510-1519. <https://doi.org/10.2741/1635>
- Pufulete, M., Al-Ghnaniem, R., Leather, A. J., Appleby, P., Gout, S., Terry, C., Emery, P. W., & Sanders, T. A. (2003). Folate status, genomic DNA hypomethylation, and risk of colorectal adenoma and cancer: a case control study. *Gastroenterology*, *124*(5), 1240-1248. [https://doi.org/10.1016/s0016-5085\(03\)00279-8](https://doi.org/10.1016/s0016-5085(03)00279-8)
- Pufulete, M., Al-Ghnaniem, R., Rennie, J. A., Appleby, P., Harris, N., Gout, S., Emery, P. W., & Sanders, T. A. (2005). Influence of folate status on genomic DNA methylation in colonic mucosa of subjects without colorectal adenoma or cancer. *Br J Cancer*, *92*(5), 838-842. <https://doi.org/10.1038/sj.bjc.6602439>
- Qi, M., & Xiong, X. (2018). Promoter hypermethylation of RAR β 2, DAPK, hMLH1, p14, and p15 is associated with progression of breast cancer: A PRISMA-compliant meta-analysis. *Medicine (Baltimore)*, *97*(51), e13666. <https://doi.org/10.1097/md.00000000000013666>
- Qian, N., Chen, X., Han, S., Qiang, F., Jin, G., Zhou, X., Dong, J., Wang, X., Shen, H., & Hu, Z. (2010). Circulating IL-1beta levels, polymorphisms of IL-1B, and risk of cervical cancer in Chinese women. *J Cancer Res Clin Oncol*, *136*(5), 709-716. <https://doi.org/10.1007/s00432-009-0710-5>
- Qiang, Y., Li, Q., Xin, Y., Fang, X., Tian, Y., Ma, J., Wang, J., Wang, Q., Zhang, R., Wang, J., & Wang, F. (2018). Intake of dietary one-carbon metabolism-related B vitamins and the risk of esophageal cancer: a dose-response meta-analysis. *Nutrients*, *10*(7). <https://doi.org/10.3390/nu10070835>
- Qin, X., Cui, Y., Shen, L., Sun, N., Zhang, Y., Li, J., Xu, X., Wang, B., Xu, X., Huo, Y., & Wang, X. (2013). Folic acid supplementation and cancer risk: a meta-analysis of randomized controlled trials. *Int J Cancer*, *133*(5), 1033-1041. <https://doi.org/10.1002/ijc.28038>
- Qu, G., Dubeau, L., Narayan, A., Yu, M. C., & Ehrlich, M. (1999). Satellite DNA hypomethylation vs. overall genomic hypomethylation in ovarian epithelial tumors of different malignant potential. *Mutat Res*, *423*(1-2), 91-101. [https://doi.org/10.1016/s0027-5107\(98\)00229-2](https://doi.org/10.1016/s0027-5107(98)00229-2)
- Rahmani, M., Talebi, M., Hagh, M. F., Feizi, A. A. H., & Solali, S. (2018). Aberrant DNA methylation of key genes and Acute Lymphoblastic Leukemia. *Biomed Pharmacother*, *97*, 1493-1500. <https://doi.org/10.1016/j.biopha.2017.11.033>
- Ramana, C. V., Chatterjee-Kishore, M., Nguyen, H., & Stark, G. R. (2000). Complex roles of STAT1 in regulating gene expression. *Oncogene*, *19*(21), 2619-2627. <https://doi.org/10.1038/sj.onc.1203525>

- Ramanakumar, A. V., Goncalves, O., Richardson, H., Tellier, P., Ferenczy, A., Coutlée, F., & Franco, E. L. (2010). Human papillomavirus (HPV) types 16, 18, 31, 45 DNA loads and HPV-16 integration in persistent and transient infections in young women. *BMC Infect Dis*, *10*, 326. <https://doi.org/10.1186/1471-2334-10-326>
- Ramassone, A., Pagotto, S., Veronese, A., & Visone, R. (2018). Epigenetics and MicroRNAs in Cancer. *Int J Mol Sci*, *19*(2). <https://doi.org/10.3390/ijms19020459>
- Rampersaud, G. C., Bailey, L. B., & Kauwell, G. P. (2002). Relationship of folate to colorectal and cervical cancer: review and recommendations for practitioners. *J Am Diet Assoc*, *102*(9), 1273-1282. <http://www.ncbi.nlm.nih.gov/pubmed/12792626>
- Ravanel, S., Gakière, B., Job, D., & Douce, R. (1998). The specific features of methionine biosynthesis and metabolism in plants. *Proc Natl Acad Sci U S A*, *95*(13), 7805-7812. <https://doi.org/10.1073/pnas.95.13.7805>
- Ray, J. G., Cole, D. E., & Boss, S. C. (2000). An Ontario-wide study of vitamin B12, serum folate, and red cell folate levels in relation to plasma homocysteine: is a preventable public health issue on the rise? *Clin Biochem*, *33*(5), 337-343. [https://doi.org/10.1016/s0009-9120\(00\)00083-7](https://doi.org/10.1016/s0009-9120(00)00083-7)
- Regina, M., Korhonen, V. P., Smith, T. K., Alakuijala, L., & Eloranta, T. O. (1993). Methionine toxicity in the rat in relation to hepatic accumulation of S-adenosylmethionine: prevention by dietary stimulation of the hepatic transsulfuration pathway. *Arch Biochem Biophys*, *300*(2), 598-607. <https://doi.org/10.1006/abbi.1993.1083>
- Rhee, I., Bachman, K. E., Park, B. H., Jair, K. W., Yen, R. W., Schuebel, K. E., Cui, H., Feinberg, A. P., Lengauer, C., Kinzler, K. W., Baylin, S. B., & Vogelstein, B. (2002). DNMT1 and DNMT3b cooperate to silence genes in human cancer cells. *Nature*, *416*(6880), 552-556. <https://doi.org/10.1038/416552a>
- Ritchie, M. E., Smyth, G. K., Phipson, B., Wu, D., Hu, Y., Shi, W., & Law, C. W. (2015). Limma powers differential expression analyses for RNA-sequencing and microarray studies. *Nucleic Acids Research*, *43*(7), e47-e47. <https://doi.org/10.1093/nar/gkv007>
- Robertson, J., Iemolo, F., Stabler, S. P., Allen, R. H., & Spence, J. D. (2005). Vitamin B12, homocysteine and carotid plaque in the era of folic acid fortification of enriched cereal grain products. *Cmaj*, *172*(12), 1569-1573. <https://doi.org/10.1503/cmaj.045055>
- Rogers, L. M., Cordero, A. M., Pfeiffer, C. M., Hausman, D. B., Tsang, B. L., De-Regil, L. M., Rosenthal, J., Razzaghi, H., Wong, E. C., Weakland, A. P., & Bailey, L. B. (2018). Global folate status in women of reproductive age: a systematic review with emphasis on methodological issues. *Ann N Y Acad Sci*, *1431*(1), 35-57. <https://doi.org/10.1111/nyas.13963>

- Roje, S. (2006). S-Adenosyl-L-methionine: beyond the universal methyl group donor. *Phytochemistry*, 67(15), 1686-1698. <https://doi.org/10.1016/j.phytochem.2006.04.019>
- Romaguera, D., Vergnaud, A. C., Peeters, P. H., van Gils, C. H., Chan, D. S., Ferrari, P., Romieu, I., Jenab, M., Slimani, N., Clavel-Chapelon, F., Fagherazzi, G., Perquier, F., Kaaks, R., Teucher, B., Boeing, H., von Rűsten, A., Tjűnneland, A., Olsen, A., Dahm, C. C., Overvad, K., Quirűs, J. R., Gonzalez, C. A., Snchez, M. J., Navarro, C., Barricarte, A., Dorronsoro, M., Khaw, K. T., Wareham, N. J., Crowe, F. L., Key, T. J., Trichopoulou, A., Lagiou, P., Bamia, C., Masala, G., Vineis, P., Tumino, R., Sieri, S., Panico, S., May, A. M., Bueno-de-Mesquita, H. B., Bűchner, F. L., Wirflt, E., Manjer, J., Johansson, I., Hallmans, G., Skeie, G., Benjaminsen Borch, K., Parr, C. L., Riboli, E., & Norat, T. (2012). Is concordance with World Cancer Research Fund/American Institute for Cancer Research guidelines for cancer prevention related to subsequent risk of cancer? Results from the EPIC study. *Am J Clin Nutr*, 96(1), 150-163. <https://doi.org/10.3945/ajcn.111.031674>
- Ronco, G., Dillner, J., Elfstrűm, K. M., Tunesi, S., Snijders, P. J., Arbyn, M., Kitchener, H., Segnan, N., Gilham, C., Giorgi-Rossi, P., Berkhof, J., Peto, J., & Meijer, C. J. (2014). Efficacy of HPV-based screening for prevention of invasive cervical cancer: follow-up of four European randomised controlled trials. *Lancet*, 383(9916), 524-532. [https://doi.org/10.1016/s0140-6736\(13\)62218-7](https://doi.org/10.1016/s0140-6736(13)62218-7)
- Rositch, A. F., Koshiol, J., Hudgens, M. G., Razzaghi, H., Backes, D. M., Pimenta, J. M., Franco, E. L., Poole, C., & Smith, J. S. (2013). Patterns of persistent genital human papillomavirus infection among women worldwide: a literature review and meta-analysis. *Int J Cancer*, 133(6), 1271-1285. <https://doi.org/10.1002/ijc.27828>
- Rositch, A. F., Soeters, H. M., Offutt-Powell, T. N., Wheeler, B. S., Taylor, S. M., & Smith, J. S. (2014). The incidence of human papillomavirus infection following treatment for cervical neoplasia: a systematic review. *Gynecol Oncol*, 132(3), 767-779. <https://doi.org/10.1016/j.ygyno.2013.12.040>
- Roura, E., Castellsagu, X., Pawlita, M., Travier, N., Waterboer, T., Margall, N., Bosch, F. X., de Sanjos, S., Dillner, J., Gram, I. T., Tjűnneland, A., Munk, C., Pala, V., Palli, D., Khaw, K. T., Barnabas, R. V., Overvad, K., Clavel-Chapelon, F., Boutron-Ruault, M. C., Fagherazzi, G., Kaaks, R., Lukanova, A., Steffen, A., Trichopoulou, A., Trichopoulos, D., Klinaki, E., Tumino, R., Sacerdote, C., Panico, S., Bueno-de-Mesquita, H. B., Peeters, P. H., Lund, E., Weiderpass, E., Redondo, M. L., Snchez, M. J., Tormo, M. J., Barricarte, A., Larranaga, N., Ekstrűm, J., Hortlund, M., Lindquist, D., Wareham, N., Travis, R. C., Rinaldi, S., Tommasino, M., Franceschi, S., & Riboli, E. (2014). Smoking as a major risk factor for cervical cancer and pre-cancer: results from the EPIC cohort. *Int J Cancer*, 135(2), 453-466. <https://doi.org/10.1002/ijc.28666>

- Roura, E., Travier, N., Waterboer, T., de Sanjosé, S., Bosch, F. X., Pawlita, M., Pala, V., Weiderpass, E., Margall, N., Dillner, J., Gram, I. T., Tjønneland, A., Munk, C., Palli, D., Khaw, K.-T., Overvad, K., Clavel-Chapelon, F., Mesrine, S., Fournier, A., Fortner, R. T., Ose, J., Steffen, A., Trichopoulou, A., Lagiou, P., Orfanos, P., Masala, G., Tumino, R., Sacerdote, C., Polidoro, S., Mattiello, A., Lund, E., Peeters, P. H., Bueno-de-Mesquita, H. B. a., Quirós, J. R., Sánchez, M.-J., Navarro, C., Barricarte, A., Larrañaga, N., Ekström, J., Lindquist, D., Idahl, A., Travis, R. C., Merritt, M. A., Gunter, M. J., Rinaldi, S., Tommasino, M., Franceschi, S., Riboli, E., & Castellsagué, X. (2016). The influence of hormonal factors on the risk of developing cervical cancer and pre-cancer: results from the EPIC cohort. *PLoS One*, *11*(1), e0147029-e0147029. <https://doi.org/10.1371/journal.pone.0147029>
- Rowling, M. J., McMullen, M. H., Chipman, D. C., & Schalinske, K. L. (2002). Hepatic glycine N-methyltransferase is up-regulated by excess dietary methionine in rats. *J Nutr*, *132*(9), 2545-2550. <https://doi.org/10.1093/jn/132.9.2545>
- Roy, D. G., Chen, J., Mamane, V., Ma, E. H., Muhire, B. M., Sheldon, R. D., Shorstova, T., Koning, R., Johnson, R. M., Esaulova, E., Williams, K. S., Hayes, S., Steadman, M., Samborska, B., Swain, A., Daigneault, A., Chubukov, V., Roddy, T. P., Foulkes, W., Pospisilik, J. A., Bourgeois-Daigneault, M. C., Artyomov, M. N., Witcher, M., Krawczyk, C. M., Larochelle, C., & Jones, R. G. (2020). Methionine metabolism shapes T helper cell responses through regulation of epigenetic reprogramming. *Cell Metab*, *31*(2), 250-266.e259. <https://doi.org/10.1016/j.cmet.2020.01.006>
- Sabra, S., Gratacós, E., & Gómez Roig, M. D. (2017). Smoking induced changes in the maternal immune, endocrine, and metabolic pathways and their impact on fetal growth: a topical review. *Fetal Diagn Ther*, *41*(4), 241-250. <https://doi.org/10.1159/000457123>
- Sadler, A. J., & Williams, B. R. G. (2008). Interferon-inducible antiviral effectors. *Nature Reviews Immunology*, *8*, 559. <https://doi.org/10.1038/nri2314>
- Saijo, Y., Tanaka, M., Miki, M., Usui, K., Suzuki, T., Maemondo, M., Hong, X., Tazawa, R., Kikuchi, T., Matsushima, K., & Nukiwa, T. (2002). Proinflammatory cytokine IL-1 beta promotes tumor growth of Lewis lung carcinoma by induction of angiogenic factors: in vivo analysis of tumor-stromal interaction. *J Immunol*, *169*(1), 469-475.
- Saito, Y., Iwatsuki, K., Hanyu, H., Maruyama, N., Aihara, E., Tadaishi, M., Shimizu, M., & Kobayashi-Hattori, K. (2017). Effect of essential amino acids on enteroids: methionine deprivation suppresses proliferation and affects differentiation in enteroid stem cells. *Biochem Biophys Res Commun*, *488*(1), 171-176. <https://doi.org/10.1016/j.bbrc.2017.05.029>
- Saito, Y., Kanai, Y., Nakagawa, T., Sakamoto, M., Saito, H., Ishii, H., & Hirohashi, S. (2003). Increased protein expression of DNA methyltransferase (DNMT) 1 is significantly correlated with the malignant potential and poor prognosis of human hepatocellular carcinomas. *Int J Cancer*, *105*(4), 527-532. <https://doi.org/10.1002/ijc.11127>

- Samblas, M., Martínez, J. A., & Milagro, F. (2018). Folic acid improves the inflammatory response in LPS-activated THP-1 macrophages. *Mediators Inflamm*, 2018, 1312626. <https://doi.org/10.1155/2018/1312626>
- Sandhu, R., Roll, J. D., Rivenbark, A. G., & Coleman, W. B. (2015). Dysregulation of the epigenome in human breast cancer: contributions of gene-specific DNA hypermethylation to breast cancer pathobiology and targeting the breast cancer methylome for improved therapy. *Am J Pathol*, 185(2), 282-292. <https://doi.org/10.1016/j.ajpath.2014.12.003>
- Sanjoaquin, M. A., Allen, N., Couto, E., Roddam, A. W., & Key, T. J. (2005). Folate intake and colorectal cancer risk: a meta-analytical approach. *Int J Cancer*, 113(5), 825-828. <https://doi.org/10.1002/ijc.20648>
- Sankaranarayanan, R., Nene, B. M., Shastri, S. S., Jayant, K., Muwonge, R., Budukh, A. M., Hingmire, S., Malvi, S. G., Thorat, R., Kothari, A., Chinoy, R., Kelkar, R., Kane, S., Desai, S., Keskar, V. R., Rajeshwarkar, R., Panse, N., & Dinshaw, K. A. (2009). HPV screening for cervical cancer in rural India. *N Engl J Med*, 360(14), 1385-1394. <https://doi.org/10.1056/NEJMoa0808516>
- Sapienza, C., & Issa, J. P. (2016). Diet, nutrition, and cancer epigenetics. *Annu Rev Nutr*, 36, 665-681. <https://doi.org/10.1146/annurev-nutr-121415-112634>
- Sasaki, M., Anast, J., Bassett, W., Kawakami, T., Sakuragi, N., & Dahiya, R. (2003). Bisulfite conversion-specific and methylation-specific PCR: a sensitive technique for accurate evaluation of CpG methylation. *Biochem Biophys Res Commun*, 309(2), 305-309.
- Sato, Y., Goto, Y., Narita, N., & Hoon, D. S. (2009). Cancer cells expressing toll-like receptors and the tumor microenvironment. *Cancer Microenviron*, 2(1), 205-214. <https://doi.org/10.1007/s12307-009-0022-y>
- Schiffman, M., Doorbar, J., Wentzensen, N., de Sanjosé, S., Fakhry, C., Monk, B. J., Stanley, M. A., & Franceschi, S. (2016). Carcinogenic human papillomavirus infection. *Nat Rev Dis Primers*, 2, 16086. <https://doi.org/10.1038/nrdp.2016.86>
- Schneider, W. M., Chevillotte, M. D., & Rice, C. M. (2014). Interferon-stimulated genes: a complex web of host defenses. *Annual Review of Immunology*, 32(1), 513-545. <https://doi.org/10.1146/annurev-immunol-032713-120231>
- Schroecksnadel, S., Jenny, M., & Fuchs, D. (2011). Myelomonocytic THP-1 cells for in vitro testing of immunomodulatory properties of nanoparticles. *Journal of Biomedical Nanotechnology*, 7(1), 209-210. <https://doi.org/10.1166/jbn.2011.1272>

- Schwab, U., Törrönen, A., Toppinen, L., Alfthan, G., Saarinen, M., Aro, A., & Uusitupa, M. (2002). Betaine supplementation decreases plasma homocysteine concentrations but does not affect body weight, body composition, or resting energy expenditure in human subjects. *Am J Clin Nutr*, *76*(5), 961-967. <https://doi.org/10.1093/ajcn/76.5.961>
- Schwartz, S. M., Daling, J. R., Shera, K. A., Madeleine, M. M., McKnight, B., Galloway, D. A., Porter, P. L., & McDougall, J. K. (2001). Human papillomavirus and prognosis of invasive cervical cancer: a population-based study. *J Clin Oncol*, *19*(7), 1906-1915. <https://doi.org/10.1200/jco.2001.19.7.1906>
- Scott, M. E., Shvetsov, Y. B., Thompson, P. J., Hernandez, B. Y., Zhu, X., Wilkens, L. R., Killeen, J., Vo, D. D., Moscicki, A. B., & Goodman, M. T. (2013). Cervical cytokines and clearance of incident human papillomavirus infection: Hawaii HPV cohort study. *Int J Cancer*, *133*(5), 1187-1196. <https://doi.org/10.1002/ijc.28119>
- Sen, P., Ganguly, P., & Ganguly, N. (2018). Modulation of DNA methylation by human papillomavirus E6 and E7 oncoproteins in cervical cancer. *Oncol Lett*, *15*(1), 11-22. <https://doi.org/10.3892/ol.2017.7292>
- Shafie, M. (2014). Unpublished work on methyl donors and cervical cancer. The University of Sheffield Laboratory Notebook.
- Shannon, P., Markiel, A., Ozier, O., Baliga, N. S., Wang, J. T., Ramage, D., Amin, N., Schwikowski, B., & Ideker, T. (2003). Cytoscape: a software environment for integrated models of biomolecular interaction networks. *Genome Res*, *13*(11), 2498-2504. <https://doi.org/10.1101/gr.1239303>
- Sharma, A., Rajappa, M., Satyam, A., & Sharma, M. (2009). Cytokines (TH1 and TH2) in patients with advanced cervical cancer undergoing neoadjuvant chemoradiation: correlation with treatment response. *Int J Gynecol Cancer*, *19*(7), 1269-1275. <https://doi.org/10.1111/IGC.0b013e3181a8efcc>
- Shaveta, G., Shi, J., Chow, V. T., & Song, J. (2010). Structural characterization reveals that viperin is a radical S-adenosyl-L-methionine (SAM) enzyme. *Biochem Biophys Res Commun*, *391*(3), 1390-1395. <https://doi.org/10.1016/j.bbrc.2009.12.070>
- Shi, C., & Pamer, E. G. (2011). Monocyte recruitment during infection and inflammation. *Nat Rev Immunol*, *11*(11), 762-774. <https://doi.org/10.1038/nri3070>
- Shin, E., Lee, Y., & Koo, J. S. (2016). Differential expression of the epigenetic methylation-related protein DNMT1 by breast cancer molecular subtype and stromal histology. *J Transl Med*, *14*, 87. <https://doi.org/10.1186/s12967-016-0840-x>

- Shiraki, N., Shiraki, Y., Tsuyama, T., Obata, F., Miura, M., Nagae, G., Aburatani, H., Kume, K., Endo, F., & Kume, S. (2014). Methionine metabolism regulates maintenance and differentiation of human pluripotent stem cells. *Cell Metab*, 19(5), 780-794. <https://doi.org/10.1016/j.cmet.2014.03.017>
- Shivapurkar, N., & Poirier, L. A. (1983). Tissue levels of S-adenosylmethionine and S-adenosylhomocysteine in rats fed methyl-deficient, amino acid-defined diets for one to five weeks. *Carcinogenesis*, 4(8), 1051-1057. <https://doi.org/10.1093/carcin/4.8.1051>
- Shivapurkar, N., Sherman, M. E., Stastny, V., Echebiri, C., Rader, J. S., Nayar, R., Bonfiglio, T. A., Gazdar, A. F., & Wang, S. S. (2007). Evaluation of candidate methylation markers to detect cervical neoplasia. *Gynecol Oncol*, 107(3), 549-553. <https://doi.org/10.1016/j.ygyno.2007.08.057>
- Shuangshoti, S., Hourpai, N., Pumsuk, U., & Mutirangura, A. (2007). Line-1 hypomethylation in multistage carcinogenesis of the uterine cervix. *Asian Pac J Cancer Prev*, 8(2), 307-309.
- Shukeir, N., Stefanska, B., Parashar, S., Chik, F., Arakelian, A., Szyf, M., & Rabbani, S. A. (2015). Pharmacological methyl group donors block skeletal metastasis in vitro and in vivo. *Br J Pharmacol*, 172(11), 2769-2781. <https://doi.org/10.1111/bph.13102>
- Shuvalov, O., Petukhov, A., Daks, A., Fedorova, O., Vasileva, E., & Barlev, N. A. (2017). One-carbon metabolism and nucleotide biosynthesis as attractive targets for anticancer therapy. *Oncotarget*, 8(14), 23955-23977. <https://doi.org/10.18632/oncotarget.15053>
- Sie, K. K., Medline, A., van Weel, J., Sohn, K. J., Choi, S. W., Croxford, R., & Kim, Y. I. (2011). Effect of maternal and postweaning folic acid supplementation on colorectal cancer risk in the offspring. *Gut*, 60(12), 1687-1694. <https://doi.org/10.1136/gut.2011.238782>
- Singh, G. K., Azuine, R. E., & Siahpush, M. (2012). Global inequalities in cervical cancer incidence and mortality are linked to deprivation, low socioeconomic status, and human development. *Int J MCH AIDS*, 1(1), 17-30. <https://doi.org/10.21106/ijma.12>
- Sinha, R., Cooper, T. K., Rogers, C. J., Sinha, I., Turbitt, W. J., Calcagnotto, A., Perrone, C. E., & Richie, J. P., Jr. (2014). Dietary methionine restriction inhibits prostatic intraepithelial neoplasia in TRAMP mice. *Prostate*, 74(16), 1663-1673. <https://doi.org/10.1002/pros.22884>
- Smith, Z. D., & Meissner, A. (2013). DNA methylation: roles in mammalian development. *Nat Rev Genet*, 14(3), 204-220. <https://doi.org/10.1038/nrg3354>
- Soda, K. (2018). Polyamine metabolism and gene methylation in conjunction with one-carbon metabolism. *Int J Mol Sci*, 19(10). <https://doi.org/10.3390/ijms19103106>

- Solomon, D., & Nayar, R. (2004). *The Bethesda System for reporting Cervical Cytology: Definition, Criteria & Explanatory Notes (2nd Ed.)*. Springer-Verlag.
- Song, C. X., & He, C. (2012). Balance of DNA methylation and demethylation in cancer development. *Genome Biol*, *13*(10), 173. <https://doi.org/10.1186/gb-2012-13-10-2012>
- Song, J., Sohn, K. J., Medline, A., Ash, C., Gallinger, S., & Kim, Y. I. (2000). Chemopreventive effects of dietary folate on intestinal polyps in Apc⁺/-Msh2^{-/-} mice. *Cancer Res*, *60*(12), 3191-3199.
- Song, X., Voronov, E., Dvorkin, T., Fima, E., Cagnano, E., Benharroch, D., Shendler, Y., Bjorkdahl, O., Segal, S., Dinarello, C. A., & Apte, R. N. (2003). Differential effects of IL-1 alpha and IL-1 beta on tumorigenicity patterns and invasiveness. *J Immunol*, *171*(12), 6448-6456.
- Sowińska, A., & Jagodzinski, P. P. (2007). RNA interference-mediated knockdown of DNMT1 and DNMT3B induces CXCL12 expression in MCF-7 breast cancer and AsPC1 pancreatic carcinoma cell lines. *Cancer Lett*, *255*(1), 153-159. <https://doi.org/10.1016/j.canlet.2007.04.004>
- Speirs, V., Kerin, M. J., Newton, C. J., Walton, D. S., Green, A. R., Desai, S. B., & Atkin, S. L. (1999). Evidence for transcriptional activation of ERalpha by IL-1beta in breast cancer cells. *Int J Oncol*, *15*(6), 1251-1254.
- Sproul, D., & Meehan, R. R. (2013). Genomic insights into cancer-associated aberrant CpG island hypermethylation. *Brief Funct Genomics*, *12*(3), 174-190. <https://doi.org/10.1093/bfgp/els063>
- Stanley, M., Pinto, L. A., & Trimble, C. (2012). Human papillomavirus vaccines-immune responses. *Vaccine*, *30*(5), F83-87. <https://doi.org/10.1016/j.vaccine.2012.04.106>
- Stanley, M. A., Pett, M. R., & Coleman, N. (2007). HPV: from infection to cancer. *Biochem Soc Trans*, *35*(Pt 6), 1456-1460. <https://doi.org/10.1042/bst0351456>
- Stanley, M. A., & Sterling, J. C. (2014). Host responses to infection with human papillomavirus. *Curr Probl Dermatol*, *45*, 58-74. <https://doi.org/10.1159/000355964>
- Stark, G. R., Kerr, I. M., Williams, B. R., Silverman, R. H., & Schreiber, R. D. (1998). How cells respond to interferons. *Annu Rev Biochem*, *67*, 227-264. <https://doi.org/10.1146/annurev.biochem.67.1.227>
- Stefanska, B., Karlic, H., Varga, F., Fabianowska-Majewska, K., & Haslberger, A. (2012). Epigenetic mechanisms in anti-cancer actions of bioactive food components--the implications in cancer prevention. *Br J Pharmacol*, *167*(2), 279-297. <https://doi.org/10.1111/j.1476-5381.2012.02002.x>

- Steluti, J., Selhub, J., Paul, L., Reginaldo, C., Fisberg, R. M., & Marchioni, D. M. L. (2017). An overview of folate status in a population-based study from São Paulo, Brazil and the potential impact of 10 years of national folic acid fortification policy. *Eur J Clin Nutr*, *71*(10), 1173-1178. <https://doi.org/10.1038/ejcn.2017.60>
- Stempak, J. M., Sohn, K. J., Chiang, E. P., Shane, B., & Kim, Y. I. (2005). Cell and stage of transformation-specific effects of folate deficiency on methionine cycle intermediates and DNA methylation in an in vitro model. *Carcinogenesis*, *26*(5), 981-990. <https://doi.org/10.1093/carcin/bgi037>
- Stevens, V. L., Rodriguez, C., Pavluck, A. L., McCullough, M. L., Thun, M. J., & Calle, E. E. (2006). Folate nutrition and prostate cancer incidence in a large cohort of US men. *Am J Epidemiol*, *163*(11), 989-996. <https://doi.org/10.1093/aje/kwj126>
- Stubenrauch, F., & Laimins, L. A. (1999). Human papillomavirus life cycle: active and latent phases. *Semin Cancer Biol*, *9*(6), 379-386. <https://doi.org/10.1006/scbi.1999.0141>
- Su, B., Qin, W., Xue, F., Wei, X., Guan, Q., Jiang, W., Wang, S., Xu, M., & Yu, S. (2018). The relation of passive smoking with cervical cancer: a systematic review and meta-analysis. *Medicine (Baltimore)*, *97*(46), e13061. <https://doi.org/10.1097/md.00000000000013061>
- Su, L. J., & Arab, L. (2001). Nutritional status of folate and colon cancer risk: evidence from NHANES I epidemiologic follow-up study. *Ann Epidemiol*, *11*(1), 65-72. [https://doi.org/10.1016/s1047-2797\(00\)00188-5](https://doi.org/10.1016/s1047-2797(00)00188-5)
- Sugawara, Y., Tsuji, I., Mizoue, T., Inoue, M., Sawada, N., Matsuo, K., Ito, H., Naito, M., Nagata, C., Kitamura, Y., Sadakane, A., Tanaka, K., Tamakoshi, A., Tsugane, S., & Shimazu, T. (2019). Cigarette smoking and cervical cancer risk: an evaluation based on a systematic review and meta-analysis among Japanese women. *Jpn J Clin Oncol*, *49*(1), 77-86. <https://doi.org/10.1093/jjco/hyy158>
- Sugiyama, Y., Hatano, N., Sueyoshi, N., Suetake, I., Tajima, S., Kinoshita, E., Kinoshita-Kikuta, E., Koike, T., & Kameshita, I. (2010). The DNA-binding activity of mouse DNA methyltransferase 1 is regulated by phosphorylation with casein kinase 1delta/epsilon. *Biochem J*, *427*(3), 489-497. <https://doi.org/10.1042/bj20091856>
- Sullivan, D. E., Gabbard, J. L., Jr., Shukla, M., & Sobral, B. (2010). Data integration for dynamic and sustainable systems biology resources: challenges and lessons learned. *Chem Biodivers*, *7*(5), 1124-1141. <https://doi.org/10.1002/cbdv.200900317>
- Sun, S., Li, X., Ren, A., Du, M., Du, H., Shu, Y., Zhu, L., & Wang, W. (2016). Choline and betaine consumption lowers cancer risk: a meta-analysis of epidemiologic studies. *Sci Rep*, *6*, 35547. <https://doi.org/10.1038/srep35547>

- Sung, H., Ferlay, J., Siegel, R. L., Laversanne, M., Soerjomataram, I., Jemal, A., & Bray, F. (2021). Global cancer statistics 2020: GLOBOCAN estimates of incidence and mortality worldwide for 36 cancers in 185 countries. *CA Cancer J Clin.* <https://doi.org/10.3322/caac.21660>
- Swann, J. B., & Smyth, M. J. (2007). Immune surveillance of tumors. *J Clin Invest*, *117*(5), 1137-1146. <https://doi.org/10.1172/jci31405>
- Szalmas, A., & Konya, J. (2009). Epigenetic alterations in cervical carcinogenesis. *Semin Cancer Biol*, *19*(3), 144-152. <https://doi.org/10.1016/j.semcancer.2009.02.011>
- Szarewski, A., Maddox, P., Royston, P., Jarvis, M., Anderson, M., Guillebaud, J., & Cuzick, J. (2001). The effect of stopping smoking on cervical Langerhans' cells and lymphocytes. *BJOG*, *108*(3), 295-303. <http://www.ncbi.nlm.nih.gov/pubmed/11281472>
- Tachezy, R., Mikysková, I., Ludvíková, V., Rob, L., Kucera, T., Slavík, V., Beková, A., Robová, H., Pluta, M., & Hamsíková, E. (2006). Longitudinal study of patients after surgical treatment for cervical lesions: detection of HPV DNA and prevalence of HPV-specific antibodies. *Eur J Clin Microbiol Infect Dis*, *25*(8), 492-500. <https://doi.org/10.1007/s10096-006-0172-5>
- Tahiliani, M., Koh, K. P., Shen, Y., Pastor, W. A., Bandukwala, H., Brudno, Y., Agarwal, S., Iyer, L. M., Liu, D. R., Aravind, L., & Rao, A. (2009). Conversion of 5-Methylcytosine to 5-Hydroxymethylcytosine in mammalian DNA by MLL partner TET1. *Science*, *324*(5929), 930. <https://doi.org/10.1126/science.1170116>
- Takaoka, A., Hayakawa, S., Yanai, H., Stoiber, D., Negishi, H., Kikuchi, H., Sasaki, S., Imai, K., Shibue, T., Honda, K., & Taniguchi, T. (2003). Integration of interferon-alpha/beta signalling to p53 responses in tumour suppression and antiviral defence. *Nature*, *424*(6948), 516-523. <https://doi.org/10.1038/nature01850>
- Tamandani, D. M., Shekari, M., & Suri, V. (2009). Interleukin-12 gene polymorphism and cervical cancer risk. *Am J Clin Oncol*, *32*(5), 524-528. <https://doi.org/10.1097/COC.0b013e318192519a>
- Tanaka, Y., Furuta, T., Suzuki, S., Orito, E., Yeo, A. E., Hirashima, N., Sugauchi, F., Ueda, R., & Mizokami, M. (2003). Impact of interleukin-1beta genetic polymorphisms on the development of hepatitis C virus-related hepatocellular carcinoma in Japan. *J Infect Dis*, *187*(11), 1822-1825. <https://doi.org/10.1086/375248>
- Tao, M. H., Mason, J. B., Marian, C., McCann, S. E., Platek, M. E., Millen, A., Ambrosone, C., Edge, S. B., Krishnan, S. S., Trevisan, M., Shields, P. G., & Freudenheim, J. L. (2011). Promoter methylation of E-cadherin, p16, and RAR- β (2) genes in breast tumors and dietary intake of nutrients important in one-carbon metabolism. *Nutr Cancer*, *63*(7), 1143-1150. <https://doi.org/10.1080/01635581.2011.605982>

- Tate, P. H., & Bird, A. P. (1993). Effects of DNA methylation on DNA-binding proteins and gene expression. *Curr Opin Genet Dev*, 3(2), 226-231. [https://doi.org/10.1016/0959-437x\(93\)90027-m](https://doi.org/10.1016/0959-437x(93)90027-m)
- Teschendorff, A. E., Marabita, F., Lechner, M., Bartlett, T., Tegner, J., Gomez-Cabrero, D., & Beck, S. (2013). A beta-mixture quantile normalization method for correcting probe design bias in Illumina Infinium 450 k DNA methylation data. *Bioinformatics*, 29(2), 189-196. <https://doi.org/10.1093/bioinformatics/bts680>
- Thivat, E., Durando, X., Demidem, A., Farges, M. C., Rapp, M., Cellarier, E., Guenin, S., D'Incan, M., Vasson, M. P., & Chollet, P. (2007). A methionine-free diet associated with nitrosourea treatment down-regulates methylguanine-DNA methyl transferase activity in patients with metastatic cancer. *Anticancer Res*, 27(4c), 2779-2783.
- Tian, Z., Shen, X., Feng, H., & Gao, B. (2000). IL-1 beta attenuates IFN-alpha beta-induced antiviral activity and STAT1 activation in the liver: involvement of proteasome-dependent pathway. *J Immunol*, 165(7), 3959-3965.
- Tibbetts, A. S., & Appling, D. (2010). Compartmentalization of Mammalian folate-mediated one-carbon metabolism. *Annu Rev Nutr*, 30, 57-81.
- Tjiong, M. Y., van der Vange, N., ter Schegget, J. S., Burger, M. P., ten Kate, F. W., & Out, T. A. (2001). Cytokines in cervicovaginal washing fluid from patients with cervical neoplasia. *Cytokine*, 14(6), 357-360. <https://doi.org/10.1006/cyto.2001.0909>
- Toh, T. B., Lim, J. J., & Chow, E. K. (2017). Epigenetics in cancer stem cells. *Mol Cancer*, 16(1), 29. <https://doi.org/10.1186/s12943-017-0596-9>
- Tomita, L. Y., Horta, B. L., da Silva, L. L. S., Malta, M. B., Franco, E. L., & Cardoso, M. A. (2021). Fruits and vegetables and cervical cancer: a systematic review and meta-analysis. *Nutr Cancer*, 73(1), 62-74. <https://doi.org/10.1080/01635581.2020.1737151>
- Tommasino, M. (2014). The human papillomavirus family and its role in carcinogenesis. *Semin Cancer Biol*, 26, 13-21. <https://doi.org/10.1016/j.semcancer.2013.11.002>
- Torre, L. A., Bray, F., Siegel, R. L., Ferlay, J., Lortet-Tieulent, J., & Jemal, A. (2015). Global cancer statistics, 2012. *CA Cancer J Clin*, 65(2), 87-108. <https://doi.org/10.3322/caac.21262>
- Torres-Poveda, K., Bahena-Román, M., Madrid-González, C., Burguete-García, A. I., Bermúdez-Morales, V. H., Peralta-Zaragoza, O., & Madrid-Marina, V. (2014). Role of IL-10 and TGF-β1 in local immunosuppression in HPV-associated cervical neoplasia. *World J Clin Oncol*, 5(4), 753-763. <https://doi.org/10.5306/wjco.v5.i4.753>

- Torres-Poveda, K., Burguete-Garcia, A. I., Bahena-Roman, M., Mendez-Martinez, R., Zurita-Diaz, M. A., Lopez-Estrada, G., Delgado-Romero, K., Peralta-Zaragoza, O., Bermudez-Morales, V. H., Cantu, D., Garcia-Carranca, A., & Madrid-Marina, V. (2016). Risk allelic load in Th2 and Th3 cytokines genes as biomarker of susceptibility to HPV-16 positive cervical cancer: a case control study. *BMC Cancer*, *16*, 330. <https://doi.org/10.1186/s12885-016-2364-4>
- Troen, A. M., Mitchell, B., Sorensen, B., Wener, M. H., Johnston, A., Wood, B., Selhub, J., McTiernan, A., Yasui, Y., Oral, E., Potter, J. D., & Ulrich, C. M. (2006). Unmetabolized folic acid in plasma is associated with reduced natural killer cell cytotoxicity among postmenopausal women. *J Nutr*, *136*(1), 189-194. <https://doi.org/10.1093/jn/136.1.189>
- Tryndyak, V. P., Han, T., Muskhelishvili, L., Fuscoe, J. C., Ross, S. A., Beland, F. A., & Pogribny, I. P. (2011). Coupling global methylation and gene expression profiles reveal key pathophysiological events in liver injury induced by a methyl-deficient diet. *Mol Nutr Food Res*, *55*(3), 411-418. <https://doi.org/10.1002/mnfr.201000300>
- Tsang, B. L., Devine, O. J., Cordero, A. M., Marchetta, C. M., Mulinare, J., Mersereau, P., Guo, J., Qi, Y. P., Berry, R. J., Rosenthal, J., Crider, K. S., & Hamner, H. C. (2015). Assessing the association between the methylenetetrahydrofolate reductase (MTHFR) 677C>T polymorphism and blood folate concentrations: a systematic review and meta-analysis of trials and observational studies. *Am J Clin Nutr*, *101*(6), 1286-1294. <https://doi.org/10.3945/ajcn.114.099994>
- Tsuchiya, S., Yamabe, M., Yamaguchi, Y., Kobayashi, Y., Konno, T., & Tada, K. (1980). Establishment and characterization of a human acute monocytic leukemia cell line (THP-1). *Int J Cancer*, *26*(2), 171-176.
- Tsujiuchi, T., Tsutsumi, M., Sasaki, Y., Takahama, M., & Konishi, Y. (1999). Hypomethylation of CpG sites and c-myc gene overexpression in hepatocellular carcinomas, but not hyperplastic nodules, induced by a choline-deficient L-amino acid-defined diet in rats. *Jpn J Cancer Res*, *90*(9), 909-913. <https://doi.org/10.1111/j.1349-7006.1999.tb00834.x>
- Tummers, B., Goedemans, R., Jha, V., Meyers, C., Melief, C. J. M., van der Burg, S. H., & Boer, J. M. (2014). CD40-mediated amplification of local immunity by epithelial cells is impaired by HPV. *J Invest Dermatol*, *134*(12), 2918-2927. <https://doi.org/10.1038/jid.2014.262>
- Uekawa, A., Katsushima, K., Ogata, A., Kawata, T., Maeda, N., Kobayashi, K., Maekawa, A., Tadokoro, T., & Yamamoto, Y. (2009). Change of epigenetic control of cystathionine beta-synthase gene expression through dietary vitamin B12 is not recovered by methionine supplementation. *J Nutrigenet Nutrigenomics*, *2*(1), 29-36. <https://doi.org/10.1159/000165374>
- Ueland, P. M. (2011). Choline and betaine in health and disease. *J Inherit Metab Dis*, *34*(1), 3-15. <https://doi.org/10.1007/s10545-010-9088-4>

- Vergnaud, A. C., Romaguera, D., Peeters, P. H., van Gils, C. H., Chan, D. S., Romieu, I., Freisling, H., Ferrari, P., Clavel-Chapelon, F., Fagherazzi, G., Dartois, L., Li, K., Tikk, K., Bergmann, M. M., Boeing, H., Tjønneland, A., Olsen, A., Overvad, K., Dahm, C. C., Redondo, M. L., Agudo, A., Sánchez, M. J., Amiano, P., Chirlaque, M. D., Ardanaz, E., Khaw, K. T., Wareham, N. J., Crowe, F., Trichopoulou, A., Orfanos, P., Trichopoulos, D., Masala, G., Sieri, S., Tumino, R., Vineis, P., Panico, S., Bueno-de-Mesquita, H. B., Ros, M. M., May, A., Wirfält, E., Sonestedt, E., Johansson, I., Hallmans, G., Lund, E., Weiderpass, E., Parr, C. L., Riboli, E., & Norat, T. (2013). Adherence to the World Cancer Research Fund/American Institute for Cancer Research guidelines and risk of death in Europe: results from the European Prospective Investigation into Nutrition and Cancer cohort study. *Am J Clin Nutr*, *97*(5), 1107-1120. <https://doi.org/10.3945/ajcn.112.049569>
- Verhoeven, Y., Tilborghs, S., Jacobs, J., De Waele, J., Quatannens, D., Deben, C., Prenen, H., Pauwels, P., Trinh, X. B., Wouters, A., Smits, E. L. J., Lardon, F., & van Dam, P. A. (2020). The potential and controversy of targeting STAT family members in cancer. *Semin Cancer Biol*, *60*, 41-56. <https://doi.org/10.1016/j.semcancer.2019.10.002>
- Verlaet, W., Snijders, P. J. F., Novianti, P. W., Wilting, S. M., De Strooper, L. M. A., Trooskens, G., Vandersmissen, J., Van Criekinge, W., Wisman, G. B. A., Meijer, C., Heideman, D. A. M., & Steenbergen, R. D. M. (2017). Genome-wide DNA methylation profiling reveals methylation markers associated with 3q gain for detection of cervical precancer and cancer. *Clin Cancer Res*, *23*(14), 3813-3822. <https://doi.org/10.1158/1078-0432.Ccr-16-2641>
- Verlaet, W., Van Leeuwen, R. W., Novianti, P. W., Schuurin, E., Meijer, C., Van Der Zee, A. G. J., Snijders, P. J. F., Heideman, D. A. M., Steenbergen, R. D. M., & Wisman, G. B. A. (2018). Host-cell DNA methylation patterns during high-risk HPV-induced carcinogenesis reveal a heterogeneous nature of cervical pre-cancer. *Epigenetics*, *13*(7), 769-778. <https://doi.org/10.1080/15592294.2018.1507197>
- Vidal, A. C., Grant, D. J., Williams, C. D., Masko, E., Allott, E. H., Shuler, K., McPhail, M., Gaines, A., Calloway, E., Gerber, L., Chi, J. T., Freedland, S. J., & Hoyo, C. (2012). Associations between intake of folate, methionine, and vitamins B12, B6 and prostate cancer risk in American veterans. *J Cancer Epidemiol*, *2012*, 957467. <https://doi.org/10.1155/2012/957467>
- Vila-del Sol, V., Punzón, C., & Fresno, M. (2008). IFN-gamma-induced TNF-alpha expression is regulated by interferon regulatory factors 1 and 8 in mouse macrophages. *J Immunol*, *181*(7), 4461-4470. <https://doi.org/10.4049/jimmunol.181.7.4461>
- Vilain, A., Bernardino, J., Gerbault-Seureau, M., Vogt, N., Niveleau, A., Lefrançois, D., Malfoy, B., & Dutrillaux, B. (2000). DNA methylation and chromosome instability in lymphoblastoid cell lines. *Cytogenetic and Genome Research*, *90*(1-2), 93-101. <https://doi.org/10.1159/000015641>

- Vilain, A., Vogt, N., Dutrillaux, B., & Malfoy, B. (1999). DNA methylation and chromosome instability in breast cancer cell lines. *FEBS Letters*, *460*(2), 231-234. [https://doi.org/https://doi.org/10.1016/S0014-5793\(99\)01358-7](https://doi.org/https://doi.org/10.1016/S0014-5793(99)01358-7)
- Vilgelm, A. E., Washington, M. K., Wei, J., Chen, H., Prassolov, V. S., & Zaika, A. I. (2010). Interactions of the p53 protein family in cellular stress response in gastrointestinal tumors. *Mol Cancer Ther*, *9*(3), 693-705. <https://doi.org/10.1158/1535-7163.mct-09-0912>
- Vineis, P., Chuang, S. C., Vaissiere, T., Cuenin, C., Ricceri, F., Johansson, M., Ueland, P., Brennan, P., & Herceg, Z. (2011). DNA methylation changes associated with cancer risk factors and blood levels of vitamin metabolites in a prospective study. *Epigenetics*, *6*(2), 195-201.
- Wagner, T. C., Velichko, S., Chesney, S. K., Biroc, S., Harde, D., Vogel, D., & Croze, E. (2004). Interferon receptor expression regulates the antiproliferative effects of interferons on cancer cells and solid tumors. *Int J Cancer*, *111*(1), 32-42. <https://doi.org/10.1002/ijc.20236>
- Wallace, K., Grau, M. V., Levine, A. J., Shen, L., Hamdan, R., Chen, X., Gui, J., Haile, R. W., Barry, E. L., Ahnen, D., McKeown-Eyssen, G., Baron, J. A., & Issa, J. P. (2010). Association between folate levels and CpG Island hypermethylation in normal colorectal mucosa. *Cancer Prev Res (Phila)*, *3*(12), 1552-1564. <https://doi.org/10.1158/1940-6207.Capr-10-0047>
- Wallin, K. L., Wiklund, F., Angström, T., Bergman, F., Stendahl, U., Wadell, G., Hallmans, G., & Dillner, J. (1999). Type-specific persistence of human papillomavirus DNA before the development of invasive cervical cancer. *N Engl J Med*, *341*(22), 1633-1638. <https://doi.org/10.1056/nejm199911253412201>
- Wang, X., Che, Y., Chen, B., Zhang, Y., Nakagawa, M., & Wang, X. (2018). Evaluation of immune responses induced by a novel human papillomavirus type 16 E7 peptide-based vaccine with Candida skin test reagent as an adjuvant in C57BL/6 mice. *Int Immunopharmacol*, *56*, 249-260. <https://doi.org/10.1016/j.intimp.2018.01.037>
- Warde-Farley, D., Donaldson, S. L., Comes, O., Zuberi, K., Badrawi, R., Chao, P., Franz, M., Grouios, C., Kazi, F., Lopes, C. T., Maitland, A., Mostafavi, S., Montojo, J., Shao, Q., Wright, G., Bader, G. D., & Morris, Q. (2010). The GeneMANIA prediction server: biological network integration for gene prioritization and predicting gene function. *Nucleic Acids Res*, *38*(Web Server issue), W214-220. <https://doi.org/10.1093/nar/gkq537>
- Warren, G. W., & Singh, A. K. (2013). Nicotine and lung cancer. *J Carcinog*, *12*, 1. <https://doi.org/10.4103/1477-3163.106680>

- Wasson, G. R., McGlynn, A. P., McNulty, H., O'Reilly, S. L., McKelvey-Martin, V. J., McKerr, G., Strain, J. J., Scott, J., & Downes, C. S. (2006). Global DNA and p53 region-specific hypomethylation in human colonic cells is induced by folate depletion and reversed by folate supplementation. *J Nutr*, *136*(11), 2748-2753. <https://doi.org/10.1093/jn/136.11.2748>
- Wei, E. K., Giovannucci, E., Selhub, J., Fuchs, C. S., Hankinson, S. E., & Ma, J. (2005). Plasma vitamin B6 and the risk of colorectal cancer and adenoma in women. *J Natl Cancer Inst*, *97*(9), 684-692. <https://doi.org/10.1093/jnci/dji116>
- Wentzensen, N., Sherman, M. E., Schiffman, M., & Wang, S. S. (2009). Utility of methylation markers in cervical cancer early detection: appraisal of the state-of-the-science. *Gynecol Oncol*, *112*(2), 293-299. <https://doi.org/10.1016/j.ygyno.2008.10.012>
- WHO. (2020). Human papillomavirus (HPV) and cervical cancer. World Health Organization. Retrieved 1 Aug 2021 from [https://www.who.int/news-room/fact-sheets/detail/human-papillomavirus-\(hpv\)-and-cervical-cancer](https://www.who.int/news-room/fact-sheets/detail/human-papillomavirus-(hpv)-and-cervical-cancer)
- Widschwendter, A., Tonko-Geymayer, S., Welte, T., Daxenbichler, G., Marth, C., & Doppler, W. (2002). Prognostic significance of signal transducer and activator of transcription 1 activation in breast cancer. *Clin Cancer Res*, *8*(10), 3065-3074.
- Wilding, S., Wighton, S., Halligan, D., West, R., Conner, M., & O'Connor, D. B. (2020). What factors are most influential in increasing cervical cancer screening attendance? An online study of UK-based women. *Health Psychology and Behavioral Medicine*, *8*(1), 314-328. <https://doi.org/10.1080/21642850.2020.1798239>
- Wilke, C. M., Hall, B. K., Hoge, A., Paradee, W., Smith, D. I., & Glover, T. W. (1996). FRA3B extends over a broad region and contains a spontaneous HPV16 integration site: direct evidence for the coincidence of viral integration sites and fragile sites. *Hum Mol Genet*, *5*(2), 187-195. <https://doi.org/10.1093/hmg/5.2.187>
- Wilson, A. S., Power, B. E., & Molloy, P. L. (2007). DNA hypomethylation and human diseases. *Biochimica et Biophysica Acta (BBA) - Reviews on Cancer*, *1775*(1), 138-162. <https://doi.org/https://doi.org/10.1016/j.bbcan.2006.08.007>
- Winer, R. L., Kiviat, N. B., Hughes, J. P., Adam, D. E., Lee, S. K., Kuypers, J. M., & Koutsky, L. A. (2005). Development and duration of human papillomavirus lesions, after initial infection. *J Infect Dis*, *191*(5), 731-738. <https://doi.org/10.1086/427557>
- Woodman, C. B., Collins, S. I., & Young, L. S. (2007). The natural history of cervical HPV infection: unresolved issues. *Nat Rev Cancer*, *7*(1), 11-22. <https://doi.org/10.1038/nrc2050>

- World Cancer Research Fund/American Institute for Cancer Research. (1997). Diet, nutrition, physical activity and cancer: a global perspective.
- World Cancer Research Fund/American Institute for Cancer Research. (2007). Diet, nutrition, physical activity and cancer: a global perspective. Continuous update project expert report.
- World Cancer Research Fund/American Institute for Cancer Research. (2018). Diet, nutrition, physical activity and cancer: a global perspective. Continuous update project report 2018. <https://www.wcrf.org/wp-content/uploads/2021/02/Summary-of-Third-Expert-Report-2018.pdf>
- Wu, C. H., Huang, T. C., & Lin, B. F. (2017). Folate deficiency affects dendritic cell function and subsequent T helper cell differentiation. *J Nutr Biochem*, *41*, 65-72. <https://doi.org/10.1016/j.jnutbio.2016.11.008>
- Wu, H., Liu, J., Li, W., Liu, G., & Li, Z. (2016). LncRNA-HOTAIR promotes TNF- α production in cardiomyocytes of LPS-induced sepsis mice by activating NF- κ B pathway. *Biochem Biophys Res Commun*, *471*(1), 240-246. <https://doi.org/10.1016/j.bbrc.2016.01.117>
- Wu, W., Kang, S., & Zhang, D. (2013). Association of vitamin B6, vitamin B12 and methionine with risk of breast cancer: a dose-response meta-analysis. *Br J Cancer*, *109*(7), 1926-1944. <https://doi.org/10.1038/bjc.2013.438>
- Wu, Z., & Zhao, P. (2018). Epigenetic alterations in anesthesia-induced neurotoxicity in the developing brain. *Front Physiol*, *9*, 1024. <https://doi.org/10.3389/fphys.2018.01024>
- Xu, W., Xu, M., Wang, L., Zhou, W., Xiang, R., Shi, Y., Zhang, Y., & Piao, Y. (2019). Integrative analysis of DNA methylation and gene expression identified cervical cancer-specific diagnostic biomarkers. *Signal Transduct Target Ther*, *4*, 55. <https://doi.org/10.1038/s41392-019-0081-6>
- Yamashita, K., Hosoda, K., Nishizawa, N., Katoh, H., & Watanabe, M. (2018). Epigenetic biomarkers of promoter DNA methylation in the new era of cancer treatment. *Cancer Sci*, *109*(12), 3695-3706. <https://doi.org/10.1111/cas.13812>
- Yang, H.-J. (2013). Aberrant DNA methylation in cervical carcinogenesis. *Chinese journal of cancer*, *32*(1), 42-48. <https://doi.org/10.5732/cjc.012.10033>
- Yang, N., Nijhuis, E. R., Volders, H. H., Eijnsink, J. J., Lendvai, A., Zhang, B., Hollema, H., Schuurin, E., Wisman, G. B., & van der Zee, A. G. (2010). Gene promoter methylation patterns throughout the process of cervical carcinogenesis. *Cell Oncol*, *32*(1-2), 131-143. <https://doi.org/10.3233/clo-2009-0510>

- Yang, S. H., Kong, S. K., Lee, S. H., Lim, S. Y., & Park, C. Y. (2014). Human papillomavirus 18 as a poor prognostic factor in stage I-IIA cervical cancer following primary surgical treatment. *Obstet Gynecol Sci*, 57(6), 492-500. <https://doi.org/10.5468/ogs.2014.57.6.492>
- Yi, K., Yang, L., Lan, Z., & Xi, M. (2016). The association between MTHFR polymorphisms and cervical cancer risk: a system review and meta analysis. *Arch Gynecol Obstet*, 294(3), 579-588. <https://doi.org/10.1007/s00404-016-4037-6>
- Yu, F., Xie, D., Ng, S. S., Lum, C. T., Cai, M. Y., Cheung, W. K., Kung, H. F., Lin, G., Wang, X., & Lin, M. C. (2015). IFITM1 promotes the metastasis of human colorectal cancer via CAV-1. *Cancer Lett*, 368(1), 135-143. <https://doi.org/10.1016/j.canlet.2015.07.034>
- Yu, W., Wang, Z., Zhang, K., Chi, Z., Xu, T., Jiang, D., Chen, S., Li, W., Yang, X., Zhang, X., Wu, Y., & Wang, D. (2019). One-carbon metabolism supports s-adenosylmethionine and histone methylation to drive inflammatory macrophages. *Mol Cell*, 75(6), 1147-1160.e1145. <https://doi.org/10.1016/j.molcel.2019.06.039>
- Yuan, Y., Cai, X., Shen, F., & Ma, F. (2021). HPV post-infection microenvironment and cervical cancer. *Cancer Lett*, 497, 243-254. <https://doi.org/10.1016/j.canlet.2020.10.034>
- Zeisel, S. (2017). Choline, other methyl-donors and epigenetics. *Nutrients*, 9(5). <https://doi.org/10.3390/nu9050445>
- Zeng, F. F., Xu, C. H., Liu, Y. T., Fan, Y. Y., Lin, X. L., Lu, Y. K., Zhang, C. X., & Chen, Y. M. (2014). Choline and betaine intakes are associated with reduced risk of nasopharyngeal carcinoma in adults: a case-control study. *Br J Cancer*, 110(3), 808-816. <https://doi.org/10.1038/bjc.2013.686>
- Zerbino, D. R., Achuthan, P., Akanni, W., Amode, M. R., Barrell, D., Bhai, J., Billis, K., Cummins, C., Gall, A., Giron, C. G., Gil, L., Gordon, L., Haggerty, L., Haskell, E., Hourlier, T., Izuogu, O. G., Janacek, S. H., Juettemann, T., To, J. K., Laird, M. R., Lavidas, I., Liu, Z., Loveland, J. E., Maurel, T., McLaren, W., Moore, B., Mudge, J., Murphy, D. N., Newman, V., Nuhn, M., Ogeh, D., Ong, C. K., Parker, A., Patricio, M., Riat, H. S., Schuilenburg, H., Sheppard, D., Sparrow, H., Taylor, K., Thormann, A., Vullo, A., Walts, B., Zadissa, A., Frankish, A., Hunt, S. E., Kostadima, M., Langridge, N., Martin, F. J., Muffato, M., Perry, E., Ruffier, M., Staines, D. M., Trevanion, S. J., Aken, B. L., Cunningham, F., Yates, A., & Flicek, P. (2018). Ensembl 2018. *Nucleic Acids Res*, 46(D1), D754-d761. <https://doi.org/10.1093/nar/gkx1098>
- Zhang, J. F., Chen, Y., Lin, G. S., Zhang, J. D., Tang, W. L., Huang, J. H., Chen, J. S., Wang, X. F., & Lin, Z. X. (2016). High IFIT1 expression predicts improved clinical outcome, and IFIT1 along with MGMT more accurately predicts prognosis in newly diagnosed glioblastoma. *Hum Pathol*, 52, 136-144. <https://doi.org/10.1016/j.humpath.2016.01.013>

- Zhang, N. (2018). Role of methionine on epigenetic modification of DNA methylation and gene expression in animals. *Anim Nutr*, 4(1), 11-16. <https://doi.org/10.1016/j.aninu.2017.08.009>
- Zhang, W., & Xu, J. (2017). DNA methyltransferases and their roles in tumorigenesis. *Biomark Res*, 5, 1-1. <https://doi.org/10.1186/s40364-017-0081-z>
- Zhang, X., Li, X., Tan, F., Yu, N., & Pei, H. (2017). STAT1 inhibits MiR-181a expression to suppress colorectal cancer cell proliferation through PTEN/Akt. *J Cell Biochem*, 118(10), 3435-3443. <https://doi.org/10.1002/jcb.26000>
- Zhang, Y., & Liu, Z. (2017). STAT1 in cancer: friend or foe? *Discov Med*, 24(130), 19-29.
- Zhang, Y., Molavi, O., Su, M., & Lai, R. (2014). The clinical and biological significance of STAT1 in esophageal squamous cell carcinoma. *BMC Cancer*, 14, 791. <https://doi.org/10.1186/1471-2407-14-791>
- Zhang, Y. F., Shi, W. W., Gao, H. F., Zhou, L., Hou, A. J., & Zhou, Y. H. (2014). Folate intake and the risk of breast cancer: a dose-response meta-analysis of prospective studies. *PLoS One*, 9(6), e100044. <https://doi.org/10.1371/journal.pone.0100044>
- Zhao, S. L., Zhu, S. T., Hao, X., Li, P., & Zhang, S. T. (2011). Effects of DNA methyltransferase 1 inhibition on esophageal squamous cell carcinoma. *Dis Esophagus*, 24(8), 601-610. <https://doi.org/10.1111/j.1442-2050.2011.01199.x>
- Zhao, Y., Guo, C., Hu, H., Zheng, L., Ma, J., Jiang, L., Zhao, E., & Li, H. (2017). Folate intake, serum folate levels and esophageal cancer risk: an overall and dose-response meta-analysis. *Oncotarget*, 8(6), 10458-10469. <https://doi.org/10.18632/oncotarget.14432>
- Zhou, H., Wang, Y., Lv, Q., Zhang, J., Wang, Q., Gao, F., Hou, H., Zhang, H., Zhang, W., & Li, L. (2016). Overexpression of ribosomal RNA in the development of human cervical cancer is associated with rDNA promoter hypomethylation. *PLoS One*, 11(10), e0163340. <https://doi.org/10.1371/journal.pone.0163340>
- Zhou, R. F., Chen, X. L., Zhou, Z. G., Zhang, Y. J., Lan, Q. Y., Liao, G. C., Chen, Y. M., & Zhu, H. L. (2017). Higher dietary intakes of choline and betaine are associated with a lower risk of primary liver cancer: a case-control study. *Sci Rep*, 7(1), 679. <https://doi.org/10.1038/s41598-017-00773-w>
- Zhou, W., Laird, P. W., & Shen, H. (2017). Comprehensive characterization, annotation and innovative use of Infinium DNA methylation BeadChip probes. *Nucleic Acids Res*, 45(4), e22. <https://doi.org/10.1093/nar/gkw967>

- Zhou, Z. Y., Wan, X. Y., & Cao, J. W. (2013). Dietary methionine intake and risk of incident colorectal cancer: a meta-analysis of 8 prospective studies involving 431,029 participants. *PLoS One*, 8(12), e83588. <https://doi.org/10.1371/journal.pone.0083588>
- Zielinski, G. D., Snijders, P. J., Rozendaal, L., Voorhorst, F. J., van der Linden, H. C., Runsink, A. P., de Schipper, F. A., & Meijer, C. J. (2001). HPV presence precedes abnormal cytology in women developing cervical cancer and signals false negative smears. *Br J Cancer*, 85(3), 398-404. <https://doi.org/10.1054/bjoc.2001.1926>
- Zuo, F., Liang, W., Ouyang, Y., Li, W., Lv, M., Wang, G., Ding, M., Wang, B., Zhao, S., Liu, J., Jiang, Z., & Li, M. (2011). Association of TNF- α gene promoter polymorphisms with susceptibility of cervical cancer in southwest China. *Laboratory Medicine*, 42(5), 287-290. <https://doi.org/10.1309/LM532DSPDUXIRJVN>
- zur Hausen, H. (2002). Papillomaviruses and cancer: from basic studies to clinical application. *Nat Rev Cancer*, 2(5), 342-350. <https://doi.org/10.1038/nrc798>
- zur Hausen, H. (2009). Papillomaviruses in the causation of human cancers - a brief historical account. *Virology*, 384(2), 260-265. <https://doi.org/10.1016/j.virol.2008.11.046>

APPENDIX

Appendix 1 Functional clustering analysis of upregulated DEGs from methyl donor depleted dataset



DAVID Bioinformatics Resources 6.8
Laboratory of Human Retrovirology and Immunoinformatics (LHRI)

*** Welcome to DAVID 6.8 ***

*** If you are looking for DAVID 6.7, please visit our development site. ***

Functional Annotation Clustering

[Help and Manual](#)

Current Gene List: List_1

Current Background: Homo sapiens

2869 DAVID IDs

Options Classification Stringency High

Rerun using options Create Sublist



















381 Cluster(s)

[Download File](#)

Annotation Cluster	Enrichment Score	GO Term	RT	Count	P_Value	Benjamini
Annotation Cluster 1	22.84					
<input type="checkbox"/> GOTERM_BP_ALL		cellular macromolecule metabolic process	RT	1497	2.3E-32	2.2E-28
<input type="checkbox"/> GOTERM_BP_ALL		macromolecule metabolic process	RT	1577	1.2E-26	2.8E-23
<input type="checkbox"/> GOTERM_BP_ALL		cellular metabolic process	RT	1713	1.2E-23	1.8E-20
<input type="checkbox"/> GOTERM_BP_ALL		organic substance metabolic process	RT	1763	7.6E-20	6.1E-17
<input type="checkbox"/> GOTERM_BP_ALL		primary metabolic process	RT	1698	9.1E-20	6.2E-17
<input type="checkbox"/> GOTERM_BP_ALL		metabolic process	RT	1813	1.0E-19	6.6E-17
Annotation Cluster 2	20.83					
<input type="checkbox"/> GOTERM_BP_ALL		RNA metabolic process	RT	904	7.6E-27	2.4E-23
<input type="checkbox"/> GOTERM_BP_ALL		nucleic acid metabolic process	RT	976	4.6E-25	8.8E-22
<input type="checkbox"/> GOTERM_BP_ALL		cellular nitrogen compound metabolic process	RT	1167	5.5E-22	7.5E-19
<input type="checkbox"/> GOTERM_BP_ALL		nitrogen compound metabolic process	RT	1227	8.3E-21	8.8E-18
<input type="checkbox"/> GOTERM_BP_ALL		nucleobase-containing compound metabolic process	RT	1052	9.0E-21	8.6E-18
<input type="checkbox"/> GOTERM_BP_ALL		heterocycle metabolic process	RT	1065	1.1E-19	6.5E-17
<input type="checkbox"/> GOTERM_BP_ALL		cellular aromatic compound metabolic process	RT	1069	3.6E-19	2.0E-16
<input type="checkbox"/> GOTERM_BP_ALL		organic cyclic compound metabolic process	RT	1084	1.6E-16	5.6E-14
Annotation Cluster 3	19.28					
<input type="checkbox"/> GOTERM_BP_ALL		regulation of macromolecule metabolic process	RT	1058	2.8E-21	3.4E-18
<input type="checkbox"/> GOTERM_BP_ALL		regulation of metabolic process	RT	1105	5.7E-20	5.0E-17
<input type="checkbox"/> GOTERM_BP_ALL		regulation of cellular metabolic process	RT	1054	8.9E-20	6.6E-17
<input type="checkbox"/> GOTERM_BP_ALL		regulation of primary metabolic process	RT	1042	6.3E-19	3.4E-16
Annotation Cluster 4	13.8					
<input type="checkbox"/> GOTERM_BP_ALL		protein ubiquitination	RT	195	2.5E-15	9.0E-13
<input type="checkbox"/> GOTERM_BP_ALL		protein modification by small protein conjugation or removal	RT	241	2.0E-14	6.7E-12
<input type="checkbox"/> GOTERM_BP_ALL		protein modification by small protein conjugation	RT	212	8.1E-14	2.2E-11
Annotation Cluster 5	12.88					
<input type="checkbox"/> GOTERM_BP_ALL		cellular macromolecule biosynthetic process	RT	904	1.3E-15	4.9E-13
<input type="checkbox"/> GOTERM_BP_ALL		cellular nitrogen compound biosynthetic process	RT	892	2.3E-15	8.9E-13
<input type="checkbox"/> GOTERM_BP_ALL		macromolecule biosynthetic process	RT	927	2.9E-15	1.0E-12
<input type="checkbox"/> GOTERM_BP_ALL		cellular biosynthetic process	RT	1048	6.6E-12	1.1E-9
<input type="checkbox"/> GOTERM_BP_ALL		organic substance biosynthetic process	RT	1061	1.8E-11	2.7E-9
<input type="checkbox"/> GOTERM_BP_ALL		biosynthetic process	RT	1070	8.1E-11	9.7E-9
Annotation Cluster 6	11.7					
<input type="checkbox"/> GOTERM_BP_ALL		macromolecule modification	RT	745	6.7E-14	1.9E-11
<input type="checkbox"/> GOTERM_BP_ALL		cellular protein modification process	RT	692	1.1E-11	1.7E-9
<input type="checkbox"/> GOTERM_BP_ALL		protein modification process	RT	692	1.1E-11	1.7E-9
Annotation Cluster 7	11.66					
<input type="checkbox"/> GOTERM_BP_ALL		regulation of gene expression	RT	802	5.0E-16	2.5E-13
<input type="checkbox"/> GOTERM_BP_ALL		transcription, DNA-templated	RT	675	2.2E-14	7.0E-12
<input type="checkbox"/> GOTERM_BP_ALL		regulation of nitrogen compound metabolic process	RT	800	3.7E-14	1.1E-11
<input type="checkbox"/> GOTERM_BP_ALL		nucleic acid-templated transcription	RT	698	7.9E-14	2.2E-11
<input type="checkbox"/> GOTERM_BP_ALL		regulation of cellular macromolecule biosynthetic process	RT	731	1.6E-13	3.8E-11

	Annotation Cluster	Enrichment Score			Count	P_Value	Benjamini
<input type="checkbox"/>	Annotation Cluster 1	22.84	G				
<input type="checkbox"/>	GOTERM_BP_ALL	regulation of macromolecule biosynthetic process	RT		749	1.7E-13	4.0E-11
<input type="checkbox"/>	GOTERM_BP_ALL	regulation of RNA metabolic process	RT		690	9.2E-13	1.9E-10
<input type="checkbox"/>	GOTERM_BP_ALL	RNA biosynthetic process	RT		709	3.3E-12	6.4E-10
<input type="checkbox"/>	GOTERM_BP_ALL	regulation of nucleobase-containing compound metabolic process	RT		740	3.9E-12	7.2E-10
<input type="checkbox"/>	GOTERM_BP_ALL	regulation of nucleic acid-templated transcription	RT		661	1.2E-11	1.8E-9
<input type="checkbox"/>	GOTERM_BP_ALL	regulation of RNA biosynthetic process	RT		663	1.7E-11	2.6E-9
<input type="checkbox"/>	GOTERM_BP_ALL	regulation of transcription, DNA-templated	RT		656	2.0E-11	3.0E-9
<input type="checkbox"/>	GOTERM_BP_ALL	heterocycle biosynthetic process	RT		782	2.4E-11	3.6E-9
<input type="checkbox"/>	GOTERM_BP_ALL	aromatic compound biosynthetic process	RT		784	2.5E-11	3.7E-9
<input type="checkbox"/>	GOTERM_BP_ALL	nucleobase-containing compound biosynthetic process	RT		772	4.4E-11	6.1E-9
<input type="checkbox"/>	GOTERM_BP_ALL	regulation of biosynthetic process	RT		769	4.9E-11	6.5E-9
<input type="checkbox"/>	GOTERM_BP_ALL	regulation of cellular biosynthetic process	RT		760	5.0E-11	6.6E-9
<input type="checkbox"/>	GOTERM_BP_ALL	organic cyclic compound biosynthetic process	RT		791	6.3E-10	6.0E-8
<input type="checkbox"/>	Annotation Cluster 8	10.75	G				
<input type="checkbox"/>	GOTERM_BP_ALL	programmed cell death	RT		377	1.4E-12	2.8E-10
<input type="checkbox"/>	GOTERM_BP_ALL	cell death	RT		393	3.4E-12	6.4E-10
<input type="checkbox"/>	GOTERM_BP_ALL	apoptotic process	RT		356	6.2E-12	1.1E-9
<input type="checkbox"/>	GOTERM_BP_ALL	regulation of apoptotic process	RT		291	8.6E-11	1.0E-8
<input type="checkbox"/>	GOTERM_BP_ALL	regulation of programmed cell death	RT		293	9.7E-11	1.1E-8
<input type="checkbox"/>	GOTERM_BP_ALL	regulation of cell death	RT		309	1.2E-10	1.3E-8
<input type="checkbox"/>	Annotation Cluster 9	10.73	G				
<input type="checkbox"/>	GOTERM_BP_ALL	response to biotic stimulus	RT		202	8.5E-12	1.4E-9
<input type="checkbox"/>	GOTERM_BP_ALL	response to other organism	RT		192	2.7E-11	3.9E-9
<input type="checkbox"/>	GOTERM_BP_ALL	response to external biotic stimulus	RT		192	2.7E-11	3.9E-9
<input type="checkbox"/>	Annotation Cluster 10	10.47	G				
<input type="checkbox"/>	GOTERM_BP_ALL	negative regulation of cellular metabolic process	RT		455	9.3E-12	1.5E-9
<input type="checkbox"/>	GOTERM_BP_ALL	negative regulation of macromolecule metabolic process	RT		449	3.1E-11	4.2E-9
<input type="checkbox"/>	GOTERM_BP_ALL	negative regulation of metabolic process	RT		477	1.4E-10	1.5E-8
<input type="checkbox"/>	Annotation Cluster 11	10.15	G				
<input type="checkbox"/>	GOTERM_BP_ALL	response to type I interferon	RT		37	2.8E-11	3.9E-9
<input type="checkbox"/>	GOTERM_BP_ALL	cellular response to type I interferon	RT		35	1.1E-10	1.3E-8
<input type="checkbox"/>	GOTERM_BP_ALL	type I interferon signaling pathway	RT		35	1.1E-10	1.3E-8
<input type="checkbox"/>	Annotation Cluster 12	8.38	G				
<input type="checkbox"/>	GOTERM_BP_ALL	multi-organism cellular process	RT		214	2.7E-10	2.8E-8
<input type="checkbox"/>	GOTERM_BP_ALL	viral process	RT		212	4.0E-10	4.0E-8
<input type="checkbox"/>	GOTERM_BP_ALL	symbiotic, encompassing mutualism through parasitism	RT		217	5.7E-10	5.5E-8
<input type="checkbox"/>	GOTERM_BP_ALL	interspecies interaction between organisms	RT		217	5.7E-10	5.5E-8
<input type="checkbox"/>	Annotation Cluster 13	8.3	G				
<input type="checkbox"/>	GOTERM_BP_ALL	negative regulation of gene expression	RT		307	4.5E-11	6.0E-9
<input type="checkbox"/>	GOTERM_BP_ALL	negative regulation of macromolecule biosynthetic process	RT		295	5.6E-11	7.1E-9
<input type="checkbox"/>	GOTERM_BP_ALL	negative regulation of RNA metabolic process	RT		261	2.6E-10	2.7E-8
<input type="checkbox"/>	GOTERM_BP_ALL	negative regulation of cellular biosynthetic process	RT		302	2.9E-10	3.0E-8
<input type="checkbox"/>	GOTERM_BP_ALL	negative regulation of RNA biosynthetic process	RT		252	4.3E-10	4.2E-8
<input type="checkbox"/>	GOTERM_BP_ALL	negative regulation of biosynthetic process	RT		305	5.0E-10	4.9E-8
<input type="checkbox"/>	GOTERM_BP_ALL	negative regulation of nitrogen compound metabolic process	RT		305	5.6E-10	5.3E-8
<input type="checkbox"/>	GOTERM_BP_ALL	negative regulation of cellular macromolecule biosynthetic process	RT		273	8.5E-10	7.8E-8
<input type="checkbox"/>	GOTERM_BP_ALL	negative regulation of nucleic acid-templated transcription	RT		246	1.9E-9	1.6E-7
<input type="checkbox"/>	GOTERM_BP_ALL	negative regulation of nucleobase-containing compound metabolic process	RT		278	3.4E-9	2.7E-7
<input type="checkbox"/>	GOTERM_BP_ALL	negative regulation of transcription, DNA-templated	RT		236	4.4E-9	3.5E-7
<input type="checkbox"/>	Annotation Cluster 14	8.88	G				
<input type="checkbox"/>	GOTERM_BP_ALL	positive regulation of macromolecule metabolic process	RT		532	1.0E-10	1.1E-8
<input type="checkbox"/>	GOTERM_BP_ALL	positive regulation of metabolic process	RT		556	1.3E-9	1.1E-7

	Annotation Cluster	Enrichment Score			Count	P_Value	Benjamini
<input type="checkbox"/>	GOTERM_BP_ALL	positive regulation of cellular metabolic process	RT		514	1.8E-8	1.3E-6
	Annotation Cluster 16	Enrichment Score: 8.37			Count	P_Value	Benjamini
<input type="checkbox"/>	GOTERM_BP_ALL	regulation of signal transduction	RT		511	1.2E-10	1.3E-8
<input type="checkbox"/>	GOTERM_BP_ALL	regulation of cell communication	RT		543	1.7E-8	1.2E-6
<input type="checkbox"/>	GOTERM_BP_ALL	regulation of signaling	RT		548	4.0E-8	2.6E-6
	Annotation Cluster 18	Enrichment Score: 8.34			Count	P_Value	Benjamini
<input type="checkbox"/>	GOTERM_BP_ALL	positive regulation of cell death	RT		143	3.8E-9	3.0E-7
<input type="checkbox"/>	GOTERM_BP_ALL	positive regulation of programmed cell death	RT		137	4.9E-9	3.8E-7
<input type="checkbox"/>	GOTERM_BP_ALL	positive regulation of apoptotic process	RT		136	5.1E-9	3.9E-7
	Annotation Cluster 17	Enrichment Score: 8.07			Count	P_Value	Benjamini
<input type="checkbox"/>	GOTERM_BP_ALL	proteolysis involved in cellular protein catabolic process	RT		153	2.4E-9	2.1E-7
<input type="checkbox"/>	GOTERM_BP_ALL	modification-dependent protein catabolic process	RT		139	3.6E-9	2.9E-7
<input type="checkbox"/>	GOTERM_BP_ALL	modification-dependent macromolecule catabolic process	RT		140	4.8E-9	3.8E-7
<input type="checkbox"/>	GOTERM_BP_ALL	cellular protein catabolic process	RT		157	7.0E-9	5.2E-7
<input type="checkbox"/>	GOTERM_BP_ALL	ubiquitin-dependent protein catabolic process	RT		136	9.1E-9	6.6E-7
<input type="checkbox"/>	GOTERM_BP_ALL	cellular macromolecule catabolic process	RT		205	3.3E-8	2.2E-6
<input type="checkbox"/>	GOTERM_BP_ALL	protein catabolic process	RT		176	3.5E-8	2.3E-6
	Annotation Cluster 18	Enrichment Score: 7.87			Count	P_Value	Benjamini
<input type="checkbox"/>	GOTERM_BP_ALL	positive regulation of innate immune response	RT		82	4.0E-9	3.2E-7
<input type="checkbox"/>	GOTERM_BP_ALL	activation of innate immune response	RT		72	1.3E-8	9.0E-7
<input type="checkbox"/>	GOTERM_BP_ALL	innate immune response-activating signal transduction	RT		69	4.8E-8	3.1E-6
	Annotation Cluster 19	Enrichment Score: 8.22			Count	P_Value	Benjamini
<input type="checkbox"/>	GOTERM_BP_ALL	positive regulation of signal transduction	RT		280	8.0E-8	5.0E-6
<input type="checkbox"/>	GOTERM_BP_ALL	positive regulation of cell communication	RT		293	1.6E-6	8.3E-5
<input type="checkbox"/>	GOTERM_BP_ALL	positive regulation of signaling	RT		294	1.7E-6	9.1E-5
	Annotation Cluster 20	Enrichment Score: 8.21			Count	P_Value	Benjamini
<input type="checkbox"/>	GOTERM_BP_ALL	regulation of viral process	RT		72	9.9E-8	6.0E-6
<input type="checkbox"/>	GOTERM_BP_ALL	regulation of symbiosis, encompassing mutualism through parasitism	RT		75	3.4E-7	2.0E-5
<input type="checkbox"/>	GOTERM_BP_ALL	regulation of multi-organism process	RT		88	7.1E-6	3.2E-4
	Annotation Cluster 21	Enrichment Score: 8.82			Count	P_Value	Benjamini
<input type="checkbox"/>	GOTERM_BP_ALL	negative regulation of response to stimulus	RT		271	5.7E-8	3.6E-6
<input type="checkbox"/>	GOTERM_BP_ALL	negative regulation of signal transduction	RT		217	8.6E-7	4.7E-5
<input type="checkbox"/>	GOTERM_BP_ALL	negative regulation of cell communication	RT		229	3.6E-6	1.8E-4
<input type="checkbox"/>	GOTERM_BP_ALL	negative regulation of signaling	RT		229	4.5E-6	2.2E-4
	Annotation Cluster 22	Enrichment Score: 6.86			Count	P_Value	Benjamini
<input type="checkbox"/>	GOTERM_BP_ALL	negative regulation of programmed cell death	RT		171	1.7E-6	9.0E-5
<input type="checkbox"/>	GOTERM_BP_ALL	negative regulation of cell death	RT		182	2.3E-6	1.2E-4
<input type="checkbox"/>	GOTERM_BP_ALL	negative regulation of apoptotic process	RT		168	2.9E-6	1.4E-4
	Annotation Cluster 23	Enrichment Score: 6.08			Count	P_Value	Benjamini
<input type="checkbox"/>	GOTERM_BP_ALL	regulation of kinase activity	RT		163	2.6E-6	1.3E-4
<input type="checkbox"/>	GOTERM_BP_ALL	regulation of transferase activity	RT		191	3.3E-6	1.6E-4
<input type="checkbox"/>	GOTERM_BP_ALL	regulation of protein kinase activity	RT		145	7.9E-5	2.8E-3
	Annotation Cluster 24	Enrichment Score: 6.04			Count	P_Value	Benjamini
<input type="checkbox"/>	GOTERM_BP_ALL	negative regulation of viral genome replication	RT		23	8.4E-7	4.6E-5
<input type="checkbox"/>	GOTERM_BP_ALL	regulation of viral genome replication	RT		30	1.8E-6	9.3E-5
<input type="checkbox"/>	GOTERM_BP_ALL	viral genome replication	RT		30	4.8E-4	1.3E-2
	Annotation Cluster 25	Enrichment Score: 6.01			Count	P_Value	Benjamini
<input type="checkbox"/>	GOTERM_BP_ALL	positive regulation of proteasomal ubiquitin-dependent protein catabolic process	RT		28	2.0E-6	1.0E-4
<input type="checkbox"/>	GOTERM_BP_ALL	regulation of proteasomal ubiquitin-dependent protein catabolic process	RT		36	6.0E-6	2.8E-4
<input type="checkbox"/>	GOTERM_BP_ALL	positive regulation of proteasomal protein catabolic process	RT		28	7.7E-5	2.8E-3
	Annotation Cluster 28	Enrichment Score: 4.88			Count	P_Value	Benjamini
<input type="checkbox"/>	GOTERM_BP_ALL	immune system development	RT		165	1.3E-5	5.4E-4
<input type="checkbox"/>	GOTERM_BP_ALL	hematopoietic or lymphoid organ development	RT		156	2.5E-5	1.0E-3
<input type="checkbox"/>	GOTERM_BP_ALL	hemopoiesis	RT		149	2.9E-5	1.2E-3
	Annotation Cluster 27	Enrichment Score: 4.32			Count	P_Value	Benjamini

Annotation Cluster 1		Enrichment Score: 22.84	G		Count	P_Value	Benjamini
<input type="checkbox"/>	GOTERM_BP_ALL	peptide biosynthetic process	RT		140	6.5E-6	3.0E-4
<input type="checkbox"/>	GOTERM_BP_ALL	translation	RT		135	8.0E-6	3.6E-4
<input type="checkbox"/>	GOTERM_BP_ALL	amide biosynthetic process	RT		148	3.6E-5	1.4E-3
<input type="checkbox"/>	GOTERM_BP_ALL	peptide metabolic process	RT		158	1.6E-4	5.2E-3
<input type="checkbox"/>	GOTERM_BP_ALL	cellular amide metabolic process	RT		182	8.1E-4	2.0E-2
Annotation Cluster 28		Enrichment Score: 4.22	G		Count	P_Value	Benjamini
<input type="checkbox"/>	GOTERM_BP_ALL	stress-activated protein kinase signaling cascade	RT		65	6.1E-6	2.8E-4
<input type="checkbox"/>	GOTERM_BP_ALL	stress-activated MAPK cascade	RT		62	9.8E-6	4.3E-4
<input type="checkbox"/>	GOTERM_BP_ALL	regulation of stress-activated protein kinase signaling cascade	RT		51	8.6E-5	3.1E-3
<input type="checkbox"/>	GOTERM_BP_ALL	regulation of stress-activated MAPK cascade	RT		50	1.5E-4	4.9E-3
<input type="checkbox"/>	GOTERM_BP_ALL	regulation of JNK cascade	RT		40	1.1E-3	2.5E-2
Annotation Cluster 28		Enrichment Score: 4.82	G		Count	P_Value	Benjamini
<input type="checkbox"/>	GOTERM_BP_ALL	positive regulation of gene expression	RT		312	4.8E-6	2.3E-4
<input type="checkbox"/>	GOTERM_BP_ALL	positive regulation of macromolecule biosynthetic process	RT		295	7.9E-6	3.6E-4
<input type="checkbox"/>	GOTERM_BP_ALL	positive regulation of nitrogen compound metabolic process	RT		316	5.3E-5	2.0E-3
<input type="checkbox"/>	GOTERM_BP_ALL	positive regulation of RNA metabolic process	RT		258	7.9E-5	2.9E-3
<input type="checkbox"/>	GOTERM_BP_ALL	positive regulation of nucleic acid-templated transcription	RT		247	8.8E-5	3.1E-3
<input type="checkbox"/>	GOTERM_BP_ALL	positive regulation of transcription, DNA-templated	RT		247	8.8E-5	3.1E-3
<input type="checkbox"/>	GOTERM_BP_ALL	positive regulation of RNA biosynthetic process	RT		250	9.5E-5	3.3E-3
<input type="checkbox"/>	GOTERM_BP_ALL	positive regulation of cellular biosynthetic process	RT		304	2.7E-4	8.2E-3
<input type="checkbox"/>	GOTERM_BP_ALL	positive regulation of biosynthetic process	RT		308	3.3E-4	9.4E-3
<input type="checkbox"/>	GOTERM_BP_ALL	positive regulation of nucleohase-containing compound metabolic process	RT		291	4.2E-4	1.1E-2
<input type="checkbox"/>	GOTERM_BP_ALL	positive regulation of transcription from RNA polymerase II promoter	RT		188	1.3E-3	2.8E-2
Annotation Cluster 30		Enrichment Score: 3.88	G		Count	P_Value	Benjamini
<input type="checkbox"/>	GOTERM_BP_ALL	activation of cysteine-type endopeptidase activity involved in apoptotic process	RT		29	2.7E-5	1.1E-3
<input type="checkbox"/>	GOTERM_BP_ALL	positive regulation of endopeptidase activity	RT		40	4.4E-5	1.7E-3
<input type="checkbox"/>	GOTERM_BP_ALL	positive regulation of peptidase activity	RT		42	8.5E-5	3.1E-3
<input type="checkbox"/>	GOTERM_BP_ALL	positive regulation of cysteine-type endopeptidase activity	RT		34	6.6E-4	1.7E-2
<input type="checkbox"/>	GOTERM_BP_ALL	positive regulation of cysteine-type endopeptidase activity involved in apoptotic process	RT		32	7.8E-4	1.9E-2
Annotation Cluster 31		Enrichment Score: 3.77	G		Count	P_Value	Benjamini
<input type="checkbox"/>	GOTERM_BP_ALL	cellular response to lipopolysaccharide	RT		40	1.6E-4	5.1E-3
<input type="checkbox"/>	GOTERM_BP_ALL	cellular response to biotic stimulus	RT		45	1.7E-4	5.4E-3
<input type="checkbox"/>	GOTERM_BP_ALL	cellular response to molecule of bacterial origin	RT		41	1.8E-4	5.7E-3
Annotation Cluster 32		Enrichment Score: 3.72	G		Count	P_Value	Benjamini
<input type="checkbox"/>	GOTERM_BP_ALL	protein localization to nucleus	RT		83	2.9E-5	1.2E-3
<input type="checkbox"/>	GOTERM_BP_ALL	protein import	RT		76	4.6E-5	1.7E-3
<input type="checkbox"/>	GOTERM_BP_ALL	nuclear import	RT		67	3.3E-4	9.5E-3
<input type="checkbox"/>	GOTERM_BP_ALL	protein import into nucleus	RT		63	4.6E-4	1.2E-2
<input type="checkbox"/>	GOTERM_BP_ALL	protein targeting to nucleus	RT		63	4.6E-4	1.2E-2
<input type="checkbox"/>	GOTERM_BP_ALL	single-organism nuclear import	RT		63	5.0E-4	1.3E-2
Annotation Cluster 33		Enrichment Score: 3.71	G		Count	P_Value	Benjamini
<input type="checkbox"/>	GOTERM_BP_ALL	regulation of cell migration	RT		139	4.0E-5	1.5E-3
<input type="checkbox"/>	GOTERM_BP_ALL	regulation of cell motility	RT		144	1.7E-4	5.5E-3
<input type="checkbox"/>	GOTERM_BP_ALL	regulation of locomotion	RT		148	2.9E-4	8.4E-3
<input type="checkbox"/>	GOTERM_BP_ALL	regulation of cellular component movement	RT		151	7.2E-4	1.8E-2
Annotation Cluster 34		Enrichment Score: 3.85	G		Count	P_Value	Benjamini
<input type="checkbox"/>	GOTERM_BP_ALL	erythrocyte homeostasis	RT		32	6.8E-5	2.5E-3
<input type="checkbox"/>	GOTERM_BP_ALL	myeloid cell homeostasis	RT		34	3.6E-4	9.9E-3
<input type="checkbox"/>	GOTERM_BP_ALL	erythrocyte differentiation	RT		28	4.6E-4	1.2E-2
Annotation Cluster 35		Enrichment Score: 3.82	G		Count	P_Value	Benjamini
<input type="checkbox"/>	GOTERM_BP_ALL	cellular response to hypoxia	RT		37	1.2E-4	3.9E-3
<input type="checkbox"/>	GOTERM_BP_ALL	cellular response to oxygen levels	RT		39	3.4E-4	9.6E-3
<input type="checkbox"/>	GOTERM_BP_ALL	cellular response to decreased oxygen levels	RT		37	3.5E-4	9.8E-3

	Annotation Cluster	Enrichment Score			Count	P_Value	Benjamini
	Annotation Cluster 38	Enrichment Score: 3.47	G				
<input type="checkbox"/>	GOTERM_BP_ALL	regulation of phosphorylation	RT		254	9.2E-5	3.2E-3
<input type="checkbox"/>	GOTERM_BP_ALL	regulation of phosphorus metabolic process	RT		283	4.8E-4	1.3E-2
<input type="checkbox"/>	GOTERM_BP_ALL	regulation of protein phosphorylation	RT		233	5.0E-4	1.3E-2
<input type="checkbox"/>	GOTERM_BP_ALL	regulation of phosphate metabolic process	RT		282	5.9E-4	1.5E-2
	Annotation Cluster 37	Enrichment Score: 3.41	G				
<input type="checkbox"/>	GOTERM_BP_ALL	negative regulation of phosphorylation	RT		90	3.1E-4	9.0E-3
<input type="checkbox"/>	GOTERM_BP_ALL	negative regulation of phosphate metabolic process	RT		110	3.1E-4	9.0E-3
<input type="checkbox"/>	GOTERM_BP_ALL	negative regulation of phosphorus metabolic process	RT		110	3.1E-4	9.0E-3
<input type="checkbox"/>	GOTERM_BP_ALL	negative regulation of protein phosphorylation	RT		82	7.4E-4	1.9E-2
	Annotation Cluster 38	Enrichment Score: 3.2	G				
<input type="checkbox"/>	GOTERM_BP_ALL	positive regulation of T cell cytokine production	RT		10	6.6E-5	2.4E-3
<input type="checkbox"/>	GOTERM_BP_ALL	T cell cytokine production	RT		12	6.0E-4	1.5E-2
<input type="checkbox"/>	GOTERM_BP_ALL	positive regulation of cytokine production involved in immune response	RT		13	1.7E-3	3.5E-2
<input type="checkbox"/>	GOTERM_BP_ALL	regulation of T cell cytokine production	RT		10	2.5E-3	4.8E-2
	Annotation Cluster 38	Enrichment Score: 3.16	G				
<input type="checkbox"/>	GOTERM_BP_ALL	activation of immune response	RT		110	4.8E-4	1.3E-2
<input type="checkbox"/>	GOTERM_BP_ALL	immune response-regulating signaling pathway	RT		106	6.4E-4	1.6E-2
<input type="checkbox"/>	GOTERM_BP_ALL	immune response-activating signal transduction	RT		99	1.1E-3	2.6E-2
	Annotation Cluster 40	Enrichment Score: 3.08	G				
<input type="checkbox"/>	GOTERM_BP_ALL	regulation of MAPK cascade	RT		133	2.8E-4	8.4E-3
<input type="checkbox"/>	GOTERM_BP_ALL	MAPK cascade	RT		156	1.1E-3	2.6E-2
<input type="checkbox"/>	GOTERM_BP_ALL	signal transduction by protein phosphorylation	RT		160	2.1E-3	4.2E-2
	Annotation Cluster 41	Enrichment Score: 2.98	G				
<input type="checkbox"/>	GOTERM_BP_ALL	response to oxygen levels	RT		68	8.0E-4	2.0E-2
<input type="checkbox"/>	GOTERM_BP_ALL	response to hypoxia	RT		63	8.1E-4	2.0E-2
<input type="checkbox"/>	GOTERM_BP_ALL	response to decreased oxygen levels	RT		63	1.8E-3	3.7E-2
	Annotation Cluster 42	Enrichment Score: 2.98	G				
<input type="checkbox"/>	GOTERM_BP_ALL	maturation of SSU-rRNA from tricistronic rRNA transcript (SSU-rRNA, 5.8S rRNA, LSU-rRNA)	RT		15	4.4E-4	1.2E-2
<input type="checkbox"/>	GOTERM_BP_ALL	maturation of SSU-rRNA	RT		17	9.1E-4	2.1E-2
<input type="checkbox"/>	GOTERM_BP_ALL	ribosomal small subunit biogenesis	RT		20	3.3E-3	6.0E-2
	Annotation Cluster 43	Enrichment Score: 2.8	G				
<input type="checkbox"/>	GOTERM_BP_ALL	positive regulation of stress-activated protein kinase signaling cascade	RT		37	4.0E-4	1.1E-2
<input type="checkbox"/>	GOTERM_BP_ALL	positive regulation of stress-activated MAPK cascade	RT		36	7.3E-4	1.8E-2
<input type="checkbox"/>	GOTERM_BP_ALL	positive regulation of JNK cascade	RT		29	6.5E-3	1.0E-1
	Annotation Cluster 44	Enrichment Score: 2.8	G				
<input type="checkbox"/>	GOTERM_BP_ALL	tRNA aminoacylation	RT		18	1.0E-3	2.4E-2
<input type="checkbox"/>	GOTERM_BP_ALL	amino acid activation	RT		18	1.3E-3	2.9E-2
<input type="checkbox"/>	GOTERM_BP_ALL	tRNA aminoacylation for protein translation	RT		17	1.5E-3	3.2E-2
	Annotation Cluster 45	Enrichment Score: 2.88	G				
<input type="checkbox"/>	GOTERM_BP_ALL	mitochondrial translational elongation	RT		25	8.8E-4	2.1E-2
<input type="checkbox"/>	GOTERM_BP_ALL	translational termination	RT		27	1.1E-3	2.5E-2
<input type="checkbox"/>	GOTERM_BP_ALL	mitochondrial translational termination	RT		24	2.4E-3	4.7E-2
	Annotation Cluster 48	Enrichment Score: 2.88	G				
<input type="checkbox"/>	GOTERM_BP_ALL	regulation of biological process	RT		1668	1.0E-3	2.4E-2
<input type="checkbox"/>	GOTERM_BP_ALL	regulation of cellular process	RT		1604	1.4E-3	3.0E-2
<input type="checkbox"/>	GOTERM_BP_ALL	biological regulation	RT		1744	7.5E-3	1.2E-1
	Annotation Cluster 47	Enrichment Score: 2.83	G				
<input type="checkbox"/>	GOTERM_BP_ALL	positive regulation of cell migration	RT		82	8.7E-4	2.1E-2
<input type="checkbox"/>	GOTERM_BP_ALL	positive regulation of cell motility	RT		82	2.5E-3	4.8E-2
<input type="checkbox"/>	GOTERM_BP_ALL	positive regulation of locomotion	RT		84	2.7E-3	5.1E-2
<input type="checkbox"/>	GOTERM_BP_ALL	positive regulation of cellular component movement	RT		82	5.0E-3	8.5E-2
	Annotation Cluster 48	Enrichment Score: 2.82	G				
<input type="checkbox"/>	GOTERM_BP_ALL	RNA splicing, via transesterification reactions	RT		64	2.2E-3	4.4E-2
<input type="checkbox"/>	GOTERM_BP_ALL	mRNA splicing, via spliceosome	RT		63	2.5E-3	4.8E-2

Appendix 2 Functional clustering analysis of downregulated DEGs from methyl donor depleted dataset



87.2%

*** Welcome to DAVID 6.8 ***
*** If you are looking for DAVID 6.7, please visit our [development site](#). ***

Functional Annotation Clustering

[Help and Manual](#)

Current Gene List: [List_1](#)
Current Background: [Homo sapiens](#)
1673 DAVID IDs

Options Classification Stringency [High](#) ▼
[Rerun using options](#) [Create Sublist](#)

316 Cluster(s)

[Download File](#)

Annotation Cluster	Enrichment Score	GO Term	RT	Bar	Count	P_Value	Benjamini
Annotation Cluster 1 Enrichment Score: 31.98 G							
<input type="checkbox"/> GOTERM_BP_ALL		mitotic cell cycle	RT		185	8.4E-34	6.1E-30
<input type="checkbox"/> GOTERM_BP_ALL		mitotic cell cycle process	RT		174	5.4E-33	2.0E-29
<input type="checkbox"/> GOTERM_BP_ALL		cell cycle process	RT		224	2.9E-31	5.2E-28
Annotation Cluster 2 Enrichment Score: 29.02 G							
<input type="checkbox"/> GOTERM_BP_ALL		nuclear division	RT		132	2.1E-31	5.2E-28
<input type="checkbox"/> GOTERM_BP_ALL		organelle fission	RT		135	3.8E-30	5.5E-27
<input type="checkbox"/> GOTERM_BP_ALL		mitotic nuclear division	RT		105	1.1E-27	1.1E-24
Annotation Cluster 3 Enrichment Score: 28.33 G							
<input type="checkbox"/> GOTERM_BP_ALL		chromosome segregation	RT		93	3.3E-29	4.0E-26
<input type="checkbox"/> GOTERM_BP_ALL		sister chromatid segregation	RT		71	4.8E-26	3.9E-23
<input type="checkbox"/> GOTERM_BP_ALL		nuclear chromosome segregation	RT		81	6.6E-26	4.8E-23
Annotation Cluster 4 Enrichment Score: 7.78 G							
<input type="checkbox"/> GOTERM_BP_ALL		negative regulation of mitotic cell cycle	RT		47	1.2E-10	2.9E-8
<input type="checkbox"/> GOTERM_BP_ALL		negative regulation of mitotic cell cycle phase transition	RT		35	8.4E-9	1.3E-6
<input type="checkbox"/> GOTERM_BP_ALL		negative regulation of cell cycle phase transition	RT		35	6.1E-8	7.9E-6
<input type="checkbox"/> GOTERM_BP_ALL		negative regulation of cell cycle process	RT		41	1.4E-6	1.4E-4
Annotation Cluster 5 Enrichment Score: 7.45 G							
<input type="checkbox"/> GOTERM_BP_ALL		spindle checkpoint	RT		18	7.0E-10	1.5E-7
<input type="checkbox"/> GOTERM_BP_ALL		regulation of mitotic sister chromatid separation	RT		20	7.9E-10	1.6E-7
<input type="checkbox"/> GOTERM_BP_ALL		metaphase/anaphase transition of cell cycle	RT		20	1.2E-9	2.3E-7
<input type="checkbox"/> GOTERM_BP_ALL		regulation of mitotic sister chromatid segregation	RT		21	1.6E-9	2.8E-7
<input type="checkbox"/> GOTERM_BP_ALL		chromosome segregation	RT		24	1.6E-9	2.9E-7
<input type="checkbox"/> GOTERM_BP_ALL		mitotic sister chromatid separation	RT		20	1.8E-9	3.0E-7
<input type="checkbox"/> GOTERM_BP_ALL		regulation of mitotic metaphase/anaphase transition	RT		19	2.8E-9	4.6E-7
<input type="checkbox"/> GOTERM_BP_ALL		metaphase/anaphase transition of mitotic cell cycle	RT		18	2.8E-9	4.5E-7
<input type="checkbox"/> GOTERM_BP_ALL		regulation of metaphase/anaphase transition of cell cycle	RT		19	4.2E-9	6.5E-7
<input type="checkbox"/> GOTERM_BP_ALL		regulation of sister chromatid segregation	RT		22	9.2E-9	1.4E-6
<input type="checkbox"/> GOTERM_BP_ALL		negative regulation of sister chromatid segregation	RT		15	2.0E-7	2.2E-5
<input type="checkbox"/> GOTERM_BP_ALL		negative regulation of chromosome segregation	RT		15	2.9E-7	3.3E-5
<input type="checkbox"/> GOTERM_BP_ALL		negative regulation of mitotic sister chromatid separation	RT		14	3.1E-7	3.4E-5
<input type="checkbox"/> GOTERM_BP_ALL		mitotic spindle checkpoint	RT		14	3.1E-7	3.4E-5
<input type="checkbox"/> GOTERM_BP_ALL		negative regulation of mitotic metaphase/anaphase transition	RT		14	3.1E-7	3.4E-5
<input type="checkbox"/> GOTERM_BP_ALL		negative regulation of metaphase/anaphase transition of cell cycle	RT		14	4.6E-7	5.1E-5
<input type="checkbox"/> GOTERM_BP_ALL		negative regulation of mitotic sister chromatid segregation	RT		14	6.9E-7	7.4E-5
<input type="checkbox"/> GOTERM_BP_ALL		negative regulation of mitotic nuclear division	RT		14	1.3E-5	9.2E-4
<input type="checkbox"/> GOTERM_BP_ALL		negative regulation of nuclear division	RT		15	4.8E-5	2.6E-3
Annotation Cluster 8 Enrichment Score: 7.08 G							
<input type="checkbox"/> GOTERM_BP_ALL		meiotic cell cycle	RT		44	2.0E-8	2.8E-6
<input type="checkbox"/> GOTERM_BP_ALL		meiotic nuclear division	RT		36	1.5E-7	1.9E-5

	Enrichment Score: 31.88			Count	P_Value	Benjamini
<input type="checkbox"/> Annotation Cluster 1						
<input type="checkbox"/> GOTERM_BP_ALL	meiotic cell cycle process	RT		37	1.7E-7	2.1E-5
<input type="checkbox"/> Annotation Cluster 7	Enrichment Score: 8.32					
<input type="checkbox"/> GOTERM_BP_ALL	carboxylic acid catabolic process	RT		39	3.7E-8	4.8E-6
<input type="checkbox"/> GOTERM_BP_ALL	organic acid catabolic process	RT		41	1.7E-7	2.1E-5
<input type="checkbox"/> GOTERM_BP_ALL	small molecule catabolic process	RT		49	1.7E-5	1.1E-3
<input type="checkbox"/> Annotation Cluster 8	Enrichment Score: 6.62					
<input type="checkbox"/> GOTERM_BP_ALL	cilium organization	RT		40	8.8E-7	8.9E-5
<input type="checkbox"/> GOTERM_BP_ALL	cilium morphogenesis	RT		41	3.0E-6	2.7E-4
<input type="checkbox"/> GOTERM_BP_ALL	cilium assembly	RT		35	1.1E-5	8.0E-4
<input type="checkbox"/> Annotation Cluster 9	Enrichment Score: 6.4					
<input type="checkbox"/> GOTERM_BP_ALL	macromolecular complex assembly	RT		185	1.7E-7	2.0E-5
<input type="checkbox"/> GOTERM_BP_ALL	protein complex assembly	RT		155	3.5E-6	3.1E-4
<input type="checkbox"/> GOTERM_BP_ALL	protein complex biogenesis	RT		155	3.7E-6	3.2E-4
<input type="checkbox"/> GOTERM_BP_ALL	protein complex subunit organization	RT		166	1.2E-4	5.7E-3
<input type="checkbox"/> Annotation Cluster 10	Enrichment Score: 4.91					
<input type="checkbox"/> GOTERM_BP_ALL	cholesterol biosynthetic process	RT		16	1.3E-6	1.2E-4
<input type="checkbox"/> GOTERM_BP_ALL	secondary alcohol biosynthetic process	RT		16	1.7E-6	1.6E-4
<input type="checkbox"/> GOTERM_BP_ALL	sterol biosynthetic process	RT		16	6.5E-6	5.2E-4
<input type="checkbox"/> GOTERM_BP_ALL	alcohol biosynthetic process	RT		18	1.6E-3	5.4E-2
<input type="checkbox"/> Annotation Cluster 11	Enrichment Score: 4.8					
<input type="checkbox"/> GOTERM_BP_ALL	establishment of chromosome localization	RT		18	9.5E-6	7.3E-4
<input type="checkbox"/> GOTERM_BP_ALL	chromosome localization	RT		18	1.2E-5	8.5E-4
<input type="checkbox"/> GOTERM_BP_ALL	metaphase plate congression	RT		14	3.6E-5	2.1E-3
<input type="checkbox"/> Annotation Cluster 12	Enrichment Score: 4.38					
<input type="checkbox"/> GOTERM_BP_ALL	centromere complex assembly	RT		17	1.2E-6	1.2E-4
<input type="checkbox"/> GOTERM_BP_ALL	chromatin remodeling at centromere	RT		14	2.8E-5	1.8E-3
<input type="checkbox"/> GOTERM_BP_ALL	DNA replication-independent nucleosome assembly	RT		15	3.1E-5	1.9E-3
<input type="checkbox"/> GOTERM_BP_ALL	DNA replication-independent nucleosome organization	RT		15	3.9E-5	2.3E-3
<input type="checkbox"/> GOTERM_BP_ALL	CFNP-A containing nucleosome assembly	RT		13	5.2E-5	2.8E-3
<input type="checkbox"/> GOTERM_BP_ALL	CFNP-A containing chromatin organization	RT		13	5.2E-5	2.8E-3
<input type="checkbox"/> GOTERM_BP_ALL	histone exchange	RT		15	8.9E-5	4.5E-3
<input type="checkbox"/> GOTERM_BP_ALL	ATP-dependent chromatin remodeling	RT		16	7.9E-4	3.0E-2
<input type="checkbox"/> Annotation Cluster 13	Enrichment Score: 4.37					
<input type="checkbox"/> GOTERM_BP_ALL	catabolic process	RT		200	1.7E-5	1.2E-3
<input type="checkbox"/> GOTERM_BP_ALL	cellular catabolic process	RT		164	3.9E-5	2.2E-3
<input type="checkbox"/> GOTERM_BP_ALL	organic substance catabolic process	RT		184	1.2E-4	5.8E-3
<input type="checkbox"/> Annotation Cluster 14	Enrichment Score: 4.36					
<input type="checkbox"/> GOTERM_BP_ALL	organic acid metabolic process	RT		102	3.4E-5	2.0E-3
<input type="checkbox"/> GOTERM_BP_ALL	carboxylic acid metabolic process	RT		94	4.6E-5	2.5E-3
<input type="checkbox"/> GOTERM_BP_ALL	oxoacid metabolic process	RT		94	5.7E-5	3.0E-3
<input type="checkbox"/> Annotation Cluster 15	Enrichment Score: 4.2					
<input type="checkbox"/> GOTERM_BP_ALL	secondary alcohol metabolic process	RT		24	2.9E-5	1.8E-3
<input type="checkbox"/> GOTERM_BP_ALL	cholesterol metabolic process	RT		23	3.9E-5	2.3E-3
<input type="checkbox"/> GOTERM_BP_ALL	sterol metabolic process	RT		23	2.3E-4	1.0E-2
<input type="checkbox"/> Annotation Cluster 16	Enrichment Score: 3.84					
<input type="checkbox"/> GOTERM_BP_ALL	reproductive process	RT		141	8.7E-5	4.4E-3
<input type="checkbox"/> GOTERM_BP_ALL	reproduction	RT		141	9.1E-5	4.6E-3
<input type="checkbox"/> GOTERM_BP_ALL	single organism reproductive process	RT		121	1.5E-3	5.1E-2
<input type="checkbox"/> Annotation Cluster 17	Enrichment Score: 3.34					
<input type="checkbox"/> GOTERM_BP_ALL	peptide metabolic process	RT		93	5.2E-5	2.8E-3
<input type="checkbox"/> GOTERM_BP_ALL	translation	RT		73	3.5E-4	1.5E-2
<input type="checkbox"/> GOTERM_BP_ALL	peptide biosynthetic process	RT		75	4.2E-4	1.8E-2
<input type="checkbox"/> GOTERM_BP_ALL	cellular amide metabolic process	RT		101	1.5E-3	5.0E-2
<input type="checkbox"/> GOTERM_BP_ALL	amide biosynthetic process	RT		78	1.7E-3	5.6E-2
<input type="checkbox"/> Annotation Cluster 18	Enrichment Score: 3.32					
<input type="checkbox"/> GOTERM_BP_ALL	fatty acid catabolic process	RT		20	1.9E-5	1.2E-3
<input type="checkbox"/> GOTERM_BP_ALL	fatty acid beta-oxidation	RT		17	3.9E-5	2.2E-3
<input type="checkbox"/> GOTERM_BP_ALL	fatty acid oxidation	RT		20	6.8E-5	3.6E-3

Appendix 3 Functional clustering analysis of common DEGs between methyl donor depleted and Epi-stage of HPV integration dataset



DAVID Bioinformatics Resources 6.8
Laboratory of Human Retrovirology and Immunoinformatics (LHRI)

*** Welcome to DAVID 6.8 ***

*** If you are looking for DAVID 6.7, please visit our [development site](#). ***

Functional Annotation Clustering

[Help and Manual](#)

Current Gene List: List_1

Current Background: Homo sapiens

565 DAVID IDs

Options Classification Stringency High

Rerun using options

Create Sublist

226 Cluster(s)

[Download File](#)

Annotation Cluster	Enrichment Score	GO Term	Count	P-Value	Benjamini
Annotation Cluster 1	Enrichment Score: 8.02				
<input type="checkbox"/> GOTERM_BP_ALL	interspecies interaction between organisms	RT	66	6.6E-10	6.2E-7
<input type="checkbox"/> GOTERM_BP_ALL	symbiosis, encompassing mutualism through parasitism	RT	66	6.6E-10	6.2E-7
<input type="checkbox"/> GOTERM_BP_ALL	viral process	RT	64	1.2E-9	9.7E-7
<input type="checkbox"/> GOTERM_BP_ALL	multi-organism cellular process	RT	64	1.6E-9	1.1E-6
Annotation Cluster 2	Enrichment Score: 8.00				
<input type="checkbox"/> GOTERM_BP_ALL	organellar fission	RT	47	5.8E-9	2.7E-6
<input type="checkbox"/> GOTERM_BP_ALL	nuclear division	RT	45	6.9E-9	3.0E-6
<input type="checkbox"/> GOTERM_BP_ALL	mitotic nuclear division	RT	37	1.3E-8	4.4E-6
Annotation Cluster 3	Enrichment Score: 8.00				
<input type="checkbox"/> GOTERM_BP_ALL	response to biotic stimulus	RT	58	7.8E-9	3.1E-6
<input type="checkbox"/> GOTERM_BP_ALL	response to external biotic stimulus	RT	56	8.4E-9	2.9E-6
<input type="checkbox"/> GOTERM_BP_ALL	response to other organism	RT	56	8.4E-9	2.9E-6
Annotation Cluster 4	Enrichment Score: 7.84				
<input type="checkbox"/> GOTERM_BP_ALL	response to type I interferon	RT	16	5.7E-9	2.9E-6
<input type="checkbox"/> GOTERM_BP_ALL	cellular response to type I interferon	RT	15	2.3E-8	7.2E-6
<input type="checkbox"/> GOTERM_BP_ALL	type I interferon signaling pathway	RT	15	2.3E-8	7.2E-6
Annotation Cluster 6	Enrichment Score: 8.82				
<input type="checkbox"/> GOTERM_BP_ALL	interferon-gamma-mediated signaling pathway	RT	16	8.2E-9	3.1E-6
<input type="checkbox"/> GOTERM_BP_ALL	response to interferon-gamma	RT	20	2.2E-7	6.3E-5
<input type="checkbox"/> GOTERM_BP_ALL	cellular response to interferon-gamma	RT	17	1.9E-6	4.1E-4
Annotation Cluster 8	Enrichment Score: 8.03				
<input type="checkbox"/> GOTERM_BP_ALL	response to cytokine	RT	51	2.9E-7	7.8E-5
<input type="checkbox"/> GOTERM_BP_ALL	cytokine-mediated signaling pathway	RT	40	3.1E-7	8.1E-5
<input type="checkbox"/> GOTERM_BP_ALL	cellular response to cytokine stimulus	RT	43	8.7E-6	1.5E-3
Annotation Cluster 7	Enrichment Score: 6.00				
<input type="checkbox"/> GOTERM_BP_ALL	chromosome segregation	RT	27	5.2E-6	1.1E-3
<input type="checkbox"/> GOTERM_BP_ALL	sister chromatid segregation	RT	21	8.8E-6	1.5E-3
<input type="checkbox"/> GOTERM_BP_ALL	nuclear chromosome segregation	RT	24	1.1E-5	1.8E-3
Annotation Cluster 8	Enrichment Score: 4.47				
<input type="checkbox"/> GOTERM_BP_ALL	regulation of cell communication	RT	125	1.8E-5	2.7E-3
<input type="checkbox"/> GOTERM_BP_ALL	regulation of signal transduction	RT	114	3.4E-5	4.5E-3
<input type="checkbox"/> GOTERM_BP_ALL	regulation of signaling	RT	124	6.1E-5	7.4E-3
Annotation Cluster 9	Enrichment Score: 4.21				
<input type="checkbox"/> GOTERM_BP_ALL	regulation of viral process	RT	22	2.7E-5	3.8E-3
<input type="checkbox"/> GOTERM_BP_ALL	regulation of symbiosis, encompassing mutualism through parasitism	RT	23	3.1E-5	4.2E-3
<input type="checkbox"/> GOTERM_BP_ALL	regulation of multi-organism process	RT	25	2.8E-4	2.6E-2
Annotation Cluster 10	Enrichment Score: 3.47				
<input type="checkbox"/> GOTERM_BP_ALL	cellular response to oxygen levels	RT	15	1.1E-4	1.2E-2
<input type="checkbox"/> GOTERM_BP_ALL	cellular response to hypoxia	RT	13	4.6E-4	3.4E-2
<input type="checkbox"/> GOTERM_BP_ALL	cellular response to decreased oxygen levels	RT	13	7.4E-4	4.8E-2
Annotation Cluster 11	Enrichment Score: 3.2				
<input type="checkbox"/> GOTERM_BP_ALL	response to oxygen levels	RT	22	3.5E-4	2.8E-2
<input type="checkbox"/> GOTERM_BP_ALL	response to hypoxia	RT	20	7.1E-4	4.7E-2

<input type="checkbox"/>	GOTERM_BP_ALL	response to decreased oxygen levels	RT		20	1.0E-3	5.9E-2					
	Annotation Cluster 12	Enrichment Score: 3.16	G		Count	P_Value	Benjamini					
<input type="checkbox"/>	GOTERM_BP_ALL	protein complex subunit organization	RT		75	1.5E-4	1.5E-2					
<input type="checkbox"/>	GOTERM_BP_ALL	protein complex assembly	RT		63	1.1E-3	6.3E-2					
<input type="checkbox"/>	GOTERM_BP_ALL	protein complex biogenesis	RT		63	1.2E-3	6.3E-2					
<input type="checkbox"/>	GOTERM_BP_ALL	macromolecular complex assembly	RT		72	1.2E-3	6.5E-2					
	Annotation Cluster 13	Enrichment Score: 3.11	G		Count	P_Value	Benjamini					
<input type="checkbox"/>	GOTERM_BP_ALL	catabolic process	RT		85	3.4E-4	2.9E-2					
<input type="checkbox"/>	GOTERM_BP_ALL	organic substance catabolic process	RT		79	7.9E-4	4.9E-2					
<input type="checkbox"/>	GOTERM_BP_ALL	cellular catabolic process	RT		68	1.8E-3	7.8E-2					
	Annotation Cluster 14	Enrichment Score: 2.81	G		Count	P_Value	Benjamini					
<input type="checkbox"/>	GOTERM_BP_ALL	metabolic process	RT		357	3.5E-4	2.8E-2					
<input type="checkbox"/>	GOTERM_BP_ALL	cellular metabolic process	RT		332	4.9E-4	3.6E-2					
<input type="checkbox"/>	GOTERM_BP_ALL	organic substance metabolic process	RT		343	1.3E-3	6.8E-2					
<input type="checkbox"/>	GOTERM_BP_ALL	primary metabolic process	RT		323	1.0E-2	2.2E-1					
	Annotation Cluster 15	Enrichment Score: 2.83	G		Count	P_Value	Benjamini					
<input type="checkbox"/>	GOTERM_BP_ALL	protein ubiquitination	RT		39	1.0E-3	5.9E-2					
<input type="checkbox"/>	GOTERM_BP_ALL	protein modification by small protein conjugation or removal	RT		48	1.4E-3	7.0E-2					
<input type="checkbox"/>	GOTERM_BP_ALL	protein modification by small protein conjugation	RT		42	2.2E-3	8.8E-2					
	Annotation Cluster 18	Enrichment Score: 2.87	G		Count	P_Value	Benjamini					
<input type="checkbox"/>	GOTERM_BP_ALL	interferon-beta production	RT		7	1.4E-3	6.9E-2					
<input type="checkbox"/>	GOTERM_BP_ALL	regulation of interferon-beta production	RT		7	1.8E-3	7.8E-2					
<input type="checkbox"/>	GOTERM_BP_ALL	positive regulation of interferon-beta production	RT		6	1.8E-3	7.9E-2					
<input type="checkbox"/>	GOTERM_BP_ALL	positive regulation of type I interferon production	RT		8	4.4E-3	1.4E-1					
	Annotation Cluster 17	Enrichment Score: 2.82	G		Count	P_Value	Benjamini					
<input type="checkbox"/>	GOTERM_BP_ALL	apoptotic process	RT		73	1.4E-3	6.8E-2					
<input type="checkbox"/>	GOTERM_BP_ALL	regulation of apoptotic process	RT		61	1.4E-3	7.0E-2					
<input type="checkbox"/>	GOTERM_BP_ALL	regulation of programmed cell death	RT		61	1.7E-3	7.7E-2					
<input type="checkbox"/>	GOTERM_BP_ALL	programmed cell death	RT		75	2.6E-3	1.0E-1					
<input type="checkbox"/>	GOTERM_BP_ALL	regulation of cell death	RT		63	3.2E-3	1.1E-1					
<input type="checkbox"/>	GOTERM_BP_ALL	cell death	RT		76	7.0E-3	1.8E-1					
	Annotation Cluster 18	Enrichment Score: 2.68	G		Count	P_Value	Benjamini					
<input type="checkbox"/>	GOTERM_BP_ALL	positive regulation of cell communication	RT		66	1.7E-3	7.6E-2					
<input type="checkbox"/>	GOTERM_BP_ALL	positive regulation of signaling	RT		66	1.9E-3	8.2E-2					
<input type="checkbox"/>	GOTERM_BP_ALL	positive regulation of signal transduction	RT		59	5.6E-3	1.6E-1					
	Annotation Cluster 19	Enrichment Score: 2.68	G		Count	P_Value	Benjamini					
<input type="checkbox"/>	GOTERM_BP_ALL	pattern recognition receptor signaling pathway	RT		17	1.6E-5	2.4E-3					
<input type="checkbox"/>	GOTERM_BP_ALL	positive regulation of innate immune response	RT		22	1.3E-4	1.4E-2					
<input type="checkbox"/>	GOTERM_BP_ALL	activation of innate immune response	RT		19	3.8E-4	2.9E-2					
<input type="checkbox"/>	GOTERM_BP_ALL	innate immune response-activating signal transduction	RT		18	7.6E-4	4.9E-2					
<input type="checkbox"/>	GOTERM_BP_ALL	positive regulation of defense response	RT		24	1.6E-3	7.5E-2					
<input type="checkbox"/>	GOTERM_BP_ALL	activation of immune response	RT		25	3.2E-2	4.1E-1					
<input type="checkbox"/>	GOTERM_BP_ALL	positive regulation of immune response	RT		29	4.2E-2	4.6E-1					
<input type="checkbox"/>	GOTERM_BP_ALL	immune response-activating signal transduction	RT		22	5.6E-2	5.2E-1					
<input type="checkbox"/>	GOTERM_BP_ALL	immune response-regulating signaling pathway	RT		22	9.4E-2	6.2E-1					
	Annotation Cluster 20	Enrichment Score: 2.65	G		Count	P_Value	Benjamini					
<input type="checkbox"/>	GOTERM_BP_ALL	regulation of protein serine/threonine kinase activity	RT		29	3.3E-4	2.8E-2					
<input type="checkbox"/>	GOTERM_BP_ALL	regulation of transferase activity	RT		44	2.8E-3	1.0E-1					
<input type="checkbox"/>	GOTERM_BP_ALL	regulation of protein kinase activity	RT		34	8.0E-3	1.9E-1					
<input type="checkbox"/>	GOTERM_BP_ALL	regulation of kinase activity	RT		36	8.3E-3	1.9E-1					
	Annotation Cluster 21	Enrichment Score: 2.48	G		Count	P_Value	Benjamini					
<input type="checkbox"/>	GOTERM_BP_ALL	xenobiotic metabolic process	RT		10	2.2E-3	8.8E-2					
<input type="checkbox"/>	GOTERM_BP_ALL	cellular response to xenobiotic stimulus	RT		10	3.0E-3	1.1E-1					
<input type="checkbox"/>	GOTERM_BP_ALL	response to xenobiotic stimulus	RT		10	5.0E-3	1.5E-1					
	Annotation Cluster 22	Enrichment Score: 2.38	G		Count	P_Value	Benjamini					
<input type="checkbox"/>	GOTERM_BP_ALL	negative regulation of apoptotic process	RT		39	2.9E-3	1.1E-1					

<input type="checkbox"/>	GOTERM_BP_ALL	negative regulation of programmed cell death	RT		39	3.6E-3	1.2E-1
<input type="checkbox"/>	GOTERM_BP_ALL	negative regulation of cell death	RT		40	7.8E-3	1.9E-1
	Annotation Cluster 23	Enrichment Score: 2.31	G		Count	P_Value	Benjamini
<input type="checkbox"/>	GOTERM_BP_ALL	immune system development	RT		39	3.2E-3	1.1E-1
<input type="checkbox"/>	GOTERM_BP_ALL	hematopoietic or lymphoid organ development	RT		37	4.0E-3	1.3E-1
<input type="checkbox"/>	GOTERM_BP_ALL	hemopoiesis	RT		34	9.4E-3	2.0E-1
	Annotation Cluster 24	Enrichment Score: 2.18	G		Count	P_Value	Benjamini
<input type="checkbox"/>	GOTERM_BP_ALL	regulation of protein phosphorylation	RT		56	3.0E-3	1.1E-1
<input type="checkbox"/>	GOTERM_BP_ALL	regulation of protein modification process	RT		68	3.5E-3	1.2E-1
<input type="checkbox"/>	GOTERM_BP_ALL	regulation of phosphorylation	RT		58	5.0E-3	1.5E-1
<input type="checkbox"/>	GOTERM_BP_ALL	regulation of phosphate metabolic process	RT		65	5.8E-3	1.6E-1
<input type="checkbox"/>	GOTERM_BP_ALL	regulation of phosphorus metabolic process	RT		65	5.8E-3	1.6E-1
<input type="checkbox"/>	GOTERM_BP_ALL	protein phosphorylation	RT		67	4.5E-2	4.7E-1
	Annotation Cluster 25	Enrichment Score: 2.17	G		Count	P_Value	Benjamini
<input type="checkbox"/>	GOTERM_BP_ALL	positive regulation of programmed cell death	RT		29	5.6E-3	1.6E-1
<input type="checkbox"/>	GOTERM_BP_ALL	positive regulation of cell death	RT		30	6.0E-3	1.6E-1
<input type="checkbox"/>	GOTERM_BP_ALL	positive regulation of apoptotic process	RT		28	9.4E-3	2.0E-1
	Annotation Cluster 26	Enrichment Score: 2.12	G		Count	P_Value	Benjamini
<input type="checkbox"/>	GOTERM_BP_ALL	negative regulation of cellular metabolic process	RT		89	6.1E-3	1.6E-1
<input type="checkbox"/>	GOTERM_BP_ALL	negative regulation of macromolecule metabolic process	RT		88	6.9E-3	1.7E-1
<input type="checkbox"/>	GOTERM_BP_ALL	negative regulation of metabolic process	RT		93	1.0E-2	2.2E-1
	Annotation Cluster 27	Enrichment Score: 2.11	G		Count	P_Value	Benjamini
<input type="checkbox"/>	GOTERM_BP_ALL	centromere complex assembly	RT		8	9.0E-4	5.4E-2
<input type="checkbox"/>	GOTERM_BP_ALL	DNA replication-independent nucleosome assembly	RT		7	4.6E-3	1.4E-1
<input type="checkbox"/>	GOTERM_BP_ALL	DNA replication-independent nucleosome organization	RT		7	5.0E-3	1.5E-1
<input type="checkbox"/>	GOTERM_BP_ALL	histone exchange	RT		7	7.1E-3	1.8E-1
<input type="checkbox"/>	GOTERM_BP_ALL	CENP-A containing nucleosome assembly	RT		6	7.8E-3	1.9E-1
<input type="checkbox"/>	GOTERM_BP_ALL	CENP-A containing chromatin organization	RT		6	7.8E-3	1.9E-1
<input type="checkbox"/>	GOTERM_BP_ALL	ATP-dependent chromatin remodeling	RT		8	8.5E-3	2.0E-1
<input type="checkbox"/>	GOTERM_BP_ALL	chromatin remodeling at centromere	RT		6	1.1E-2	2.3E-1
<input type="checkbox"/>	GOTERM_BP_ALL	chromatin remodeling	RT		9	1.1E-1	6.6E-1
	Annotation Cluster 28	Enrichment Score: 2.00	G		Count	P_Value	Benjamini
<input type="checkbox"/>	GOTERM_BP_ALL	proteolysis involved in cellular protein catabolic process	RT		32	5.6E-3	1.6E-1
<input type="checkbox"/>	GOTERM_BP_ALL	cellular protein catabolic process	RT		33	6.0E-3	1.6E-1
<input type="checkbox"/>	GOTERM_BP_ALL	modification-dependent protein catabolic process	RT		29	6.8E-3	1.7E-1
<input type="checkbox"/>	GOTERM_BP_ALL	protein catabolic process	RT		37	7.4E-3	1.8E-1
<input type="checkbox"/>	GOTERM_BP_ALL	modification-dependent macromolecule catabolic process	RT		29	8.1E-3	1.9E-1
<input type="checkbox"/>	GOTERM_BP_ALL	ubiquitin-dependent protein catabolic process	RT		28	1.0E-2	2.2E-1
<input type="checkbox"/>	GOTERM_BP_ALL	cellular macromolecule catabolic process	RT		41	1.7E-2	2.9E-1
	Annotation Cluster 29	Enrichment Score: 1.80	G		Count	P_Value	Benjamini
<input type="checkbox"/>	GOTERM_BP_ALL	cellular biosynthetic process	RT		208	2.9E-3	1.1E-1
<input type="checkbox"/>	GOTERM_BP_ALL	biosynthetic process	RT		210	8.7E-3	2.0E-1
<input type="checkbox"/>	GOTERM_BP_ALL	organic substance biosynthetic process	RT		207	9.3E-3	2.0E-1
<input type="checkbox"/>	GOTERM_BP_ALL	cellular macromolecule biosynthetic process	RT		168	1.8E-2	2.9E-1
<input type="checkbox"/>	GOTERM_BP_ALL	macromolecule biosynthetic process	RT		171	2.8E-2	3.8E-1
	Annotation Cluster 30	Enrichment Score: 1.80	G		Count	P_Value	Benjamini
<input type="checkbox"/>	GOTERM_BP_ALL	negative regulation of phosphorus metabolic process	RT		27	9.0E-3	2.0E-1
<input type="checkbox"/>	GOTERM_BP_ALL	negative regulation of phosphate metabolic process	RT		27	9.0E-3	2.0E-1
<input type="checkbox"/>	GOTERM_BP_ALL	negative regulation of protein phosphorylation	RT		21	1.1E-2	2.3E-1
<input type="checkbox"/>	GOTERM_BP_ALL	negative regulation of phosphorylation	RT		22	1.4E-2	2.5E-1
	Annotation Cluster 31	Enrichment Score: 1.84	G		Count	P_Value	Benjamini
<input type="checkbox"/>	GOTERM_BP_ALL	positive regulation of cellular catabolic process	RT		17	6.0E-3	1.6E-1
<input type="checkbox"/>	GOTERM_BP_ALL	regulation of cellular catabolic process	RT		20	1.4E-2	2.6E-1
<input type="checkbox"/>	GOTERM_BP_ALL	positive regulation of catabolic process	RT		18	1.8E-2	2.9E-1

	Enrichment Score: 1.81			Count	P_Value	Benjamini
Annotation Cluster 32						
<input type="checkbox"/> GOTERM_BP_ALL	positive regulation of cellular protein catabolic process	RT		13	8.2E-3	1.9E-1
<input type="checkbox"/> GOTERM_BP_ALL	positive regulation of proteolysis involved in cellular protein catabolic process	RT		12	1.1E-2	2.3E-1
<input type="checkbox"/> GOTERM_BP_ALL	regulation of cellular protein catabolic process	RT		15	1.5E-2	2.7E-1
<input type="checkbox"/> GOTERM_BP_ALL	regulation of proteolysis involved in cellular protein catabolic process	RT		14	1.7E-2	2.9E-1
<input type="checkbox"/> GOTERM_BP_ALL	positive regulation of protein catabolic process	RT		14	3.7E-2	4.4E-1
Annotation Cluster 33	Enrichment Score: 1.78	G		Count	P_Value	Benjamini
<input type="checkbox"/> GOTERM_BP_ALL	cellular protein modification process	RT		133	1.2E-2	2.4E-1
<input type="checkbox"/> GOTERM_BP_ALL	protein modification process	RT		133	1.2E-2	2.4E-1
<input type="checkbox"/> GOTERM_BP_ALL	macromolecule modification	RT		139	1.9E-2	3.0E-1
<input type="checkbox"/> GOTERM_BP_ALL	cellular protein metabolic process	RT		163	2.6E-2	3.7E-1
Annotation Cluster 34	Enrichment Score: 1.77	G		Count	P_Value	Benjamini
<input type="checkbox"/> GOTERM_BP_ALL	regulation of macromolecule metabolic process	RT		194	1.1E-2	2.3E-1
<input type="checkbox"/> GOTERM_BP_ALL	regulation of cellular metabolic process	RT		193	1.7E-2	2.9E-1
<input type="checkbox"/> GOTERM_BP_ALL	regulation of primary metabolic process	RT		191	2.0E-2	3.2E-1
<input type="checkbox"/> GOTERM_BP_ALL	regulation of metabolic process	RT		202	2.1E-2	3.2E-1
Annotation Cluster 35	Enrichment Score: 1.71	G		Count	P_Value	Benjamini
<input type="checkbox"/> GOTERM_BP_ALL	nitric oxide biosynthetic process	RT		7	1.2E-2	2.4E-1
<input type="checkbox"/> GOTERM_BP_ALL	nitric oxide metabolic process	RT		7	1.6E-2	2.8E-1
<input type="checkbox"/> GOTERM_BP_ALL	reactive nitrogen species metabolic process	RT		7	2.0E-2	3.2E-1
<input type="checkbox"/> GOTERM_BP_ALL	reactive oxygen species biosynthetic process	RT		7	3.7E-2	4.4E-1
Annotation Cluster 36	Enrichment Score: 1.68	G		Count	P_Value	Benjamini
<input type="checkbox"/> GOTERM_BP_ALL	blood vessel morphogenesis	RT		24	1.7E-2	2.9E-1
<input type="checkbox"/> GOTERM_BP_ALL	angiogenesis	RT		21	1.8E-2	2.9E-1
<input type="checkbox"/> GOTERM_BP_ALL	blood vessel development	RT		26	3.0E-2	3.9E-1
<input type="checkbox"/> GOTERM_BP_ALL	vasculature development	RT		26	5.3E-2	5.0E-1
Annotation Cluster 37	Enrichment Score: 1.67	G		Count	P_Value	Benjamini
<input type="checkbox"/> GOTERM_BP_ALL	regulation of MAPK cascade	RT		34	2.6E-3	1.0E-1
<input type="checkbox"/> GOTERM_BP_ALL	MAPK cascade	RT		33	7.1E-2	5.6E-1
<input type="checkbox"/> GOTERM_BP_ALL	signal transduction by protein phosphorylation	RT		33	1.1E-1	6.5E-1
Annotation Cluster 38	Enrichment Score: 1.48	G		Count	P_Value	Benjamini
<input type="checkbox"/> GOTERM_BP_ALL	organic acid metabolic process	RT		38	2.3E-2	3.4E-1
<input type="checkbox"/> GOTERM_BP_ALL	carboxylic acid metabolic process	RT		34	3.8E-2	4.4E-1
<input type="checkbox"/> GOTERM_BP_ALL	oxoacid metabolic process	RT		34	4.3E-2	4.6E-1
Annotation Cluster 39	Enrichment Score: 1.47	G		Count	P_Value	Benjamini
<input type="checkbox"/> GOTERM_BP_ALL	regulation of hematopoietic progenitor cell differentiation	RT		4	7.0E-3	1.7E-1
<input type="checkbox"/> GOTERM_BP_ALL	regulation of stem cell differentiation	RT		5	1.8E-2	2.9E-1
<input type="checkbox"/> GOTERM_BP_ALL	stem cell differentiation	RT		5	3.2E-1	9.0E-1
Annotation Cluster 40	Enrichment Score: 1.42	G		Count	P_Value	Benjamini
<input type="checkbox"/> GOTERM_BP_ALL	negative regulation of G1/S transition of mitotic cell cycle	RT		9	6.7E-3	1.7E-1
<input type="checkbox"/> GOTERM_BP_ALL	negative regulation of cell cycle G1/S phase transition	RT		9	8.6E-3	2.0E-1
<input type="checkbox"/> GOTERM_BP_ALL	negative regulation of mitotic cell cycle phase transition	RT		10	3.6E-2	4.3E-1
<input type="checkbox"/> GOTERM_BP_ALL	negative regulation of cell cycle phase transition	RT		10	5.3E-2	5.0E-1
<input type="checkbox"/> GOTERM_BP_ALL	regulation of G1/S transition of mitotic cell cycle	RT		9	5.3E-2	5.0E-1
<input type="checkbox"/> GOTERM_BP_ALL	regulation of cell cycle G1/S phase transition	RT		9	7.8E-2	5.8E-1
<input type="checkbox"/> GOTERM_BP_ALL	negative regulation of cell cycle process	RT		10	2.6E-1	8.6E-1
Annotation Cluster 41	Enrichment Score: 1.41	G		Count	P_Value	Benjamini
<input type="checkbox"/> GOTERM_BP_ALL	cardiac muscle tissue growth	RT		7	1.3E-2	2.5E-1
<input type="checkbox"/> GOTERM_BP_ALL	heart growth	RT		7	1.8E-2	2.9E-1
<input type="checkbox"/> GOTERM_BP_ALL	regulation of organ growth	RT		6	9.3E-2	6.2E-1
<input type="checkbox"/> GOTERM_BP_ALL	organ growth	RT		8	1.1E-1	6.5E-1
Annotation Cluster 42	Enrichment Score: 1.39	G		Count	P_Value	Benjamini
<input type="checkbox"/> GOTERM_BP_ALL	negative regulation of signal transduction	RT		43	3.6E-2	4.3E-1
<input type="checkbox"/> GOTERM_BP_ALL	negative regulation of cell communication	RT		46	3.8E-2	4.4E-1

<input type="checkbox"/>	GOTERM_BP_ALL	negative regulation of signaling	RT		46	3.9E-2	4.4E-1	
<input type="checkbox"/>	GOTERM_BP_ALL	negative regulation of response to stimulus	RT		51	5.4E-2	5.1E-1	
	Annotation Cluster 43		Enrichment Score: 1.39			Count	P_Value	Benjamini
<input type="checkbox"/>	GOTERM_BP_ALL	mitotic metaphase, plate congression	RT		5	2.2E-2	3.3E-1	
<input type="checkbox"/>	GOTERM_BP_ALL	establishment of chromosome localization	RT		6	5.0E-2	4.9E-1	
<input type="checkbox"/>	GOTERM_BP_ALL	metaphase, plate congression	RT		5	5.0E-2	4.9E-1	
<input type="checkbox"/>	GOTERM_BP_ALL	chromosome localization	RT		6	5.2E-2	5.0E-1	
	Annotation Cluster 44		Enrichment Score: 1.37			Count	P_Value	Benjamini
<input type="checkbox"/>	GOTERM_BP_ALL	positive regulation of cellular protein metabolic process	RT		54	3.4E-2	4.2E-1	
<input type="checkbox"/>	GOTERM_BP_ALL	positive regulation of protein metabolic process	RT		56	4.6E-2	4.8E-1	
<input type="checkbox"/>	GOTERM_BP_ALL	positive regulation of protein modification process	RT		44	4.8E-2	4.9E-1	
	Annotation Cluster 45		Enrichment Score: 1.37			Count	P_Value	Benjamini
<input type="checkbox"/>	GOTERM_BP_ALL	positive regulation of macromolecule metabolic process	RT		101	2.3E-2	3.4E-1	
<input type="checkbox"/>	GOTERM_BP_ALL	positive regulation of metabolic process	RT		104	5.0E-2	4.9E-1	
<input type="checkbox"/>	GOTERM_BP_ALL	positive regulation of cellular metabolic process	RT		96	6.9E-2	5.6E-1	
	Annotation Cluster 48		Enrichment Score: 1.35			Count	P_Value	Benjamini
<input type="checkbox"/>	GOTERM_BP_ALL	cellular nitrogen compound biosynthetic process	RT		169	8.3E-3	1.9E-1	
<input type="checkbox"/>	GOTERM_BP_ALL	transcription, DNA-templated	RT		125	1.9E-2	3.0E-1	
<input type="checkbox"/>	GOTERM_BP_ALL	regulation of gene expression	RT		147	2.2E-2	3.3E-1	
<input type="checkbox"/>	GOTERM_BP_ALL	regulation of nitrogen compound metabolic process	RT		148	2.6E-2	3.7E-1	
<input type="checkbox"/>	GOTERM_BP_ALL	heterocycle biosynthetic process	RT		147	3.4E-2	4.2E-1	
<input type="checkbox"/>	GOTERM_BP_ALL	regulation of RNA metabolic process	RT		127	3.7E-2	4.3E-1	
<input type="checkbox"/>	GOTERM_BP_ALL	aromatic compound biosynthetic process	RT		147	3.8E-2	4.4E-1	
<input type="checkbox"/>	GOTERM_BP_ALL	nucleic acid-templated transcription	RT		127	3.9E-2	4.4E-1	
<input type="checkbox"/>	GOTERM_BP_ALL	regulation of nucleic acid-templated transcription	RT		122	4.5E-2	4.7E-1	
<input type="checkbox"/>	GOTERM_BP_ALL	nucleobase-containing compound biosynthetic process	RT		144	4.7E-2	4.8E-1	
<input type="checkbox"/>	GOTERM_BP_ALL	regulation of transcription, DNA-templated	RT		121	4.8E-2	4.9E-1	
<input type="checkbox"/>	GOTERM_BP_ALL	regulation of nucleobase-containing compound metabolic process	RT		136	5.0E-2	4.9E-1	
<input type="checkbox"/>	GOTERM_BP_ALL	regulation of RNA biosynthetic process	RT		122	5.1E-2	5.0E-1	
<input type="checkbox"/>	GOTERM_BP_ALL	organic cyclic compound biosynthetic process	RT		148	6.2E-2	5.4E-1	
<input type="checkbox"/>	GOTERM_BP_ALL	regulation of macromolecule biosynthetic process	RT		135	6.3E-2	5.5E-1	
<input type="checkbox"/>	GOTERM_BP_ALL	regulation of cellular macromolecule biosynthetic process	RT		131	7.0E-2	5.6E-1	
<input type="checkbox"/>	GOTERM_BP_ALL	RNA biosynthetic process	RT		128	7.6E-2	5.8E-1	
<input type="checkbox"/>	GOTERM_BP_ALL	regulation of cellular biosynthetic process	RT		139	8.2E-2	5.9E-1	
<input type="checkbox"/>	GOTERM_BP_ALL	regulation of biosynthetic process	RT		139	1.1E-1	6.6E-1	
<input type="checkbox"/>	GOTERM_BP_ALL	RNA metabolic process	RT		148	1.2E-1	6.7E-1	
	Annotation Cluster 47		Enrichment Score: 1.34			Count	P_Value	Benjamini
<input type="checkbox"/>	GOTERM_BP_ALL	regulation of cell migration	RT		30	2.8E-2	3.8E-1	
<input type="checkbox"/>	GOTERM_BP_ALL	regulation of cell motility	RT		31	3.9E-2	4.4E-1	
<input type="checkbox"/>	GOTERM_BP_ALL	regulation of locomotion	RT		31	6.1E-2	5.4E-1	
<input type="checkbox"/>	GOTERM_BP_ALL	regulation of cellular component movement	RT		32	6.5E-2	5.5E-1	
	Annotation Cluster 48		Enrichment Score: 1.34			Count	P_Value	Benjamini
<input type="checkbox"/>	GOTERM_BP_ALL	nitrogen compound metabolic process	RT		229	7.8E-3	1.9E-1	
<input type="checkbox"/>	GOTERM_BP_ALL	cellular nitrogen compound metabolic process	RT		211	2.5E-2	3.6E-1	
<input type="checkbox"/>	GOTERM_BP_ALL	organic cyclic compound metabolic process	RT		198	4.2E-2	4.6E-1	
<input type="checkbox"/>	GOTERM_BP_ALL	heterocycle metabolic process	RT		188	7.7E-2	5.8E-1	
<input type="checkbox"/>	GOTERM_BP_ALL	cellular aromatic compound metabolic process	RT		189	8.2E-2	5.9E-1	
<input type="checkbox"/>	GOTERM_BP_ALL	nucleic acid metabolic process	RT		165	8.4E-2	6.0E-1	
<input type="checkbox"/>	GOTERM_BP_ALL	nucleobase-containing compound metabolic process	RT		183	9.7E-2	6.3E-1	
	Annotation Cluster 48		Enrichment Score: 1.33			Count	P_Value	Benjamini
<input type="checkbox"/>	GOTERM_BP_ALL	DNA replication-independent nucleosome assembly	RT		7	4.6E-3	1.4E-1	
<input type="checkbox"/>	GOTERM_BP_ALL	DNA replication-independent nucleosome organization	RT		7	5.0E-3	1.5E-1	
<input type="checkbox"/>	GOTERM_BP_ALL	DNA packaging	RT		12	3.7E-2	4.4E-1	

<input type="checkbox"/>	GOTERM_BP_ALL	nucleosome assembly	RT		9	7.3E-2	5.7E-1
<input type="checkbox"/>	GOTERM_BP_ALL	nucleosome organization	RT		10	7.5E-2	5.7E-1
<input type="checkbox"/>	GOTERM_BP_ALL	protein-DNA complex assembly	RT		12	8.1E-2	5.9E-1
<input type="checkbox"/>	GOTERM_BP_ALL	chromatin assembly	RT		9	1.1E-1	6.6E-1
<input type="checkbox"/>	GOTERM_BP_ALL	DNA conformation change	RT		13	1.2E-1	6.9E-1
<input type="checkbox"/>	GOTERM_BP_ALL	chromatin assembly or disassembly	RT		9	1.9E-1	7.9E-1
	Annotation Cluster 60	Enrichment Score: 1.32	G		Count	P_Value	Benjamini
<input type="checkbox"/>	GOTERM_BP_ALL	primary alcohol metabolic process	RT		6	9.5E-3	2.0E-1
<input type="checkbox"/>	GOTERM_BP_ALL	retinol metabolic process	RT		5	1.1E-2	2.2E-1
<input type="checkbox"/>	GOTERM_BP_ALL	isoprenoid metabolic process	RT		8	7.9E-2	5.9E-1
<input type="checkbox"/>	GOTERM_BP_ALL	terpenoid metabolic process	RT		7	8.8E-2	6.1E-1
<input type="checkbox"/>	GOTERM_BP_ALL	retinoid metabolic process	RT		6	1.2E-1	6.7E-1
<input type="checkbox"/>	GOTERM_BP_ALL	diterpenoid metabolic process	RT		6	1.5E-1	7.2E-1
	Annotation Cluster 61	Enrichment Score: 1.23	G		Count	P_Value	Benjamini
<input type="checkbox"/>	GOTERM_BP_ALL	positive regulation of nitric oxide biosynthetic process	RT		5	3.5E-2	4.3E-1
<input type="checkbox"/>	GOTERM_BP_ALL	positive regulation of nitric oxide metabolic process	RT		5	3.5E-2	4.3E-1
<input type="checkbox"/>	GOTERM_BP_ALL	positive regulation of reactive oxygen species biosynthetic process	RT		5	5.7E-2	5.2E-1
<input type="checkbox"/>	GOTERM_BP_ALL	regulation of nitric oxide biosynthetic process	RT		5	7.5E-2	5.7E-1
<input type="checkbox"/>	GOTERM_BP_ALL	regulation of reactive oxygen species biosynthetic process	RT		5	1.4E-1	7.1E-1
	Annotation Cluster 62	Enrichment Score: 1.21	G		Count	P_Value	Benjamini
<input type="checkbox"/>	GOTERM_BP_ALL	cardiac muscle cell proliferation	RT		5	3.0E-2	4.0E-1
<input type="checkbox"/>	GOTERM_BP_ALL	striated muscle cell proliferation	RT		5	6.4E-2	5.4E-1
<input type="checkbox"/>	GOTERM_BP_ALL	regulation of cardiac muscle cell proliferation	RT		4	8.0E-2	5.9E-1
<input type="checkbox"/>	GOTERM_BP_ALL	regulation of organ growth	RT		6	9.3E-2	6.2E-1
	Annotation Cluster 63	Enrichment Score: 1.2	G		Count	P_Value	Benjamini
<input type="checkbox"/>	GOTERM_BP_ALL	positive regulation of cell motility	RT		19	5.2E-2	5.0E-1
<input type="checkbox"/>	GOTERM_BP_ALL	positive regulation of cellular component movement	RT		19	6.4E-2	5.5E-1
<input type="checkbox"/>	GOTERM_BP_ALL	positive regulation of locomotion	RT		19	6.7E-2	5.5E-1
<input type="checkbox"/>	GOTERM_BP_ALL	positive regulation of cell migration	RT		18	7.0E-2	5.6E-1
	Annotation Cluster 64	Enrichment Score: 1.2	G		Count	P_Value	Benjamini
<input type="checkbox"/>	GOTERM_BP_ALL	reproductive process	RT		52	4.0E-2	4.5E-1
<input type="checkbox"/>	GOTERM_BP_ALL	reproduction	RT		52	4.1E-2	4.5E-1
<input type="checkbox"/>	GOTERM_BP_ALL	single organism reproductive process	RT		43	1.6E-1	7.4E-1
	Annotation Cluster 65	Enrichment Score: 1.18	G		Count	P_Value	Benjamini
<input type="checkbox"/>	GOTERM_BP_ALL	hepatocyte proliferation	RT		3	6.1E-2	5.4E-1
<input type="checkbox"/>	GOTERM_BP_ALL	epithelial cell proliferation involved in liver morphogenesis	RT		3	6.1E-2	5.4E-1
<input type="checkbox"/>	GOTERM_BP_ALL	liver morphogenesis	RT		3	7.7E-2	5.8E-1
	Annotation Cluster 66	Enrichment Score: 1.18	G		Count	P_Value	Benjamini
<input type="checkbox"/>	GOTERM_BP_ALL	positive regulation of protein phosphorylation	RT		35	6.4E-2	5.4E-1
<input type="checkbox"/>	GOTERM_BP_ALL	positive regulation of phosphate metabolic process	RT		40	6.6E-2	5.5E-1
<input type="checkbox"/>	GOTERM_BP_ALL	positive regulation of phosphate metabolic process	RT		40	6.6E-2	5.5E-1
<input type="checkbox"/>	GOTERM_BP_ALL	positive regulation of phosphorylation	RT		36	7.0E-2	5.6E-1
	Annotation Cluster 67	Enrichment Score: 1.18	G		Count	P_Value	Benjamini
<input type="checkbox"/>	GOTERM_BP_ALL	cardiac muscle tissue development	RT		12	2.0E-2	3.1E-1
<input type="checkbox"/>	GOTERM_BP_ALL	muscle tissue development	RT		16	1.2E-1	6.7E-1
<input type="checkbox"/>	GOTERM_BP_ALL	striated muscle tissue development	RT		15	1.4E-1	7.2E-1
	Annotation Cluster 68	Enrichment Score: 1.14	G		Count	P_Value	Benjamini
<input type="checkbox"/>	GOTERM_BP_ALL	transforming growth factor beta receptor signalling pathway	RT		10	4.2E-2	4.6E-1
<input type="checkbox"/>	GOTERM_BP_ALL	cellular response to transforming growth factor beta stimulus	RT		11	9.2E-2	6.2E-1
<input type="checkbox"/>	GOTERM_BP_ALL	response to transforming growth factor beta	RT		11	9.7E-2	6.3E-1
	Annotation Cluster 69	Enrichment Score: 1.11	G		Count	P_Value	Benjamini
<input type="checkbox"/>	GOTERM_BP_ALL	epithelial cell migration	RT		12	6.9E-2	5.6E-1
<input type="checkbox"/>	GOTERM_BP_ALL	epithelium migration	RT		12	7.4E-2	5.7E-1
<input type="checkbox"/>	GOTERM_BP_ALL	endothelial cell migration	RT		9	8.0E-2	5.9E-1
<input type="checkbox"/>	GOTERM_BP_ALL	amphoidal-type cell migration	RT		15	8.4E-2	6.0E-1

Appendix 4 Functional clustering analysis of common DEGs between methyl donor depleted and Int-stage of HPV integration dataset



82.9%

*** Welcome to DAVID 6.8 ***
*** If you are looking for DAVID 6.7, please visit our [development site](#). ***

Functional Annotation Clustering

[Help and Manual](#)

Current Gene List: [List_1](#)

Current Background: **Homo sapiens**

495 DAVID IDs

Options Classification Stringency **High** ▼

224 Cluster(s)

[Download File](#)

Annotation Cluster	Enrichment Score	GO Term	RT	Bar	Count	P_Value	Benjamini
Annotation Cluster 1	10.8		G				
<input type="checkbox"/> GOTERM_BP_ALL		response to external biotic stimulus	RT		57	8.1E-12	1.1E-8
<input type="checkbox"/> GOTERM_BP_ALL		response to other organism	RT		57	8.1E-12	1.1E-8
<input type="checkbox"/> GOTERM_BP_ALL		response to biotic stimulus	RT		57	6.1E-11	5.6E-8
Annotation Cluster 2	10.78		G				
<input type="checkbox"/> GOTERM_BP_ALL		response to type I interferon	RT		18	5.9E-12	1.1E-8
<input type="checkbox"/> GOTERM_BP_ALL		cellular response to type I interferon	RT		17	2.8E-11	3.1E-8
<input type="checkbox"/> GOTERM_BP_ALL		type I interferon signaling pathway	RT		17	2.8E-11	3.1E-8
Annotation Cluster 3	8.38		G				
<input type="checkbox"/> GOTERM_BP_ALL		viral process	RT		59	3.5E-10	2.1E-7
<input type="checkbox"/> GOTERM_BP_ALL		interspecies interaction between organisms	RT		60	4.3E-10	2.4E-7
<input type="checkbox"/> GOTERM_BP_ALL		symbiosis, encompassing mutualism through parasitism	RT		60	4.3E-10	2.4E-7
<input type="checkbox"/> GOTERM_BP_ALL		multi-organism cellular process	RT		59	4.6E-10	2.3E-7
Annotation Cluster 4	6.84		G				
<input type="checkbox"/> GOTERM_BP_ALL		negative regulation of cellular metabolic process	RT		94	2.1E-6	4.3E-4
<input type="checkbox"/> GOTERM_BP_ALL		negative regulation of metabolic process	RT		96	1.4E-5	2.1E-3
<input type="checkbox"/> GOTERM_BP_ALL		negative regulation of macromolecule metabolic process	RT		89	2.7E-5	3.5E-3
Annotation Cluster 5	4.88		G				
<input type="checkbox"/> GOTERM_BP_ALL		regulation of viral process	RT		21	9.3E-6	1.6E-3
<input type="checkbox"/> GOTERM_BP_ALL		regulation of symbiosis, encompassing mutualism through parasitism	RT		22	9.6E-6	1.6E-3
<input type="checkbox"/> GOTERM_BP_ALL		regulation of multi-organism process	RT		25	2.6E-5	3.5E-3
Annotation Cluster 6	4.8		G				
<input type="checkbox"/> GOTERM_BP_ALL		catabolic process	RT		83	3.5E-6	6.7E-4
<input type="checkbox"/> GOTERM_BP_ALL		cellular catabolic process	RT		68	1.9E-5	2.7E-3
<input type="checkbox"/> GOTERM_BP_ALL		organic substance catabolic process	RT		72	2.3E-4	1.9E-2
Annotation Cluster 7	3.79		G				
<input type="checkbox"/> GOTERM_BP_ALL		immune system development	RT		40	8.2E-5	8.4E-3
<input type="checkbox"/> GOTERM_BP_ALL		hemopoiesis	RT		36	2.0E-4	1.7E-2
<input type="checkbox"/> GOTERM_BP_ALL		hematopoietic or lymphoid organ development	RT		37	2.6E-4	2.0E-2
Annotation Cluster 8	3.6		G				
<input type="checkbox"/> GOTERM_BP_ALL		regulation of signal transduction	RT		96	2.8E-4	2.1E-2
<input type="checkbox"/> GOTERM_BP_ALL		regulation of cell communication	RT		104	3.1E-4	2.3E-2
<input type="checkbox"/> GOTERM_BP_ALL		regulation of signaling	RT		105	3.7E-4	2.6E-2
Annotation Cluster 9	3.43		G				
<input type="checkbox"/> GOTERM_BP_ALL		metabolic process	RT		312	7.4E-5	7.8E-3
<input type="checkbox"/> GOTERM_BP_ALL		organic substance metabolic process	RT		302	1.4E-4	1.3E-2
<input type="checkbox"/> GOTERM_BP_ALL		cellular metabolic process	RT		285	9.8E-4	5.0E-2
<input type="checkbox"/> GOTERM_BP_ALL		primary metabolic process	RT		284	1.9E-3	7.6E-2
Annotation Cluster 10	3.38		G				
<input type="checkbox"/> GOTERM_BP_ALL		positive regulation of signaling	RT		62	2.6E-4	2.0E-2
<input type="checkbox"/> GOTERM_BP_ALL		positive regulation of cell communication	RT		61	3.9E-4	2.7E-2
<input type="checkbox"/> GOTERM_BP_ALL		positive regulation of signal transduction	RT		56	7.2E-4	4.2E-2
Annotation Cluster 11	3.22		G				
<input type="checkbox"/> GOTERM_BP_ALL		regulation of viral genome replication	RT		10	1.8E-4	1.5E-2

<input type="checkbox"/>	GOTERM_BP_ALL	negative regulation of viral genome replication	RT		8	2.5E-4	2.0E-2
<input type="checkbox"/>	GOTERM_BP_ALL	viral genome replication	RT		9	4.9E-3	1.4E-1
	Annotation Cluster 12	Enrichment Score: 3.18	G		Count	P_Value	Benjamini
<input type="checkbox"/>	GOTERM_BP_ALL	response to oxygen levels	RT		20	3.4E-4	2.4E-2
<input type="checkbox"/>	GOTERM_BP_ALL	response to hypoxia	RT		18	8.4E-4	4.6E-2
<input type="checkbox"/>	GOTERM_BP_ALL	response to decreased oxygen levels	RT		18	1.2E-3	5.5E-2
	Annotation Cluster 13	Enrichment Score: 3.03	G		Count	P_Value	Benjamini
<input type="checkbox"/>	GOTERM_BP_ALL	mitotic cell cycle process	RT		40	4.3E-4	2.8E-2
<input type="checkbox"/>	GOTERM_BP_ALL	mitotic cell cycle	RT		42	5.8E-4	3.5E-2
<input type="checkbox"/>	GOTERM_BP_ALL	cell cycle process	RT		51	3.2E-3	1.1E-1
	Annotation Cluster 14	Enrichment Score: 3	G		Count	P_Value	Benjamini
<input type="checkbox"/>	GOTERM_BP_ALL	system development	RT		139	3.0E-4	2.2E-2
<input type="checkbox"/>	GOTERM_BP_ALL	anatomical structure development	RT		169	5.0E-4	3.2E-2
<input type="checkbox"/>	GOTERM_BP_ALL	multicellular organism development	RT		152	8.1E-4	4.5E-2
<input type="checkbox"/>	GOTERM_BP_ALL	developmental process	RT		169	2.1E-3	8.0E-2
<input type="checkbox"/>	GOTERM_BP_ALL	single-organism developmental process	RT		163	3.8E-3	1.2E-1
	Annotation Cluster 15	Enrichment Score: 2.88	G		Count	P_Value	Benjamini
<input type="checkbox"/>	GOTERM_BP_ALL	cell death	RT		74	2.4E-4	1.9E-2
<input type="checkbox"/>	GOTERM_BP_ALL	programmed cell death	RT		66	2.5E-3	9.3E-2
<input type="checkbox"/>	GOTERM_BP_ALL	apoptotic process	RT		62	3.9E-3	1.2E-1
	Annotation Cluster 16	Enrichment Score: 2.72	G		Count	P_Value	Benjamini
<input type="checkbox"/>	GOTERM_BP_ALL	negative regulation of phosphorus metabolic process	RT		27	1.2E-3	5.5E-2
<input type="checkbox"/>	GOTERM_BP_ALL	negative regulation of phosphate metabolic process	RT		27	1.2E-3	5.5E-2
<input type="checkbox"/>	GOTERM_BP_ALL	negative regulation of phosphorylation	RT		21	5.3E-3	1.4E-1
	Annotation Cluster 17	Enrichment Score: 2.7	G		Count	P_Value	Benjamini
<input type="checkbox"/>	GOTERM_BP_ALL	cellular biosynthetic process	RT		184	9.1E-4	4.8E-2
<input type="checkbox"/>	GOTERM_BP_ALL	organic substance biosynthetic process	RT		186	1.2E-3	5.5E-2
<input type="checkbox"/>	GOTERM_BP_ALL	biosynthetic process	RT		187	1.9E-3	7.5E-2
<input type="checkbox"/>	GOTERM_BP_ALL	macromolecule biosynthetic process	RT		153	7.4E-3	1.8E-1
	Annotation Cluster 18	Enrichment Score: 2.47	G		Count	P_Value	Benjamini
<input type="checkbox"/>	GOTERM_BP_ALL	regulation of primary metabolic process	RT		174	1.6E-3	7.1E-2
<input type="checkbox"/>	GOTERM_BP_ALL	regulation of cellular metabolic process	RT		174	2.4E-3	9.0E-2
<input type="checkbox"/>	GOTERM_BP_ALL	regulation of macromolecule metabolic process	RT		171	4.8E-3	1.4E-1
<input type="checkbox"/>	GOTERM_BP_ALL	regulation of metabolic process	RT		179	6.7E-3	1.7E-1
	Annotation Cluster 19	Enrichment Score: 2.29	G		Count	P_Value	Benjamini
<input type="checkbox"/>	GOTERM_BP_ALL	gluconeogenesis	RT		8	2.2E-3	8.4E-2
<input type="checkbox"/>	GOTERM_BP_ALL	regulation of gluconeogenesis	RT		6	2.6E-3	9.4E-2
<input type="checkbox"/>	GOTERM_BP_ALL	hexose biosynthetic process	RT		8	2.8E-3	9.6E-2
<input type="checkbox"/>	GOTERM_BP_ALL	monosaccharide biosynthetic process	RT		8	3.7E-3	1.2E-1
<input type="checkbox"/>	GOTERM_BP_ALL	carbohydrate biosynthetic process	RT		10	5.6E-2	4.7E-1
	Annotation Cluster 20	Enrichment Score: 2.24	G		Count	P_Value	Benjamini
<input type="checkbox"/>	GOTERM_BP_ALL	vasculature development	RT		28	2.8E-3	9.7E-2
<input type="checkbox"/>	GOTERM_BP_ALL	angiogenesis	RT		21	3.6E-3	1.2E-1
<input type="checkbox"/>	GOTERM_BP_ALL	blood vessel development	RT		25	9.6E-3	2.0E-1
<input type="checkbox"/>	GOTERM_BP_ALL	blood vessel morphogenesis	RT		22	1.1E-2	2.1E-1
	Annotation Cluster 21	Enrichment Score: 2.21	G		Count	P_Value	Benjamini
<input type="checkbox"/>	GOTERM_BP_ALL	positive regulation of cell death	RT		27	5.1E-3	1.4E-1
<input type="checkbox"/>	GOTERM_BP_ALL	positive regulation of programmed cell death	RT		26	5.2E-3	1.4E-1
<input type="checkbox"/>	GOTERM_BP_ALL	positive regulation of apoptotic process	RT		25	8.9E-3	1.9E-1
	Annotation Cluster 22	Enrichment Score: 2.2	G		Count	P_Value	Benjamini
<input type="checkbox"/>	GOTERM_BP_ALL	negative regulation of biosynthetic process	RT		58	8.4E-4	4.5E-2
<input type="checkbox"/>	GOTERM_BP_ALL	negative regulation of cellular biosynthetic process	RT		57	9.8E-4	5.0E-2
<input type="checkbox"/>	GOTERM_BP_ALL	negative regulation of macromolecule biosynthetic process	RT		54	1.8E-3	7.3E-2
<input type="checkbox"/>	GOTERM_BP_ALL	negative regulation of nitrogen compound metabolic process	RT		55	3.8E-3	1.2E-1
<input type="checkbox"/>	GOTERM_BP_ALL	negative regulation of gene expression	RT		53	7.1E-3	1.7E-1
<input type="checkbox"/>	GOTERM_BP_ALL	negative regulation of cellular macromolecule biosynthetic process	RT		48	8.5E-3	1.9E-1

<input type="checkbox"/>	GOTERM_BP_ALL	negative regulation of RNA biosynthetic process	RT		44	8.9E-3	1.9E-1
<input type="checkbox"/>	GOTERM_BP_ALL	negative regulation of nucleic acid-templated transcription	RT		43	1.1E-2	2.1E-1
<input type="checkbox"/>	GOTERM_BP_ALL	negative regulation of RNA metabolic process	RT		44	1.7E-2	2.6E-1
<input type="checkbox"/>	GOTERM_BP_ALL	negative regulation of transcription, DNA-templated	RT		40	2.3E-2	3.0E-1
<input type="checkbox"/>	GOTERM_BP_ALL	negative regulation of nucleobase-containing compound metabolic process	RT		45	4.8E-2	4.4E-1
	Annotation Cluster 23	Enrichment Score: 2.16	G		Count	P_Value	Benjamini
<input type="checkbox"/>	GOTERM_BP_ALL	transforming growth factor beta receptor signaling pathway	RT		11	6.4E-3	1.6E-1
<input type="checkbox"/>	GOTERM_BP_ALL	cellular response to transforming growth factor beta stimulus	RT		13	7.1E-3	1.7E-1
<input type="checkbox"/>	GOTERM_BP_ALL	response to transforming growth factor beta	RT		13	7.6E-3	1.8E-1
	Annotation Cluster 24	Enrichment Score: 2.68	G		Count	P_Value	Benjamini
<input type="checkbox"/>	GOTERM_BP_ALL	cellular response to nutrient levels	RT		11	6.4E-3	1.6E-1
<input type="checkbox"/>	GOTERM_BP_ALL	cellular response to extracellular stimulus	RT		12	7.4E-3	1.8E-1
<input type="checkbox"/>	GOTERM_BP_ALL	cellular response to external stimulus	RT		14	1.2E-2	2.2E-1
	Annotation Cluster 25	Enrichment Score: 2.67	G		Count	P_Value	Benjamini
<input type="checkbox"/>	GOTERM_BP_ALL	proteolysis involved in cellular protein catabolic process	RT		30	2.1E-3	8.0E-2
<input type="checkbox"/>	GOTERM_BP_ALL	protein catabolic process	RT		34	3.7E-3	1.2E-1
<input type="checkbox"/>	GOTERM_BP_ALL	cellular macromolecule catabolic process	RT		39	4.0E-3	1.2E-1
<input type="checkbox"/>	GOTERM_BP_ALL	cellular protein catabolic process	RT		30	4.1E-3	1.2E-1
<input type="checkbox"/>	GOTERM_BP_ALL	modification-dependent protein catabolic process	RT		24	2.1E-2	2.8E-1
<input type="checkbox"/>	GOTERM_BP_ALL	modification-dependent macromolecule catabolic process	RT		24	2.4E-2	3.1E-1
<input type="checkbox"/>	GOTERM_BP_ALL	ubiquitin-dependent protein catabolic process	RT		22	5.3E-2	4.5E-1
	Annotation Cluster 26	Enrichment Score: 2.68	G		Count	P_Value	Benjamini
<input type="checkbox"/>	GOTERM_BP_ALL	response to defenses of other organism involved in symbiotic interaction	RT		3	8.6E-3	1.9E-1
<input type="checkbox"/>	GOTERM_BP_ALL	response to host	RT		3	8.6E-3	1.9E-1
<input type="checkbox"/>	GOTERM_BP_ALL	response to host defenses	RT		3	8.6E-3	1.9E-1
	Annotation Cluster 27	Enrichment Score: 2.82	G		Count	P_Value	Benjamini
<input type="checkbox"/>	GOTERM_BP_ALL	collagen metabolic process	RT		9	6.1E-3	1.6E-1
<input type="checkbox"/>	GOTERM_BP_ALL	multicellular organismal macromolecule metabolic process	RT		9	8.0E-3	1.8E-1
<input type="checkbox"/>	GOTERM_BP_ALL	multicellular organism metabolic process	RT		9	1.8E-2	2.7E-1
	Annotation Cluster 28	Enrichment Score: 2.61	G		Count	P_Value	Benjamini
<input type="checkbox"/>	GOTERM_BP_ALL	protein targeting to nucleus	RT		16	4.5E-3	1.3E-1
<input type="checkbox"/>	GOTERM_BP_ALL	protein import into nucleus	RT		16	4.5E-3	1.3E-1
<input type="checkbox"/>	GOTERM_BP_ALL	single-organism nuclear import	RT		16	4.6E-3	1.3E-1
<input type="checkbox"/>	GOTERM_BP_ALL	nuclear import	RT		16	8.0E-3	1.8E-1
<input type="checkbox"/>	GOTERM_BP_ALL	protein import	RT		17	8.4E-3	1.9E-1
<input type="checkbox"/>	GOTERM_BP_ALL	protein localization to nucleus	RT		17	1.9E-2	2.8E-1
<input type="checkbox"/>	GOTERM_BP_ALL	nucleocytoplasmic transport	RT		20	2.4E-2	3.0E-1
<input type="checkbox"/>	GOTERM_BP_ALL	nuclear transport	RT		20	2.7E-2	3.3E-1
	Annotation Cluster 29	Enrichment Score: 1.88	G		Count	P_Value	Benjamini
<input type="checkbox"/>	GOTERM_BP_ALL	positive regulation of reactive oxygen species metabolic process	RT		9	1.4E-3	6.3E-2
<input type="checkbox"/>	GOTERM_BP_ALL	regulation of reactive oxygen species metabolic process	RT		10	1.4E-2	2.4E-1
<input type="checkbox"/>	GOTERM_BP_ALL	reactive oxygen species metabolic process	RT		11	5.1E-2	4.5E-1
	Annotation Cluster 30	Enrichment Score: 1.88	G		Count	P_Value	Benjamini
<input type="checkbox"/>	GOTERM_BP_ALL	regulation of phosphate metabolic process	RT		59	2.5E-3	9.2E-2
<input type="checkbox"/>	GOTERM_BP_ALL	regulation of phosphorus metabolic process	RT		59	2.6E-3	9.3E-2
<input type="checkbox"/>	GOTERM_BP_ALL	regulation of phosphorylation	RT		50	8.3E-3	1.8E-1
<input type="checkbox"/>	GOTERM_BP_ALL	regulation of protein phosphorylation	RT		47	9.6E-3	2.0E-1
<input type="checkbox"/>	GOTERM_BP_ALL	regulation of protein modification process	RT		55	2.4E-2	3.0E-1
<input type="checkbox"/>	GOTERM_BP_ALL	protein phosphorylation	RT		55	1.2E-1	6.4E-1
	Annotation Cluster 31	Enrichment Score: 1.83	G		Count	P_Value	Benjamini
<input type="checkbox"/>	GOTERM_BP_ALL	regulation of cell migration	RT		29	7.1E-3	1.7E-1
<input type="checkbox"/>	GOTERM_BP_ALL	regulation of cell motility	RT		30	9.9E-3	2.0E-1
<input type="checkbox"/>	GOTERM_BP_ALL	regulation of locomotion	RT		30	1.7E-2	2.6E-1
<input type="checkbox"/>	GOTERM_BP_ALL	regulation of cellular component movement	RT		31	1.7E-2	2.6E-1

	Annotation Cluster	Enrichment Score: 1.89	G		Count	P_Value	Benjamini
<input type="checkbox"/>	GOTERM_BP_ALL	regulation of cell death	RT		53	1.0E-2	2.0E-1
<input type="checkbox"/>	GOTERM_BP_ALL	regulation of apoptotic process	RT		49	1.4E-2	2.4E-1
<input type="checkbox"/>	GOTERM_BP_ALL	regulation of programmed cell death	RT		49	1.6E-2	2.5E-1
	Annotation Cluster 33	Enrichment Score: 1.83	G		Count	P_Value	Benjamini
<input type="checkbox"/>	GOTERM_BP_ALL	regulation of cholesterol storage	RT		4	3.6E-3	1.2E-1
<input type="checkbox"/>	GOTERM_BP_ALL	cholesterol storage	RT		4	5.5E-3	1.5E-1
<input type="checkbox"/>	GOTERM_BP_ALL	regulation of macrophage derived foam cell differentiation	RT		3	1.6E-1	7.2E-1
	Annotation Cluster 34	Enrichment Score: 1.78	G		Count	P_Value	Benjamini
<input type="checkbox"/>	GOTERM_BP_ALL	positive regulation of stress-activated MAPK cascade	RT		10	7.9E-3	1.8E-1
<input type="checkbox"/>	GOTERM_BP_ALL	positive regulation of stress-activated protein kinase signaling cascade	RT		10	8.3E-3	1.8E-1
<input type="checkbox"/>	GOTERM_BP_ALL	regulation of stress-activated MAPK cascade	RT		12	1.2E-2	2.2E-1
<input type="checkbox"/>	GOTERM_BP_ALL	regulation of stress-activated protein kinase signaling cascade	RT		12	1.2E-2	2.2E-1
<input type="checkbox"/>	GOTERM_BP_ALL	stress-activated MAPK cascade	RT		12	4.0E-2	4.0E-1
<input type="checkbox"/>	GOTERM_BP_ALL	stress-activated protein kinase signaling cascade	RT		12	5.3E-2	4.6E-1
	Annotation Cluster 35	Enrichment Score: 1.77	G		Count	P_Value	Benjamini
<input type="checkbox"/>	GOTERM_BP_ALL	cellular response to oxygen levels	RT		10	1.2E-2	2.2E-1
<input type="checkbox"/>	GOTERM_BP_ALL	cellular response to hypoxia	RT		9	1.7E-2	2.6E-1
<input type="checkbox"/>	GOTERM_BP_ALL	cellular response to decreased oxygen levels	RT		9	2.3E-2	3.0E-1
	Annotation Cluster 38	Enrichment Score: 1.78	G		Count	P_Value	Benjamini
<input type="checkbox"/>	GOTERM_BP_ALL	positive regulation of cell motility	RT		19	1.4E-2	2.4E-1
<input type="checkbox"/>	GOTERM_BP_ALL	positive regulation of cellular component movement	RT		19	1.8E-2	2.7E-1
<input type="checkbox"/>	GOTERM_BP_ALL	positive regulation of locomotion	RT		19	1.9E-2	2.8E-1
<input type="checkbox"/>	GOTERM_BP_ALL	positive regulation of cell migration	RT		18	2.0E-2	2.8E-1
	Annotation Cluster 37	Enrichment Score: 1.75	G		Count	P_Value	Benjamini
<input type="checkbox"/>	GOTERM_BP_ALL	positive regulation of p38MAPK cascade	RT		4	6.7E-3	1.7E-1
<input type="checkbox"/>	GOTERM_BP_ALL	p38MAPK cascade	RT		4	2.6E-2	3.2E-1
<input type="checkbox"/>	GOTERM_BP_ALL	regulation of p38MAPK cascade	RT		4	3.1E-2	3.6E-1
	Annotation Cluster 38	Enrichment Score: 1.75	G		Count	P_Value	Benjamini
<input type="checkbox"/>	GOTERM_BP_ALL	protein ubiquitination	RT		31	1.0E-2	2.0E-1
<input type="checkbox"/>	GOTERM_BP_ALL	protein modification by small protein conjugation	RT		33	2.2E-2	2.9E-1
<input type="checkbox"/>	GOTERM_BP_ALL	protein modification by small protein conjugation or removal	RT		37	2.5E-2	3.1E-1
	Annotation Cluster 39	Enrichment Score: 1.73	G		Count	P_Value	Benjamini
<input type="checkbox"/>	GOTERM_BP_ALL	muscle cell proliferation	RT		10	1.5E-2	2.5E-1
<input type="checkbox"/>	GOTERM_BP_ALL	smooth muscle cell proliferation	RT		8	1.9E-2	2.7E-1
<input type="checkbox"/>	GOTERM_BP_ALL	regulation of smooth muscle cell proliferation	RT		8	2.3E-2	3.0E-1
	Annotation Cluster 40	Enrichment Score: 1.72	G		Count	P_Value	Benjamini
<input type="checkbox"/>	GOTERM_BP_ALL	macromolecular complex assembly	RT		59	8.8E-3	1.9E-1
<input type="checkbox"/>	GOTERM_BP_ALL	protein complex subunit organization	RT		57	1.3E-2	2.3E-1
<input type="checkbox"/>	GOTERM_BP_ALL	protein complex assembly	RT		48	3.3E-2	3.7E-1
<input type="checkbox"/>	GOTERM_BP_ALL	protein complex biogenesis	RT		48	3.4E-2	3.7E-1
	Annotation Cluster 41	Enrichment Score: 1.88	G		Count	P_Value	Benjamini
<input type="checkbox"/>	GOTERM_BP_ALL	regulation of cytokine production involved in immune response	RT		6	1.5E-2	2.5E-1
<input type="checkbox"/>	GOTERM_BP_ALL	regulation of production of molecular mediator of immune response	RT		8	1.7E-2	2.6E-1
<input type="checkbox"/>	GOTERM_BP_ALL	cytokine production involved in immune response	RT		6	3.5E-2	3.8E-1
	Annotation Cluster 42	Enrichment Score: 1.83	G		Count	P_Value	Benjamini
<input type="checkbox"/>	GOTERM_BP_ALL	cell migration	RT		44	7.8E-3	1.8E-1
<input type="checkbox"/>	GOTERM_BP_ALL	localization of cell	RT		46	2.0E-2	2.8E-1
<input type="checkbox"/>	GOTERM_BP_ALL	cell motility	RT		46	2.0E-2	2.8E-1
<input type="checkbox"/>	GOTERM_BP_ALL	locomotion	RT		50	3.8E-2	4.0E-1
<input type="checkbox"/>	GOTERM_BP_ALL	movement of cell or subcellular component	RT		56	5.8E-2	4.8E-1
	Annotation Cluster 43	Enrichment Score: 1.69	G		Count	P_Value	Benjamini
<input type="checkbox"/>	GOTERM_BP_ALL	regulation of nitrogen compound metabolic process	RT		134	5.2E-3	1.4E-1
<input type="checkbox"/>	GOTERM_BP_ALL	aromatic compound biosynthetic process	RT		132	1.1E-2	2.1E-1
<input type="checkbox"/>	GOTERM_BP_ALL	nucleobase-containing compound biosynthetic process	RT		130	1.2E-2	2.2E-1

<input type="checkbox"/>	GOTERM_BP_ALL	heterocycle biosynthetic process	RT			131	1.3E-2	2.3E-1
<input type="checkbox"/>	GOTERM_BP_ALL	regulation of macromolecule biosynthetic process	RT			123	1.3E-2	2.3E-1
<input type="checkbox"/>	GOTERM_BP_ALL	regulation of biosynthetic process	RT			129	1.4E-2	2.4E-1
<input type="checkbox"/>	GOTERM_BP_ALL	regulation of nucleobase-containing compound metabolic process	RT			122	1.7E-2	2.6E-1
<input type="checkbox"/>	GOTERM_BP_ALL	regulation of cellular macromolecule biosynthetic process	RT			119	1.7E-2	2.6E-1
<input type="checkbox"/>	GOTERM_BP_ALL	organic cyclic compound biosynthetic process	RT			133	1.9E-2	2.7E-1
<input type="checkbox"/>	GOTERM_BP_ALL	regulation of cellular biosynthetic process	RT			126	2.1E-2	2.9E-1
<input type="checkbox"/>	GOTERM_BP_ALL	cellular nitrogen compound biosynthetic process	RT			143	2.2E-2	3.0E-1
<input type="checkbox"/>	GOTERM_BP_ALL	regulation of gene expression	RT			126	3.1E-2	3.6E-1
<input type="checkbox"/>	GOTERM_BP_ALL	regulation of RNA metabolic process	RT			110	3.8E-2	4.0E-1
<input type="checkbox"/>	GOTERM_BP_ALL	regulation of transcription, DNA-templated	RT			105	4.7E-2	4.4E-1
<input type="checkbox"/>	GOTERM_BP_ALL	transcription, DNA-templated	RT			105	4.8E-2	4.4E-1
<input type="checkbox"/>	GOTERM_BP_ALL	regulation of nucleic acid-templated transcription	RT			105	5.4E-2	4.6E-1
<input type="checkbox"/>	GOTERM_BP_ALL	RNA biosynthetic process	RT			112	5.8E-2	4.7E-1
<input type="checkbox"/>	GOTERM_BP_ALL	regulation of RNA biosynthetic process	RT			105	6.1E-2	4.8E-1
<input type="checkbox"/>	GOTERM_BP_ALL	nucleic acid-templated transcription	RT			108	6.5E-2	5.0E-1
<input type="checkbox"/>	GOTERM_BP_ALL	RNA metabolic process	RT			128	1.1E-1	6.3E-1
	Annotation Cluster 44	Enrichment Score: 1.68	G			Count	P_Value	Benjamini
<input type="checkbox"/>	GOTERM_BP_ALL	positive regulation of macromolecule metabolic process	RT			88	2.2E-2	2.9E-1
<input type="checkbox"/>	GOTERM_BP_ALL	positive regulation of metabolic process	RT			93	2.4E-2	3.0E-1
<input type="checkbox"/>	GOTERM_BP_ALL	positive regulation of cellular metabolic process	RT			86	3.4E-2	3.7E-1
	Annotation Cluster 45	Enrichment Score: 1.64	G			Count	P_Value	Benjamini
<input type="checkbox"/>	GOTERM_BP_ALL	regulation of MAPK cascade	RT			30	3.2E-3	1.1E-1
<input type="checkbox"/>	GOTERM_BP_ALL	MAPK cascade	RT			29	7.1E-2	5.2E-1
<input type="checkbox"/>	GOTERM_BP_ALL	signal transduction by protein phosphorylation	RT			29	1.0E-1	6.1E-1
	Annotation Cluster 48	Enrichment Score: 1.64	G			Count	P_Value	Benjamini
<input type="checkbox"/>	GOTERM_BP_ALL	chromatin remodeling at centromere	RT			6	6.0E-3	1.6E-1
<input type="checkbox"/>	GOTERM_BP_ALL	centromere complex assembly	RT			6	1.1E-2	2.1E-1
<input type="checkbox"/>	GOTERM_BP_ALL	CENP-A containing chromatin organization	RT			5	2.2E-2	2.9E-1
<input type="checkbox"/>	GOTERM_BP_ALL	CENP-A containing nucleosome assembly	RT			5	2.2E-2	2.9E-1
<input type="checkbox"/>	GOTERM_BP_ALL	DNA replication-independent nucleosome assembly	RT			5	4.5E-2	4.3E-1
<input type="checkbox"/>	GOTERM_BP_ALL	DNA replication-independent nucleosome organization	RT			5	4.7E-2	4.4E-1
<input type="checkbox"/>	GOTERM_BP_ALL	histone exchange	RT			5	5.9E-2	4.8E-1
<input type="checkbox"/>	GOTERM_BP_ALL	ATP-dependent chromatin remodeling	RT			5	1.4E-1	6.8E-1
	Annotation Cluster 47	Enrichment Score: 1.61	G			Count	P_Value	Benjamini
<input type="checkbox"/>	GOTERM_BP_ALL	negative regulation of response to stimulus	RT			48	1.4E-2	2.4E-1
<input type="checkbox"/>	GOTERM_BP_ALL	negative regulation of signal transduction	RT			38	3.3E-2	3.7E-1
<input type="checkbox"/>	GOTERM_BP_ALL	negative regulation of cell communication	RT			40	4.3E-2	4.2E-1
<input type="checkbox"/>	GOTERM_BP_ALL	negative regulation of signaling	RT			40	4.3E-2	4.2E-1
	Annotation Cluster 48	Enrichment Score: 1.6	G			Count	P_Value	Benjamini
<input type="checkbox"/>	GOTERM_BP_ALL	cellular protein modification process	RT			113	2.6E-2	3.2E-1
<input type="checkbox"/>	GOTERM_BP_ALL	protein modification process	RT			113	2.6E-2	3.2E-1
<input type="checkbox"/>	GOTERM_BP_ALL	macromolecule modification	RT			117	4.8E-2	4.4E-1
	Annotation Cluster 49	Enrichment Score: 1.46	G			Count	P_Value	Benjamini
<input type="checkbox"/>	GOTERM_BP_ALL	nitrogen compound metabolic process	RT			199	6.2E-3	1.6E-1
<input type="checkbox"/>	GOTERM_BP_ALL	organic cyclic compound metabolic process	RT			173	2.7E-2	3.3E-1
<input type="checkbox"/>	GOTERM_BP_ALL	cellular nitrogen compound metabolic process	RT			182	2.7E-2	3.3E-1
<input type="checkbox"/>	GOTERM_BP_ALL	cellular aromatic compound metabolic process	RT			166	4.6E-2	4.3E-1
<input type="checkbox"/>	GOTERM_BP_ALL	nucleobase-containing compound metabolic process	RT			160	6.4E-2	5.0E-1
<input type="checkbox"/>	GOTERM_BP_ALL	heterocycle metabolic process	RT			163	6.7E-2	5.0E-1
<input type="checkbox"/>	GOTERM_BP_ALL	nucleic acid metabolic process	RT			143	7.6E-2	5.3E-1
	Annotation Cluster 60	Enrichment Score: 1.44	G			Count	P_Value	Benjamini
<input type="checkbox"/>	GOTERM_BP_ALL	positive regulation of nitric oxide metabolic process	RT			5	2.2E-2	2.9E-1

<input type="checkbox"/>	GOTERM_BP_ALL	positive regulation of nitric oxide biosynthetic process	RT		5	2.2E-2	2.9E-1
<input type="checkbox"/>	GOTERM_BP_ALL	nitric oxide biosynthetic process	RT		6	2.4E-2	3.1E-1
<input type="checkbox"/>	GOTERM_BP_ALL	nitric oxide metabolic process	RT		6	3.0E-2	3.5E-1
<input type="checkbox"/>	GOTERM_BP_ALL	positive regulation of reactive oxygen species biosynthetic process	RT		5	3.5E-2	3.8E-1
<input type="checkbox"/>	GOTERM_BP_ALL	reactive nitrogen species metabolic process	RT		6	3.7E-2	3.9E-1
<input type="checkbox"/>	GOTERM_BP_ALL	regulation of nitric oxide biosynthetic process	RT		5	4.7E-2	4.4E-1
<input type="checkbox"/>	GOTERM_BP_ALL	reactive oxygen species biosynthetic process	RT		6	6.0E-2	4.8E-1
<input type="checkbox"/>	GOTERM_BP_ALL	regulation of reactive oxygen species biosynthetic process	RT		5	9.2E-2	5.8E-1
	Annotation Cluster 61	Enrichment Score: 1.41	G		Count	P_Value	Benjamini
<input type="checkbox"/>	GOTERM_BP_ALL	regulation of protein transport	RT		29	2.0E-2	2.8E-1
<input type="checkbox"/>	GOTERM_BP_ALL	regulation of establishment of protein localization	RT		30	3.5E-2	3.8E-1
<input type="checkbox"/>	GOTERM_BP_ALL	regulation of protein localization	RT		32	8.3E-2	5.5E-1
	Annotation Cluster 62	Enrichment Score: 1.41	G		Count	P_Value	Benjamini
<input type="checkbox"/>	GOTERM_BP_ALL	myeloid leukocyte migration	RT		11	6.4E-3	1.6E-1
<input type="checkbox"/>	GOTERM_BP_ALL	leukocyte chemotaxis	RT		10	5.3E-2	4.6E-1
<input type="checkbox"/>	GOTERM_BP_ALL	cell chemotaxis	RT		10	1.7E-1	7.4E-1
	Annotation Cluster 63	Enrichment Score: 1.38	G		Count	P_Value	Benjamini
<input type="checkbox"/>	GOTERM_BP_ALL	regulation of protein import into nucleus	RT		11	1.1E-2	2.1E-1
<input type="checkbox"/>	GOTERM_BP_ALL	regulation of protein import	RT		11	1.2E-2	2.2E-1
<input type="checkbox"/>	GOTERM_BP_ALL	regulation of nucleocytoplasmic transport	RT		12	1.8E-2	2.7E-1
<input type="checkbox"/>	GOTERM_BP_ALL	regulation of protein localization to nucleus	RT		12	2.1E-2	2.8E-1
<input type="checkbox"/>	GOTERM_BP_ALL	regulation of protein targeting	RT		12	1.3E-1	6.6E-1
<input type="checkbox"/>	GOTERM_BP_ALL	regulation of intracellular protein transport	RT		14	1.4E-1	6.8E-1
<input type="checkbox"/>	GOTERM_BP_ALL	regulation of intracellular transport	RT		16	2.0E-1	7.7E-1
	Annotation Cluster 64	Enrichment Score: 1.38	G		Count	P_Value	Benjamini
<input type="checkbox"/>	GOTERM_BP_ALL	protein K11-linked deubiquitination	RT		3	2.4E-2	3.1E-1
<input type="checkbox"/>	GOTERM_BP_ALL	protein K63-linked deubiquitination	RT		4	2.6E-2	3.2E-1
<input type="checkbox"/>	GOTERM_BP_ALL	protein K48-linked deubiquitination	RT		3	1.4E-1	6.8E-1
	Annotation Cluster 65	Enrichment Score: 1.35	G		Count	P_Value	Benjamini
<input type="checkbox"/>	GOTERM_BP_ALL	secondary alcohol metabolic process	RT		8	3.1E-2	3.6E-1
<input type="checkbox"/>	GOTERM_BP_ALL	steroid metabolic process	RT		8	4.2E-2	4.1E-1
<input type="checkbox"/>	GOTERM_BP_ALL	cholesterol metabolic process	RT		7	6.7E-2	5.0E-1
	Annotation Cluster 66	Enrichment Score: 1.35	G		Count	P_Value	Benjamini
<input type="checkbox"/>	GOTERM_BP_ALL	cellular response to lipopolysaccharide	RT		9	3.3E-2	3.7E-1
<input type="checkbox"/>	GOTERM_BP_ALL	cellular response to molecule of bacterial origin	RT		9	4.0E-2	4.0E-1
<input type="checkbox"/>	GOTERM_BP_ALL	cellular response to biotic stimulus	RT		9	7.1E-2	5.2E-1
	Annotation Cluster 67	Enrichment Score: 1.33	G		Count	P_Value	Benjamini
<input type="checkbox"/>	GOTERM_BP_ALL	negative regulation of endothelial cell differentiation	RT		3	8.6E-3	1.9E-1
<input type="checkbox"/>	GOTERM_BP_ALL	negative regulation of epithelial cell differentiation	RT		4	7.2E-2	5.2E-1
<input type="checkbox"/>	GOTERM_BP_ALL	regulation of endothelial cell differentiation	RT		3	1.6E-1	7.2E-1
	Annotation Cluster 68	Enrichment Score: 1.32	G		Count	P_Value	Benjamini
<input type="checkbox"/>	GOTERM_BP_ALL	glucose metabolic process	RT		11	2.1E-2	2.9E-1
<input type="checkbox"/>	GOTERM_BP_ALL	hexose metabolic process	RT		11	6.3E-2	4.9E-1
<input type="checkbox"/>	GOTERM_BP_ALL	monosaccharide metabolic process	RT		11	8.2E-2	5.5E-1
	Annotation Cluster 69	Enrichment Score: 1.29	G		Count	P_Value	Benjamini
<input type="checkbox"/>	GOTERM_BP_ALL	positive regulation of pathway-restricted SMAD protein phosphorylation	RT		5	3.1E-2	3.6E-1
<input type="checkbox"/>	GOTERM_BP_ALL	regulation of pathway-restricted SMAD protein phosphorylation	RT		5	6.5E-2	5.0E-1
<input type="checkbox"/>	GOTERM_BP_ALL	pathway-restricted SMAD protein phosphorylation	RT		5	6.8E-2	5.0E-1
	Annotation Cluster 80	Enrichment Score: 1.27	G		Count	P_Value	Benjamini
<input type="checkbox"/>	GOTERM_BP_ALL	regulation of viral release from host cell	RT		4	4.4E-2	4.3E-1
<input type="checkbox"/>	GOTERM_BP_ALL	viral release from host cell	RT		4	5.2E-2	4.5E-1
<input type="checkbox"/>	GOTERM_BP_ALL	negative regulation of viral release from host cell	RT		3	6.5E-2	5.0E-1
	Annotation Cluster 81	Enrichment Score: 1.24	G		Count	P_Value	Benjamini
<input type="checkbox"/>	GOTERM_BP_ALL	regulation of transferase activity	RT		33	5.2E-2	4.5E-1
<input type="checkbox"/>	GOTERM_BP_ALL	regulation of kinase activity	RT		28	5.7E-2	4.7E-1